



Albashaireh, Khawlah Zakareyya (2022) *Microbial interkingdom interaction in endodontic biofilms and the quest for novel antimicrobial treatments*. PhD thesis.

<https://theses.gla.ac.uk/83186/>

Copyright and moral rights for this work are retained by the author

A copy can be downloaded for personal non-commercial research or study, without prior permission or charge

This work cannot be reproduced or quoted extensively from without first obtaining permission from the author

The content must not be changed in any way or sold commercially in any format or medium without the formal permission of the author

When referring to this work, full bibliographic details including the author, title, awarding institution and date of the thesis must be given

Enlighten: Theses

<https://theses.gla.ac.uk/>
research-enlighten@glasgow.ac.uk



University
of Glasgow

**Microbial interkingdom interaction in endodontic
biofilms and the quest for novel antimicrobial
treatments.**

Khawlah Zakareyya Albashaireh
BDS, MClintDent/ Endodontics

Submitted in fulfilment of the requirements for the degree
of Doctor of Philosophy

School of Medicine, Dentistry and Nursing
College of Medical, Veterinary and Life Sciences

University of Glasgow

May 2022

Abstract

Candida albicans and *Enterococcus faecalis* are two commensal microorganisms in the human microflora. Both are opportunistic pathogens that are frequently coisolated from nosocomial, bloodstream, and root canal infections. Biofilm formation is one of the key features of both microorganisms. Inter-species interaction can induce behavioural changes in microorganisms residing within a polymicrobial biofilm, which will eventually affect the overall pathogenicity of the biofilm. Interkingdom interactions are complex and can exacerbate infection. Moreover, these complex communities can result in enhanced tolerance to antimicrobial agents. With the rise of antimicrobial resistance worldwide, coupled with tolerant biofilm communities, then there is a great demand for finding alternative treatment modalities that can manage complex infection.

Endodontic infection is a polymicrobial biofilm disease, with *C. albicans* and *E. faecalis* frequently coisolated from clinical samples of this infection. It is believed that *E. faecalis* exert an antagonistic impact on *C. albicans* by inhibiting its hyphal formation, which results in preserving commensalism within normal microbiome niches. However, their common coisolation in different disease entities indicates a complex interaction beyond antagonism.

One of the aims of the experimental work reported in this thesis was to investigate this interkingdom interaction and employ different tools to unravel key behavioural changes that would help in understanding cross-kingdom communications. Interkingdom interaction was first investigated phenotypically by assessing metabolic activity using XTT assay, then by assessing biofilm biomass using a crystal violet assay, and by microscopic analysis wherein dual-species biofilm was visualised. Molecular analysis using qPCR was employed to quantify cell number and assess growth of microorganisms in dual-species biofilm. Gene expression analysis was then performed using real-time quantitative polymerase chain reaction (RT-qPCR) to assess key virulence gene expression in *C. albicans* and *E. faecalis* at different biofilm formation stages. Next, whole *C. albicans* RNA-sequencing was implemented to investigate differential gene expression of the microorganism in response to *E. faecalis* presence at 8 hours and 24 hours. Finally, novel therapeutic agents, including nanodiamonds and small molecules screened

from FDA approved drug library, were employed to target virulence mechanisms and assess microorganism behaviour within dual-species biofilm compared to single species biofilm.

E. faecalis was shown to induce phenotypic changes on *C. albicans*. It inhibited hyphal morphogenesis, growth and reduced its biofilm biomass. Phenotypic results showed antagonism against *C. albicans* but *E. faecalis* remained unchanged. At molecular levels, *E. faecalis* downregulated key genes involved in *C. albicans* virulence, whilst *C. albicans* upregulated genes involved in *E. faecalis* adhesion and biofilm formation. In addition, the transcriptome of *C. albicans* was significantly altered in the presence of *E. faecalis*. Stress responses, oxidoreductase activity, amino acid biosynthesis and the fungal biofilm matrix were the most significantly upregulated pathways in *C. albicans*. Glucose sensation and transportation, glycerol biosynthesis process and arginine catabolic pathway were the most significantly downregulated pathways in *C. albicans*. Finally, the coexistence of both microorganisms in dual-species biofilm altered their response to novel therapeutic agents compared to each species alone by increasing each microorganism's tolerance to different types of treatments.

This research can be seen as a starting point to investigate further mechanisms relevant to *C. albicans* and *E. faecalis* complex interkingdom relationship using advanced tools. In addition, this research provides a significant input to the current knowledge that repurposing drugs and nanomaterials can be suitable candidates to be used as broad antimicrobial agents.

Table of Contents

Abstract.....	ii
Table of Contents	iv
List of Tables.....	viii
List of Figures.....	ix
List of Publications.....	xiv
List of Accompanying Materials.....	xv
Acknowledgement	xvi
Author’s Declaration.....	xviii
Definitions/Abbreviations.....	xix
Chapter 1: General Introduction	1
1.1 Endodontic Microbiology	2
1.1.1 The dental pulp	2
1.1.2 Pathogenesis of endodontic infections.....	4
1.1.3 Root canal ecology as a factor to drive composition and virulence of polymicrobial community in endodontic infections	8
1.1.4 Endodontic infection as a biofilm induced disease.....	9
1.1.5 Technical advancements in microbial identification.....	16
1.1.6 Microbial interaction within a biofilm	23
1.1.7 Interkingdom interaction in biofilms.....	26
1.2 Management of endodontic infections	35
1.2.1 Novel approaches to root canal disinfection	36
1.3 Hypothesis and aims	55
Chapter 2: Characterisation of <i>Candida albicans</i> and <i>Enterococcus faecalis</i> dual-species biofilm and the reciprocal effect on their virulence	56
2.1 Introduction.....	57
2.2 Hypotheses and Aims	63
2.3 Materials and methods	64
2.3.1 Culture conditions and standardisation.....	64
2.3.2 <i>E. faecalis</i> standardisation using serial dilution and standard curve	65
2.3.3 Haemolysis assay.....	66

2.3.4	Gelatinase assay	67
2.3.5	Metabolic activity assay.....	67
2.3.6	Biofilm biomass assay	68
2.3.7	Adherence assay	68
2.3.8	Assessment of <i>C. albicans</i> phenotypic characteristics when cocultured with <i>E. faecalis</i>	69
2.3.9	Metabolic activity and biofilm biomass assessment of single and dual-species biofilm	70
2.3.10	Microbial load assessment using quantitative PCR.....	70
2.3.11	Transcriptional analysis of virulence related genes in <i>C. albicans</i> and <i>E. faecalis</i>	71
2.3.12	Statistical Analysis	75
2.4	Results	75
2.4.1	<i>E. faecalis</i> virulence characterisation.	75
2.4.2	<i>E. faecalis</i> standardisation	75
2.4.3	<i>C. albicans</i> biofilm characterisation	88
2.4.4	<i>C. albicans</i> and <i>E. faecalis</i> dual-species biofilm characterisation ...	88
2.5	Discussion	103
2.6	Conclusion.....	108

Chapter 3: Transcriptomic analysis of *C. albicans* response to *E. faecalis* in dual-species biofilm 109

3.1	Introduction.....	110
3.2	Hypothesis and Aims	112
3.3	Materials and methods	113
3.3.1	Strain and culture conditions	113
3.3.2	Media preparation	113
3.3.3	<i>In vitro</i> transcriptomic analysis of <i>C. albicans</i> interactions with <i>E. faecalis</i>	113
3.3.4	RNA extraction from <i>C. albicans</i> and <i>E. faecalis</i> biofilms.....	114
3.3.5	RNA-seq and analysis pipeline	115
3.3.6	Statistical Analysis.....	116
3.4	Results	117

3.4.1 <i>E. faecalis</i> induced major transcriptomic changes in <i>C. albicans</i> in mixed-species biofilms.....	117
3.4.2 <i>E. faecalis</i> downregulated key genes involved in virulence, growth and biofilm formation.....	139
3.5 Discussion	148
3.6 Conclusion.....	160

Chapter 4: Response of Dual-species biofilm to novel treatment strategies: a window to understanding interkingdom interactions 161

4.1 Introduction.....	162
4.2 Hypotheses and Aims	167
4.3 Materials and methods	168
4.3.1 Culture conditions and standardisation.....	168
4.3.2 Assessment of the antimicrobial activity of nanodiamonds	168
4.3.3 Transcriptional analysis of biofilm related genes	170
4.3.4 Nanodiamonds disc preparation	170
4.3.5 Biofilm inhibition screen.....	171
4.3.6 Compound library and selected drugs stock preparation.....	172
4.3.7 Planktonic minimum inhibitory concentration of small molecule compounds against <i>E. faecalis</i> and <i>C. albicans</i> isolates	172
4.3.8 KHS101 hydrochloride and darapladib biofilm inhibition, and disruption susceptibility against single-species and dual-species biofilm of <i>C. albicans</i> and <i>E. faecalis</i>	173
4.3.9 Statistical Analysis.....	174
4.4 Results.....	175
4.4.1 Nanodiamonds showed no fungicidal and bactericidal activity against <i>C. albicans</i> and <i>E. faecalis</i> biofilms.	175
4.4.2 Microscopic analysis of nanodiamonds interaction with <i>C. albicans</i> and <i>E. faecalis</i>	178
4.4.3 Nanodiamonds exhibited anti-adhesion and biofilm inhibition effect against <i>C. albicans</i> clinical and lab isolates.....	181
4.4.4 Nanodiamonds exhibited biofilm inhibition effect against <i>E. faecalis</i> .	

4.4.5	Nanodiamonds showed dual-species biofilm inhibition.	185
4.4.6	Nanodiamonds altered the virulence behaviour of <i>C. albicans</i> in single and dual-species biofilm	194
4.4.7	<i>C. albicans</i> and <i>E. faecalis</i> response to Biodentine incorporated with NDs was altered when in dual-species biofilm.	196
4.4.8	Screening antifungal activity of FDA approved drugs against <i>C. albicans</i> SC5314	200
4.4.9	Minimum inhibitory concentration of 11 candidate compounds against <i>C. albicans</i> and <i>E. faecalis</i> isolates.....	212
4.4.10	Biofilm inhibition activity of KHS101 hydrochloride against single and dual-species biofilm of <i>C. albicans</i> and <i>E. faecalis</i>	217
4.4.11	Biofilm inhibition activity of darapladib against single and dual-species biofilm of <i>C. albicans</i> and <i>E. faecalis</i>	227
4.4.12	Biofilm disruption activity of KHS101 and darapladib against single and dual-species biofilm combined with NDs	237
4.5	Discussion	251
4.6	Conclusion.....	259
Chapter 5: General Discussion		260
5.1	Introduction.....	261
5.2	Building dual-species biofilm model.....	263
5.3	Antagonism in health, but synergy in disease	263
5.4	Does antagonism increase sensitivity of microbial cells towards treatment? 268	
5.5	Concluding remarks and future work.....	269
List of References.....		271

List of Tables

Table 2.1: List of <i>C. albicans</i> and <i>E. faecalis</i> isolates.....	65
Table 2.2: Volumes used from each component to prepare the master mix for the cDNA.	73
Table 2.3: List of primers used in this chapter	74
Table 4.1: NDs percentages incorporated into Biodentine™.....	171
Table 4.2: Biofilm inhibition MIC of <i>C. albicans</i> , <i>E. faecalis</i> clinical and lab isolates to NaOCl, EDTA, Chitosan and nanodiamonds. Numbers represent metabolic activity MIC values. a (-) indicates MIC value not detected.	176
Table 4.3: Biofilm inhibition MIC of <i>C. albicans</i> , <i>E. faecalis</i> clinical and lab isolates to NaOCl, EDTA, Chitosan and NDs. Numbers represent biofilm biomass MIC values. a (-) indicates MIC value not detected.....	177
Table 4.4: Hit compounds identified from library screening and their mechanism of action.....	206
Table 4.5: MIC of planktonic cells of eleven compounds against three <i>C. albicans</i> isolates and three <i>E. faecalis</i> strains. (-) indicates not detected	214

List of Figures

Figure 1.1: Pathogenesis of pulpal and periapical infection	5
Figure 1.2: Stages of biofilm formation.....	14
Figure 1.3: NDs properties, types, and production methods	41
Figure 1.4: Approaches in drug repurposing.....	47
Figure 2.1: Standardization of <i>E. faecalis</i> ATCC 29212.	76
Figure 2.2: Haemolytic phenotypes identified among <i>E. faecalis</i> isolates under different incubation conditions for 24 hours.	77
Figure 2.3: Quantitative haemolysis analysis of <i>E. faecalis</i> strains under different incubation conditions for 24h.	78
Figure 2.4: Gelatinase enzyme identification in <i>E. faecalis</i> strains.	79
Figure 2.5: Quantitative identification of gelatinase enzyme activity in <i>E. faecalis</i> strains	80
Figure 2.6: Metabolic activity of <i>E. faecalis</i> strains.	82
Figure 2.7: Quantification of biofilm biomass of <i>E. faecalis</i> strains.....	84
Figure 2.8: Percentage of adherent <i>E. faecalis</i> cells to Collagen I ECM protein.	86
Figure 2.9: Heatmap analysis of all <i>E. faecalis</i> strains showing enhanced virulence under anaerobic conditions.	87
Figure 2.10: Characterisation of <i>C. albicans</i> isolates according to their biofilm forming capability.....	88
Figure 2.11: <i>E. faecalis</i> inhibits yeast to hyphae switch in <i>C. albicans</i>	90
Figure 2.12: Alteration of dual-species biofilm metabolic activity compared to each strain in a mono-species biofilm.....	92
Figure 2.13: Alteration of dual-species biofilm biomass compared to each mono-species biofilm biomass.	93
Figure 2.14: The effect of <i>E. faecalis</i> and <i>C. albicans</i> on each other's growth in dual-species biofilm compared to single species biofilm.	95
Figure 2.15: <i>E. faecalis</i> high and low virulent strains induces changes in <i>C. albicans</i> key virulence genes at early and late dual-species biofilm.....	97
Figure 2.16: <i>C. albicans</i> induces changes in <i>E. faecalis</i> key virulence genes at early and late dual-species biofilm.	98
Figure 2.17: Gene expression analysis of virulence related genes in <i>C. albicans</i> at biofilm adhesion phase of dual-species biofilm formation.	100

Figure 2.18: Gene expression analysis of virulence related genes in <i>E. faecalis</i> at biofilm adhesion phase of dual-species biofilm formation.	102
Figure 3.1: Experimental pipeline.	114
Figure 3.2: Bioinformatics analysis pipeline.	116
Figure 3.3: Presence of <i>E. faecalis</i> determines mature biofilm transcriptome.	118
Figure 3.4: <i>Enterococcus faecalis</i> induces specific gene upregulation in <i>C. albicans</i> at 8 hours and 24 hours.	119
Figure 3.5: <i>Enterococcus faecalis</i> induces specific gene downregulation in <i>C. albicans</i> at 8 hours and 24 hours.	120
Figure 3.6: Heatmap and Volcano plot for <i>C. albicans</i> in mono-species biofilm transcription profile	123
Figure 3.7: Heatmap and Volcano plot for <i>C. albicans</i> in dual-species biofilm transcription profile.	125
Figure 3.8: <i>E. faecalis</i> induces significant changes in different metabolic pathways in <i>C. albicans</i> at 8 hours and 24 hours compared to <i>C. albicans</i> mono-species biofilm.	127
Figure 3.9: Heatmap and Volcano plot for <i>C. albicans</i> + <i>E. faecalis</i> dual-species vs. <i>C. albicans</i> mono-species biofilm transcription profile at 8 hours.	130
Figure 3.10: <i>E. faecalis</i> induced significant upregulation and downregulation of different metabolic pathways in <i>C. albicans</i> at 8 hours.	132
Figure 3.11: Heatmap and Volcano plot for <i>C. albicans</i> and <i>E. faecalis</i> dual-species VS <i>C. albicans</i> mono-species biofilm transcription profile at 24 hours.	137
Figure 3.12: <i>E. faecalis</i> induced significant upregulation and downregulation of different metabolic pathways in <i>C. albicans</i> at 24 hours.	138
Figure 3.13: Heatmaps showing upregulated and downregulated genes involved in <i>C. albicans</i> virulence mechanism in dual-species compared to single species biofilm.	142
Figure 3.14: Heatmaps showing differentially expressed genes involved in <i>C. albicans</i> Growth.	146
Figure 3.15: <i>E. faecalis</i> downregulates the septin gene family.	147
Figure 3.16: Summary of arginine biosynthetic pathway and nitrogen utilization in <i>C. albicans</i> indicating acidic environment.	154
Figure 4.1: Disk diffusion assay for NDs.	178

Figure 4.2: Light microscopic images of <i>C. albicans</i> biofilm after incubation with NDs.	179
Figure 4.3: Light microscopic images of <i>E. faecalis</i> biofilm after incubation with NDs.	180
Figure 4.4: NDs prevented <i>C. albicans</i> isolates cell attachment.....	182
Figure 4.5: NDs prevented <i>E. faecalis</i> strains cell attachment. Mean colony forming units (CFU) of twelve strains of <i>E. faecalis</i>	184
Figure 4.6: Light microscope images of single and dual-species biofilm of <i>C. albicans</i> SC5314 with and without treatment with NDs.	186
Figure 4.7: Light microscope images of single and dual-species biofilm of <i>C. albicans</i> LBF BC023 with and without treatment with NDs.	187
Figure 4.8: Light microscope images of single and dual-species biofilm of <i>C. albicans</i> HBF BC146 with and without treatment with NDs.....	188
Figure 4.9: NDs effect on colony forming ability of <i>C. albicans</i> isolates in dual-species biofilm.	191
Figure 4.10: NDs effect on colony forming ability of <i>E. faecalis</i> strains in dual-species biofilm.	193
Figure 4.11: Relative gene expression analysis of key virulence genes in <i>C. albicans</i> SC5314 in the presence of NDs compared to untreated control.....	195
Figure 4.12: Relative gene expression analysis of key virulence genes in <i>C. albicans</i> SC5314 in dual-species biofilm in the presence of NDs compared to untreated control.	196
Figure 4.13: <i>C. albicans</i> lab strain SC5314 mean colony forming units in single and dual-species biofilms grown on bovine dentine, Biodentine™, Biodentine™ and NDs discs.	198
Figure 4.14: <i>E. faecalis</i> clinical strains ER5/1 and E2 mean colony forming units in single and dual-species biofilms grown on bovine dentine, Biodentine™, Biodentine™ and NDs discs.	199
Figure 4.15: Heatmaps showing metabolic activity and biofilm biomass values of Tocriscreen™ library plates for <i>C. albicans</i> SC5314 (Plate 1 - Plate 4):.....	201
Figure 4.16: Heatmaps showing metabolic activity and biofilm biomass values of Tocriscreen™ library plates for <i>C. albicans</i> SC5314 (Plate 5 - Plate 8):.....	202
Figure 4.17: Heatmaps showing metabolic activity and biofilm biomass values of Tocriscreen™ library plates for <i>C. albicans</i> SC5314 (Plate 9 - Plate 12):	203

Figure 4.18: Heatmaps showing metabolic activity and biofilm biomass values of Tocriscreen™ library plates for <i>C. albicans</i> SC5314 (Plate 13 - Plate 16):	204
Figure 4.19: Hits identified by screening a library of biologically active compounds for biofilm inhibition effect on <i>C. albicans</i>	205
Figure 4.20: Metabolic activity and biofilm biomass of <i>C. albicans</i> and <i>E. faecalis</i> HVS ER5/1 single and dual-species biofilms with and without KHS101 hydrochloride treatment.	218
Figure 4.21: Metabolic activity and biofilm biomass of <i>C. albicans</i> and <i>E. faecalis</i> HVS E2 single and dual-species biofilms with and without KHS101 hydrochloride treatment.	219
Figure 4.22: KHS101 hydrochloride inhibitory effect on single and dual-species biofilm formation by viable plate count.	221
Figure 4.23: Light microscope images of <i>C. albicans</i> single-species biofilm inhibition before and after treatment with KHS101 hydrochloride.....	222
Figure 4.24: Light microscope images of <i>E. faecalis</i> ER5/1 single-species biofilm inhibition before and after treatment with KHS101 hydrochloride.....	223
Figure 4.25: Light microscope images of <i>C. albicans</i> and <i>E. faecalis</i> ER5/1 dual-species biofilm inhibition before and after treatment with KHS101 hydrochloride.	224
Figure 4.26: Light microscope images of <i>E. faecalis</i> E2 single-species biofilm inhibition before and after treatment with KHS101 hydrochloride.....	225
Figure 4.27: Light microscope images of <i>C. albicans</i> and <i>E. faecalis</i> E2 dual-species biofilm inhibition before and after treatment with KHS101 hydrochloride.	226
Figure 4.28: Metabolic activity and biofilm biomass of <i>C. albicans</i> and <i>E. faecalis</i> HVS ER5/1 single and dual-species with and without darapladib treatment....	228
Figure 4.29: Metabolic activity and biofilm formation of <i>C. albicans</i> and <i>E. faecalis</i> LVS E2 single and dual-species with and without darapladib treatment.	229
Figure 4.30: Darapladib inhibitory effect on single and dual-species biofilm formation based on viable plate counts.....	231
Figure 4.31: Light microscope images of <i>C. albicans</i> single-species biofilm inhibition with and without treatment with darapladib.	232

Figure 4.32: Light microscope images of <i>E. faecalis</i> ER5/1 single-species biofilm inhibition with and without treatment with darapladib.	233
Figure 4.33: Light microscope images of <i>C. albicans</i> and <i>E. faecalis</i> ER5/1 dual-species biofilm inhibition with and without treatment with darapladib.	234
Figure 4.34: Light microscope images of <i>E. faecalis</i> E2 single-species biofilm inhibition with and without treatment with darapladib.	235
Figure 4.35: Light microscope images of <i>C. albicans</i> and <i>E. faecalis</i> E2 dual-species biofilm inhibition with and without treatment with darapladib.	236
Figure 4.36: Metabolic activity of <i>C. albicans</i> and two <i>E. faecalis</i> strains single and dual-species after biofilm disruption treatment by KHS101 hydrochloride, Darapadib, NDs and combinational treatment.	239
Figure 4.37: Biofilm biomass of <i>C. albicans</i> and two <i>E. faecalis</i> strains single and dual-species after biofilm disruption treatment by KHS101 hydrochloride, Darapadib, NDs and combinational treatment.	240
Figure 4.38: <i>C. albicans</i> colony forming units after biofilm disruption treatment by KHS101 hydrochloride, darapadib, NDs and combinational treatment.	242
Figure 4.39: <i>E. faecalis</i> colony forming units after biofilm disruption treatment by KHS101 hydrochloride, darapadib, NDs and combinational treatment.	244
Figure 4.40: Light microscope images of single-species biofilm disruption of <i>C. albicans</i> with and without different treatment conditions.	246
Figure 4.41: Light microscope images of single-species biofilm disruption of <i>E. faecalis</i> ER5/1 with and without different treatment conditions.	247
Figure 4.42: Light microscope images of <i>C. albicans</i> and <i>E. faecalis</i> ER5/1 dual-species biofilm disruption with and without different treatment conditions. ..	248
Figure 4.43: Light microscope images of single-species biofilm disruption of <i>E. faecalis</i> E2 with and without different treatment conditions.	249
Figure 4.44: Light microscope images of <i>C. albicans</i> and <i>E. faecalis</i> E2 dual-species biofilm disruption with and without treatment conditions	250
Figure 5.1: Spatial patterning of microorganisms (microbiogeography) determines the fate of infection	262

List of Publications

Publications related to this thesis:

Abusrewil S, Alshanta OA, Albashaireh K, *et al.* Detection, treatment and prevention of endodontic biofilm infections: what's new in 2020?. *Crit Rev Microbiol.* 2020;46(2):194-212. DOI: [10.1080/1040841X.2020.1739622](https://doi.org/10.1080/1040841X.2020.1739622)

Alshanta OA, Albashaireh K, McKloud E, *et al.* *Candida albicans* and *Enterococcus faecalis* biofilm frenemies: When the relationship sours. *Biofilm.* 2022;4:100072. Published 2022 Mar 14. DOI: [10.1016/j.bioflm.2022.100072](https://doi.org/10.1016/j.bioflm.2022.100072)

Submitted papers related to this thesis:

A paper was submitted to APMIS journal under the title “Screening the Tocriscreen™ bioactive compound library in search for inhibitors of *Candida* biofilm formation”.

List of Accompanying Materials

- I. Supplementary Data: Gene counts from RNA-Sequencing data set of *C. albicans* at 8 hours and 24 hours' time points.
- II. High resolution versions of figures.

Acknowledgement

All praises be to Allah who has given me patience and granted me willpower and strength to continue my PhD journey until the very end. I would like to express my gratitude to Dr William Mclean and Professor Gordon Ramage for their useful guidance and extensive help during this project and thesis preparation. Thanks to you, this project has survived the challenging times of COVID. Your valuable advice and feedback have helped shaping my academic personality.

Many thanks and gratitude go to Jordan University of Science and Technology for their financial support of my PhD and to University of Glasgow MVLS Graduate School for their financial support in the last months of my PhD due to COVID impact.

I want to also thank Mr. Steve Milligan for his help with all technical issues in the lab.

I was blessed to have a wonderful and cooperative colleagues in Glasgow dental hospital and school who supported me throughout my PhD whether in or outside the lab. Dr Tracy Young, my lab role model, I am so grateful for your help in the last year, I have learned a lot from you. Dr Christopher Delaney, thank you for your support in the Bioinformatics chapter of my thesis, data analysis and proofreading. Mark Butcher, Bryn Short, Dr Emily McCloud, Dr Ryan Kean, Ryan Stewart, Dr William Johnston, Dr Lais Arias, EJay Bakri, Krystyna Piela and the GEG group: Sumayya AbuSreweil, Om-Alkhair Alshanta, Suror Shaban, Hafsa AbdulJaleel and Saeed AlQahtani. I will always remember our chats, lunches, birthdays, and Christmas parties. Thank you for being a part of a nice memory and for making my lab days enjoyable. Jamie Kidd, thank you for your kind support during lockdown and Matt Brennand-Roper, thank you for being a good friend and a good listener.

Special thanks go to Dr Jason Brown for providing a great support in the lab since day one until the last days in my PhD and for the reassurance whenever I was in doubt. I will always remember you telling me, “just keep doing what you’re

doing”. I would also like to thank my dear friend Lina Mowafi for making (Figure 1.1 and Figure 3.16) in my thesis.

I am so grateful to have earned a friend for life, Abeer Alghamdi, your presence was invaluable and helped me going through the very difficult times. Yusra, you made my life in the UK so much fun! Yara Jubran, my childhood friend, thank you for taking care of me and supporting me on day-to-day basis. Uncle Suli and Auntie Mary, thank you for being my second family in Glasgow. My friends in Glasgow, thank you for all the adventures we had in Scotland. Ikram, thank you for being a good listener.

Finally, to my mom and dad words can never describe my ultimate gratitude. Thank you for your endless love and encouragement. I wouldn't be able to do what I have done without you in my life. My brothers and sisters, Derar, Arwa, Dhoha, Alaa, Roqayyah and Yahya. Your unconditional love and support have helped me through my difficult times. Lina, the best friend anyone can have, thank you for making my thesis look prettier and for being in my life!

Author's Declaration

I declare that I have carried out the work described in this thesis unless otherwise acknowledged or cited, under the supervision of Dr William Mclean and Professor Gordon Ramage. I further declare that this thesis has not been submitted for any other degree at the University of Glasgow or any other institution.

Khawlah Albashaireh

May 2022

Definitions/Abbreviations

AgNPs:	Silver nanoparticles
ALS:	Agglutinin-like sequence
ANOVA :	Analysis of Variance
BHI:	Brain heart infusion
BP:	Biological processes
BSA:	Bovine serum albumin
CBA:	Columbia blood agar
CC:	cellular components
cDNA:	Complementary DNA
CFE:	Colony forming equivalents
CHX:	Chlorhexidine
cND:	Carboxylated nanodiamond
CV:	Crystal violet
DLC:	Diamond-like carbon
DNDs:	Detonated nanodiamonds
ECM:	Extracellular matrix
eDNA:	Extracellular DNA
EDTA:	Ethylenediaminetetraacetic acid
EHRs:	Electronic health records
EntV:	Enterocin V583
EPS:	Extracellular polymeric substances
eRNA:	Enhancing RNA
GO:	gene ontology
GPI:	Glycosylphosphatidylinositol

GPX:	Glutathione peroxidases
HBF:	High biofilm former
HPHT:	High pressure - high temperature
HSPs:	Heat shock proteins
HTS:	High throughput screening
HVS:	High virulent strain
IBF:	Intermediate biofilm former
LBF:	Low biofilm former
Log ₂ FC:	log ₂ fold change
LPS:	Lipopolysaccharide
LTA:	Lipoteichoic acid
LVS:	Low virulent strain
MF:	Molecular functions
MIC:	Minimal inhibitory circulation
MIC:	Minimum inhibitory concentration
MNDs:	Milled nanodiamonds
NADPH:	Nicotinamide adenine dinucleotide phosphate
NaOCl:	Sodium hypochlorite
NC	Negative control
NDGP:	Nanodiamonds gutta percha
NDs:	Nanodiamonds
NGS:	Next generation sequencing
ONT:	Oxford Nanopore Technologies
OTU:	Operational taxonomic units
Padj:	adjusted p value
PAP:	Primary apical periodontitis

PBS:	Phosphate buffer sodium chloride
PC:	Positive control
PCA:	principal component analysis
PCR:	Polymerase chain reaction
PMMA:	Polymethyl-methacrylate
qRT-PCR:	Real-time polymerase chain reaction
REDOX	Oxidation-reduction
RNA-seq:	RNA sequencing
ROS:	Reactive oxygen species
RPMI:	Roswell Park Memorial Institute
rRNA:	Ribosomal RNA
RT:	Reverse transcription
SAB:	Sabouraud's dextrose agar
SAP:	Secondary apical periodontitis
SEM:	Scanning electron microscopy
sEntV:	Synthetic EntV
SMRT:	Single molecule real time
SOD:	Superoxide dismutase
TEM:	Transmission electron microscope
THA:	Todd-Hewitt Agar
THB :	Todd-Hewitt Broth
UV:	Ultraviolet
YPD:	Yeast peptone dextrose
ZnONPs:	Zinc oxide nanoparticles

Chapter 1: General Introduction

1.1 Endodontic Microbiology

1.1.1 The dental pulp

The dental pulp is the highly vascularized and innervated mass of loose connective tissue in the centre of the tooth. The main cells of the pulp are the odontoblasts, fibroblasts, undifferentiated ectomesenchymal cells, macrophages, and other immunocompetent cells. Its extracellular matrix (ECM) consists of collagen fibres and ground substance. The primary function of the dental pulp is providing vitality and protection to the tooth. The odontoblasts are protective and reparative cells present at the interface of the dentine-pulp complex. These very specialised cells can form reparative dentine in response to a noxious stimulus. The pulpal blood vessels supply nutrients that are essential for dentine formation and for maintaining the integrity of the dentine-pulp complex. Pulp also can identify various microbial species and their toxins, and provoke an immune response to combat them (Walton and Torabinejad, 2015). Under normal conditions, the dental pulp is sterile and sealed by overlying enamel, dentine, and cementum. These calcified tissues covering the pulp form natural barriers against external stimuli and prevent access to the pulp by oral microbiota. However, these protective layers may be breached as a result of dental caries, crown cracks and fractures, restorative procedures, scaling and root planning and tooth wear. Consequently, the dentine-pulp complex is exposed to the oral environment. Microorganisms in saliva bathing the exposed area, and in dental plaque invade the exposed dentine-pulp complex. Moreover, microorganisms from subgingival biofilms associated with periodontal disease may also have access to the pulp via any existing lateral canals, dentinal tubules at the cervical region of the tooth and lateral or apical foramina. They may also have access to the root canal any time during or after endodontic procedures.

One of the main objectives of dental practice is to maintain pulpal vitality, preserve and restore the natural integrity of the tooth should it be compromised. However, the ability of pulp microcirculation is limited in dealing with pulpal injuries because of a restricted low compliance environment in the root canal. Thus, the surrounding defence system encounters an irresistible challenge of pathogenic microorganisms which will lead to necrosis of the pulp (Heyeraas, 1989). Subsequently, bacteria and their by-products pass out of the canal system

via apical and lateral foramina and initiate inflammation and resorption in the periapical tissues in the form of symptomatic apical periodontitis (Siqueira and Rocas, 2007). Apical periodontitis is a dynamic encounter between microbial factors and host defences at the interface between infected radicular pulp and periodontal ligament that results in local inflammation, resorption of hard tissues, destruction of other periapical tissues, and eventual formation of various histopathological categories of periapical lesions (Wong *et al.*, 2021a). Should the dental pulp succumb to microbial insult, endodontic procedures that involve the use of instruments, irrigants and dressings are employed to disinfect the root canal system. The disinfected space is then filled as completely as possible using obturation materials and a coronal restoration is placed to seal the tooth and prevent re-entry of microorganisms. Despite substantial progress in modern endodontics root canal infections and their associated apical periodontitis remain remarkably prevalent (Persoon and Ozok, 2017). This might be attributed in part to clinical strategies being focused more on preparing canals to achieve a radiographically favourable outcome, rather than on the removal of microbes and effective debridement of the complex root canal systems. Focusing on “canal shaping” alone deviates the endodontic treatment target away from the microbial aetiopathogenesis of apical periodontitis, which drives the need for effective chemo-mechanical disinfection (Wong *et al.*, 2021a). To date, persistent infections remain a problematic issue in endodontic practice which is attributed in part to microorganisms that survived the clinical procedures or found their way back into root canal space to evoke infection of different magnitudes. With this in mind, some factors form a significant proportion of the foundations of endodontic practice and provide the framework for effective therapy. These factors include a detailed knowledge of the multi-microbial-driven aetiology of infections, complete awareness of the antimicrobial challenges faced within root canals (Wong *et al.*, 2021a); and thoughtful utilization of drug repurposing to develop new drugs and medicaments to combat new infection and fight resistant microbes (Birjandi *et al.*, 2020).

The following sections will provide a literature review pertaining to pathogenesis of endodontic diseases, biofilm induced infections, technical advancement of microbial identification, microbiota of root canal infections, microbial, interspecies and interkingdom interactions. Consideration will also be made to

management of endodontic infections, novel approaches to root canal disinfection and drug repurposing and phenotypic screening will be presented.

1.1.2 Pathogenesis of endodontic infections

When dentine is exposed, microorganism gain a relatively easy pathway via the dentinal tubules towards the pulp as the smallest tubule diameter (mean 0.9 μm) (Garberoglio and Brannstrom, 1976) is compatible with the cell diameter of most oral bacterial species, which usually ranges from 0.2-0.7 μm (Siqueira and Fouad, 2014). The status of the pulp plays an important role in the process of bacterial invasion of dentinal tubules. Invasion occurs at significantly higher rate in teeth with a non-vital pulp than in those with a vital pulp (Nagaoka *et al.*, 1995). Because of the presence of tubular contents in vital teeth, the functional or physiologic diameter of the tubules is only 5-10% of the anatomic diameter seen by microscopy (Michelich *et al.*, 1978). The risk of pulpal infection is increased with increased permeability and reduced thickness of the dentine overlying the pulp.

Microorganisms, dental trauma, or restorative procedures are some of the factors which can cause inflammation in the dental pulp and periapical tissues. Microbial insults are considered amongst the most common causes of root canal infections (Nair, 2006). The most common route for microorganisms to gain access to the root canal system is through deep carious lesions. After invading the pulp, the microorganisms, or their by-products affect the pulp. The infection in the root canal may further spread via the apical foramen to affect the periapical tissues causing apical periodontitis (Nair, 2004) (Figure 1.1)

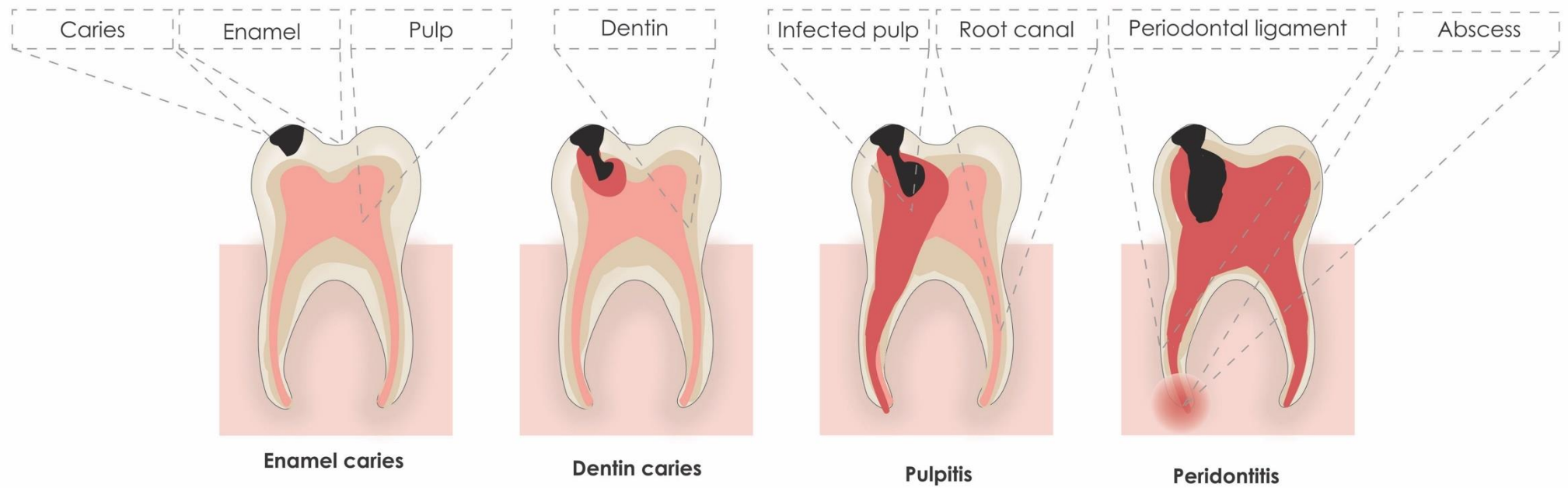


Figure 1.1: Pathogenesis of pulpal and periapical infection. Enamel caries can progress into dentin caries causing the breach of the hard tissues overlying the pulp which eventually cause pulpitis. When left untreated pulpal infection can lead to apical periodontitis.

The prevalence of root canal infections varies greatly depending on the type of infection. In primary apical periodontitis (PAP), prevalence varies between 7 - 86%, while in the case of secondary apical periodontitis (SAP), it varies between 10 - 62% (Persoon and Ozok, 2017). It has been shown that bacteria are the major domain involved in the aetiology of root canal infections although fungi, Archaea, and viruses have been found in association with some forms of apical periodontitis (Siqueira and Rocas, 2009b, Ramachandran Nair, 1987).

Kakehashi *et al.* (1965) has proved in his landmark study that bacterial colonisation is the cause of pulpal and periapical diseases. They studied the outcome of pulpal exposures in germ free rats and rats with normal flora. The pulps of germ-free rats remained vital and evidence of dentinal bridge formation overlying the exposed area was seen after 28 days. In contrast, the group of rats with normal flora developed pulpal inflammation; and abscesses associated with infected- teeth were noticed (Kakehashi *et al.*, 1965). These findings were further confirmed by the report of Sundqvist *et al.* (1976), who used anaerobic culturing technique to isolate bacteria from necrotic pulps of teeth with intact crowns in patients with a history of traumatic injury. They reported that 88 bacterial strains were isolated from teeth with periapical pathosis (Sundqvist, 1976). Likewise, Moller *et al.*, (2004) affirmed the cause-and-effect relationship between bacteria and apical periodontitis. Their study was performed on monkey's teeth. The results demonstrated periapical pathosis on the apices of infected teeth whereas no periapical lesions were noticed on the apices of teeth with healthy pulps (Moller *et al.*, 2004).

The human commensal microbiota that populates oral mucosa have evolved to tolerate the host defence mechanisms. However, bacteria can undergo a commensal organism to pathogen transition. When commensal microorganisms invade a different and previously sterile space like that of the dental pulp, they develop pathogenic mechanisms potent enough to cause infection inside the pulp chamber and root canal space. When in the pulp space, commensal microorganisms become pathogenic and acquire the ability to adhere, colonise, and survive the harsh environment inside the root canal. Simultaneously, they are capable of evading host defence mechanisms including, neutrophils, macrophages, the complement system, and antibodies. Pathogens in the root

canal system can release harmful enzymes and metabolites that can inflict direct damage to the pulp and periodontium. In addition, in response to microbial invasion a host immune reaction initiates the release of lipopolysaccharide (LPS), peptidoglycan, lipoteichoic acid (LTA), extracellular vesicles, and membrane proteins. Eventually, such products will bring about indirect tissue damage (Nair, 2004).

The ability of pulp microcirculation is limited in dealing with injuries because of a restricted low compliance environment in the root canal. Thus, the defence system becomes overwhelmed by the challenge of pathogenic microorganisms which will lead to necrosis of the pulp (Heyeraas, 1989). Subsequently, bacteria and their by-products pass out of the canal system via apical and lateral foramina. They initiate inflammation and resorption in the periapical tissues in the form of apical periodontitis (Siqueira and Rocas, 2007).

Intra-radicular infection was deemed the commonest factor for persistent apical periodontitis (Nair, 2006) and it was affirmed by Siqueira *et al.* 2014 who listed six biological factors that lead to asymptomatic radiolucencies persisting after root canal treatment. The six factors are: “(i) intraradicular infection persisting in the complex apical root canal system; (Cousin *et al.*) extraradicular infection, generally in the form of periapical actinomycosis; (iii) extruded root canal filling or other exogenous materials that cause a foreign body reaction; (iv) accumulation of endogenous cholesterol crystals that irritate periapical tissues; (v) true cystic lesions, and (vi) scar tissue healing of the lesion” (Siqueira *et al.*, 2014). Persistent apical periodontitis may occur because of endodontic procedural shortcomings that may include inadequate aseptic control, poor access cavity design, missed canals, inadequate instrumentation and debridement and leaking temporary or permanent restorations. Even when the most rigorous endodontic procedures are followed, peri-apical lesions may persist, remain active and show no clinical or radiographic signs of healing (Nair, 2006, Siqueira *et al.*, 2014).

1.1.3 Root canal ecology as a factor to drive composition and virulence of polymicrobial community in endodontic infections

Historically, little was known about the microbiota of the oral cavity and traditionally, it was believed that apical periodontitis resulted from specific species of pathogens (Gutmann and Manjarres, 2018). The premise of specific species causing apical periodontitis might have prevailed due to past shortcomings in cultivating techniques which favoured certain species. A ground-breaking study was done by Åke J. R. Möller in 1966 who established the framework for future microbiological studies in particular (Moller, 1966). This was the first large and significant microbiological examination of root canals and the periapical tissues of human teeth. He designed culture techniques to maximize the recovery of anaerobes and bacteria in small numbers under stress of root canal medicaments in treatment cases (Bergenholtz, 2004). However, a major shift towards the theory of a polymicrobial cause of apical periodontitis occurred (Machado de Oliveira et al., 2007, Siqueira and Rocas, 2009a, Burmolle et al., 2014). Evidence suggests that no single species exerts their pathogenic effect on tissues, but it is rather a community behaviour that causes tissue injury (Siqueira *et al.*, 2004). In addition, microbial load is also an important factor to consider when determining the degree of pathogenicity (Wilson *et al.*, 2002). However, the high prevalence of a given microbial species does not necessarily ensure a causal relationship between the species and peri-radicular disease (Siqueira, 2002). The microbial composition of polymicrobial communities evolves over time depending on changes in root canal ecology and inter-species interaction. At early stages of pulpal infection, the pulp has higher levels of oxygen tension and greater availability of nutrients which are essential for facultative microorganisms to thrive. This initial favourable environment results in a high microbial count and a greater overall microbial diversity (Fabricius *et al.*, 1982a). Later, more anaerobic microbes start to dominate due to a drop in oxygen levels, carbohydrate depletion and increased protein quantity. These factors favour asaccharolytic, obligate anaerobes especially in the apical third of root canal system (Fabricius *et al.*, 1982b). The obligate anaerobes are rather easily eradicated during root canal treatment. On the other hand, facultative bacteria such as streptococci, enterococci, and lactobacilli, once established, are more likely to survive chemomechanical instrumentation and root canal medication (Chavez De Paz *et al.*, 2003).

Microbial succession is a dynamic process that can be influenced by the introduction of root canal antibacterial irrigants, medicaments and changes to oxygen tension. The new pulpal ecology promotes selective species to survive this harsh environment and have the potential to form persistent infection (Haapasalo *et al.*, 2008).

The ability of bacteria to survive RCT procedures and to reinstate infections might be attributed to the bacterial ability to form biofilm, remain in dentinal tubules and the complexities of the root canal system. Moreover, bacteria acquire virulence potential and thus can escape the host response and exhibit resistance to antimicrobial medicaments (Siqueira and Rocas, 2008). Alterations in ecological status change the virulence behaviour of microorganisms and ultimately change their phenotypic traits (Sundqvist, 1994). Bacterial virulence is a significant factor in determining the polymicrobial community behaviour inside root canals. Virulence is defined as the degree of a pathogenicity or disease of a microorganism (Sparling, 1983). The ecology of the root canal can potentiate such virulence of microorganisms invading the root canal. Bacterial virulence may be influenced by several factors which include the degree of anaerobiosis, pH level, and the availability of nutrients and nonspecific and specific immune defences (Sparling, 1983, Sundqvist, 1994).

1.1.4 Endodontic infection as a biofilm induced disease

1.1.4.1 What is a biofilm?

Biofilms are defined as sessile communities of microorganisms arranged systematically and enclosed in their own extracellular polymeric matrix that adheres to either biotic (living) or abiotic (physical) surfaces (Flemming and Wingender, 2010). The local biofilm environment provides its microorganisms with the nutrients necessary for their survival and enables them to adapt to ecological changes such as nutrient scarcity.

Numerous studies have been designed to examine biofilms and their clinical significance in endodontic disease. It has been reported that biofilms induce apical periodontitis infection (Ricucci and Siqueira, 2010) and are the primary cause of endodontic treatment failure (Ricucci *et al.*, 2009) which was attributed to the

adaptive mechanisms of bacteria in biofilms that significantly increase microbial survival (Chavez de Paz, 2007). Biofilm formation may trigger drug resistance and inflammation, resulting in persistent infections (Chen and Wen, 2011). Studies on dental plaque demonstrate bacterial adherence to solid or liquid surfaces and underlying mechanisms and nutrient acquisition from the surrounding environment (Vinogradov *et al.*, 2004). Dental caries is a prime example of a plaque-dependent disease (Koo *et al.*, 2013) and is considered a polymicrobial biofilm disease driven by the diet and microbiota-matrix interactions (Bowen *et al.*, 2018).

Biofilms cause up to 60% of human infectious diseases (Chen and Wen, 2011) and mediate many human infectious diseases (Hall-Stoodley *et al.*, 2004). Endocarditis, cystic fibrosis, middle ear infections, caries, gingivitis are all common examples of biofilm induced infections (Moreillon and Que, 2004, Akyildiz *et al.*, 2013, Koo *et al.*, 2013, Murakami *et al.*, 2018).

1.1.4.2 Biofilm Composition

Biofilms consist of microbial cells embedded in a 3D structural ECM. The ECM is composed of Extracellular Polymeric Substances (EPS) (Serrage *et al.*, 2021) that contains exopolysaccharides, nucleic acids (extracellular DNA (eDNA) and enhancer RNA (eRNA)), proteins, lipids, and other biomolecules. The EPS make biofilms stable, mediate their adhesion to surfaces and form a cohesive, three-dimensional polymer network that interconnects and transiently immobilizes biofilm cells (Flemming and Wingender, 2010). The EPS play a key role in determining the evolving properties of the forming biofilm. The composition and configuration of EPS vary according to the microorganisms present, the shear stress experienced, temperature and the availability of nutrients (Flemming and Wingender, 2010). The distinctive features of biofilms, such as social cooperation between communities, resource capture and enhanced survival following exposure to antimicrobials, all depend on the structural and functional properties of the matrix (Flemming *et al.*, 2016).

The composition and spatial organization of mono-species microbial communities may differ from that of their multi-species counterparts (Bowen *et al.*, 2018). The EPS components can be produced by the microbial community or acquired from the host or surrounding environment such as saliva which can assist in microbial

attachment as well as provide nutrients for microbes (Marsh *et al.*, 2016). Minerals are essential components of EPS and can provide structural support for morphogenesis of microbial colonies. They also act as scaffold to protect microbial cells from shear forces and antimicrobial agents (Oppenheimer-Shaanan *et al.*, 2016). A distinct feature of the biofilm matrix is the presence of interstitial voids or water channels separating bacterial microcolonies in the biofilm. These channels help deliver nutrients to microcolonies and serves as their waste drainage system (Evans, 2000).

The functions of EPS can be divided into physical and chemical (Dragos and Kovacs, 2017). The physical EPS functions include adhesion-cohesion, scaffolding, mechanical stability, and protection. The chemical functions of EPS may include the promotion of cell adhesion to solid substrates; and improvement of cohesion among bacterial cells which eventually leads to the development of structured cell clusters, often termed microcolonies. The EPS also promotes cell-cell cohesion including inter-species recognition to serve as an anchor for further colonization and facilitates microbial aggregation (Bowen *et al.*, 2018, Flemming *et al.*, 2016).

In addition, EPS can sequester substances while at the same time influencing the diffusion of various molecules inside the biofilm. Thus, nutritional and chemical gradients can form within the biofilm. These gradients include oxygen, pH, inorganic ions, metabolites, and other solutes. A prominent chemical role of the biofilm ECM is that it acts as a local nutrient reservoir of various biomolecules such as exopolysaccharides and provides heterogeneous microenvironments differing in diffusion properties, stiffness, pH, oxygen and metabolites or nutrient levels (Koo and Yamada, 2016, Cugini *et al.*, 2019).

The nucleic acids, eDNA and eRNA, are important components of EPS. The eDNA may be actively secreted or produced by cell lysis (Turnbull *et al.*, 2016). The eDNA may interact with different EPS constituents of biofilms and contribute to the biofilm structural organization, serve as a nutrient source, while promoting protection against antimicrobials and allowing horizontal gene transfer (Karygianni *et al.*, 2020). The eDNA is considered as a carbon source that can influence biofilm dispersal (DeFrancesco *et al.*, 2017). Interestingly, anionic EPS

components and eDNA can become cation chelators and even make the microbial ecosystem cation-deficient, thereby promoting antimicrobial resistance (Okshevsky and Meyer, 2015).

1.1.4.3 Stages of biofilm development

Biofilm formation involves a cascade of events. The stages of biofilm formation differ between Gram-positive, Gram negative and species from different kingdoms such as *Candida albicans*. Generally, its formation starts by the attachment of planktonic cells to a surface. The initial bacterial adhesion often involves the classic adhesin-receptor interactions and surface-scanning and sensing processes (Karygianni *et al.*, 2020). Some species use extracellular appendages such as flagella, pilli and curli, as mechanosensors to scan surfaces as shown in *Vibrio cholerae* and *Bacillus subtilis* (Teschler *et al.*, 2015, Vlamakis *et al.*, 2013). Some bacteria may sense adhesion forces over a specific distance above the substratum surface by way of quorum sensing (Wang *et al.*, 2019). In the case of the Gram-positive bacterium *Enterococcus faecalis*, several virulence factors are utilised that are well known to be related to biofilm formation. The enterococcal surface protein has been found to adhere to and colonize abiotic surfaces, playing an important role in *E. faecalis* biofilm formation (Toledo-Arana *et al.*, 2001). *E. faecalis* gelatinase is an extracellular metalloprotease. It can hydrolyse gelatine, collagen, and haemoglobin which were reported to be involved in bacterial adherence and biofilm formation (Park *et al.*, 2007). *E. faecalis* biofilm formation has been shown to be DNA-dependent (Serrage *et al.*, 2021). The actively secreted version of eDNA or the by-product of cell lysis seems to play a role in biofilm formation. A combination of eDNA and cell wall-anchored proteins e.g PrgB was required for extensive cellular aggregation and the addition of PrgA was necessary for extensive binding of *E. faecalis* to abiotic surfaces and development of robust biofilms (Bhatty *et al.*, 2015). Moreover, inhibition of eDNA leads to decreased of *E. faecalis* biofilm formation (Yu *et al.*, 2019a).

The EPS promote microbial adhesion to biotic and abiotic surfaces. Once attached, microbial aggregation is achieved by further production of EPS which surround, cement, and promote cell-cell cohesion including inter-species recognition (Donlan, 2002, Flemming *et al.*, 2016). Other inter-species interactions and aggregations depend on mechanosensors or specific adhesin (protein)-receptor

(saccharide) pairs. Continuous EPS production *in situ* further expands the matrix in three-dimensions while forming a core of EPS-bacterial-cells meshwork. This core acts as a supporting framework and facilitates the development of 3D clusters, aggregates or microcolonies (Karygianni *et al.*, 2020).

Bacterial aggregation is followed by the stage of microcolony formation, in which large quantities of EPS are secreted. Bacterial cells divide and form multi-layered clusters, produce more EPS and thus, the attachment becomes irreversible (Figure 1.2). The final stages involve biofilm maturation and dispersion. In the dispersion state, microbial cells detach because of certain microbial enzymes that degrade ECM. The microbial cells disperse and colonize new surfaces. (Figure 1.2)(Boles and Horswill, 2011, Vasudevan, 2014).

In *Candida* species, the process of biofilm formation is complex, and controlled by a variety of transcription factors including Bcr1p, Ace2p, Efg1p and Zap1p, all of which are involved in complex molecular pathways (Finkel and Mitchell, 2011, Nobile and Mitchell, 2006, Fanning *et al.*, 2012). Initial surface attachment occurs when yeast cells use adhesins including, agglutinin like sequence protein ALS3 and the cell wall protein EAP1 (Green *et al.*, 2005, Li *et al.*, 2007). Subsequently, microcolonies form and *C. albicans* morphology switches to pseudo- and true-hyphae under the control of the regulator Efg1p (Ramage *et al.*, 2002), to form a network of hyphal structures with yeast distributed in this “net”.

As biofilm matures, *Candida* starts depositing glucan rich EPS which encompasses *Candida* cells (Nett *et al.*, 2010). Thus, the cells live behind a protective barrier against host defence responses, antimicrobial agents, and environmental stresses. A hypoxic environment develops as the biofilm matures. This environment induces the up-regulation of glycolytic genes that control filamentation (Bonhomme *et al.*, 2011). Later, planktonic yeast cells are able to disperse from the mature biofilm and colonise a new surface to begin the development of a new biofilm (Uppuluri *et al.*, 2010a).

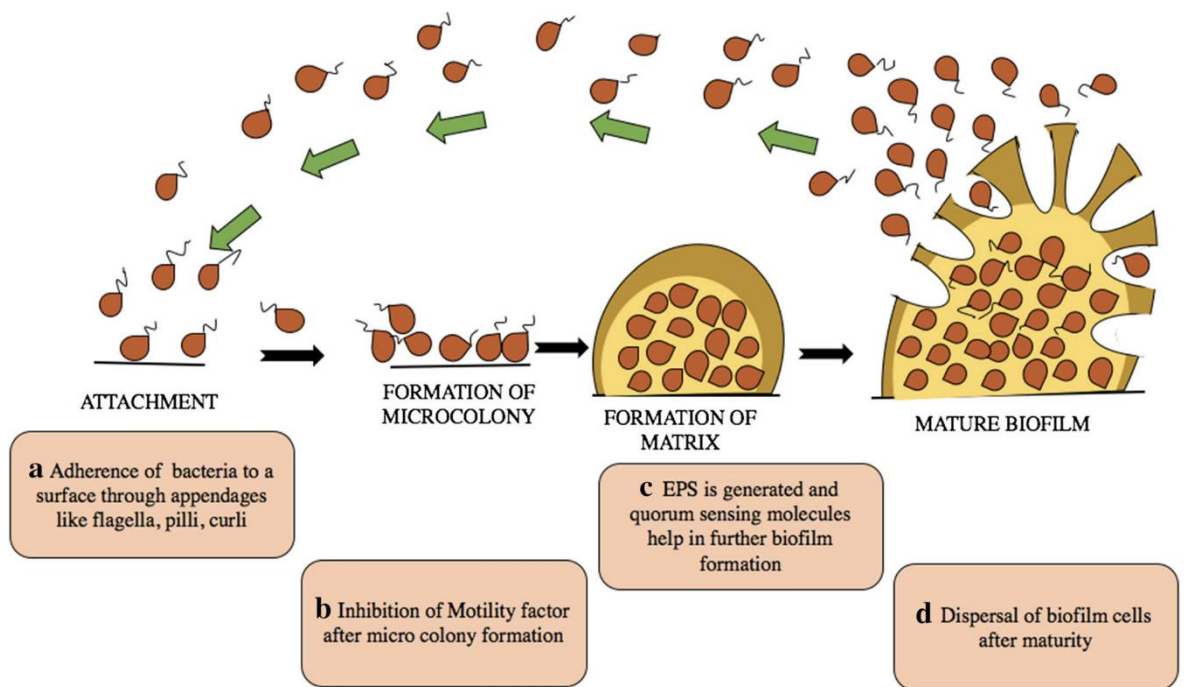


Figure 1.2: Stages of biofilm formation. (a) planktonic cells attach to surfaces via different mechanisms. (b) the beginning of formation microcolonies by cell- cell adhesion and inter-species recognition. (C) EPS deposition and the start multi-layer formation. (d) Mature biofilm formation and the release of mature cells to seed different locations (Banerjee *et al.*, 2020).

1.1.4.4 Biofilm resistance to host defence mechanisms and treatment

Biofilm is endowed with a variety of mechanisms which make it difficult to be eradicated by host defence responses, antimicrobials or even by mechanical means. The viscoelasticity of mature biofilms provided by exopolysaccharides and eDNA makes separation of biofilms from the substrate a challenging task even under vigorous mechanical pressure and shear stresses (Peterson *et al.*, 2015). The EPS also promotes protection against antimicrobials and enhances drug tolerance via different mechanisms and serves as a physical barrier that limits the ingress of various antimicrobial agents into the biofilm structure. Thus, a limited antimicrobial drugs access into the deep layers of the biofilm occurs (Karygianni *et al.*, 2014). In addition, access of antimicrobials may be hindered by EPS-antimicrobial interactions, with positively charged agents likely to bind to negatively charged polymers thus contributing to biofilm antimicrobial tolerance (Karygianni *et al.*, 2014). These interactions may isolate the antimicrobial agents and inhibit their arrival to their target sites (Fux *et al.*, 2005). Another factor that contributes to the antimicrobial tolerance of biofilms is the presence of enzymes in the biofilm matrix. These enzymes may participate in degradation or

inactivation of antimicrobial agents. Interaction of antimicrobials with biofilm matrix can also alter specific genetic determinants of antimicrobial tolerance (Taglialegna *et al.*, 2016, Hall and Mah, 2017). Additionally, microorganisms differ phenotypically when organized in biofilms compared to their planktonic counterparts. When in biofilm state, microbial cells express genes to switch to the biofilm phenotype. The virulent biofilm phenotypes are capable of producing glucans that can bind to antimicrobials and physically sequester them; a mechanism that leads to reduction of antimicrobial efficacy (Donlan, 2000).

It is well established that antimicrobial agents are highly effective against actively growing cells (Davies, 2003). The importance of slow growing bacterial cells and their ability to escape the adverse effects of antimicrobial agents has been highlighted (Proctor *et al.*, 2006). Cells within microbial communities can enter a dormant state during adverse conditions that enables them to endure hostile environments. These cells are referred to as persister cells. They represent a small population that accounts for 0.1-10% of the microbial population in biofilms. These persisters are specialized survivor cells which can evade host response, resist antimicrobial agents and serve as initiator cells to resume the infection process once conditions become favourable (Keren *et al.*, 2004).

1.1.4.5 Biofilms in endodontic infections

It has been documented that microorganisms invade and colonize the necrotic pulp tissue and cause primary intraradicular infections (Wong *et al.*, 2021a, Walton and Torabinejad, 2015). Microorganisms of infected root canals exist in biofilms in a similar fashion to those in other locations. Evidence as shown by scanning electron microscopy (SEM) and transmission electron microscope (TEM) suggests that infected root canal biofilms comprise microbial communities of several species embedded in their own EPS and attached to root canal dentine (Schaudinn *et al.*, 2009). Infection in the main root canal lumen can spread to other areas of the root canal system (Siqueira and Rocas, 2021). Biofilm is primarily present in the root canal adhering to the intraradicular dentinal walls, lateral or apical ramifications and isthmuses of root canal, (Ricucci and Siqueira, 2010) and in other areas that are difficult to access using endodontic instrumentations, irrigants, and medicaments (Molven *et al.*, 1991). Both PAP and SAP are caused by biofilms as shown by SEMs (Nair, 1987).

One of the main challenges encountered while exploring root canal biofilms that cause apical periodontitis, is the coexistence of biofilm and planktonic cells. The old sampling, processing, and culturing techniques have been criticised for their inherent limitations. Morse, 1970 was critical of the old technology and claimed that inaccessible areas of the root canal system did not permit appropriate sampling (Morse, 1970). Ricucci and Siqueira (2010) studied biofilms inside root canals and apical tissues using histological methods. Samples were obtained by apical surgery or extraction. Additionally, they studied the histopathologic nature of apical periodontitis. Biofilms were evident in 74% of secondary or post-treatment root canal infections and in 80% of primary root canal infections. However, histopathologic studies alone are insufficient to understand the role of biofilm in root canal infections. In addition, visualising the organisation of the biofilm and its adhesion strength would add important details to the role of biofilm in root canal infections (Ricucci and Siqueira, 2010)

1.1.5 Technical advancements in microbial identification

Extensive research has been done on the relationship between bacterial biofilms and various factors, such as nutrient availability, temperature, substrate and hydrodynamics, to understand their behaviour under various growth and environmental conditions. The understanding gleaned from this research can potentially be utilized to develop control strategies. High throughput sequencing has enabled scientists to examine the human microbiome and provide insights into microbial interactions, as well as microbial host interactions (Molobela and Ilunga, 2012).

Oral biofilms are good examples of the diversity of the human microbiome. It has been estimated that oral biofilms have over 700 species of biofilm producing organisms which are associated with several oral infections (Paster *et al.*, 2006, Narayanan and Vaishnavi, 2010). Identification of microbes involved in root canal infections is important to further understand the pathogenicity of the disease and help in developing strategies to combat them.

Culture based methodologies were traditionally used to identify microbial species in root canal infections. One of the key limitations of culture-based methodologies is the underestimation of microbial diversity within the microbial population.

Therefore, despite the existence of Archaea, viruses, and fungi; bacteria remain the main microorganisms frequently isolated from root canal infections using traditional techniques (Wong *et al.*, 2021a). This has resulted in the emergence of a belief that certain sets of species were the main cause of apical periodontitis. Other disadvantages are that culture methods are costly and it can take several days to weeks to identify fastidious anaerobes (Morse, 1970). Furthermore, it is impossible to cultivate many bacterial species due to the lack of knowledge of their growing requirements and if cultivated they will be difficult to identify (Bonnet *et al.*, 2020). In some cases, nutrient depletion in root canal environment induces phenotypic changes and altered genes expression which render bacteria inactive and unsusceptible to antibiotics targeting their metabolic pathways. In such state, the bacteria are alive, but cannot be detected using culture-based methods (Li *et al.*, 2014).

Due to these limitations, close ended DNA based molecular microbiology techniques like polymerase chain reaction (PCR) have been used to expand the range of identifiable microorganisms and to further confirm the prevalence of the already cultured bacteria. These methods have allowed the identification of certain species that could not be cultivated (Gatti *et al.*, 2000, Siqueira and Rocas, 2004, Fernandes Cdo *et al.*, 2014). Studies based on 16S ribosomal RNA (rRNA) genes have revealed that 40-60% of the bacterial species in the oral cavity represent as-yet-uncultivated (phylotype) and uncharacterized bacteria (Siqueira and Rocas, 2013a). Using molecular technology, high bacterial diversity in samples isolated from root canals and low abundance of species have also been reported. Molecular based methods of bacterial identification have their own limitations which are mostly attributable to technical procedures during cell lysis and DNA extraction (Manoil *et al.*, 2020).

There has been a remarkable advancement in sequencing technologies over the last five decades. Traditionally, 16S rRNA sequences were generated using Sanger sequencing which is a “first-generation” DNA sequencing technology, this offered high accuracy but was a difficult and laborious process when dealing with identification of mixed bacterial communities (Sanger *et al.*, 1977). Applying this technology directly on mixed species would result in overlapping signals. Thus, an intermediate culturing step is required to isolate the different bacterial species

(Weisburg *et al.*, 1991, Winand *et al.*, 2019). The less abundant micro-organisms that constitute the majority of the biodiversity cannot be selected for sequencing (Petrosino *et al.*, 2009). Therefore, the Sanger sequencing technique is considered expensive and labour intensive with limited in-depth coverage, and unable to characterise bacteria in complex mixed samples (Weisburg *et al.*, 1991). Despite its limitations, clonal analysis of the 16S rRNA gene has identified 700 - 1000 species in the human oral cavity (Paster *et al.*, 2006). The application of this method in endodontic microbiota identification studies revealed previously unrecognized bacterial diversity (Rolph *et al.*, 2001, Munson *et al.*, 2002, Sakamoto *et al.*, 2006).

With the introduction of “next-generation” sequencing (NGS) technologies, it has become possible to generate 16S rRNA sequences from organisms in mixed complex samples without the intermediate culturing step (Winand *et al.*, 2019). As a result, NGS technology has gained popularity because of the high sequence data throughput generated in one reaction which made the procedure more cost effective. It allows rapid identification of organisms involved in a variety of clinical conditions of interest (Lefterova *et al.*, 2015).

High-throughput NGS approaches such as pyrosequencing and the Illumina system have been recently adopted in clinical research studies (Di Resta *et al.*, 2018). These molecular methods are now broadly implemented in identification of microbiota in any human body site including the oral cavity. This method was employed to identify taxa that other approaches could not discover in oral microbiota samples (Keijser *et al.*, 2008). Over 1000 distinct species-level taxa have been detected from oral samples using culture-independent technologies and studies using next-generation DNA sequencing and it is projected that the breadth of bacterial diversity may be even much larger (Siqueira and Rocas, 2017).

Pyrosequencing facilitates metagenomic investigations through high-throughput, deep-coverage, massively parallel and multiplex barcoded approaches (Ronaghi *et al.*, 1998). It provides long base pair read lengths. However, it was associated with high error rates as addition of more than five identical nucleotides cannot be detected efficiently (Fakruddin *et al.*, 2012). An improved second generation

technology, Illumina technology, was developed to eliminate the error disadvantage and deliver high quality and accuracy (Reuter *et al.*, 2015).

Second generation NGS methods have become popular nowadays due to their inherent advantages. Illumina technologies have been referred to as “short-read” sequencing technologies because achievable read lengths are relatively limited. The technology offers greater sequencing coverage with lower sequencing error rates. The Illumina MiSeq instrument is capable of sequencing maximum 2×300 bp, which is insufficient to cover the entire 16S rRNA gene. However, it permits sequencing one or more variable regions, rendering gene region selection paramount due to variable gene regions differences within and among species (Di Bella *et al.*, 2013).

The capability of second-generation sequencing platforms is limited to short read lengths that has to be assembled with the assistance of bioinformatic tools/pipelines into an original length template. Another disadvantage is the PCR bias introduced by clonal amplification, for detection of signal. The search for improved sequencing technology has led to the introduction of “third generation of high throughput NGS technology” or single molecule real time (SMRT) sequencing which emerged to obviate the limitations of the second generation approaches. It comprises sequencers with SMRT technology platforms like Helicos’ Genetic Analysis System, Pacific Biosciences and Oxford Nanopore Technologies (ONT) sequencing. In addition to other complete genomics by Beijing Genomics Institute and GnuBio by BioRad (Ambardar *et al.*, 2016).

The third generation NGS platforms such as ONT (MinION, Oxford Nanopore Technologies, Oxford, UK), and SMRT sequencing developed by Pacific Biosciences, (PacBio, Menlo Park, CA), (Rhoads and Au, 2015) have been used to sequence the entire rRNA. It is anticipated that there would be a shift towards using whole gene sequencing in NGS technology rather than rely on selected hypervariable region sequencing. With entire 16S gene sequencing, the taxonomic annotation at species level will become possible and this will provide microbiome data with greater resolution (Shin *et al.*, 2016).

A recent review of previous studies that used NGS to profile the microbial communities of root canals, reported that the commonest NGS platforms used were 454 pyrosequencing (Roche Diagnostic Corporation, Risch-Rotkreuz, Switzerland) and Illumina-based technology (Illumina Inc, San Diego, CA). In addition, most sequenced hypervariable regions were between v1 and v6 regions (Shin *et al.*, 2018)

1.1.5.1 The microbiota of root canal infections

Advanced identification methodologies have revealed substantial evidence that root canal infections are initiated as a polymicrobial community (Narayanan and Vaishnavi, 2010). Thus, the traditional belief that apical periodontitis was caused by a set of specific species has been abandoned (Morse, 1970, Gutmann and Manjarres, 2018). In a remarkable account of historical and contemporary perspectives on the microbiological aspects of endodontics, Gutmann and Manjarres (2018) highlighted the many studies that sought to identify specific bacteria related to necrotic pulps and infection of the periradicular tissues (Gutmann and Manjarres, 2018). Siqueira and Rôças (2009c) studied bacterial diversity in root canal infections and pooled the data obtained from culture dependent and culture independent datasets. They identified 460 taxa belonging to 100 genera and 9 phyla in different types of endodontic infections (Siqueira and Rôças, 2009c). The phyla with the highest species richness were, *Firmicutes*, *Bacteroidetes*, *Actinobacteria*, *Proteobacteria*. They concluded that bacterial diversity varied considerably according to the type of infection. Moreover, the taxa disclosed from molecular based studies were significantly more than that obtained from culture-based studies. Cultivable and as-yet-uncultivated phylotypes have emerged as candidate pathogens (Siqueira and Rôças, 2009c).

Several studies have used pyrosequencing to explore the microbiota of root canals. One study compared two sequencing methods, where they used 454 pyrosequencing technology and the conventional Sanger capillary sequencing. Pyrosequencing obtained 28590 sequences compared to only 47 sequences generated by Sanger sequencing per sample. In addition, pyrosequencing provided 600 times depth of coverage; and detected more bacterial genera and phyla compared to Sanger sequencing methodology. Pyrosequencing was able to identify

179 bacterial genera in 13 phyla and the phylum *Bacteroidetes* was the most prevalent one (Li *et al.*, 2010).

One study used second generation platform Illumina MiSeq to study the microbial community in post treatment apical periodontitis cases (Siqueira *et al.*, 2016). More than 500 bacterial operational taxonomic units (OTU), 11 phyla and 103 genera were identified. More than 85% belonged to phyla *Proteobacteria*, *Firmicutes*, *Fusobacteria*, *Actinobacteria*. *Proteobacteria* were the most abundant phyla while *Fusobacterium* and *Pseudomonas* were the most dominant genera. *E. faecalis* was found in only 4 cases (Siqueira *et al.*, 2016).

Fungi have been found in the oral cavity of healthy individuals and in association with many oral diseases (de Carvalho *et al.*, 2006, Dagistan *et al.*, 2009). It has been reported that fungi may be involved in root canal infections and was identified in between 0.5-55% of the infections and that their contribution to periapical disease might be significant (Egan *et al.*, 2002). Fungi are commonly found in persistent root canal infections as well as in individuals with immunocompromised health status (Gomes *et al.*, 2017). A literature review indicated that fungi contributed to 7.5% of root canal infections, and identified no specific factor influencing this prevalence (Persoon *et al.*, 2017b). Another study identified the mycobiome and microbiome in root canal infections. *Candida* and *Malassezia* were the most frequently isolated species. There were no differences between bacteriome and mycobiome profiles of apical and coronal root segments. Fungal diversity is limited, but when fungi are present the composition of the bacteriome is clearly different (Persoon *et al.*, 2017a). NGS and qPCR methods detected species that were previously unknown. When performing treatment some species were reduced and other species relative abundance increased (Persoon *et al.*, 2017a).

1.1.5.2 Microbial community diversity and root canal infection type. Are they equally diverse?

It has been long claimed that the microbial community within a secondary root canal infections is less diverse compared to primary root canal infections (Cheung and Ho, 2001, Siqueira and Rocas, 2009c). Using a combination of culture-dependent and culture-independent methods, it has been shown that persistent

root canal infections harbour much the same diversity of microbial community as primary infections and low abundant microorganisms constituted the majority of endodontic microbiota (Anderson *et al.*, 2012).

One study investigated the microbial composition in groups of primary and persistent root canal infections in a Greek population and reported that *Bacteroidetes* was the most abundant phylum in both infection types. *Proteobacteria* and *Tenericutes* were significantly more enriched in persistent infections than in primary ones. Increased enrichment in persistent infections for *Lactobacillus*, *Streptococcus* and *Sphingomonas* were reported (Tzanetakis *et al.*, 2015). Hong *et al.* (2013) utilised the pyrosequencing method to detect microbiota in primary and persistent endodontic infections and reported that *Bacteroidetes* was the most abundant phylum in both primary and persistent infections. This study suggested that the microbial community of primary and secondary infections have almost similar diversity (Hong *et al.*, 2013). This finding is consistent with the results of the previous study (Tzanetakis *et al.*, 2015) where no significant differences were found between bacterial community profiles of primary and persistent infection groups. A more recent study also compared primary and persistent endodontic infections using high throughput pyrosequencing from pulverised samples. The data revealed 15 phyla and 160 genera and 368 species. No significant differences between the two primary and persistent groups were found in terms of diversity and richness of OTUs (Keskin *et al.*, 2017).

A comparison was made between the bacterial microbiota in primary chronic apical periodontitis, secondary chronic apical periodontitis and apical abscess using Illumina sequencing. The data showed that communities were individually different and the most numerous were *Firmicutes* and *Bacteroidetes*. *E. faecalis* was found in one case of secondary chronic apical periodontitis. One periapical abscess case sample displayed a significantly high proportion (47%) of *Proteobacteria* (Vengerfeldt *et al.*, 2014). A more recent study confirmed the polymicrobial aetiology of apical periodontitis and reported some distinct bacterial communities found in PAP and SAP. The most abundant and prevalent OTU was *F. nucleatum*, and *E. faecalis* was higher in secondary root canal infections than in primary ones (Bouillaguet *et al.*, 2018). In summary, the literature reported no clear distinction between the microbial community of

primary and secondary infections. However, enough evidence suggests that the microbial community is diverse and *Bacteroidetes* is the most abundant phylum in primary and secondary infections. Several studies reported similar diversity in both.

1.1.6 Microbial interaction within a biofilm

In multispecies biofilm, communities are arranged in a spatial organization that is influenced by varied interaction between different species, genera, and even kingdoms within the biofilm. The interactions comprise physical cell-cell associations known as co-aggregation, inter-species signalling, secretion and turnover of antimicrobial compounds and the sharing of ECM (Rickard *et al.*, 2003, Giaouris *et al.*, 2015). In addition, the influence of metabolic synergies to utilize available metabolites is important for biofilm structure and stratification. Collective properties of biofilms, such as the collective migration and spreading property is attributed to, cell-cell interactions. It helps microbial masses to adapt effectively and withstand harsh environmental conditions (Preda and Săndulescu, 2019). Microorganisms can communicate via quorum sensing within a biofilm (Donlan, 2002). The release and detection of certain signalling molecules and their accumulation at threshold level induces gene expression in microbes to act differently in terms of virulence, resistance to host defences and biofilm formation (Rutherford and Bassler, 2012). This dynamic state within the biofilm necessitates assessing transcriptomic, proteomic, and metabolic changes rather than just evaluating phenotypic changes in the biofilm. Assessing the metabolic changes may be more informative in delineating endodontic biofilms.

1.1.6.1 Omics as a means to understand inter-species interactions

The last few years have witnessed a rapid increase in the use of high-throughput omics techniques that can question the abundance levels of many biological molecules concurrently. They include amplicon analysis, transcriptomics, proteomics, and metabolomics, among others (McClure, 2019).

The endodontic biofilm community is polymicrobial in nature and contains several microorganisms. It is difficult to attribute specific roles to individual species because all species present and living interact with host and other species; and

have the potential to contribute to the infection process (Göran Sundqvist and Figdor, 2003). Interactions in a biofilm can be competitive which promotes microbes' adaptation in the biofilm environment and as a result lead to the production of toxic molecules. The interactions can also be cooperative, whereby microbes survive by maintaining a stable equilibrium with the host and its associated microbial communities. Accordingly, these microbial interactions may shape host health and can potentially result in disease (Baishya *et al.*, 2021). These interactions may serve one or more of the following functions. They can influence the growth of specific organisms or groups of related organisms (Kuramitsu *et al.*, 2007). They can form the spatial architecture of the biofilm, determine the distribution of microorganisms within its structure, protect the interacting microbial cells from lethal challenges or antimicrobial agents, (Marsh, 2005) and most importantly regulate the virulence and pathogenicity of the microbial community (Antunes *et al.*, 2010). Microorganisms interact together by inducing reciprocal transcriptomic and proteomic changes. These microbial interactions can lead to regulation of nutrient acquisition, metabolic processes, and other activities, including synergy, spore formation, bacteriocin production and genetic competence (Antunes *et al.*, 2010). Inter-species interactions within a community are complex, and the task of identifying them and assimilating their impact on the overall community is critical, and can be complicated (McClure, 2019). Nevertheless, with the plentiful availability of omics analysis, scientists have the tools to use network inference to predict and understand interspecies interactions in natural microbial communities. The analysis of such interaction within multi-species biofilms using a combination of multi-omics technologies, *vide supra*, may help unravel key inter-species interactions that contribute to the spatial organization of the community. Hence, obtaining a detailed description of spatial organization in multispecies biofilm using a blend of advanced *in situ* imaging techniques and recently developed multi-omics technologies can disclose the molecular mechanisms behind inter-species interactions and put biofilm research an important step forward (Liu *et al.*, 2016). Moreover, interaction analyses can also provide better understanding of microorganisms' virulence and disease pathogenesis (Jakubovics, 2015, Shokeen *et al.*, 2021).

Advanced technical approaches such as DNA sequencing have been used to identify several taxonomies in health and disease, and have helped scientists to

understand the genomic functional role of microorganisms in shifting the healthy status into a diseased one (Wang *et al.*, 2013, Belda-Ferre *et al.*, 2012, Griffen *et al.*, 2012, Park *et al.*, 2015). However, the contribution of such approaches to the actual understanding of inter-microbial interactions is still controversial as some species might share the same ecological niche as a preference (Hirano and Takemoto, 2019). Furthermore, comprehensive RNA sequencing (RNA-seq) has been used to understand communities function expressed during health and disease (Jorth *et al.*, 2014, Tanner *et al.*, 2017, Duran-Pinedo *et al.*, 2014). Metabolomics is one of the omics technologies that has been applied successfully (Pinu *et al.*, 2019b) to further understand the functional potential of these communities by analysing all metabolites produced by a cell or system in healthy and diseased patients (Gawron *et al.*, 2019, Liebsch *et al.*, 2019, Fiehn, 2002). Attempts were made using advanced bioinformatics methods to analyse existing large genomic/metagenomic datasets to extrapolate inter-species interactions, and discover the hidden laws of the microbial ecosystem from available data (Pinu *et al.*, 2019b). However, for some authors this approach is still controversial (McClure, 2019, McClure *et al.*, 2018), as many inference approaches are superior to others, thus it is still difficult to identify the proper network method for the right experiment (McClure, 2019). Furthermore, collection and storage techniques, required quantity and choice of biological samples, used for genomics investigations may not be suitable for metabolomics, proteomics, or transcriptomics. In addition, carefully integrated multi-omics data must be transformed into single data sets before depositing them into omics-specific databases to make it publicly available (Pinu *et al.*, 2019a).

The transcriptome is the set of all RNA molecules, including mRNA, rRNA, tRNA, and non-coding RNA produced in one or a population of cells. Transcriptome sequencing has become an important tool in studying inter-species relationships (Wolf *et al.*, 2018). Currently, RNA-seq has emerged as an applicable tool alternative to the traditional microarray platforms used for conducting transcriptional profiling. The main difference between both technologies lies in the ability of RNA-seq to fully sequence the whole transcriptome, while microarray-based technology allows only predefined transcripts profiling. Despite that, both technologies have provided important insights to the complex nature of inter-species interactions (Shokeen *et al.*, 2021).

The term proteomics describes the study and characterization of the complete set of proteins present in a cell, organ, or organism at a given time (Wilkins *et al.*, 1996). Proteomics approaches are complementary to transcriptomics. They measure the abundance of proteins present at a given point of time depending on mRNA turnover or protein half-life length. In addition, post-translational modifications can be discovered using proteomics along with the processed forms of proteins. Some studies utilised metaproteomic approaches to capture the complex proteomic composition of oral microbial communities, but comparable to other omics approaches, the complexities of inter-species interactions cannot yet be captured using readily available tools (Belda-Ferre *et al.*, 2015, Belstrøm *et al.*, 2016, Grassl *et al.*, 2016, Rabe *et al.*, 2019).

In the context of endodontic research, culture and molecular biology technology advancements have demonstrated that bacterial communities residing in the root canal are mixed polymicrobial communities and vary in species richness which is the number of species in an ecological environment and in abundance i.e. the number of individuals in a species, and that is dependent upon the histopathological/clinical diagnosis (Siqueira and Rocas, 2009b). Moreover, advanced omics technologies can assist in developing further insight into the microbial ecology. However, it should be noted that often multi-omics lack the ability to perform subpopulation analysis (Burmeister and Grunberger, 2020, Noor *et al.*, 2019). Furthermore, studies can be limited to certain species which comprise only a small proportion of the countless species that inhabit infected root canals. Omics approaches have already started to provide insight into the complexities of inter-species interactions; but elucidating the mechanisms underlying these relationships, as well as comprehensive metabolomic investigations, remains a challenge (Muller *et al.*, 2013).

1.1.7 Interkingdom interaction in biofilms

As stated, it is recognised that endodontic infections are polymicrobial, and may contain *Candida spp.* (Abusrewil *et al.*, 2020). However, the focus of many endodontic microbiological studies has been *E. faecalis* (Swimberghe *et al.*, 2019). The advent of culture independent technology such as NGS combined with appropriate sampling methods has revealed that *Candida spp.* play an important,

yet neglected role in supporting these complex communities (Delaney *et al.*, 2018). Indeed, more than 100 fungal species have been reported to colonise the oral cavity and coexist within complex biofilm populations closely alongside neighbouring bacterial microbiomes (Ghannoum *et al.*, 2010). Apparently, cross-kingdom interactions are essential for modulating their coexistence and for pathogenesis of dental diseases involving bacterial-fungal biofilms. The most studied pathogen in the fungi kingdom is *C. albicans*. The interactions between *C. albicans* and the bacteria in biofilms found on biotic and abiotic surfaces comprise diverse types including synergistic, antagonistic, and neutral relationships (Ponde *et al.*, 2021, Delaney *et al.*, 2018, Alshanta *et al.*, 2022). The interactions of *C. albicans* with other microorganisms can occur via co-aggregation and co-adhesion. *C. albicans* key adhesins like (ALS1, ALS2, ALS3, HWP1), enable interactions with other bacterial species such as *Streptococcus gordonii* and *Staphylococcus aureus* (Peters *et al.*, 2012, Hoyer *et al.*, 2014).

Plaque biofilms are an excellent example of synergistic interkingdom relationship between *C. albicans* and *Streptococcus mutans*. Within plaque biofilms, *S. mutans* glucosyltransferases bind directly to mannans which are polysaccharides on the surface of *C. albicans* yeast and hyphal cell walls which promote the deposition of ECM (Hwang *et al.*, 2015, Ellepola *et al.*, 2017). Another example of co-adhesion is the one between *C. albicans* and *S. gordonii*. It was shown that *sspA* and *sspB* in *S. gordonii* mutants exhibit reduced expression of streptococcal adhesins for *C. albicans*, which leads to less co-aggregation of *C. albicans* with these *S. gordonii* mutants (Klotz *et al.*, 2007)

Several studies have utilised new technologies like RNA-seq for studying interkingdom interactions between *C. albicans* and several bacterial species within oral biofilms (Hwang *et al.*, 2015). *C. albicans* transcriptomic changes were studied when cocultured with the key periodontal pathogen *Porphyromonas gingivalis* (Sztukowska *et al.*, 2018) or *S. gordonii* (Dutton *et al.*, 2016).

One *in vitro* study incubated *S. gordonii* and *C. albicans* together for different time intervals mimicking the formation of a biofilm. The aim was to outline the transcriptional responses of *C. albicans* and *S. gordonii* in the early stages of their interaction. The results demonstrated that the *C. albicans* yeast to hyphal

transition was prompted by *S. gordonii* interaction, with 75 *C. albicans* genes implicated in responses to chemical stimuli, regulation, homeostasis, protein modification and cell cycle significantly ($P \leq 0.05$) up regulated. The transcriptional response of *S. gordonii* to *C. albicans* was less noticeable, with only 8 out of 72 *S. gordonii* genes being significantly ($p \leq 0.05$) up-regulated (Dutton *et al.*, 2016).

Another *in vitro* study investigated interactions of *C. albicans* and *P. gingivalis*; and reported that both microorganisms co-adhere in both planktonic and sessile phases and their interaction is mediated by In1J and an adhesin expressed on *C. albicans* hyphae Als3. This finding was further confirmed by RNA-Seq transcriptional profiling data which revealed that genes were upregulated in an In1J-dependant manner in *P. gingivalis*-*C. albicans* communities, with a disproportionately large number of those corresponding to genes related to growth, division and virulence (Sztukowska *et al.*, 2018).

In addition, a recent study employed proteomics and transcriptomic profiling to unravel molecular pathways of *C. albicans* when cocultured with *S. mutans* in mixed biofilms. Data analyses revealed that *C. albicans* genes and proteins associated with carbohydrate metabolism including sugar transport, aerobic respiration, pyruvate breakdown and the glyoxylate cycle were significantly enhanced. Another gene set related to cell wall components was upregulated which indicates enhanced biofilm activity in mixed species biofilm. More data analyses revealed that *S. mutans* -derived exoenzyme glucosyltransferase B (GtfB) binds to the fungal cell surface and promote co-adhesion. Subsequently the coenzyme can break down sucrose into glucose and fructose which can be readily metabolized by *C. albicans* enhancing growth and acid production (Ellepola *et al.*, 2019a).

One drawback of NGS approaches is that the investigation of two partner species does not fully reflect the complex polymicrobial environments. Zhang *et al.*, (2019) have employed meta transcriptomics sequencing to investigate multispecies oral communities under prolonged incubation time under different conditions (Zhang *et al.*, 2019). Although this was a study of bacterial interspecies interactions, such studies will unravel the intricate polymicrobial interactions

happening inside multispecies biofilm to better understand what occurs in clinical scenarios.

1.1.7.1 *Candida albicans* and *Enterococcus faecalis* interkingdom interactions

C. albicans and *E. faecalis* are well known commensal microorganisms that coexist in the gastrointestinal tract, oral cavity, and vagina of healthy individuals (Rindum *et al.*, 1994). Both microorganisms are opportunistic pathogens when in immunocompromised patients, or if any physiological perturbations occur (Garsin and Lorenz, 2013). *Enterococcus* species are the third commonest nosocomial infectious pathogens and *Candida* species are the fourth (Wisplinghoff *et al.*, 2004, Cruz *et al.*, 2013). They inhabit many of the same niches including the oral cavity; and have been frequently isolated concurrently from clinical samples of polymicrobial infections (Hermann *et al.*, 1999), this indicates similarities in biological mechanisms which might be synergistic within the host. Indeed, it has been shown that the co-infection between *C. albicans* and *E. faecalis*, using a nematode infection model resulted in less pathology and less mortality than infection with either species alone, (Garsin and Lorenz, 2013). Interestingly, lactobacilli decrease the virulence of *C. albicans* by a low pH generated through the production of short chain fatty acids and by preventing the formation of hyphae which is essential for penetrating and infecting host tissues, (Noverr and Huffnagle, 2004). Similarly, it has been reported that the presence of *E. faecalis* has dramatically inhibited hyphal morphogenesis of *C. albicans* in worm hosts. In addition, coinfection with *E. faecalis* and *C. albicans* caused less tissue damage than with the monomicrobial infection due to the prevention of hyphal formation in *C. albicans* and the cell death of *E. faecalis* (Cruz *et al.*, 2013).

***Candida albicans* and *Enterococcus faecalis* a deeper understanding**

Fungi are frequently involved in endodontic infections and have been isolated from approximately (3-18%) of infected root canals with a predominance of the *Candida* species (Siqueira and Fouad, 2014). Some studies (Egan *et al.*, 2002, Persoon *et al.*, 2017b) and systematic review and meta-analysis (Mergoni *et al.*, 2018) reported that the prevalence of *Candida* species in infected root canals ranged between (0.5-55%). A recent systematic review reported that *C. albicans*

is the fungus most frequently isolated from endodontic root canal infections (Yoo *et al.*, 2020). Another study reported that the combined prevalence of *Candida* species in root canal infections was (8.2%) and *C. albicans* was the most prevalent species and was reported in (68.4%) 39 out of 57 reviewed studies (Mergoni *et al.*, 2018). In general, *C. albicans* was the most frequently isolated fungal species in hospital settings worldwide (Lindberg *et al.*, 2019). *C. albicans* and to a lesser extent other *Candida* species are present in the oral cavity of up to 75% of the population (Mayer *et al.*, 2013).

C. albicans is a diploid, Gram-positive fungus that may exist in a unicellular (yeast) or multicellular (hyphae, pseudohyphae) forms. A distinctive feature of this microbe is that it can switch between different phenotypes (Jacobsen *et al.*, 2012). This morphological transformation is spontaneous and reversible and can happen multiple times depending on environmental alterations including pH and temperature changes.

C. albicans was believed to be only asexual, and simply existing as an obligate diploid. Yet, a mating locus was identified that was homologous to those in sexually reproducing fungi, and mating of *C. albicans* strains was subsequently demonstrated *in vitro* (Bennett and Johnson, 2005). For efficient mating, microbes must switch from their white form (white, round cells forming dome-shaped colonies) to the opaque form (opaque, elongated cells forming flatter colonies) (Bennett and Johnson, 2003).

It has been reported that *C. albicans* can develop in at least three different morphological forms namely: a budding yeast, pseudohyphae, and filamentous hyphae. Further morphologies include white and opaque cells, formed during switching, and chlamydozoospores, which are thick-walled spore-like structures. The shape of *C. albicans* cells varies according to its form; thus, they are oblong in opaque phase, oval in yeasts cells and elongated when with pseudohyphae or hyphae. The hyphae formation and morphological shape of *C. albicans* may be determined by a few conditions. Starvation, the presence of serum or N-acetylglucosamine, physiological temperature and CO₂ help the formation of hyphae (Sudbery, 2011). Morphogenesis of *C. albicans* may be regulated by quorum sensing that is to say the communication mechanism between microbial cells

(Albuquerque and Casadevall, 2012). The interactions of quorum sensing molecules, such as farnesol, tyrosol and dodecanol encourage cells in high cell densities ($> 10^7$ cells ml⁻¹) to form yeast and promote those in low cell densities ($< 10^7$ cells ml⁻¹) to develop hyphal formation (Hall *et al.*, 2011). The transition between both growth forms, dimorphism is a determinant factor for pathogenicity (Jacobsen *et al.*, 2012). The hyphal form is more invasive than the yeast form (Berman and Sudbery, 2002), and the yeast form is believed to be primarily involved in dissemination (Saville *et al.*, 2003). *C. albicans* has a specialized set of proteins (adhesins) which enable it to adhere to similar cells, different microorganisms, abiotic surfaces and to biotic host cells (Verstrepen and Klis, 2006). Agglutinin-like sequence (ALS) proteins form a family consisting of eight members (Als1-7 and Als9). The ALS3 gene expression is upregulated during infection and Hwp1 (surface protein that promotes adherence) may covalently link *C. albicans* hyphae to host cells. It has been reported that Hwp1 and Als3 participate in biofilm formation by acting as complementary adhesins (Nobile *et al.*, 2008).

The ability of *C. albicans* to infect a wide range of host tissues has been attributed to multitude of virulence factors and health qualities (Mayer *et al.*, 2013). The virulence factors include morphological shift between yeast and hyphal forms, the expression of adhesins and invasins on the cell surface, the formation of biofilms, and the secretion of hydrolytic enzymes. Additionally, the relatively instant adaptation to the continuous variations in environmental pH and temperature, metabolic flexibility, effective nutrient acquisition systems and robust stress response are a few of the *C. albicans* strength attributes (Bennett and Johnson, 2005, Mayer *et al.*, 2013, Nicholls *et al.*, 2011).

C. albicans must be able to adapt to pH changes ranging from slightly alkaline to severely acidic. It has been claimed that neutral to alkaline pH can cause severe stresses to *C. albicans*, including malfunctioning of pH-sensitive proteins, and impaired nutrient acquisition (Davis, 2009). However, *C. albicans* can also modulate extracellular pH, actively alkalinizing its surrounding environment, endure nutrient starvation and, thereby, autoinducing hyphae formation (Mayer *et al.*, 2012). Therefore, *C. albicans* senses, adapts to and strikingly, also actively modulates extracellular pH (Mayer *et al.*, 2013).

Invasion into host cells by *C. albicans* is probably dependent on two complementary mechanisms: firstly, induced endocytosis mediated by two surface protein invasins, Als3 and Ssa1, and secondly, active penetration mediated by yet undefined molecular mechanisms (Maciel *et al.*, 2020). In endocytosis the fungal cell is engulfed by the host and in active penetration viable *C. albicans* hyphae is essential (Mayer *et al.*, 2013). Hyphal forms are thought to be more virulent since expression of toxins, including the recently discovered Candidalysin (Naglik *et al.*, 2019), are associated with this morphology. Candidalysin is a cytolytic peptide toxin secreted by the invasive form of *C. albicans*. The toxin damages epithelial cells, and thus may allow *C. albicans* to penetrate barrier tissues and establish infections. It is considered as the first real classical virulence factor of *C. albicans* but also induces protective immune responses (Naglik *et al.*, 2019).

C. albicans biofilm is made primarily of mannans and glucans, but also contains polynucleotides that are primarily DNA and RNA, polypeptides, proteins, the glycogen complex fibrinogen, and polysaccharide carbohydrate glucans (Staib and Morschhauser, 2007). Fibrinogen and fibronectin are used as anchor substances which are jelled together by lignans with stickiness properties. The biofilm of *C. albicans* is formed in four steps. First, there is the initial adherence step, wherein the yeast-form cells adhere to the substrate. The second step is called Intermediate step, where the cells propagate to form microcolonies, and yield hyphae. In the maturation step, the biomass expands in size as the ECM accumulates. In the last step, the yeast-form cells disperse to colonize the surrounding environment (Ponde *et al.*, 2021). Yeast cells released from a biofilm have novel properties, like increased virulence and drug tolerance (McCall *et al.*, 2019). An *in vivo* study revealed that dispersion of yeast cells from the mature biofilm can directly contribute to virulence, as dispersed cells were more virulent in a mouse model of disseminated infection (Uppuluri *et al.*, 2010a). It has been reported that contact sensing or thigmotropism is an important factor that can trigger *C. albicans* to form biofilm and hyphae (Kumamoto, 2008). The hyphae can invade a living tissue like the tooth pulp or form a biofilm on a solid surface like a denture. Moreover, *C. albicans* induces directional growth when it encounters a surface with depressions or ridges such as found in dentine (Brand *et al.*, 2007). Following adhesion to the surface, the hyphae of *C. albicans* secretes hydrolases

such as proteases, phospholipases and lipases, that facilitate penetration into living tissue and enable acquisition of extracellular nutrients, (Naglik *et al.*, 2003).

The main nutrient sources for *C. albicans* are obtained from the host environment and may include glucose, lipids, proteins and amino acids. *C. albicans* is able to use these nutrients individually and to react and adapt to the dynamic changes in the host and to those induced by pathogens in micro-environmental nutrient availability. All these features of adaptability to pH, nutrient shortage and avoiding host defences contribute to its astonishing capacity to coexist as a commensal, and to triumph as a fungal pathogen in humans. Subsequently, a robust stress response contributes to the survival, virulence, and readiness of *C. albicans* to respond to harsh host-derived stresses for instance, heat shock, osmotic and oxidative stresses (Mayer *et al.*, 2013).

The heat shock response is a reaction of living organisms to stressful high temperature. Such a stress causes protein unfolding and nonspecific protein aggregation which may lead to cell death. In order to counteract this detrimental fate, cells react by producing heat shock proteins (HSPs) (Lindquist, 1992). These specialized proteins guard the microbes and prevent protein unfolding and aggregation by binding to microbial cells and stabilizing them (Richter *et al.*, 2010). These proteins generated a lot of research interest especially as some of them for example (HSP21) are absent in humans but present in *Candida* which make them potential drug targets. A further issue is that trace metals such as iron, zinc and manganese are required for the growth and survival of all living organisms. Pathogenic microorganisms, and also their respective hosts, have developed mechanisms to give or deny access to these metals (Hood and Skaar, 2012).

C. albicans possesses virulence factors that might contribute to the severity and the onset of endodontic infections. This clade can adjust to changing environmental conditions and adhere to biotic pulpal or periodontal tissues, and to abiotic surfaces such as those of dental prostheses and coronal or radicular dentine as well as root filling materials (Narayanan and Vaishnavi, 2010). Fungi have occasionally been found in primary root canal infections, but they seem to occur more often in the root canals of teeth in which RCT has failed (Siqueira and

Sen, 2004). In one study, *C. albicans* was detected in 5 out of 24 samples (21%) (Baumgartner *et al.*, 2000). A more recent meta-analysis study reported that the prevalence of *Candida* species was (9.0%) in primary and (9.3%) in secondary root canal infections (Alberti *et al.*, 2021).

E. faecalis is a non-spore forming, fermentative, facultatively anaerobic, Gram-positive coccus. The *E. faecalis* cell shape is ovoid, and its diameter is 0.5 to 1 µm. These cells occur singly, in pairs, or in short chains, and are frequently elongated in the direction of the chain. Most strains are non-haemolytic and non-motile (Schleifer and Kilpperbalz, 1984). Enterococci are resilient and versatile species and can withstand harsh environmental conditions. For example, *E. faecalis* has been shown to be less sensitive to normally lethal levels of ethanol, hydrogen peroxide, acidity, hyperosmolarity, heat, acidity, and alkalinity (Flahaut *et al.*, 1997, Flahaut *et al.*, 1996). It can also starve for prolonged periods and become resistant to various disinfection protocols, such as ultraviolet (Bonhomme *et al.*) irradiation and heat or sodium hypochlorite (NaOCl) treatment (Giard *et al.*, 1996). Moreover, *E. faecalis* can enter a viable but not cultivable state which is a way of survival in an unfavourable environment (Lleo *et al.*, 2001). Subsequently, they become able to endure limited-nutrient environments such as root canals (Kayaoglu and Orstavik, 2004). Indeed, it has been reported that in contrast to many other bacteria, *E. faecalis* was capable of invading tubules in root canal dentine (Akpatá and Blechman, 1982, Love *et al.*, 1997). Furthermore, it has been found that *E. faecalis* could survive independently without the cooperation of other bacteria when colonizing root canals (Fabricius *et al.*, 1982a). *E. faecalis* exhibit an effective proton pump mechanism which adjusts its cytoplasmic pH to optimum levels. Thus, *E. faecalis* avoids the potential deleterious effects of high alkalinity medicaments such as calcium hydroxide that has been used routinely as root canal antimicrobial dressing and forms part of the final obturation material (Orstavik and Haapasalo, 1990). Moreover, *E. faecalis* has an inherent or acquired advantage to resist a wide range of antibiotics; which if used, may shift the microbial flora in its favour (Hunt, 1998). *E. faecalis* displays its virulence through colonization of the host, competition with other bacteria and resistance to a wide range of antibiotics. *E. faecalis* can also evade host immune responses and show resistance against defence mechanism of the host and production of pathological changes directly through production of toxins or

indirectly through induction of inflammation (Kayaoglu and Orstavik, 2004). Some of the most extensively studied virulence factors of *E. faecalis* are aggregation substance, surface adhesins, sex pheromones, LTA, extracellular superoxide, gelatinase, hyaluronidase and cytolysin (hemolysin).

It is apparent that *C. albicans* and *E. faecalis* are capable of colonizing the root canal system and influencing the health of the periapical tissues via the apical foramen or lateral canals. As outlined, they are capable of forming a biofilm on different surfaces, evading the host immune system, and withstanding rigorous treatment procedures. Understanding the pathogenic mechanisms these species use during infection is crucial for developing diagnostic procedures and therapies (Kayaoglu and Orstavik, 2004). Several virulence factors, such as dimorphism, the secretion of proteases and the expression of adhesins and invasins, have been suggested as attractive targets. Another research avenue is to study the polymicrobial nature of root canal biofilms and explore the interplay between these two microorganisms, *C. albicans* and *E. faecalis*, and others harboured within the root canal. As our understanding of endodontic microbiology improves, the potential for developing novel clinical procedures, and therapeutics is enhanced. Thus, the scientific endeavours to eradicate the microbes may succeed and the prognosis of endodontic treatment may further improve.

1.2 Management of endodontic infections

Endodontic treatment attempts to resolve pulpal and periapical diseases, prevent relapse and improve long-term tooth prognosis (Ricucci *et al.*, 2009). Clinicians use chemical agents and mechanical instrumentation to eliminate microorganisms from root canals and hopefully achieve a sterile space. However, the traditional instruments do not achieve full contact with root canal walls and thus not all infected root canal surfaces are well debrided. Despite these laborious procedures, biofilm islands remain in areas such as isthmuses, fins, deltas and lateral canals that are difficult to access (Metzger *et al.*, 2013).

In order to manage the shortfall in mechanical debridement, it has been stated that irrigation of the root canal system is important, in fact it is considered the most important determinant in the healing of the periapical tissues (Kandaswamy and Venkateshbabu, 2010). An ideal root canal irrigation solution should kill

microorganisms and flush out debris whilst not injuring the periapical tissues in cases of material extrusion (Kandaswamy and Venkateshbabu, 2010).

One of the irrigating solutions that have been widely used in endodontic practice is NaOCl. It is a nonspecific proteolytic chemical which has been shown to have a wide spectrum of activity against microorganisms (Mohammadi and Shalavi, 2013). The clinical efficacy of NaOCl depends on its concentration, contact time, volume used and its continuous replenishment (Leclerc, 1990). Despite its many advantages, the use NaOCl in endodontics is hampered by several drawbacks. It is very irritating to soft tissues (Spencer *et al.*, 2007) and unstable when combined with other irrigants (Mohammadi *et al.*, 2017). In addition, SEM images demonstrated that NaOCl lacks the ability to dissolve and remove the inorganic part of smear layer (Garberoglio and Becce, 1994). Ethylenediaminetetraacetic acid (EDTA), a chelating agent is commonly being used to remove the inorganic component of smear layer (Aktener and Bilkay, 1993).

Chlorhexidine (CHX) is another disinfectant compound used as an endodontic irrigant (Mohammadi and Abbott, 2009). It is a potent antiseptic agent and is a widely used as a mouthwash for the management of periodontal diseases. It has been reported that CHX has a wide spectrum of antimicrobial activity and the contact time required for 1.0% and 2.0% CHX liquid to eliminate all microorganisms was the same necessary for 5.25% NaOCl (Vianna *et al.*, 2004). The action of CHX can be either bacteriostatic or bactericidal depending on the concentration; at a higher concentration (0.2% v/v) CHX is bactericidal, while at a lower concentration (0.02% v/v) it is bacteriostatic (Sassone *et al.*, 2003). It has been recommended to use CHX in treating root canal infections as a final irrigant because of its continuing therapeutic or substantivity effect (Komorowski *et al.*, 2000). However, its main drawback is its inability to dissolve organic materials (Naenni *et al.*, 2004).

1.2.1 Novel approaches to root canal disinfection

The term nano-dentistry was first introduced in the 21st century (Izadi *et al.*, 2020) and has developed very quickly in the past decades giving rise to several applications in different biomedical fields including the field of endodontics. Nanoparticles have numerous applications (Wong *et al.*, 2021b). They have been

used for various biomedical applications such as in therapeutics, diagnostics, imaging, and drug delivery. Nanomaterials are also used as scaffolds in tissue engineering (Chatterjee *et al.*, 2014). In dentistry, they have been incorporated into direct restorative materials, dental prosthesis, used in guided tissue regeneration and for modifying the surface of implants (Abiodun-Solanke *et al.*, 2014).

According to EU recommendations, a "Nanomaterial" is: a natural, incidental or manufactured material containing particles, in an unbound state or as an aggregate or as an agglomerate and where, for 50 % or more of the particles in the number size distribution, one or more external dimensions is in the size range (1-100) nm (European-Commission, 2011). Nanoparticles are classified according to their dimensions and their material origin. They are composed of three layers: the **core**, is essentially the centre of the nanoparticle and usually used to refer to the original material of the nanoparticle itself; the **shell layer**, is the intermediate layer and it is chemically different from the core. Then, there is the external **surface layer** that can be functionalized with other particles via surface interactions to create better catalysts and support the "functionalization" of nanoscale material surfaces for applications ranging from drug delivery to more affordable modes of producing and storing energy (Khan *et al.*, 2019). Owing to their size, nanoparticles have distinctive physicochemical properties compared to their bulk counterparts. Nanoscale materials have larger surface areas which increases their reactivity, offers greater solubility, provide biomimetic features and support their own functionalization with other materials like drugs, bioactive molecules and photosensitizers (Jeevanandam *et al.*, 2018). In addition, antimicrobial nanoparticles can penetrate biofilms that may help deliver drugs like antibiotics more efficiently allowing closer contact with microbial cells (Li *et al.*, 2015). Many nanoparticles exhibit antimicrobial activities, mediated through mechanisms such as interacting electrostatically with bacterial cell walls leading to cell membrane damage, increasing cell permeability, generation of reactive oxygen species (ROS), interfering with cellular functions, destruction of proteins, DNA damage and ultimately cell death (Beyth *et al.*, 2015, Bapat *et al.*, 2018).

As highlighted briefly above, due to their many favourable characteristics, the application of nanoparticles in the fields of dentistry has gathered substantial

interest (Freitas, 2000). Nanoparticles have been considered for use as potential endodontic irrigants, incorporation into intracanal medicaments, inclusion in obturation materials, and in root canal sealers. In addition, nanoparticles have been studied for use in regenerative endodontic procedures, and for likely incorporation into scaffolds, as a means of sustained release of bioactive molecules (Shrestha and Kishen, 2017), which are crucial for modulating cellular activity such as proliferation, migration and differentiation (Lee *et al.*, 2011).

Silver nanoparticles

Silver nanoparticles (AgNPs) have been widely investigated in dentistry, and the literature indicates that they are a promising system with antimicrobial, anti-inflammatory and antitumor activity capabilities. (Noronha *et al.*, 2017, Yin *et al.*, 2020). They can interact electrostatically with cell walls and disrupt them, alter metabolic processes, generate ROS, and disable enzyme activity (Bapat *et al.*, 2018). AgNPs exhibit antimicrobial and antifungal properties and enhance the antimicrobial effects of antifungal agents which, in turn lowers the doses of antibiotics necessary for killing microbes, and thus reducing their cytotoxic effects on human cells and overcoming the antibiotic resistance issue (Patra and Baek, 2017). However, some bacterial species might develop resistance to AgNPs after repetitive exposure to antimicrobial medicaments by producing flagellin which initiates aggregation of the nanoparticles (Panáček *et al.*, 2018).

AgNPs have been investigated as a possible nanoparticle-based irrigant for use in the field of endodontics (Wong *et al.*, 2021b). It has been demonstrated that AgNPs as a medicament, but not as a solution possess antimicrobial and antibiofilm effectiveness against *E. faecalis* and could eliminate residual bacterial biofilms during root canal disinfection (Wu *et al.*, 2014). The irrigant's antibiofilm efficacy was further enhanced when combined with ultrasonic energy which improved the contact of the irrigant with hard-to-reach regions of the root canal system (Ioannidis *et al.*, 2019). Surface-charge and contact-time were important determinants of the antimicrobial effectiveness, with positively charged nanoparticles taking the shortest time to inhibit planktonic *E. faecalis* growth compared to neutral and negatively charged particles (Abbaszadegan *et al.*, 2015). Their antimicrobial properties were comparable to conventional

endodontic irrigants (Ertem *et al.*, 2017), though some studies disagree with these findings (Rodrigues *et al.*, 2018). Improved physical and structural properties of root dentine have been associated with AgNPs. Using an AgNPs-based irrigant as a final rinse in RCT enhanced the fracture resistance by two folds compared to when NaOCl was used (Jowkar *et al.*, 2020). AgNPs-based irrigants had no adverse effect on the hardness and elastic modulus of dentine (Suzuki *et al.*, 2019) bond strength and interface permeability of resin-bonded glass-fibre posts (Farshad *et al.*, 2017). On the other hand, AgNPs proved to be cytotoxic to human cells. The generation of ROS initiates pro-inflammatory host responses which depends on their concentration, dimension, and aggregation of AgNPs (Ahamed *et al.*, 2008).

Chitosan nanoparticles

Chitosan is a natural, organic compound derived from chitin that can be obtained from the shells of crabs and shrimp (Dutta *et al.*, 2004). Chitosan is a cationic broad spectrum antimicrobial compound that can interact with the negatively charged bacterial cell membrane causing an increase in its permeability and ultimately cell death. In addition to their antimicrobial potential, chitosan particles are biocompatible, biodegradable and have chelating abilities which make possible their use as irrigants in RCT procedures. (Kong *et al.*, 2010). The antimicrobial use of chitosan in endodontics has been widely investigated (Dutta *et al.*, 2004). Chitosan-based irrigants exhibited antibacterial efficacy against *E. faecalis*. However, their efficacy was enhanced when irrigation was followed by diode laser irradiation (Roshdy *et al.*, 2019). Applying 0.2% carboxymethyl chitosan particles on root canal dentine as a final irrigation step effectively removed smear layer from the middle and apical thirds of the root, improved disinfection and prevented recolonisation to root dentine surfaces prior to root canal obturation (Silva *et al.*, 2013). In addition, chitosan was shown to enhance dentine wettability and stabilise dentine collagen by providing resistance to bacterial collagenase degradation (Kishen *et al.*, 2016).

Metal and metal oxide nanoparticles

Zinc oxide nanoparticles (ZnONPs) have bactericidal properties like that of AgNPs. It has been reported that using a combination of both ZnONPs and AgNPs in a polymeric irrigation solution produced superior antimicrobial activity against *E. faecalis* more than when each was used independently. However, 2.5% NaOCl was still proven to be superior to both in reducing colony forming units (Samiei *et al.*, 2015). Further studies have confirmed that, ZnONPs exhibited lower antimicrobial efficacy compared to conventional endodontic irrigants (Shrestha *et al.*, 2010). Nanoparticles of magnesium oxide, titanium oxide, and iron oxide, all have been shown to have antimicrobial properties (Beyth *et al.*, 2015, Nguyen *et al.*, 2018). Albeit fewer experiments have been designed to explore the potential use of these nanomaterials as irrigants in endodontic treatments (Wong *et al.*, 2021b). One study showed that nano-magnesium oxide solution had long-term antimicrobial effect in *in vitro* and *ex vivo* models against *E. faecalis* (Monzavi *et al.*, 2015). Iron oxide nanoparticles were incorporated into an irrigant solution with hydrogen peroxide. It was reported that the irrigant demonstrated peroxidase-like action resulting in antibiofilm and bactericidal activity against *E. faecalis* (Bukhari *et al.*, 2018). Metal and metal oxides nanoparticles possess a degree of cytotoxicity, thus risk assessment and biocompatibility experiments are required before proceeding to translational studies (Beyth *et al.*, 2015, Wong *et al.*, 2021b).

1.2.1.1 Nanodiamonds

Nanodiamonds (NDs), a new class of nanoparticles in the carbon family, were first described in 1963 (Danilenko, 2004). They were “re-discovered” in Russia in 1983 and were commercially available in 1988 for the first time in the United States of America (Mochalin *et al.*, 2012). Nanoscale diamonds, are usually smaller than 100 nm (Chaudhary *et al.*, 2010). Owing to their biocompatibility and being tolerated by human tissues, they have been used for drug delivery and imaging applications, coatings for implantable materials; and biosensors and biomedical nanorobots (Schrand *et al.*, 2007).

NDs can be produced on a large scale using relatively inexpensive synthetic techniques and their surfaces can be functionalised (Passeri *et al.*, 2015).

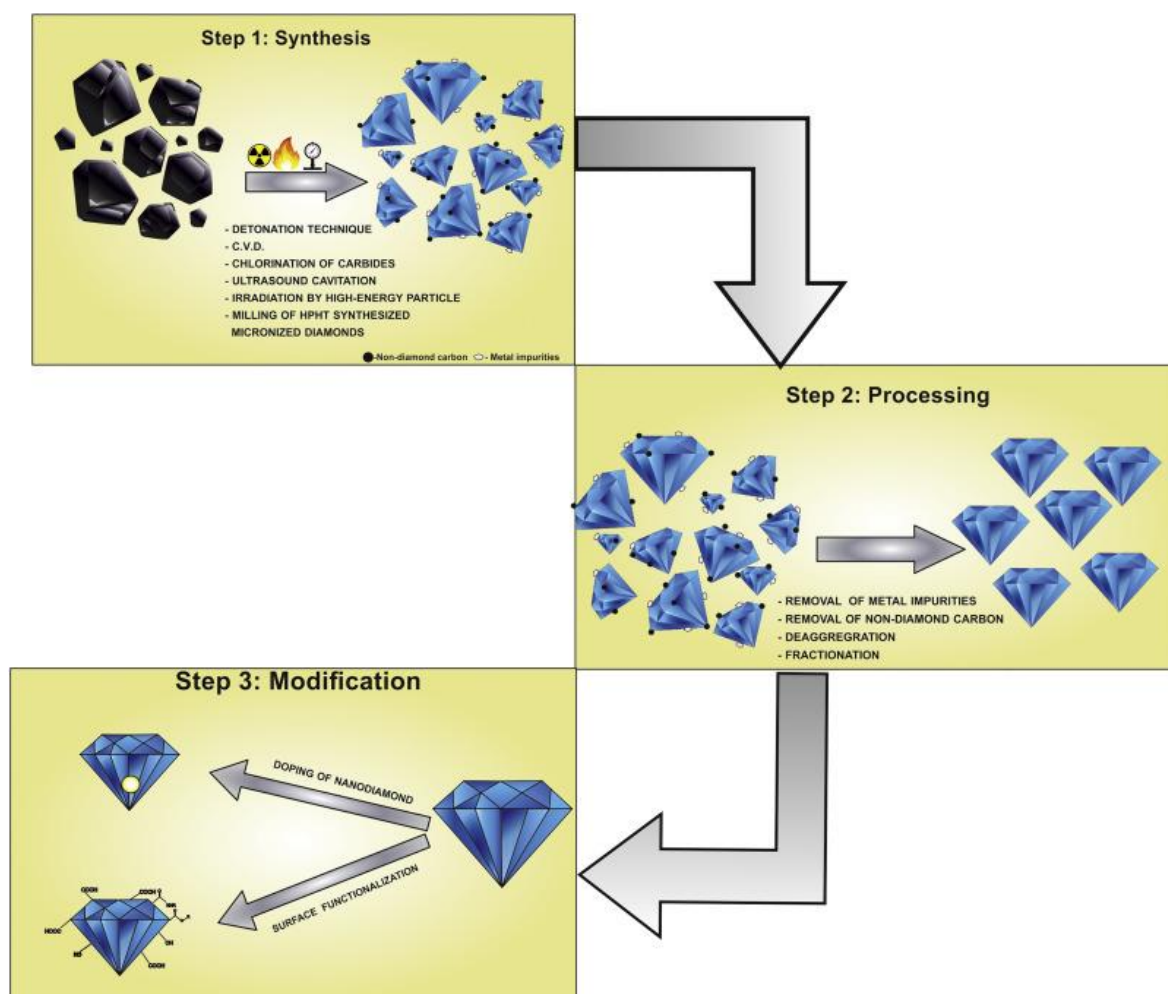


Figure 1.3: NDs properties, types, and production methods. Production process of different types of NDs (Tinwala and Wairkar, 2019).

Nanodiamond structure consists of an inert core material and a surface shell that is partially graphite (Passeri *et al.*, 2015). They can be formed by applying special methods like detonation technique, high pressure - high temperature (HPHT) methods, chemical vapor deposition (CVD) technique, ultrasonic synthesis, hydrothermal synthesis, ion and laser bombardment and electro-chemical synthesis (Figure 1.3) (Kharisov *et al.*, 2010). These techniques determine the size, shape, groups attached on the surface, and quality of NDs (Chauhan *et al.*, 2019). The detonated type of ND has sp^2 carbon on its surface with functional groups and large surface area, which enables the attachment of drug molecules, thus establishing an excellent drug carrier system and improving drug efficiency (Chauhan *et al.*, 2019). Moreover, NDs have a strong affinity towards proteins and antibodies, thus allowing an effective and stable protein loading on their surfaces (Kong *et al.*, 2005). Detonated nanodiamonds (DND) have been shown to lead to

significant reductions of viability in different bacterial strains, including Gram negative *E. coli* and Gram-positive *B. subtilis* (Wehling *et al.*, 2014).

Milled nanodiamonds (MND) are typically made by milling HPHT synthesized bulk diamond into particles of a few tens of nanometres in size producing diamond nanoparticles with varying distributions of shapes and sizes (Ong *et al.*, 2018). One advantage of MNDs over DNDs is that they are more biocompatible because of less carbon allotropes (Zhu *et al.*, 2012). The MNDs have angular and flake-like geometries with larger facets in contrast to DNDs being round and small (Ong *et al.*, 2017). The sharp edges of these MND make them able to pierce biological membranes and the crystallographic orientation of the facets determines their chemical affinities (Chu *et al.*, 2014). NDs act as a potent antibacterial agent by destroying bacterial barriers and have the potency to bind with several viruses like hepatitis B or C (Chauhan *et al.*, 2019, Torres Sangiao *et al.*, 2019).

In dentistry, NDs have been incorporated in dental composites, polymers, and used as implant coatings to improve their mechanical and biological properties. They also have been employed in the oral medicine field, where they have been used for imaging and as drug delivery agents to treat oral infections and cancerous lesions (Najeeb *et al.*, 2016).

In endodontics, the antimicrobial capability of NDs have not been studied extensively. NDs can be embedded in gutta percha forming (NDGP) which can be functionalized with commonly used broad spectrum antibiotics like amoxicillin (Lee *et al.*, 2015). The NDGP was employed in a laboratory study and the results demonstrated improved mechanical properties of NDGP over unmodified GP. In addition, bacterial growth inhibition assays validated drug functionality of NDGP functionalized with amoxicillin. It was concluded that obturation of root canals with NDGP could be achieved using clinically relevant techniques (Lee *et al.*, 2015). A clinical study was conducted to validate the results of the *in vitro* study (Lee *et al.*, 2017). Follow-up examinations after 3 months and 6 months, revealed no adverse events, and lesion healing was confirmed in teeth treated with NDGP (Lee *et al.*, 2017).

Do nanodiamonds possess antimicrobial activity?

One study explored the mechanism of antibacterial action of NDs. The study compared the antibacterial activity of Diamond-like carbon (DLC) films and DLC films doped with DNDs against *E. coli* (Conceição *et al.*, 2019). The DLC films coated with NDs were able to significantly reduce bacterial growth by 95%. It was claimed that DNDs were able to penetrate the cell wall, cause damage to its genetic content and induce oxidative stress which resulted in bacterial death (Conceição *et al.*, 2019). Wehling *et al.* (2014) proposed that when the NDs surface is partially oxidized and negatively charged, it would gain an antibacterial group namely acid anhydride and be the most effective against Gram-positive and Gram-negative bacteria. On other hand, highly purified NDs obtained using detonation technique were not able to exhibit antibacterial properties due to less oxidised surface. Moreover, surface functionalization of NDs with protein molecules increased the NDs bactericidal property (Wehling *et al.*, 2014). Another research group investigated the antibacterial activity of ultrafine nanodiamond against *E. coli*. They functionalised NDs surface with carboxyl group to form carboxylated nanodiamond (cND) and was placed in rich nutritious media. SEM photomicrographs showed cND attached to a damaged bacterial cell wall surface (Chatterjee *et al.*, 2015). When the surface of NDs is functionalized with glycan, it displayed an effect specifically against adhesion and biofilm formation of type 1 fimbriae-mediated *E. coli*. It was suggested that the NDs form covalent bonds with cell wall molecules, or they bind to intracellular components inhibiting vital enzymes and proteins and leading to a rapid collapse of the bacterial metabolism and eventually cell death (Szunerits *et al.*, 2016).

Chwalibog *et al.* (2010) explored the activity of ND and metallic nanoparticles against Gram-positive and Gram-negative bacteria and reported that ND did not show any destruction against Gram-positive *S. aureus*. This variable effect was explained by the positive zeta potential of NDs. Visualization of the morphologic interaction between the nanoparticles and microorganisms showed that NDs bound closely and non-specifically to *S. aureus* surface and surround *C. albicans* without causing visible damage to both cells, demonstrating self-assembly ability. These findings contrast with that seen with metal nanoparticles with negative zeta potential which had cell damaging properties. For instance, nano-Ag established

contact at a specific point of the cell wall and attached to substances released by *S. aureus* and *C. albicans* causing distorted cells and disintegrated cell wall of *C. albicans*. Platinum nanoparticles damaged cell walls and caused the release of cell contents. The non-specific attachment of NDs to *S. aureus* cell wall was attributed to their high affinity to the peptidoglycan layer. In addition, NDs could be seen within the cell and cell wall (Chwalibog *et al.*, 2010).

NDs have been investigated with simple chemical surface functionalisation to enhance their antibacterial properties. The NDs functionalised with an anhydride functional group were able to kill bacteria owing to their higher reactivity. Meanwhile, NDs functionalised with lower reactivity carboxylic groups were less able to eradicate bacteria. This has been attributed to differences in surface isotropy and homogeneity of the surface charge distribution. The more interesting being an anisotropic surface with inhomogeneous surface charge distribution (Wehling *et al.*, 2014). These findings were confirmed in another study which demonstrated the importance of oxidation state and the surface group charge at the surface of NDs (Szunerits *et al.*, 2016). A study explored different types of surface oxidation, such as -H, -F, -O, on ND coated films (Dunseath *et al.*, 2019). Other studies have used germanium (Robertson *et al.*, 2017), molecules like glycan (Barras *et al.*, 2013) or essential oils (Turcheniuk *et al.*, 2015) for functionalization. Moreover, NDs have been functionalised with larger molecules like glycol molecules. Glyco-conjugate NDs and mannose-functionalised NDs (Mannose-ND) have been tested against *E. coli* and the results demonstrated that the bacteria had high affinity to adhere to Mannose-ND and polysaccharides (Hartmann *et al.*, 2012).

Several studies have tested the antifungal activity of NDs. A recent study has evaluated the effect of different concentrations of NDs added to polymethyl-methacrylate (PMMA) denture base material on *C. albicans* adhesion. Their results showed that the addition of NDs decreased *C. albicans* count significantly more than in the control group (Fouda *et al.*, 2019). Zhang *et al.* (2021) evaluated the antimicrobial activity of NDs fabricated using HPHT technique against biofilms. They reported a major role of NDs in inhibiting biofilm growth as well as their disrupting effect on preformed biofilm of oral bacteria *S. mutans* and *P. gingivalis* and fungi *C. albicans* and *C. glabrata*. Gene expression analysis revealed that NDs

were able to inhibit biofilm growth and modulate virulence of *C. albicans* (Zhang *et al.*, 2021b).

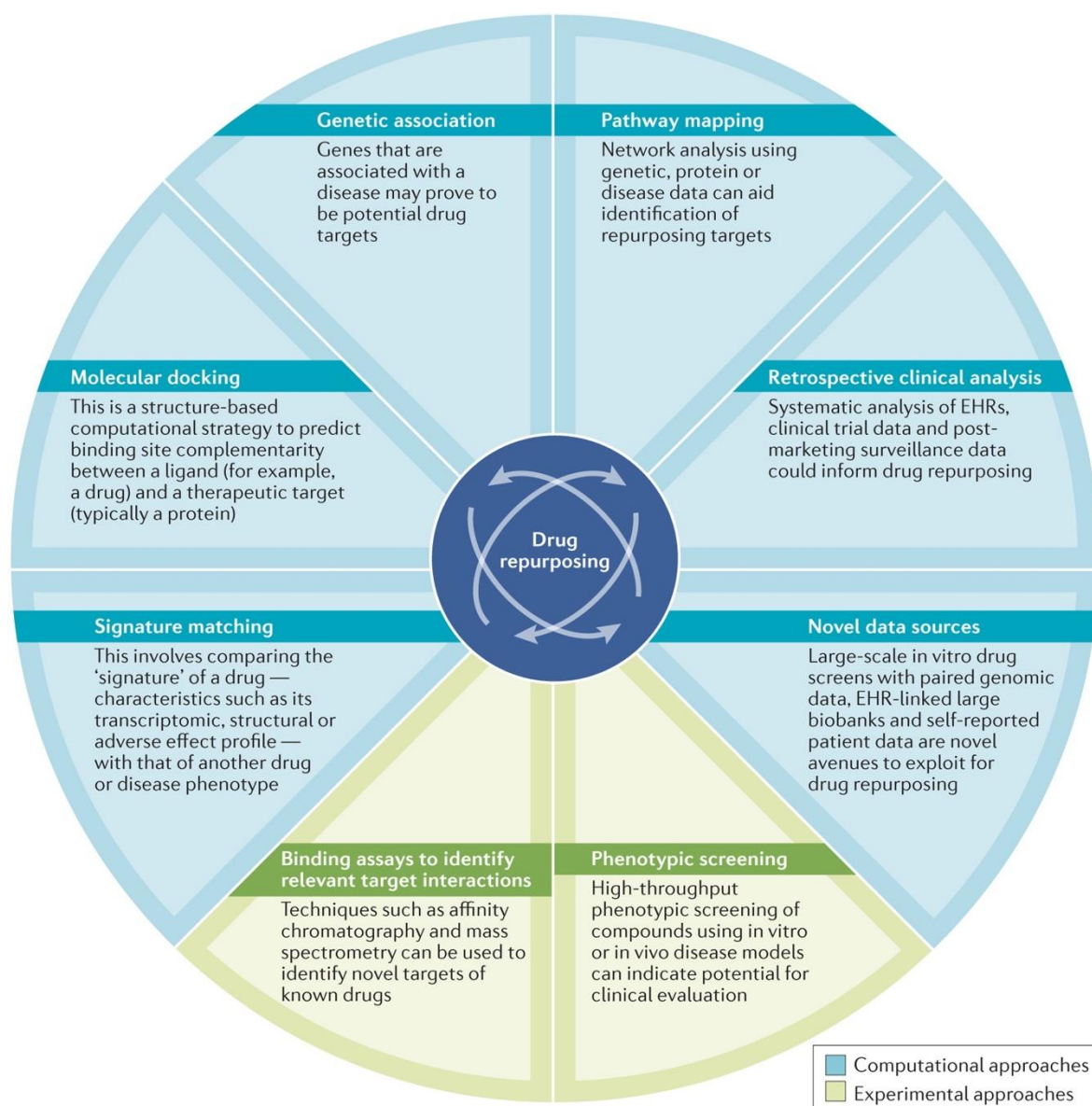
(Norouzi *et al.*, 2020) looked at the interaction between microbial strains, nanoparticle size and surface chemistries. They observed particle aggregation and bacterial clumping. Such behaviour could explain reduced colony counts, which may have been wrongly interpreted as a bactericidal effect (Ong *et al.*, 2018). The study also showed no mechanism to be linked to specific material property. They hypothesized that aggregation is an important factor in reducing the *in vitro* colony forming ability of *E. coli*, *S. aureus* and *S. epidermidis* when exposed to MND and proposed a model to prove their assumption. In the model, they showed that the effect of the NDs is two-fold. When NDs attach to the bacterial cell wall in ample concentration, they prevent the proliferation of bacteria into colonies and facilitate the formation of larger crystals of mixed bacteria and NDs reducing the number of loose bacteria that can form separate colonies. They also showed that NDs does not aggregate in water but tend to aggregate immediately when adding salt and protein. This observation which, was used to refute the “contact killing”, behaviour seen and misinterpreted in previous work of same authors (Ong *et al.*, 2018), can be ascribed to a multifactorial process of aggregation (Norouzi *et al.*, 2020).

1.2.1.2 Drug Repurposing

Various synonyms have been used for drug repurposing such as drug repositioning, reprofiling or re-tasking. The term describes a strategy developed for identifying new horizons of uses for already approved or trial drugs that are outside the scope of their intended original medical indication (Ashburn and Thor, 2004). This strategy assures maximum success and drug safety because the drug has already been tested in preclinical models in human early-stage clinical trials. Drug development is achievable in a relatively short time frame because safety assessment and formulation development data are already in place. In addition, the cost of drug repurposing is lower than developing a new drug. There are substantial savings in preclinical and phase I and phase II costs (Breckenridge and Jacob, 2019). Lastly, repurposed drugs may reveal new targets and pathways that can be further exploited (Pushpakom *et al.*, 2019).

Drug repurposing techniques comprise computational, experimental or mixed approaches (Figure 1.4). Systematic analysis of data such as gene expression and chemical structure are an example of a computational approach (Hurle *et al.*, 2013). Experimental approaches on the other hand, include molecular docking, signature matching, pathway mapping and genetic association (Iorio *et al.*, 2013).

The success of drug repurposing in history encouraged the development of a systematic approaches to identify more repurposed compounds. The drug repurposing strategy requires three preliminary steps: generation of a hypothesis in which a candidate molecule is identified for a given indication; systematic assessment of the candidate drug effect in preclinical models; and evaluation of drug efficacy in clinical trials.



Nature Reviews | **Drug Discovery**

Figure 1.4: Approaches in drug repurposing. Computational and experimental approaches can be used alone or synergistically to identify repurposing opportunities (Pushpakom *et al.*, 2019).

Computational approaches

Generally, computational approaches depend on collection and analysis of data. They involve systematic analysis of data of, amongst others, soft copies of health records, gene expression, transcriptomic and proteomics data. This collection of information guides researcher in generating an appropriate drug hypothesis. The most used computational approaches are:

1. **Signature matching:** this approach compares the unique characteristics (signature) pertaining to a particular drug molecule to those of another drug, disease, or clinical phenotype (Keiser *et al.*, 2009). Three types of data can assist in identifying a drug signature, namely: transcriptomic, proteomic, or metabolic data; chemical structures; or profiles of reported adverse event. Matching transcriptomic signatures can be utilised for estimating drug-disease similarities (Dudley *et al.*, 2011) and for drug-drug comparisons (lorio *et al.*, 2013). In the case of drug-disease similarities, the transcriptomic signature of a drug is elicited by comparing the gene expression profile of biological material, for example a tissue, before and after treatment with the drug. The resultant differential gene expression is called (the molecular signature of the drug). The disease-associated expression profile is obtained in a similar way via differential expression analysis of disease versus healthy conditions. Comparisons are then made between the resultant gene expression signature of the drug and that of the disease to assess the extent of negative correlation between them; in other words, the extent of gene increase in the disease state compared to that of gene decrease with the drug treatment and *vice versa*. This correlation would then imply whether the drug may have a probable impact on the disease (Sirota *et al.*, 2011). It has been reported that a hypothesis of drug-repurposing can be generated based on negatively correlated profiles, whereas positively correlated profiles may be used to infer side effects of drugs. This computational approach relies on the signature reversion principle (Pushpakom *et al.*, 2019). This approach identifies drugs with inverted transcriptomic signatures relating to the signature of a disease. Treatment of patients with such drugs could thus result in rectifying (reversing) the disease transcriptomic signature, presumably

restoring the healthy phenotype (Pushpakom *et al.*, 2019, Dudley *et al.*, 2011). As for drug-drug similarity, the goal of the approach is to identify shared transcriptomic signatures of drugs that are of different chemical structure or listed in another drug class (Chiang and Butte, 2009). It can help in identifying alternative targets of current drugs or unravel off-target effects which can be tested for clinical therapies (Keiser *et al.*, 2009). It could be deduced that a shared transcriptomic signature between two drugs could therefore indicate that they share similar therapeutic application, irrespective of the differences in their chemical structures (Iorio *et al.*, 2010). Both drug-disease and drug-drug similarity approaches rely extensively on publicly accessible gene expression data for matching of transcriptomic signatures. Several accessible databases have been produced to serve as a reference like connectivity map databases available in the US National Institutes of Health (Lamb *et al.*, 2006). Other important public sources of transcriptomic data, such as the Gene Expression Omnibus and Array Express contain raw gene expression data from hundreds of disease conditions in human and animal models, are available for drug repurposing research (Wang *et al.*, 2016).

Another type of signature matching is based on chemical structures and their role in biological activity, and the wide use of data analysis simulation tools (Oprea *et al.*, 2007). Comparisons are conducted between a chemical signature of one drug with that of another to elucidate if the two drugs are chemically similar. Chemical similarities, if present, may indicate some shared biological activities. The process involves choosing a set of chemical features for each drug and then assembling networks based on the shared chemical features (Keiser *et al.*, 2009). Finally, matching the adverse effect signature of drugs is another approach used for drug repurposing (Campillos *et al.*, 2008). Every drug has its own specific adverse effect profile that could be used as an alternative for its phenotype. It has been hypothesised that two drugs triggering the same adverse effects may be acting on a shared target or protein or on the same pathway (Campillos *et al.*, 2008, Dudley *et al.*, 2011). Shared pathways and physiology by both the drug and the disease will occur when the adverse effect phenotype of a particular drug resemble that of a disease (Campillos *et al.*, 2008).

2. **Computational molecular docking:** this is a computational approach used for predicting a binding site complementarity between the ligand (a drug) and the target (a receptor). If one target receptor in a certain disease is known beforehand then multiple ligands (drugs) could be tested against this target; a process known as conventional docking which involves one target and multiple ligands (Kitchen *et al.*, 2004). Another docking method is called inverse docking in which drug libraries are explored against a range of target receptors to detect new interactions that can be taken into consideration for repurposing. High-throughput computational docking has been used for performing molecular fit computations on many FDA approved drugs and screening them against human protein crystal structures to discover potential repurposed drugs (Dakshanamurthy *et al.*, 2012).
3. **Genome-wide association studies (GWAS):** this approach aims to identify genetic variants involved in common diseases. It enables researchers to have a comprehensive view of the disease biology and identify potential novel targets. The data obtained may be beneficial in identifying of receptors, some of which could be shared between diseases treated by drugs and disease phenotypes thereby be valuable for repositioning of drugs (Sanseau *et al.*, 2012).
4. **Pathway or network mapping:** When potential targets are discovered by GWAS, they make themselves directly amenable as drug targets. In such situations, a pathway strategy can be used to deliver information on genes that are either upstream or downstream of the GWAS associated target and could be exploited for repurposing opportunities (Smith *et al.*, 2012a, Greene and Voight, 2016a).
5. **Retrospective clinical analysis:** this approach is based on using electronic health records (EHRs). It furnishes repurposing opportunities that may arise from retrospective clinical or pharmacological analyses (Cavalla and Singal, 2012). Retrospective clinical data can be obtained from EHRs, post marketing surveillance data and clinical trial data (Greene and Voight, 2016b). EHRs contain a huge amount of structured and unstructured data

on patient outcomes. An example of structured results are laboratory tests results and drug prescribing data. Nevertheless, EHRs encompass considerable amounts of unstructured information, such as detailed descriptions of clinical features, and imaging data. Apparently, this wealth of data present in EHRs represent a rich source for identifying signals for drug repurposing (Hurle *et al.*, 2013). In addition, the data also provide high statistical power (Paik *et al.*, 2015) and reduce the probability of false conclusions. However, a variety of ethical, legal and technical hurdles currently impede the systematic deposition of these data in EHRs and hinder their mining (Jensen *et al.*, 2012).

6. **Novel Sources of data for drug repurposing:** Immortalized human cancer cell lines (CCLs) have been employed in high-throughput drug screening against hundreds of approved and experimental compounds to examine their effectiveness on cell's ability to live (Huang and Vakoc, 2016). Mining available data sets containing paired genomic and pharmacological data on large groups of CCLs has been considered as a pioneer project for identifying drug and accelerating repositioning opportunities (Weinstein, 2012). The resulting pharmacological data from these screens have been paired with comprehensive genomic characterization of the probed CCLs which allows the identification of pharmacogenomic interactions between molecular features of the cell and drug response (Seashore-Ludlow *et al.*, 2015).

Experimental approaches

In an era of chemical biology for target validation, analyses of the targets and “off-targets” of drugs and drug repurposing have become natural associates (Molina *et al.*, 2013). One of the methods used is to identify target interactions using binding assays. It relies on proteomic techniques like affinity chromatography and quantitative mass spectrometry techniques to identify binding target partners for an increasing number of drugs (Brehmer *et al.*, 2005, Molina *et al.*, 2013). Advances in the development of highly specific chemical probes, in conjunction with improved structural biology, are accelerating target identification (Pushpakom *et al.*, 2019).

Phenotypic screening to discover antimicrobial activity of repurposed drugs

Phenotypic screening can identify compounds that exhibit disease-relevant effects in an experimental model system without previous knowledge of the target affected (Moffat *et al.*, 2017). Small molecules are organic compounds of low molecular weight (<900 Dalton). Owing to their small size, these molecules have the advantage of passing across cell membranes to reach targets, rendering them suitable for many targeted therapies. *In vitro* phenotypic screens use a series of assays in a 96-well format. Phenotypic screens have been used to identify novel small-molecule compounds that possess antineoplastic actions (Iljin *et al.*, 2009). *In vivo* models have been utilized in drug repurposing to evaluate 39 FDA-approved medications for use in tobacco dependence (Cousin *et al.*, 2014). Large drug and compound libraries have been screened for new activities and alternate uses which can facilitate rapid identification of new therapies (Iljin *et al.*, 2009, Cousin *et al.*, 2014). Recently, library screening methods have been used to identify new antimicrobial agents. This type of screening method explores many small-molecules compounds and identifies candidate antimicrobial agents (Ayon and Gutheil, 2019). Small-molecule compounds enjoy many valuable merits namely their high chemical stability and relatively low costs compared to organic compounds and their uncomplicated synthesis.

E. faecalis and *C. albicans* species were reported as antimicrobial resistant pathogens (Weiner-Lastinger *et al.*, 2020). There is an obvious need to discover compounds that can aid in managing these and other organisms that represent a developing public health crisis. The antihistamine compounds terfenadine and its analogues have been investigated as potential antibacterial drugs. Terfenadine has shown acceptable activity against *S. aureus*. The drug activity was enhanced by manufacturing eighty-four derivatives that have presented greater minimal inhibitory circulation (MIC) values against *S. aureus* (1 mg/L) as well as activity against *E. faecalis* (Perlmutter *et al.*, 2014). In another study, the antibacterial activity of Penfluridol (Harpf *et al.*), an oral long-acting antipsychotic drug, has been investigated by drug repurposing against *E. faecalis*; and it was concluded that after structural optimization, PF has potential as a new antibacterial agent against *E. faecalis* (Zeng *et al.*, 2021). Bithionol (BT) is a clinically approved anthelmintic drug which has been repurposed in an *in vitro* and *in vivo*

antimicrobial and antibiofilm study. BT demonstrated significant antimicrobial and antibiofilm effects against *E. faecalis in vitro*, in a dose-dependent manner, by disrupting the integrity of the bacterial cell membranes. Moreover, BT effectively decreased the bacterial load in *in vivo* when combined with conventional antibiotics in a peritonitis infection model (She *et al.*, 2021).

Many studies have explored repurposed drugs to combat *C. albicans* biofilms. In one such study, flucytosine, also known as 5-fluorocytosine (5-FC). This drug was synthesized in 1957, as a potential anti-tumour agent (Duschinsky *et al.*, 1957). Later, it was repurposed to treat human candidosis and cryptococcosis in 1968 (Tassel and Madoff, 1968). Moreover, small-molecule antifungal compounds were identified using library screening methods with *C. albicans*. Their antifungal effects on *Candida* biofilms and cytotoxic effects on human cells were evaluated (Watanoto *et al.*, 2015). This screening identified an agent, CV-3988 that was formerly unknown to have antifungal activity, which could be a useful medicament for treating superficial mucosal candidiasis. Another study investigated the antifungal activity of the compound Bay-11-7085 against *C. albicans* biofilm. The results demonstrated that the Bay-11 compound inhibited and eradicated biofilm formation of antifungal resistant *Candida* isolates (Escobar *et al.*, 2021). Other potential repurposed anti *C. albicans* drugs include Haloperidol or benzocyclane derivative; Aripiprazole; Alexidinedihydrochloride; Sulfonamide drugs; and Aspirin (Kim *et al.*, 2020a).

The attractive characteristics of small molecules makes them ideal for dental applications (Birjandi *et al.*, 2020). Drug repurposing has been used in dentistry to apply small molecules in dentine repair by stimulating Wnt/ β -catenin signalling; stimulating signalling in a tooth cavity with pulp exposure induces odontogenesis and prompts reparative dentine formation (Alaohali *et al.*, 2022) . A noteworthy study (Birjandi *et al.*, 2020) investigated a range of small molecules that are currently used for treatment of various medical conditions and reported that Tivantinib, a c-Met inhibitor, has the ability to stimulate Wnt/ β -catenin pathway in dental pulp cells *in vitro* at low concentrations. Such approach hasn't been utilised in the field of endodontics yet. Various *in vitro* and *in vivo* studies including drug repurposing ones need to be done to investigate potential

antimicrobial agents to manage endodontically relevant microorganisms and inhibit biofilm formation inside root canals.

1.3 Hypothesis and aims

The hypothesis of this thesis is that *C. albicans* and *E. faecalis* interact with each other in dual-species biofilm which can affect each other's virulence behaviour and impact the overall virulence of the biofilm in responding to treatment.

The aims of this thesis are:

1. To characterise biofilms of *Candida albicans* and *Enterococcus faecalis* at a phenotypic and molecular level.
2. To investigate the transcriptome of *C. albicans* when in coculture with *E. faecalis*.
3. To assess both species response to novel therapeutics when in dual-species to help understanding interkingdom interaction.

Chapter 2: Characterisation of *Candida albicans* and *Enterococcus faecalis* dual-species biofilm and the reciprocal effect on their virulence

2.1 Introduction

The state of pulpal and periapical infection plays an important role in modifying root canal ecology. The untreated infected pulp has an abundance of nutrients from oral cavity which allows facultative bacteria to thrive and support a diverse mixture of species. In contrast, root filled teeth exhibit a nutrient deficient environment, and a drop in oxygen levels (Shepard and Gilmore, 1999). Oxygen tension levels differ across the root canal and depend on the vitality of the tooth. Necrotic tissue is conducive for anaerobic bacteria to thrive (Siqueira and Rocas, 2013b). It has been also shown that the existence of *C. albicans* in a biofilm could promote a hypoxic condition where many anaerobic bacteria could successfully grow (Fox *et al.*, 2014). Therefore, certain species can withstand such harsh environments and modulate their virulence factors accordingly and contribute further to the virulence of diseases (Fabricius *et al.*, 1982b). *E. faecalis* have shown an ability to inhabit an undernourished environment of root-filled canals within a biofilm by virtue of their own properties; and the synergistic and antagonistic interactions between species (Bouillaguet *et al.*, 2018). In addition, *E. faecalis* can express certain virulence factors that enables it to withstand different environmental stresses. For example, *E. faecalis* can produce a high-molecular-weight surface protein Esp that aids in colonization and persistence of *E. faecalis* and helps its primary attachment and biofilm formation (Toledo-Arana *et al.*, 2001). Several studies have shown the expression of the gene *esp* among endodontic isolates (Sedgley *et al.*, 2005a, Reynaud af Geijersstam *et al.*, 2007, Zoletti *et al.*, 2011). Gelatinase is an extracellular zinc containing metalloproteinase enzyme that can hydrolyse gelatine, collagen, fibrinogen and other proteins. Gelatinases of *E. faecalis* may play an important role in the pathogenesis of periapical inflammation. Phenotypic gelatinase activity has been reported in 47-70% of positive endodontic isolates (Sedgley *et al.*, 2005a, Reynaud af Geijersstam *et al.*, 2007, Zoletti *et al.*, 2011), which contrasts with Anderson *et al.* (2015) who revealed gelatinase activity in only 3.3% of endodontic isolates. However, upon gene analysis, the gene *gelE* was present in all clinical endodontic isolates (Anderson *et al.*, 2015). In addition, cytolysin (formerly called haemolysin) is considered the most frequently plasmid-encoded toxin (Van Tyne *et al.*, 2013). Cytolysin was frequently found in *E. faecalis* isolated from root canal

infections (Reynaud af Geijersstam *et al.*, 2007, Sedgley *et al.*, 2004). Finally, *E. faecalis* produces a small protein, EntV, that is a potent inhibitor of the ability of *C. albicans* to form biofilms and reduces fungal virulence in several models (Cruz *et al.*, 2013).

Studies have shown that *C. albicans* and *E. faecalis* were the most frequently isolated microorganisms in recurrent endodontic infections (Peciuliene *et al.*, 2001, Dumani *et al.*, 2012). *C. albicans* is well suited for survival in nutrient limited conditions, and *E. faecalis* possesses a similar capacity for starvation survival and growth (Richards *et al.*, 2010, Gao *et al.*, 2016).

Fungi and bacteria interkingdom interaction can significantly influence the virulence of a mixed-species biofilm. *C. albicans* can interact with different bacterial species that can either enhance or antagonise its virulence. This interaction can be physical or by quorum sensing molecules and other soluble mediators. For example, *S. gordonii* expresses surface antigen SspA and SspB to attach to mucosal surfaces but also to other microorganisms' surfaces. *C. albicans* uses this antigen to coaggregate with *S. gordonii* which allows proximal cell to cell communication via secreted signals (Bamford *et al.*, 2009). Another important example of interkingdom synergism is when *S. aureus* utilises hyphae specific ALS3 to bind to *C. albicans* and promote its colonisation to host tissues and biofilm formation (Peters *et al.*, 2012). In addition, farnesol a quorum sensing molecule produced by *C. albicans* can enhance *S. aureus* tolerance to antimicrobials by inducing the upregulation of efflux pump genes (Kong *et al.*, 2017). Moreover, the existence of *C. albicans* amongst oral bacteria has significantly enhanced its hyphal formation and virulence and upregulated genes involved in adherence and biofilm formation (Morse *et al.*, 2019).

In contrast, microbial interactions between *C. albicans* and bacterial species can be detrimental to the fungal organism. An example on the strong antagonistic relationship that exists between *C. albicans* and *P. aeruginosa* is that *P. aeruginosa* produces quorum sensing molecule that inhibits hyphal morphogenesis of *C. albicans* and prevents its growth. This molecule regulates *P. aeruginosa* adherence to *C. albicans* hyphae by triggering the synthesis of surface adherence proteins (Fourie *et al.*, 2016). Once adhered, quorum sensing system starts

producing redox-active (oxidation-reduction) phenazines which generates ROS that can directly kill *C. albicans* cells. In doing so, *P. aeruginosa* weakens *C. albicans* cell wall integrity and stops hyphal morphogenesis. Moreover, farnesol produced by *C. albicans* prevents the formation of hyphae and thus provides protection against killing by *P. aeruginosa* (Hogan and Kolter, 2002, Fourie *et al.*, 2016).

It has been shown that *C. albicans* and *E. faecalis* have an antagonistic relationship when they coexist together in mixed species biofilm (Alshanta *et al.*, 2022). One study isolated anti-*Candida* protein from *E. faecalis* strains and reported that this protein could inhibit the growth of many *C. albicans* strains including the multi resistant *C. albicans*; and it concluded that anti-*Candida* protein could be utilised in the treatment of candidiasis specially in the immunocompromised patients (Shekh and Roy, 2012). Moreover, it has been reported that *E. faecalis* bacteriocin, EntV, is necessary and sufficient for the reduction of *C. albicans* biofilm formation and virulence by inhibiting hyphal morphogenesis (Graham *et al.*, 2017b). Furthermore, a more recent study assessed the antifungal capability of heat-killed *E. faecalis* in oral candidiasis patients and showed that the bacterium significantly decreased the load of oral *Candida* in those patients by inhibiting mycelial growth (Yamazaki *et al.*, 2019). In addition, it has been demonstrated that the relationship of both microorganisms caused less pathology and mortality than either species alone; a finding that was attributed, in part, to an interkingdom signalling event by a bacterial-derived product that inhibited hyphal morphogenesis of *C. albicans* (Garsin and Lorenz, 2013). Indeed, nematodes treated with the bacteriocin peptide were completely resistant to killing by *C. albicans* (Graham *et al.*, 2017b). This killing resistance might indicate that a level of antagonism exists between the microorganisms.

In contrast, a recent article by our research group evaluated the relevance of pH to dual-species biofilm interactions and demonstrated that *E. faecalis* rapidly and significantly impacted *C. albicans* morphogenesis and biofilm formation. These results suggested that the anti-*Candida* effect of *E. faecalis* is not completely based on a single mechanism but may rather involve various mechanisms, which

collectively reflect the complexity of interactions between *C. albicans* and *E. faecalis* (Alshanta *et al.*, 2022).

The literature review reveals that interkingdom interaction between *E. faecalis* and *C. albicans* occurs when coexisting together. This interaction has been considered a determinant in shaping biofilm formation, reducing the growth of *C. albicans* and influencing its virulence. The interaction is two-sided and might be reciprocal as both synergistic and antagonistic effects have been reported, *vide supra*. This project comprised studies that were conducted to build on the observations of colleagues (Alshanta *et al.*, 2022), and to explore further the interactions between *C. albicans* and different *E. faecalis* clinical isolates.

the most frequently isolated microorganisms in recurrent infections (Peciuliene *et al.*, 2001, Dumani *et al.*, 2012). *C. albicans* is well suited for survival in nutrient limited conditions, and *E. faecalis* possesses a similar capacity for starvation survival and growth (Richards *et al.*, 2010, Gao *et al.*, 2016).

Fungi and bacteria interkingdom interaction can significantly influence the virulence of a mixed-species biofilm. *C. albicans* can interact with different bacterial species that can either enhance or antagonise its virulence. This interaction can be physical or by quorum sensing molecules and other soluble mediators. For example, *S. gordonii* expresses surface antigen SspA and SspB to attach to mucosal surfaces but also to other microorganisms' surfaces. *C. albicans* uses this antigen to coaggregate with *S. gordonii* which allows proximal cell to cell communication via secreted signals (Bamford *et al.*, 2009). Another important example on interkingdom synergism is when *S. aureus* utilises hyphae specific ALS3 to bind to *C. albicans* and promote its colonisation of host tissues and biofilm formation (Peters *et al.*, 2012). In addition, farnesol a quorum sensing molecule produced by *C. albicans* can enhance *S. aureus* tolerance to antimicrobials by inducing the upregulation of efflux pump genes (Kong *et al.*, 2017). Moreover, the existence of *C. albicans* amongst oral bacteria has significantly enhanced its hyphal formation and virulence and upregulated genes involved in adherence and biofilm formation (Morse *et al.*, 2019).

In contrast, microbial interactions between *C. albicans* and bacterial species can be detrimental to the fungal organism. An example on the strong antagonistic relationship that exists between *C. albicans* and *P. aeruginosa* is that *P. aeruginosa* produces quorum sensing molecule that inhibits hyphal morphogenesis of *C. albicans* and prevents its growth. This molecule regulates *P. aeruginosa* adherence to *C. albicans* hyphae by triggering the synthesis of surface adherence proteins (Fourie *et al.*, 2016). Once adhered, quorum sensing system starts producing redox-active (oxidation-reduction) phenazines which generates ROS that can directly kill *C. albicans* cells. In doing so, *P. aeruginosa* weakens *C. albicans* cell wall integrity and stops hyphal morphogenesis. Moreover, farnesol produced by *C. albicans* prevents the formation of hyphae and thus provides protection against killing by *P. aeruginosa* (Hogan and Kolter, 2002, Fourie *et al.*, 2016).

It has been shown that *C. albicans* and *E. faecalis* have antagonistic relationship when they coexist together in mixed species biofilm (Alshanta *et al.*, 2022). One study isolated anti-Candida protein from *E. faecalis* strains and reported that this protein could inhibit the growth of many *C. albicans* strains including the multi resistant *C. albicans*; and it concluded that anti-Candida protein could be utilised in the treatment of candidiasis specially in the immunocompromised patients (Shekh and Roy, 2012). Moreover, it has been reported that *E. faecalis* bacteriocin, EntV, is necessary and sufficient for the reduction of *C. albicans* biofilm formation and virulence by inhibiting hyphal morphogenesis (Graham *et al.*, 2017b). Furthermore, a more recent study assessed the antifungal capability of heat-killed *E. faecalis* in oral candidiasis patients and showed that the bacterium significantly decreased the load of oral Candida in those patients by inhibiting mycelial growth (Yamazaki *et al.*, 2019). In addition, it has been demonstrated that the relationship of both microorganisms caused less pathology and mortality than either species alone; a finding that was attributed, in part, to an interkingdom signalling event by a bacterial-derived product that inhibited hyphal morphogenesis of *C. albicans* (Garsin and Lorenz, 2013). Indeed, nematodes treated with the bacteriocin peptide were completely resistant to killing by *C. albicans* (Graham *et al.*, 2017b). This killing resistance might indicate that a level of antagonism exists between the microorganisms.

On the contrary, a recent article of our research group evaluated the relevance of pH to dual-species biofilm interactions and demonstrated that *E. faecalis* rapidly and significantly impacted *C. albicans* morphogenesis and biofilm formation. These results suggested that the anti-Candida effect of *E. faecalis* is not completely based on a single mechanism but may rather involve various mechanisms, which collectively reflect the complexity of interactions between *C. albicans* and *E. faecalis* (Alshanta *et al.*, 2022).

The literature review reveals that interkingdom interaction between *E. faecalis* and *C. albicans* is a reality when coexisting together. This interaction has been considered a determinant factor in shaping biofilm formation, reducing the growth of *C. albicans* and influencing its virulence. The interaction is two-sided and might be reciprocal as both synergistic and antagonistic effects have been reported, *vide supra*. This project comprised studies that were conducted to build on the observations of colleagues (Alshanta *et al.*, 2022), and to explore further the interactions between *C. albicans* and different *E. faecalis* clinical isolates.

2.2 Hypotheses and Aims

Clinical isolates of *E. faecalis* can be characterised according to virulence. This virulence varies according to source of infection and niche inhabited. It is therefore hypothesised that virulence in *E. faecalis* species is strain-dependent and is influenced by oxygen tension level which varies according to anatomical location and pathological conditions in root canals. Moreover, it was hypothesised that *C. albicans* and *E. faecalis* has an antagonistic relationship when they exist together. This relationship depends on the anatomical location and the source of infection within the host. This antagonism may be manifested by virulence inhibition exerted by the actions of lactic acid producing *E. faecalis* on *C. albicans*. Based on this, it is hypothesised that a reciprocal alteration of virulence exists in both species and is demonstrated in morphology, viability, and biofilm formation at phenotypic and molecular levels.

The aims of this chapter are to :

- Characterise the virulence behaviour of twelve *E. faecalis* strains under different incubation conditions.
- Characterise biofilm forming ability of different *C. albicans* isolates.
- Characterise dual-species biofilm model phenotypically at different stages of biofilm formation.
- To assess virulence genes modulation of *C. albicans* and *E. faecalis* in dual-species biofilm at different stages of biofilm formation.

2.3 Materials and methods

2.3.1 Culture conditions and standardisation

C. albicans clinical isolates were obtained from an oral rinse from patients attending restorative clinics at Glasgow Dental Hospital and School for routine dental care, as previously described (Coco *et al.*, 2008a). The strains were revived from -80°C storage and sub-cultured on Sabouraud's dextrose agar (SAB (Sigma-Aldrich, Dorset, UK)) plates and maintained aerobically at 30°C for 48 hours. Afterwards, plates were kept at 4°C until required for experimental use. For growth in liquid media, an overnight culture was prepared in a sterile universal tube (Sterilin® Limited, Cambridge UK) by adding a 10 µL loopful of yeast colonies in 10 mL yeast peptone dextrose (1% w/v yeast extract, 2% w/v peptone, 2% w/v dextrose, 1.5% agar (YPD (Sigma-Aldrich, Dorset, UK)) and incubated at 30°C at 120 rpm in an orbital shaker (IKA KS 4000 i control, Berlin, Germany). After 18 hours, the yeast cells were pelleted by centrifugation at 3000rpm for 5 minutes, the supernatant was discarded and the pellet was washed twice with sterile phosphate buffered saline (10 mM phosphate buffer, 2.7 mM potassium chloride, 137 mM sodium chloride, pH 7.4) (PBS (Sigma-Aldrich, UK)) and resuspended in 10 mL of PBS. 100 times dilution of the cells was then obtained by adding 10 µL cell suspension to 990 µL PBS in a sterile 1.5 mL microcentrifuge tube and counted using a haemocytometer. The concentration of cells in the original suspension was calculated back according to the above dilution factor.

All *E. faecalis* strains were sub-cultured on Columbia blood agar (CBA (BA + 5% defibrinated horse blood (Fisher Chemicals, UK)) and plates were incubated at 37°C, 5% CO₂ for 48 hours. Afterwards, plates were kept at 4°C until required for experimental use. An overnight culture was then prepared in a sterile universal tube (Sterilin® Limited, Cambridge UK) by adding a 10 µL loopful of *E. faecalis* colonies in 10 mL Brain heart infusion (Fakruddin *et al.*) growth media ((BHI), Sigma-Aldrich, Dorset, UK) and incubated at 37° C, 5% CO₂. Cells then pelleted by centrifugation at 4400rpm for 5 minutes, washed twice with PBS and standardized using spectrophotometry at OD₆₀₀ nm of 0.3 to give a cell density of 1X10⁸ cells/mL. The full list of *C. albicans* and *E. faecalis* isolates are listed in **Error! Not a valid bookmark self-reference.**

Table 2.1: List of *C. albicans* and *E. faecalis* isolates

<i>C. albicans</i>		<i>E. faecalis</i>	
Name	Reference	Name	Reference
SC5314	(Fonzi and Irwin, 1993)	ATCC-29212	(Kim <i>et al.</i> , 2012)
3513A	Obtained from the National Collection of Pathogenic Fungi (NCPF, Bristol, UK)	NCTCC 5957	National Collection of Type Cultures, Public Health Laboratory Service (www.phe-culturecollections.org.uk).
BC020	(Coco <i>et al.</i> , 2008b)	E1	(Johnson <i>et al.</i> , 2006, Sedgley <i>et al.</i> , 2004)
BC146	(Coco <i>et al.</i> , 2008b)	E2	(Johnson <i>et al.</i> , 2006, Sedgley <i>et al.</i> , 2004)
BC023	(Coco <i>et al.</i> , 2008b)	E3	(Johnson <i>et al.</i> , 2006, Sedgley <i>et al.</i> , 2004)
BC145	(Coco <i>et al.</i> , 2008b)	ER5/1	(Johnson <i>et al.</i> , 2006)
BC037	(Coco <i>et al.</i> , 2008b)	ER35	GDS culture collection
BC136	(Coco <i>et al.</i> , 2008b)	OS-16	(Sedgley <i>et al.</i> , 2005b)
BC038	(Coco <i>et al.</i> , 2008b)	V583	(Sahm <i>et al.</i> , 1989)
BC117	(Coco <i>et al.</i> , 2008b)	OGX-1	(Didem <i>et al.</i> , 2021)
BC039	(Coco <i>et al.</i> , 2008b)	J 42-7	GDS culture collection
BC040	(Coco <i>et al.</i> , 2008b)	AA-OR 34	(Sedgley <i>et al.</i> , 2006)

2.3.2 *E. faecalis* standardisation using serial dilution and standard curve

To assess the number of *E. faecalis* ATCC29212, a suspension of McFarland standard OD₆₀₀ 0.3, overnight broth was washed twice with PBS. Cells suspended in PBS were adjusted to an optical density (OD₆₀₀) of 0.1, 0.2, 0.3, 0.4. Appropriate agar plates (CBA+ 5% horse blood) were prepared in advance and ensured to be dry before use to reduce spreading of liquid over the agar. The adjusted cell suspension of each OD was serially diluted 10-fold in PBS from neat to 10⁶ within microcentrifuge tubes and 100 µL of 10⁻⁴, 10⁻⁵, 10⁻⁶ dilutions was spread on CBA

plates. Plates were then incubated at 37°C, 5% CO₂ for 24 h after which the number of CFUs/mL was counted. Standard curve created using GraphPad Prism (version 9.3.1) and the corresponding number of CFUs/ml for each OD₆₀₀ was determined.

2.3.3 Haemolysis assay

2.3.3.1 Plate method

A single *E. faecalis* colony was taken from a stock plate and streaked onto a fresh 5% CBA plate under aseptic conditions. Plates were incubated under three different conditions for 24 hours: aerobically, 5% CO₂ and anaerobically. After retrieving the plates from incubators, plates were checked for signs of haemolysis which was a clearance halo surrounding *E. faecalis* colonies.

2.3.3.2 Quantitative haemolysis assay

A single *E. faecalis* colony was taken from a stock plate and streaked onto a fresh CBA plate under aseptic conditions. Plates were incubated under three different conditions; aerobically, 5% CO₂ and anaerobically for 24h. Plates with no culture were incubated in parallel to act as a positive control (PC). After retrieving the plates from the incubators. A total of two extracts from the blood agar plate were taken aseptically from zones of haemolysis, removed as plugs using the widest ends of a sterile 250 µL tip. Two extracts were also taken from control plates. These plugs were suspended in 1 mL of PBS and freeze-thawed between room temperature and -20°C for a total of three cycles. The agar was pelleted by centrifugation (13,000 x g for 10 minutes at room temperature), yielding a haemoglobin-containing supernatant, which was analysed spectroscopically according to (Brown *et al.*, 2018). Supernatants of 100 µL were transferred into a 96 well plate and absorbance was measured at 410nm wavelength, the maximum spectra peak for haemoglobin. The percentage of haemolysis was calculated as follows:

$$\% \text{ haemolysis} = (\text{OD test} / \text{OD PC}) \times 100\%$$

2.3.4 Gelatinase assay

2.3.4.1 Plate method

An *E. faecalis* colony was taken from the single colony plate and streaked onto 3% gelatine Todd-Hewitt Agar ((THA), Merck UK) plates under aseptic conditions. Plates were incubated under three different conditions: aerobic, 5% CO₂ and anaerobically for 24 hours. Plates were retrieved out of the incubator and inspected for an opaque halo surrounding the colonies indicating the presence of gelatinase activity.

2.3.4.2 Quantitative gelatinase assay

A single *E. faecalis* colony was taken from the stock plate and used to inoculate 10 mL of BHI broth and incubated in CO₂ incubator at 37°C overnight. The suspension of *E. faecalis* was then washed 2 times with PBS and diluted in PBS to achieve an OD of 0.3 which gives a suspension of 1X10⁸ CFU. Sterile disks (Watman international, Maidstone, UK) were loaded with 15 µL of each *E. faecalis* suspension and the disks were aseptically applied on to a 3% gelatine THA plate. Plates were placed in an O₂ incubator at 37°C, 5% CO₂ incubator at 37°C or in the anaerobic cabinet at 37°C for 24 hours. The diameter of the opaque halo produced was measured according to standard methodologies (Pires-Boucas *et al.*, 2010, Janda *et al.*, 1980). Relative enzyme activity was calculated as the ratio of the big diameter of the halo surrounding the disc (R) to the small diameter of the halo (r).

2.3.5 Metabolic activity assay

E. faecalis strains were standardised to the desired cellular density of 1X10⁷ cells/mL into BHI medium and the biofilms formed onto pre-sterilised, polystyrene, 96-well flat-bottom microtiter plates. The plates were incubated at 37°C for 24 h. After incubation, the biofilms were washed once with 200 µL with PBS to remove the loosely attached cells using a multi-channel pipette. Biofilms were analysed for metabolic activity using AlamarBlue™ cell viability dye (Invitrogen, UK) (Yajko *et al.*, 1995). After treatment and neutralisation, AlamarBlue™ was added at 1:10 dilution with growth media, then 200 µL were

added to each well in dark conditions. Plates were then incubated at 37°C 5% CO₂, a change from blue to pink indicates a reduction in the fluorogenic dye resazurin to resorufin by reductase enzymes in normal cellular respiration. The colour change was read when the growth control reached a sufficient pink to allow this to be used as a 100% viability control or max 3 hours, depending on which occurred first. 100 µL from each well was transferred to a fresh 96 well flat bottom microtiter plate and top read using fluorescence 530/590nm (FLOUstar™, BMG lab tech, UK). A negative sterility control was used on the same plate whereby no biofilm growth was evident to use as a blank to normalise the fluorescence by taking the average of this value.

2.3.6 Biofilm biomass assay

Biofilm biomass of all strains was quantified using the crystal violet (CV) assay (Jose *et al.*, 2010) after they were grown as in 0. A stock solution of 1% CV (Sigma-Aldrich, UK) was made using ddH₂O and diluted to 0.05% for use. 100 µL of 0.05% CV solution was added to each well and incubated at room temperature for 20 minutes. CV was then removed by multichannel pipette, and biofilms gently washed twice with multichannel pipette using ddH₂O removing excess dye. 100 µL of 100% ethanol was used to de-stain the biofilm, this was mixed well with a pipette five times and 75 µL transferred to a fresh flat bottom microtiter plate for measurement. Biomass was quantified by reading absorbance at 570nm (FLOUstar™, BMG lab tech, UK). A negative sterility control was used on the same plate whereby no biofilm growth was evident to use as a blank to normalise the absorbance by taking the average of this value.

2.3.7 Adherence assay

Adherence to Collagen I was tested using a previously described method with some modifications (Xiao *et al.*, 1998). A single *E. faecalis* colony was taken from the stock plate for each strain and used to inoculate 10 mL of BHI broth and incubated in CO₂ incubator at 37°C overnight. The suspension of *E. faecalis* was then washed twice with PBS and diluted in PBS to achieve an OD₆₀₀ of 0.3 which gives a suspension of 1x10⁸ CFU/mL. The cultures were centrifuged at 4400 rpm for 10 minutes. The cell pellets were resuspended in 0.1% Tween® 80 (Sigma-Aldrich, UK)

-0.1% bovine serum albumin (BSA) (source) in PBS. Collagen I solution (Sigma-Aldrich, Dorset, UK), contained 20 µg of ECM per mL of PBS. A 50 µL ECM solution was added to a 96-well Nunc™ Maxisorp® flat-bottomed high affinity protein binding microtiter plates (Fisher Scientific, Loughborough, UK) to coat the surface with ECM, and the microtiter plates were incubated at 4°C overnight. After decanting, the wells were blocked with 200 µL of 0.2% BSA in PBS at 4°C for 2 hours and then washed with PBS three times. A total volume of 50 µL of bacteria was added to each well and incubated at room temperature for 2 hours adherence with gentle shaking at 70 rpm. The wells were washed with 0.1% Tween® 80 -0.1% BSA in PBS three times to remove supernatants. Each well was treated with 50 µL of trypsin, and the bacterial cells were suspended by vigorous pipetting. Plates were examined under the microscope to ensure removal of *E. faecalis* adherent cells. Serial dilutions of suspended bacteria were plated on CBA plates. Adhesion data were expressed as percentages calculated from three independent experiments, as follows: $100 \times (\text{number of adhering bacteria} / \text{number of bacteria inoculated})$. Isolates were considered to adhere to ECM proteins if >5% of total inoculated cells bound to the well.

2.3.8 Assessment of *C. albicans* phenotypic characteristics when cocultured with *E. faecalis*

For phenotypic evaluation, *C. albicans* SC5314 and *E. faecalis* ER5/1 high virulent strain (HVS) and *E. faecalis* E2 low virulent strain (LVS) were standardized to 1×10^6 cells/mL for *C. albicans* and 1×10^7 cells/mL for *E. faecalis* in Todd-Hewitt broth (THB) (Merck UK) supplemented with 10mM menadione and 10mg/mL hemin. These were subsequently mixed 1:1 v/v with Roswell Park Memorial Institute (RPMI-1640) (Sigma-Aldrich, Dorset, UK), a medium which has been shown to support the coculture of *C. albicans* and bacterial species (Montelongo-Jauregui *et al.*, 2016). Mono-cultures of *C. albicans* and cocultures of *C. albicans* with *E. faecalis* were created in a 24 well microtiter plates (Corning Incorporated, Corning, NY, USA) for 4, 6, 8 and 24h in 5% CO₂ at 37°C. After incubation, biofilms were washed with PBS and were then imaged using EVOS FL Cell Imaging system (Thermo Fisher Scientific, Waltham, MA, USA).

2.3.9 Metabolic activity and biofilm biomass assessment of single and dual-species biofilm

Single and dual-species biofilms of *C. albicans* (SC5314) and *E. faecalis* HVS and LVS were prepared as described in 0. For metabolic activity assessment, biofilms were washed twice with 500 μ L of PBS to remove non adherent cells. Immediately after washing, the XTT (2,3-bis(2-methoxy-4-nitro-5-sulfophenyl)-2H-tetrazolium-5-carboxanilide salt) (Sigma-Aldrich, UK) metabolic reduction assay was used to assess cell viability (Pierce *et al.*, 2008). Briefly, XTT was prepared as a solution of 0.25 g/L in ddH₂O. The solution was then filtered through a 0.22 μ m filter, aliquoted and stored at -80°C. Prior to use, XTT was thawed and menadione ((Sigma-Aldrich, Dorset, UK), 10 mM prepared in acetone) added to a final concentration of 1 μ M. A 100 μ L aliquot of the XTT/menadione solution was subsequently added to each pre-washed biofilm, and to control wells (for measurement of background XTT-reduction levels). Plates were then incubated in the dark for 2 hours at 37°C. A colorimetric change in the XTT reduction assay, representing a direct correlation of metabolic activity of the biofilm, was then measured at 492 nm in a microtitre plate reader (FluoStar Omega, BMG Labtech, Aylesbury, Buckinghamshire, UK). A negative sterility control was used on the same plate whereby no biofilm growth was evident to use as a blank to normalise the fluorescence by taking the average of this value.

The biomass of the biofilms was quantified using CV stain. After metabolic assessment the remaining cell volume was discarded by inverting quickly to remove solution and wells were then washed once with PBS and airdried overnight at room temperature. The staining procedure was as described in section 2.3.6.

2.3.10 Microbial load assessment using quantitative PCR

Mono- and dual-species biofilms of *C. albicans* SC5314 and *E. faecalis* ER5/1 and E2 were grown as described above in 6 well microtiter plates for 4, 6, 8 and 24h in 5% CO₂ at 37°C. Biofilms were then removed by scraping into 1mL of PBS before DNA extraction using QIAamp DNA mini kit, as per manufacturer's instructions (Qiagen, Crawley, UK). For qPCR, in one sample, 1 μ L of extracted DNA was added to a MicroAmp™ optical 96-well PCR plate (ThermoFisher, UK) and 19 μ L of a

mastermix containing 10 μ L Fast SYBR GreenER™ (Thermo Fisher Scientific, Paisley, UK), 7 μ L ultraviolet (UV)-treated RNase-free water and 1 μ L each of a 10 μ M forward and reverse primers for each species. Standard curves for each strain were also included. The used thermal cycles were 50°C for 2 min, 95°C for 2 min, 40 cycles of 95°C for 3 s and 60°C for 30 seconds using Step-One plus real time PCR machine and StepOne software V2.3 (Life Technologies, Paisley, UK). Colony forming equivalents (CFE) was calculated in relation to each species standard curve, as previously described (O'Donnell *et al.*, 2016). Data obtained is from triplicates from three independent experiments.

2.3.11 Transcriptional analysis of virulence related genes in *C. albicans* and *E. faecalis*

2.3.11.1 RNA extraction from *in vitro* biofilms

For assessment of *C. albicans* related genes, biofilms of *C. albicans* SC5314, *E. faecalis* ER5/1 alone or in coculture were developed for 30, 60 and 120 minutes, 4 and 24 hours. Biofilms of *C. albicans* SC5314, *E. faecalis* E2 alone or in coculture were developed for for 4 and 24 hours. Biofilms were grown in T75 cell culture flasks in THB:RPMI and incubated in 5% CO₂ at 37°C. Following incubation, supernatants were discarded, and biofilms were carefully washed with PBS. One mL of PBS was added to each flask and biofilm was scraped and kept in sterile 1.5 mL microcentrifuge tube. Cells were centrifuged at 13,000 rpm for 10 minutes (Hettich, Germany) and supernatant discarded. One mL of TRIzol™ solution (Invitrogen, Paisley, UK) was added to each 1.5 mL microcentrifuge tube containing cell pellet. The resulting biomass was transferred to an O-ring screw-cap microcentrifuge tube (Stratech, Newmarket, UK) and approximately 250 μ L of 0.5 mm diameter sterile glass microbeads (BioSpec, Bartlesville, Oklahoma, USA) were added to each tube and placed on ice. Cells within the TRIzol™ solution were mechanically disrupted in the bead beater using a BeadBug™ 3 Position Bead Homogenizer (Benchmark scientific, USA) at 350 rpm for 3 cycles of 30 seconds. Samples were placed on ice in between each cycle and 100 μ L of 1-bromo-3-chloropropane (Sigma-Aldrich, Dorset, UK) was added to each sample before they were vortexed for 30 seconds. Samples were left at room temperature for 5 minutes, with occasional inversion, before centrifuged at 13,000 rpm for 15

minutes at 4 °C and then placed on ice. The upper aqueous layer of each sample was transferred to a sterile microfuge tube and 500 µL of ice-cold isopropanol was added to precipitate the RNA. The solution was placed at -20 °C overnight to maximise precipitation of RNA.

Following overnight precipitation, all samples were centrifuged for 10 minutes at 10,000 rpm at 4 °C. The supernatant was discarded, and the remaining pellet washed with 500 µL of ice cold 70% ethanol. Samples were inverted 40 times then centrifuged at 10,000 rpm for 5 minutes at 4 °C. The ethanol was carefully removed, and samples were air dried for 30 minutes. The RNA was finally resuspended in 25 µL of RNase free distilled water and incubated at 65 °C in a heat block (Techne, Staffordshire, UK) for 5 minutes to aid the recovery of RNA.

2.3.11.1 DNase digestion of total RNA

To ensure the extracted RNA was free from DNA contamination, a DNase digestion kit was used, as per manufacturer's instructions (Qiagen Ltd, Crawley, West Sussex, UK). Briefly, 10 µL of RDD buffer was mixed with 10 µL of DNase before being added to the extracted RNA. Finally, 55 µL of RNase-free distilled water was added to the reaction to make a final volume of 100 µL and samples were incubated at room temperature for 20 min. The RNA was quantified using a NanoDrop™ spectrophotometer (Labtech, UK). 1 µL of elute was used and samples with a 260/280nm ratio of between ≥ 1.8 and ≤ 2.2 were deemed of high enough quality to be used for RT-qPCR.

2.3.11.2 cDNA synthesis from total RNA

RNA concentrations were standardised, and complementary DNA (cDNA) was synthesised using High-Capacity cDNA™ reverse transcription (RT) kit (Fisher Scientific, Loughborough, UK). 2 x RT master mix were prepared for each sample according to manufacturer's instructions (Table 2.2). A negative control (-CT) which did not contain the reverse transcriptase enzyme to detect genomic DNA contamination was included. For each reverse transcription reaction, a mixture of 10 µL RT master mix and 10 µL RNA sample were mixed, sealed, and briefly centrifuged to eliminate air bubbles. Finally, samples were loaded into a MWG-

Biotech Primus 96 plus thermal cycler to generate cDNA under the following thermal cycling conditions: 25°C for 10 minutes, 37°C for 120 minutes, and finally, 85°C for 5 minutes. Samples were stored at - 20°C for long term storage or processed for PCR analysis immediately

Table 2.2: Volumes used from each component to prepare the master mix for the cDNA.

Component	Volume/ Reaction (µL)	
	-CT	+CT
10× RT Buffer	2	2
20x dNTP Mix (100mM)	0.8	0.8
10x RT random primers	2	2
MultiScribe™ reverse transcriptase	-	1
Nuclease-free H ₂ O	5.2	4.2
Total master mix/ reaction (µl)	10	10

2.3.11.3 Assessing gene expression using real time PCR

The level of expression of the genes of interest within the samples, were calculated all relative to the standard housekeeping gene ACT1 in *C. albicans* gene expression analysis and DDL in *E. faecalis* gene expression analysis. For qPCR, a mastermix containing Fast SYBR GreenER™ (Thermo Fisher Scientific, Paisley, UK), forward/reverse primers (Table 2.3), and UV treated RNase-free water was prepared, to which extracted DNA was added. The used thermal cycles were 50°C for 2 minutes, 95°C for 2 minutes, 40 cycles of 95°C for 3 seconds and 60°C for 30 seconds using Step-One plus real time PCR machine and StepOne software V2.3 (Life Technologies, Paisley, UK). No RT and no template controls were also included. Each parameter was analysed in duplicate. Expression of the genes of interest were normalised to the housekeeping ACT1 and relative expression quantified using the $2^{-\Delta\Delta Ct}$ method (O'Donnell *et al.*, 2016). Data obtained is from triplicates from three independent experiments.

Table 2.3: List of primers used in this chapter

Primer	Gene name	Sequence (5'– 3')	Function
<i>C. albicans</i>	18S region	F- CTCGTAGTTGAACCTTGGGC	For <i>C. albicans</i> quantification
		R - GGCCTGCTTTGAACACTCTA	
	ACT1	F - AAGAATTGATTTGGCTGGTAGAGA	Housekeeping
		R - TGGCAGAAGATTGAGAAGAAGTTT	
	HWP1	F - GCTCAACTTATTGCTATCGCTTATTACA	Hyphal wall protein
		R - GACCGTCTACCTGTGGGACAGT	
	ALS3	F - CAACTTGGGTTATTGAAACAAAACA	Adhesion
		R - AGAAACAGAAACCAAGAACAACCT	
	ECE1	F - GCTGGTATCATTGCTGATAT	Hyphae specific protein
		R - TTCGATGGATTGTTGAACAC	
	SAP2	F - GAATTAAGAATTAGTTTGGGTTTCAGTTGA	Secreted aspartyl protease
		R - CCACAAGAACATCGACATTATCAGT	
SAP5	F - CCAGCATCTTCCCGCACTT	Secreted aspartyl protease	
	R - GCGTAAGAACCGTCACCATATTTAA		
BCR1	F - ATTGCCACCAATACCTGCTC	Transcription factor	
	R - GGCTGTCCATGTTGTTGTTG		
EFG1	F - CCAGTGGTGGCAGTAATGTG	Transcription factor	
	R - CAGTGGCAGCCTTGGTATTT		
<i>E. faecalis</i>	16S region	F - CGCTAGTAATCGTGGATCAGAATG	For <i>E. faecalis</i> quantification
		R - TGTGACGGGCGGTGTA	
	ddl	F - CAACTG TTGGCATTCCACAA	housekeeping
		R - TGGATTTCTTTCCAGTC ACTTC	
	entV	F - AGCTGCACAAAAGAAAGCCTG	Secreted bacteriocin
		R- GCTTAGCCCACATTGAACTGC	
	gelE	F- ACCCCGTATCATTGGTTT	Gelatinase enzyme
		R- ACGCATTGCTTTTCCATC	
	esp	F- TGGTGATGGAAACCCTGACG	Surface protein
		R- GTTGCCTTTGTGACCTGTT	
	cyl	F- CCGCAGGAGGATATGGTGAC	Cytolysin
		R- AGCAGCTTTGCCTAGTGGAG	

2.3.12 Statistical Analysis

Graph production, data distribution and statistical analysis were performed using GraphPad Prism (Version 9.3.1; La Jolla, CA, USA). One-way Analysis of Variance (ANOVA) or non-parametric Kruskal-Wallis were used to investigate significant differences between independent groups of data. A Dunnett's and Dunn's post-comparison test was applied to the p value to account for multiple comparisons of smaller datasets. Statistical significance was $P < 0.05$. Two-way ANOVA was used to assess significance between treatment group samples under different conditions with Tukey multiple comparison test was used for tests with more parameters.

2.4 Results

2.4.1 *E. faecalis* virulence characterisation.

In the following sections twelve strains of *E. faecalis* were characterised - 10 clinical isolates and two laboratory strains listed in Table 2.1. First, a series of phenotypic assays were carried out under different incubation conditions to determine the virulence of *E. faecalis* strains using standardised cultures. These tests were haemolysis, gelatinase, metabolic activity, biofilm biomass and adhesion to collagen type I. Then, based on their results a HVS and a LVS were selected to be used in subsequent experiments.

2.4.2 *E. faecalis* standardisation

Using serial dilutions and standard curve, the number of *E. faecalis* colonies in a McFarland standard of OD₆₀₀ 0.3 was determined. Results showed that at OD 0.3, an *E. faecalis* suspension has approximately 1×10^8 colonies per mL (Figure 2.1)

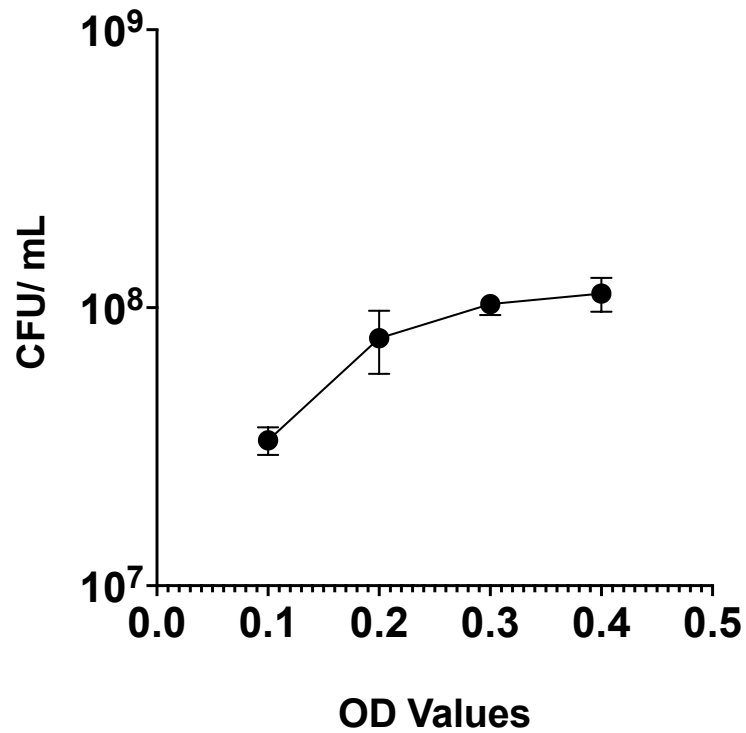


Figure 2.1: Standardization of *E. faecalis* ATCC 29212. Miles and Misra technique was done to determine the number of *E. faecalis* colonies at McFarland Standard OD_{600} 0.3. Data plotted represents mean \pm SD, performed in triplicate from three independent experiments.

2.4.2.1 Identification of haemolysis phenotypes for *E. faecalis* strains under different incubation conditions.

The twelve strains of *E. faecalis* were cultured on CBA plates and incubated under 3 different conditions: aerobic, 5% CO₂ and anaerobic for 24 hours. Only two laboratory strains had positive haemolysin activity under all incubation conditions (Figure 2.2). Results also showed variability in haemolytic activity among *E. faecalis* strains. This variability was most pronounced in CO₂ incubation conditions; The lab strain ATCC 29212 haemolytic activity was significantly higher than the other strains (ER35 $p < 0.05$, ER5/1, E3, OS-16 $p < 0.01$, OGX, J42-17, V583, E1, $p < 0.001$, E2, AAOR34 $p < 0.0001$) except for NCTCC5947. Under anaerobic conditions, all strains showed increased haemolytic activity compared to aerobic and CO₂ incubation conditions (Figure 2.3: A-C). In summary, it was observed that haemolytic activity of *E. faecalis* strains was variable among incubation conditions. The level of haemolytic activity was increased significantly as conditions were more anaerobic compared to CO₂ and aerobic conditions ($p < 0.0001$) (Figure 2.3: D)

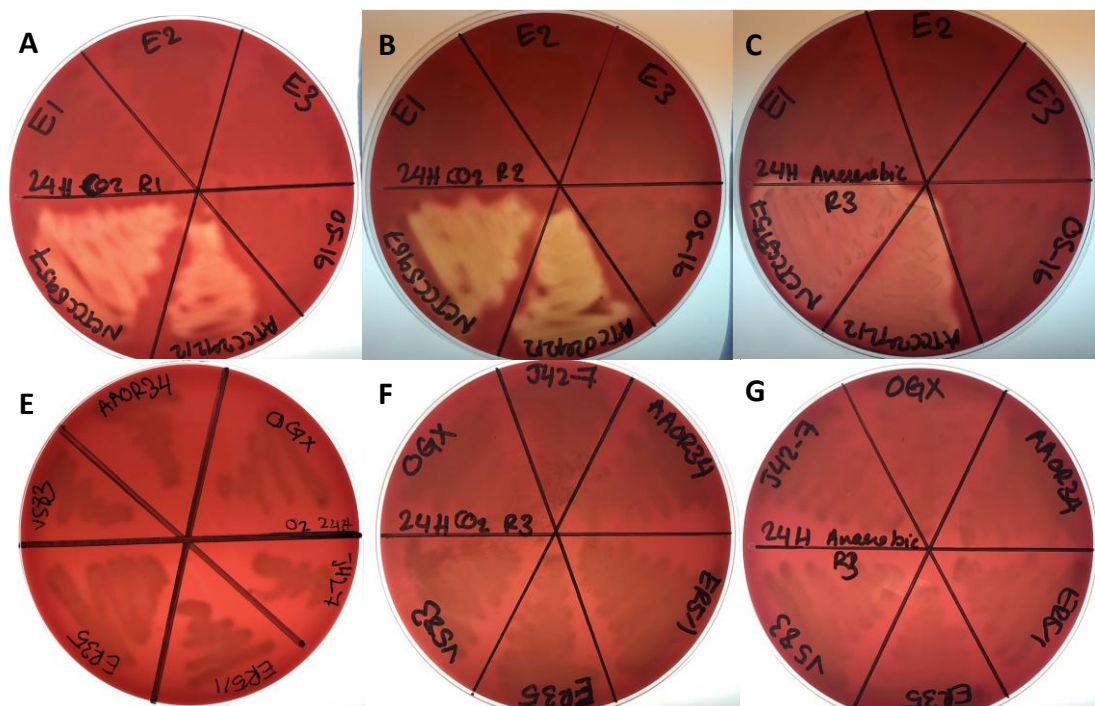


Figure 2.2: Haemolytic phenotypes identified among *E. faecalis* isolates under different incubation conditions for 24 hours. A-C: shows the two lab strains (ATCC 29212, NCTCC 5957) with haemolytic activity described by a clear halo around *E. faecalis* colonies which was increased under anaerobic conditions. E1, E2, E3, OS-16 did not show any signs of haemolytic activity under O₂, CO₂ and anaerobic condition. E-G: OGX, J42-7, AAOR34, ER5/1, ER35, V583 showed non-haemolytic activity under O₂, CO₂ and anaerobic conditions.

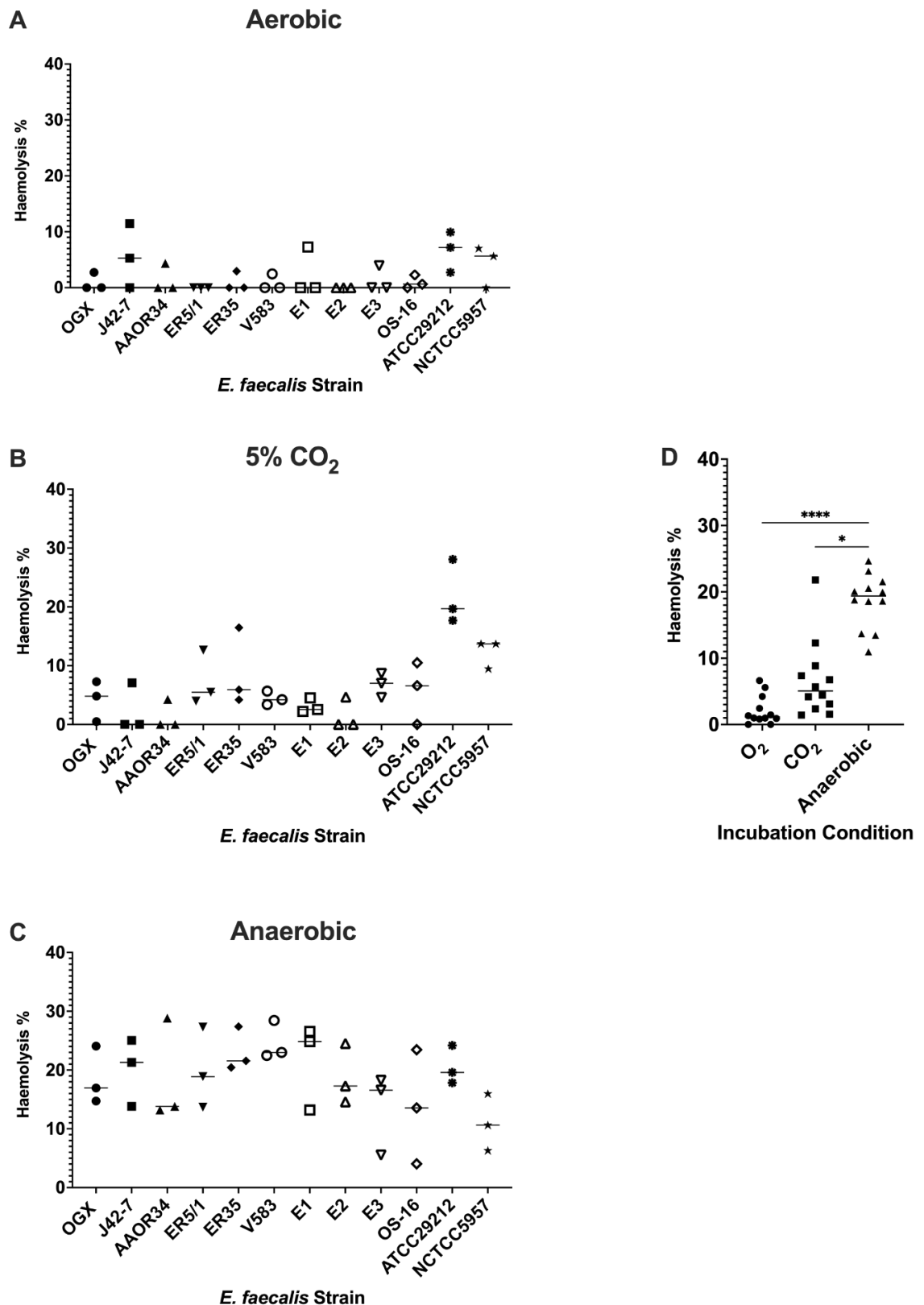


Figure 2.3: Quantitative haemolysis analysis of *E. faecalis* strains under different incubation conditions for 24h. Heterogeneity in expressing haemolytic activity amongst *E. faecalis* strains for 24h under (A) aerobic condition (B) 5% CO₂ condition (C) Anaerobic condition. Significant difference was found between each incubation conditions at 24H (D). Statistical analysis was done using one-way ANOVA with Tukey's multiple comparison post-test (* P<0.05, **P<0.01, ***P<0.001 ****P<0.0001). Data represents mean ± SD, performed in triplicate from three independent experiments.

2.4.2.2 Identification of gelatinase activity among *E. faecalis* strains under different incubation conditions.

Twelve *E. faecalis* strains were screened for the presence/ absence of gelatinase enzyme under different incubation conditions by streaking *E. faecalis* colonies on 3% TSA plates. Amongst the twelve strains, only three produced gelatinase. E1, ER5/1 and V583 strains demonstrated gelatinase activity as it was evident on agar plates by showing an opaque halo surrounding *E. faecalis* colonies (Figure 2.4: A-F, Figure 2.5: A). The gelatinase enzyme activity was significantly reduced when plates were incubated under anaerobic conditions (Figure 2.5: D). This was observed by measuring the zones of enzymatic activity around the discs of *E. faecalis* (Figure 2.5: A, B).

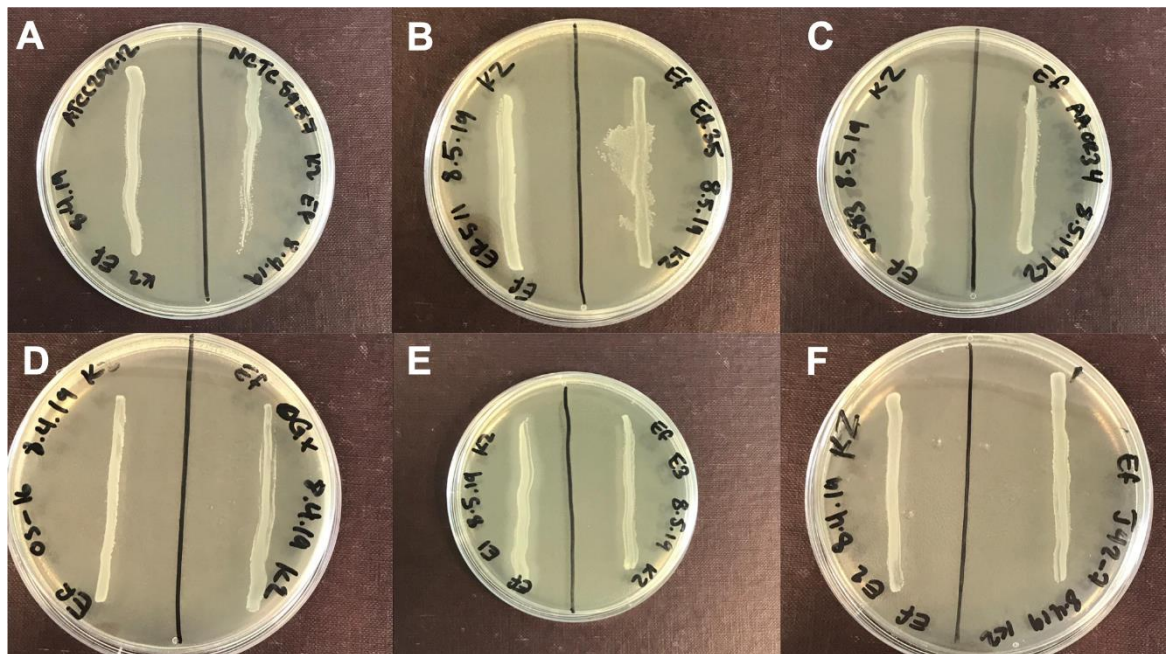


Figure 2.4: Gelatinase enzyme identification in *E. faecalis* strains. A: No opaque halo was found surrounding ATCC29212 and NCTC5957. B: Opaque halo surrounding ER5/1 colonies but not ER35. C: opaque halo surrounding V583 *E. faecalis* colonies but not AAOR34. D: No opaque halo was found surrounding OS-16 and OGX. E: Opaque halo was found surrounding E1 colonies but not E3. F: No opaque halo was found surrounding E2 and J42-7 *E. faecalis* colonies.

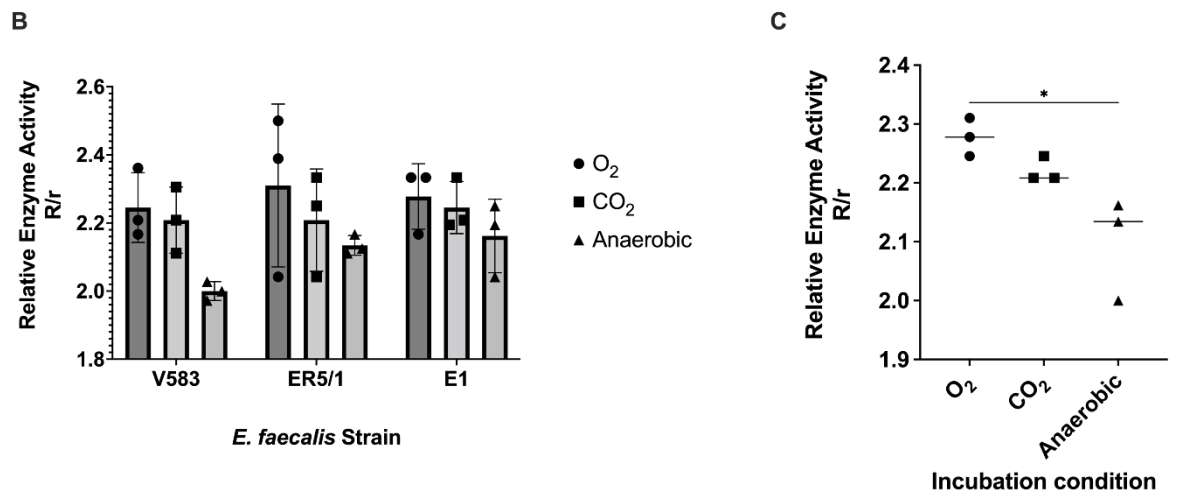
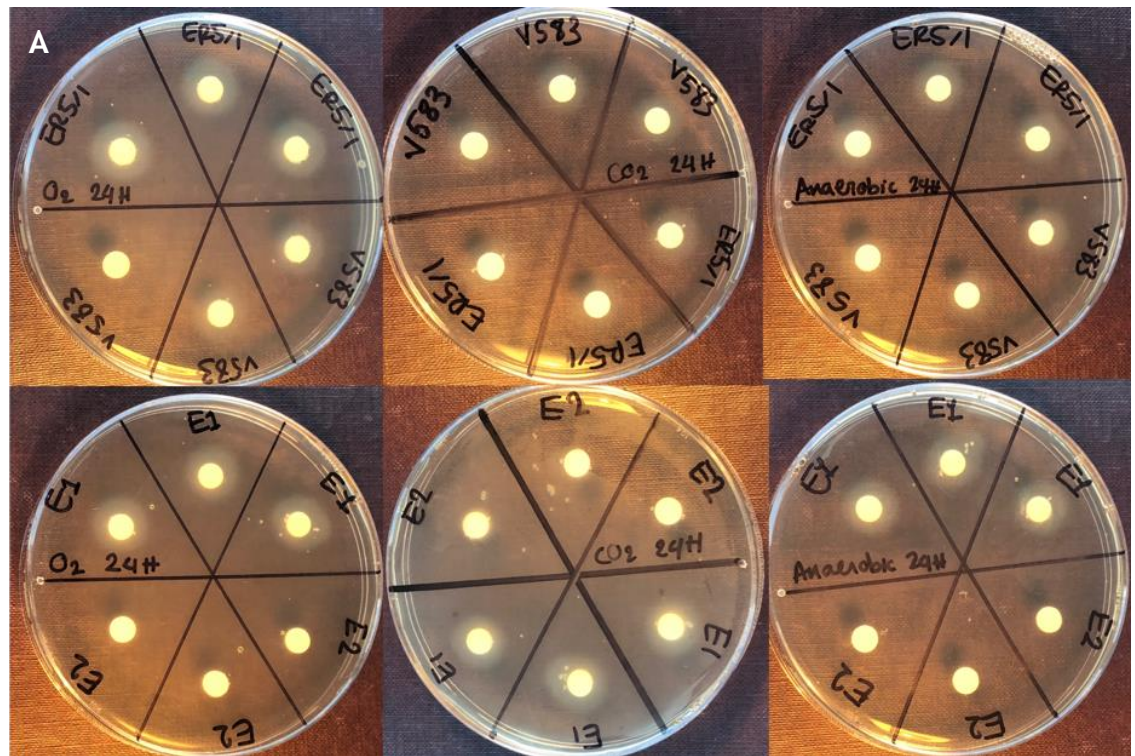


Figure 2.5: Quantitative identification of gelatinase enzyme activity in *E. faecalis* strains. Sterile discs were loaded with *E. faecalis* suspension and incubated in 3% THA plates. A: A halo was produced around discs. (B+C) the relative enzymatic activity was measured by dividing the largest diameter (R) by the smallest diameter (r) surrounding the disc. Statistical analysis was done using one-way ANOVA. (* P<0.01) with Tukey's multiple comparison post-test to assess difference between incubation conditions and two-way ANOVA to assess difference between strain types and incubation conditions variables. Data represents mean \pm SD, performed in triplicate from three independent experiments.

2.4.2.3 Biofilm metabolic activity and biomass assessment of *E. faecalis* strains under different incubation conditions

The metabolic activity of the various *E. faecalis* isolates were compared under different atmospheric conditions. *E. faecalis* strains showed slight variability in metabolic activity under O₂ and anaerobic conditions although it was not statistically significant (Figure 2.6: A,C). Under CO₂ conditions, J42-7, AAOR34, ER5/1, E2, E3 metabolic activity was significantly higher than OGX ($p < 0.01$) in addition to V583, E1, OS-16, ATCC 29212 and NCTCC 5957 ($p < 0.001$) (Figure 2.6: B). Moreover, *E. faecalis* strains metabolic activity did not differ between incubation conditions (Figure 2.6: B).

0.77) or greater than the third quartile (Q3 $OD_{570} = 1.16$), respectively. Those isolates in between the first and third quartile (Q1-Q3) were defined with intermediate biofilm formation (IBF). This heterogeneity in biofilm formation among strains were not significant when plates incubated under CO₂ conditions (Figure 2.7: B). However, under aerobic conditions (Figure 2.7: A), strain J42-7 was significantly lower than strain AAOR34 ($p < 0.05$) which proved to be a HBF strain in all incubation conditions. Under anaerobic conditions, the variation among strains increased. AAOR34 ($p < 0.0001$), ER35 ($p < 0.001$), E2 ($p < 0.01$) and OS-16 ($p < 0.05$) biofilm biomass was significantly higher than J42-7. In addition, AAOR34 ($p < 0.001$), ER35 ($p < 0.01$), E2 ($p < 0.01$) and OS-16 ($p < 0.05$) biofilm biomass was also significantly higher than OGX (Figure 2.7: C). The incubation condition affected the ability of *E. faecalis* to produce biofilm, 5% CO₂ showed the highest biofilm formation in *E. faecalis* strains (Figure 2.7: D).

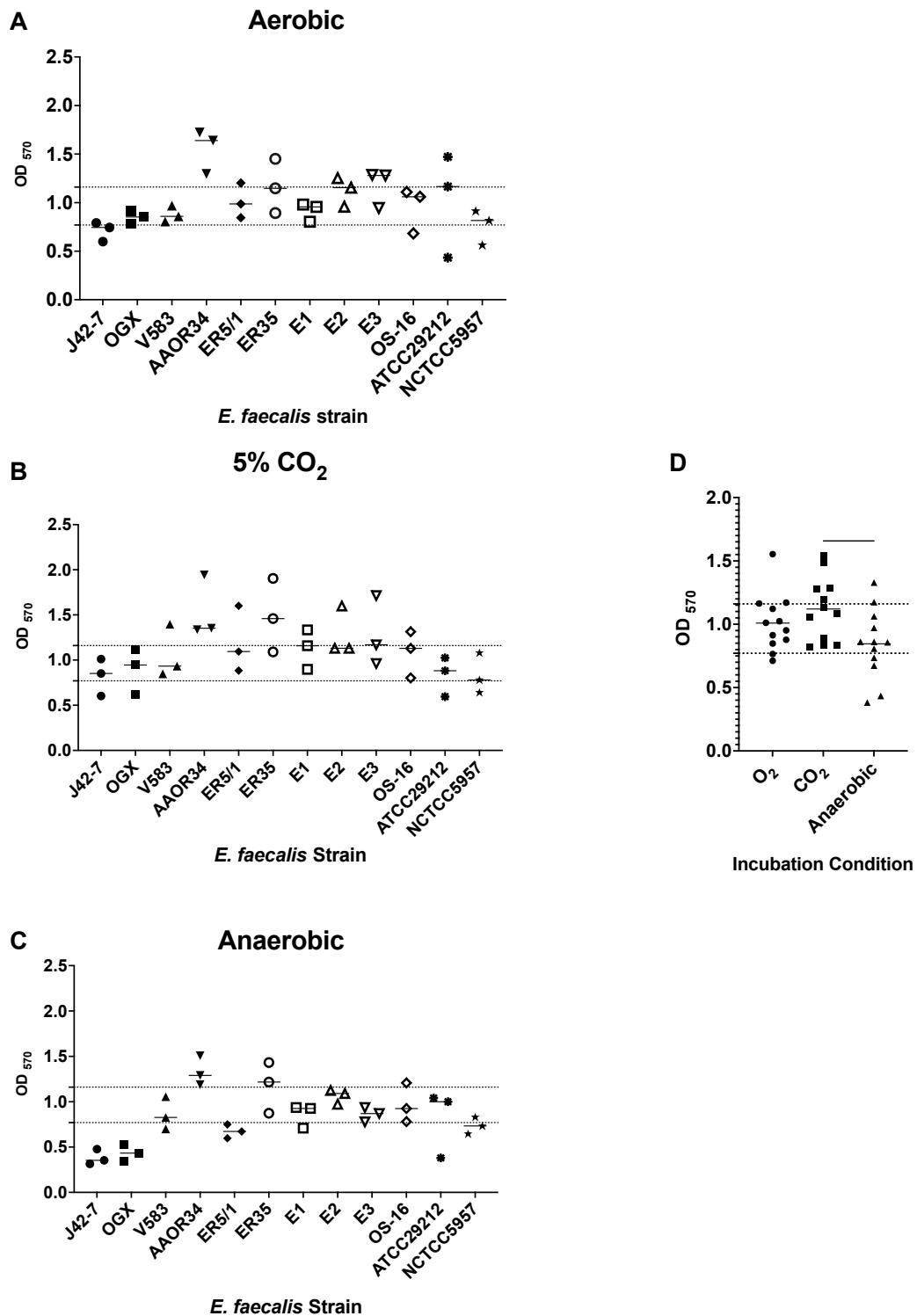


Figure 2.7: Quantification of biofilm biomass of *E. faecalis* strains. After assessment of metabolic activity, biofilms were left to dry overnight, and CV staining used to measure differences in biofilm biomass formation among *E. faecalis* strains under oxygenated conditions (A) 5% CO₂ (B) and anaerobic conditions (C). Growing biofilms under 5% CO₂ showed the highest biofilm biomass in *E. faecalis* strains (D). Statistical analysis was done using one-way ANOVA with Tukey's multiple comparison post-test and Kruskal-Wallis test and Dunn's multiple comparison post-test (* P<0.01, ** P<0.01, ***P<0.001). Data represents mean ± SD, performed in triplicate from three independent experiments.

2.4.2.4 Adhesion to collagen assessment for *E. faecalis* strains under different incubation conditions

To assess the adhesion potential of *E. faecalis*, wells of a high affinity 96 well plates with Collagen type 1 was coated. Collagen type 1 was chosen because it is the major protein of intertubular dentine (90%) (Goldberg *et al.*, 2011). *E. faecalis* cells showed the lowest adhesion to collagen I ECM protein under aerobic conditions. except for the lab strain NCTCC 5957 which showed the highest adhesion compared to other strains ($p < 0.0001$) (Figure 2.8: A). Under CO₂ incubation condition, higher variability amongst *E. faecalis* strains adhesion was observed. E1 showed increased adhesion compared to V583 ($p < 0.05$), ER35 showed higher adhesion percentage compared to E2, E3 ($p < 0.05$), OGX also showed increased adhesion compared to E2, E3, V583, AAOR34 ($p < 0.0001$), ER5/1 ($p < 0.001$), J42-7 (p . value < 0.01). OS-16 adhesion was increased compared to E2, E3, V583, AAOR34 (p . value < 0.05). NCTCC 5957 adhesion was also increased compared to ER5/1 ($P < 0.05$), E2, E3, V583, AAOR34 ($P < 0.01$) (Figure 2.8: B). When *E. faecalis* biofilms were incubated under anaerobic conditions, E3, ER5/1, AAOR43 showed higher adhesion while lab strain ATCC 29212 and OS-16 adhesion was reduced compared to CO₂ and O₂ conditions. (Figure 2.8: C).

Generally, the level of oxygen affected *E. faecalis* adhesion to collagen type 1 ECM protein, the more adherence to collagen was observed when *E. faecalis* cells were incubated under 5% CO₂ and anaerobic conditions (Figure 2.8: D).

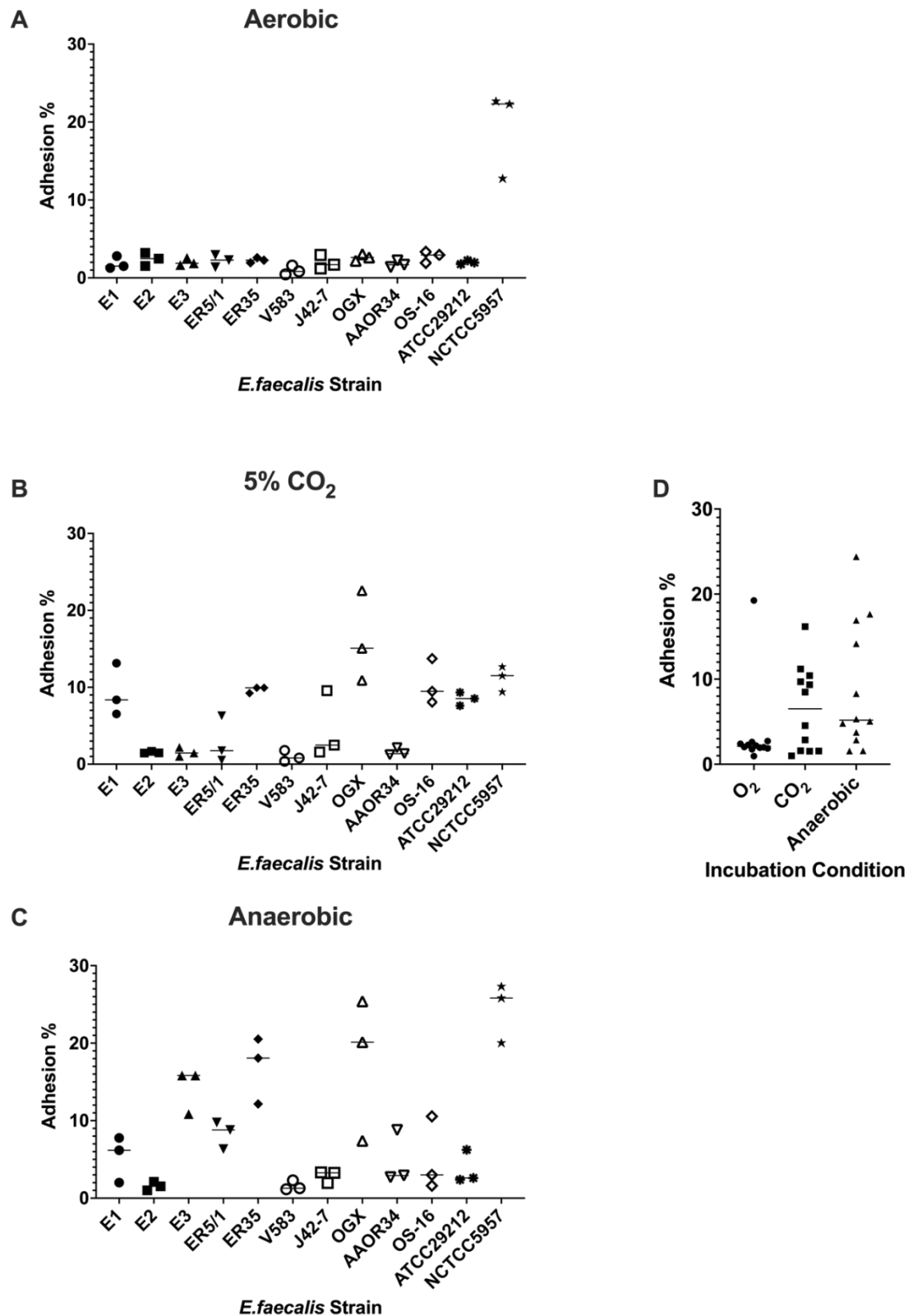


Figure 2.8: Percentage of adherent *E. faecalis* cells to Collagen I ECM protein. Adherence was tested in wells coated with 1 μ g of ECM proteins. *E. faecalis* strains were added to each designated well and washed with 0.1% Tween 80, 0.1% PBS three times. Biofilms were incubated under aerobic (A) 5% CO₂ (B) and anaerobic conditions (C) for 2 hours. Adhesion percentage was shown to be the lowest under aerobic conditions (D). Statistical analysis was done using one-way ANOVA with Tukey's multiple comparison post-test (* P<0.01, ** P<0.01, ***P<0.001, ****P<0.0001). Data represents mean \pm SD, performed in triplicate from three independent experiments.

2.4.2.5 *E. faecalis* virulence behaviour was modulated according to oxygen tension

To summarize the results presented above, each test was given a point when *E. faecalis* strain tested positive for that test in different incubation conditions. These scores were summarized in a form of a heatmap that showed gradient transition to red colour indicating increased virulence (red) under anaerobic conditions. Low virulence expressed as green colour was more on the aerobic conditions. Based on these results, ER5/1 was chosen to represent a HVS and E2 to be represented as a LVS (Figure 2.9).

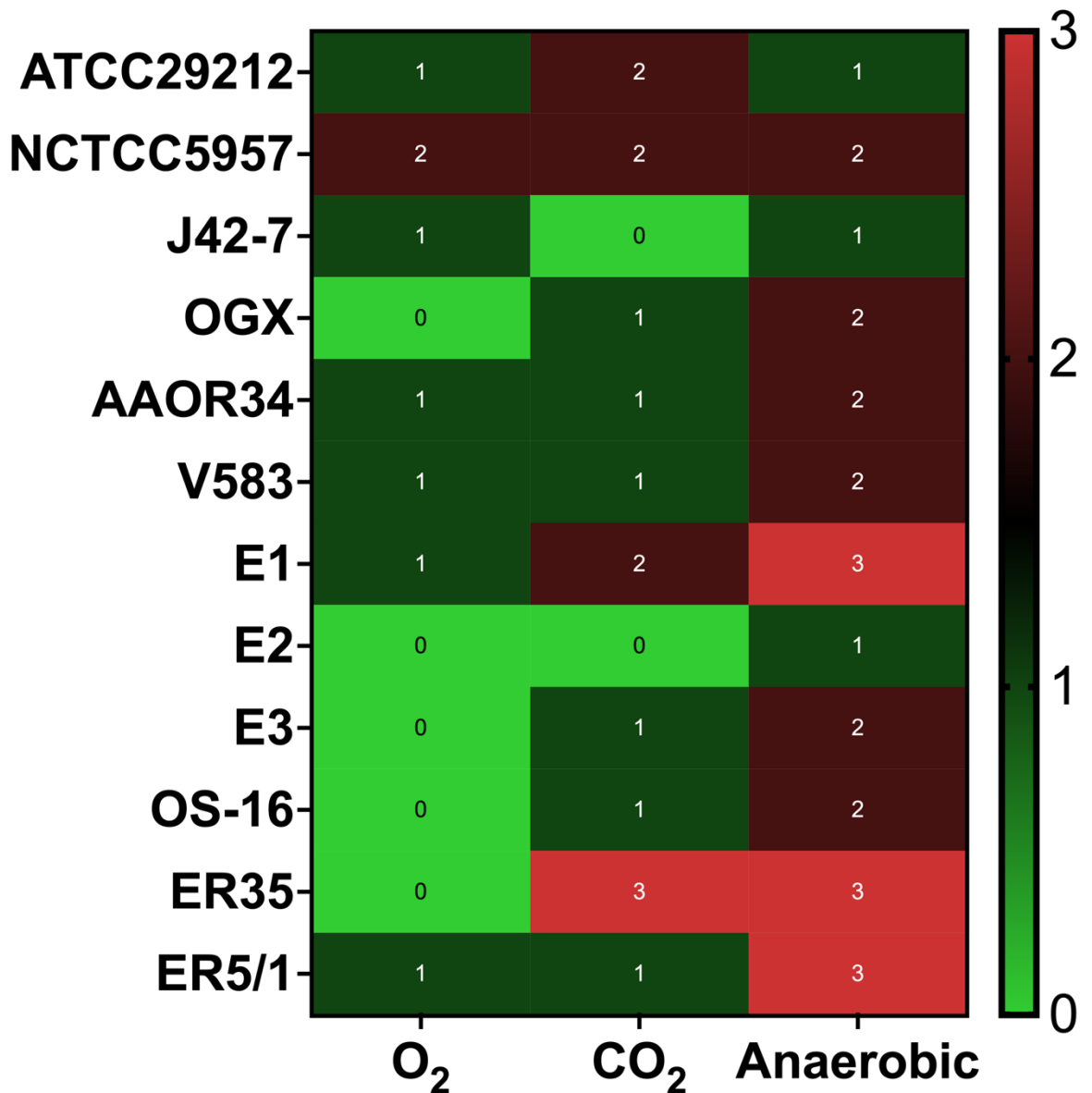


Figure 2.9: Heatmap analysis of all *E. faecalis* strains showing enhanced virulence under anaerobic conditions. Multiple *in vitro* assays were used to assess the virulence of *E. faecalis* strains; Biofilm biomass, Haemolytic activity, Gelatinase activity and Adhesion to collagen I. Each

assay was given a point wherever an *E. faecalis* tested positive for that assay. Red indicates increased virulence and green indicates low virulence.

2.4.3 *C. albicans* biofilm characterisation

To choose a strain to be cocultured with *E. faecalis* in dual-species biofilm model, biofilm biomass assessment was done to characterize isolates of in-house *C. albicans* as HBF and LBF at 4, 6, 8 and 24 hours. Results showed that the lab strain SC5314 was the highest biofilm former among *C. albicans* isolates through all time points. Thus, SC5314 was selected as the candidate strain to be used in subsequent experiments (Figure 2.10).

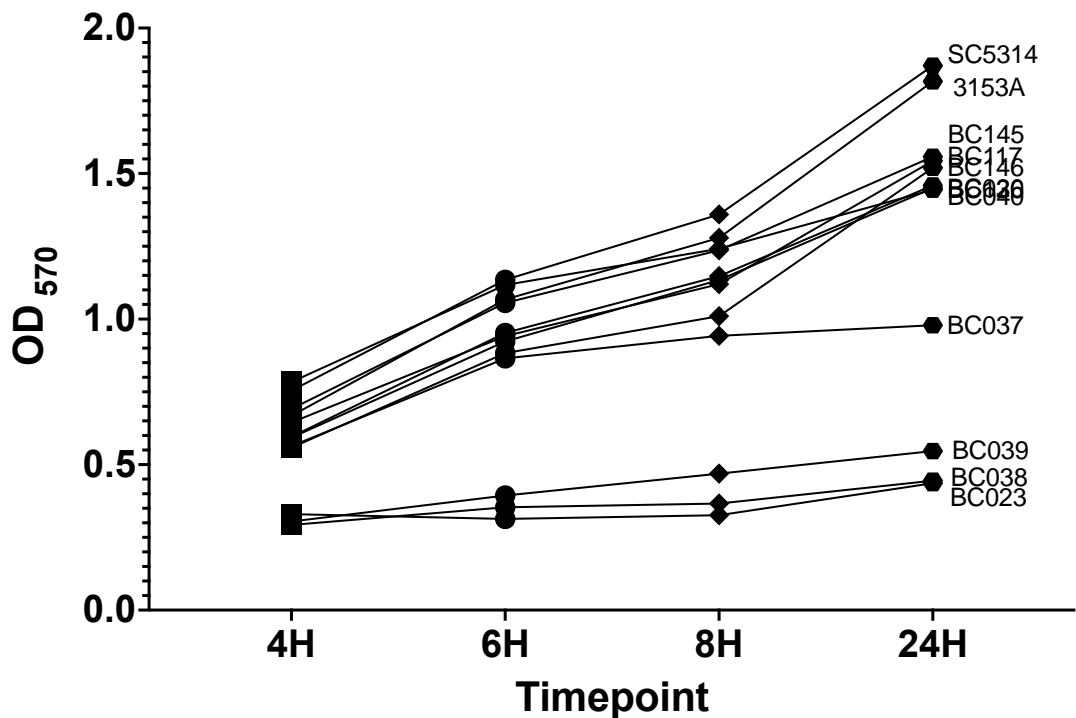


Figure 2.10: Characterisation of *C. albicans* isolates according to their biofilm forming capability. Biofilm biomass of twelve *C. albicans* isolates present in house was quantified by staining using 0.05% CV. Lab strain SC5314 was the highest biofilm former.

2.4.4 *C. albicans* and *E. faecalis* dual-species biofilm characterisation

In the following sections, dual-species biofilms were characterised at the phenotypic and molecular levels at different time points that reflects different

stages of biofilm formation. Dual-species biofilms were phenotypically assessed at 4, 6, 8 and 24 hours. Biofilm growth phase occurs at 4 - 8 hours, at this stage, *C. albicans* develops hyphal morphogenesis and ECM is actively produced. Microbial cells enter the biofilm maturation phase at nearly 24 hours. Gene expression analysis was done at 4 hours (biofilm growth phase) and 24 hours (biofilm maturation phase). Gene expression was analysed further at earliest biofilm formation stage when the biofilm adhesion occurs (30 minutes - 2 hours).

The previous work revealed that ER5/1 to be the HVS candidate and E2 was chosen as LVS. In addition, results have shown that SC5314 was the highest biofilm former throughout all time points amongst the *C. albicans* isolates. Thus, the lab strain SC5314 was chosen to be cocultured with *E. faecalis* HVS and LVS.

2.4.4.1 *E. faecalis* inhibited hyphal morphogenesis of *C. albicans*

To assess dual-species morphologically, several images were captured under the microscope at 4, 6, 8 and 24 hours (Figure 2.11) *C. albicans* biofilm started at 4h and initial hyphal development was evident (Figure 2.11:A).

Hyphal growth continued through all time points and was more evident at 8 and 24 hours (solid black arrow) (Figure 2.11:B, C, D). When *C. albicans* was grown with ER5/1 strong hyphal growth inhibition was evident at all time points (dotted black arrow) (Figure 2.11: E-H). This inhibition was also evident in E2 LVS dual-species biofilm (Figure 2.11: I-L). This suggests that the inhibition of hyphal morphogenesis was evident regardless of the virulence of *E. faecalis*.

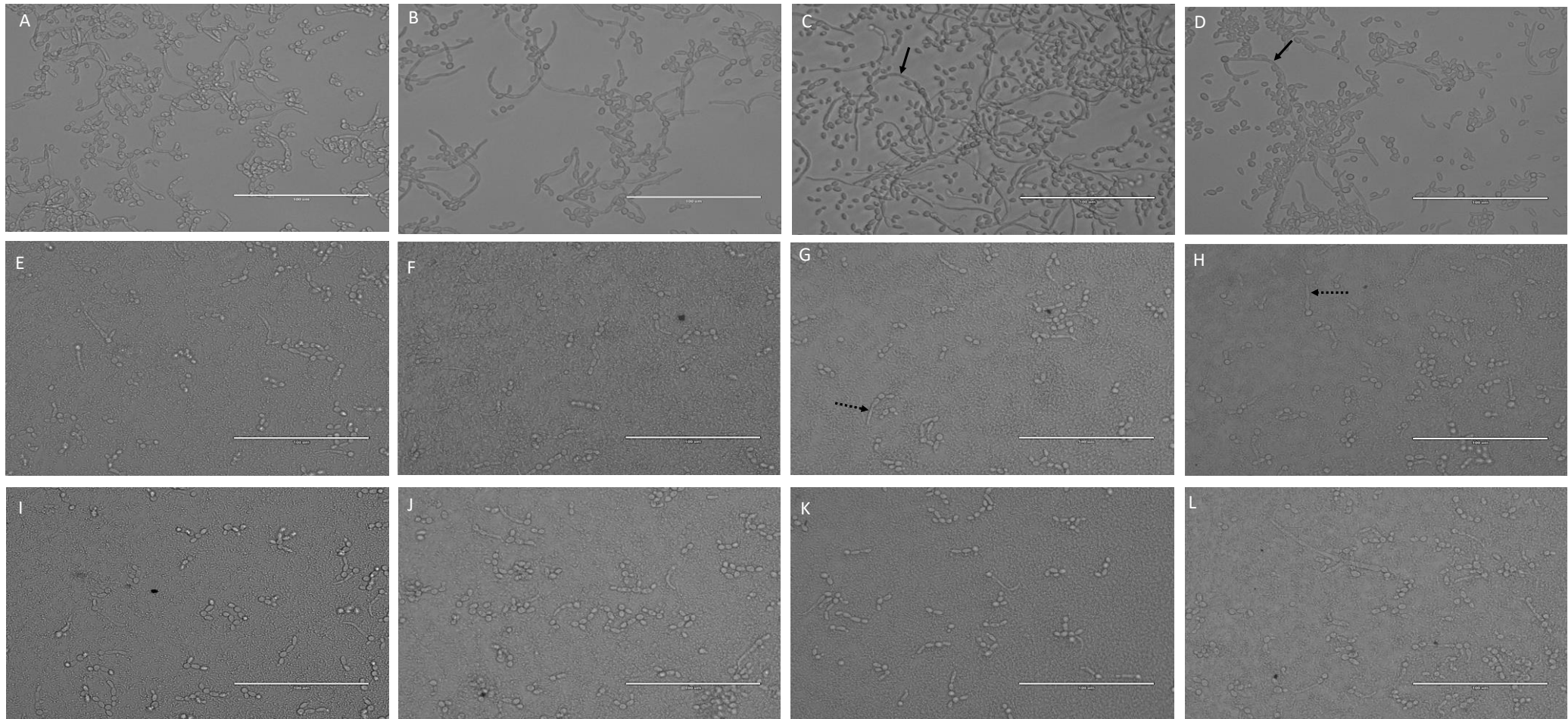


Figure 2.11: *E. faecalis* inhibits yeast to hyphae switch in *C. albicans*. Mono-species biofilm of *C. albicans* (A-D), ER5/1 *E. faecalis* + *C. albicans* dual-species biofilm (E-H) and E2 *E. faecalis* + *C. albicans* dual-species biofilm (I-L) were grown for 4h (A, E, I), 6h (B, F, J), 8h (C, G, K), and (D, H, L) in 24 well plate. Cells were washed with PBS and examined using EVOS cell imaging system at 400X magnification. Solid arrow indicated hyphal formation. Dashed arrow indicates shortened hyphae.

2.4.4.2 *E. faecalis* and *C. albicans* dual-species biofilm metabolic activity was reduced and the biofilm biomass was enhanced compared to *C. albicans* mono-species biofilm

Mono- and dual-species biofilms were quantified at 4, 6, 8 and 24 hours' time points using XTT and CV to assess total biofilm metabolic activity and biofilm biomass respectively (Figure 2.12, Figure 2.13). Dual species biofilm metabolic activity was decreased compared to *C. albicans* mono-species biofilm at 24h time point. This effect was significantly seen in ER5/1 strain dual-species biofilm ($p < 0.01$) compared to E2 strain of *E. faecalis* (Figure 2.12: A, B) suggestive that *E. faecalis* virulence plays a role in metabolic activity of dual-species biofilm.

The strain ER5/1 dual species biofilm formation was enhanced at 4 hours ($p < 0.0001$) and 8 hours ($p < 0.001$). At 24 hours, dual-species biofilm biomass was also enhanced compared to SC5314 single species biofilm ($p < 0.001$), however, it was significantly reduced compared to ER5/1 single species biofilm ($p < 0.001$) (Figure 2.13: A). In E2 LVS coculture, E2 increased dual-species biofilm biomass compared to SC5314 single species biofilm as in HVS at 8 hours ($p < 0.001$). At 24 hours, E2 also enhanced dual-species biofilm biomass compared to SC5314 mono-species biofilm ($p < 0.05$), however, SC5314 reduced dual-species biofilm compared to E2 single species biofilm as in HVS although it was less significant ($P < 0.05$) (Figure 2.13: B).

Overall, based on microscopy, metabolic activity and biofilm formation assessment, we can conclude that the presence of *C. albicans* in the mixed community did not influence *E. faecalis* biofilm-forming capability compared to *E. faecalis* mono-species biofilm except for 24 hours in which biofilm biomass was reduced. However, on the contrary, *E. faecalis* did reduce the ability of *C. albicans* to form biofilms when compared to *C. albicans* mono-species biofilm alone. Results also showed the more virulent the *E. faecalis* strain was (e.g., the HVS compared to the LVS), the more it inhibits *C. albicans* capability to contribute to biofilm deposition in dual-species biofilm (Figure 2.13: A, B)

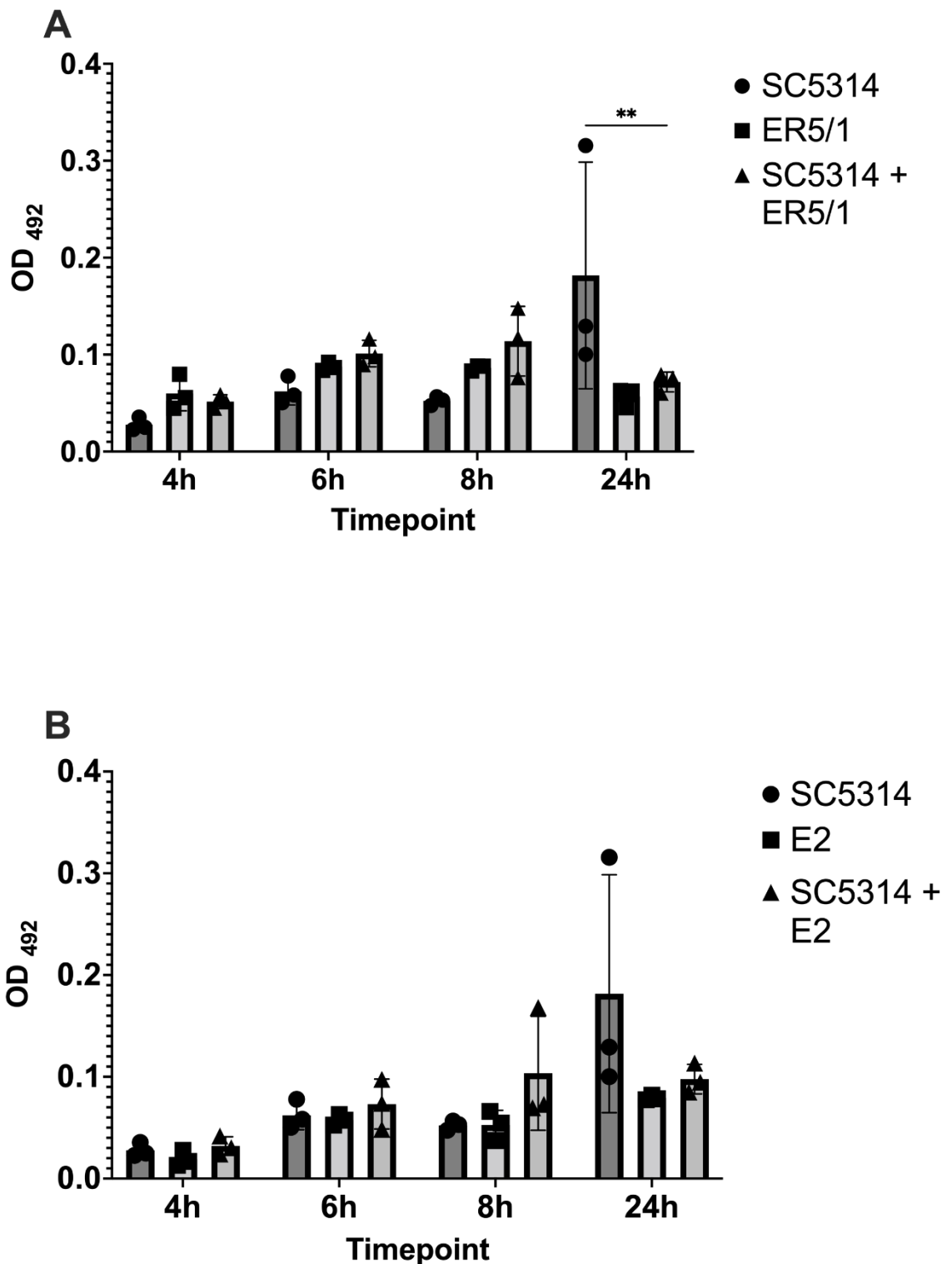


Figure 2.12: Alteration of dual-species biofilm metabolic activity compared to each strain in a mono-species biofilm. Single and multi-species biofilms containing *C. albicans* lab strain SC5314 and *E. faecalis* strains ER5/1 and E2 were grown for 4h, 6h, 8h and 24h. Metabolic activity of SC5314, ER5/1, SC5314 + ER5/1 (A), SC5314, E2, SC5314 + ER5/1 (B) was measured using XTT sodium salt. Statistical analysis was done using two-way ANOVA with Tukey's multiple comparison post-test Experiments were performed on three separate occasions and error bars represent standard deviation of the mean (**; $P < 0.01$).

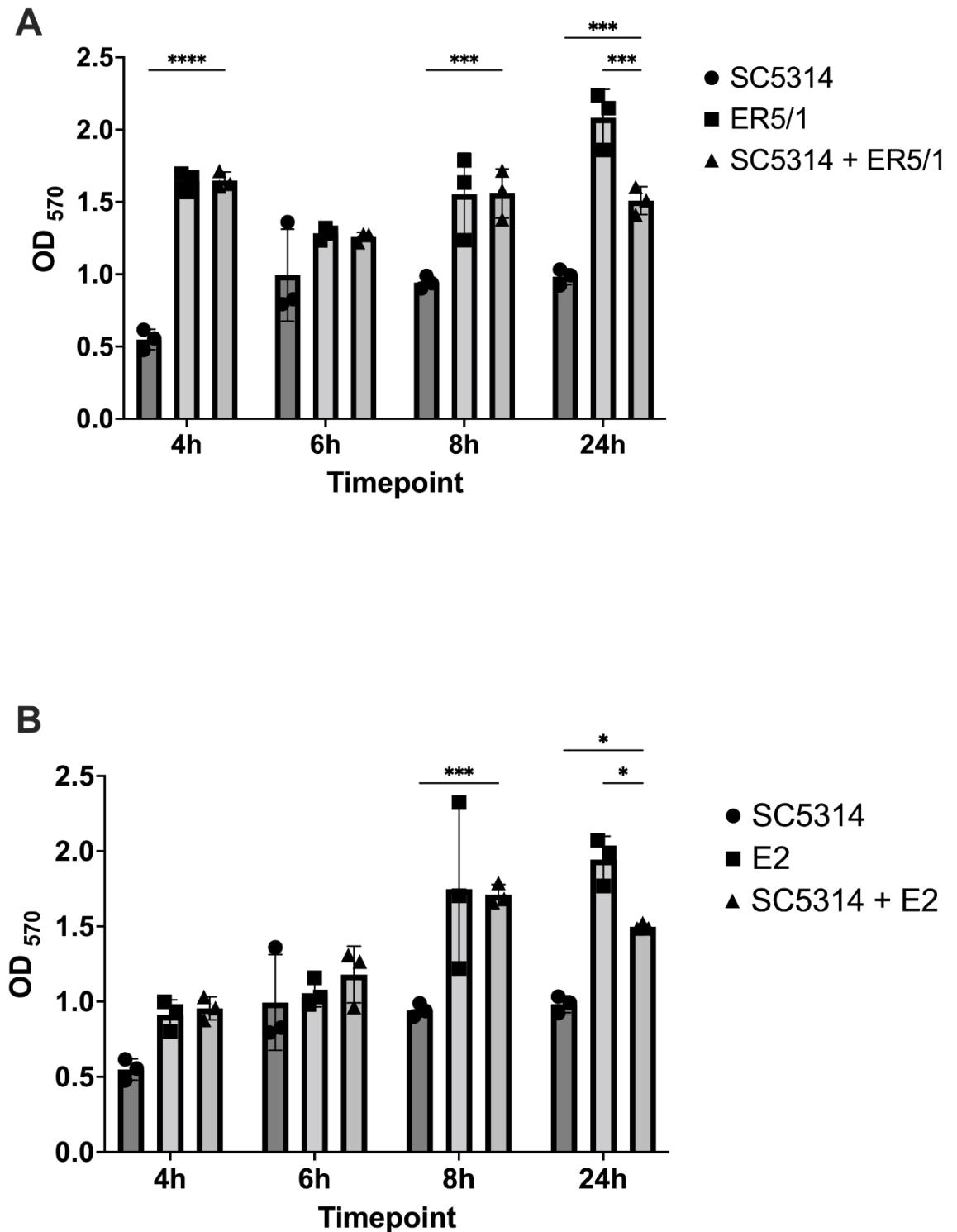


Figure 2.13: Alteration of dual-species biofilm biomass compared to each mono-species biofilm biomass. Single and multi-species biofilms containing *C. albicans* lab strain SC5314 and *E. faecalis* strains ER5/1 and E2 were grown for 4h, 6h, 8h and 24h. Biofilm biomass of SC5314, ER5/1, SC5314 + ER5/1 (A), SC5314, E2, SC5314 + E2 (B) was measured using CV. Statistical analysis was done using two-way ANOVA with Tukey's multiple comparison post-test. Experiments were performed on three separate occasions and error bars represent standard deviation of the mean (*; $P < 0.05$, ***; $P < 0.001$, ****; $P < 0.0001$).

2.4.4.3 *E. faecalis* inhibited the growth of *C. albicans* while *C. albicans* had no effect of *E. faecalis* growth.

Next, to further reveal the antagonist or synergistic effect of these two microorganisms on each other's growth and replication, the total number of cells in each biofilm was quantified using qPCR at 4, 6, 8 and 24 hours. Results showed that the number *E. faecalis* cells were not affected by the presence of *C. albicans* compared to *E. faecalis* mono-species biofilm (Figure 2.14: A,B). However, *C. albicans* cell number was significantly lower at 8 hours in ER5/1 ($P < 0.01$) and E2 ($P < 0.001$) dual-species compared to *C. albicans* single species biofilm. This was also evident at 24 hours' time point, *C. albicans* cells number was significantly lower in ER5/1 ($P < 0.001$) and E2 ($P < 0.05$) dual-species compared to *C. albicans* single species biofilm (Figure 2.14: C). Generally, in line with results shown above, the virulence of *E. faecalis* strain did have an impact on *C. albicans* growth where the HVS ER5/1 exhibited slightly more growth inhibition observed at all time points although not statistically significant at 4 hours and 6 hours (Figure 2.14: C).

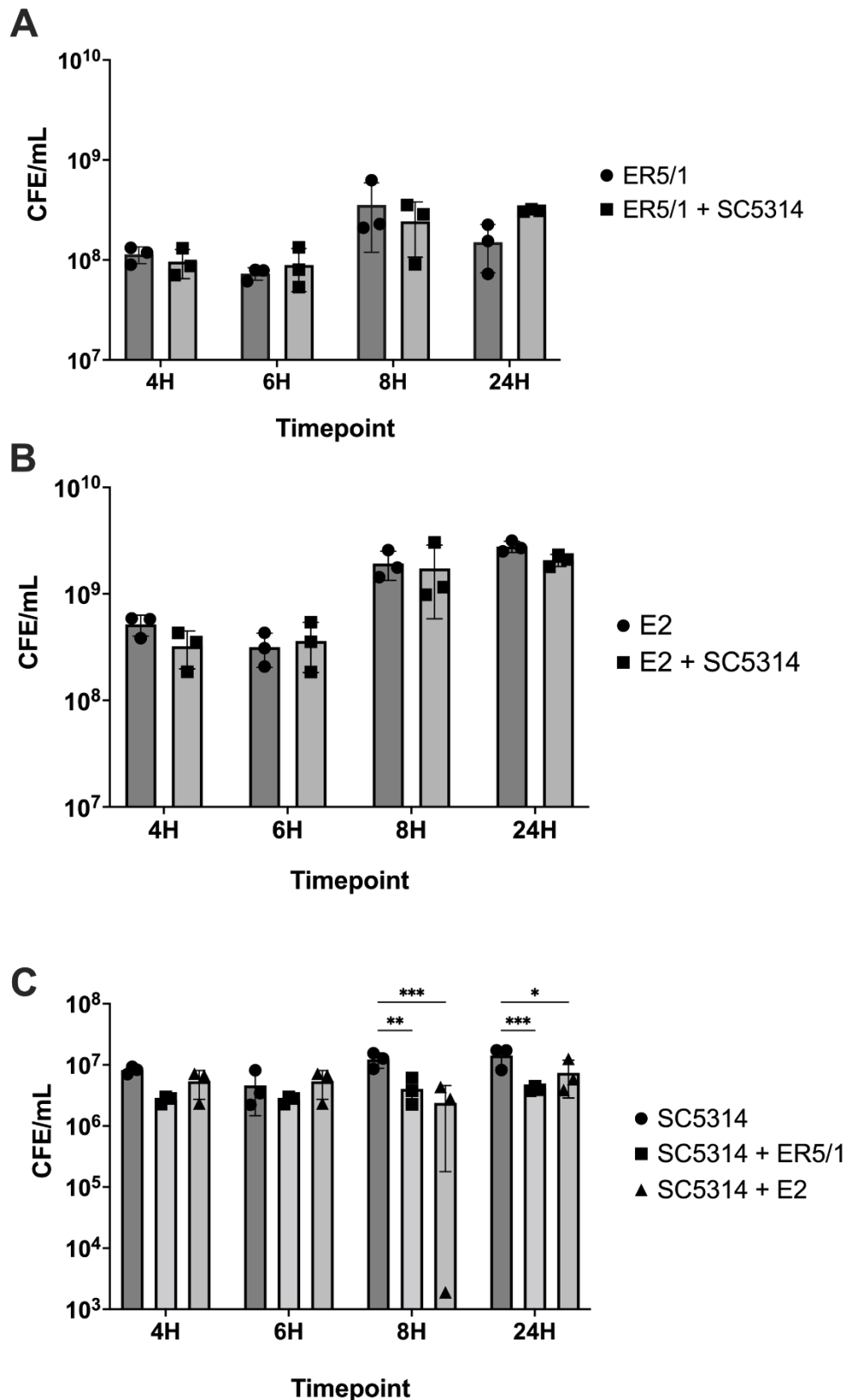


Figure 2.14: The effect of *E. faecalis* and *C. albicans* on each other's growth in dual-species biofilm compared to single species biofilm. Biofilm biomass was removed via scraping, DNA was extracted and the total number of cells in each biofilm was quantified using qPCR. The total number of *E. faecalis* ER5/1 (A) and *E. faecalis* E2 (B) and *C. albicans* SC5314 (C) cells at 4, 6, 8 and 24 hours biofilms are presented as CFE/mL. Statistical analysis was done using two-way ANOVA with Tukey's multiple comparison post-test. Experiments were performed on three separate occasions and error bars represent standard deviation of the mean (*, P < 0.05; **, P < 0.01; ***, P < 0.001).

2.4.4.4 *E. faecalis* induces changes in key virulence genes in *C. albicans* at 4- and 24-hours' time points.

Results highlighted above showed that *E. faecalis* inhibited hyphal morphogenesis, biofilm formation and growth of *C. albicans*. In this section, to further interrogate interactions between the two microorganisms, gene expression analysis was done on key genes involved in hyphal morphogenesis and biofilm formation in *C. albicans*.

Gene expression analysis revealed that *E. faecalis* downregulated key virulence genes in *C. albicans* during biofilm formation and maturation. *HWP1* encodes hyphal cell wall protein required for filamentation and adherence to substrates and biofilm formation (Martin *et al.*, 2013). This gene was slightly upregulated at 4 hours and then downregulated by 3.7 and 3.3 Log₂FCs when *C. albicans* was cocultured with *E. faecalis* HVS and LVS respectively at 24 hours (Figure 2.15: A). *ALS3* encodes a hyphae-specific adhesin that is essential for *C. albicans* adhesion and biofilm formation (Liu and Filler, 2011). This gene was also downregulated by 3 and 2.5 Log₂FCs in dual-species biofilm composed of *C. albicans* and HVS, LVS respectively (Figure 2.15: B). *SAP5*, encodes secreted aspartyl protease 5 (SAP5), a member of the SAP family proteins and considered as a biofilm specific marker (Winter *et al.*, 2016) it is known to play a role in *C. albicans* hyphal formation, adherence, and host penetration (Hube *et al.*, 1994). This gene was upregulated by 1.1 and 1.9 when *C. albicans* was cocultured with HVS and LVS, respectively. *EFG1*, encodes an important transcription factor for hyphal morphogenesis (Martin *et al.*, 2013), was upregulated at 4 hours by 1.6 and 2.2 when *C. albicans* was cocultured with HVS and LVS respectively. However, downregulation was noticed by HVS and LVS on *EFG1* by 2.3 and 2.7 respectively at 24 hours (Figure 2.15: D).

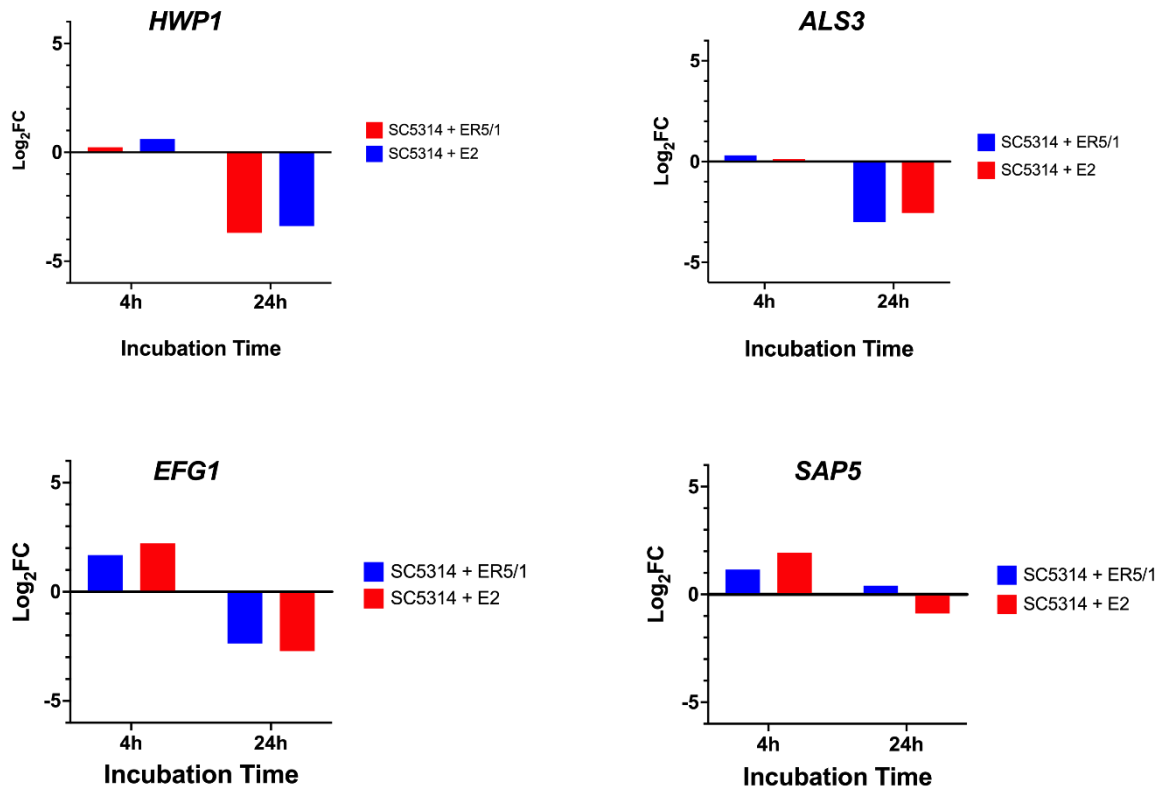


Figure 2.15: *E. faecalis* high and low virulent strains induces changes in *C. albicans* key virulence genes at early and late dual-species biofilm. Differential expression of key virulence genes in *C. albicans* SC5314 when cocultured with HVS ER5/1 and LVS E2. Genes were measured in monoculture and in presence of *E. faecalis* at 4 and 24 hours. Data was done using qRT-PCR from three independent biological repeats. Data shown is the mean Log₂FC relative to mono-species biofilms.

2.4.4.5 *C. albicans* induces changes in key virulence genes in *E. faecalis* high and low virulent strains at 4- and 24-hours' time points.

Gene expression analysis of key virulence genes in high and low virulent strains of *E. faecalis* revealed that *C. albicans* downregulated *entV* gene expression at 4 hours, which is a gene that encodes a bacteriocin that is well proven in literature to inhibit *C. albicans* hyphal morphogenesis (Graham et al., 2017a). This downregulation was more pronounced in E2 LVS by 1.5 while it was only downregulated by 0.5 Log₂FC in ER5/1 HVS. However, upregulation was induced at 24 hours in both strains. Again, the upregulation was more pronounced in E2 LVS by 1.7 Log₂FC compared to ER5/1 HVS which was upregulated by 0.6 Log₂FC only (Figure 2.16: A). *ace*; a gene that encodes collagen binding protein that's essential for biofilm formation (Nallapareddy et al., 2000); was upregulated in ER5/1 HVS when cocultured with *C. albicans* SC5314 at 4 and 24 hours by 1.2 and

2 Log₂FC respectively. However, no differential expression was found at 4 hours when the LVS E2 was cocultured with *C. albicans* SC5314 but an upregulation by 0.9 Log₂FC was noticed at 24 hours (Figure 2.16: B). In addition, *esp* gene encodes enterococcal surface protein, which is involved in the interaction between substratum and bacteria (Waar *et al.*, 2002). This gene is expressed in E2 LVS only and was upregulated by 0.9 and 0.5 Log₂FC at 4 and 24 hours respectively (Figure 2.16: C). Finally, *gelE* (gelatinase) was also proved to associated with *E. faecalis* biofilm formation (Wang *et al.*, 2011). This gene is expressed in ER5/1 HVS only and was slightly upregulated by 0.1 at 4 hours and downregulated by 0.5 Log₂FC at 24 hours (Figure 2.16: D).

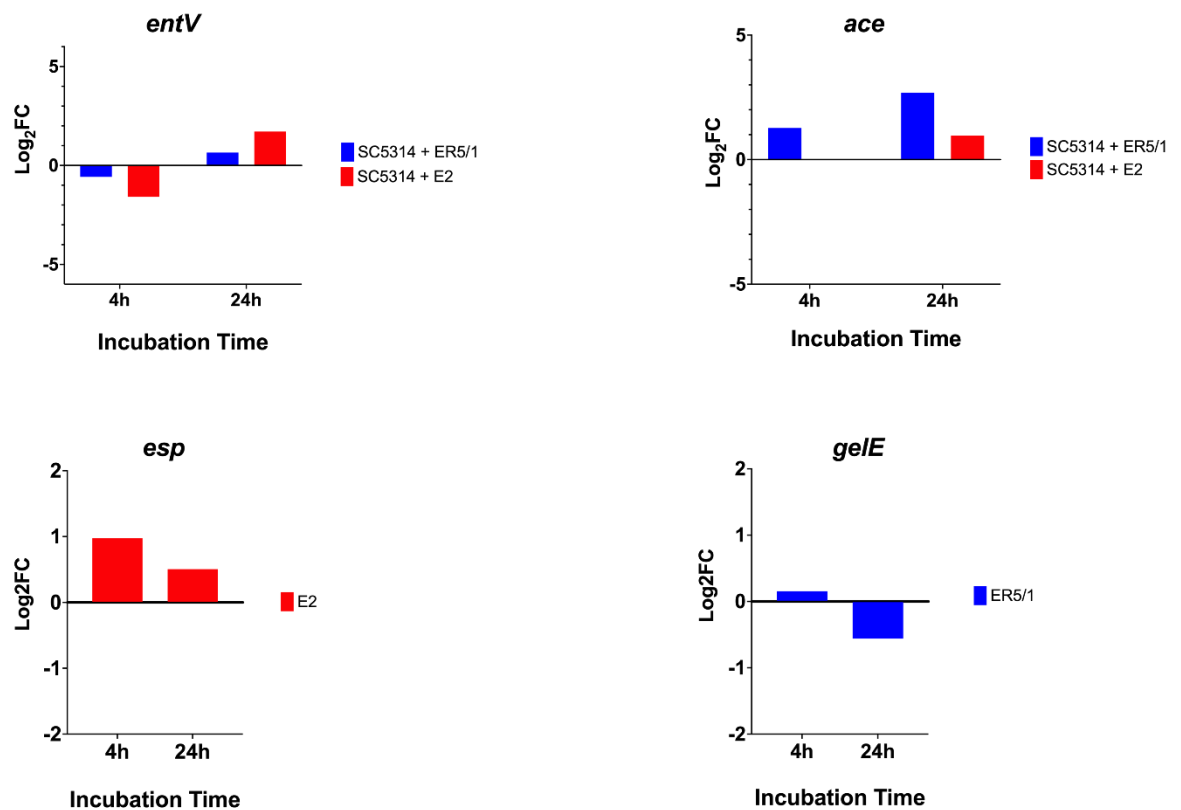


Figure 2.16: *C. albicans* induces changes in *E. faecalis* key virulence genes at early and late dual-species biofilm. Differential expression of key virulence genes in *E. faecalis* HVS ER5/1 and LVS E2 when cocultured with *C. albicans* SC5314. Genes was measured in monoculture and in presence of *C. albicans* at 4h and 24 h. Data was done using qRT-PCR from three independent biological repeats. Data shown is the mean log Log₂FC relative to mono-species biofilms.

2.4.4.6 *E. faecalis* and *C. albicans* induced changes in each other's virulence genes at biofilm adhesion stage of dual-species biofilm formation.

Coculturing *C. albicans* SC5314 and *E. faecalis* HVS ER5/1 results in a gradual upregulation of the gene HWP1 by 0.6, 0.9 and 1.7 at 30 minutes, 1 hour and 2 hours respectively (Figure 2.17: A). ALS3 gene expression was the highest at 30 minutes by 1.1 Log₂FC which remained nearly constant at 2 hours (Figure 2.17: B). *ECE1*, encodes cytolytic toxin peptide that plays a critical role in *C. albicans* pathogenicity, virulence, and promotes host tissue damage (Moyes *et al.*, 2016), was at its highest at 30 minutes by 1.3 Log₂FC and was gradually downregulated at 2 hours by 0.5 Log₂FC (Figure 2.17: C). SAP5 was downregulated at 30 minutes of coculture by 2.9 and no differential expression was detected at 1- and 2-hours' time points (Figure 2.17: D). However, SAP2 gene expression that encodes a member of the secreted aspartyl protease family was subject to gradual increase in gene expression from 30 minutes to 2 hours by 0.2, 0.6 to 1.4 Log₂FC respectively (Figure 2.17: E). In addition, two of the major transcription factors genes were differentially expressed. *EFG1* was downregulated at 30 minutes by 2.5 Log₂FC while it was gradually increased at 1 and 2 hours time points by 0.2 and 0.7 Log₂FCs respectively (Figure 2.17: F). *BCR1*, encodes a transcription factor involved in biofilm formation (Nobile *et al.*, 2012). This gene was gradually upregulated until it reached 1.9 Log₂FCs at 2 hours (Figure 2.17: G).

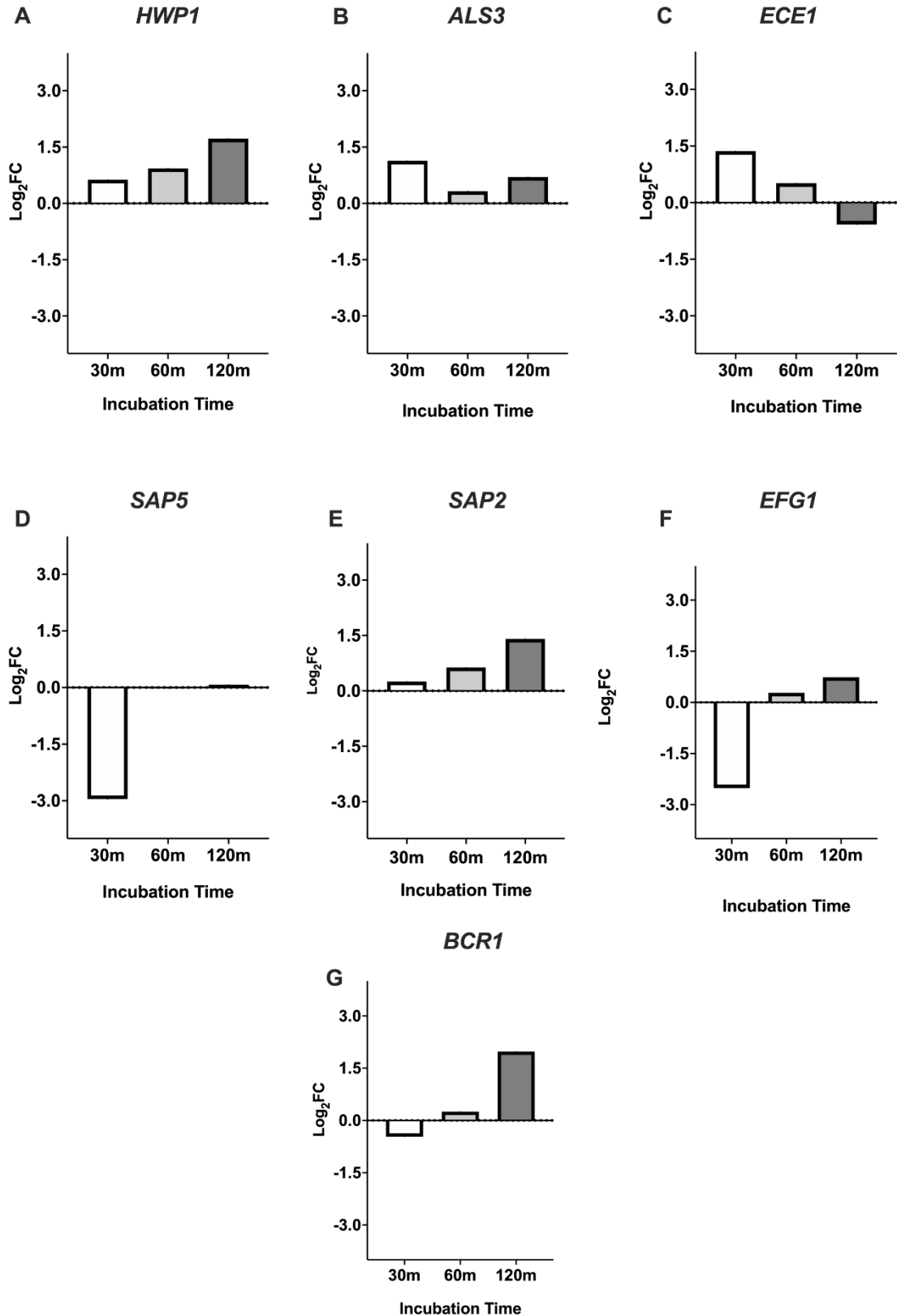


Figure 2.17: Gene expression analysis of virulence related genes in *C. albicans* at biofilm adhesion phase of dual-species biofilm formation. Differential expression of key virulence genes in *C. albicans* SC5314 when cocultured with HVS ER5/1. Genes were measured in monoculture and in presence of *E. faecalis* at 30 minutes, 1h and 2h. Data was done using qRT-PCR from three independent biological repeats. Data shown is the mean log Log₂FC relative to mono-species biofilms.

To assess *E. faecalis* virulence behaviour when cocultured with *C. albicans*, the differential expression of key virulence genes in *E. faecalis* ER5/1 HVS key virulence was assessed at 30 minutes, 1 hour and 2 hours. The results showed minimal changes happened to the three virulence genes assessed. The gene *ace* expression was downregulated at 1 hour by 1.5 Log₂FC although it remained slightly downregulated at 30 minutes and 2 hours' time points. In addition, *gelE* expression levels were slightly upregulated at 30 minutes and 2 hours while it was slightly downregulated at 2 hours by 0.1 Log₂FC. The highest upregulation in *entV* was at 30 minutes time point by 1.4 Log₂FC. This upregulation in gene expression remained constant through 1 hour and 2 hours' time points (0.8 and 0.7 Log₂FC respectively) (Figure 2.18).

Taken together, the results from this and the preceding figures suggest that both species induce changes in each other's virulence at the molecular levels. Major changes in gene expression occurs at biofilm maturation phase (24 hours) whereby downregulation of genes involved in virulence was evident in *C. albicans*. Genes that govern adhesion and biofilm formation in *C. albicans* were upregulated which suggest mutualistic relationship between both species at the establishment of biofilm formation. For *E. faecalis*, genes involved in adhesion and biofilm formation (e.g., *esp*, *ace*) were upregulated at 24 hours which implies a mutualistic relationship between both species that favours enhanced adhesion of *E. faecalis* in dual-species biofilm. At earliest time points, when *C. albicans* was introduced, adhesion was downregulated in *E. faecalis*. However, the active expression of *entV* at this stage of biofilm formation was evident which suggests antagonism from *E. faecalis* side.

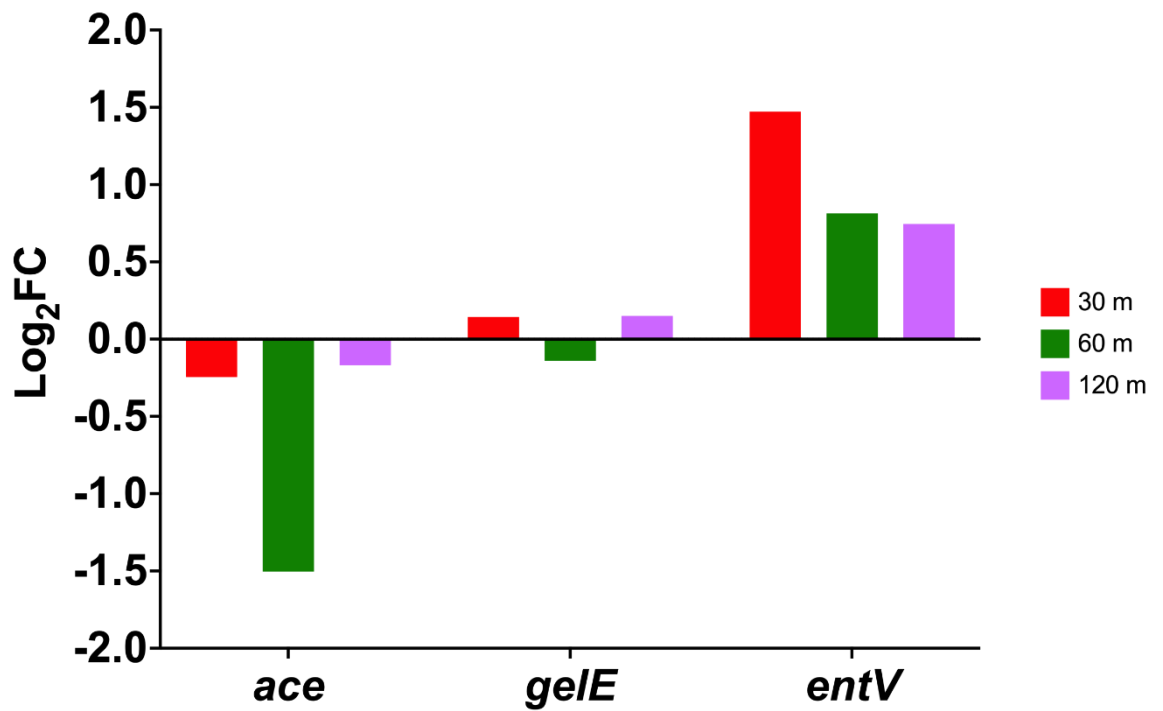


Figure 2.18: Gene expression analysis of virulence related genes in *E. faecalis* at biofilm adhesion phase of dual-species biofilm formation. Differential expression of key virulence genes in *E. faecalis* HVS ER5/1 when cocultured with *C. albicans* SC5314. Genes was measured in monoculture and in presence of *C. albicans* at 30 minutes, 1h and 2h. Data was done using qRT-PCR from three independent biological repeats. Data shown is the mean Log₂FC relative to mono-species biofilms.

2.5 Discussion

The microenvironment inside the root canal is subjected to dynamic changes according to microorganisms that reside within, anatomical location, irrigation and materials introduced inside root canals during RCT. Therefore, oxygen tension which can affect the microbial community that inhabit the root canal varies accordingly. On this note, *C. albicans* can survive harsh environments with different levels of oxygen tension whilst biofilm formation can provide anaerobic microenvironment wherein anaerobic bacteria can thrive (Fox *et al.*, 2014). A common co-colonizer of the root canal, *E. faecalis*, can also survive in challenging environments. Thus, in this research, the effect of oxygen tension levels on the virulence behaviour of *E. faecalis* was explored. Its interactions with *C. albicans* were also investigated. The data presented in this chapter shows clearly that oxygen tension modified the virulence behaviour of *E. faecalis* strains, which increased in response to anaerobiosis. It was evident that the degree of virulence of *E. faecalis* isolates varied considerably as some strains displayed low-virulence and others demonstrated high-virulence. The heterogeneity seen amongst *E. faecalis* strains was in line with previous results that showed variation in virulence behaviour amongst *E. faecalis* strains isolated from clinical infections (Barbosa-Ribeiro *et al.*, 2016, Gulhan *et al.*, 2015, Zheng *et al.*, 2017).

The virulence characterisation results showed that cytolysin activity in *E. faecalis* strains was enhanced under anaerobic conditions. These results are in line with the findings of a previous report which showed that *E. faecalis* strains exhibited greater haemolysis under anaerobic conditions compared to aerobic conditions (Day *et al.*, 2003). In addition, their results showed that cytolysin genes were regulated in response to the degree of aerobiosis where higher expression was induced under anaerobic conditions (Day *et al.*, 2003). Moreover, the current results revealed that gelatinase activity of *E. faecalis* strains was enhanced under aerobic conditions. The literature search yielded one study only (Merrill and Clark, 1928) that reported the effect of aerobiosis on gelatinase activity. They had shown that the production of gelatinase was evidently increased with the increase in aeration, (Merrill and Clark, 1928). It has been evident that microorganisms respond to their surrounding microenvironment and change EPS

compositions (Ahimou *et al.*, 2007). Therefore, their adhesion abilities vary accordingly. Oxygen-limited biofilms exhibit more cohesive structure due to their relatively greater EPS production (Applegate and Bryers, 1991) which explains results found in this chapter that showed biofilm formation and adhesion was at its highest under 5% CO₂.

Here, the present data have shown the importance of oxygen tension in modulating *E. faecalis* virulence which will affect the course of endodontic infection. The findings from *E. faecalis* characterisation under different oxygen tension conditions suggest that *E. faecalis* virulence is oxygen-dependent. When root canals are treated and sealed, any remaining *E. faecalis* cells will be subjected to low oxygen tension and limited nutrient availability which will play a significant influence on its virulence and ability to survive (Portela *et al.*, 2014, Kim *et al.*, 2020b). Some studies characterised virulence factors from endodontic isolates have reported that virulence traits were induced in *E. faecalis* (Zhu *et al.*, 2010, Patidar *et al.*, 2013, Zoletti *et al.*, 2011). Production of proteases like cytolysin and gelatinase depends on microenvironment of root canals. As a result, infection course can vary depending on the virulence of strains isolated.

In this chapter, an interkingdom dual-species biofilm model of *C. albicans* and *E. faecalis* was established. Several interkingdom interactions between *C. albicans* and other bacterial species revealed antagonistic relationship which induced hyphal morphogenesis inhibition (Bor *et al.*, 2016, Fourie *et al.*, 2016, Allonsius *et al.*, 2017). The current data have demonstrated that the metabolic activity of *C. albicans* was maintained although *C. albicans* growth was inhibited. Dual-species biofilm characterisation revealed that *E. faecalis* displayed antagonistic effect on *C. albicans* virulence which was manifested by inhibiting its hyphal morphogenesis and biofilm formation. This antagonism is consistent with previous studies that reported similar results including inhibition of *C. albicans* hyphal morphogenesis and biofilm formation (Graham *et al.*, 2017a, Cruz *et al.*, 2013).

Synergistic interactions between *C. albicans* and *E. faecalis* have been reported. One study showed that *C. albicans* and *E. faecalis* produced a thicker and a denser biofilm compared to each mono-species biofilm; and that *E. faecalis* and *C. albicans* cell load has been increased as revealed by their qPCR data (Du *et al.*,

2021). This finding was in contradiction with this chapter's results which have shown that *E. faecalis* reduced the number of *C. albicans* cells compared to the number of mono-species biofilm at both time points, 8 and 24 hours; whilst the number of *E. faecalis* cells remained unchanged. This contradiction might be attributed to methodologies and the use of dentine as a colonisation surface in the (Du et al., 2021) model.

Biofilm formation includes distinct developmental phases (Figure 1.1); adhesion phase (0-2 hours) whereby microbial cells start to adhere to surfaces. At 3-8 hours cells start to proliferate and distinct microcolonies start to appear. At 24 hours, biofilm starts to mature along with the continuous deposition of ECM and polysaccharides (Chong *et al.*, 2018, Fourie *et al.*, 2016). The biofilm model was also investigated at different time points to tackle alterations at different biofilm formation stages. At the molecular level, genes involved in *C. albicans* adhesion and biofilm formation were downregulated at 24 hours' time point matching what was observed phenotypically. This proves that major antagonistic events take place during biofilm maturation stage. However, these genes were upregulated during biofilm growth phase which indicates synergistic effects at earlier time points. Since results showed possible mutualistic relationship at early time points, it was decided to explore further possible interactions during the adhesion phase of biofilm formation at time points (30 minutes - 2 hours). Generally, *E. faecalis* enhanced expression of virulence genes related to adhesion, biofilm formation and hyphal morphogenesis during this stage of biofilm formation. This finding suggests that during adhesion and biofilm establishment phase a synergy was essential for *C. albicans* to successfully establish a biofilm and colonise substrates.

One study examined the effect of encapsulated *E. faecalis* and the lab strain ATCC29212 on ALS3 gene expression in *C. albicans*, and found it to be downregulated at 24 hours' time point (Bachtiar *et al.*, 2016) which was consistent with this chapter's findings. Another study explored the effect of *E. faecalis* on *C. albicans* virulence behaviour within an organotypic oral epithelial model, and reported that the genes involved in *C. albicans* virulence were upregulated (Krishnamoorthy *et al.*, 2020); Their results revealed marked upregulation in HWP1 as well as ALS3 along with other genes that are responsible for tissue

destruction and invasion. Their results are in disagreement with the gene expression data reported in this chapter, which revealed a marked decrease in both genes at 24 hours. This can be explained by the fact that they have used biotic surface to grow their biofilm. Hence, a different element that might have changed the response of dual-species from abiotic surfaces like polystyrene plates, catheters, or dentures.

The two-component regulatory system consisting of the *fsr* locus in *E. faecalis* is critical for establishing its virulence. *gelE* is one of the major genes that are directly dependent on *fsr* system. It has been reported that EntV bacteriocin peptide requires cleavage by GelE to generate a peptide capable of inhibiting *C. albicans* hyphal morphogenesis (Graham et al., 2017a). Krishnamoorthy *et al.*, (2020) found that *C. albicans* downregulated key genes involved in this two-component regulatory system, like *gelE* and *fsrB* and *fsrC* (Krishnamoorthy *et al.*, 2020). In contrast, another study found that the synergistic interactions between *E. faecalis* and *C. albicans* increased the adhesion of *E. faecalis* to dentine; their results revealed several adhesion and biofilm related genes like *ace*, *esp*, *gelE* were upregulated (Du *et al.*, 2021). This contradiction might be due to differences in colonization surfaces; as mucosal surface was used in one study (Krishnamoorthy *et al.*, 2020) while in another study dentine was used as a colonisation surface (Du *et al.*, 2021). Gene expression data in this chapter were in direct agreement with the results of Du *et al.*, (2021) who confirmed the synergistic interactions between *E. faecalis* and *C. albicans* that favours biofilm formation, possibly by promoting initial adhesion of *E. faecalis*. In addition, the data here revealed a higher expression of *entV* in dual-species biofilm which can be the reason behind *C. albicans* morphogenesis inhibition as proven by another study (Graham et al., 2017a).

Insights from other interkingdom interactions can provide a framework for future research on *C. albicans* and *E. faecalis*. Studies that investigated the interkingdom interaction between *C. albicans* and *P. aeruginosa* revealed that antagonistic interaction existed between these two species (Hogan and Kolter, 2002, Fourie *et al.*, 2016). There is a complex relationship behind this antagonism wherein a synergistic virulence might exist under certain conditions and during different

stages of the fungi-bacteria interaction (Fourie and Pohl, 2019). The results detailed in this chapter showed a clear phenotypic antagonism on *C. albicans* exerted by the bacterium, while *E. faecalis* was less affected when grown alongside the fungal microorganism. However, detecting alterations in each species behaviour at different time points of biofilm formation stages at molecular levels indicates complex relationships between both species. Given that this interkingdom interaction remains vastly understudied, other tools should be utilised to decode further this relationship. Nevertheless, the results in this chapter highlight a dynamic relationship between these two organisms that are commonly isolated from root canal infections and provide a fundamental platform for future studies into the endodontic landscape.

2.6 Conclusion

Virulence factors of *E. faecalis* may enable the bacterium to establish an endodontic infection and maintain periapical inflammation. The preliminary findings present in this chapter suggest that:

- There is a strain heterogeneity in virulence factors and the microorganism can modulate virulence factors that depend on the microenvironment in which they reside.
- In anaerobic conditions, *E. faecalis* changes its behaviour and modifies its virulence factors. In this context, the findings may be of a clinical importance as the root canal space comprises three parts namely: coronal, middle and apical, with the microenvironment being most anaerobic in apical part.
- Major changes occurred in both species at phenotypic and molecular levels wherein *C. albicans* was most affected.

However, despite the clinical cooccurrence of *E. faecalis* and *C. albicans* and being common in hospital settings and dental clinics, there is still a gap of knowledge in understanding their biological interactions. Exploiting the interplay between these microorganisms and their antagonistic interacting partners will enhance the efficacy of existing antimicrobials in treating opportunistic microbial infections.

The findings detailed in this chapter can contribute significantly little to the scarce research investigating the mechanisms of interactions of these two microorganisms.

Chapter 3: Transcriptomic analysis of *C. albicans* response to *E. faecalis* in dual-species biofilm

3.1 Introduction

Biofilm communities are polymicrobial in nature with complex inter-species interactions that shapes the communities' structure and function. Traditionally, studies have used species co-occurrence to infer potential connection between two species. Coexistence does not give exact evidence on their interactions as information at phenotypic and functional levels is still required. Examples of inter-species interaction that are reported in literature includes adherence, metabolic interaction, signalling and competition for resources (Rickard *et al.*, 2003, Giaouris *et al.*, 2015, Ellepola *et al.*, 2019a). Omics approaches have revealed important information about microorganisms' cellular response in the presence of another microbial partner (Shokeen *et al.*, 2021, Zhang *et al.*, 2019). Some of these studies focused on the microbial transcriptional response followed by proteomic investigations. In addition, metabolomic approaches have been employed to investigate metabolites in different oral sites. However, the studies examining the metabolic response of interacting species were limited to exploring specific metabolites rather than broad metabolomic approach (McClure *et al.*, 2018).

The transcriptome of a cell is defined as all the mRNA transcripts within a cell and their quantity at a given point in time. One of the changes that occur at the molecular level during inter-microorganism interactions is changes in the transcriptome. Transcriptomics offers a comprehensive way to study all changes in gene expression of an organism under different conditions and different time points (Pinu *et al.*, 2019a). This change can be monitored and studied using high-throughput technologies such as RNA-Seq or microarrays (Wang *et al.*, 2009).

In addition, the adaptation of gene expression to environmental changes within a microorganism is mediated through complex regulatory networks (Vandermeulen and Cullen, 2022). Network inference predicts gene regulatory interactions based on transcriptome data. The need to analyse and understand the large data sets produced from RNA-seq can be addressed using bioinformatics which combines mathematics, computer science and biological techniques in the management of the data (Consortium, 2015).

The transcriptome of *C. albicans* during interaction with other species has been reported in literature. The periodontal pathogen *S. gordonii* is an example of how it impacts the transcriptional response in *C. albicans*. Many transcriptional changes that occurred in *C. albicans* when in dual-species with *S. gordonii* involved genes expressing proteins resulting in hyphae formation and cellular processes especially those related to oxidative stress and adhesins. Simultaneously, other genes were also involved in transport and translation (Dutton *et al.*, 2016). Another example that impacts the transcriptional response is the cariogenic species *S. mutans*. The presence of *S. mutans* altered the *C. albicans* transcriptome. *C. albicans* genes and proteins associated with carbohydrate metabolism including sugar transport, aerobic respiration, pyruvate breakdown, and the glyoxylate cycle were significantly upregulated. Other *C. albicans* genes directly and indirectly related to cell morphogenesis and cell wall components such as mannan and glucan were also upregulated, indicating enhanced fungal activity in mixed-species biofilm (Ellepola *et al.*, 2019b). Moreover, upregulated genes in dual-species biofilms of *C. albicans* and *S. aureus* were related to gene ontology (GO) involved in virulence, biofilm formation and protein binding such as ACE2 and multiple HSPs (Short *et al.*, 2021).

The inter-species and interkingdom interactions of multispecies biofilms in root-filled canals are poorly understood, and further information on inter-species interactions is needed. Therefore, more in-depth analyses of these interactions are required. In this chapter, transcriptomics has been used to study cell-cell interactions between *C. albicans* and *E. faecalis*. This could be beneficial in revealing the effects that *E. faecalis* has on fungal behaviour.

3.2 Hypothesis and Aims

It has been shown in chapter 2 that *E. faecalis* reduces the virulence of *C. albicans* by inhibiting its growth, biofilm formation and hyphal morphogenesis. As a result, it is logical to speculate that it is very likely that *E. faecalis* will induce significant changes in *C. albicans* transcriptome.

The aims of this chapter were to:

- Investigate and reveal changes that *E. faecalis* may impose on *C. albicans* at the transcriptomic levels using RNA-Seq technology.
- To explore pathways developed in *C. albicans* in response to *E. faecalis*.
- To investigate changes in *C. albicans* virulence, adhesion, and biofilm formation by manually extracting genes involved in these changes.

Publications pertaining to this chapter:

Alshanta OA, Albashaireh K, McKloud E, *et al.* *Candida albicans* and *Enterococcus faecalis* biofilm frenemies: When the relationship sours. *Biofilm*. 2022;4:100072. Published 2022 Mar 14. DOI: 10.1016/j.bioflm.2022.100072

3.3 Materials and methods

3.3.1 Strain and culture conditions

Candida albicans SC5314 and *Enterococcus faecalis* clinical strain ER5/1 were used in this chapter. *C. albicans* was cultured on SAB agar for 48 hours at 30°C. *E. faecalis* ER5/1 was cultured in 5% CO₂ incubator on 5% BA plates for 48 hours. For biofilm formation, overnight cultures of *C. albicans* and *E. faecalis* were grown in YPD and BHI media, respectively, under appropriate culture conditions. Cultures were washed twice with PBS and standardised to 1x10⁶ for *C. albicans* and 1x10⁷ for *E. faecalis*.

3.3.2 Media preparation

The medium THB was supplemented with 10µM menadione and 10µg/mL hemin (ThermoFisher) and mixed 1:1 with RPMI (referred to as 1:1 medium).

3.3.3 *In vitro* transcriptomic analysis of *C. albicans* interactions with *E. faecalis*

Overnight cultures were standardised in 1:1 broth as described above, and *Candida* biofilms grown in T75 cell culture flasks (Corning, USA) for 4 h in 5% CO₂. After incubation, media was removed, and biofilms washed with PBS before *E. faecalis* was added for an additional 4 or 20 hours. At each time point the media was removed and biofilms washed with PBS before being imaged to ensure no contamination and scraped into 1 mL of RNAlater (ThermoScientific, Loughborough, UK). A graphical illustration of the experimental methodology can be found in (Figure 3.1)

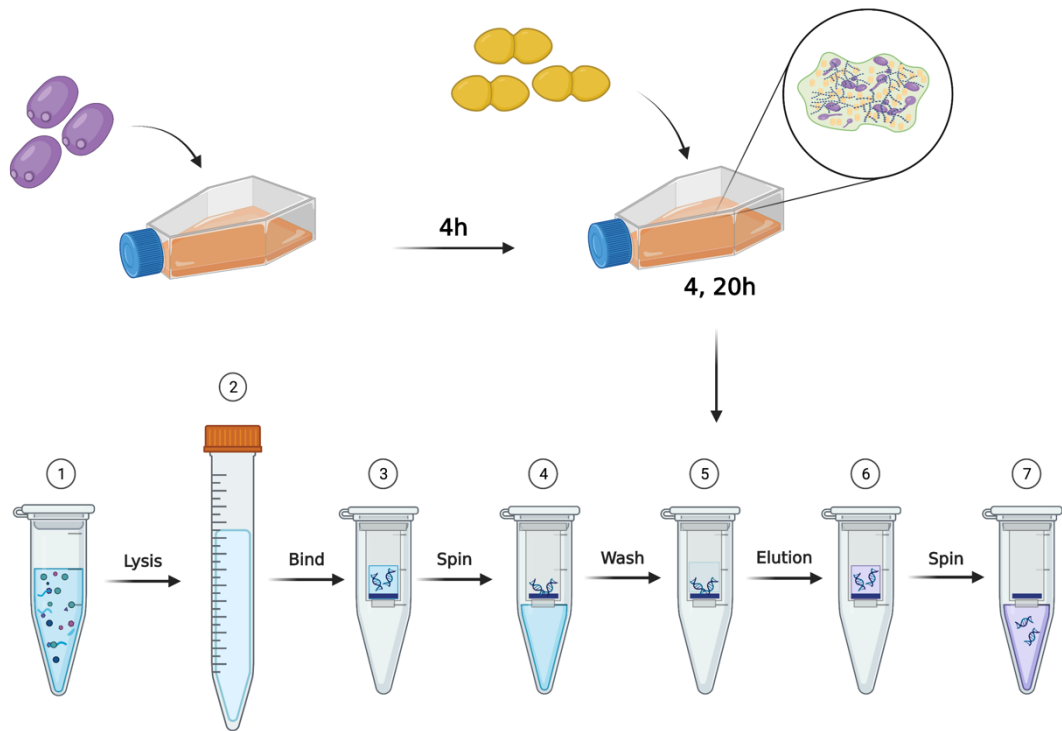


Figure 3.1: Experimental pipeline. *C. albicans* was incubated for 4 hours and then *E. faecalis* strain ER5/1 was added for further 4 hours and 20 hours to make a dual-species biofilm of 8 hours and 24 hours respectively in T75 cell culture flask. Biofilm was scraped into RNA later suspension for RNA extraction. Extractions were performed following manufacturers' instructions. First, biofilm cells were extracted in zirconia beads, then RNA was purified, and bound spin columns and contaminants were washed using manufacturer's buffers. RNA was eluted using 100 μ L nuclease free water. Image was generated using BioRender.

3.3.4 RNA extraction from *C. albicans* and *E. faecalis* biofilms

RNA was extracted from microbial biofilms using the RiboPure™ RNA Purification Kit for yeast (ThermoScientific, Loughborough, UK), following the manufacturer's instructions. Biofilms were centrifuged at >12,000 g for 5 minutes to pellet cells and supernatants were discarded. To each sample, 480 μ L lysis buffer, 48 μ L 10% SDS and 480 μ L of Phenol:Chloroform:IAA were added before the pellet was resuspended by vortexing and the full mixture transferred to bead beating tubes containing 750 μ L of ice-cold zirconia beads. Samples were then beaten for 3x30 seconds-cycles using a BeadBug™ microtube homogenizer (Merck, Gillingham, UK) and centrifuged at 16,100 g for 5 minutes to separate the RNA containing aqueous layer. The aqueous layer was then transferred to a sterile tube before 1.9 mL of binding buffer and 1.25 mL of 100% ethanol was added and gently mixed. The entire sample was then passed through a filter cartridge placed in a collection

tube and the eluate discarded. The filter was then washed with 700 μ L of wash solution 1, followed by washing twice with 500 μ L of wash buffer 2/3. The filter cartridge was then transferred to a fresh collection tube and 25 μ L of pre-heated elution solution added before the sample was centrifuged for 1 minute to collect RNA. Finally, a DNase treatment reaction was assembled and added to each sample for 5 minutes. The reaction was then pelleted and purified and RNA was transferred to a sterile 1.5 mL microcentrifuge tube before being stored at -80°C until analysis. Integrity of RNA was assessed using a Bioanalyser system (Aligent, USA) to ensure highly intact RNA was sent for sequencing analysis. Samples were deemed acceptable if they obtained a minimum RNA integrity number of 7.0 and a minimum quantity of 2.5 μ g. Genome-wide *Candida* transcripts were sequenced using the Illumina NOVASeq6000 sequencing platform (Edinburgh Genomics) to obtain 100bp paired-end reads.

3.3.5 RNA-seq and analysis pipeline

RNA-seq was performed by Edinburgh Genomics (genomics.ed.ac.uk) using a NovaSeq 6000 platform and produced 100 bp paired end reads. FastQC v.1.8.0 was used to assess sequence data quality and produce quality control scores for the produced reads (Wingett and Andrews, 2018). RNA-seq reads were processed by first quality controlled using the software Trimmomatic v0.38 (Bolger *et al.*, 2014) to remove Illumina adapters low quality bases leading=3 and trailing=3 and reads with remaining length of less than 30 bases. Then, HISAT2 (v2.1.0) was used to align and map the reads to a reference *C. albicans* genome (Candidagenomedatabase.org) (Javorka *et al.*, 2019). Samtools (v1.7) (Li *et al.*, 2009) was used to coordinate and sort the SAM files containing the aligned reads which were then converted to BAM format using the same tool. Quality of the alignments was assessed using the software Qualimap (v.2.2.2) and the BAM files for each sample were counted to obtain gene counts with the use of the program HTSeq-count (0.11.0) (Anders *et al.*, 2015, Okonechnikov *et al.*, 2016). A Feature Counts table was gathered and subsequently read into RStudio (version 3.6.3). Differentially expressed genes for pairwise comparisons were analysed using DESeq2 package (v1.26) (Love *et al.*, 2014). The Bioinformatics pipeline is summarised in (Figure 3.2). Quality control, sequence trimming, read alignment

and enumeration were performed with the assistance of Dr Christopher Delaney (University of Glasgow).

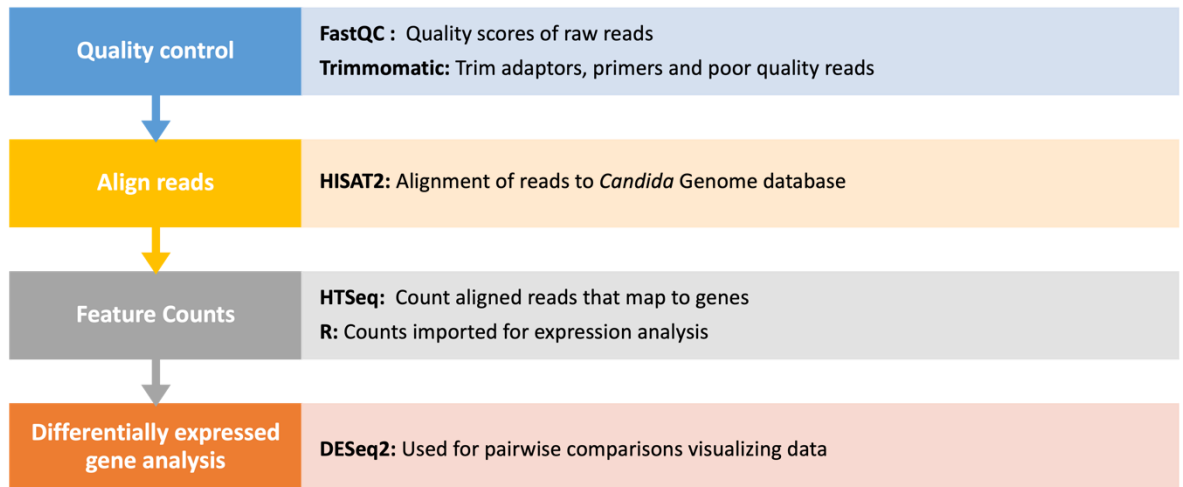


Figure 3.2: Bioinformatics analysis pipeline. A schematic diagram showing the bioinformatics pipeline used in RNA-Seq analysis. Sequences were first assessed and trimmed to achieve high quality reads. Next, reads were aligned to a reference *C. albicans* genome and the number of aligned genes were counted. Then, DESeq2 package was used to perform pairwise analysis to assess differentially expressed genes.

3.3.6 Statistical Analysis

Figures in this chapter were produced using different packages in Rstudio to visualize differential gene expression analysis. Pairwise comparisons were performed between samples using the DESeq2 package (v1.26). Genes were considered significantly differentially expressed between both conditions when the cut-off \log_2 fold change (Log_2FC) ≥ 1.5 and adjusted p-value of ≤ 0.05 were met. Following that, ClueGo application in Cytoscape (v3.7.2) (cytoscape.com) was used to display gene interaction networks. ClueGO (v2.5.7) plugin was used to annotate and group the genes functionally using GO into categories represented by the most significant term utilizing the hypergeometric test. CluePedia (v1.5.8) was used to integrate genes into networks. Functional categories were considered enriched when the adjusted p value (P_{adj}) was ≤ 0.05 . ClueGO genes interaction networks were grouped by function, considering their three GO terms; molecular functions (MF), cellular components (CC) and biological processes (BP) (Bindea *et al.*, 2009, Shannon *et al.*, 2003).

3.4 Results

3.4.1 *E. faecalis* induced major transcriptomic changes in *C. albicans* in mixed-species biofilms

Previous data from this PhD (Chapter 2) showed that *E. faecalis* has had a clear impact on *C. albicans* by reducing its metabolic activity, biofilm biomass and growth in the dual-species biofilm. This effect was distinct at 8 hours and 24 hours' time points. In contrast, *E. faecalis* was less affected by *C. albicans* presence; a finding that made the focus more on the transcriptomic changes in the eukaryotic pathogen *C. albicans*. In addition, HVS ER5/1 was chosen because it is a clinical strain retrieved from root canal treated teeth and the *C. albicans* virulence response was strain dependent.

3.4.1.1 Differential Expression Analysis

Differential expression analysis was performed to identify transcriptional changes in *C. albicans* biofilms when interacting with *E. faecalis*. Multivariate principal component analysis (PCA) shows a variance (67%) between samples by time points (8 hours and 24 hours) in the presence of *E. faecalis*. The second variance between samples was 20% at 24 hours (single species and dual-species) (Figure 3.3).

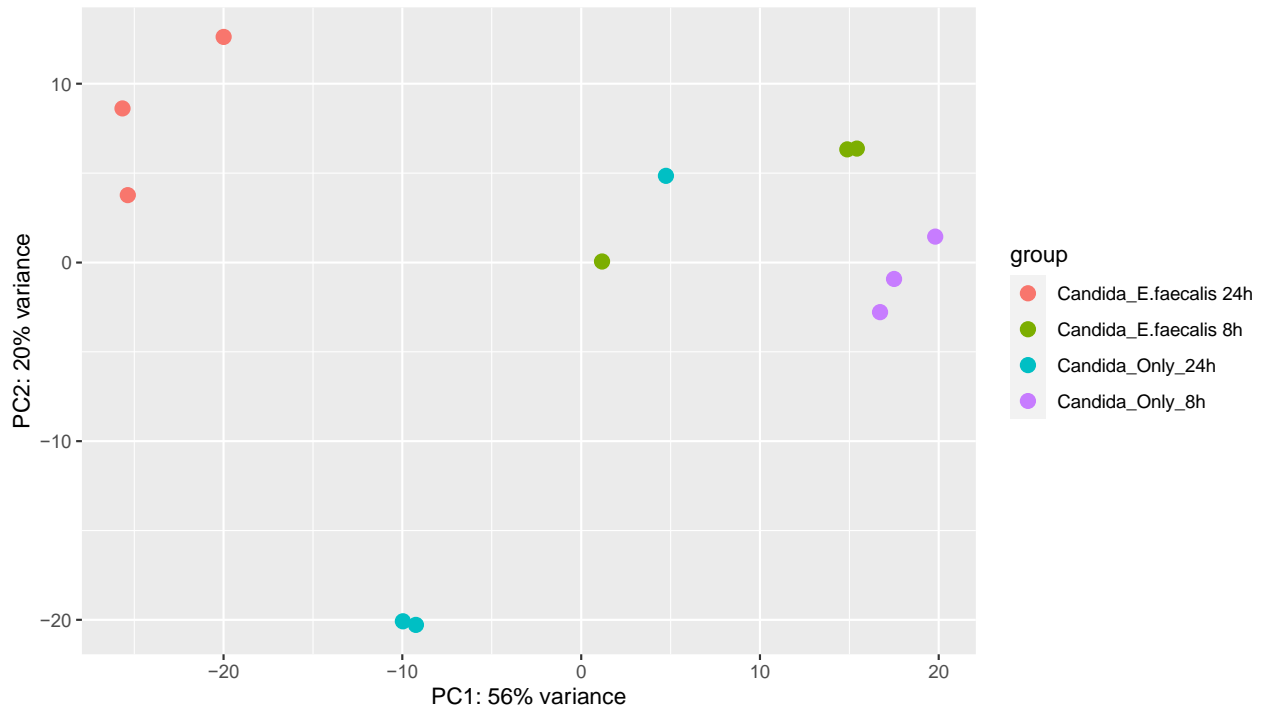


Figure 3.3: Presence of *E. faecalis* determines mature biofilm transcriptome. PCA plot shows distinct grouping of each sample. PCA plot displays variables of largest variance along PC1 (56%) and second largest along PC2 (20%).

3.4.1.2 Co-expression Venn diagram

The co-expression Venn diagram presents the number of genes that were upregulated (Figure 3.4) and downregulated (Figure 3.5) in each time point of 8 hours and 24 hours. A total of 69 genes were upregulated at 8 hours and 24 hours; 6 of these genes were only upregulated in 8 hours and 60 genes were upregulated only in 24 hours. Three genes were upregulated at both time points. A total of 32 genes were downregulated at 8 hours and 24 hours; 12 genes were downregulated only at 8 hours and 17 genes were downregulated at 24 hours only. This was based on the False Detection Rate (FDR) (P_{adj}) cut-off applied with a statistical significance of $P_{adj} \leq 0.05$. Another filtering technique was used to identify the highly upregulated and downregulated genes based on the Log_2FC . All the genes with a Log_2FC more than 1.5 were considered overly upregulated and all genes with a Log_2FC less than -1.5 were considered overly downregulated (Figure 3.4).

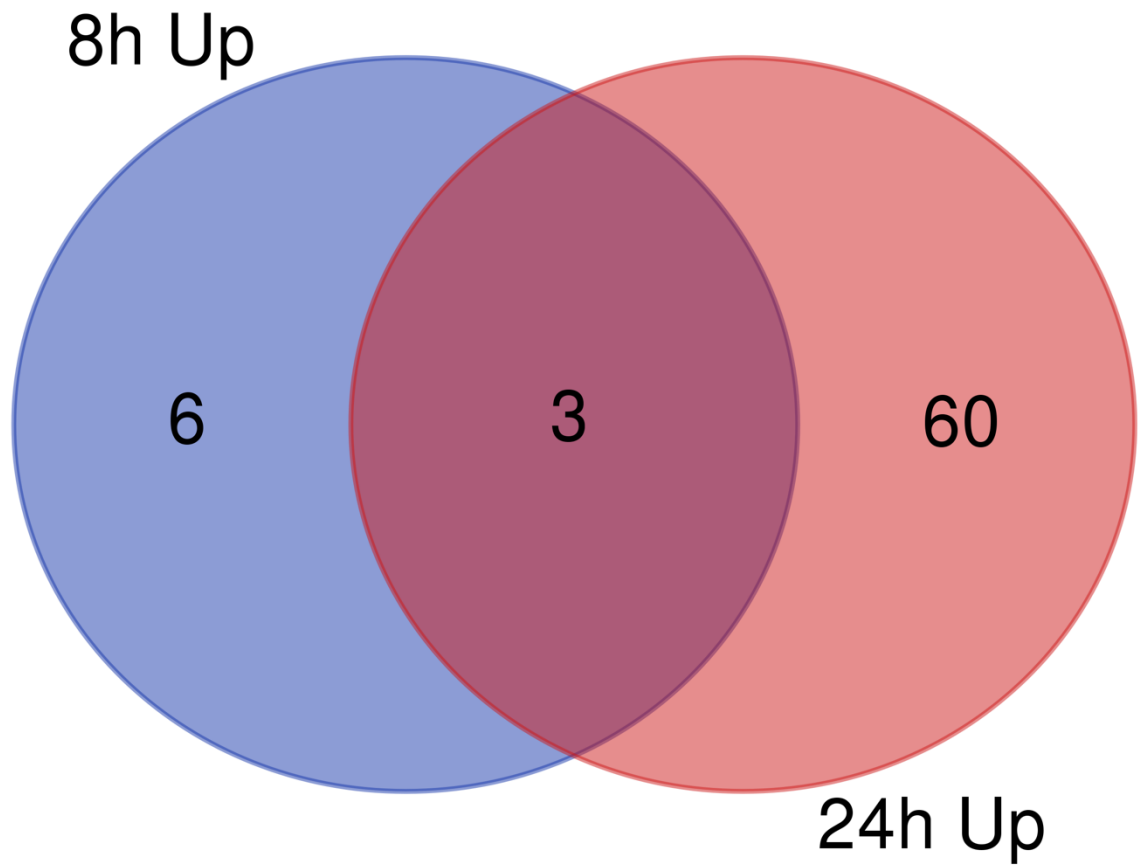


Figure 3.4: *Enterococcus faecalis* induces specific gene upregulation in *C. albicans* at 8 hours and 24 hours. Venn diagram showing the number of genes upregulated in dual-species biofilm at 8 hours and 24 hours. Blue circle represents upregulated genes at 8 hours' time point, and red circle represents upregulated genes at 24 hours' time point. (h denotes hour)

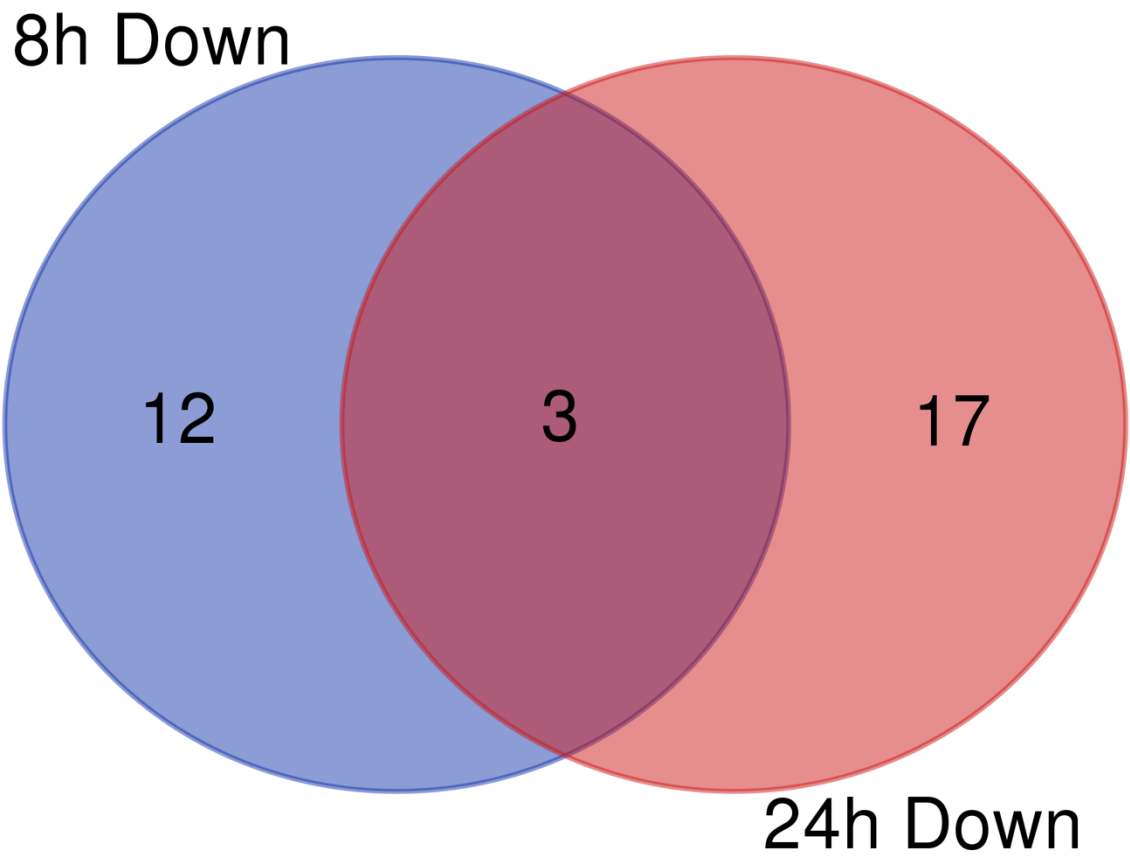
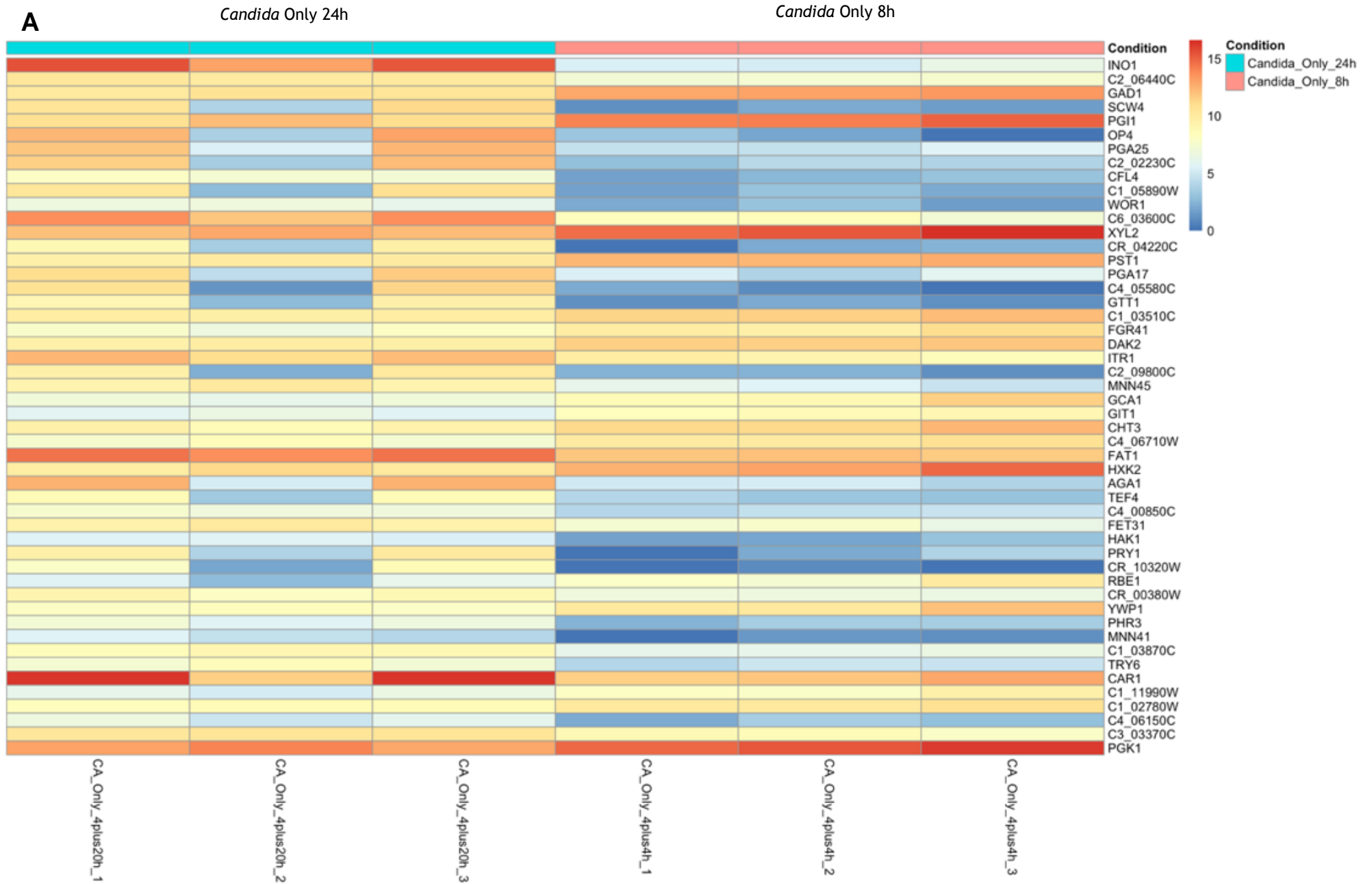


Figure 3.5: *Enterococcus faecalis* induces specific gene downregulation in *C. albicans* at 8 hours and 24 hours. Venn diagrams showing the number of genes differentially expressed in dual and single species biofilm at 8 hours and 24 hours. Blue circle represents downregulated genes at 8 hours time point, and red circle represents downregulated genes at 24 hours' time point. (h denotes hour)

3.4.1.3 Heatmaps and Volcano plots reveal different transcriptomic profile at 8 hours and 24 hours in *C. albicans* when in dual-species compared to mono-species biofilm.

The heatmap in (Figure 3.6: A) shows the first 50 most differentially expressed genes in *C. albicans* mono-species biofilm at 8 hours and 24 hours and the volcano plot in (Figure 3.6: B) shows the genes differentially expressed at 8 hours and 24 hours in *C. albicans* mono-species biofilm. *C. albicans* had different gene profiles differentially expressed when in single-species biofilm at both time points (Figure 3.6: A, B) compared to dual-species biofilm (Figure 3.7: A, B). Further elaboration on these genes will be given when each time point is discussed.

ClueGO tool created gene interaction networks that were grouped by function. These networks revealed the distinct pathways involving these genes. It is clear that the transcription profile of *C. albicans* when cocultured with *E. faecalis* (Figure 3.8: A) is different from that in *C. albicans* mono-species biofilm (Figure 3.8: B). The interaction networks show that genes involved in transmembrane transport activity, chaperone cofactor-dependent protein refolding, fungal biofilm matrix, oxidoreductase activity, co-enzyme binding and neurotransmitter catabolic process were differentially expressed in dual-species biofilm. Oxidoreductase activity and fungal biofilm matrix pathways were the most significantly expressed ($P < 0.0005$) in dual-species biofilm followed by transmembrane transport activity and genes that encodes proteins mainly function at plasma membrane in addition to heat shock response pathway (Figure 3.8: A). However, in *C. albicans* mono-species biofilm, genes involved in heme-binding and cellular carbohydrate metabolic process were upregulated (Figure 3.8: B).

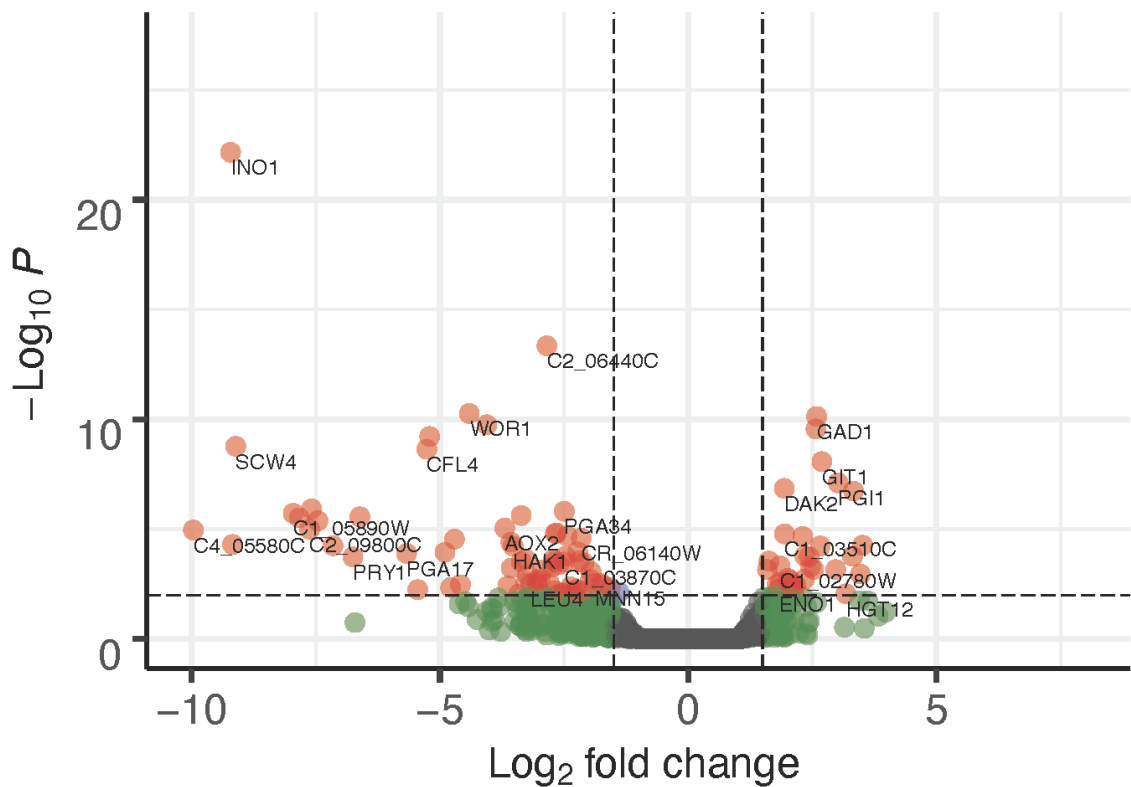


B

Candida_Only_24h_vs_Candida_Only_8h

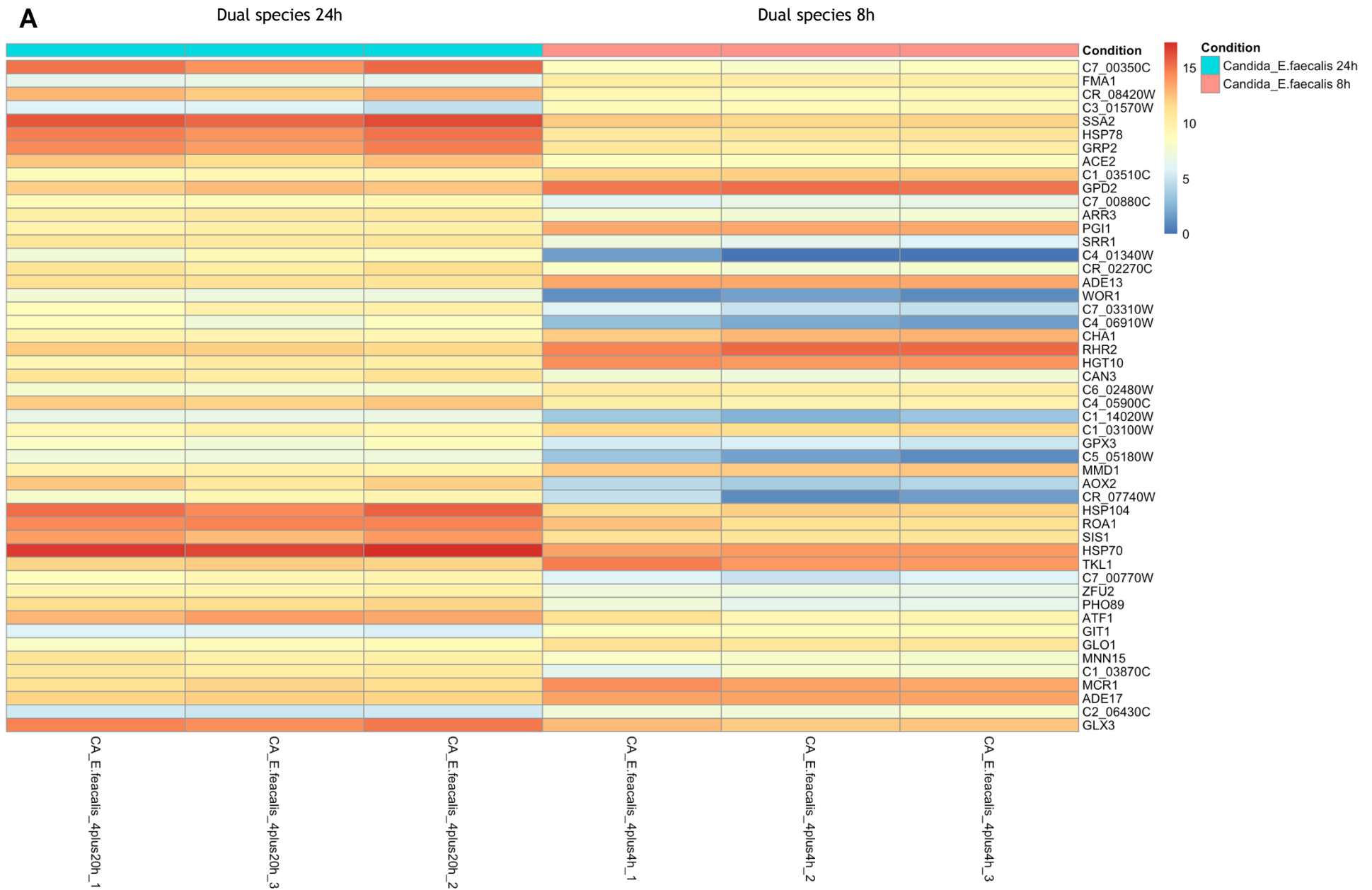
Volcano Plot Candida_Only_24h = -ve Candida_Only_8h = +ve

● NS ● Log₂ FC ● p-value ● p-value and log₂ FC



FC cutoff, 1.5; p-value cutoff, 10e-3

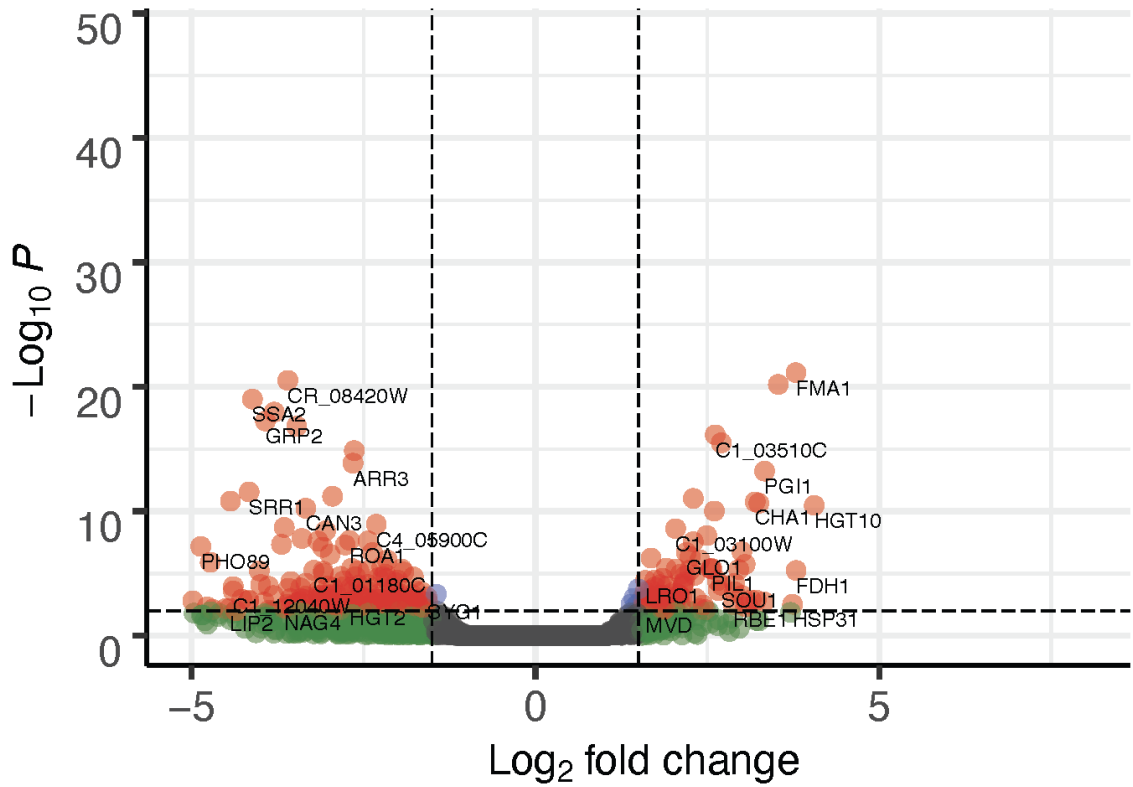
Figure 3.6: Heatmap and Volcano plot for *C. albicans* in mono-species biofilm transcription profile. (A) heatmap showing top 50 differentially expressed genes in *C. albicans* mono-species biofilm at 8 hours and 24 hours (B) Volcano plot depicting upregulated genes in *C. albicans* mono-species biofilm at 8 hours and 24 hours. Volcano plot shows Log₂FC versus the negative Log₁₀ of the Padj. Genes of interest can be identified where expression levels are above or below the Log₂FC cut-offs of -1.5 and 1.5 (green) and those that are also highly significant (P < 0.01; red). (H denotes hour)



B Candida_E.faecalis 24h_vs_Candida_E.faecalis 8h

Volcano Plot Candida_E.faecalis 24h = -ve Candida_E.faecalis 8h = +

● NS ● Log₂ FC ● p-value ● p-value and log₂ FC



FC cutoff, 1.5; p-value cutoff, 10e-3

Figure 3.7: Heatmap and Volcano plot for *C. albicans* in dual-species biofilm transcription profile. (A) heatmap showing top 50 differentially expressed genes in *C. albicans* dual-species biofilm at 8 hours and 24 hours (B) Volcano plot depicting upregulated genes in *C. albicans* dual biofilm at 8 hours and 24 hours. Volcano plot shows Log₂FC versus the negative Log₁₀ of the Padj. Genes of interest can be identified where expression levels are above or below the Log₂FC cut-offs of -1.5 and 1.5 (green) and those that are also highly significant (P < 0.01; red). (H denotes hour).

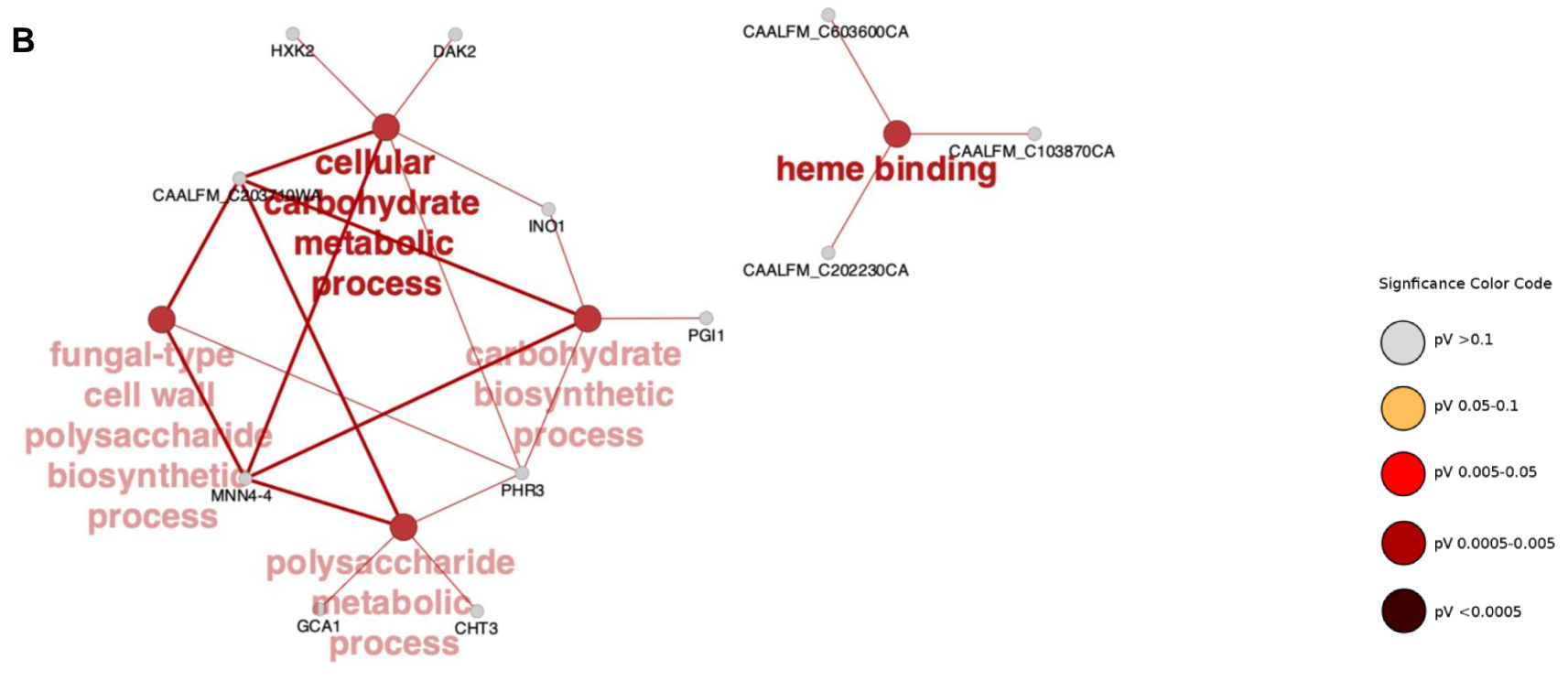
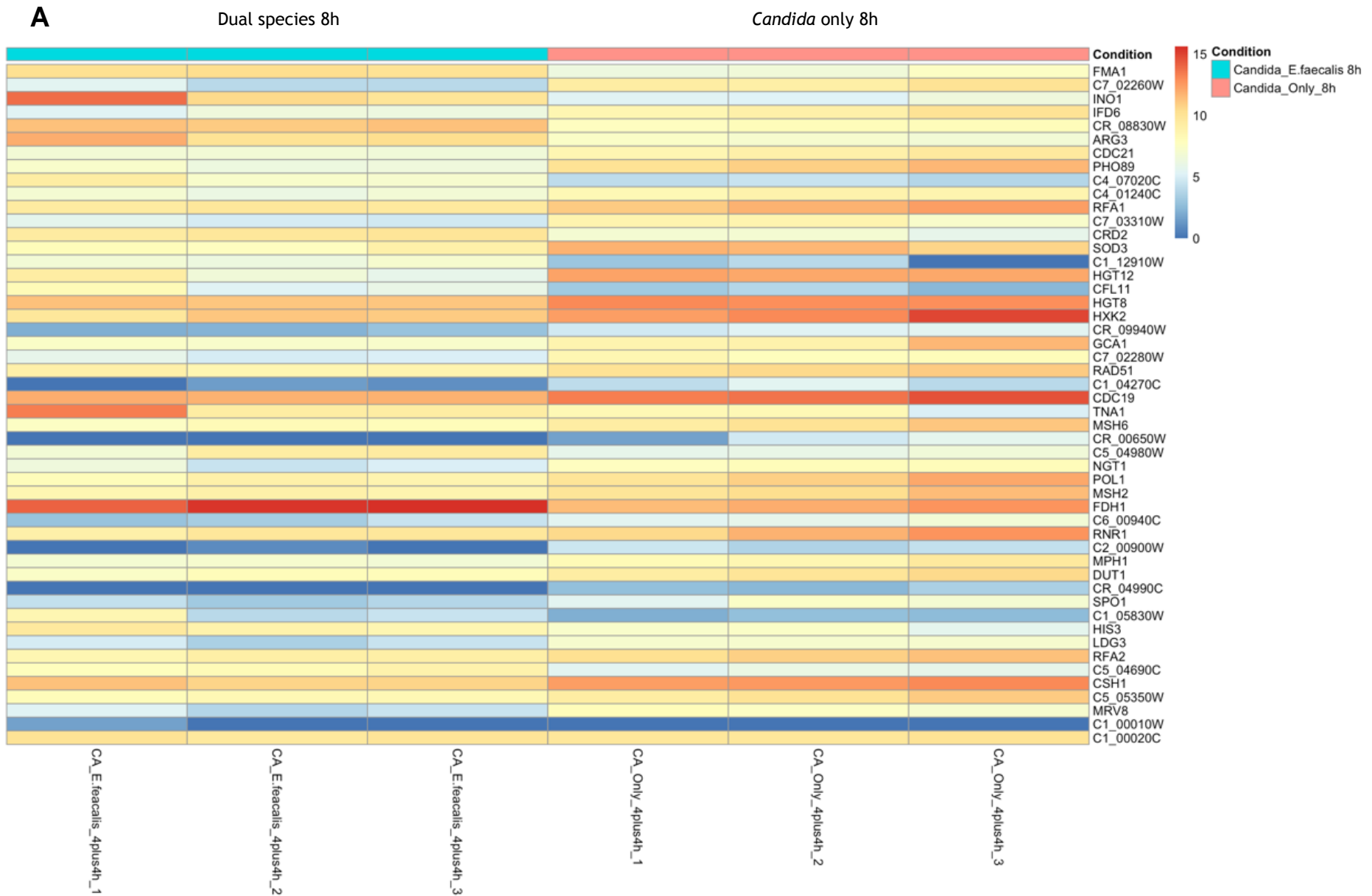


Figure 3.8: *E. faecalis* induces significant changes in different metabolic pathways in *C. albicans* at 8 hours and 24 hours compared to *C. albicans* mono-species biofilm. Gene networks show interactions between upregulated genes specific to *C. albicans* in dual-species biofilm (A) and *C. albicans* mono-species biofilm (B) at 8 hours and 24 hours. Genes of similar function are grouped together to form nodes (circles) and nodes with similar functions are linked by edges lines. Nodes are coloured by levels of significance and node size increases

3.4.1.4 *E. faecalis* reduced carbohydrate metabolic process and sugar transport activity and enhanced oxidoreductase activity, fungal biofilm matrix and arginine biosynthetic process in *C. albicans* at 8 hours' time point.

Heatmaps and volcano plots show the differentially expressed genes at 8 hours' time point (Figure 3.9: A, B). Heatmap shows the 50 first genes that were significantly differentially expressed with Log_2FC cut-off = 1.5. Genes that were significantly downregulated are genes encoding glucose transporters; HGT8, HGT12 and hexokinase HXK2 and the pyruvate kinase CDC19. In addition, genes encoding the phosphate transporter PHO89, superoxide dismutase 3 SOD3, and the aldo-keto reductase (AKR) IFD6 and thymidylate synthase CDC21 are significantly downregulated. Genes encoding oxidoreductase FMA1, formate dehydrogenase FDH1 and INO1, arginase ARG3, and enzyme of histidine biosynthesis HIS3 were amongst the significantly upregulated genes (Figure 3.9: A, B).

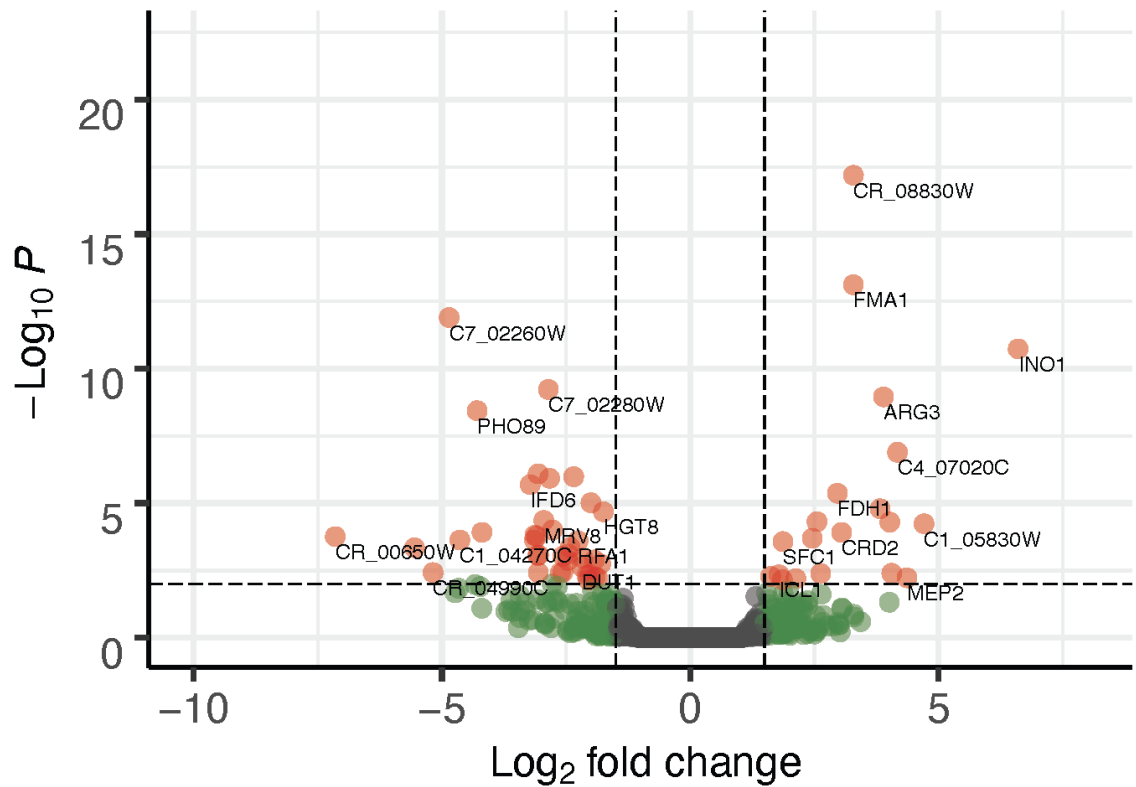


Candida_Only_8h_vs_Candida_E.faecalis_8h

Volcano Plot Candida_Only_8h = -ve Candida_E.faecalis 8h = +ve

B

● NS ● Log₂ FC ● p-value and log₂ FC



FC cutoff, 1.5; p-value cutoff, 10e-3

Figure 3.9: Heatmap and Volcano plot for *C. albicans* + *E. faecalis* dual-species vs. *C. albicans* mono-species biofilm transcription profile at 8 hours. (A) heatmap showing top 50 differentially expressed genes in *C. albicans* mono-species biofilm at 8 hours (B) Volcano plot depicting upregulated (right) and downregulated genes (left) in *C. albicans* mono-species biofilm at 8 hours. Volcano plot shows Log₂FC versus the negative Log₁₀ of the P_{adj}. Genes of interest can be identified where expression levels are above or below the Log₂FC cut-offs of -1.5 and 1.5 (green) and those that are also highly significant (P < 0.01; red). (h denotes hour).

The Gene Ontology analysis of differentially expressed genes revealed several groups were significantly upregulated at 8 hours' time point (Figure 3.10:B). Genes involved in oxidoreductase activity pathway were amongst the most significantly upregulated ($P= 0.0005 - 005$). These included genes *CFL11*, *CRD2* and *FMA1*. The gene *CFL11* encodes nicotinamide adenine dinucleotide phosphate (NADPH) oxidase for generating a burst of ROS. Furthermore, *CRD2* encodes a metallothionein that is produced during oxidative stress and well known to protect *C. albicans* against heavy metals is expressed in the presence of copper. *FMA1* is a gene involved in catalysis of redox reaction.

Moreover, amongst the pathways that were significantly upregulated was the arginine biosynthesis. *ARG3* which encodes an ornithine carbamoyltransferase, is a sub pathway in the arginine biosynthesis pathway. In addition, *INO*, a gene that encodes inositol-7-phosphate synthase was also upregulated.

The GO analysis revealed that pathways associated with carbohydrate metabolism were significantly downregulated ($P<0.0005$) (Figure 3.10:A). This pathway involves genes that encode sugar sensing and transportation like *HGT8* which encodes a high affinity glucose transporter, and *HGT12* which encodes glucose, fructose, and mannose transporter. The gene *HXK2* encodes hexokinase which is the main glucose phosphorylating enzyme in the glycolytic pathway. The *GCA1* gene that encodes a glucoamylase, an enzyme involved in carbohydrate metabolism, was also downregulated. The gene *PHO89*, that encodes phosphate permease responsible for inorganic phosphate ion transportation across the plasma membrane, was also downregulated. In addition, the *SOD3* gene encodes a superoxide dismutase that plays a vital role in ROS catalysis. *IFD6*, a gene that encodes an alcohol dehydrogenase was also downregulated.

Furthermore, genes involved in DNA stabilisation and repair pathways were significantly downregulated; *RFA1*, a gene that encodes DNA replication factor involved in DNA replication, repair, and recombination, in addition to *CDC21*, a gene that encodes single stranded DNA binding protein.

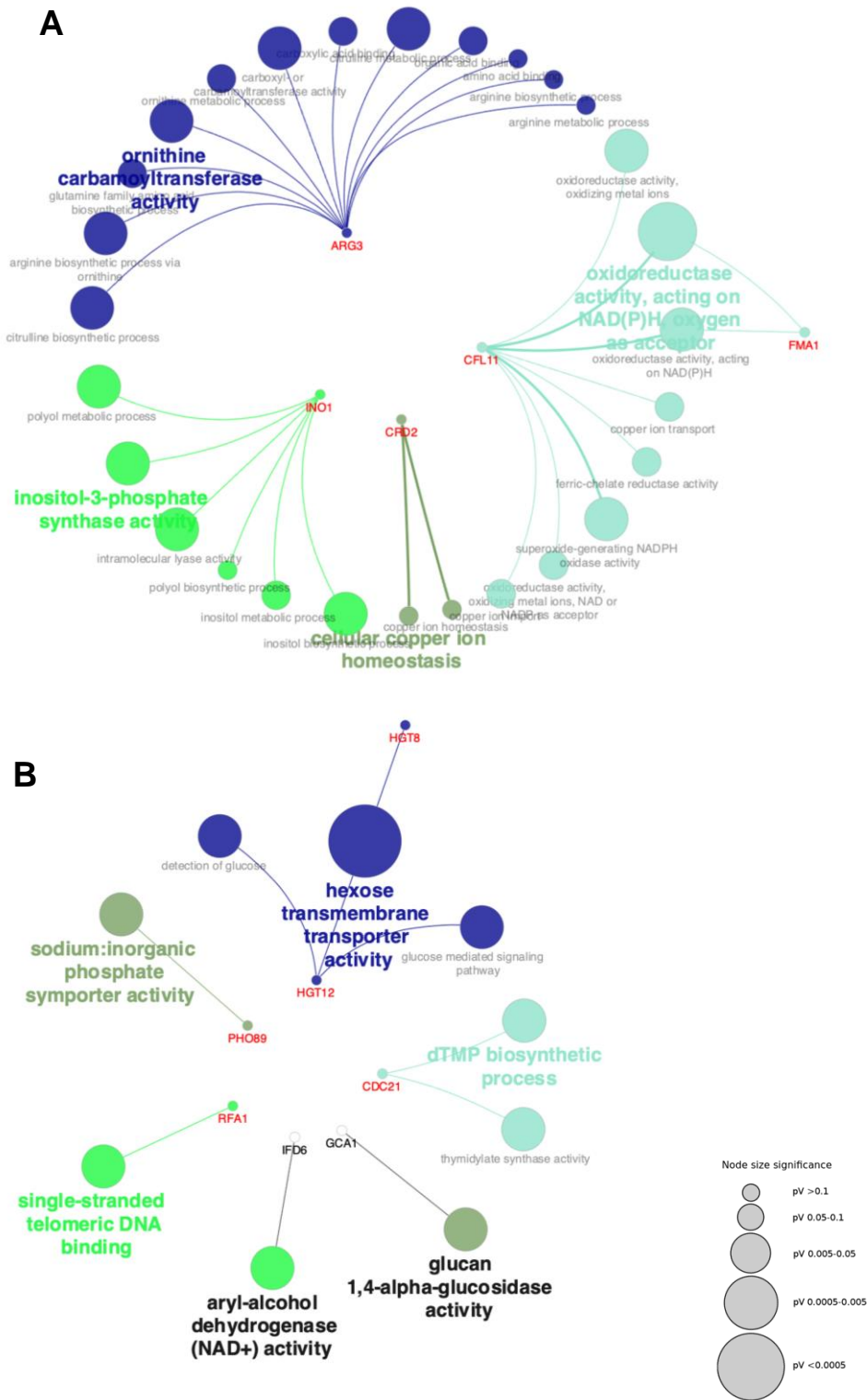


Figure 3.10: *E. faecalis* induced significant upregulation and downregulation of different metabolic pathways in *C. albicans* at 8 hours. Gene networks show interactions between upregulated genes (A) and downregulated genes (B) specific to *C. albicans* in dual-species biofilm at 8 hours. Genes of similar function are grouped together to form nodes (circles) and nodes with similar functions are linked by edges (lines). Nodes are coloured by group cluster node size increases with significance and the number of genes involved in each function. Networks were created using ClueGO and CluePedia

3.4.1.5 *E. faecalis* enhanced stress response, transmembrane transport activity and induced amino acid starvation while reducing arginine catabolic process in *C. albicans* at 24 hours' time point.

Heatmaps and volcano plots show the differentially expressed genes at 24 hours' time point as demonstrated in (Figure 3.11: A, B and Figure 3.12). The heatmap shows the first 50 genes that were significantly differentially expressed with Log_2FC cut-off = 1.5 (Figure 3.11:A). The genes HSP78, SIS1, SSA2, HSP104, HSP90, LYS22, ARO3, HIS5, HIS4, MEP2, ATF, GPX, GOR1 were amongst the ones that were significantly downregulated. Moreover, GPD2, RHR2, HGT8, 10, LDG3, LRO1 were also significantly downregulated (Figure 3.11: A, B). GO analysis using ClueGO was used to further explore pathways and biological functions of these genes and the results are depicted in (Figure 3.12).

The GO analysis revealed the upregulation of amino acid biosynthesis related genes (Figure 3.12: RED); *ARG3*, *LYS22*, *HIS4*, *HIS5*, *ARO3*, *LEY42*, in addition to genes that encodes aminotransferases *BAT21*, *BAT22*. One gene, *MEP2*, which encodes ammonium transferase enzyme responsible for amino acid transfer was significantly upregulated. In addition, another gene that was significantly upregulated is *PCL5* which encodes a cyclin for PHO85 kinase. The latter, PHO85 kinase, is responsible for the degradation of the transcription factor GCN4 which is mainly involved in amino acid starvation response to encourage amino acid biosynthesis.

Also, GO analysis for differentially expressed genes revealed the upregulation of oxidoreductase activity pathway. Several genes were differentially expressed in this oxidative response. *GLX3*, a gene that codes glutathione independent glyoxalase which is part of the glutathione glyoxalases that mainly detoxify the highly toxic methylglyoxal to D-lactate. *GPX3* is a gene that encodes Glutathione peroxidase; an enzyme that protects the organisms from oxidative damage. *GRP2*, is also and NAD(H) methylglyoxal oxidoreductase enzyme involved in methylglyoxal metabolism (Figure 3.12).

Amongst the genes that were significantly upregulated are the genes involved in alcohol metabolic process. *GOR1*, a gene that encodes an enzyme involved in glyoxylate catabolic process in the glyoxylate cycle. CR_06770 is L-azetidine-2-

carboxylic acid transferase that reduces alcohol. *ATF1* which encodes an alcohol acetyltransferase.

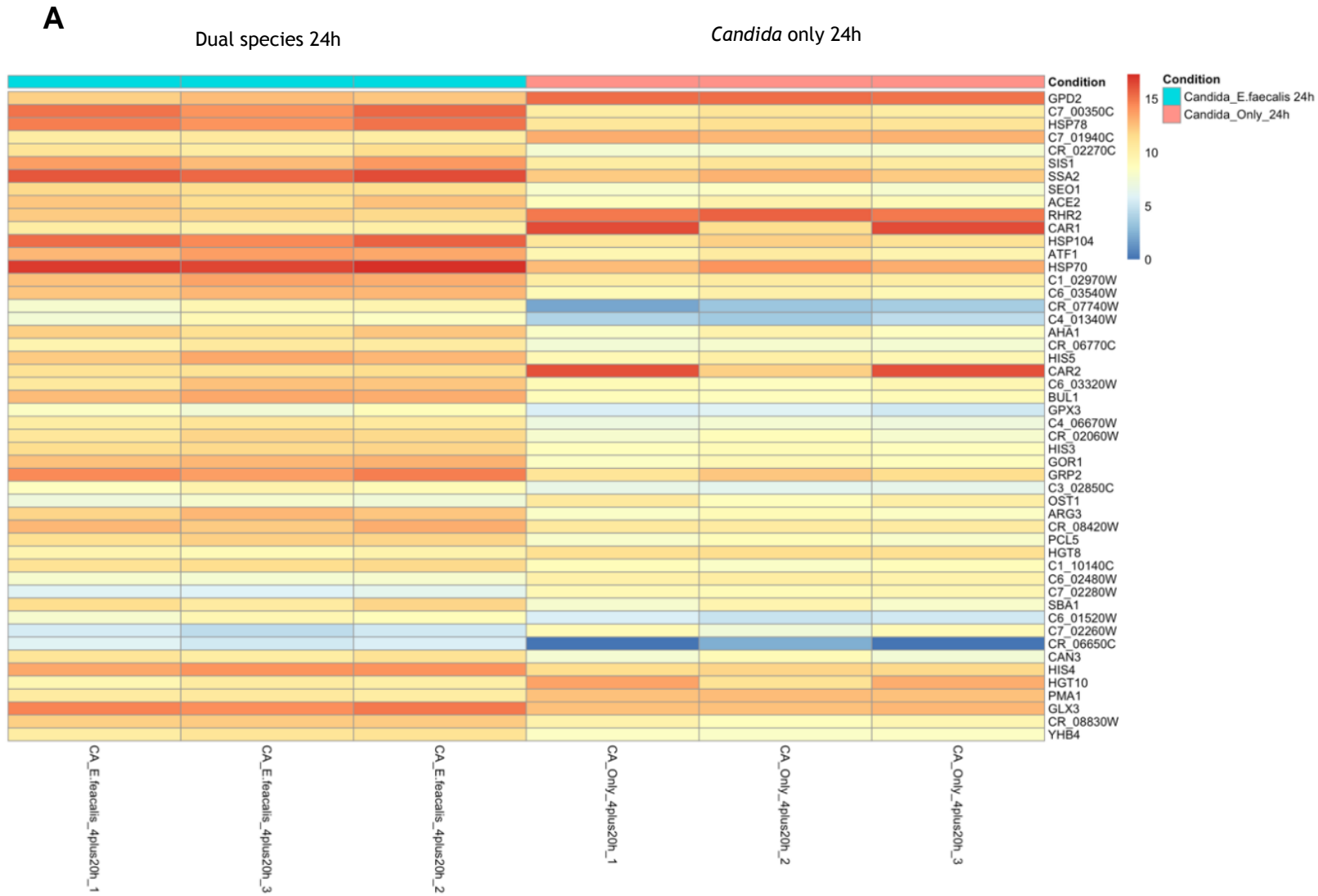
In addition, a series of heat shock response genes were significantly upregulated. *CDC37*, *AHA1* encoding HSP90 co-chaperones were upregulated in *C. albicans* in the mixed-species biofilm. In addition, genes encoding other HSPs such as *HSP70*, *HSP104*, *HSP78*, *SSA1*, *SSA2* were also upregulated. *HSP78* acts in concert with mitochondrial *HSP70*, for the dissociation, solubilization and refolding of damaged proteins aggregates in the mitochondrial matrix after heat stress. Moreover, *HSP90* was amongst the HSPs that were significantly upregulated. *ACE2*, a gene that encodes a cell wall protein transcription factor was also upregulated.

Lastly, *YHB4* and *C4_06910* genes were upregulated. *YHB4* encodes a putative flavohemoglobin which is a protein that has been shown to be induced during nitrosative stress. *C4_06910* encodes PDR-subfamily ABC transporter.

Several genes were downregulated at 24 hours' time point as shown in (Figure 3.12: Blue). The most significant being those involved in arginine catabolism pathway ($p = 0.005-0.05$); *CAR1* gene that encodes arginase and *CAR2* gene that encodes ornithine transferase enzyme. Moreover, GO analysis of data showed that the genes involved in glycerol biosynthesis pathway were downregulated. Genes involved in this pathway are *RHR2* and *GPD2* which encode glycerol 3 phosphatase and glycerol 3-P dehydrogenase enzymes respectively. Furthermore, *HGT10* a gene that encodes glycerol permease which enhances glycerol uptake was downregulated. In addition, *LRO1* that encodes triacylglycerol formation by an acyl-CoA independent pathway was also downregulated (Figure 3.12: Blue).

Genes involved in the cell wall mannoprotein biosynthetic process were downregulated (Figure 3.12: Blue). Data showed that genes involved in the N-glycosylation of proteins catalytic process involved the presence of oligosaccharyl transferase, OST protein were downregulated. *OST1* which encodes a subunit of the OST complex and mainly involved in the catalytic process for N-glycosylation of proteins was downregulated in addition to *PMI* which encodes a mannose-6-phosphate isomerase. Moreover, the gene *PLB4.5* that encodes a phospholipase was also downregulated. Lastly, *PMA1*, a gene that encodes a plasma membrane

H⁺ ATPase was also downregulated in addition to *HGT8* which as mentioned previously encodes is a high affinity glucose transporter.



B *Candida_Only_24h_vs_Candida_E.faecalis_24h*

Volcano Plot *Candida_Only_24h* = -ve *Candida_E.faecalis_24h* = +ve

● NS ● Log_2 FC ● p-value and log_2 FC

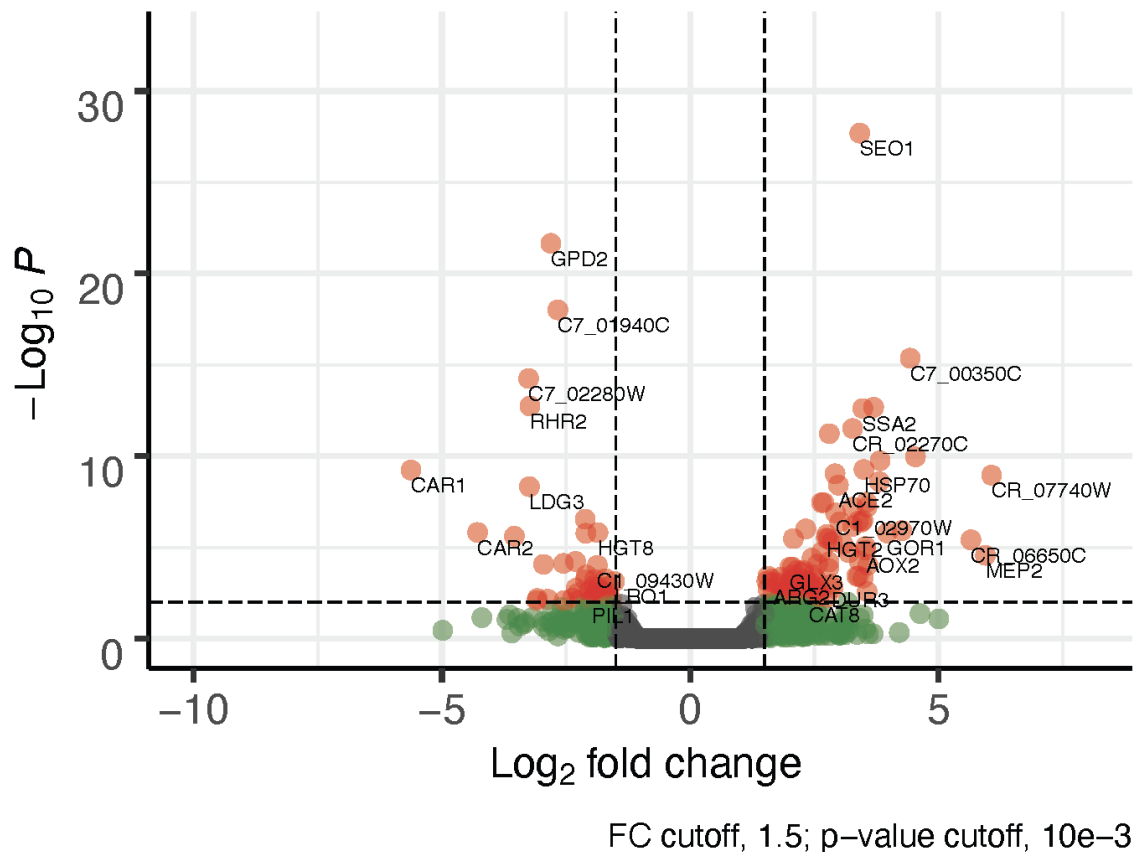


Figure 3.11: Heatmap and Volcano plot for *C. albicans* and *E. faecalis* dual-species VS *C. albicans* mono-species biofilm transcription profile at 24 hours. (A) heatmap showing top 50 differentially expressed genes in *C. albicans* mono-species biofilm at 24 hours (B) Volcano plot of upregulated genes in *C. albicans* mono-species biofilm at 24 hours. Volcano plot depicting Log_2FC versus the negative Log_{10} of the P_{adj} . Genes of interest can be identified where expression levels are above or below the Log_2FC cut-offs of -1.5 and 1.5 (green) and those that are also highly significant ($P < 0.01$; red). (h denotes hour).

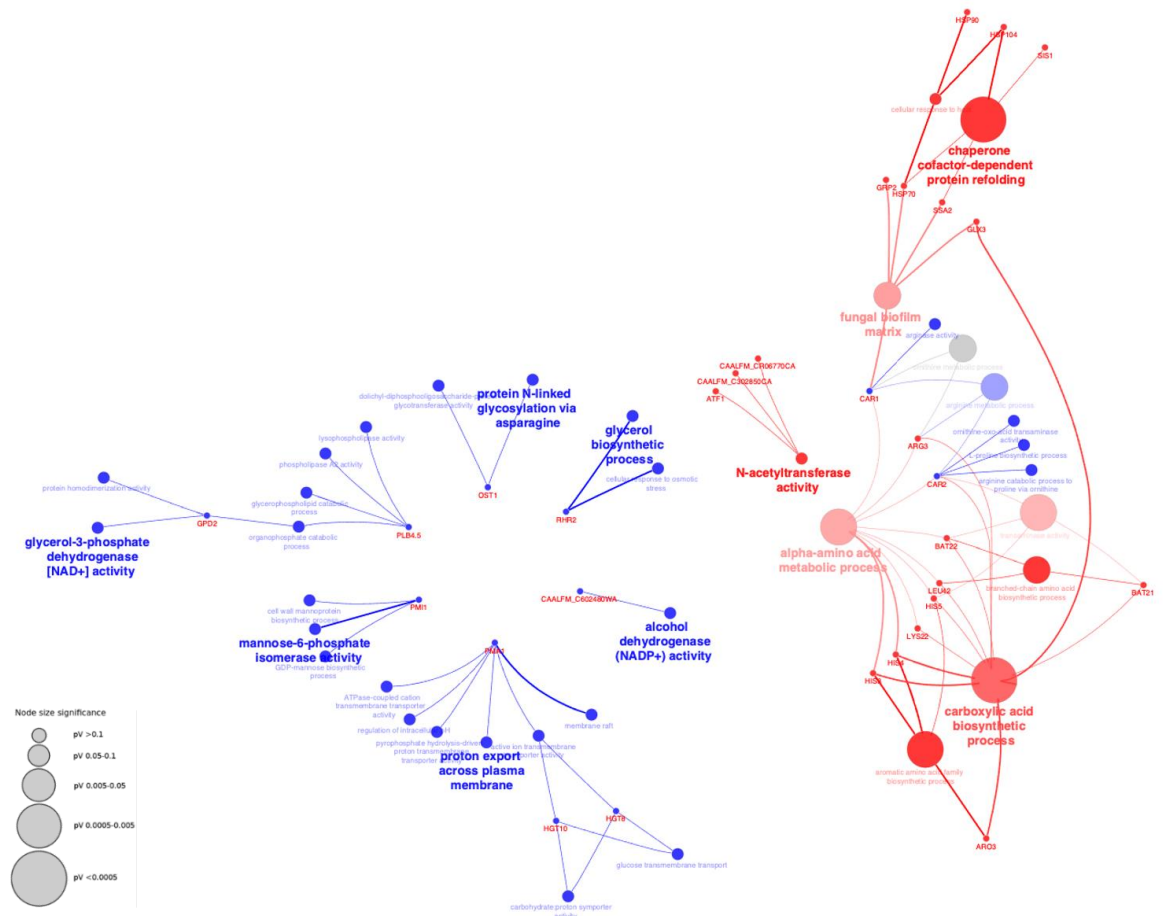


Figure 3.12: *E. faecalis* induced significant upregulation and downregulation of different metabolic pathways in *C. albicans* at 24 hours. Gene networks show interactions between upregulated genes (Red) and downregulated genes (Blue) specific to *C. albicans* in dual-species at 24 hours. Genes of similar function are grouped together to form nodes (circles) and nodes with similar functions are linked by edges (lines). Nodes are coloured by group cluster node size increases with significance and the number of genes involved in each function. Networks were created using ClueGO and CluePedia

3.4.2 *E. faecalis* downregulated key genes involved in virulence, growth and biofilm formation

As detailed in the previous results section. *E. faecalis* induced major changes on *C. albicans* metabolic pathways in a dual-species biofilm compared to mono-species. Although metabolic adaptability is a key factor in determining *C. albicans* virulence behaviour, further exploration of *E. faecalis* effect on other virulence mechanism in *C. albicans* like adhesion, biofilm formation, hydrolase enzyme secretion and growth was carried out. Key genes involved in these virulence mechanisms were manually extracted from data table generated by performing DESeq2 analysis. Genes that passed the 1 Log₂FC were chosen and plotted in the following sections.

3.4.2.1 *E. faecalis* altered the expression of genes involved in *C. albicans* biofilm formation, adhesion, and hydrolytic enzyme secretion.

Some genes involved in biofilm formation were selected (Figure 3.13: A). Amongst these genes a set of GPI anchored adhesins that were shown to contribute to biofilm formation (Nobile *et al.*, 2012) were downregulated; *FAV2*, *PGA6*, *PGA32* were downregulated by more than one Log₂FC at 24 hours' time point. *PGA6* was also downregulated by 1.4 Log₂FC at 8 hours and by 1 log₂FC at 24 hours. *PGA32* was downregulated by 1.4 at 24 hours. A gene that encodes the transcriptional repressor involved in biofilm formation, *NRG1*, was also downregulated at 24 hours' time point by 1.1 Log₂FC. This transcription factor is involved in true biofilm formation and virulence regulation of *Candida albicans* (Uppuluri *et al.*, 2010b). Moreover, it directs transcriptional repression of a subset of filament-specific genes such as *HWP1*, *HYR1* (Murad *et al.*, 2001) which were also shown to be downregulated at 24 hours by 1.9- and 1.5 Log₂FC respectively. The PBR1 protein that is required for adhesion, cohesion, and biofilm formation (Nett *et al.*, 2009) was downregulated by 3.1 Log₂FC. The transcriptional regulatory protein, *UME6* controls the level and duration of gene expression in filamentous growth program and promotes filamentous biofilms and is specifically important for hyphal elongation and germ tube formation (Banerjee *et al.*, 2008). *UME6* was downregulated by 1.6 Log₂FC at 24 hours.

One of the main genes involved in biofilm formation is *CHK1*, it encodes a histidine protein kinase. This gene regulates cell wall mannan and glucan biosynthesis (Kruppa *et al.*, 2003). It also regulates hyphal formation, biofilm formation and virulence (Nobile *et al.*, 2012). It participates in covering beta glucans underneath dense mannan layer which helps in evading immune system (Klippel *et al.*, 2010). This *CHK1* gene was upregulated by 1.2 Log₂FC at 24 hours. In addition, *TEC1* transcription factor which regulates genes involved in hyphal development, cell adhesion, biofilm development, and virulence (Nobile *et al.*, 2012). This *TEC1* gene was upregulated by 1.6 Log₂FC at 8 hours' time point. *GCN4* is an amino acid starvation response transcription factor. It has positive response to biofilm formation (Nobile *et al.*, 2012). The gene that encodes *GCN4* was upregulated at 8 and 24 hours by 1.3 and 2 Log₂FC respectively. *PGA10* is a heme binding protein that acquires iron from host tissue and is involved in biofilm formation as well; this gene was upregulated at 24 hours by 1.4 Log₂FC (Weissman and Kornitzer, 2004, Nett *et al.*, 2009).

Regarding biofilm matrix regulation, the results showed that the *C. albicans* zinc-response transcription factor *CSH1*, the negative regulator of biofilm matrix (Nobile *et al.*, 2012, Nobile *et al.*, 2009) was downregulated by 1.3 Log₂FC at 8 hours. Glucoamylases, *GCA1* and *GCA2* are two genes that have positive roles in matrix production and may function through hydrolysis of insoluble β -1,3 glucan chains (Nobile *et al.*, 2009). The gene *GCA1* was downregulated by 3 Log₂FC at 8 hours and upregulated by 1.1 Log₂FC at 24 hours. It was also shown that genes encoding alcohol dehydrogenases *CSH1* and *IFD6* have roles in matrix production wherein *Csh1* and *Ild6* acts negatively (Nobile *et al.*, 2009). *CSH1* and *IFD6* were downregulated at 8 hours by 1.8- and 3.2 Log₂FC respectively and by 0.4 and 1.4 Log₂FC at 24 hours respectively.

Genes involved in adhesion include the well- studied ALS family (*ALS1-7* and *9*) adhesins (Hoyer, 2001) which encode glycosylphosphatidylinositol (GPI)-linked cell surface glycoproteins, as well as *HWP1* (Martin *et al.*, 2013). Amongst these genes, *ALS3* that encodes the hyphal-associated adhesin of *C. albicans* was upregulated by 1.3 Log₂FC at 8 hours and downregulated by almost 1.5 Log₂FC at 24 hours. *ALS4* was downregulated by 1 Log₂FC at 8 hours. *HWP1*, which is also a hypha-associated GPI-linked protein was downregulated by 1.9 Log₂FC at 24 hours.

However, one gene *SSA1*; a cell surface expressed protein and a member of the HSP70 family that was found to be involved in biofilm formation (Nobile *et al.*, 2012) was highly upregulated by 3.4 Log₂FC (Figure 3.13:B).

The fungus *C. albicans* is equipped with sets of hydrolytic enzymes that facilitates its invasion to host tissues. Amongst those are the secreted aspartyl protease family (Hube *et al.*, 1994). Amongst the genes that were differentially expressed that belong to this family are *SAP2*, *SAP5*, and *SAP7*. *SAP2* was found to be upregulated by approximately 1.5 Log₂FC at 8 hours and 24 hours. *SAP6* upregulated by 1.3 Log₂FC at 8 hours. However, *SAP5* was downregulated by approximately 1 Log₂FC at 24 hours. In addition, *SAP7* was also downregulated by 2 Log₂FC at 8 hours (Figure 3.13: D). Another set of hydrolase enzymes is the lipase gene family (Hube *et al.*, 2000). Most of lipase genes were downregulated at 8 hours by more than 1 Log₂FC except for *LIP1* which was downregulated at 24 hours by approximately 5 Log₂FC. However, *LIP10* was the only lipase that was upregulated at 8 and 24 hours by 1- and 2.3 Log₂FC respectively. Amongst the phospholipase's gene family (Ghannoum, 2000), only PLB4.5 which is a GPI anchored phospholipase was downregulated by 1.7 Log₂FC (Figure 3.13: C).

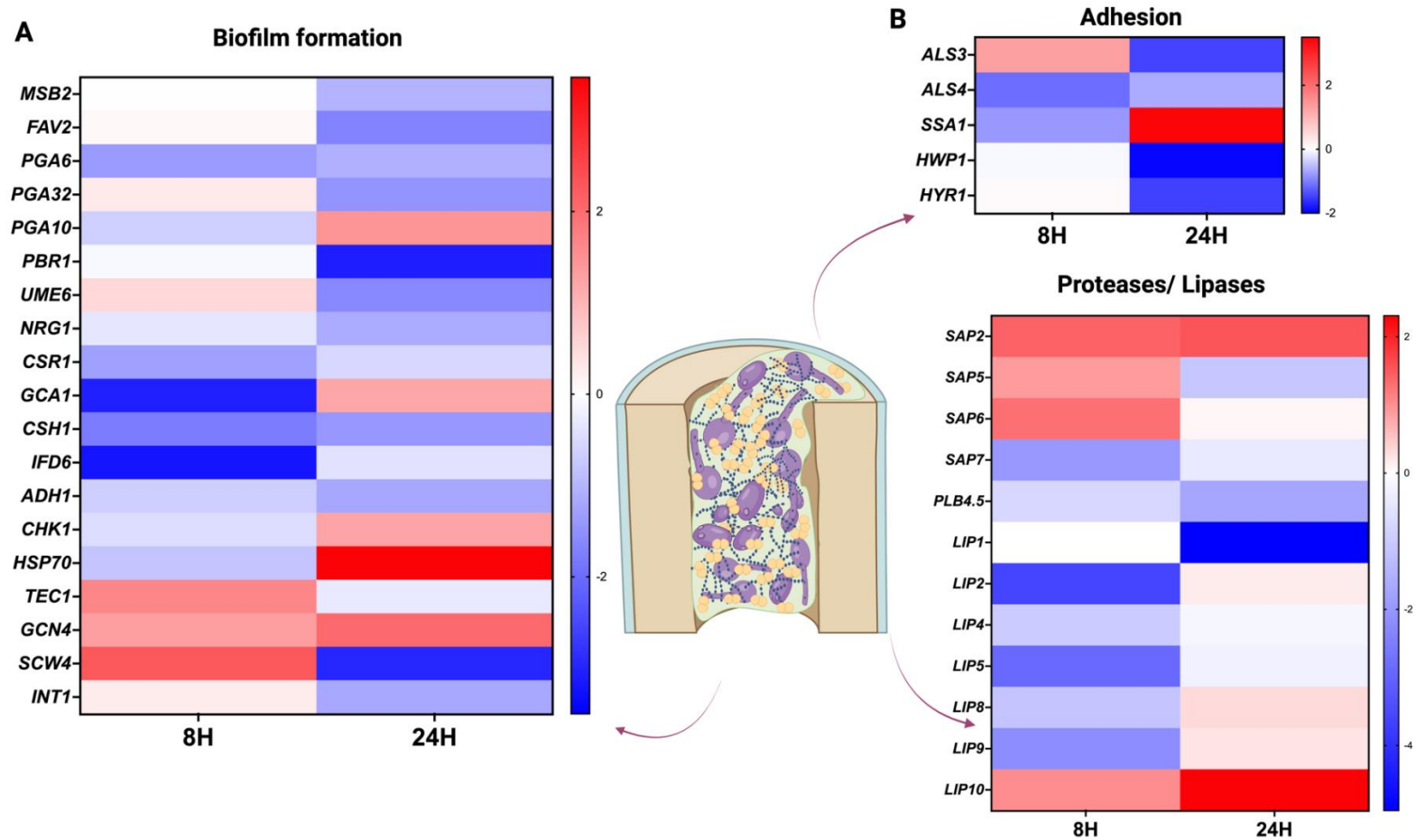


Figure 3.13: Heatmaps showing upregulated and downregulated genes involved in *C. albicans* virulence mechanism in dual-species compared to single species biofilm. Genes involved in biofilm formation (A), adhesion (B), proteases and lipases (C) were manually extracted after performing DESeq2 analysis. Upregulation of gene expression is represented in red and a downregulation in gene expression is represented by blue at 8 hours and 24 hours' time points. heatmaps were generated using GraphPad Prism. Figure was created using BioRender. : *C. albicans*, : *E. faecalis*, : ECM, : Dentinal tubule.

3.4.2.2 *E. faecalis* downregulated genes involved in *C. albicans* growth

Cell cycle progression is linked to proliferation, morphogenesis and consequently the virulence of *C. albicans*. Regulation of the physiological processes making up the cell cycle requires cyclins and their associated kinases as well as cell cycle checkpoints. At the transcriptional level, periodic expression of cell-cycle-specific factors and checkpoints regulate cell cycle events. All genes in this section were selected based on (Cote et al., 2009) unless citation states otherwise.

The first cluster of genes is expressed during the transition from the first growth phase (G1) to the synthesis phase (S), where all the chromosomes are being replicated. The genes encode mainly DNA polymerase subunits, such as *POL1*, *POL2*, and *POL3*. These genes were mainly downregulated at 8 hours by 2.5, 1.3, 1.2 Log₂FC respectively. At 24 hours, only *POL1* was downregulated by 1.5 Log₂FC. Genes encoding DNA replication factor elements; *RFA1* and *RFA2* were downregulated by 2.2 and 1.9 Log₂FC at 8 hours' time point and were downregulated to a lesser and insignificant extent at 24 hours. Other replication factors that peak at G1/ S phase are *RFC2* and *RFC4*. The gene that encodes *RFC2* was downregulated by 1 Log₂FC at 24 hours whilst *RFC4* was downregulated by 1.2 Log₂FC at 8 hours. Ribonuclease reductase (*RNR1*) gene was also downregulated by 2.4 and 1.1 Log₂FC at 8 hours and 24 hours respectively. The DNA clamp loader PCNA orthologue (*POL30*) gene was downregulated by a decrease of nearly 1.9 and 1 Log₂FC at 8 and 24 hours respectively (Nobile *et al.*, 2012). The genes encoding for the cell cycle progression such as G1 cyclins (*CCN1* and *PCL2*) are activated. *CCN1* was downregulated by 1.5 Log₂FC at 24 hours and *PCL2* was also downregulated by 2 Log₂FC change. *MSH2,6* are components of the post-replicative DNA mismatch repair system (Tzung *et al.*, 2001), their genes were downregulated by nearly 1 Log₂FC at 8 and 24 hours. *YOX1* that encodes a DNA transcription factor that peaks at G1/S phase was also downregulated at 24 hours by 2 Log₂FC decrease (Figure 3.14:A). *HGC1* is a gene that encodes hypha-specific G1 cyclin-related protein involved in regulation of morphogenesis, biofilm formation (Zheng *et al.*, 2004). This gene was upregulated by 1.1 at 8 hours and the downregulated by 1.9 at 24 hours' time point.

During the next periodic phase, after completion of DNA replication (S) and start of the second growth phase (G2), the cell starts preparing for mitosis by transcribing some periodic genes involved in spindle formation (*CDC14*, *ESP1*, *MPS1*, and *SPC98*) and in chromosome organization and condensation (*SMC2*, *APC1*, *CDC27*, and *TUB2* and *-4*). These genes were generally downregulated. Genes that passed 1 Log₂FC cut-off were *CDC14* which encodes a tyrosine protein kinase involved in exit from mitosis and morphogenesis. This gene was downregulated by 1.1 and 1.4 Log₂FC at 8 hours and 24 hours respectively. Other genes involved in morphogenesis determination are *HSL1*, *SWE1* (Gale *et al.*, 2009, Wightman *et al.*, 2004). *HSL1* which is a protein kinase involved in determination of morphology during the cell cycle of both yeast-form and hyphal cells via regulation of *SWE1*. The gene *HSL1* was downregulated by approximately 1.3 Log₂FC at 8- and 24-hours' time point. *SWE1* was downregulated at by 1.1 Log₂FC at 8 hours' time point (Figure 3.14: B). Lastly, *TUB1*, a gene that encodes alpha-tubulin was downregulated by 1.2 Log₂FC.

The G2/M phase genes are composed of the components of the mitotic exit network (*MOB1*), cytokinesis related genes (*HOF1*), mitotic spindle associated genes (*KIP2* and *ASE1*), the anaphase- promoting complex regulatory subunit (*CDC20*), and the polo- like kinase (*CDC5*). Of the G2/M phase genes, *HOF1* was downregulated by 1 Log₂FC, *CDC5* was downregulated at 24 hours by approximately 1.5 Log₂FC. *C. albicans* has a set of four chitin synthases enzymes that deposit chitin at sites of growth, which includes the polarized tips of buds and hyphae, and sites of septation (Munro *et al.*, 2003). *CHS8* was downregulated by 1.4 Log₂FC at 24 hours. *ACE2* is a transcription factor involved in the RAM (Regulation of *ACE2* transcription factor and Morphogenesis) signalling network that regulates polarized morphogenesis. It is also involved in regulating the expression of genes implicated in cell separation (Weiss *et al.*, 2002). Furthermore, *ACE2* is required for adherence, biofilm formation and invasion in *C. albicans* (Kelly *et al.*, 2004). The data demonstrated that the *ACE2* gene was upregulated by 2.9 Log₂FC at 24 hours (Figure 3.14: C).

The genes *CLB2* and *CLB4* encode a mitotic-specific cyclins that is essential for the control of cell cycle at this stage (Bensen *et al.*, 2005). G2/M cyclins accumulate steadily during G2 and are abruptly destroyed at mitosis. This degradation is

necessary for the cell to exit from mitosis (Figure 3.14: D). *CLB2* was downregulated at 24 hours by 1.4 and *CLB4* was also downregulated at 8 and 24 hours by nearly 1 and 1.1 Log₂FC respectively.

Upon exit from mitosis, the phase of cell division and formation of a new cell is activated. During this phase, the transcription of genes involved in cell bud or cell wall development and cell wall proteins (*SCW4*, 11) are differentially expressed. The results showed that *SCW4* was upregulated by 2.2 Log₂FC and downregulated by 2.9 Log₂FC at time points, 8 and 24 hours respectively. Also, genes that encodes the components of cell division (*MCM3*, *MCM6*, *CDC46* and *CDC54*) were differentially expressed. This set of gene family was downregulated by nearly 1 to 1.7 Log₂FC at 8 and 24 hours. The DNA prereplication subunit (*CDC6*) gene was downregulated at 24 hours by 2 Log₂FC.

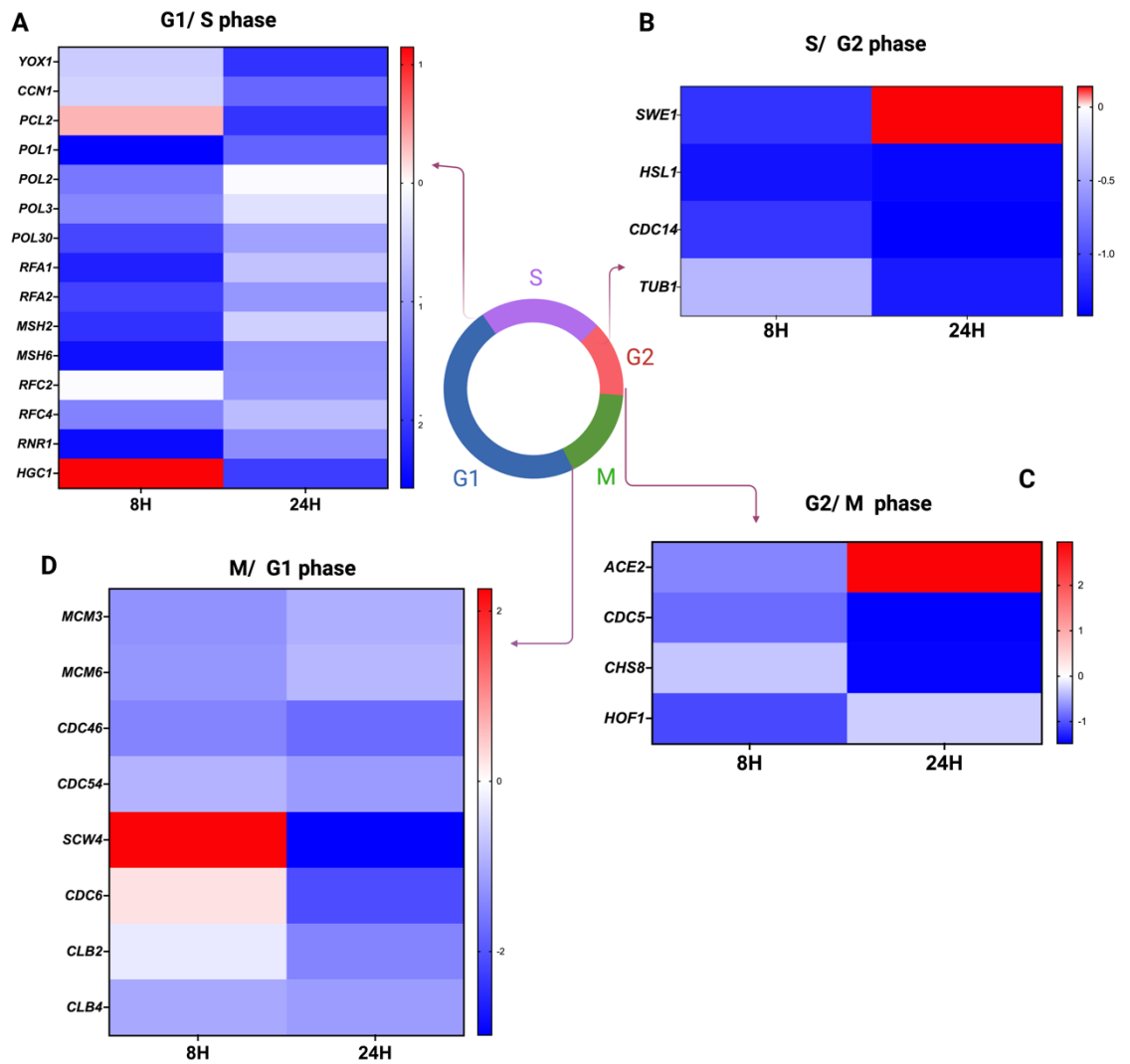


Figure 3.14: Heatmaps showing differentially expressed genes involved in *C. albicans* Growth. Differential expression of genes involved in *C. albicans* cell cycle progression in G1/ S phase (A), S/ G2 phase (B), G2/ M phase (C) and M/ G1 phase (D). Increased expression of genes is shown in red, and a decreased expression is represented in blue at 8 hours and 24 hours' time points. Analysis was done using DESeq2. Data were manually extracted and plotted as heatmaps using GraphPad Prism. Figure was created using BioRender.

3.4.2.3 *E. faecalis* inhibited septin gene family at 24 hours' time point.

A further set of four genes which belong to the septins family were downregulated at 24 hours. These CDC10, CDC11 and CDC12 septins are assembled in a ring at the future site of septation during budding, pseudohyphal and hyphal growth of *C. albicans*. Septins are also involved in morphogenesis, chitin deposition, bud site selection, cell cycle regulation (Warenda and Konopka, 2002). *CDC10*, encodes a septin that plays a role in the cell cycle was downregulated by 1.5 Log₂FC. *CDC11* encodes a septin that plays a key role in invasive growth and virulence was

downregulated by 2 Log₂FC. *CDC12* was downregulated by 1.5 Log₂FC and *CCN1* a gene that encodes G1/S-specific cyclin was downregulated by 1.5 G1/S-specific cyclin (Figure 3.15)

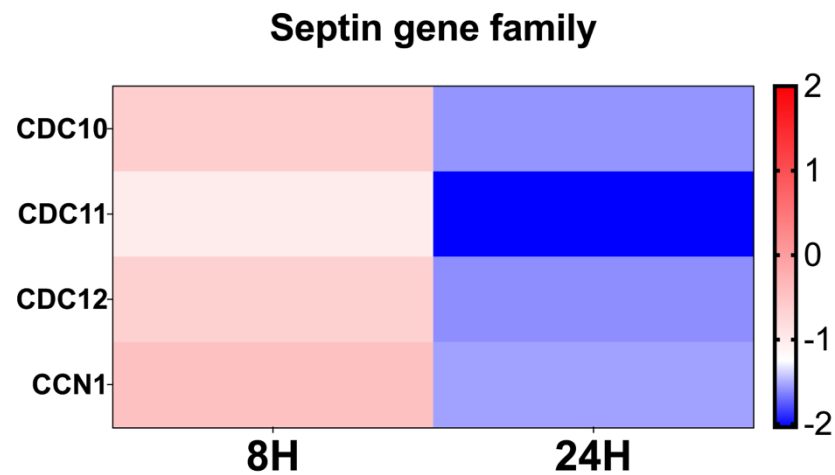


Figure 3.15: *E. faecalis* downregulates the septin gene family. Differential expression of genes involved in the septin family. Increased expression of genes is shown in red, and a decreased expression is represented in blue at 8 hours and 24 hours' time points. Analysis was done using DESeq2. Data were manually extracted and plotted as heatmaps using GraphPad Prism. Figure was created using BioRender.

3.5 Discussion

The previous chapter demonstrated that *E. faecalis* affected *C. albicans* virulence behaviour by reducing its growth and hyphal morphogenesis as well as reducing its virulence by downregulating key genes involved in adhesion and biofilm formation. The results reported in this chapter, revealed major transcriptomic changes that affected *C. albicans* behaviour in the presence of *E. faecalis*.

C. albicans relies on metabolic flexibility to grow and thrive in a wide range of conditions. Therefore, it must be able to assimilate various carbon and nitrogen sources from available nutrients. Carbohydrates are the primary and preferred source of carbon for *C. albicans* to generate energy and produce biomolecules. The central carbohydrate metabolism in *C. albicans* is glycolysis which is commonly used for fermentation and respiration. Glycolysis is responsible for converting hexose phosphates that are converted from sugars, into the key metabolite pyruvate and simultaneously yielding ATP and NADH. Since glycolysis is critical for carbon assimilation, this pathway is upregulated during infections and is important to *C. albicans* virulence (Brown *et al.*, 2006). Glycolytic enzymes are transcriptionally regulated in response to environmental conditions, such as oxygen levels and carbon sources changes (Brown *et al.*, 2006). At 8 hours' time point, the current results showed that genes involved in glycolysis pathway were downregulated; and the genes that encode sugar sensing and transportation enzymes like hexokinases were significantly downregulated as well as *GCA1* that encodes glucoamylase was downregulated. *GCA1* is known to be upregulated when *C. albicans* cells are grown on fermentable sugars (Sturtevant *et al.*, 1999). The contradiction suggests that *C. albicans* does not rely exclusively on glycolysis for carbohydrate metabolism but rather depends on alternative carbon sources except glucose when it is cocultured with *E. faecalis* (Ene *et al.*, 2012). Interestingly, *ICL1* that encodes isocitrate lyase an enzyme involved in a glyoxylate cycle was significantly upregulated at 8 hours by 1.7-Log₂FC (P<0.02). This gene has been reported to be upregulated when *C. albicans* cells are grown on lactate and oleic acid (Sandai *et al.*, 2018). This result supports the speculation that as carbon fermentable sugar sources becomes limited, *C. albicans* shifts its metabolism from the central metabolic pathway to alternative carbon metabolism. Results were in line with a previous study that showed *ICL1* was to

be upregulated in *C. albicans* when cocultured with *S. gordonii* (Dutton *et al.*, 2016). On the other hand, *C. albicans* carbohydrate metabolism was upregulated when cocultured with *P. aeruginosa*. These variation in results along with this chapter's data indicates the flexibility in *C. albicans* carbon assimilation from available sources which differs depending on its interacting partner.

The data analysis showed that a key gene, *PHO89* was downregulated at 8 hours. Since this enzyme requires an alkaline media to function efficiently, the downregulation might indicate that the environment has become acidic when *C. albicans* and *E. faecalis* coexist in dual-species biofilm. Indeed, an acidic pH for the dual *C. albicans* and *E. faecalis* biofilm has been reported (Alshanta *et al.*, 2021). Moreover, the downregulation of *PHO89* might indicate that *C. albicans* ambient media was high in phosphate, which is consistent with previous reports (Serra-Cardona *et al.*, 2014, Kohler *et al.*, 2020).

Another set of genes that are expressed when *C. albicans* is subject to oxidative stress is alcohol dehydrogenases which are also involved in biofilm matrix regulation. The gene *IFD6* encodes aldo-keto reductase has been proven to have a negative impact on biofilm matrix production (Mukherjee *et al.*, 2006). Furthermore, one study proposed that this alcohol dehydrogenase and *CSH1* generate quorum-sensing aryl and acyl alcohols that govern multiple events in biofilm maturation (Nobile *et al.*, 2009). Thus, *IFD6* and *CSH1* (-1.8 Log₂FC p = 0.006) downregulation reported in this chapter indicates that matrix production of *C. albicans* is higher and that helps in biofilm maturation. This is in agreement with previous reports (Mukherjee *et al.*, 2006, Nobile *et al.*, 2009)

On the other hand, transcriptomic results revealed that several key genes involved in metabolic pathways were upregulated. The ROS are natural by-products of cellular aerobic metabolism and are synthesized by ROS generating enzymes. One source of ROS is mitochondrial respiration via oxidative phosphorylation (Murphy, 2009). Leakage of electrons from the respiratory chain results in the reduction of oxygen, which generates ROS in the cells. Another way to generate ROS is by xanthine oxidase and NADPH oxidases (Murphy, 2009, Babior *et al.*, 1973). A key gene that encodes one of the NADPH oxidases is *CFL11*. This gene was highly upregulated in this chapters' data which indicates that *C. albicans* is actively

generating ROS when cocultured with *E. faecalis* in contrast to *S. gordonii* in which this gene was downregulated. These negating results can be explained by the fact that *C. albicans* responded to oxidative stress to *S. gordonii* differently by upregulating other genes involved oxidative stress response (Dutton *et al.*, 2016). This chapter's results were in agreement with a previous report, whereby *CFL11* was induced when *C. albicans* were cocultured with hepatocytes (Huang *et al.*, 2020)

One of the key mechanisms for protection against oxidative stress is the generation of metallothioneins which are expressed to protect *C. albicans* against heavy metal ions (Palmiter, 1998). Copper is an essential element in many enzymes involved in biological processes, however, high levels of copper is toxic and catalyses the synthesis of ROS (Linder and Hazegh-Azam, 1996). *CRD2* encodes a metallothionein that is essential for *C. albicans* adaptative growth in media rich in copper. Mutants of this gene showed reduced growth in increasing copper concentration (Riggle and Kumamoto, 2000). The current data showed that transcripts of the *CRD2*, were highly expressed at 8 hours; a finding which might indicate that *C. albicans* is subjected to oxidative stress by increased amount of copper when cocultured with *E. faecalis*. In addition, one of the key oxidative stress enzymes, *SOD3* was downregulated at 8 hours. It has been reported that *SOD3* is induced during copper starvation to overcome *SOD1* activity that depends on copper as catalytic cofactor (Broxton and Culotta, 2016). The current data analysis revealed that *SOD3* was significantly downregulated which might indicate that *C. albicans* relies on alternative oxidative enzymes to combat oxidative stress in response to the available metal ions. This finding with in line with a previous study that reported the downregulation of *SOD3* in *C. albicans* when cocultured with *P. aeruginosa* (Fourie *et al.*, 2021).

The current transcriptomic data revealed major changes of metabolic pathway in *C. albicans* when cocultured with *E. faecalis* compared to those when in a single-species biofilm at 24 hours. These changes might have occurred because *C. albicans* requires a source of nitrogen to synthesize essential proteins to carry out important cellular functions and to generate nucleotide bases for DNA and RNA synthesis (Silao and Ljungdahl, 2021). Moreover, *C. albicans* can assimilate nitrogen from the surrounding environment, for example, amino acids, urea,

peptides, proteins, and N-acetyl glucosamine (GlcNAc) and ammonia. It has been reported that *C. albicans* prefers amino acid as a nitrogen source to assimilate and use as nitrogen and carbon sources (Garbe and Vylkova, 2019).

A number of amino acid sensors and transporters are located on the plasma membrane of *C. albicans* (Garbe and Vylkova, 2019). CAN3 is a basic amino acid permease and GAP2 involved in amino acid sensing. Genes encoding these proteins were upregulated by 1.6 Log₂FC. Moreover, another gene involved in amino acid uptake is AAP was also insignificantly upregulated by 1.7 Log₂FC. MEP2 is a gene that encodes a plasma membrane protein involved in the sensation of nitrogen sources availability and is an ammonium transporter. This enzyme is known to be regulated in response to nitrogen starvation which might indicate nitrogen limiting sources for *C. albicans* when upregulated (Biswas and Morschhauser, 2005). The significant upregulation of this gene in this chapters' data indicates that *C. albicans* was subjected to nitrogen starvation when cocultured with *E. faecalis*.

In addition, results showed that genes involved in amino acid biosynthesis were strongly upregulated at 24 hours. The upregulation of these genes indicates amino acid starvation state in *C. albicans* which is supported by a previous report (Tripathi *et al.*, 2002). One of the key transcriptional factors that are induced during amino acid starvation is GCN4 (Tripathi *et al.*, 2002) which is consistent with the current data that showed significant upregulation of *GCN4* by 2 Log₂FC (p <0.005). One cyclin that is GCN4-dependent is PCL5. The gene that encodes PCL5 protein was strongly upregulated at 24 hours. *PCL5* is transcriptionally induced in the presence of GCN4 and it is part of its homeostatic mechanism (Shemer *et al.*, 2002). Moreover, the high upregulation in genes involved in amino acid biosynthesis as well as transportation that indicates amino acid starvation agreed with previous studies when *C. albicans* was cocultured with other species like *Lactobacilli* (McKloud *et al.*, 2021).

The metabolic pathway of arginine biosynthetic process was upregulated at 8 and 24 hours. *ARG3* encodes ornithine carbamoyltransferase, a sub pathway in the arginine biosynthesis pathway. This gene was upregulated at 8 and 24 hours but was more expressed at the latter. *ARG3* converts ornithine and carbamoyl-P (which is synthesised from ammonia) to citrulline which in turn is converted L-

arginosuccinate via ARG1 enzyme. ARG4 converts L-arginosuccinate to arginine amino acid. All these enzymes involved in the synthesis of arginine were shown to be upregulated at 24 hours' time point. However, data showed arginine catabolic pathway was downregulated at 24 hours. This pathway involves key genes that encodes enzymes involved in the catabolic process of arginine which were shown to be strongly downregulated in this chapters' results; CAR1 is an arginase enzyme that converts arginine to urea and ornithine, CAR2 is ornithine-oxo-acid transaminase which converts ornithine to L-glutamate 5- semialdehyde which will eventually be converted to proline amino acid via the enzyme action of PRO3. Results here were also reported in previous studies whereby *C. albicans* arginine biosynthetic pathway was upregulated when cocultured with other species as in *Lactobacillus* spp. (McKloud *et al.*, 2021) and *S. gordonii* (Dutton *et al.*, 2016). Moreover, arginine biosynthetic genes are induced under conditions of mild oxidative stress as those which might occur within phagocytes (Jiménez-López *et al.*, 2013)

Glutamate serves as a building block for amino acid synthesis. It is converted to N-acetyl glutamate via ARG2 which in turn will be converted to N-acetyl glutamate P via ARG5 which will also convert N-acetyl glutamate to N-acetyl glutamate semialdehyde which will be converted to N-acetyl ornithine by ARG8 and eventually to ornithine. All the genes encoding these enzymes mentioned in ornithine biosynthesis pathway were upregulated.

In addition, glutamate can be generated from glutamine through different pathways. Ammonia can be protonated to NH_4^+ for as long as the cytosolic pH remains neutral. Ammonium can then be reassimilated to generate glutamate by the NADPH dependent glutamate dehydrogenase (GDH3) which uses alpha-ketoglutarate as a substrate (Han *et al.*, 2019). This enzyme, GDH3, was shown to be upregulated in the present transcriptomics results by 1.8 Log_2FC although not statistically significant. This finding was further confirmed by the present results because, a gene that encodes GDH2 enzyme (NAD⁺-dependent glutamate dehydrogenase) was significantly downregulated by 1.6 Log_2FC ($P < 0.01$). This enzyme catalyses the reaction that leads to ammonia generation from glutamate by converting cytosolic glutamate to alpha-ketoglutarate (Silao *et al.*, 2021). If the cytosolic pH is maintained near neutrality (pH 6.5), most ammonia is

converted to its protonated form ammonium. Free ammonia is membrane-permeable and can readily exit cells, where it contributes to the alkalization of the growth environment (Fernandes *et al.*, 2017). Since current data indicate that ammonium transferases were highly expressed this further support that ammonium is being transferred from extracellular environment to compensate for nitrogen starvation and that the ambient environment surrounding *C. albicans* is acidic when *C. albicans* is cocultured with *E. faecalis*. To support this, ARG3 is repressed in alkalinising medium, however, it was significantly upregulated as demonstrated in the present data. The upregulation might be attributed to an acidic pH of the *C. albicans* biofilm environment (Serrano *et al.*, 2002). A summary of arginine biosynthetic pathway and nitrogen utilization in *C. albicans* is provided in (Figure 3.16)

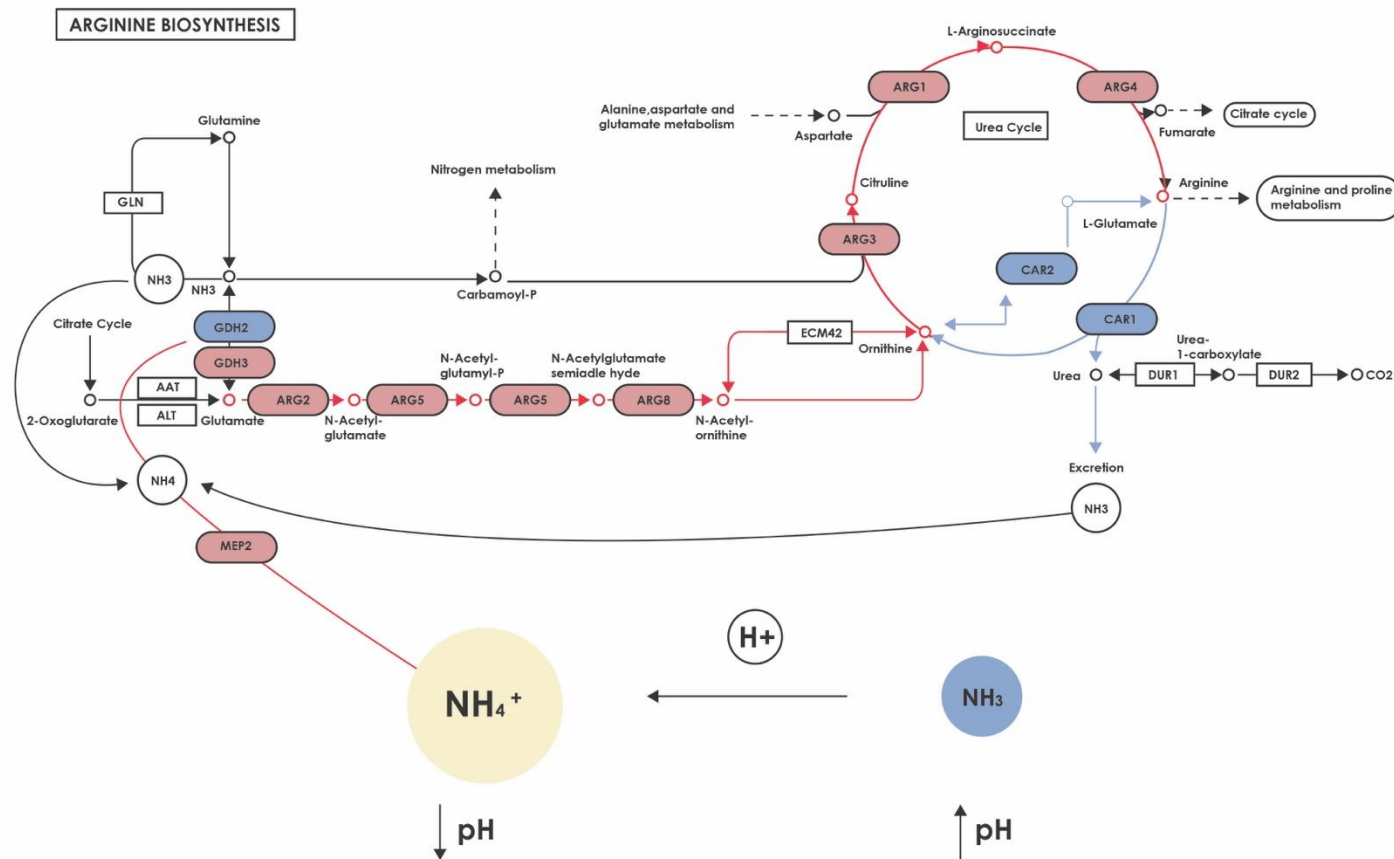


Figure 3.16: Summary of arginine biosynthetic pathway and nitrogen utilization in *C. albicans* indicating acidic environment. Genes encode enzymes involved in ornithine biosynthesis subpathway from glutamate were upregulated (*ARG2*, *ARG5*, *ARG8*). Genes encode enzymes involved arginine biosynthetic pathway were upregulated (*ARG3*, *ARG1*, *ARG4*). Genes encode enzymes involved in arginine catabolic process (*CAR1*, *CAR2*) were downregulated. Ammonia by product is generated from urea and glutamate when converted to glutamine by the catalytic action of *GDH2*. Excess ammonia produced in the cytosol should be removed due to its toxic effects, most of it is converted to ammonium (NH_4^+) which is assimilated by central nitrogen metabolism via *GDH3* enzyme and *GLN1*. Free ammonia is converted to the protonated form ammonium for as long as the cytosolic pH is maintained near neutrality (pH ~ 6.5). In acidic media (low pH) the ammonium form predominates. Ammonium can be imported from extracellular media via the ammonium transporter *MEP2*. Red boxes and lines indicate upregulated genes and pathways respectively. Blue boxes and lines indicate downregulated genes and pathway respectively. Figure was adopted from KEGG pathway maps: www.genome.jp and redrawn.

It is well known that *C. albicans* utilizes various nitrogen sources with ammonia, glutamine, asparagine and glutamate the preferred sources. However, when the primary nitrogen sources are limited, *C. albicans* can also use the less-preferred nitrogen sources like isoleucine, tyrosine and tryptophan (Wong *et al.*, 2008). In the extreme case of nitrogen depletion, cells cease growing, even with all other nutrients available in excess, and enter a nitrogen-specific quiescent state (Klosinska *et al.*, 2011). Such quiescent cells retain viability for an extended period of time and suppress catabolism in a way that prevents consumption of ambient glucose in the medium (Brauer *et al.*, 2008). Thus, yeast cells cope their synthetic capacity and growth rate to the quality and amount of available metabolizable nitrogen which might explain the cease in growth shown in the previous chapter.

An efficient oxidative stress response is an important metabolic process for *C. albicans* to survive within different environments within human host. It has been shown that virulence of *C. albicans* was attenuated in the presence of defective stress response mechanisms. Therefore, *C. albicans* must cope with ROS like superoxide radicals and hydrogen peroxide generated during oxidative burst for survival (Patterson *et al.*, 2013, Jain *et al.*, 2013). Antioxidant genes following exposure to H₂O₂ are upregulated including genes encoding catalases, glutathione peroxidases (GPX) and superoxide dismutases (SOD) (Enjalbert *et al.*, 2003, Enjalbert *et al.*, 2006). The current data revealed one gene that encodes GPX3 enzyme; a glutathione peroxidase involved in CAP1 dependent oxidative response to H₂O₂ to be significantly upregulated in addition to *GLX3* that encodes glutathione-independent glyoxalase that is upregulated when *C. albicans* cells are subject to H₂O₂ oxidative stress. A proposed explanation to the upregulation in these genes involved in oxidative stress response might be that *C. albicans* will encounter ROS produced by the H₂O₂-producing *E. faecalis*. *E. faecalis* secretes ROS into its surroundings that may have inhibitory effect on the growth of *C. albicans* (Huycke *et al.*, 2002). The upregulation of *GPX3* was confirmed in other study where *C. albicans* responded to the presence of *S. gordonii* by the upregulation of antioxidant genes (Dutton *et al.*, 2016).

One of the gene sets that were highly upregulated in *C. albicans* at 24 hours is HSPs. They are usually expressed in response to thermal stress and control basic physiological activities and virulence via interaction with various regulators in cellular signalling pathways. In addition, HSPs can help in drug resistance. HSPs can be activated by additional non - thermal stressors like heavy metals and oxidative stress (Burnie *et al.*, 2006, Cuéllar-Cruz *et al.*, 2014). Furthermore, many studies have revealed important roles for HSPs in the growth and virulence of *C. albicans* (Becherelli *et al.*, 2013b, O'Meara and Cowen, 2014). Therefore, targeting HSPs pharmacologically or genetically could enhance the sensitivity of *C. albicans* to traditional antifungal drugs and reduce its pathogenicity (Li and Sun, 2016, Fiori *et al.*, 2012). One of the key genes in this family is *HSP104* which encodes HSP104 protein that has an important role in thermotolerance. In addition, Fiori *et al.* has showed that mutation in these genes demonstrated attenuated pathogenicity in *C. elegans* infection models. Their results also showed that it is required for efficient biofilm formation and *C. albicans* virulence (Fiori *et al.*, 2012). Other studies have shown the potential involvement of heat shock response in *C. albicans* biofilm development (Becherelli *et al.*, 2013a), specifically HSP90. HSP90 is the most studied HSP in *C. albicans* due to its involvement as a transcription factor in several virulence pathways such as biofilm formation, hyphal morphogenesis and virulence (O'Meara *et al.*, 2017). The upregulation of HSP104 and HSP90 in this chapter was in line with Short *et al.* who showed that these two genes were upregulated *C. albicans* when in coculture with *S. aureus* (Short *et al.*, 2021). Their results showed that *S. aureus* drives *C. albicans* towards a pathogenic genotype. Thus, it can be deduced that *E. faecalis* has a virulent synergistic effect when it is cocultured with *C. albicans*.

In addition, SSA1 and SSA2 are major members of the HSP70 family; their genes were found to be upregulated in the present results. It has been suggested that SSA1 and SSA2 contribute positively to *C. albicans* virulence by inducing host cell endocytosis. In addition, they act as invasins. They combine with host cell cadherins and facilitate host cell endocytosis allowing *C. albicans* to invade host cells (Sun *et al.*, 2010).

The current data analysis showed that genes involved in glycerol biosynthesis were downregulated. In cases of glucose limitation, *C. albicans* adapts to this situation by relying on nonfermentable sources such as glycerol for its growth and energy production in addition to the necessity of glycerol for maintaining intracellular osmotic pressure (Desai *et al.*, 2013). Results here were in contrast with a previous study who found that this pathway was upregulated when *C. albicans* was cocultured with *S. gordonii* (Dutton *et al.*, 2016). Specifically, the gene *RHR2* encoding the glycerol biosynthetic enzyme glycerol-3-phosphatase was highly upregulated (Dutton *et al.*, 2016) in contrast to this chapters results which was highly downregulated (-3.2 Log₂FC). These contradicting results may be attributed to the fact that *S. gordonii* respond to glycerol production by utilising it as an alternate carbon source indicating a beneficial relationship in contrast to *E. faecalis*.

The macromolecular composition, molecular organization, and thickness of *C. albicans* cell wall varies considerably depending on environmental changes. *C. albicans* cell wall is a complex dynamic structure based on a core assembly of β -glucans and chitins and an outer layer of mannose-glycosylated proteins. The outer layer of the fungal cell wall is mainly composed of mannoproteins and phosphopeptidomannan, which is a polymer of O-linked mannoses and N-linked mannoses. This outer layer shields the glucan polysaccharide matrix. Most of the cell surface glycoproteins are extensively glycosylated and harbour both N-linked and O-linked oligosaccharides. The N-glycosylation of proteins catalytic process involved the presence of OST protein (Aebi, 2013, Roman *et al.*, 2016). *OST1* which encodes a subunit of the oligosaccharyl transferase complex is mainly involved in the catalytic process for N- glycosylation of proteins was downregulated. *PMI* which encodes a mannose-6-phosphate isomerase that's essential in cell wall mannoprotein biosynthesis was also downregulated. In addition, PMT family genes were downregulated; these genes encode protein O-mannosyltransferases that initiate O-mannosylation of secretory proteins. Mutants in *PMT1* and *PMT4* showed significant decrease in cell wall mannoproteins (Prill *et al.*, 2005). At 24 hours, the current results showed than *PMT1* was significantly downregulated by 2 Log₂FC (p=0.01), *PMT2* and *PMT4* were also significantly downregulated by 2.3 Log₂FC (p=0.002). Another gene that's associated with β -mannosylation is *RHD1* which encodes β -mannosyltransferase, this gene was upregulated by 2.2 Log₂FC (p =

0.008) at 24 hours. The alterations in *OST*, *PMI*, *PMT* gene family and *RHD1* expression indicates some form of cell wall remodelling in *C. albicans* when cocultured with *E. faecalis*. These results were in accordance with Didem *et al.* who showed a significant alteration *C. albicans* cell wall when cocultured with *E. faecalis* upon examination under TEM (Didem *et al.*, 2021).

As shown earlier, *C. albicans* showed metabolic adaptability in response to environmental changes induced by *E. faecalis*. Certain genes involved in key virulence mechanisms were manually extracted to investigate gene families involved in adhesion, invasion, phenotypic switch, proteases, lipases and biofilm formation. The main hyphae specific genes *HWP1* and *ALS3* (Fan *et al.*, 2013) were downregulated as demonstrated in the current results which confirms the inhibition of hyphal morphogenesis seen in the previous chapter. Moreover, *SAP5* is also a hyphae specific (Felk *et al.*, 2002) was downregulated amongst *SAP* family genes at 24 hours. However, *SAP5*, *SAP6* were upregulated at 8 hours whilst *SAP7* was downregulated. *SAP2* which has a very broad substrate activity was upregulated at both time points. The high expression of proteases is suggestive of enhanced synergism in virulence between *C. albicans* and *E. faecalis*.

Lipases are another set of hydrolases that hydrolyse lipids to use fatty acids and/or glycerol as substrates (Stehr *et al.*, 2004). The results showed that these genes were generally downregulated at both time points. This was in contrast with a previous result which showed that *C. albicans* lipases genes were upregulated in response to *P. aeruginosa* (Fourie *et al.*, 2021). However, one gene *LIP1* was upregulated by 10 Log₂FC in a recent study when *C. albicans* was cocultured with *E. faecalis* (Alshanta *et al.*, 2022). The reason behind these contradicting results might be that the transcriptome of *C. albicans* was investigated at a different time point (6 hours), reflecting a different biofilm formation stage from this chapters' data time points (8 hours and 24 hours)

Metabolic adaptation of *C. albicans* affects greatly its biofilm formation. Variation in biofilm formation has been observed in *C. albicans* grown in different carbon sources (Jin *et al.*, 2004, Ene *et al.*, 2012). After a closer look at genes encodes transcription factors, it was shown than *ACE2*, *GCN4* were highly upregulated. The upregulation of *ACE2* was in agreement with a recent study that investigated *C.*

albicans transcriptome with *S. aureus*. Their results showed the upregulation of *ACE2* along with other genes involved in biofilm formation and virulence. This is indicative that *E. faecalis* also acts in synergy with *C. albicans* in biofilm formation and virulence. Several other transcription factors and genes involved in adhesion biofilm formation were differentially expressed and whether upregulated or downregulated depends hugely on the underlying metabolic activity and nutrient availability for *C. albicans* to be able to produce customised biofilm at certain time point (Ene *et al.*, 2012). Generally, the most important finding is the upregulation of the transcription factor gene involved in biofilm matrix (*CSH1*) and the differential expression of genes regulated by it.

Lastly, one study used microscopy and metabolomics to investigate interkingdom interactions between *C. albicans* and *E. faecalis* (Didem *et al.*, 2021). They utilised metabolomic analysis to determine the effect of *E. faecalis* on the cell growth and hyphal formation of *C. albicans* and to understand the mechanism of *Candida* inhibition by *E. faecalis*. Their results showed alterations in carbohydrate, amino acid metabolites. This finding complements this chapters' findings, where transcripts involved in carbohydrate and amino acid metabolism were altered compared to *C. albicans* single species biofilm. Moreover, they showed thicker beta-glucan chitin and a denser and narrower fibrillar mannan layer of *C. albicans* when examining *C. albicans* cell wall under SEM. This was in line with the alteration in gene expression involved in mannoprotein synthesis at 24 hours (Didem *et al.*, 2021).

Transcriptomic analysis confirmed previous observations whereby *C. albicans* growth was dramatically downregulated. In this chapter, it was revealed that genes involved in *C. albicans* growth and cell cycle progression were downregulated which confirms the cease in growth observed earlier. Moreover, it provides a greater insight into how bacteria influence *C. albicans* behaviour in complex communities.

3.6 Conclusion

The main conclusions drawn from the results of this chapters can be summarised as follows:

- **Virulence:** the transcriptomic results confirmed chapter 2 results wherein the virulence reduction was seen in *C. albicans* at both the phenotypic and molecular levels.
- **Metabolic profiles:** the results demonstrated that *C. albicans* exhibited different metabolic profiles that contributed to the adaptation and responses of *C. albicans* to changes in the environment which it is enduring when grown with *E. faecalis*.
- **Metabolic adaptation** of *C. albicans* to amino acid and nitrogen starvation resulted in inducing HSPs, stress responses pathways, enhancing oxidoreductase activities and switching to amino acid biosynthesis pathway.
- **Metabolic adaptation** involved downregulating glucose sensation and transportation mechanisms and glycerol biosynthesis process.
- **Environmental pH changes:** arginine metabolic pathway was hugely affected by the presence of *E. faecalis* and played a significant role in responding to the environmental pH changes induced by both microorganisms in dual-species biofilm.
- **Behavioural changes** induced by *E. faecalis* presence contributed to ceasing the growth of *C. albicans* which allow it to survive longer. On the other hand, **behavioural changes** resulted in different levels of *C. albicans* virulence exhibited through expressing many genes related to biofilm formation and maturation.

With a deeper understanding of the way *E. faecalis* or other bacteria affect various aspects of *C. albicans* viability and fitness, better therapeutic strategies could be developed for *C. albicans* infections when present in polymicrobial biofilms.

Chapter 4: Response of Dual-species biofilm to novel treatment strategies: a window to understanding interkingdom interactions

4.1 Introduction

Antimicrobial resistant infections are becoming increasingly prevalent and difficult to treat due to antimicrobial misuse. It has been estimated that infections due to antimicrobial resistance claims at least 700,000 lives worldwide each year and the number could rise to 10 million annually by 2050 (Antimicrobial Resistance, 2022). It has been calculated that there was an estimated 4.95 million deaths associated with bacterial antimicrobial resistance in 2019 (Murray *et al.*, 2022).

Fungal pathogens can cause life threatening conditions like candidaemia, or recurrent and superficial infections like oral and vaginal candidiasis, especially in immunocompromised patients. The overall death toll due to fungal infections, most of which are caused by *Candida* species, has been estimated to be around 1.35 million deaths per year (Brown *et al.*, 2012). The intensive use of some antifungal drugs, such as azoles, has encouraged a shift in the epidemiology of candidiasis, in which the incidence of *C. albicans* has decreased in favour of other species that are naturally less susceptible to this drug. However, *C. albicans* remains the most common fungal species to infect humans (Quindos, 2014). Currently, available drugs are categorized into four major classes which include azoles, polyenes, pyrimidine analogues, and echinocandins. The primary targets of these antifungal drugs are the biosynthetic pathway of ergosterol, the cell wall of fungal cells, or the DNA/RNA of fungi (Sagatova *et al.*, 2016, Silva *et al.*, 2017). Resistance to azoles has increased over the last 20 years (Whaley *et al.*, 2016), and resistance towards echinocandins and other drugs is increasing and causing significant concern (Pristov and Ghannoum, 2019).

Bacteria are endowed with many intrinsic mechanisms that make them naturally resistant to certain antibiotics. Briefly, some of these mechanisms include the lack of, or possession of low affinity targets, the permeability of their cell membrane to antibiotics or the existence of multidrug efflux pumps that excrete them (Cox and Wright, 2013). Another type of resistance is acquired resistance. This occurs via many means, such as, genetic mutation, antimicrobial resistance gene gained via horizontal transfer, mobile genetic elements, or via selection upon antibiotic exposure (van Hoek *et al.*, 2011). There is an urgent need to limit

the spread of such genes, which could be transferred to opportunistic and pathogenic bacteria (Peterson and Kaur, 2018). Due to the inherent resistance of *E. faecalis* to several antibiotic agents and their natural competence for acquired resistance, treating *E. faecalis* infections has gradually become more difficult in recent years (Diekema *et al.*, 2019, Horner *et al.*, 2021). Enterococci are intrinsically resistant to many commonly used antibiotics (Hollenbeck and Rice, 2012). They exhibit resistance to penicillin and ampicillin (Conceicao *et al.*, 2014, Ono *et al.*, 2005), and they show high resistance to cephalosporins and all semi synthetic penicillins due to the expression of low-affinity penicillin-binding proteins (Arbeloa *et al.*, 2004). In addition, they are inherently resistant to clindamycin, as well as, clinically used concentrations of aminoglycosides which hinders their use as single agents (Vesić and Kristich, 2012, Eliopoulos, 1993).

The term antibiotic tolerance implies that the bacteria can be inhibited by clinically achievable concentrations but can only be killed by concentrations that far exceeds the inhibitory concentrations. Enterococci are tolerant to the bactericidal active agents like beta- lactam antibiotics and vancomycin (Frieden *et al.*, 1993). This tolerance can be overcome by combining cell wall active agents with aminoglycosides (Mederski-Samoraj and Murray, 1983, ZERVOS *et al.*, 1987). Enterococci successfully acquired resistance to many clinically used antimicrobial agents, such as chloramphenicol, erythromycin and tetracyclines (Murray, 1990, Leclercq, 1997). They also demonstrate high level aminoglycoside resistance, which negates the synergism between cell wall active agents and aminoglycosides (Murray, 1990). In addition, resistance has also been demonstrated against the newly licensed agents quinupristin-dalfopristin, linezolid, daptomycin and tigecycline (Singh and Murray, 2005, Martínez-Martínez *et al.*, 1998, Palmer *et al.*, 2010, Arias *et al.*, 2011, Lu *et al.*, 2005).

E. faecalis and *C. albicans* were amongst the 15 most frequently reported pathogens across all types of adult healthcare associated infections between 2015 and 2017. Both species were reported as antimicrobial resistant pathogens (Weiner-Lastinger *et al.*, 2020). Thus, new antimicrobial agents are much needed that can provide multi-species susceptibility. Combinational therapy also offers advantages in increased synergistic action to provide broad spectrum activity.

In recent years, the demand to find new antimicrobial agents to be utilised in the field of endodontics has increased. To overcome antimicrobial drug resistance and the potential cytotoxic effects of traditional endodontic irrigation materials, novel therapies have been proposed to be utilised as endodontic irrigants, root canal sealers and obturation materials. Fungi and bacteria are capable of adhering to different surfaces to form biofilm. *C. albicans* and *E. faecalis* are both efficient biofilm formers which exacerbates the problem of chronic infections in which they are present (Douglas, 2003, Fisher and Phillips, 2009). In endodontic infections, microorganisms can colonise dentinal walls, obturation materials, and reside within fins, isthmi and lateral canals, the areas that are difficult to reach by instrumentation and irrigation (Prada *et al.*, 2019). This raises the necessity to deliver antimicrobial drugs that enhance antimicrobial effect and penetration of the ECM surrounding them when in biofilm state.

Since treating mature biofilms is significantly more challenging. Strategies to target these pathogenic mechanisms to inhibit early development of biofilms are an attractive route for management of microbially induced disease. This has prompted the development of novel materials that exhibit an anti-adhesion effect or treatments that target certain virulence factors of pathogens that interfere with biofilm formation.

The emergence of nanomaterials science has created a host of materials with various applications demonstrated in the biomedical field. Amongst these are nanodiamonds. These have been heavily studied for imaging, as drug carriers and in sensors. Limited studies have been carried out to investigate the potential for antimicrobial activity. Owing to their unique properties and biocompatible nature they have been proposed as strong candidates as potential antimicrobial materials (Barnard *et al.*, 2003). In addition, they are amenable to the addition of functional groups or biomolecules like lysozyme or drugs to enhance their efficacy or delivery (Lai and Barnard, 2011). Moreover, they have a high affinity to proteins allowing an easy and effective protein load on their surface (Huang *et al.*, 2008). Given these features, NDs may represent an attractive target for investigation and development as anti-biofilm agents.

In addition to nanomaterials, to overcome the problem of resistance, efforts have been made to find novel anti-biofilm molecules. These molecules can have different targets that attack certain virulence mechanisms, such as inhibitors of yeast to hyphae transition, inhibitors of certain enzymes linked to host colonisation and virulence like proteases and phospholipases. To explore such molecules, high throughput screening (HTS) has been employed to discover new antibiofilm compounds. Chemical compound library screening (CLS) is the initial approach for the discovery of new bioactive agents. However, large whole cell and target-based library screening requires extensive efforts and results have been disappointing so far (Payne *et al.*, 2007). An alternative to large library screens, screening FDA approved drug libraries has become more popular for drug repurposing. The term drug repurposing is used to describe a strategy to identify new uses for approved drugs that are outside of the scope of their original intended medical use (Pushpakom *et al.*, 2019). Amongst other approaches of drug discovery that are costly, drug repurposing is now expanding because it can provide a greatly shortened path to clinical use.

HTS has been used to identify hits by screening libraries containing different drugs. Whole cell phenotypic and target-based screens are two strategies employed to identify hits in libraries. A target-based method was popular after the arrival of genomics and bioinformatics where it can provide insight into the mechanism of action of the drug which helps in identifying important disease related targets. Phenotypic screens were less favoured as mechanisms of actions were usually determined later. However, target-based approaches results were disappointing, and no new antibiotics were developed from these platforms. Whole phenotypic cell assays gained popularity again as they are more likely to produce successful leads (Payne *et al.*, 2007). Phenotypic screening methods can identify compounds that show an effect in a model system without prior knowledge of the target affected (Moffat *et al.*, 2017).

In this chapter, the antimicrobial activity of NDs was assessed. In addition, a HTS of an FDA-approved compound library was performed to identify potential novel antifungal agents, with the consideration that repurposing currently available drugs may substantially reduce the time and effort required for antifungal

development. Screening bioactive compounds can give hits which affect a particular process of interest, which in this chapter is biofilm formation. These novel approaches may allow better understanding of mechanisms underlying the process of biofilm formation.

Although some *in vitro* studies have shown an antagonistic relationship between *C. albicans* and *E. faecalis* (Graham et al., 2017a, Cruz et al., 2013), the common coisolation of *C. albicans* and *E. faecalis* from different sources of infections would suggest that a synergistic pathogenicity might exist between both species. In the previous chapter, transcriptomic analysis reflected this complex relationship, whereby results from phenotypic analysis that demonstrated antagonism were confirmed, however, several other virulence mechanisms were shown to be altered in favour of *C. albicans* survival like deposition of biofilm matrix, metabolic adaptability, and enhanced stress response. This led to speculation that *C. albicans* develops enhanced stress response in dual-species biofilm. To test this assumption and to decode further the complex behaviour of both microorganisms when they coexist together, it was decided to challenge a dual-species biofilm model with novel therapeutics to assess their response when targeting virulence mechanisms. For this purpose, antimicrobial materials were chosen to target biofilm formation of dual-species without causing a killing effect. Therefore, detonated-NDs were chosen as it was shown to produce less killing effect than other types of NDs. In addition, small molecules that would be good candidates to hit virulence targets in *C. albicans* was also identified through HTS of FDA approved drugs.

4.2 Hypotheses and Aims

C. albicans and *E. faecalis* have a complex relationship beyond antagonism. It is hypothesised that treating dual-species biofilms of these organisms with novel therapeutics targeting their virulence will help in understanding the cross-kingdom, co-infectious microbial relationship. In addition, it is hypothesised that these novel therapeutics will be effective in reducing virulence mechanisms in both species when in single and dual-species biofilm states.

The aims of this chapter were to:

1. Explore NDs antimicrobial activity against *C. albicans* and *E. faecalis* in mono-species and dual-species biofilms.
2. Investigate the effect of detonated-NDs on *C. albicans* virulence behaviour when in single and dual-species biofilm.
3. Screen FDA approved drugs for anti-fungal activity against *C. albicans* lab strain using HTS.
4. Test the effect of identified compounds against high and low biofilm formers and high and low virulence strains of *E. faecalis* in mono-species biofilm state.
5. Investigate antimicrobial activity of identified compounds against dual-species biofilm
6. Explore combinational treatments with NDs and outputs from HTS against pre-formed mono and dual-species biofilms.

A paper pertaining this chapter was submitted to APMIS journal under the title “Screening the Tocriscreen™ bioactive compound library in search for inhibitors of Candida biofilm formation”.

4.3 Materials and methods

4.3.1 Culture conditions and standardisation

As described in 2.3.1.

4.3.2 Assessment of the antimicrobial activity of nanodiamonds

4.3.2.1 Nanodiamonds and endodontic irrigants stock preparation

Different antimicrobial test agents were used in this chapter at the following stock concentration: 3% (30000 ppm) NaOCl (Parcan; Septodont, Saint-Maur-des-Fosses, France), 17% (170000 ppm) EDTA (ENDO-SoLution, Poland), and medium molecular weight Chitosan (Sigma-Aldrich, St. Louis, USA). Chitosan was prepared at 1400 µg/mL and was solubilised in 2% acetic acid under constant magnetic stirring for 24 hours at room temperature (Vieira *et al.*, 2019). Purified detonation NDs (G01 grade) were purchased from Plasmachem GmbH, Berlin, Germany (average cluster size: ca. 4nm, >97% NDs powder, non-diamond carbon content: traces, controlled admixtures, %: Fe<0.3; Zn < 0.01l Cu<0.01; Mn < 0.01: Si+Cr+Ca+Ti < 0.01). Stock concentration of NDs were prepared in 1:1 v/v THB:RPMI media at 10,000 mg/L and the mixture was sterilized by autoclaving at 121°C for 20 minutes.

4.3.2.2 Minimum biofilm inhibitory concentration agents against *C. albicans* and *E. faecalis*

The MIC was determined using a broth microdilution method according to the M27-A3 standard for fungi (Wayne, 2002) (CLSI) and M07-A10 for bacteria (Patel *et al.*, 2015) with modification. Yeast cells were adjusted to 2×10^6 yeast/mL while bacteria were adjusted to 2×10^7 cells/mL in 1:1 RPMI:THB. A 200 µL of 3% NaOCl only, 17% EDTA only, and 0.7 mg/mL Chitosan, 5000 mg/L NDs. Untreated controls were used for comparison and each drug was added to the appropriate wells of 96-well flat-bottom microtiter plates (Corning Incorporated, NY, USA) and serial doubling-dilutions were performed in RPMI:THB. After 24 hours, the MIC concentration was determined using AlamarBlue™ metabolic activity assay (Sigma-Aldrich, UK) as described in section 2.3.5. CV assay was used as previously described in section 2.3.6 to measure biofilm biomass as the lowest concentration

of treatment that prevents 80% of biofilm metabolic activity and biofilm biomass. In parallel, plates were imaged using EVOS FL Cell Imaging System (Thermo Fisher Scientific).

4.3.2.3 Agar disc diffusion test

Sterile paper discs (diameter: 6mm, thickness: 1mm) (Watman International, Maidstone, UK) were impregnated with 10 µl of NDs (5000 mg/L), NaOCl 3% as a positive control and PBS to act as a NC. CBA and SAB plates were prepared to inoculate *E. faecalis* ER5/1 strain and *C. albicans* SC5314 lab strain respectively. After inoculation with the respective strain, plates were left to dry inside the hood. Loaded discs were inserted into agar plates and incubated in 37°C and 30°C incubators overnight. Zone of inhibition was indicated by a clear halo surrounding the disc.

4.3.2.4 Metabolic analysis of biofilms

Biofilms were analysed for metabolic activity using AlamarBlue™ cell viability dye (Invitrogen, UK) (Yajko *et al.*, 1995) As described in section 2.3.5.

4.3.2.5 Assessment of biofilm biomass

The biomass of the biofilms was quantified using a CV stain (Jose *et al.*, 2010). As described in section 2.3.6.

4.3.2.6 Quantification of biofilm cells of *C. albicans* and *E. faecalis* in single and dual-species biofilm when treated with nanodiamonds

C. albicans and *E. faecalis* cultures were adjusted to a density of 2×10^6 cells/mL and 2×10^7 cells /mL respectively in THB:RPMI medium containing NDs concentration of 2500/mL. A volume of 500 µL of the microbial/ NDs mixture was then dispensed into the defined wells of the 24-well flat bottom microtitre plates and incubated in 5% CO₂ at 37°C for 24 hours. After incubation, plates were washed with PBS to remove loosely attached cells. Untreated wells were included as positive controls for comparison. The effect of treatment was assessed using light microscopy and by means of viable plate counts.

4.3.2.7 Viability assessed by colony forming units (CFU)

The Miles and Misra technique was used to assess the number of viable and culturable cells within the biofilm post maturation or treatment (Miles *et al.*, 1938). Firstly, the supernatants were removed from the designated wells and kept in sterile 1.5 mL microcentrifuge tubes. Then, biofilm removal from the surface of a substrate was achieved in the following manner: designated wells were washed to remove non-adherent cells by using a pipette angled 45° at the side of the well and washing two times with PBS. To remove the biofilm 1000µL PBS was added into the well and a 1000 µL pipette tip to disaggregate the biofilm from the surface, firstly using a circular motion within the well and finally a criss-cross pattern to ensure adequate removal. Suspensions were serially diluted 10x in PBS from neat to 10⁻⁶ within 96-well microtiter plates. Appropriate agar plates were prepared in advance and ensured to be dry before use to reduce spreading of liquid over the agar. Plates were sectioned into 6 and for each dilution 20 µL spot plated onto a section in triplicate and left to dry in the category II safety cabinet before transfer to appropriate incubator. Colonies were counted where the numbers ranged between 15-200 and CFU/mL calculated (CFU = Mean num. of colonies in spot × 50 × dilution factor per mL).

4.3.3 Transcriptional analysis of biofilm related genes

Biofilms were grown as described in section 4.3.2.7 in 24 well flat-bottom plates 24 hours at 37°C. Following incubation, the supernatant was kept in sterile 1.5 mL microcentrifuge tubes and biofilms carefully washed with PBS. One millilitre of PBS was added to each well and biofilm was scraped and kept in sterile 1.5 mL microcentrifuge tubes. RNA extraction from biofilms, DNase digestion, cDNA synthesis and gene expression using qRT-PCR was carried out as in the following sections respectively

4.3.4 Nanodiamonds disc preparation

Bovine dentine discs (Modus Laboratories, Reading, UK) used in this study were of 7 mm in diameter, 1 mm in thickness, with perpendicular dentinal tubule orientation (transverse cross section). The dentine discs were autoclaved at

122 °C, before use, for 16 min. One bioceramic material was used: Biodentine™ (Septodont, Saint-Maur-des-Fossés, France). Moulds, 1 mm in height with 7 mm diameter corresponding to the size of the bovine dentine discs, were fabricated from dental silicone-based impression materials; putty soft (Coltene, Altstätten, Switzerland); and polyvinyl siloxane impression material (Extrude, Romulus, MI, USA). The moulds were then disinfected with 70% ethanol. To investigate the effect of NDs on the antimicrobial properties of the tested material, NDs (Plasmachem GmbH, Berlin, Germany) were incorporated into Biodentine™ using two different concentrations (2.5 wt% and 5 wt%) and the resultant powder was mixed with 180 µL of the Biodentine™ Liquid (approximately 5 drops as recommended by the manufacturer) (Table 4.1), using a mixing machine for 30 seconds at 4000-4200 rpm. Unmodified Biodentine™ was mixed similarly and used as control. The material was then compacted into the aseptic moulds and allowed to set in a moist atmosphere at 37 °C for 1 h. Following incubation, the discs were disinfected using UV for 15 minutes.

Table 4.1: NDs percentages incorporated into Biodentine™

Percentage	Biodentine™ powder (g)	NDs powder (g)	Mixing liquid (Biodentine™ Liquid)
BD (Unmodified)	0.7	–	180 µL
BD + 2.5 wt%	0.6825 (0.7-0.0175)	0.0175	180 µL
BD + 5 wt%	0.665 (0.7-0.035)	0.035	200 µL

4.3.5 Biofilm inhibition screen

The FDA approved drug library from Tocriscreen™ 2.0 micro-library (Tocriscreen™, Bristol, UK) were assessed for biofilm inhibition against the *C. albicans* SC5314 wild type strain. Overnight culture was prepared as described in section 2.3.1 An initial 1:100 dilution was prepared by pipetting 1 µL of this concentrated solution into 99 µL of cells in RPMI media using the wells of presterilized, polystyrene, flat-bottomed 96 well microtiter plates (Corning Incorporated, Corning, NY). The first column of the plate, 1 µL of DMSO was added as a control. Cells were incubated

for 24 hours at 37°C. Supernatants were removed from wells and XTT metabolic reduction assay was used to assess cell viability, as described in section 0. The biomass inhibitory effect was assessed through CV assay as section 0.

4.3.6 Compound library and selected drugs stock preparation

Tocriscreen™ 2.0 Micro is a collection of 1280 biologically active compounds of 10mM pre-dissolved in DMSO solutions were dispensed in 96 well racks with 80 compounds per rack each well contained 50 µL with the first and last columns containing only empty tubes a total number of 18 plates were stored in -20°C freezer until use. The selected hit compounds were Polygodial, M62812, KHS101 hydrochloride, Toyocamycin, CD437, darapladib, Bazedoxifine acetate, CH55 purchased from Tocriscreen (Biotechnie, Bristol, UK) and LE135, Ferrostatin-1 purchased from Sigma Aldrich (Sigma - Aldrich, UK) and solubilised in 100% DMSO (w/v) according to manufacturer instruction to produce 100mM stocks. Aliquots of each compound were then stored at -20°C.

4.3.7 Planktonic minimum inhibitory concentration of small molecule compounds against *E. faecalis* and *C. albicans* isolates

Minimum inhibitory concentration (MIC) was determined using a broth microdilution method according to the M27-A3 standard for fungi (Wayne, 2002) (CLSI) and M100 for bacteria (CLSI, 2022). Briefly, yeast cells were adjusted to 2×10^4 yeast/mL while bacteria were adjusted to 2×10^5 cells/mL in 1:1 THB: RPMI. 200 µL of each drug was added to the appropriate wells of 96-well round-bottom microtiter plates (Corning Incorporated, NY, USA) and serial doubling-dilutions were performed in THB: RPMI. 100 µL of standardised cells was added to each well containing the drug and incubated at 37°C, to get a final volume of 200 µL. (Sigma-Aldrich, Dorset, UK). The plates were incubated at 37°C. After 24 hours, the MIC concentration was determined as the lowest concentration of treatment that prevents visible microbial growth.

4.3.8 KHS101 hydrochloride and darapladib biofilm inhibition, and disruption susceptibility against single-species and dual-species biofilm of *C. albicans* and *E. faecalis*

For biofilm inhibition assessment, *C. albicans* and *E. faecalis* cells were adjusted to a density of 2×10^6 cells/mL and 2×10^7 cells/mL respectively in THB: RPMI media containing KHS101 hydrochloride at 8, 16, 32 and 64 $\mu\text{g/mL}$ concentration and darapladib at 4, 8, 16 and 32 $\mu\text{g/mL}$. A volume of 500 μL of the microbial/ drugs mixture was then dispensed into the defined wells of the 24-well flat bottom microtitre plates and incubated in 5% CO_2 at 37°C for 24 hours. After incubation planktonic cells were discarded. Untreated wells were included as a PC for comparison. The effect of treatment was assessed phenotypically by microscopic images, viability assay using XTT to determine metabolic activity, biofilm biomass using CV assay and by means of viable plate counts.

For biofilm disruption assessment, *C. albicans* and *E. faecalis* cells were adjusted to a density of 1×10^6 cells/mL and 1×10^7 cells/mL, respectively, in THB:RPMI medium. Cells were then dispensed into the defined wells of the 24-well flat bottom microtitre plates and incubated in 5% CO_2 at 37°C for 24 hours. After incubation planktonic cells were discarded. Preformed biofilms were washed twice with 500 μL PBS. Treatments of KHS101 hydrochloride 64 μg , KHS101 64+ NDs 5000 mg/L, darapladib 32 $\mu\text{g/L}$, darapladib 32 + NDs 5000mg/L and NDs 5000mg/L were added to each designated well. Untreated wells were included as a PC for comparison. The effect of treatment was assessed phenotypically by microscopic images, viability assay using XTT to determine metabolic activity, biofilm biomass using CV assay and by means of viable plate counts, as described in section 2.3.

4.3.9 Statistical Analysis

Graph production, data distribution and statistical analysis were performed using GraphPad Prism (Version 9.3.1; La Jolla, CA, USA). One-way Analysis of Variance (ANOVA) or non-parametric Kruskal-Wallis were used to investigate significant differences between independent groups of data. A Dunnett's and Dunn's post-comparison tests were applied to the p value to account for multiple comparisons of smaller datasets. Statistical significance was achieved upon $P < 0.05$. Multiple t-tests were used to assess significance between treated samples and PCs of independent groups of data. Two-way ANOVA was used to assess significance between different treatment group samples under different conditions with Tukey multiple comparison test was used for tests with more parameters.

4.4 Results

4.4.1 Nanodiamonds showed no fungicidal and bactericidal activity against *C. albicans* and *E. faecalis* biofilms.

First, to determine the antimicrobial activity of NDs, a standard MIC test was carried out to assess their fungicidal and bactericidal activity against *C. albicans* and *E. faecalis* strains. This activity was compared to novel and traditional irrigants; increasing concentrations of NDs, a novel irrigant Chitosan and traditional endodontic irrigants (NaOCl and EDTA) were used. Following incubation for 24 hours, viability and biofilm biomass were assessed using AlamarBlue™ and CV respectively. Results revealed that NaOCl 3% showed MIC against all *E. faecalis* strains at a concentration range from 0.062% - 0.31%. Furthermore, NaOCl showed MIC values between 0.01%- 0.0187% against *C. albicans* isolates. Regarding biofilm biomass, NaOCl was able to inhibit biofilm formation at concentrations from 0.062% - 0.125% in *E. faecalis* strains and 0.023% - 0.187% in *C. albicans* isolates. EDTA showed MIC between 0.016%-0.066% against *E. faecalis* strains and 0.016% - 0.13% against *C. albicans* isolates. EDTA was able to inhibit biofilm biomass at the same concentrations. Chitosan showed potency against *E. faecalis* and *C. albicans*, the MIC against *E. faecalis* strains ranged between (0.02 - 0.175) mg/mL and (0.04 - 0.35) mg/mL. Regarding biofilm biomass, chitosan inhibited biofilm formation at (0.175-1.4) mg/mL for *E. faecalis* strains and (0.35-1.4) mg/mL for *C. albicans* isolates. Results showed that NDs were not able to kill *C. albicans* or *E. faecalis* strains. The MIC values for metabolic activity and biofilm biomass is listed in Table 4.2 and Table 4.3 respectively. To further confirm results, an disk diffusion assay was done. NaOCl were included a PC and PBS as a NC. The diffusion assay confirmed the inability of NDs to kill *E. faecalis* or *C. albicans* compared to NaOCl that showed zone of inhibition indicating killing activity against both species (Figure 4.1).

Table 4.2: Biofilm inhibition MIC of *C. albicans*, *E. faecalis* clinical and lab isolates to NaOCl, EDTA, Chitosan and nanodiamonds. Numbers represent metabolic activity MIC values. a (-) indicates MIC value not detected.

Metabolic Activity	Isolate name	NaOCl %	EDTA %	Chitosan mg/mL	NDs mg/L
<i>E. faecalis</i> Strains	ATCC29212	0.062	0.016-0.066	0.02-0.175	-
	NCTCC5957	0.062	0.13-0.033	0.175	-
	E1	0.06 - 0.125	0.13-0.033	0.08-0.175	-
	E3	0.06 - 0.125	0.016-0.033	0.08-0.175	-
	ER5/1	0.06 - 0.125	0.016-0.033	0.175-0.35	-
	E2	0.06 - 0.125	0.016-0.033	0.175	-
	J42-7	0.062	0.016-0.033	0.08-0.7	-
	O5-16	0.062 - 0.31	0.016-0.033	0.04-0.175	-
	OGX	0.06 - 0.125	0.016-0.033	0.08-0.175	-
	AAOR34	0.062	0.016-0.033	0.175	-
	V583	0.062	0.016-0.066	0.04-0.175	-
	ER35	0.062	0.016-0.033	0.08-0.175	-
<i>C. albicans</i> strains	BC020	0.023-0.09	0.016-0.033	0.04-0.35	-
	BC146	0.046-0.187	0.033-0.13	0.08-0.35	-
	BC023	0.09-0.187	0.033-0.066	0.175-0.35	-
	BC145	0.09 - 0.187	0.016-0.033	0.175-0.35	-
	BC037	0.011-0.187	0.016-0.066	0.35	-
	BC136	0.023-0.187	0.016-0.066	0.175-0.35	-
	BC038	0.023-0.09	0.066	0.35	-
	BC117	0.09-0.187	0.033-0.13	0.175-0.35	-
	BC039	0.023-0.187	0.066	0.35	-
	BC040	0.023-0.187	0.066-0.13	0.175-0.35	-
	SC5314	0.011-0.187	0.066	0.35	-
	3153A	0.011-0.187	0.033-0.13	0.175-0.35	-

Table 4.3: Biofilm inhibition MIC of *C. albicans*, *E. faecalis* clinical and lab isolates to NaOCl, EDTA, Chitosan and NDs. Numbers represent biofilm biomass MIC values. a (-) indicates MIC value not detected.

Biofilm Biomass	Isolate Name	NaOCl %	EDTA %	Chitosan mg/mL	NDs mg/L
<i>E. faecalis</i> strains	ATCC29212	0.09-0.187	0.016-0.033	0.175	-
	NCTCC5957	0.09-0.187	0.016-0.033	0.175-0.7	-
	E1	0.09	0.033	0.175-0.35	-
	E3	0.09	0.033	0.175-1.4	-
	ER5/1	0.09	0.033	0.175	-
	E2	0.09	0.016-0.033	0.175	-
	J42-7	0.187	0.016-0.033	0.175	-
	O5-16	0.09	0.033	0.175	-
	OGX	0.09	0.016-0.033	0.175	-
	AAOR34	0.09	0.016-0.033	0.175	-
	V583	0.09	0.016-0.033	0.175	-
	ER35	0.09	0.016-0.033	0.175	-
<i>C. albicans</i> strains	BC020	0.09	0.066	0.35	-
	BC146	0.09	0.016-0.033	0.35-1.4	-
	BC023	0.09-0.187	0.033-0.066	1.4	-
	BC145	0.09	0.033-0.13	0.35	-
	BC037	0.09	0.016-0.033	0.35-0.7	-
	BC136	0.09	0.016-0.033	0.35	-
	BC038	0.046	0.016-0.033	0.35	-
	BC117	0.023-0.187	0.016-0.066	0.35-0.7	-
	BC039	0.187	0.033	0.7	-
	BC040	0.09	0.016-0.066	0.35-1.4	-
	SC5314	0.046	0.016-0.033	0.35	-
	3153A	0.09	0.016-0.066	0.35-0.7	-

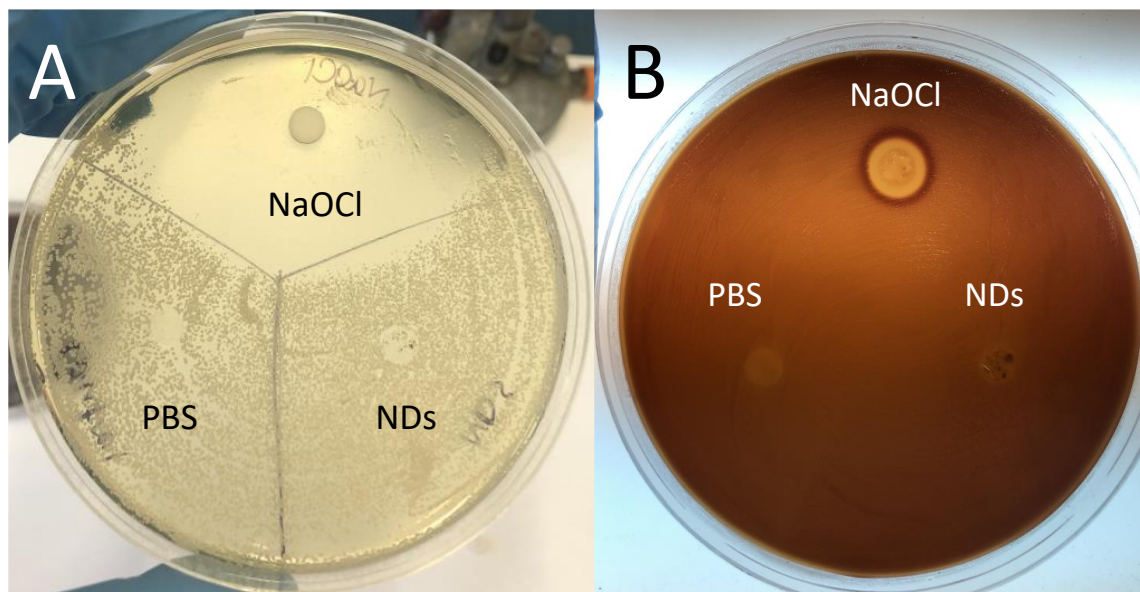


Figure 4.1: Disk diffusion assay for NDs. Kirby-Bauer disk diffusion susceptibility test on *C. albicans* SC5314 isolate (A) and *E. faecalis* strain ER5/1 (B) on Sabouraud agar (A) and Blood agar (B) plates with NaOCl 3%, NDs 5000 mg/L and PBS used as control. The zones of clearing indicate susceptibility to tested drugs.

4.4.2 Microscopic analysis of nanodiamonds interaction with *C. albicans* and *E. faecalis*

To explore any potential phenotypic changes on *C. albicans* and *E. faecalis* by NDs, microscopic images were taken to investigate the interaction of NDs with *C. albicans* and *E. faecalis*. Following incubation of *C. albicans* lab strain SC5314 and *E. faecalis* strain ER5/1 with NDs, biofilm was washed with PBS and examined under light microscopy. Images showed that NDs coated *C. albicans* cells and its hyphae in a dose dependent manner (Figure 4.2: Black arrows). Furthermore, it was observed that less cells adhered at the bottom of the plate when biofilm was incubated with NDs for 24 hours (Figure 4.2). This indicates that the presence of NDs with *C. albicans* inhibited its attachment compared to PC. In addition, microscopic images showed fewer *E. faecalis* cells attached compared to PC which also suggests prevention of biofilm formation. It was also evident that *E. faecalis* cells aggregated with NDs particles which might have contributed to the reduced attachment seen (Figure 4.3: Black arrows).

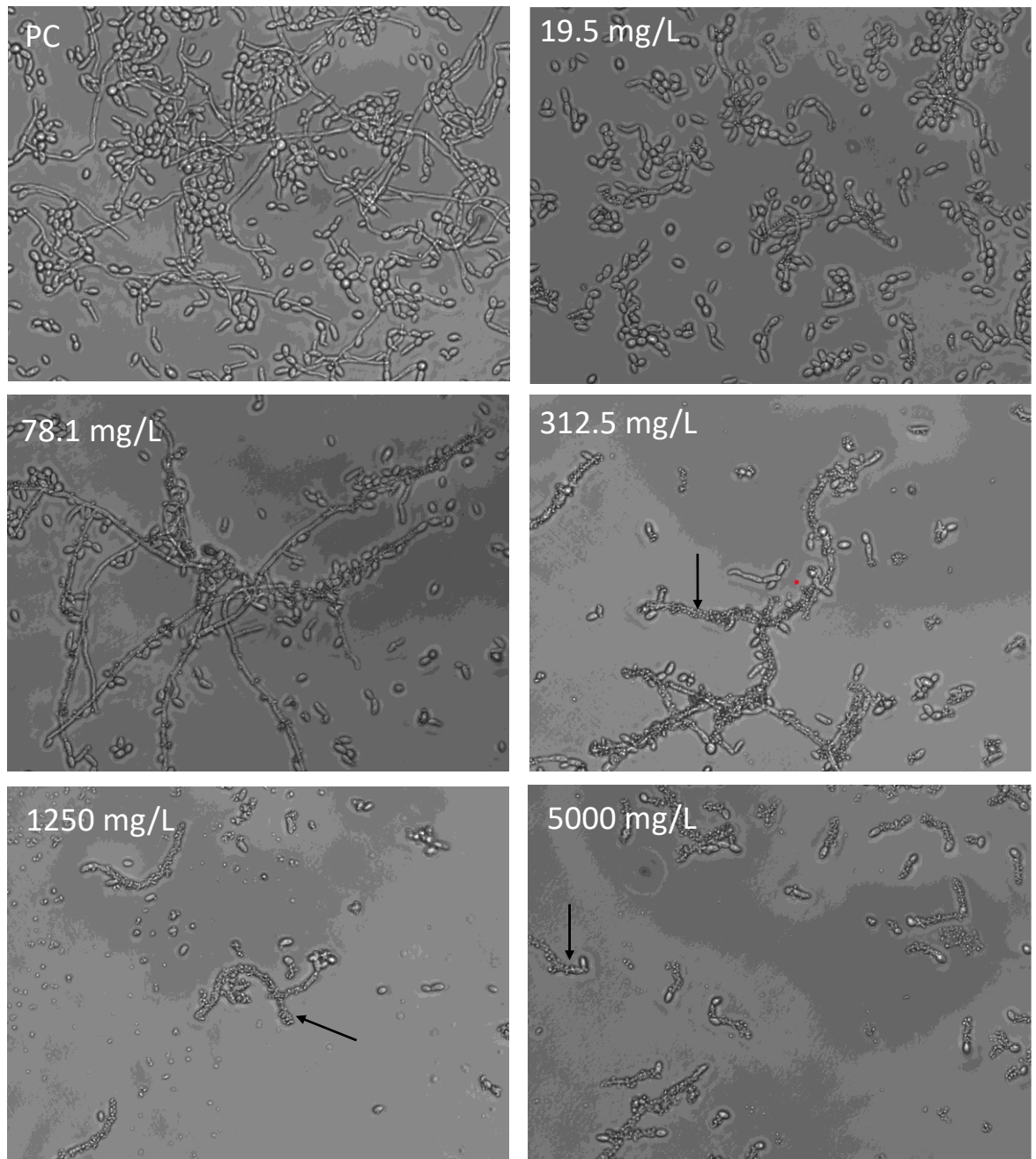


Figure 4.2: Light microscopic images of *C. albicans* biofilm after incubation with NDs. *C. albicans* SC5314 lab strain was grown in THB:RPMI media in mono-culture with NDs for 24 hours at increasing concentrations. *C. albicans* can be seen coated with NDs (Black arrows) and a decrease in *C. albicans* cell numbers as concentration of NDs increases. Biofilms were examined using EVOS cell imaging system at 400X magnification.

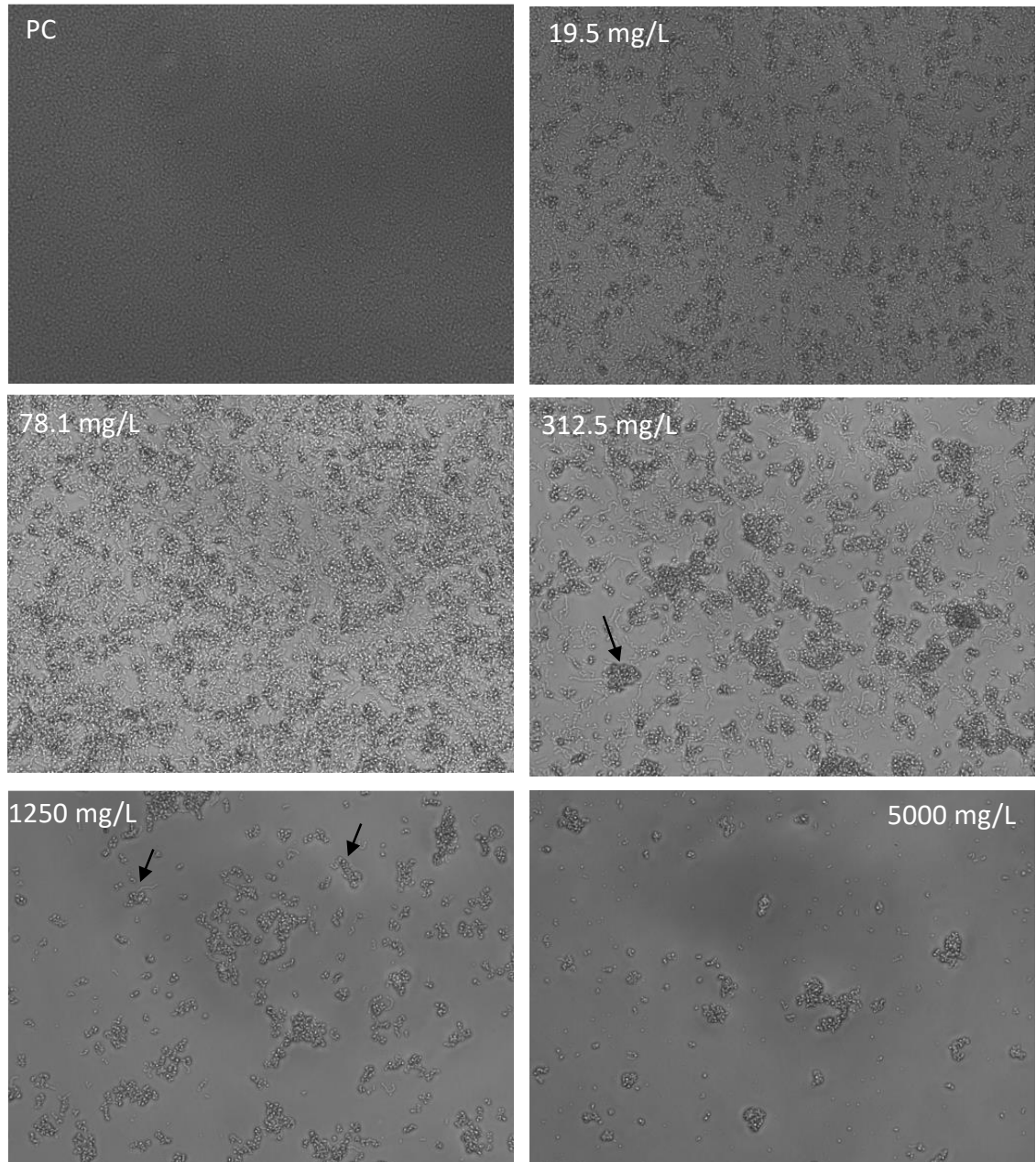


Figure 4.3: Light microscopic images of *E. faecalis* biofilm after incubation with NDs. *E. faecalis* ER5/1 strain was grown in THB:RPMI media in mono-culture with NDs for 24 hours at increasing concentrations. *E. faecalis* can be seen aggregating with NDs (Black arrows). A decrease in *E. faecalis* cell number is noted as concentration of NDs increases. Biofilms were examined using EVOS cell imaging system at 400X magnification.

4.4.3 Nanodiamonds exhibited anti-adhesion and biofilm inhibition effect against *C. albicans* clinical and lab isolates

As previously shown in microscopic images, reduced cell attachment was evident when *C. albicans* and *E. faecalis* were incubated with NDs. To explore the possibility that NDs reduce cell attachment. Mean colony forming units of *C. albicans* planktonic cells and cells that were attached at the bottom of the plate were counted for 12 *C. albicans* isolates.

Results showed that *C. albicans* planktonic cell counts were higher in treated compared to untreated cells. This effect was evident across all *C. albicans* isolates. In BC023, BC136, SC5314, BC023, BC145, 3153A, BC146 and BC117 there was an increase in planktonic cells compared to their untreated PCs. However, this increase was lower than 50% and was only statistically significant in BC146 isolate ($p < 0.01$). In BC037, BC038, BC040, BC039, planktonic cells were increased compared to their positive counterparts by more than 50%. This was statistically significant in BC037 ($p < 0.01$), BC040, BC039 ($p < 0.05$). In addition, results showed a decrease in the number of attached cells in treated cells compared to untreated. BC117, BC040 ($p < 0.05$), BC037 ($p < 0.05$), BC146, 3513A, BC020 showed reduction in cell attachment by more than 90%. In BC136, BC145 ($p < 0.05$), SC5314, BC039 ($p < 0.05$), BC023, reductions between 80% - 90% was observed in cell attachment. BC038 showed the least reduction in cell attachment (73%). In conclusion, NDs inhibit cell attachment by preventing *C. albicans* adhesion (Figure 4.4).

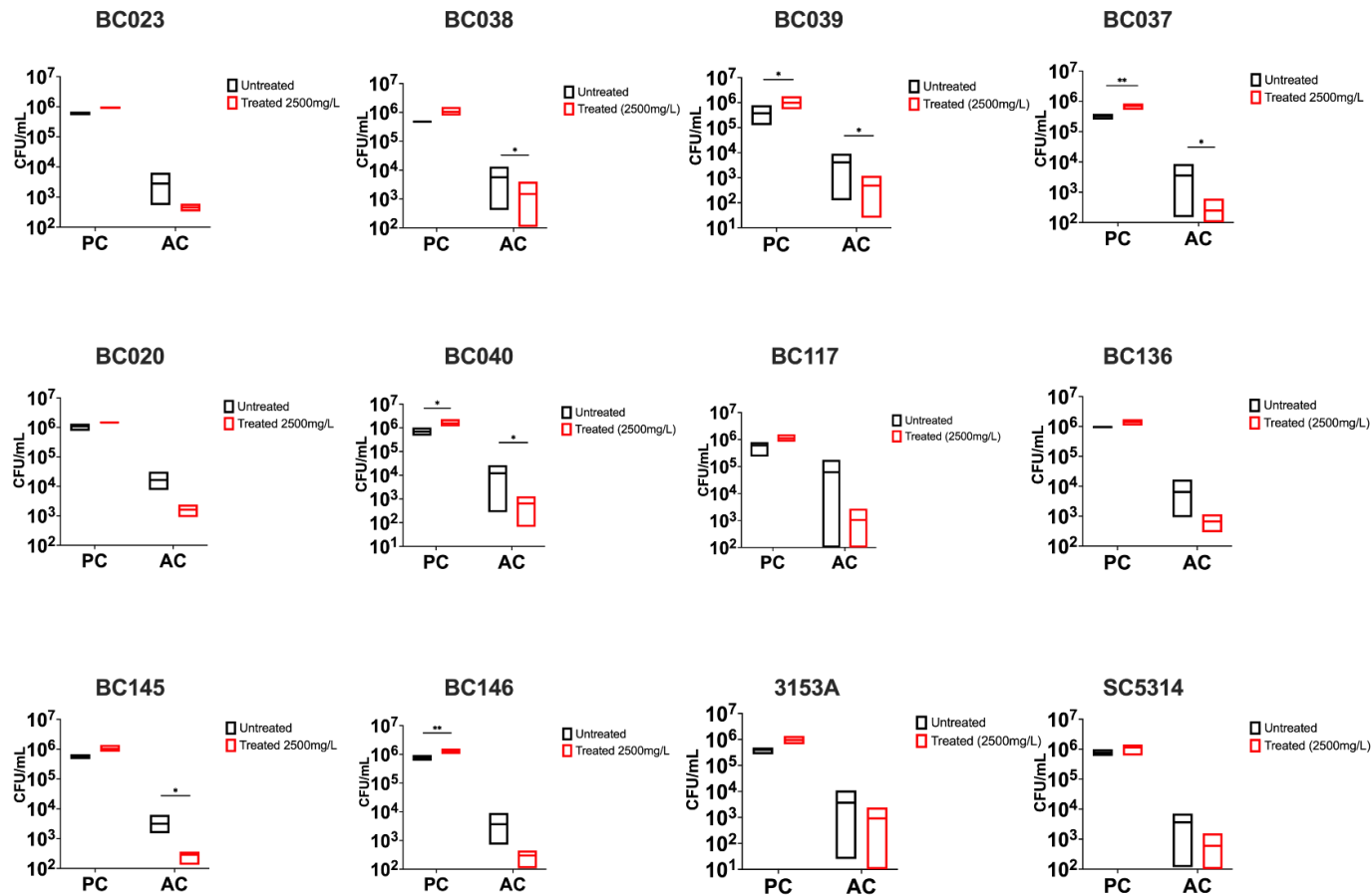


Figure 4.4: NDs prevented *C. albicans* isolates cell attachment. Mean colony forming units (CFU) of twelve strains of *C. albicans*. An increase in *C. albicans* planktonic cells when incubated with nanodiamonds and a reduction in cells attachment was observed in all twelve isolates. All samples were assayed in triplicate, on three separate occasions. Multiple t tests were used to assess significance between treated samples and PCs ($Xp < 0.05$, $**p < 0.01$). PC= Planktonic cells, AC= Attached cells.

4.4.4 Nanodiamonds exhibited biofilm inhibition effect against *E. faecalis*.

To further explore the reduction in *E. faecalis* cell attachment, viable plate counts were carried out to determine the number of planktonic and attached cells of *E. faecalis* strains with and without treatment with NDs at 2500 mg/L. Results showed that NDs reduced planktonic in *E. faecalis* cell numbers contrary to *C. albicans* isolates. More than 90% reduction was seen in NCTCC 5957 ($p < 0.001$), E3 ($p < 0.01$) and ER35 ($p < 0.05$). ATCC 29212 showed 79% decrease in planktonic cells. O5-16, V583 and OGX showed a decrease in planktonic cells between (50% - 64%) compared to their positive counterparts. In addition, a reduction in planktonic cells between 40% - 50% was also observed in J42-7, E2, E1 and ER5/1 *E. faecalis* strains. The lowest reduction was observed in AAOR34.

Moreover, reduction was also evident in attached cells of *E. faecalis* strains. OGX, ER5/1, E3 and AAOR34 showed more than 80% reduction in attachment. Less reduction in cell attachment was evident in ER35, V583, E1, E2 and O5-16 which showed reduction between 50% - 80%. However, the only significant difference was in ER5/1 and ER35 ($p < 0.05$). ATCC29212 and J42-7 showed the least reductions in cell attachment (36% and 25% respectively). However, NCTCC5957 strain was the only strain show an increase in attachment by 59%. Although results by viable cell counts showed total reduction of cells, however, according to our previous results where NDs showed no killing effect, it could be assumed that NDs exhibit a bacteriostatic effect against *E. faecalis* strains. Moreover, this suggests variation amongst *E. faecalis* strains in response to NDs treatment (Figure 4.5).

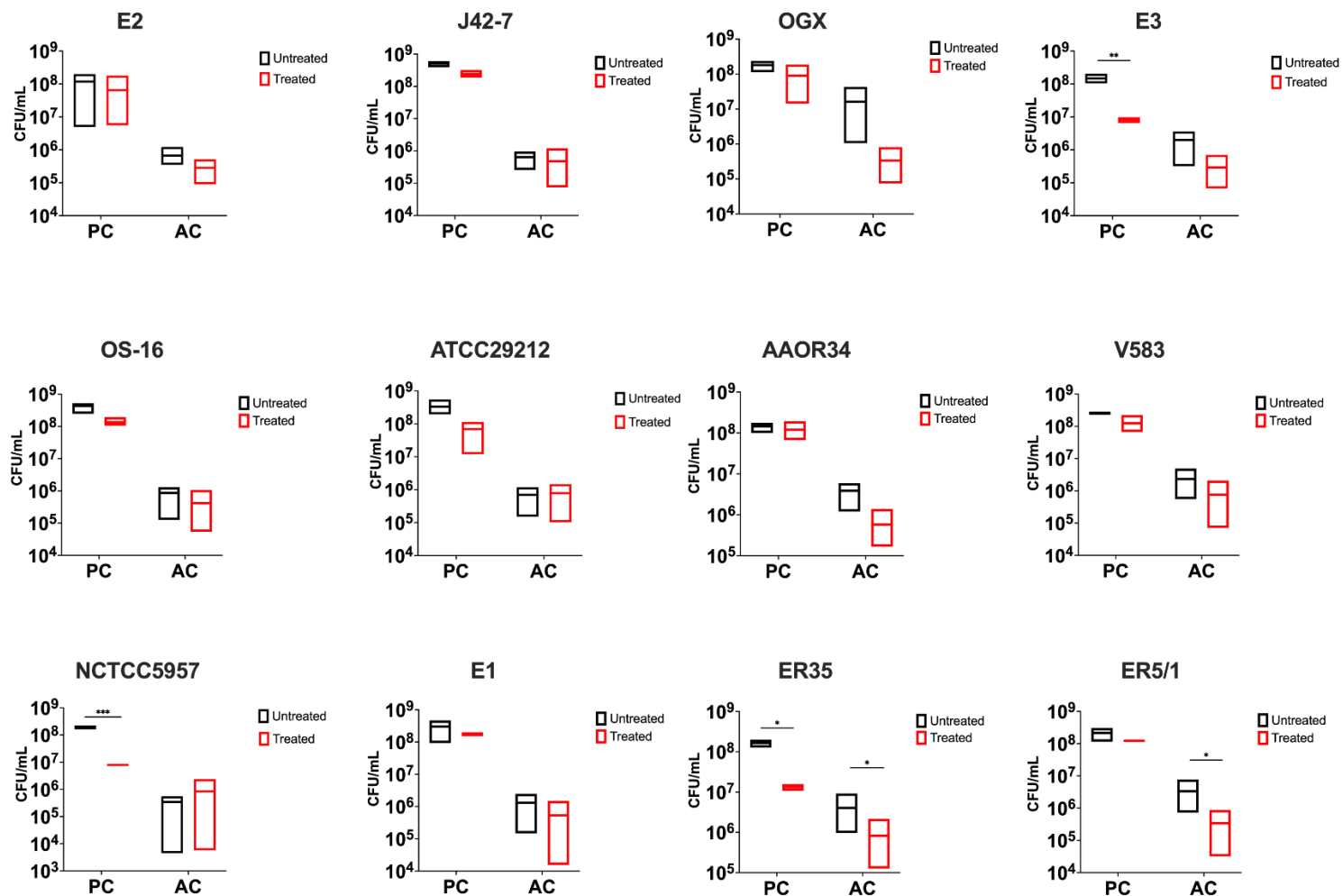


Figure 4.5: NDs prevented *E. faecalis* strains cell attachment. Mean colony forming units (CFU) of twelve strains of *E. faecalis*. A decrease in *E. faecalis* planktonic cells when incubated with nanodiamonds and a reduction in cells attachment was observed. All samples were assayed in triplicate, on three separate occasions. Multiple t tests were used to assess significance between treated samples and PCs (* $p<0.05$, ** $p<0.01$, *** $p<0.001$). PC= Planktonic cells, AC= Attached cells.

4.4.5 Nanodiamonds showed dual-species biofilm inhibition.

To assess the efficacy of NDs on *C. albicans* and *E. faecalis* dual-species biofilms, three isolates of *C. albicans* - a HBF (BC146), a LBF (BC023) and a lab strain (SC5314) were used. These were combined with two *E. faecalis* strains, a high virulent (ER5/1) and a LVS (E2). Each *C. albicans* isolate was cocultured with ER5/1 or E2 *E. faecalis* strain to establish a dual-species biofilm comprising of (BC146 + ER5/1) (BC146 + E2) (BC023 + ER5/1) (BC023 + E2) (SC5314 + ER5/1) (SC5314 + E2). Mono-species biofilm of each isolate was grown as a control. These biofilms (mono and dual-species) were co-incubated with and without NDs for 24 hours. Viable plate count assay was performed for planktonic and attached cells to enumerate *C. albicans* / *E. faecalis* cells. Furthermore, similar plates were incubated in parallel for imaging.

Microscopic analysis showed that NDs coated *C. albicans* SC5314 cells and their hyphae (Figure 4.6: B, black arrow) compared to untreated control (Figure 4.6: A) as shown previously. When *C. albicans* SC5314 was incubated with either *E. faecalis* strain, reduction in *C. albicans* cells was seen as well as inhibition of hyphal formation compared to SC5314 single-species biofilm (Figure 4.6: C, E). Upon incubation of dual-species with NDs, less *C. albicans* and *E. faecalis* cells were attached to the bottom of the plate (Figure 4.6: D, F). As seen in the images below, NDs coated *C. albicans* cells (Figure 4.6: B, solid black arrow). It was noticed that *C. albicans* hyphae were more apparent when this dual-species was treated with NDs (Figure 4.6: D, dashed black arrow) compared to untreated biofilms (Figure 4.6: C). This suggests that *C. albicans* responded differently to the presence of NDs than *E. faecalis*.

The effect on SC5314 was also evident in clinical isolates. Fewer yeast cells were attached from the LBF isolate when treated with NDs compared with PC (Figure 4.7: A, B). When LBF was incubated with ER5/1 or E2 *E. faecalis* strain, less *C. albicans* cells were seen in the dual-species compared to single-species biofilm (Figure 4.7: C, E). Upon treatment with NDs, reduction in *C. albicans* and *E. faecalis* attached cells was seen in dual-species with both strains (Figure 4.7: D, F). NDs coating yeast cells and *E. faecalis* cells was evident (Figure 4.7: F, solid black arrow). This effect was also seen in the HBF isolate. NDs were coating *C. albicans* cells as well as *E. faecalis* cells in both strains and less attached cells

were seen in both species (Figure 4.8: A, C, E) compared to their respective PCs (Figure 4.8: B, D, F).

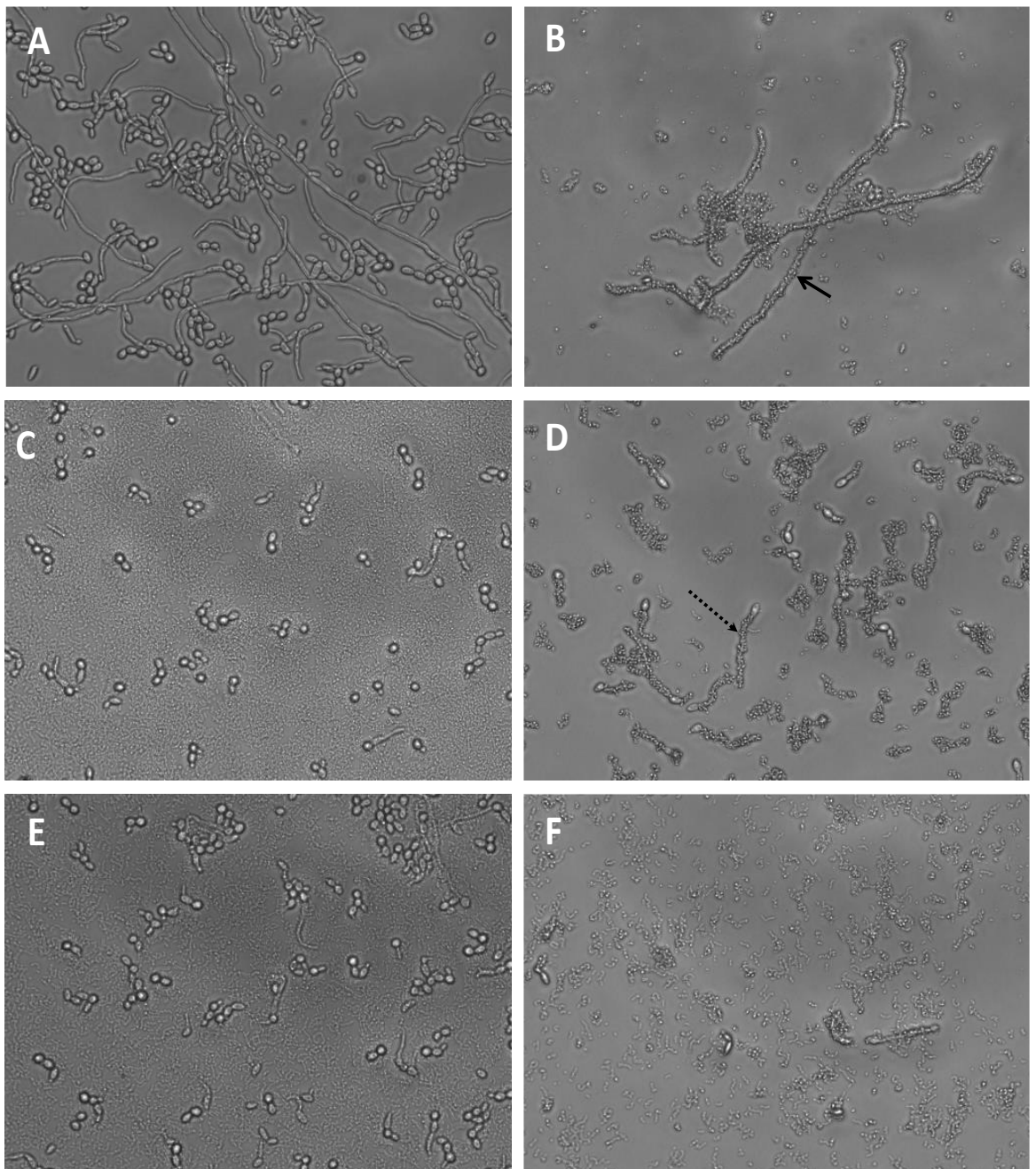


Figure 4.6: Light microscope images of single and dual-species biofilm of *C. albicans* SC5314 with and without treatment with NDs. *C. albicans* SC5314 was grown in THB:RPMI media in mono-culture not treated (A) and treated with NDs 2500 mg/L (B) or in coculture with *E. faecalis* HVS ER5/1 not treated (C) and treated with NDs 2500 mg/L (D) and *E. faecalis* LVS E2 not treated (E) and treated with 2500 mg/L (F) for 24 hours. Biofilms were examined using EVOS cell imaging system at 400X magnification. The solid arrow indicates NDs coating *C. albicans* hyphae. The dashed arrow represents increased hyphal development coated with NDs.

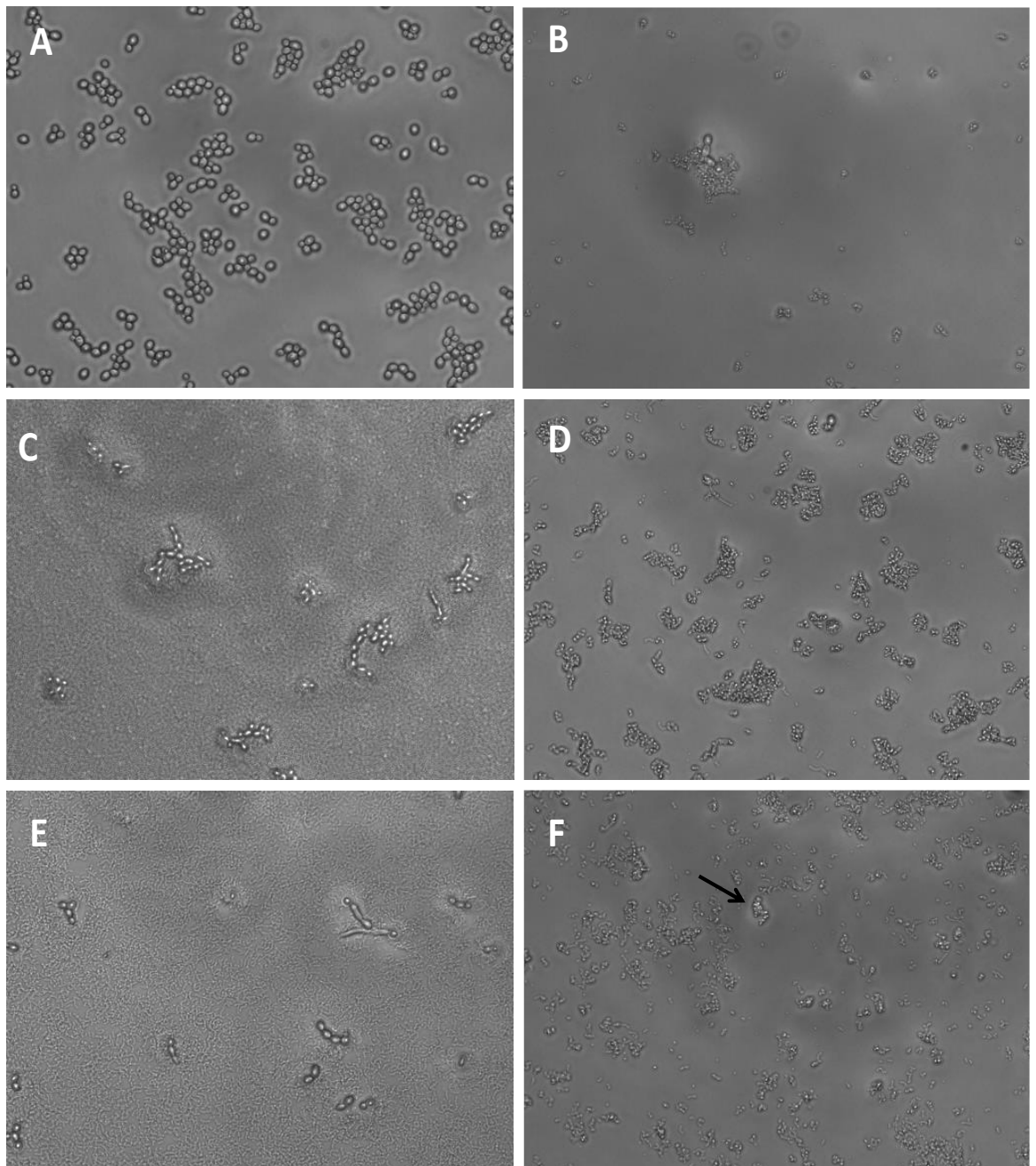


Figure 4.7: Light microscope images of single and dual-species biofilm of *C. albicans* LBF BC023 with and without treatment with NDs. *C. albicans* SC5314 was grown in THB:RPMI media in mono-culture not treated (A) and treated with NDs 2500 mg/L (B) or in coculture with *E. faecalis* HVSER5/1 not treated (C) and treated with NDs 2500 mg/L (D) and *E. faecalis* LVS E2 not treated (E) and treated with 2500 mg/L (F) for 24 hours. Biofilms were examined using EVOS cell imaging system at 400X magnification. The solid arrow indicates NDs aggregating on *E. faecalis* cells.

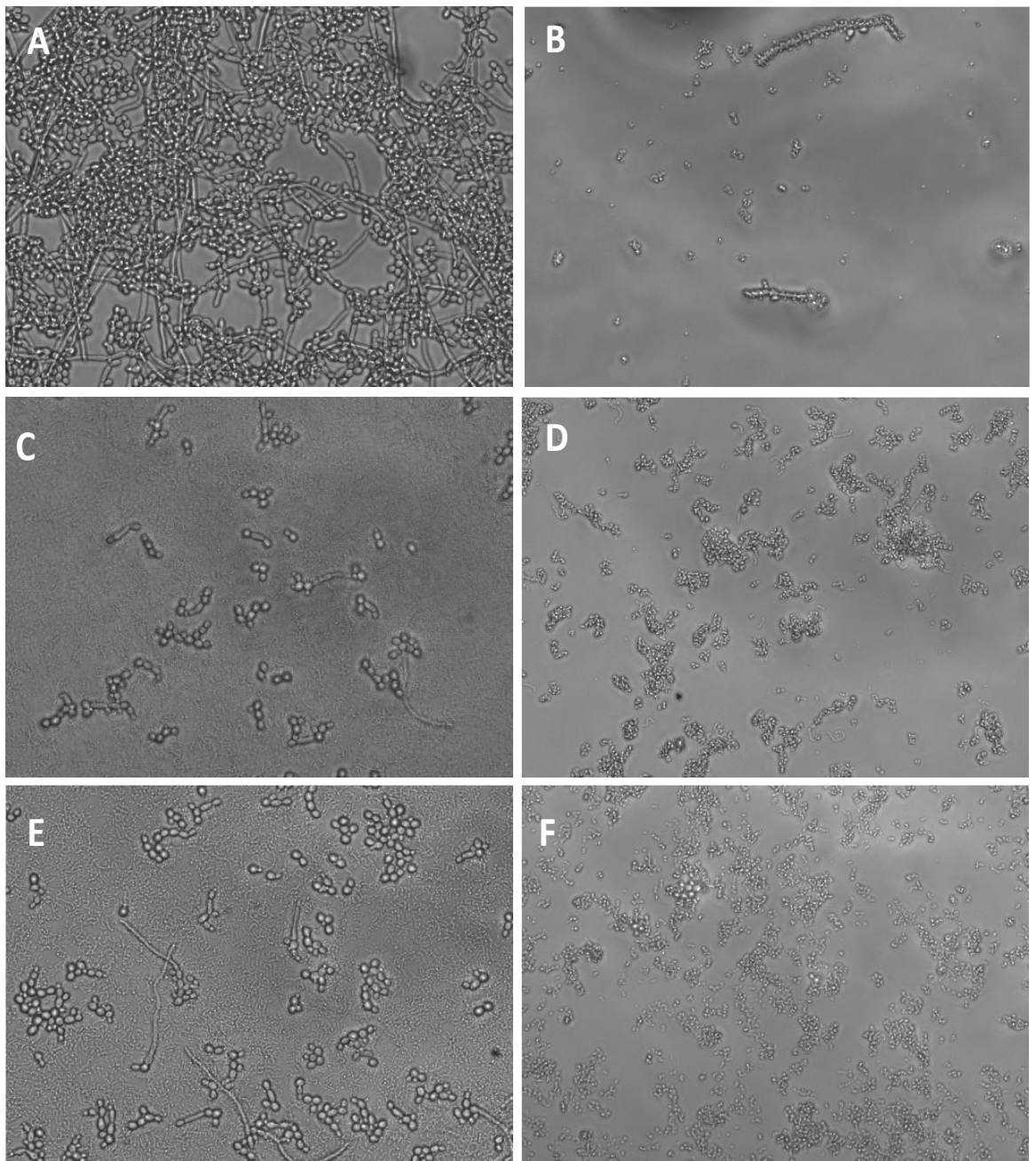


Figure 4.8: Light microscope images of single and dual-species biofilm of *C. albicans* HBF BC146 with and without treatment with NDs. *C. albicans* SC5314 was grown in THB:RPMI media in mono-culture not treated (A) and treated with NDs 2500 mg/L (B) or in coculture with *E. faecalis* HVS ER5/1 not treated (C) and treated with NDs 2500 mg/L (D) and *E. faecalis* low virulent strain E2 not treated (E) and treated with 2500 mg/L (F) for 24 hours. Biofilms were examined using EVOS cell imaging system at 400X magnification.

It was demonstrated that the total cell numbers of *C. albicans* that includes planktonic and attached cells in single and dual-species biofilms were higher when treated with NDs compared to PC. Adhesion was prevented across all biofilms composed of clinical and lab isolates cocultured with high virulent or low virulent strains of *E. faecalis*. Planktonic cells were higher in treated biofilms, whilst, attached cells were lower than untreated biofilms.

The total cell number of *C. albicans* SC5314 in treated single-species biofilm was 36% higher than the PC, planktonic cells counts were 73% higher in treated and the number of attached cells were 81% lower than untreated biofilm ($p<0.05$) (Figure 4.9: A). When SC5314 was cocultured with high virulence strain ER5/1 of *E. faecalis* the total number of *C. albicans* cells were significantly higher than the untreated biofilm by 79% ($p<0.05$). Due to the adhesion prevention seen by NDs the number of planktonic cells were significantly higher in treated than untreated biofilm by 91% ($p<0.01$). Less attached cells were seen compared to untreated biofilm by 43% (Figure 4.9: E). The same trend was seen using *E. faecalis* E2 low virulence strain dual-species biofilm. The total cell number was reduced by 55% in treated biofilm. Planktonic cells were higher by 92% ($p<0.01$) and attached cells were reduced by 57% compared to untreated controls. (Figure 4.9: H).

C. albicans LBF (BC023) single-species biofilm, comparable total cell counts were seen between treated and untreated biofilm. Planktonic cells of BC023 were slightly higher by 24% in treated biofilms compared to PC. BC023 attached cells were reduced by 91% in treated compared to untreated biofilms ($p<0.05$) (Figure 4.9: B). In dual-species biofilm (BC023 + ER5/1), a significant increase by 82% in the total cell number of BC023 was seen ($p<0.05$). Planktonic cells were significantly higher by 88% ($p<0.05$) and less attached cells were seen by 71% compared to PC (Figure 4.9: F). The same trend was seen in *E. faecalis* LVS. Total cell number of BC023 when cocultured with E2 LVS was increased by 78%. Planktonic cells were increased by 91% ($p<0.05$) and attached cells were decreased by 74% compared to PC (Figure 4.9: I).

In HBF BC146 the total cell number comprising planktonic and attached cells was increased by 67% in treated compared to untreated biofilms. Planktonic cells were increased by 85% and attached cells were reduced by 93% ($p<0.01$) (Figure 4.9: C). In dual-species biofilm, BC146 total cell number was increased by 84% when

cocultured with ER5/1 HVS ($p < 0.05$) in biofilm treated with NDs. Planktonic cells were increased by 92% ($p < 0.05$) and attached cells were reduced by 78% in treated biofilms compared to untreated biofilms (Figure 4.9: G). The same observation was seen dual-species biofilm when BC146 was cocultured with E2 LVS. Total cell number of BC146 was increased by 82% in treated compared to untreated controls. Planktonic cells were increased by 89% and attached cells were reduced by 69% in treated compared to untreated controls. (Figure 4.9:J)

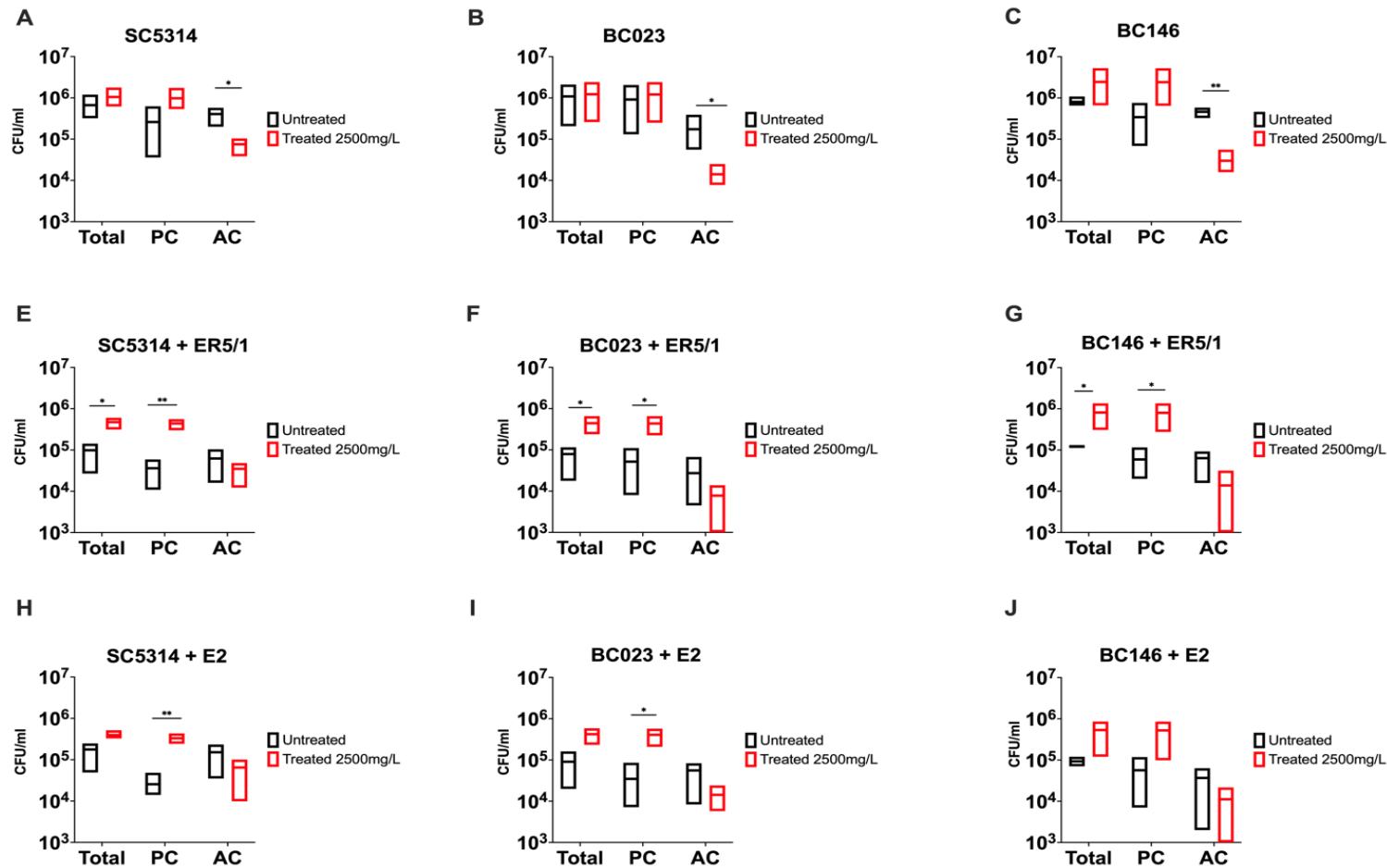


Figure 4.9: NDs effect on colony forming ability of *C. albicans* isolates in dual-species biofilm. (A - C) Mean colony forming unit (CFU) SC5314 (A), LBF BC023 (B) BC146 (C) of total, planktonic and attached cells when cocultured with HVS ER5/1 (E-G) and LVS E2 (H-J) in the presence and absence of NDs. All samples were assayed in triplicate, on three separate occasions. Multiple t tests were used to assess significance between treated samples and PCs. Data represents mean \pm SD * $p \leq 0.05$, ** $p \leq 0.01$. PC= Planktonic cells, AC= Attached cells

The response of *E. faecalis* differed according to strain type. In the case of HVS ER5/1, comparable total cell numbers were seen in single-species biofilm between treated and untreated biofilms. However, 97% reduction in cell attachment was evident in treated biofilm ($p < 0.01$) (Figure 4.10: A). In dual-species biofilm composed of ER5/1 and SC5314, a slight increase was observed in total cell number as well as planktonic cells by 33% and 38% respectively in treated biofilms. However, a reduction by 94% was seen in attached cells in treated biofilm ($p < 0.01$) (Figure 4.10: C). The same observation was seen in ER5/1 cell counts when cocultured with LBF BC023. Total cell number and planktonic cells were increased by 35% approximately in treated biofilm compared to PC. 90% reduction in attached cells in biofilm treated with NDs was observed (Figure 4.10: E). When ER5/1 was cocultured with HBF BC146, approximately 60% increase in total and planktonic cells was seen in ER5/1 in treated biofilm. In addition, 94% reduction in cells attachment in biofilm treated with NDs compared to PC ($p < 0.001$) (Figure 4.10: G).

In contrast to ER5/1, When LVS E2 was cocultured with SC5314, a decrease in its total cell number as well as planktonic cells by 93% was seen in single-species biofilm when treated with NDs ($p < 0.01$). Fewer attached cells were seen by 79% compared to PC ($p < 0.05$) (Figure 4.10: B). Less reduction in total cell number (64%) and planktonic cells in dual-species biofilm (E2 + SC5314) compared to single-species biofilm when treated with NDS. The percentage of reduction in attached cells remained the same as in single-species biofilm (79%) ($p < 0.01$) (Figure 4.10: D). When LVS E2 was cocultured with BC023 (LBF), approximately 88% reduction in total cell number and planktonic cells was seen ($p < 0.05$). However, no significant reduction in attached cells were observed in treated biofilm compared to PC (18%) (Figure 4.10: F). In LVS E2 and HBF BC146 coculture, the same reduction in total cell number and planktonic cells as LBF was seen (88%) in treated biofilm ($p < 0.01$). However, the percentage in attached cells reduction was higher (62%) compared to LBF although not statistically significant in both cases (Figure 4.10: H).

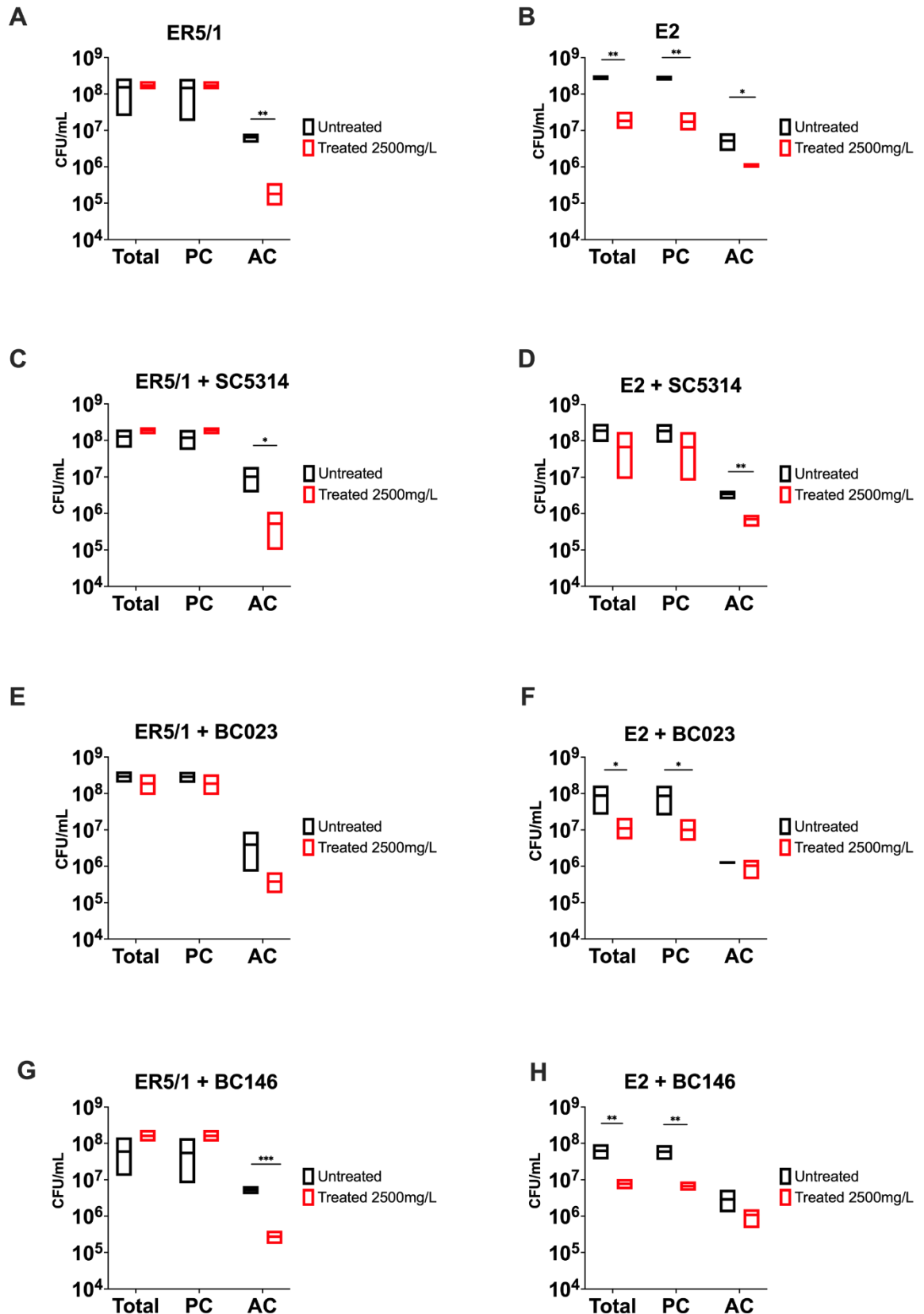


Figure 4.10: NDs effect on colony forming ability of *E. faecalis* strains in dual-species biofilm. (A and B): Mean colony forming unit (CFU) of planktonic cells of HVS (ER5/1) (A) and LVS (E2) (B) when cocultured with lab strain SC5314 (C and D) and a LBF (BC023) (E and F) and a HBF (BC146) (G and H) in the presence and absence of NDs. All samples were assayed in triplicate, on three separate occasions. Multiple t tests were used to assess significance between treated samples and PCs. Data represents mean \pm SD * $p \leq 0.05$, ** $p \leq 0.01$, *** $p \leq 0.001$. PC= Planktonic cells, AC= Attached cells.

4.4.6 Nanodiamonds altered the virulence behaviour of *C. albicans* in single and dual-species biofilm

From the previous experiments, a conclusion can be postulated that NDs physically interact with *C. albicans* thus preventing adhesion in single and dual-species biofilm. The aim was to ascertain if NDs can modulate certain genetic pathways that are involved in adhesion and biofilm formation. Therefore, gene expression analysis of key virulence genes on *C. albicans* involved in these pathways was performed. First, the effect of NDs on *C. albicans* single-species biofilm was explored, after 24 hours of incubation of *C. albicans* with NDs, downregulation of *HWP1* by 1.6 Log₂FC occurred. *HWP1* is involved in hyphal transformation and adhesion to host tissues as well as biofilm formation. In addition, *ALS3* expression was downregulated by 0.5 Log₂FC. *ALS3* is a surface adhesin specific to hyphae and plays a key role in biofilm formation. *SAP5* gene expression was downregulated by 0.3 Log₂FC. This extracellular protease is known to be upregulated in biofilm formation and a key enzyme in *C. albicans* virulence and adhesion to host tissues. Transcriptional factor *EFG1* gene was downregulated by NDs treatment by 1.4 Log₂FC. This factor contributes to virulence by regulating hyphal formation and host tissue adhesion and invasion. Gene expression data further supported the inhibition of *C. albicans* cells adhesion and biofilm formation seen in our previous phenotypic analysis and suggest that NDs can modulate virulence behaviour of *C. albicans* mono-species biofilm (Figure 4.11).

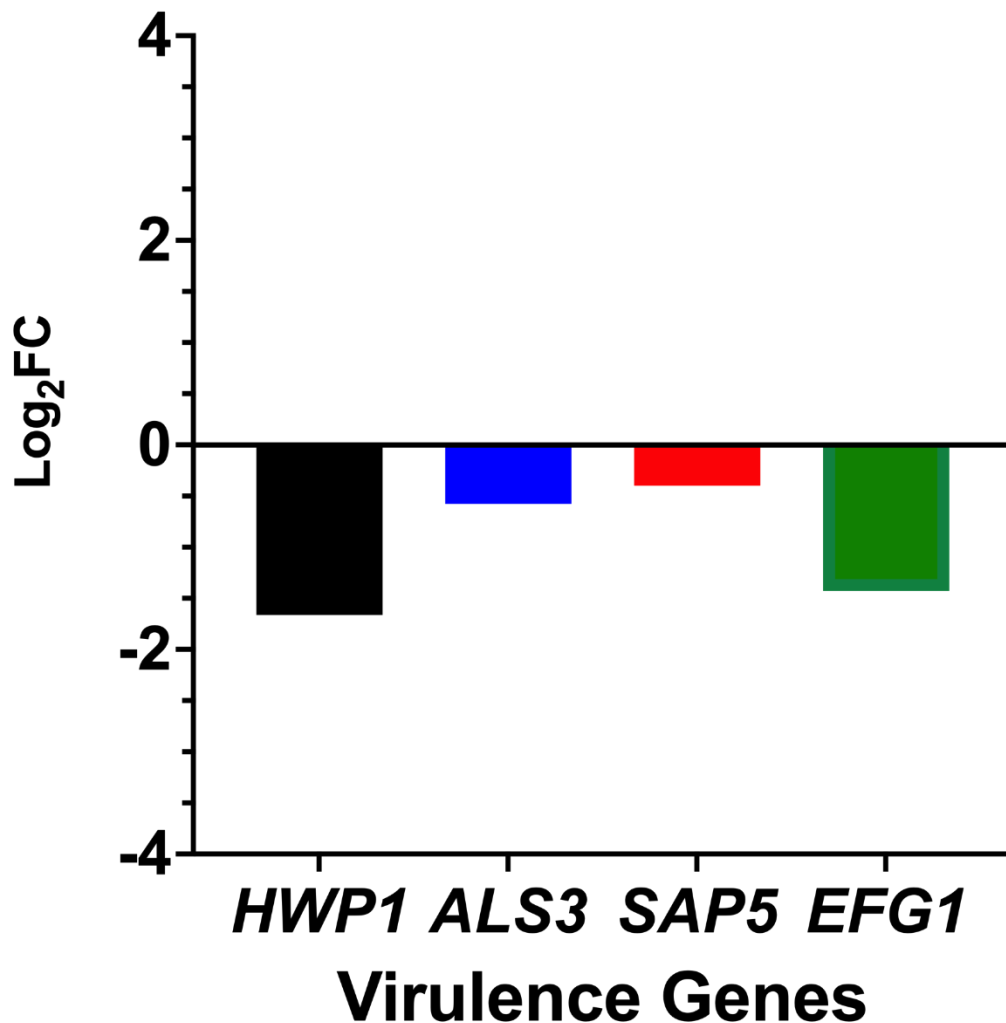


Figure 4.11: Relative gene expression analysis of key virulence genes in *C. albicans* SC5314 in the presence of NDs compared to untreated control. *C. albicans* biofilm was grown with NDs at concentration of 2500 mg/L at time point 0 for 24 hours. NDs downregulated the expression of key virulence genes in *C. albicans*. Gene expression analysis was done using qRT-PCR. ACTB was used as housekeeping gene. Fold changes were calculated using $2^{-\Delta\Delta ct}$. The experiment was done in triplicate and included appropriate no RT and non-template controls.

Further to the work above, the effect of NDs on *C. albicans* when in dual-species biofilm was explored. The same virulence genes of *C. albicans* were tested with a high or low virulence strains of *E. faecalis*. When *C. albicans* was cocultured with the HVS of *E. faecalis* (ER5/1), gene expression analysis revealed that NDs slightly downregulated genes encoding the adhesins HWP1 and ALS3 by 0.17 and 0.2 Log₂FC respectively. The transcription factor EFG1 gene was downregulated by 0.8 Log₂FC. Interestingly, SAP5 was upregulated when dual-species were treated with NDs.

When *C. albicans* was cocultured with E2 LVS, HWP1 was slightly upregulated by 0.35 Log₂FC, ALS3 and EFG1 were downregulated by 1.43 Log₂FC. The upregulation

effect seen on *SAP5* in dual-species biofilm in ER5/1 was also evident in E2 strain by 1.5 Log₂FC.

This is indicative that *C. albicans* virulence behaviour like adhesion and biofilm formation was not downregulated further by the presence of NDs however this was strain dependent. In fact, enhanced expression of protease *SAP5* gene was observed when challenged with NDs when in dual-species biofilm (Figure 4.12)

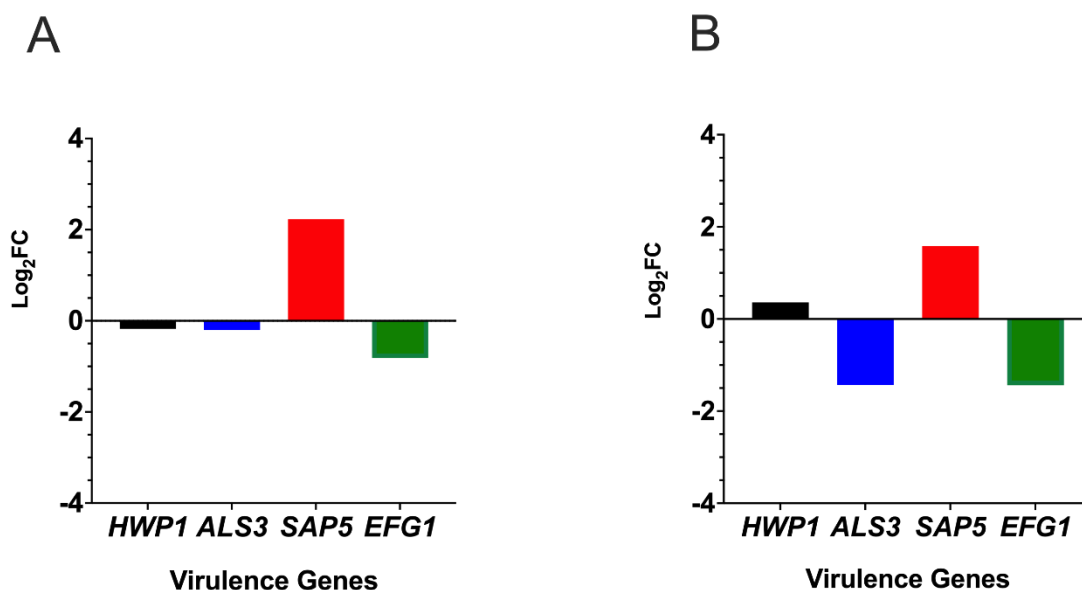


Figure 4.12: Relative gene expression analysis of key virulence genes in *C. albicans* SC5314 in dual-species biofilm in the presence of NDs compared to untreated control. Dual-species biofilm was grown with ER5/1 high virulent (A) and E2 low virulent (B) *E. faecalis* strains the presence and absence of NDs. NDs induced differential gene expression of *C. albicans* virulence genes in the presence of NDs when grown in dual-species biofilm. Gene expression analysis was done using qRT-PCR. ACTB was used as housekeeping gene. Fold changes were calculated using $2^{-\Delta\Delta ct}$.

4.4.7 *C. albicans* and *E. faecalis* response to Biodentine incorporated with NDs was altered when in dual-species biofilm.

For further assessment of the adhesion prevention of NDs on single- and dual-species biofilm, it was combined with Biodentine™ bioceramic material that is based on tricalcium silicate chemistry and has multiple applications in endodontics including perforation repairs, retrograde fillings and vital pulp therapy. Biodentine™ has previously been shown to possess some antifungal and antibacterial activity (Esteki *et al.*, 2021). Since NDs have shown anti biofilm activity, it was considered possible that combining Biodentine™ with NDs might

enhance the antimicrobial activity of Biodentine™. Therefore, NDs were incorporated into Biodentine™ at a concentration of 2.5% and 5%. Biofilms were grown for 24 hours, scraped and incubated with their respective material discs for a further 24 hours.

Results showed that *C. albicans* SC5314 colonisation of dentine was less in dual-species than in single-species biofilm by 1.6 log and 2 logs ($p < 0.05$) in ER5/1 and E2 coculture, respectively. *C. albicans* colonisation of Biodentine™ was slightly higher than dentine by 0.4 log. The colonisation of *C. albicans* in dual-species biofilm was lower by 0.9 ($p < 0.05$) and 2.9 ($p < 0.01$) for ER5/1 and E2 dual-species biofilm respectively. Reduction in colonisation of *C. albicans* between dentine and Biodentine™ + NDs 2.5% was found to be only 44%, however, it was 80% when compared to Biodentine™ alone. Reduction in *C. albicans* CFUs was also seen in Biodentine™ + NDs 2.5% when in single and dual-species biofilm by 1.1 - 1.3 logs in ER5/1 and E2 *E. faecalis* strains respectively. In Biodentine™ + NDs 5%, lower *C. albicans* colonisation on the disc surface was observed compared to dentine by 1 and 1.5 logs compared to Biodentine™ only. *C. albicans* colonised on NDs 2.5% surface by 0.7 log less than on Biodentine™ surface and by 1 log more when cocultured with ER5/1 and E2 respectively. When NDs concentration was 5%, levels of *C. albicans* colonisation was similar for single and dual-species biofilm, however, it was less when SC5314 was cocultured with E2 but comparable to Biodentine™. In this group, *C. albicans* colonisation to NDs did not differ when in single and dual-species biofilm with ER5/1, however, significant reduction in colonisation by 1.3 log when *C. albicans* was cocultured with E2 ($p < 0.05$). Finally, *C. albicans* colonisation did not differ significantly in colonisation amongst different treatment groups when in dual-species biofilm with either *E. faecalis* strains.

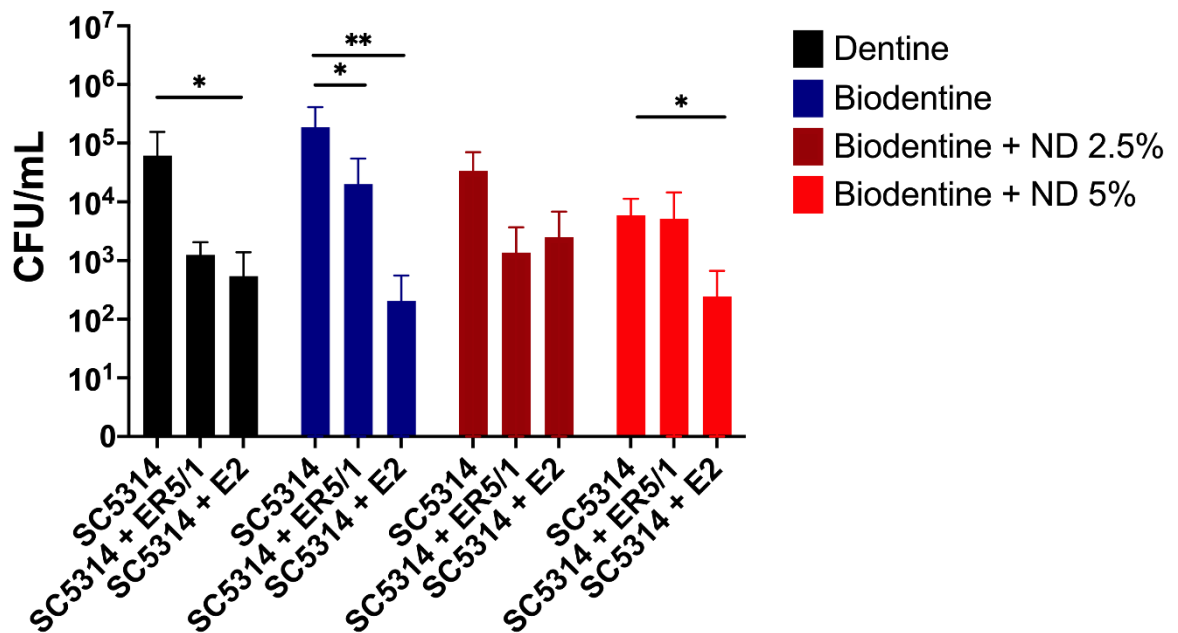


Figure 4.13: *C. albicans* lab strain SC5314 mean colony forming units in single and dual-species biofilms grown on bovine dentine, Biodentine™, Biodentine™ and NDs discs. *C. albicans* SC5314 was grown in single and ER5/1 / E2 dual-species biofilms on bovine dentine, Biodentine™, Biodentine™ + 2.5% NDs, Biodentine™ + 5% NDs discs for 24 hours. *C. albicans* SC5314 colonisation on disc surfaces was assessed by viable plate counts. Experiments were assayed in triplicate, on three separate occasions. Two-way ANOVA was used to assess significance between different treatment group samples with Benferroni multiple comparison test. Data represents mean ± SD * $p \leq 0.05$, ** $p \leq 0.01$.

E. faecalis ER5/1 colonisation on dentine surface was higher by 51% when in single-species compared to dual-species biofilm. On a Biodentine™ surface, ER5/1 colonisation was increased by 85% when cocultured with *C. albicans* compared to single-species biofilm ($p < 0.05$). Moreover, lower ER5/1 colonisation was observed on a Biodentine™ surface (85%) compared to dentine ($p < 0.05$). When NDs were combined with Biodentine™, no significant difference in ER5/1 colonisation was observed when it was in single or dual-species biofilm. However, less *E. faecalis* colonisation was observed on Biodentine™ + NDs surfaces compared to dentine (88%) ($p < 0.05$) while *E. faecalis* ER5/1 colonisation did not differ significantly in colonisation between different treatment groups when in dual-species biofilm.

For *E. faecalis* E2, comparable levels of colonisation on all surface types were seen when in single and dual-species biofilm. In addition, less colonisation of E2 on Biodentine™ surface by 70% compared to dentine was evident. 82% reduction in E2 colonisation when 2.5% NDs were incorporated into Biodentine™. A higher reduction was observed when 5% NDs were incorporated into Biodentine™ (94%). When E2 was in dual-species biofilm, the same level of colonisation was observed across all treatment groups.

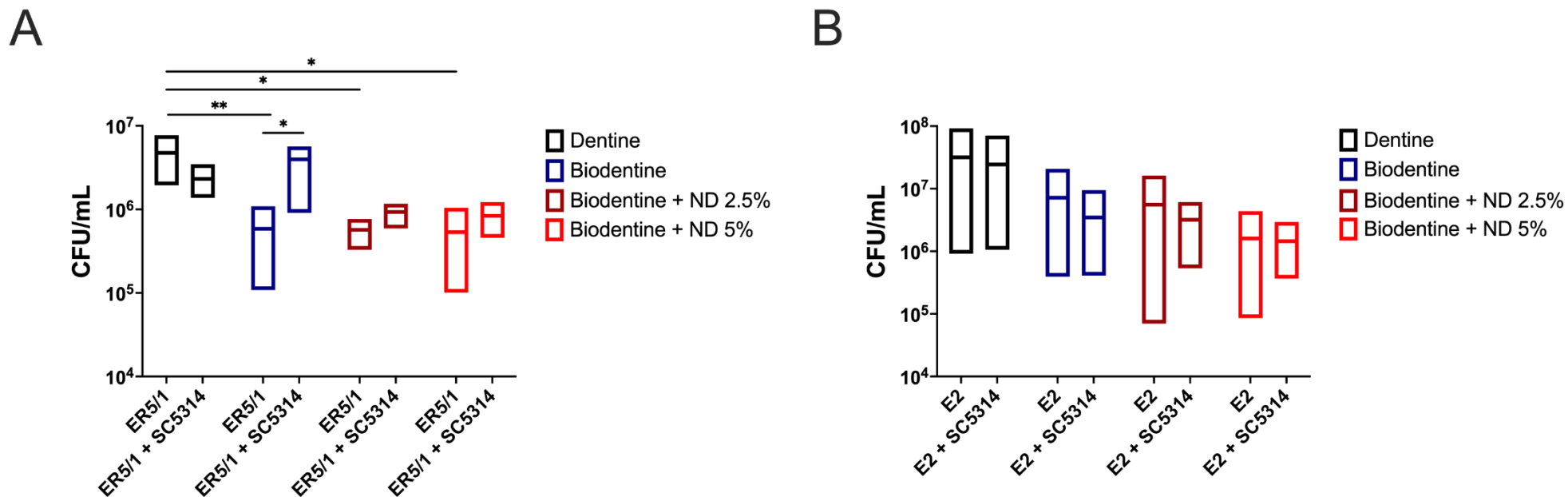


Figure 4.14: *E. faecalis* clinical strains ER5/1 and E2 mean colony forming units in single and dual-species biofilms grown on bovine dentine, Biodentine™, Biodentine™ and NDs discs. *E. faecalis* ER5/1 and E2 strains were grown in single and dual-species biofilms on bovine dentine, Biodentine™, Biodentine™ + 2.5% NDs, Biodentine™ + 5% NDs discs for 24 hours. *E. faecalis* colonisation on disc surfaces was assessed by viable plate counts. Experiments were assayed in triplicate, on three separate occasions. Two-way ANOVA was used to assess significance between different treatment group samples with Benferroni multiple comparison test. Data represents mean ± SD * p ≤ 0.05.

4.4.8 Screening antifungal activity of FDA approved drugs against *C. albicans* SC5314

Given that NDs were shown to have a biological effect on *C. albicans* and *E. faecalis*, though no clear antimicrobial effect, the aim was to find a compound with this characteristic tested. Therefore, 1289 compounds from the Tocriscreen™ micro-library were for their biofilm inhibition effect against the *C. albicans* lab strain SC5314 using the XTT reduction assay and CV to assess metabolic activity and biofilm biomass respectively (Figure 4.15, Figure 4.16, Figure 4.17, Figure 4.18). Compounds were identified as hits when they showed more than 99% inhibition in metabolic activity and biofilm biomass (Figure 4.19) at the initial concentration of 100 µM. Of the 1280 compounds, 82 were identified as initial hits: 10 belonged to the nuclear receptors target class, 17 to 7-TM receptors, 3 to transporters, 15 compounds targeted cell biology, 6 ion channels and 30 targeted enzymes and two belonged to other pharmacological categories. The full list of hit compounds with their mechanism of action are described in Table 4.4.

Chapter 4: Response of Dual-species biofilm to novel treatment strategies: a window to understanding interkingdom interactions

Plate 1: Metabolic Activity

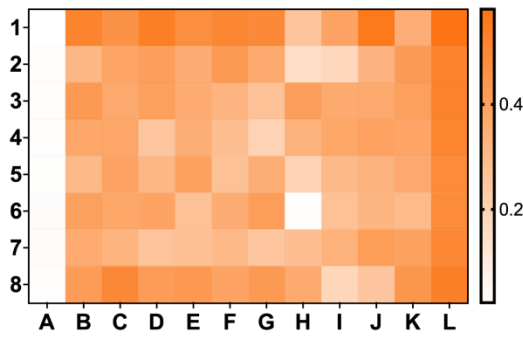


Plate 1: Biofilm Biomass

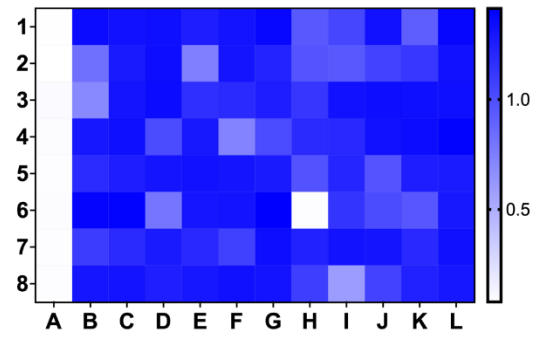


Plate 2: Metabolic Activity

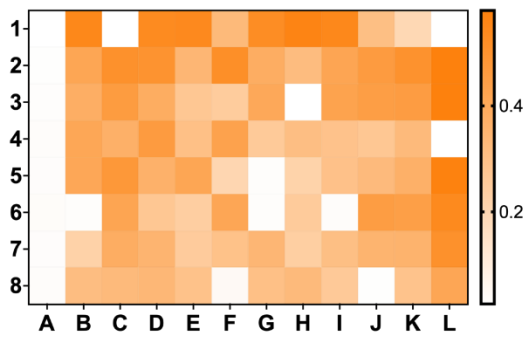


Plate 2: Biofilm Biomass

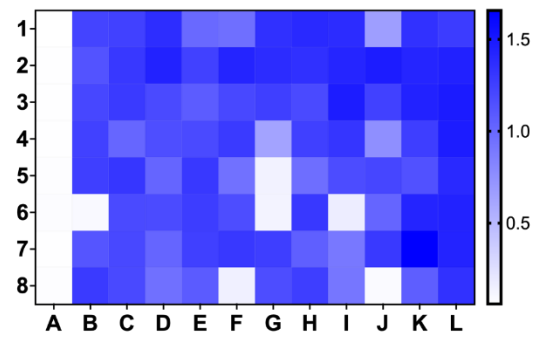


Plate 3: Metabolic Activity

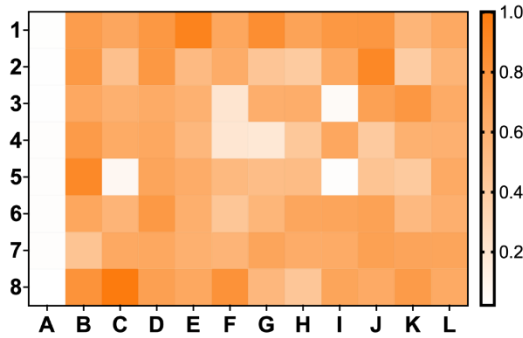


Plate 3: Biofilm Biomass

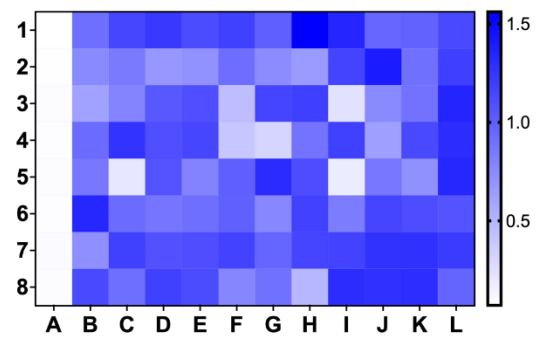


Plate 4: Metabolic Activity

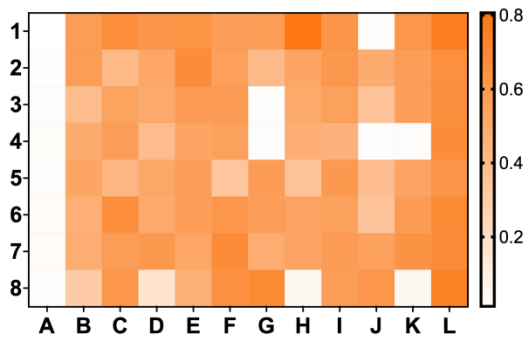


Plate 4: Biofilm Biomass

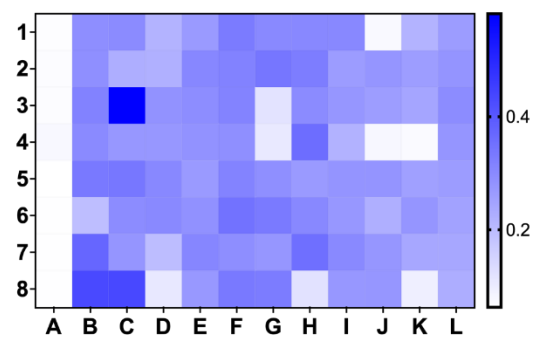


Figure 4.15: Heatmaps showing metabolic activity and biofilm biomass values of Tocriscreen™ library plates for *C. albicans* SC5314 (Plate 1 – Plate 4): Metabolic activity was assessed using XTT reduction assay (left panel – Orange) and biofilm biomass was assessed using CV assay (right panel – Blue). OD was measured at OD₄₉₂ for XTT metabolic reduction assay and OD₅₇₀ for CV were plotted and expressed as heatmaps.

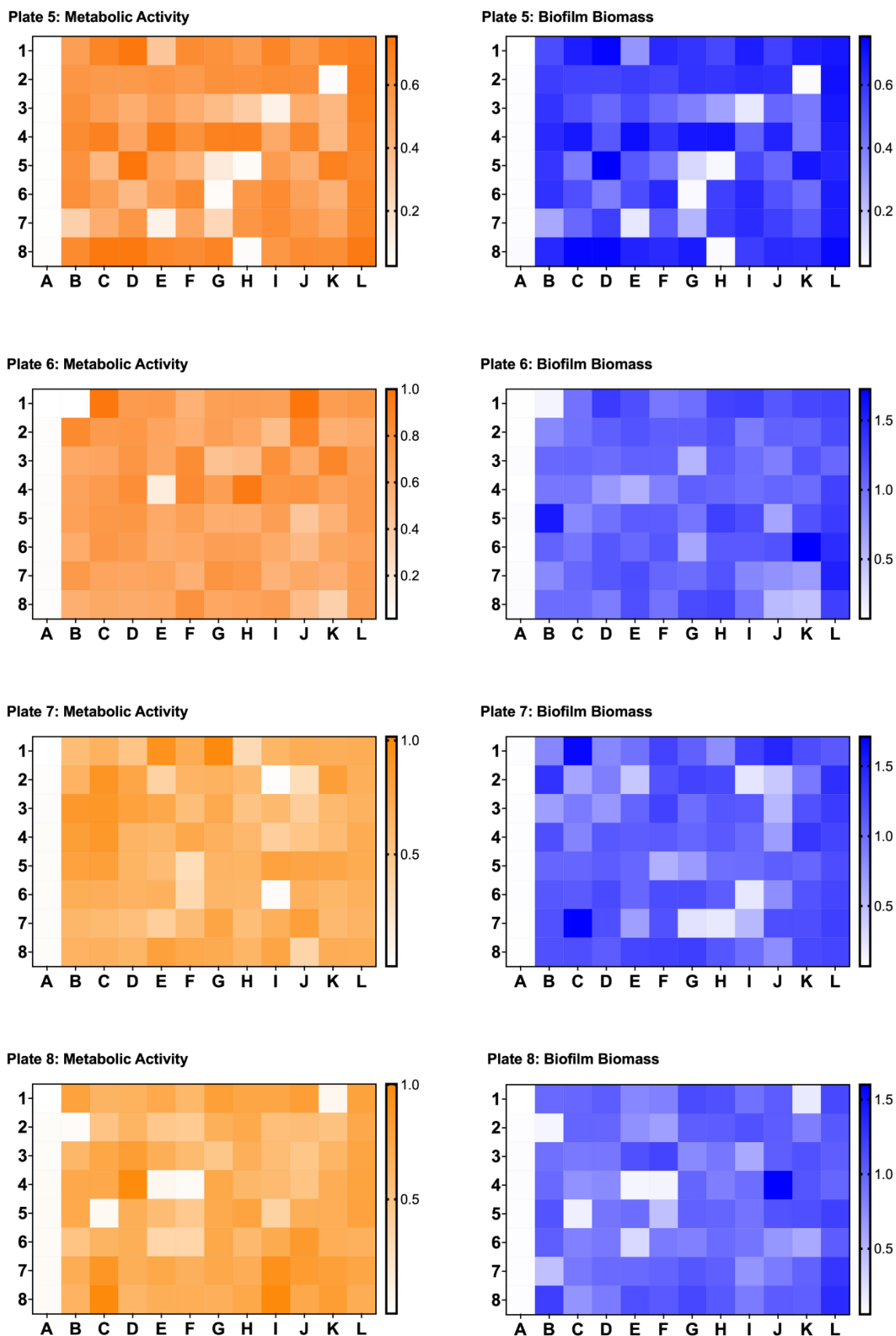


Figure 4.16: Heatmaps showing metabolic activity and biofilm biomass values of Tocriscreen™ library plates for *C. albicans* SC5314 (Plate 5 – Plate 8): Metabolic activity was assessed using XTT reduction assay (left panel – Orange) and biofilm biomass was assessed using CV assay (right panel – Blue). OD was measured at 492 for XTT metabolic reduction assay and 570 for CV were plotted and expressed as heatmaps.

Plate 9: Metabolic Activity

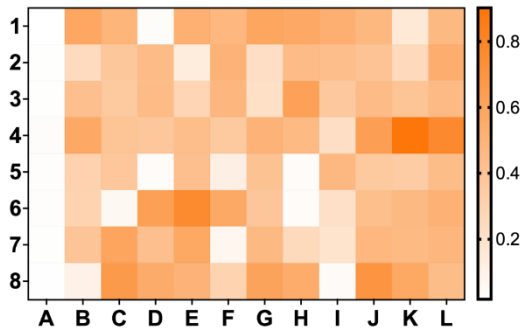


Plate 9: Biofilm Biomass

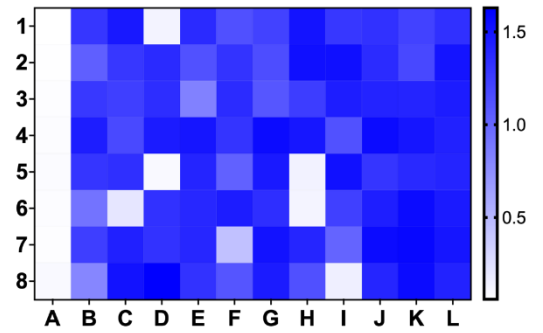


Plate 10: Metabolic Activity

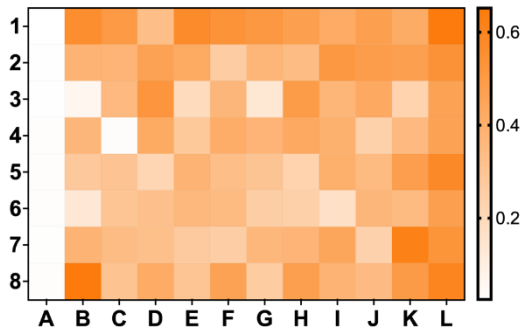


Plate 10: Biofilm Biomass

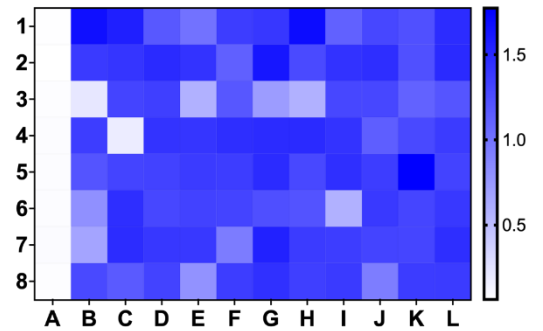


Plate 11: Metabolic Activity

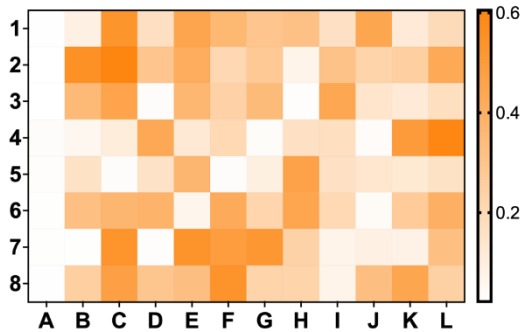


Plate 11: Biofilm Biomass

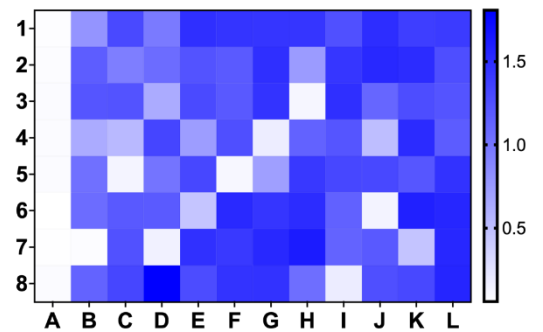


Plate 12: Metabolic Activity

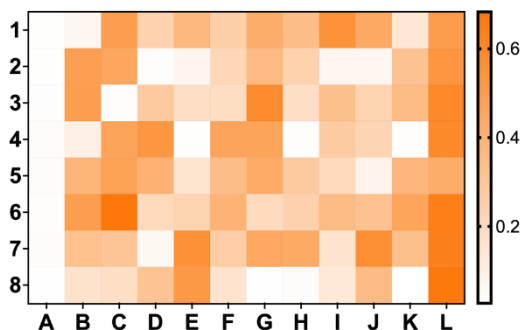


Plate 12: Biofilm Biomass

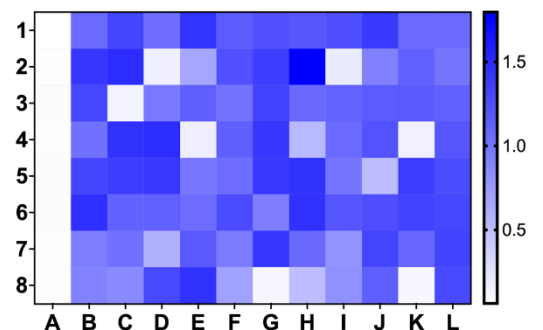


Figure 4.17: Heatmaps showing metabolic activity and biofilm biomass values of Tocriscreen™ library plates for *C. albicans* SC5314 (Plate 9 – Plate 12): Metabolic activity was assessed using XTT reduction assay (left panel – Orange) and biofilm biomass was assessed using CV assay (right panel – Blue). OD was measured at 492 for XTT metabolic reduction assay and 570 for CV were plotted and expressed as heatmaps.

Plate 13: Metabolic Activity

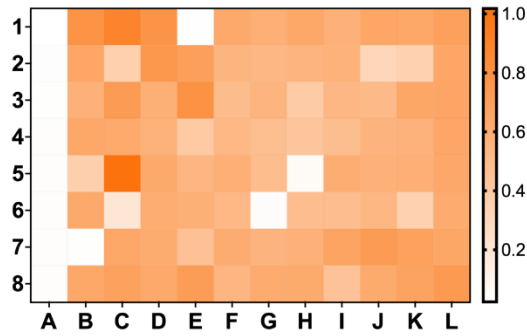


Plate 13: Biofilm Biomass

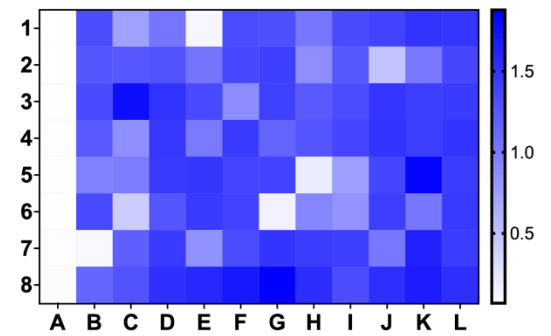


Plate 14: Metabolic Activity

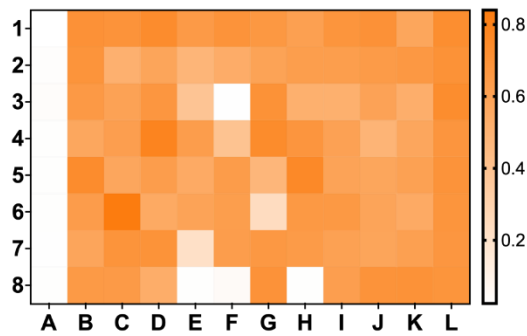


Plate 14: Biofilm Biomass

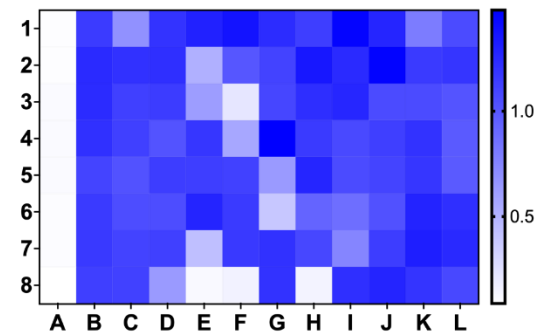


Plate 15: Metabolic Activity

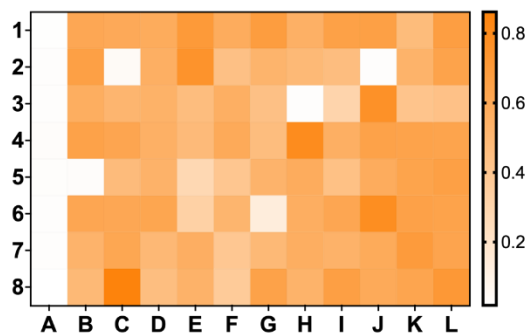


Plate 15: Biofilm Biomass

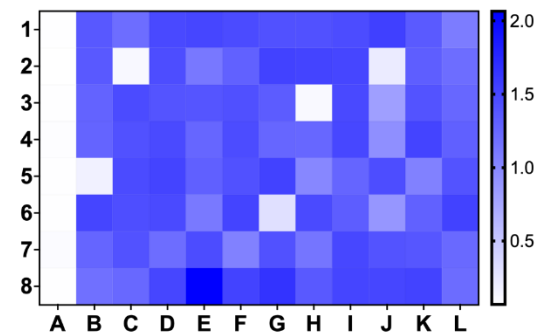


Plate 16: Metabolic Activity

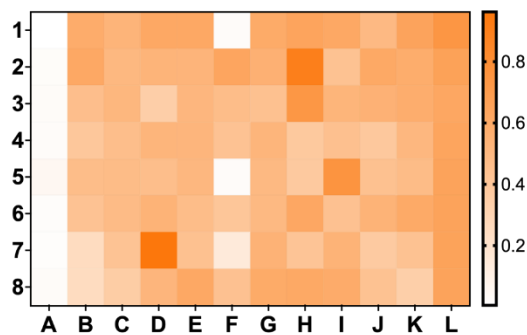


Plate 16: Biofilm Biomass

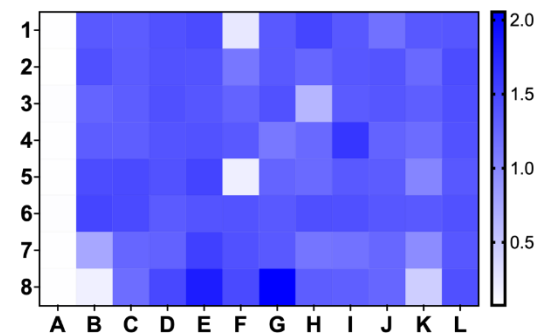


Figure 4.18: Heatmaps showing metabolic activity and biofilm biomass values of Tocriscreen™ library plates for *C. albicans* SC5314 (Plate 13 – Plate 16): Metabolic activity was assessed using XTT reduction assay (left panel – Orange) and biofilm biomass was assessed using CV assay (right panel – Blue). OD was measured at 492 for XTT metabolic reduction assay and 570 for CV were plotted and expressed as heatmaps.

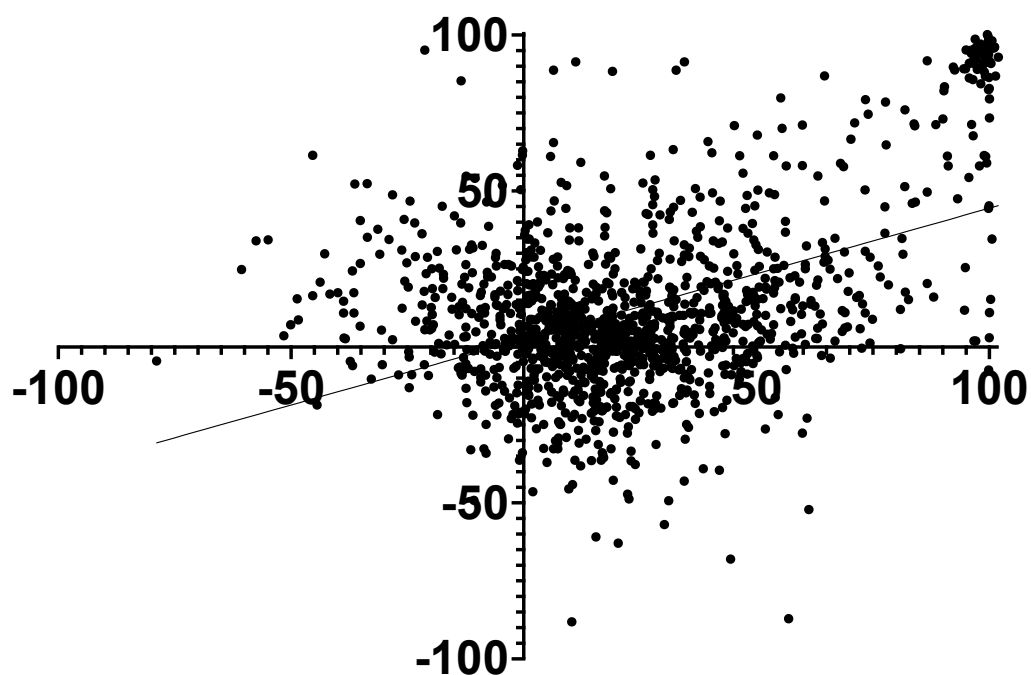


Figure 4.19: Hits identified by screening a library of biologically active compounds for biofilm inhibition effect on *C. albicans*. *C. albicans* strain SC5314 was grown in the presence of compounds at a concentration of 100 μ M for 24 hours at 37°C and their metabolic activity and biofilm biomass was assessed using XTT and CV, respectively. Results are expressed as percentage of inhibition. X and Y axes represent metabolic activity and biofilm biomass respectively.

Table 4.4: Hit compounds identified from library screening and their mechanism of action.

Drug Name	MOA: Mechanism of Action
Tamoxifen citrate	Oestrogen and Related Receptors Modulator
SR 59230A hydrochloride	Potent and selective B3 antagonist
CD 437	RAR γ -selective agonist
Indatraline hydrochloride	Potent 5-HT uptake inhibitor; also inhibits dopamine and noradrenalin uptake
SCH 79797 dihydrochloride	Potent, selective non-peptide PAR1 antagonist
Bay 11-7085	Bay 11-7085 Irreversible inhibitor of TNF- α -induced I κ B α phosphorylation
LE 135	Selective RARB antagonist
Bax channel blocker	Allosteric inhibitor of Bax channel activation
NSC 146109 hydrochloride	Cell-permeable, genotype-selective antitumor agent; activates p53-dependent transcription
JTC 801	Selective NOP antagonist
IKK 16	Selective inhibitor of IKK
CD 1530	Potent and selective RAR γ agonist
10-DEBC hydrochloride	Selective Akt/PKB inhibitor

NNC 05-2090 hydrochloride	Cell-permeable, genotype-selective antitumor agent; activates p53-dependent transcription
UCB 35625	Potent CCR1 and CCR3 antagonist
PD 146176	Selective 15-lipoxygenase inhibitor
SU 9516	Cdk inhibitor; potently inhibits cdk1 and cdk2
RS 127445 hydrochloride	High affinity and selective 5-HT _{2B} antagonist
NS 1738	Positive allosteric modulator of $\alpha 7$ nAChRs; active <i>in vivo</i>
NS 1643	KV11.1 (hERG) channel activator; antiarrhythmic
Dorsomorphin dihydrochloride	Potent AMPK inhibitor; also BMP type I receptor inhibitor
SB 699551	Selective 5-HT _{5A} antagonist
Polygodial	TRPA1 channel activator; analgesic and antifungal
NPS 2143 hydrochloride	Selective calcium-sensing receptor (CaSR) antagonist; orally active calcilytic agent
PD 166285 dihydrochloride	Potent Src inhibitor; also inhibits FGFR1, PDGFR β and Wee1
HX 531	Potent RXR antagonist
A 419259 trihydrochloride	Inhibitor of Src family kinases
SR 140333	Potent NK1 antagonist

L 760735	High affinity NK1 antagonist
Flupenthixol dihydrochloride	Dopamine antagonist
SMER 3	Selective inhibitor of E3 ubiquitin ligase
DBeQ	Selective and reversible p97 ATPase inhibitor
Wiskostatin	N-WASP inhibitor; inhibits Arp2/3 activation
YE 120	GPR35 agonist
Moclobemide	Reversible MAO-A inhibitor
P 22077	USP7 inhibitor
ML 228	HIF pathway activator
Tegaserod maleate	5-HT4 partial agonist
NSC 405020	Histone deacetylase inhibitor
AC 186	Potent and selective ERB agonist; neuroprotective
SC 144 hydrochloride	gp130 inhibitor; blocks cytokine-triggered gp130 signalling
SR 1078	ROR α / γ agonist
NSC 319726	Reactivator of mutant p53

AC 710	Potent and selective PDGFR family inhibitor
Pitavastatin calcium	HMG-CoA reductase inhibitor
RN 1 dihydrochloride	LSD1 inhibitor
PPTN hydrochloride	High affinity and selective P2Y14 antagonist
KHS 101 hydrochloride	Selective inducer of neuronal differentiation in hippocampal neural progenitors
PFI 3	Potent and selective SMARCA2/4 and polybromo 1 inhibitor
GSK 2193874	Potent and selective TRPV4 antagonist; orally active
SA 4503 dihydrochloride	Selective σ 1 receptor agonist
CASIN	Cdc42 inhibitor
DDR1-IN-1 dihydrochloride	Selective DDR1 inhibitor
TC-G 1003	High affinity somatostatin sst2 agonist
NS 9283	Positive allosteric modulator of α 4 β 2 nAChRs
Bazedoxifene acetate	Potent and selective oestrogen receptor modulator (SERM)
Furamidine dihydrochloride	Selective PRMT1 inhibitor
Perhexiline maleate	Carnitine palmitoyltransferase 1 and 2 (CPT1/2) inhibitor

Ferrostatin 1	Selective inhibitor of erastin induced ferroptosis
Toyocamycin	Adenosine analogue; antifungal antibiotic
Ro 48-8071 fumarate	2,3-Oxidosqualene cyclase (OSC) inhibitor; blocks cholesterol synthesis
NS 19504	Activator of BKCa (KCa1.1) channels
SPP 86	Potent RET inhibitor
FRAX 486	Potent PAK inhibitor; brain penetrant and orally bioavailable
Spautin 1	USP10 and USP13 inhibitor; inhibits autophagy
SP100030	NF- κ B and AP-1 dual inhibitor
SAG 21k	Hedgehog signalling activator; brain penetrant and orally bioavailable
Ispinesib	High affinity and selective allosteric KSP inhibitor
M62812	TLR-4 inhibitor
Deltarasin	High affinity PDE δ -KRas interaction inhibitor; binds to PDE δ
OSU 03012	PDPK1 (PDK1) inhibitor; inhibits Akt signaling
GN 44028	Potent HIF-1 α inhibitor Hypoxia induced
Cinacalcet hydrochloride	Allosteric activation of the calcium-sensing receptors

LY 2955303	A potent and selective 5-HT antagonist
MLS 1547	G protein-biased D2 partial agonist
FTY720	Potent S1P receptor agonist; also immunosuppressant
Dacomitinib	Selective and irreversible inhibitor of EGFR.
Tamoxifen	Selective estrogen receptor modulator used for managing breast cancer
SLM 6031434 hydrochloride	Sphk2 inhibitor
EHop 016	a novel inhibitor of Rac activity
CD 437	pan-Bcl-2 inhibitor
Darapladib	Inhibitor lipoprotein-associated phospholipase A2 (Lp-PLA2) that is in development as a drug for treatment of atherosclerosis.
GN44028	Potent HIF-1 α inhibitor
Obatoclox mesylate	Inhibitor of Bcl-2 family members; antiapoptotic
Sertraline hydrochloride	5-HT reuptake inhibitor

4.4.9 Minimum inhibitory concentration of 11 candidate compounds against *C. albicans* and *E. faecalis* isolates

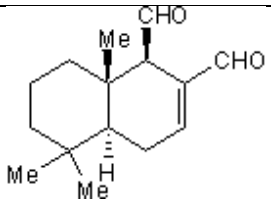
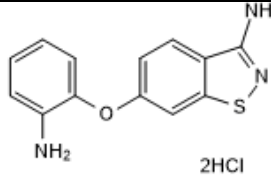
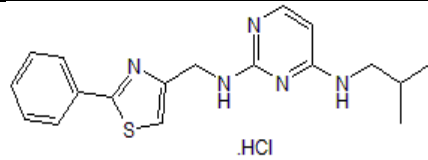
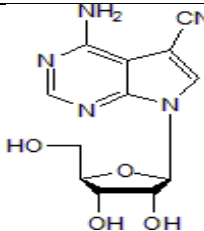
From the hit compounds identified, eleven compounds were selected with biological activities that might potentially exert favourable actions upon host cells whilst causing an inhibitory action on *C. albicans* biofilm formation. Retinoic acid compounds that mainly induce changes in cell proliferation, differentiation, and apoptosis (CD437, LE135, CH55) were chosen. Compounds that have potential anti-inflammatory effect - M62812; a TLR4 inhibitor and SP100020; that is an NF-kb and AP-1 dual inhibitor were selected. Other compounds were selected based on their proven antimicrobial properties: Toyocamycin, an adenosine analogue, antifungal and antibiotic (Nishimura *et al.*, 1956) and Polygodial, an analgesic with antifungal activity (Kubo *et al.*, 2001, Lee *et al.*, 1999, Kipanga *et al.*, 2021). Furthermore, darapladib was also selected. Darapladib is a phospholipase inhibitor that can serve as a potential inhibitor of one of the key virulence factors, phospholipase, secreted by *C. albicans*. KHS101 hydrochloride, an inducer of neurogenic differentiation that can potentially serve a dual function by being toxic to *C. albicans* whilst exhibiting favourable effects on host cells. Finally, Ferrostatin 1, a ferroptosis inhibitor that can reduce programmed cell death initiated by ferroptosis due to accumulation of lipid peroxides.

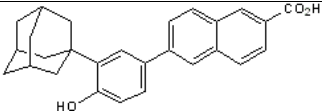
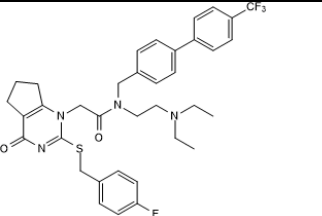
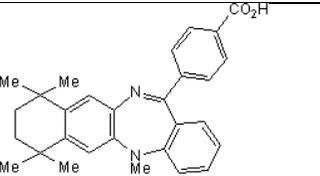
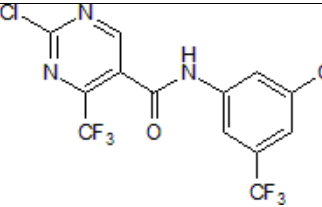
These compounds were tested against three *C. albicans* isolates: HBF (BC146), LBF (BD023), SC5314, alongside three *E. faecalis* strains, HVS (ER5/1), LVS (E2) and a ATCC 29212. Their MICs were determined against planktonic forms of the strains. The results confirmed the antifungal activity of Polygodial, M62812, KHS101 hydrochloride, Toyocamycin, CD437, darapladib and LE135; 5 of which (M62812, KHS101 hydrochloride, CD437, darapladib and LE135) were also effective against *E. faecalis* strains (Table 4.5). Polygodial had antifungal activity at concentrations ranging from 8- 16 µg/mL but did not show any anti-bacterial effect against *E. faecalis* strains. M62812 showed antifungal activity at concentrations from 16-32 µg/mL but their antibacterial effect against *E. faecalis* strains were noticed at higher concentration (128 µg/mL). KHS101 hydrochloride was potent against *C. albicans* and *E. faecalis* isolates at concentration 32 µg/mL.

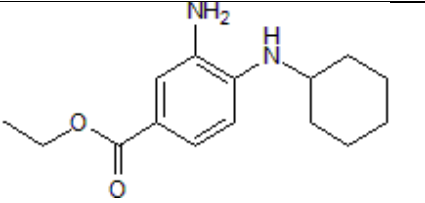
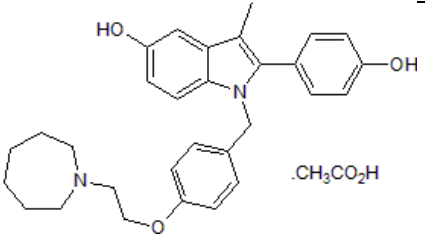
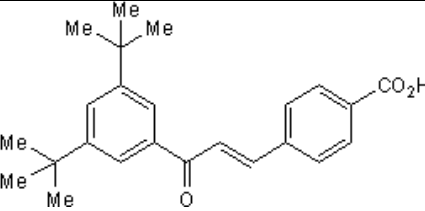
However, Toyocamycin was only effective against *C. albicans* strains at very low concentrations (0.25 µg/mL). The retinoid compound CD437 showed antifungal

activity against *C. albicans* isolates at 8 µg/mL and was very potent antibacterial against *E. faecalis* strains at 1 µg/mL. Darapladib showed both antifungal and antibacterial effects against *C. albicans* and *E. faecalis* isolates at concentrations from 4-16 µg/mL. LE135 was effective against *C. albicans* isolates at 64 µg/mL concentration, however, it showed antibacterial activity against *E. faecalis* isolates at a lower concentration (4 µg/mL). SP100030, Ferrostatin-1 and Bazedoxifine acetate did not show any antifungal or antibacterial activities. CH55 showed only antibacterial activity against *E. faecalis* strains at 8 µg/mL.

Table 4.5: MIC of planktonic cells of eleven compounds against three *C. albicans* isolates and three *E. faecalis* strains. (-) indicates not detected

Drug $\mu\text{g/mL}$	Structure	BC020	BC023	SC5314	ER5/1	E2	ATCC29212
Polygodial		16	16-64	8	-	-	-
M62812	 2HCl	16- 32	32	32	128	128	128
KHS101	 .HCl	32	32-64	32	32	32	32
Toyocamycin		0.25	0.25	0.25	-	-	-

CD437		8	8	8	1	1	1
Darapladib		4 - 8	4 - 8	4 - 8	4 - 16	4 - 16	4 - 16
LE135		64	64	64	4	4	4
SP100030		-	-	-	-	-	-

Ferrostatin-1		-	-	-	-	-	-
Bazedoxifin Acetate		-	-	-	-	-	-
CH55		-	-	-	8	8	8

4.4.10 Biofilm inhibition activity of KHS101 hydrochloride against single and dual-species biofilm of *C. albicans* and *E. faecalis*

Two drugs were selected that were proven to be effective against both *C. albicans* and *E. faecalis* to challenge dual-species biofilm inhibition at various concentrations.

Metabolic activity and the biomass of each biofilm were assessed using AlamarBlue™ and CV when treated with KHS101 hydrochloride. *C. albicans* metabolic activity was reduced by more than 65% at 8 and 16 µg/mL concentrations and by ($p<0.01$) 99% and 100% at 32 and 64 µg/mL ($p<0.001$) (Figure 4.20: A). Regarding *C. albicans* biofilm biomass, it was reduced by more than 70% at concentrations starting from 16 µg/mL to 64 µg/mL, however, significant reduction was only observed at 32 µg/mL ($p<0.05$) (Figure 4.20: D).

For *E. faecalis* single-species biofilm, metabolic activity and biofilm biomass remained the same at lower concentrations of 8 and 16 µg/mL. At 32 µg/mL concentration, metabolic activity, and biofilm biomass were reduced by only 30% and 40%, respectively. Biofilm biomass was reduced by 100% ($p<0.01$) and 88% ($P<0.05$) respectively at the highest concentration (Figure 4.20: B, E). However, for LVS E2, a greater reduction was observed in metabolic activity and biofilm biomass than for HVS ER5/1. It was observed that metabolic activity was reduced by 86% at 32 µg/mL ($p<0.0001$) and completely inhibited at 64 µg/mL ($p<0.0001$) (Figure 4.21: B). The biofilm biomass was completely inhibited at 32 µg/mL and by 78% ($p<0.01$) at 64 µg/mL in E2 single-species biofilm ($p<0.05$) (Figure 4.21: E). In dual-species biofilm composed of SC5314 + HVS ER5/1, the metabolic activity and biofilm biomass remained unchanged at 8 and 16 µg/mL but was reduced by 29% at 32 µg/mL and 100% at the highest concentration 64 µg/mL ($p<0.01$) (Figure 4.20: C). The biofilm biomass was reduced by 43% at 32 µg/mL and 98% at the highest concentration ($p<0.01$) (Figure 4.20: F). The same observation was evident in dual-species biofilm composed of SC5314 + LVS E2, however, at 32 µg/mL concentration, the metabolic activity was slightly more reduced (40%) than when cocultured with ER5/1 HVS although not statistically significant in both and It was completely inhibited at 64 µg/mL ($p<0.01$) (Figure 4.21: C). Regarding dual-

species biofilm biomass, it was more reduced in E2 LVS (70%) in coculture than HVS ER5/1, although still not statistically significant. The dual-species biomass was reduced by 92% at 64 $\mu\text{g}/\text{mL}$ (Figure 4.21: F).

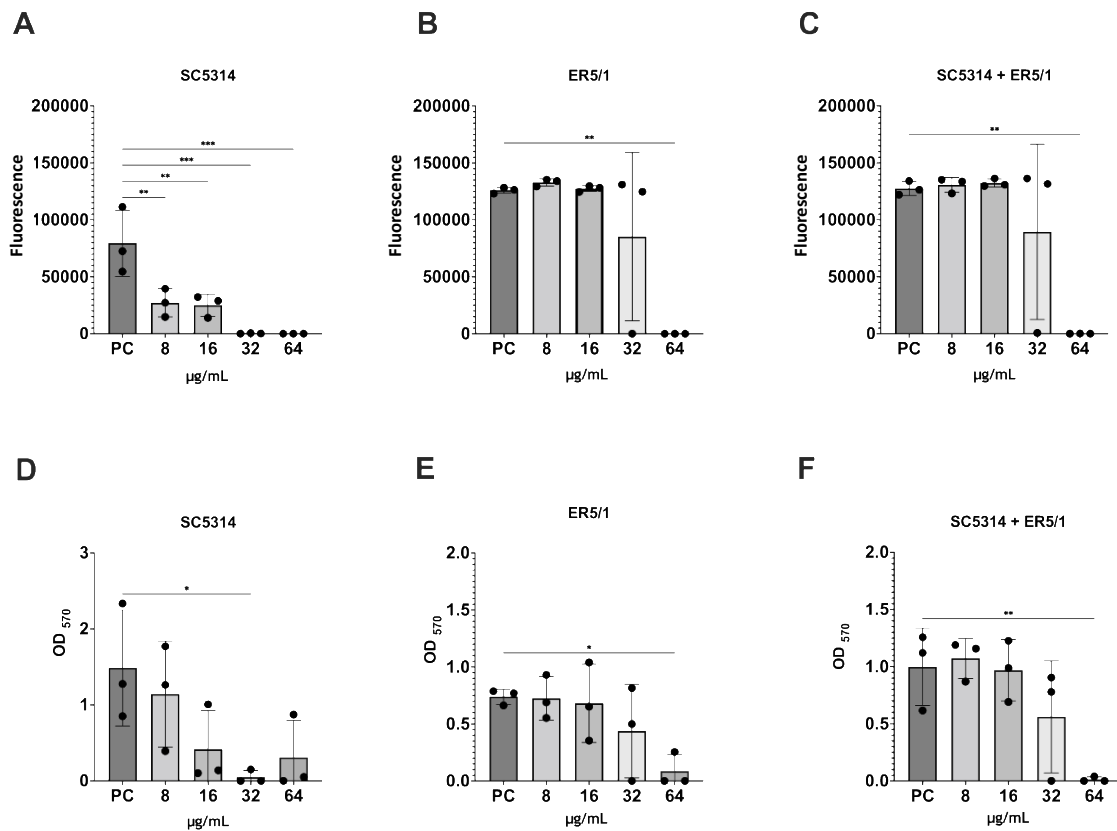


Figure 4.20: Metabolic activity and biofilm biomass of *C. albicans* and *E. faecalis* HVS ER5/1 single and dual-species biofilms with and without KHS101 hydrochloride treatment. *C. albicans* SC5314 and ER5/1 HVS were grown in (THB/RPMI) medium in 24 well plate in single (A, B, D, E) and dual-species biofilm (C,F) with their respective drug concentration. After 24 hours, biofilms metabolic activity (A-C) and biofilm biomass (D-F) were determined using AlamarBlue™ and CV respectively. Data represented as mean \pm SD in triplicate on three separate occasions. An Analysis of Variance (ANOVA) statistical test and Dunnett's post-test was used to assess significance between treated samples and PCs when data were normally distributed and A Kruskal-Wallis statistical test with Dunn's post-test was used to assess significance between treated samples and PCs (* $p < 0.05$, ** $p < 0.01$, *** $p < 0.001$, **** $p < 0.0001$).

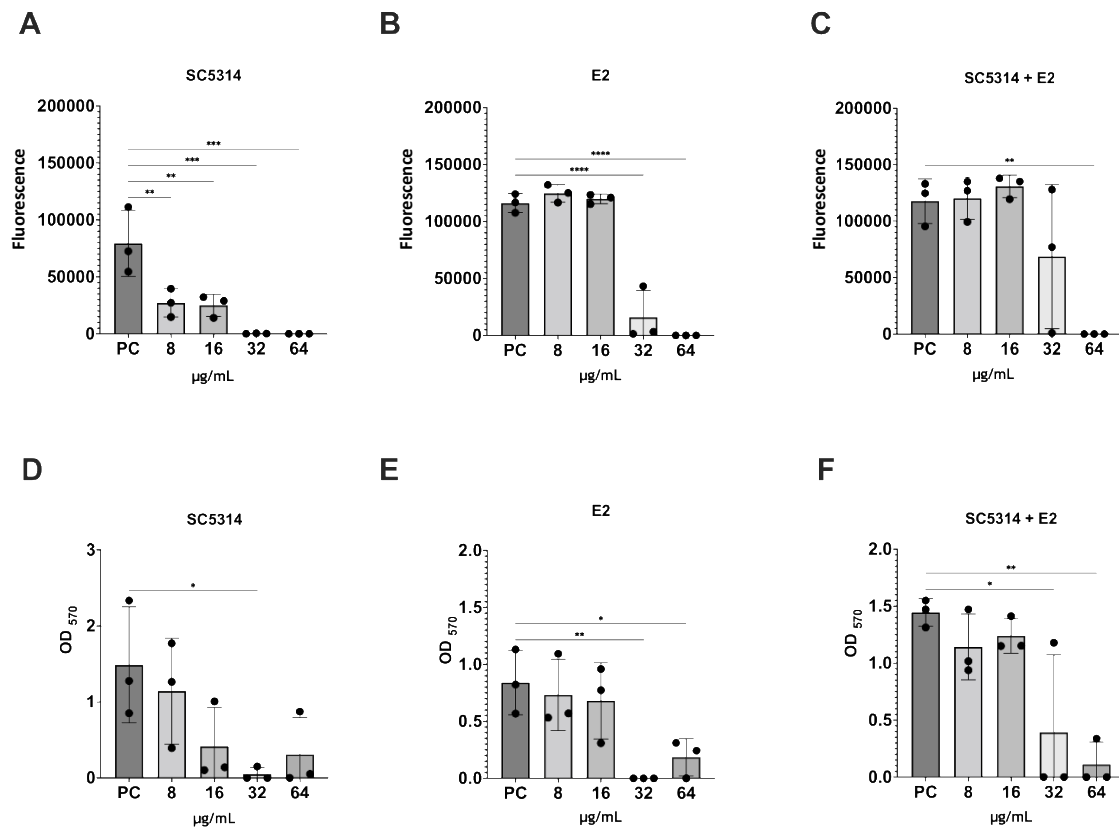


Figure 4.21: Metabolic activity and biofilm biomass of *C. albicans* and *E. faecalis* HVS E2 single and dual-species biofilms with and without KHS101 hydrochloride treatment. *C. albicans* SC5314 and E2 HVS were grown in (THB/RPMI) media in 24 well plate in single (A, B, D, E) and dual-species biofilm (C,F) with their respective drug concentration. After 24 hours, biofilms metabolic activity (A-C) and biofilm biomass (D-F) were determined using AlamarBlue™ and CV respectively. Data represented as mean \pm SD in triplicate on three separate occasions. An Analysis of Variance (ANOVA) statistical test and Dunnett's post-test was used to assess significance between treated samples and PCs when data were normally distributed and A Kruskal-Wallis statistical test with Dunn's post-test was used to assess significance between treated samples and PCs (* p <0.05, ** p <0.01, *** p <0.001, **** p <0.0001).

To determine composition of biofilms before and after treatment, *C. albicans* and *E. faecalis* cells were quantified by viable plate counts in single and dual-species biofilms. In *C. albicans* single-species biofilm, KHS101 hydrochloride reduced CFUs of *C. albicans* by 0.4 and 1 log at 8 and 16 µg/mL respectively although not statistically significant. At 32 µg/mL, a significant 4.7-log reduction was observed in CFUs, (p <0.0001) with a complete reduction at 64 µg/mL concentration (p <0.0001) (Figure 4.22: A). *C. albicans* CFUs were reduced in a dose dependent manner when cocultured with *E. faecalis* in either strain, however, a greater reduction was observed when cocultured with LVS E2 than HVS ER5/1. Log reduction by 0.3 and 0.6 was observed at 8 and 16 µg/mL respectively when SC5314 was cocultured with ER5/1 and 0.5 and 0.8 log reduction when cocultured with E2 (p <0.05). A significant reduction was observed at higher concentrations in

C. albicans CFUs when cocultured with either strain. Log reduction of 2.9 and 3.2 was observed when *C. albicans* was cocultured with ER5/1 ($p<0.05$). In E2 coculture, No CFUs were detected at 32 and 64 $\mu\text{g}/\text{mL}$ concentrations ($p<0.0001$) (Figure 4.22: B, C).

In the case of *E. faecalis*, KHS101 did not show log reductions at 8 and 16 $\mu\text{g}/\text{mL}$ in single-species biofilm in both strains (Figure 4.22: D, F). However, at these concentrations, it was more potent against *E. faecalis* when cocultured with *C. albicans* SC5314. E2 LVS was more susceptible than ER5/1 HVS, 0.7 - 0.9 log reductions were observed in E2 LVS compared to 0.3 - 0.6 in HVS ER5/1 at 8 and 16 $\mu\text{g}/\text{mL}$ concentrations respectively although not statistically significant (Figure 4.22: E, G). KHS101 hydrochloride exhibited nearly the same log reductions in ER5/1 HVS of *E. faecalis* in single and dual-species biofilm at 32 $\mu\text{g}/\text{mL}$ (0.5 and 0.4 log reduction respectively) this reduction was not statistically significant (Figure 4.22: D, E). However, at the same concentration, E2 LVS was more susceptible in single-species biofilm compared to dual-species biofilm. It showed 3.9-log reductions in single-species ($p<0.0001$), while 1.3-log reductions in dual-species biofilm ($p<0.01$) (Figure 4.22: F, G). The highest concentrations showed the highest killing against *E. faecalis* strains whether in single or dual-species biofilms. KHS101 hydrochloride demonstrated a higher level of killing against ER5/1 HVS in dual-species biofilm (4.1-log reduction) compared to single-species biofilm (2.9-log reduction) although they both were statistically significant ($p<0.01$) (Figure 4.22: D, E). In E2 LVS, a 5.1-log reduction in single-species biofilm and 4.8-log reduction in dual-species biofilm were observed at 64 $\mu\text{g}/\text{mL}$ concentration ($p<0.0001$) (Figure 4.22: F, G).

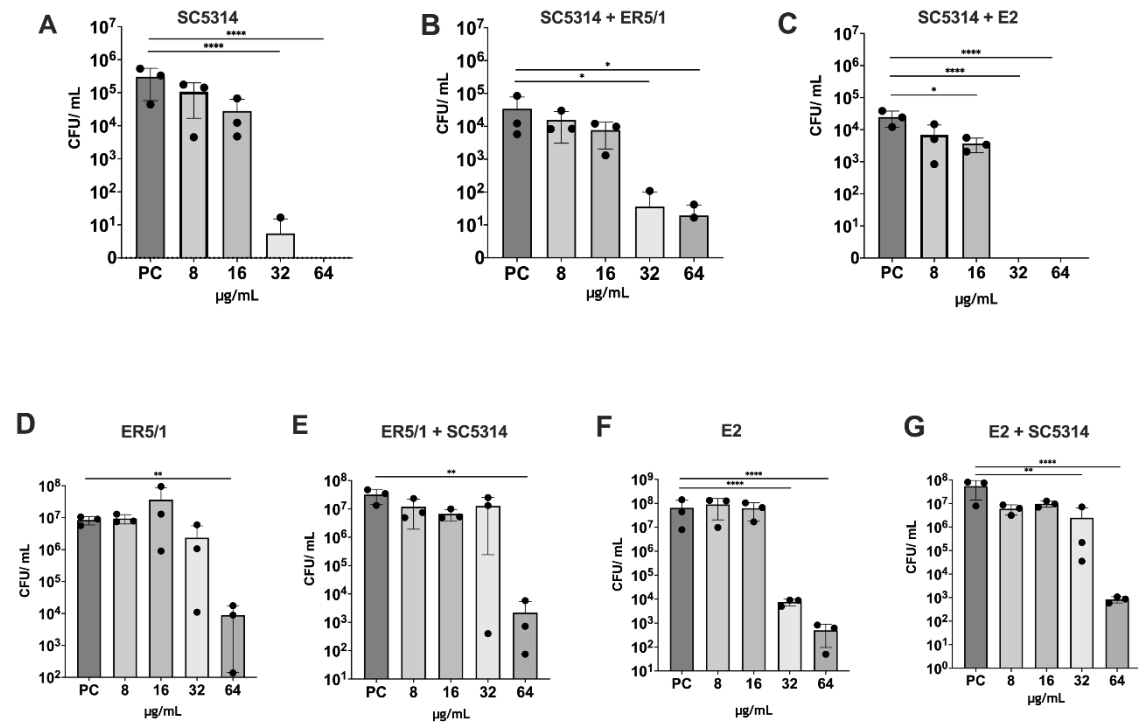


Figure 4.22: KHS101 hydrochloride inhibitory effect on single and dual-species biofilm formation by viable plate count. Biofilms were grown in (THB/ RPMI) media on 24 well plate in single and dual-species biofilm states with drug concentrations ranging from 8 - 64 µg/mL. After 24 hours, Mean colony forming units of *C. albicans* and *E. faecalis* strains were determined: (A - C) Mean colony forming unit (CFU) in SC5314 single-species biofilm (A), dual-species when cocultured with HVS ER5/1 (B), dual-species when cocultured with LVS E2 (C), (D-G) mean colony forming units of *E. faecalis* HVS ER5/1 single-species biofilm (D), HVS ER5/1 in dual-species biofilm (E), LVS E2 in single-species biofilm (F), E2 LVS in dual-species biofilm (G). Untreated biofilms were determined as PCs. Data represented as mean ± SD in triplicate on three separate occasions. An Analysis of Variance (ANOVA) statistical test and Dunnett's post-test was used to assess significance between treated samples and PCs when data were normally distributed and A Kruskal-Wallis statistical test with Dunn's post-test was used to assess significance between treated samples and PCs (* $p < 0.05$, ** $p < 0.01$, *** $p < 0.001$, **** $p < 0.0001$).

Microscopic images revealed that *C. albicans* cells were more yeast-like when treated with KHS101 hydrochloride with less biofilm production observed in a dose dependent manner (Figure 4.23: A-F). In *E. faecalis* HVS ER5/1, biofilm formation was inhibited at highest concentration only (64 µg/mL) (Figure 4.24: E). When HVS ER5/1 was cocultured with *C. albicans* SC5314, dual-species biofilm was observed at 8 and 16 µg/mL concentration (Figure 4.25: B, C). At 32 µg/mL, cells were more yeast like in single-species biofilm compared to dual-species biofilm (Figure 4.25: D). At 64 µg/mL, biofilm was inhibited compared to PC (Figure 4.25: E). The same observation was noticed in LVS E2, where single-species biofilm was completely inhibited at 64 µg/mL (Figure 4.26: E). similar results were evident in E2 and *C. albicans* dual-species biofilm, although less *C. albicans* cells were seen in a dose dependent manner compared to PC (Figure 4.27).

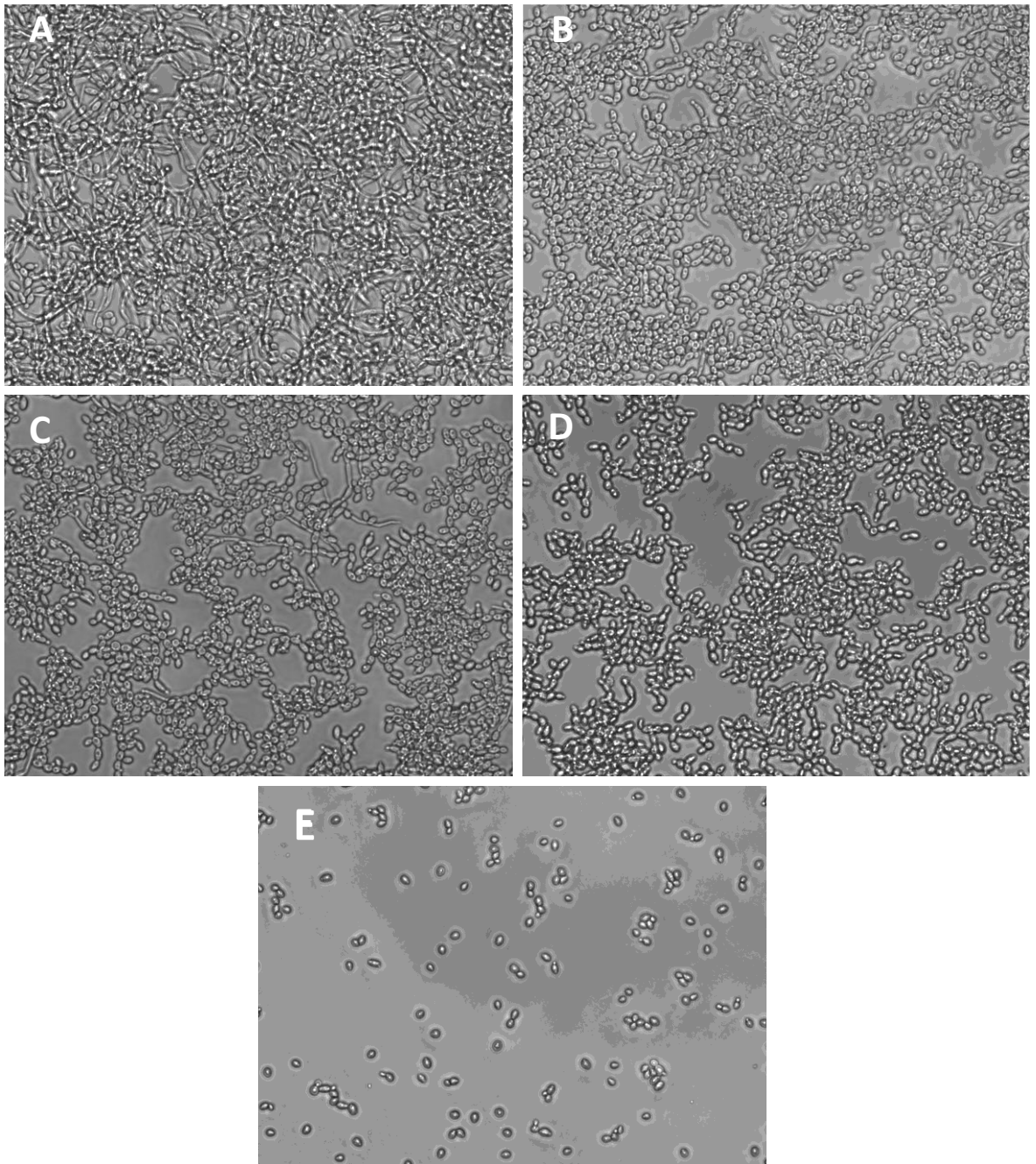


Figure 4.23: Light microscope images of *C. albicans* single-species biofilm inhibition before and after treatment with KHS101 hydrochloride. *C. albicans* laboratory strain SC5314 single-species biofilm (A-E) was grown in THB:RPMI media for 24 hours with KHS101 hydrochloride at 8 $\mu\text{g}/\text{mL}$ (B) and 16 $\mu\text{g}/\text{mL}$ (C) and 32 $\mu\text{g}/\text{mL}$ (D) and 64 $\mu\text{g}/\text{mL}$ (E) and without treatment as PCs (A). Images are representatives of three replicates. Biofilms were examined using EVOS cell imaging system at 400X magnification.

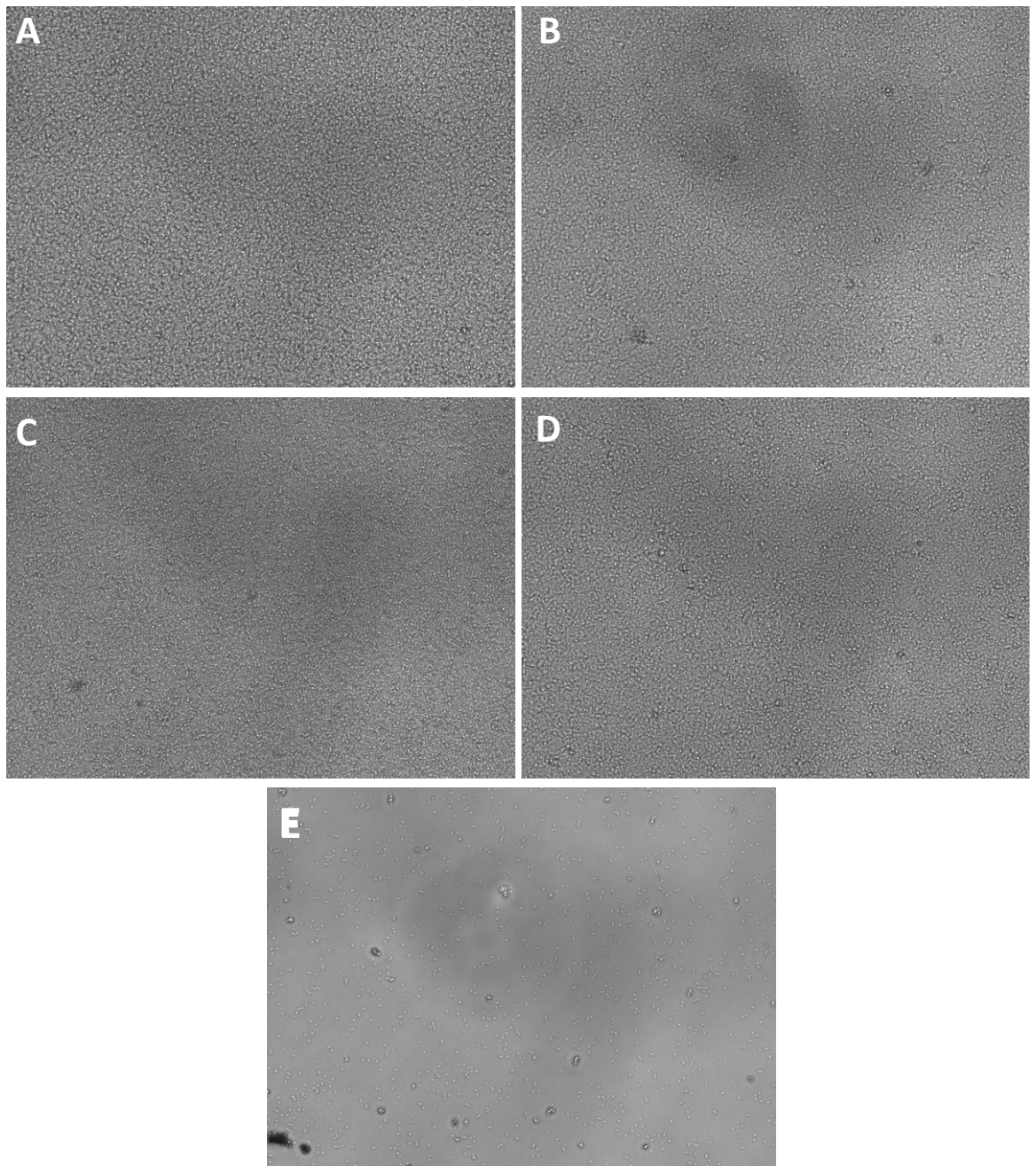


Figure 4.24: Light microscope images of *E. faecalis* ER5/1 single-species biofilm inhibition before and after treatment with KHS101 hydrochloride. *C. albicans* laboratory strain SC5314 and *E. faecalis* clinical strain ER5/1 single-species biofilm (A-E) was grown in THB:RPMI media for 24 hours with KHS101 hydrochloride at 8 µg/mL (B) and 16 µg/mL (C) and 32 µg/mL (D) and 64 µg/mL (E) and without treatment as PCs (A). Images are representatives of three replicates. Biofilms were examined using EVOS cell imaging system at 400X magnification.

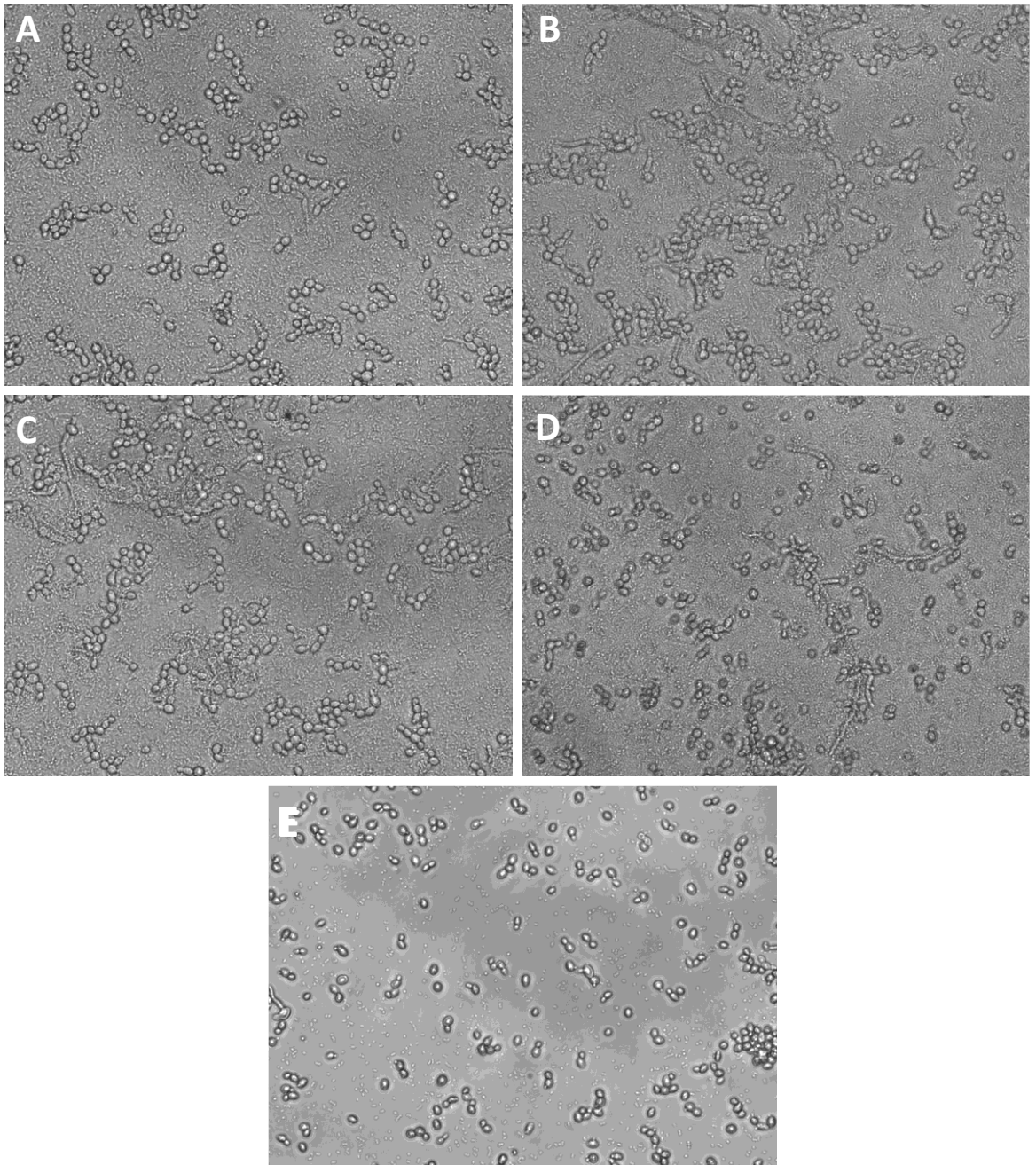


Figure 4.25: Light microscope images of *C. albicans* and *E. faecalis* ER5/1 dual-species biofilm inhibition before and after treatment with KHS101 hydrochloride. *E. faecalis* clinical strain ER5/1 single-species biofilm and *C. albicans* laboratory strain SC5314 (A-E) was grown in THB:RPMI media for 24 hours with KHS101 hydrochloride at 8 µg/mL (B) and 16 µg/mL (C) and 32 µg/mL (D) and 64 µg/mL (E) and without treatment as PCs (A). Images are representatives of three replicates. Biofilms were examined using EVOS cell imaging system at 400X magnification.

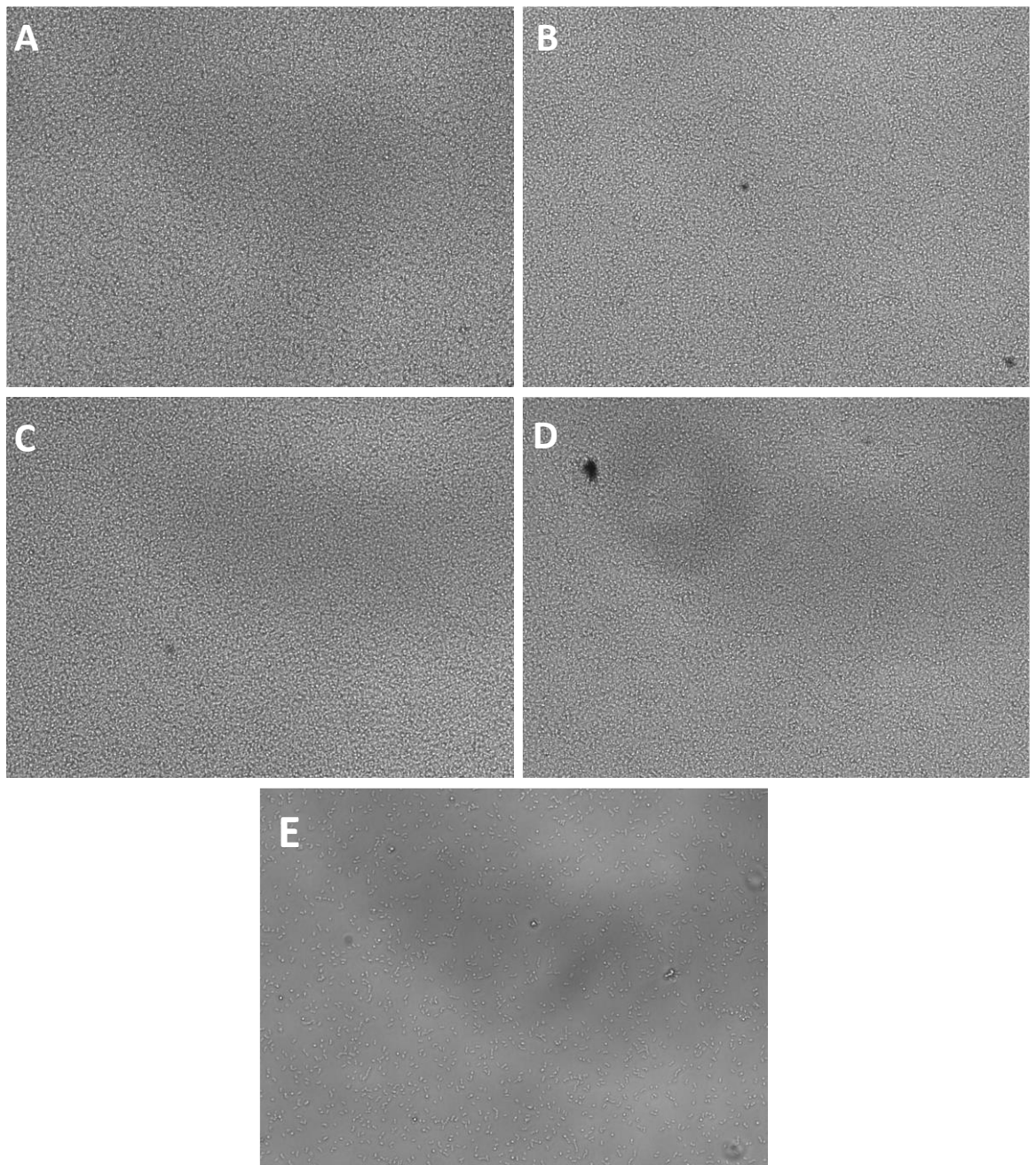


Figure 4.26: Light microscope images of *E. faecalis* E2 single-species biofilm inhibition before and after treatment with KHS101 hydrochloride. *E. faecalis* clinical strain E2 single-species biofilm (A-E) was grown in THB:RPMI media for 24 hours with KHS101 hydrochloride at 4µg/mL (B) and 8 µg/mL (C) and 32 µg/mL (D) and 64 µg/mL (E) and without treatment as PCs (A). Images are representatives of three replicates. Biofilms were examined using EVOS cell imaging system at 400X magnification.

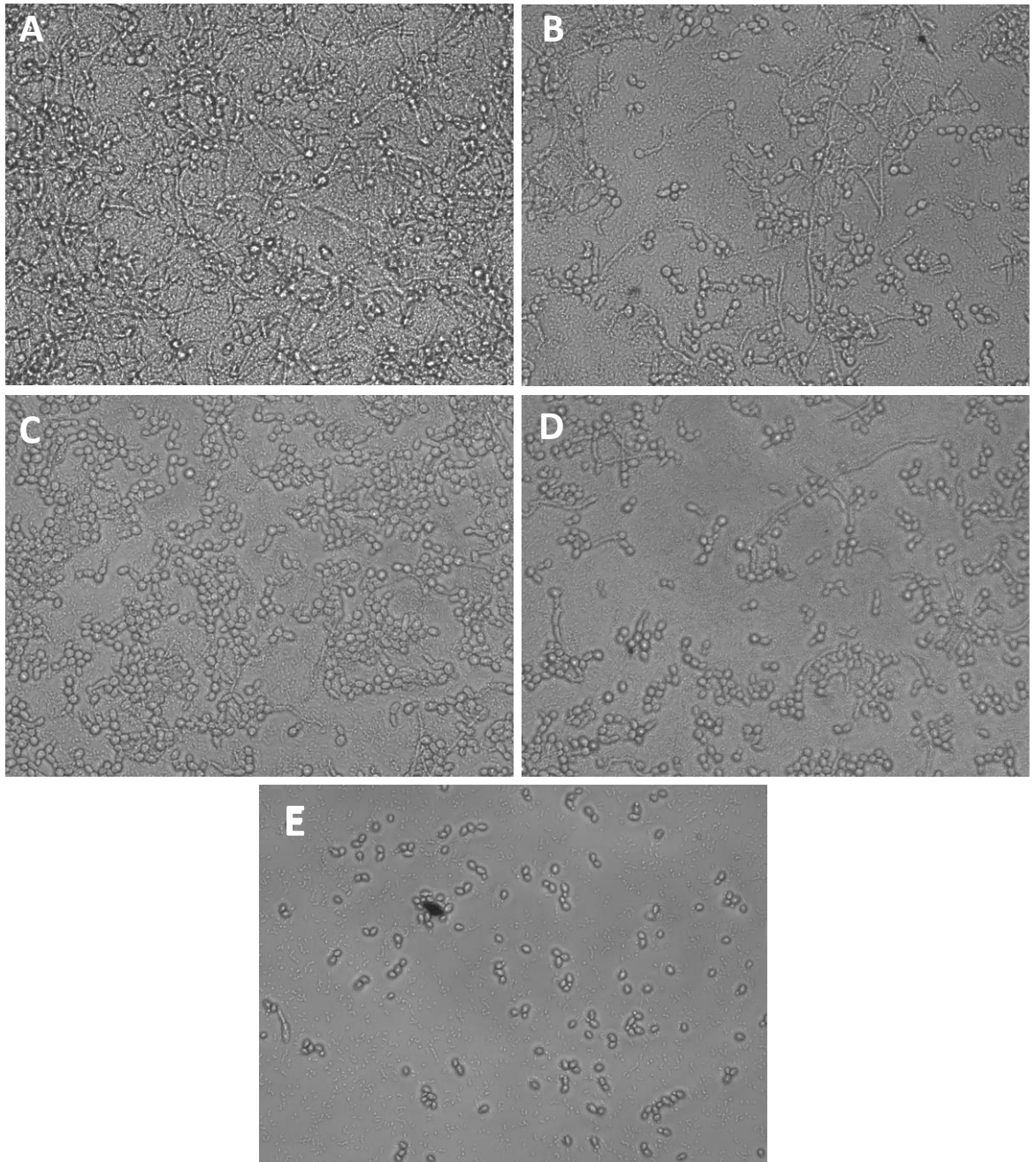


Figure 4.27: Light microscope images of *C. albicans* and *E. faecalis* E2 dual-species biofilm inhibition before and after treatment with KHS101 hydrochloride. *E. faecalis* clinical strain E2 single-species biofilm and *C. albicans* laboratory strain SC5314 (A-E) was grown in THB:RPMI media for 24 hours with KHS101 hydrochloride at 8 µg/mL (B) and 16 µg/mL (C) and 32 µg/mL (D) and 64 µg/mL (E) and without treatment as PCs (A). Images are representatives of three replicates. Biofilms were examined using EVOS cell imaging system at 400X magnification.

4.4.11 Biofilm inhibition activity of darapladib against single and dual-species biofilm of *C. albicans* and *E. faecalis*

Metabolic activity and biofilm biomass analysis revealed that at 4 and 8 µg/mL darapladib reduced the metabolic activity by 56% ($p<0.001$) and 82% ($p<0.0001$), respectively in *C. albicans* single-species biofilm. In addition, metabolic activity was inhibited by 99% at 16 and 32 µg/mL concentrations ($p<0.0001$) (Figure 4.28: A). Biofilm biomass was significantly reduced at 8, 16, 32 µg/mL by 79%, 92%, 86% respectively ($p<0.05$) (Figure 4.28: B)

For single-species ER5/1 and E2 *E. faecalis* strains, 4 µg/mL darapladib did not show any reduction in metabolic activity as well as biofilm biomass (Figure 4.28: B, E, Figure 4.29: B, E). At 8 µg/mL, metabolic activity of ER5/1 single-species biofilm was reduced by only 37% and was inhibited by 99.9% and 100% at 16 and 32 µg/mL concentrations ($p<0.01$) (Figure 4.28: B). In addition, darapladib reduced E2 single-species biofilm viability by 51% at 8 µg/mL ($p<0.05$), 95% at 16 µg/mL and 99% at concentrations at 32 µg/mL ($p<0.001$) (Figure 4.28: B). Biofilm biomass of LVS E2 was more effectively reduced by darapladib when compared to the reduction of HVS ER5/1 at concentrations 8, 16, 32 µg/mL (Figure 4.28: E, Figure 4.29: E). No significant difference was observed between ER5/1 single-species biofilm biomass treatment concentrations and untreated controls (Figure 4.28: E). In contrast, E2 demonstrated 83% biofilm biomass reduction was observed at 8 µg/mL concentration and 100% at 16 µg/mL and 79% at 32 µg/mL ($p<0.01$) (Figure 4.29: E).

In dual-species biofilm, biofilm viability and biomass were unaffected in dual-species biofilms at 4 and 8 µg/mL and remained similar to the control. However, at 16 and 32 µg/mL, complete reductions in viability was seen in *C. albicans* SC5314 and *E. faecalis* ER5/1 HVS coculture ($p<0.0001$) (Figure 4.28: C) and 99% reduction in viability was observed in E2 and SC5314 coculture ($p<0.001$) (Figure 4.29: C). Regarding biofilm biomass, complete biomass reduction was seen in dual-species biofilm composed of SC5314 and HVS ER5/1 ($p<0.0001$) (Figure 4.28: F). Biofilm biomass reduction was also observed at 16 and 32 µg/mL concentrations (85%, $p<0.001$ and 91%, $p<0.0001$ respectively) in dual-species biofilm composed of SC5314 and LVS E2 (Figure 4.29: F).

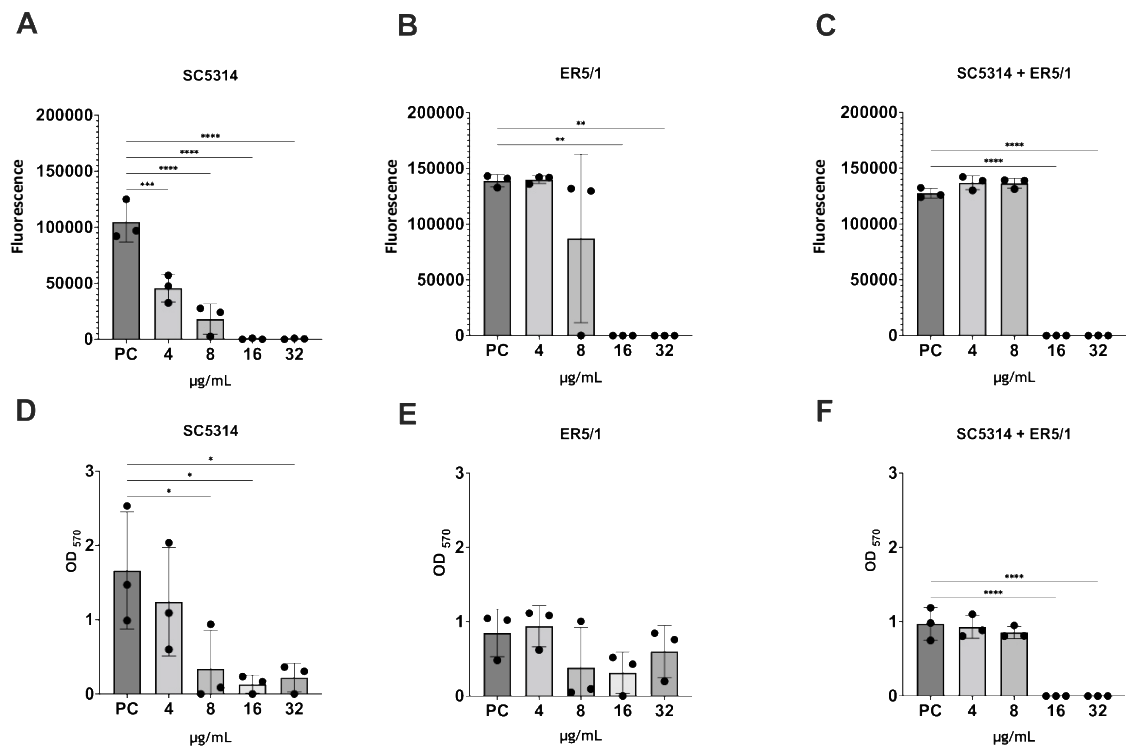


Figure 4.28: Metabolic activity and biofilm biomass of *C. albicans* and *E. faecalis* HVS ER5/1 single and dual-species with and without darapladiib treatment. *C. albicans* SC5314 and *E. faecalis* ER5/1 HVS were grown in (THB/RPMI) media in 24 well plate in single (A, B, D, E) and dual-species biofilm (C,F) with their respective drug concentration. After 24 hours, biofilms metabolic activity (A-C) and biofilm biomass (D-F) were determined using AlamarBlue™ and CV respectively. Data represented as mean ± SD in triplicate on three separate occasions. An Analysis of Variance (ANOVA) statistical test and Dunnett's post-test was used to assess significance between treated samples and PCs when data were normally distributed and A Kruskal-Wallis statistical test with Dunn's post-test was used to assess significance between treated samples and PCs (* $p < 0.05$, ** $p < 0.01$, *** $p < 0.001$, **** $p < 0.0001$).

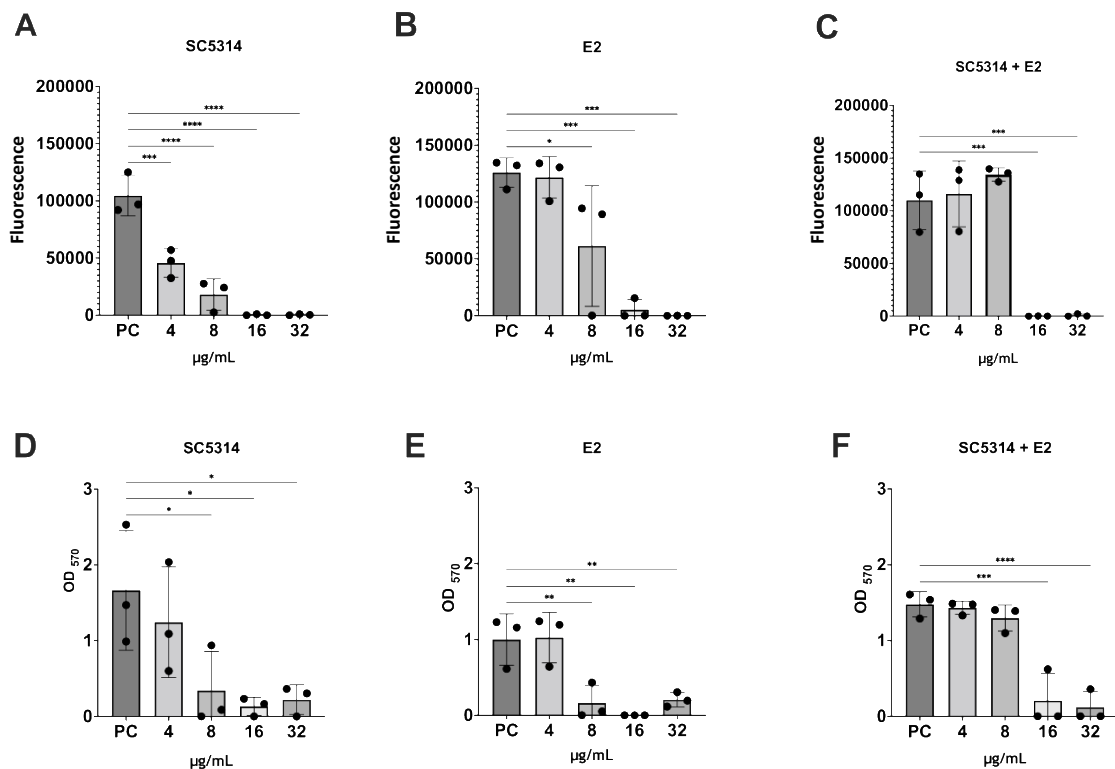


Figure 4.29: Metabolic activity and biofilm formation of *C. albicans* and *E. faecalis* LVS E2 single and dual-species with and without darapladiib treatment. *C. albicans* SC5314 and *E. faecalis* E2 LVS were grown in (THB: RPMI) media in 24 well plate in single (A, B, D, E) and dual-species biofilm (C,F) with their respective drug concentration. After 24 hours, biofilms metabolic activity (A-C) and biofilm biomass (D-F) were determined using AlamarBlue™ and CV respectively. Data represented as mean ± SD in triplicate on three separate occasions. An Analysis of Variance (ANOVA) statistical test and Dunnett's post-test was used to assess significance between treated samples and PCs when data were normally distributed and A Kruskal-Wallis statistical test with Dunn's post-test was used to assess significance between treated samples and PCs (* $p < 0.05$, ** $p < 0.01$, *** $p < 0.001$, **** $p < 0.0001$).

Following treatment with darapladiib, *C. albicans* cells was slightly reduced at 4 and 8 µg/mL by 0.3 and 0.9 log reductions. However, at higher concentrations, namely 16 and 32 µg/mL more significant reduction were seen up to 3.6 ($p < 0.01$) and 2.9 ($p < 0.01$) log reductions respectively (Figure 4.30: A). In dual-species biofilm, *C. albicans* SC5314 demonstrated no reduction when cocultured with ER5/1. In contrast, *C. albicans* CFUs were slightly reduced by 0.3 log reduction when cocultured with E2 LVS, although not statistically significant. At 8 µg/mL concentration, CFU reduction in *C. albicans* was 0.9 when cocultured with ER5/1 although not statistically significant. This was however, higher than E2 coculture which showed no significant log reduction (0.1). At 16 µg/mL concentration, darapladiib reduced CFUs of *C. albicans* by 4 log reductions when cocultured with ER5/1 HVS compared to LVS E2 which showed 2.8 log reductions ($p < 0.01$). Log

reductions were 1.6 and 1.4 when *C. albicans* was cocultured with ER5/1 and E2 ($p<0.05$) respectively (Figure 4.30: B, C).

For *E. faecalis* ER5/1 HVS single-species biofilm, CFUs remained similar when tested at 4 $\mu\text{g}/\text{mL}$. At 8 $\mu\text{g}/\text{mL}$ concentration, darapladib reduced the CFU of ER5/1 cells by 1-log in single and dual-species biofilm ($p<0.05$). The highest CFUs reduction was observed at 16 $\mu\text{g}/\text{mL}$ by more than 3-logs in single and dual-species biofilm ($p<0.01$). At 32 μg concentration, darapladib reduced colonies of ER5/1 HVS by 1.8 in single-species biofilm, however, this was not statistically significant. This reduction was higher in dual-species biofilm (2.8 log reduction) ($p<0.05$) (Figure 4.30: D, E).

In the case of *E. faecalis* E2 LVS, greater log reductions were observed in single-species biofilm. A reduction in CFUs was observed in single and dual-species biofilms at 4 $\mu\text{g}/\text{mL}$ 0.9 and 0.4 respectively. More potent reduction was seen on E2 single-species biofilm by 3.7-, 4.3-, 3.3-log reductions at 8, 16, 32 $\mu\text{g}/\text{mL}$ concentrations respectively ($p<0.0001$) (Figure 4.30: F). In dual-species, a significant reduction was observed at 16 $\mu\text{g}/\text{mL}$ (3.5 log reduction). At 8 and 32 $\mu\text{g}/\text{mL}$ concentrations, the reduction was only by 1, 1.5 respectively (Figure 4.30: G).

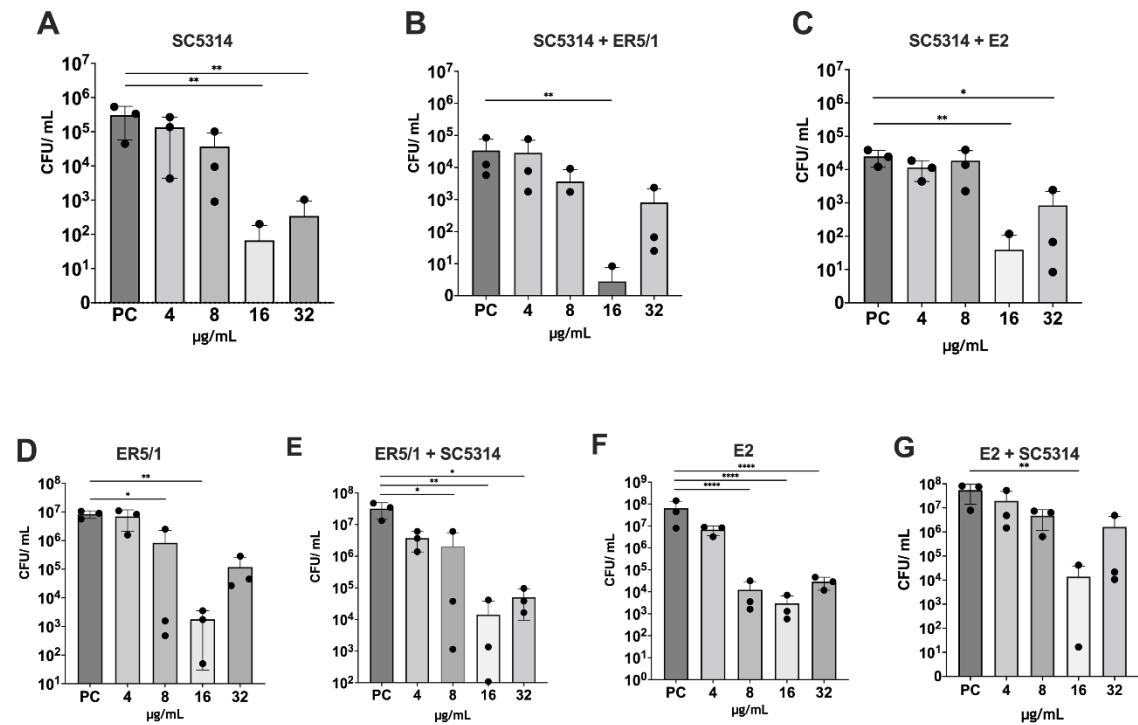


Figure 4.30: Darapladib inhibitory effect on single and dual-species biofilm formation based on viable plate counts. Biofilms were grown in (THB/ RPMI) medium in 24 well plate in single and dual-species biofilm states with drug concentrations ranging from 4 - 32 µg/mL. After 24 hours, mean colony forming units of *C. albicans* and *E. faecalis* strains were determined: (A - C) Mean colony forming unit (CFU) in *C. albicans* SC5314 single-species biofilm (A), dual-species when cocultured with *E. faecalis* HVS ER5/1 (B), dual-species when cocultured with *E. faecalis* LVS E2 (C), (D-G) mean colony forming units of *E. faecalis* HVS ER5/1 single-species biofilm (D), *E. faecalis* HVS ER5/1 in dual-species biofilm (E), *E. faecalis* LVS E2 in single-species biofilm (F), *E. faecalis* E2 LVS in dual-species biofilm (G). Untreated biofilms were determined as PCs. Data represented as mean ± SD in triplicate on three separate occasions. An Analysis of Variance (ANOVA) statistical test and Dunnett's post-test was used to assess significance between treated samples and PCs when data were normally distributed and A Kruskal-Wallis statistical test with Dunn's post-test was used to assess significance between treated samples and PCs (* $p < 0.05$, ** $p < 0.01$, *** $p < 0.001$, **** $p < 0.0001$).

Microscopic images showed that darapladib inhibited biofilm formation in a dose dependent manner. At all concentrations, yeast cells were more evident and less hyphae were observed (Figure 4.31: B- E). In addition, dose dependent biofilm inhibition was seen in both *E. faecalis* strains single-species biofilm from 8 to 32 µg/mL (Figure 4.32: B-D) (Figure 4.34: B-D), however, no inhibition was seen at 4 µg/mL (Figure 4.32: E) (Figure 4.34: E). Moreover, microscopic images revealed that at 8 µg/mL concentration, the LVS E2 was more susceptible to darapladib (Figure 4.34: C) compared to HVS ER5/1 (Figure 4.32: C). In dual-species biofilm in both strains, no biofilm inhibition was observed at 4 and 8 µg/mL concentrations (Figure 4.33: B-C, Figure 4.35: B-C). However, at 16 and 32 concentrations biofilm

was inhibited and more yeast like cells were dispersed along with *E. faecalis* colonies (Figure 4.33: D-E, Figure 4.34: D-E)

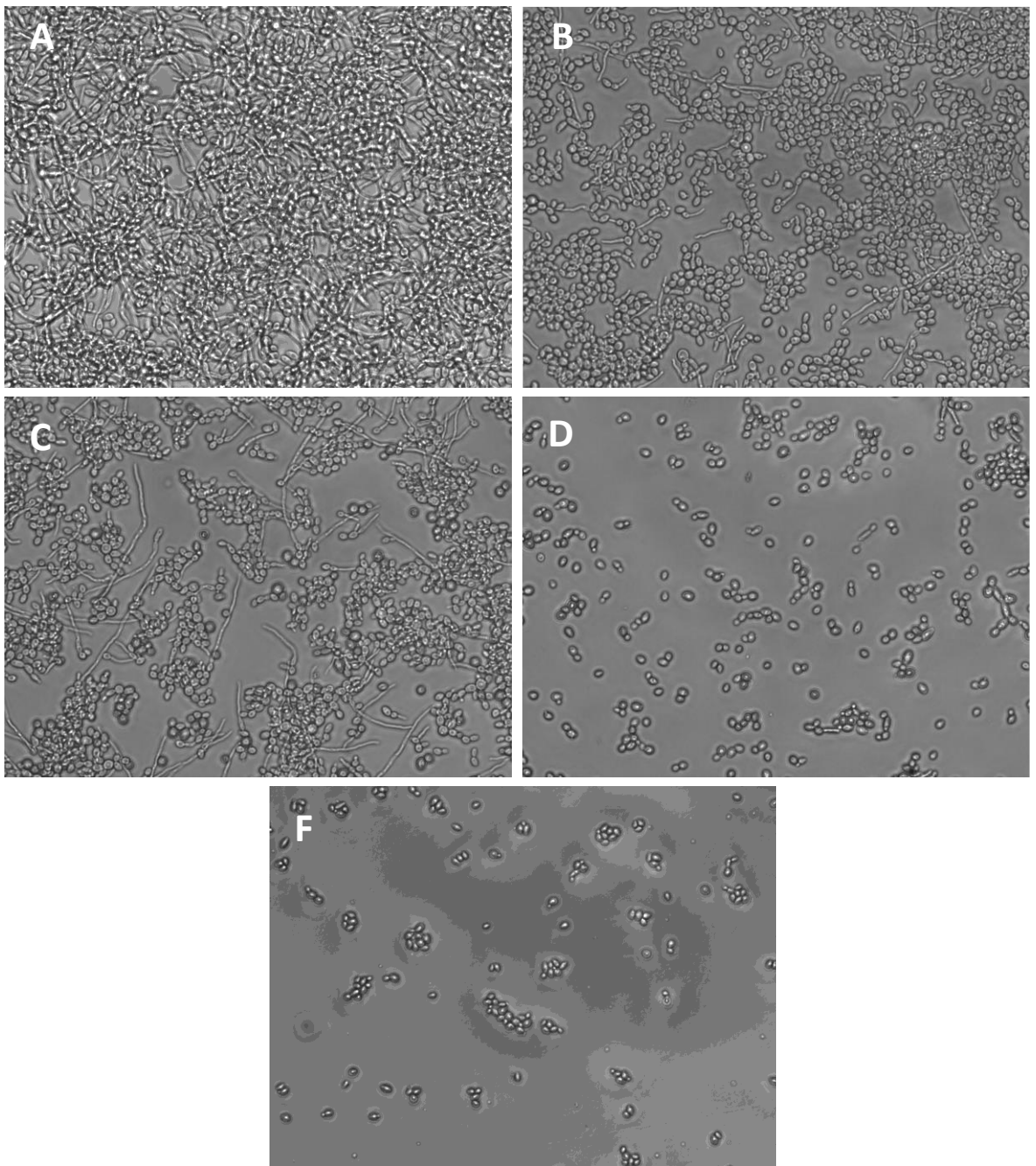


Figure 4.31: Light microscope images of *C. albicans* single-species biofilm inhibition with and without treatment with darapladib. *C. albicans* SC5314 single-species biofilm (A-E) was grown in THB:RPMI media for 24 hours with darapladib at 4 µg/mL (B) and 8 µg/mL (C) and 12 µg/mL (D) and 32 µg/mL (E) and without treatment as PCs (A). Images are representatives of three replicates. Biofilms were examined using EVOS cell imaging system at 400X magnification.

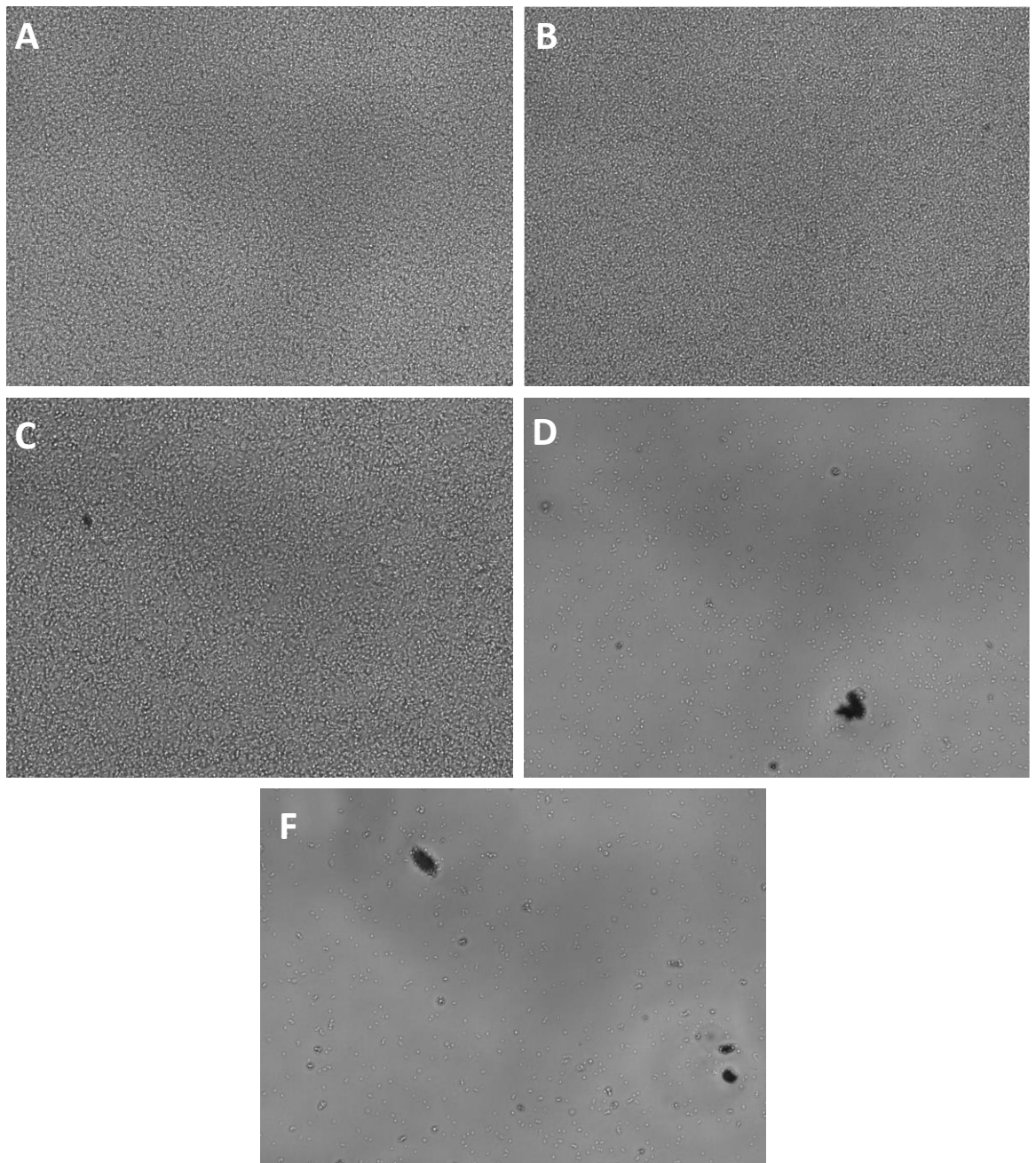


Figure 4.32: Light microscope images of *E. faecalis* ER5/1 single-species biofilm inhibition with and without treatment with darapladib. *E. faecalis* clinical strain ER5/1 single-species biofilm (A-E) was grown in THB:RPMI media for 24 hours with darapladib at 4 $\mu\text{g}/\text{mL}$ (B) and 8 $\mu\text{g}/\text{mL}$ (C) and 16 $\mu\text{g}/\text{mL}$ (D) and 32 $\mu\text{g}/\text{mL}$ (E) and without treatment as PCs (A). Images are representatives of three replicates. Biofilms were examined using EVOS cell imaging system at 400X magnification.

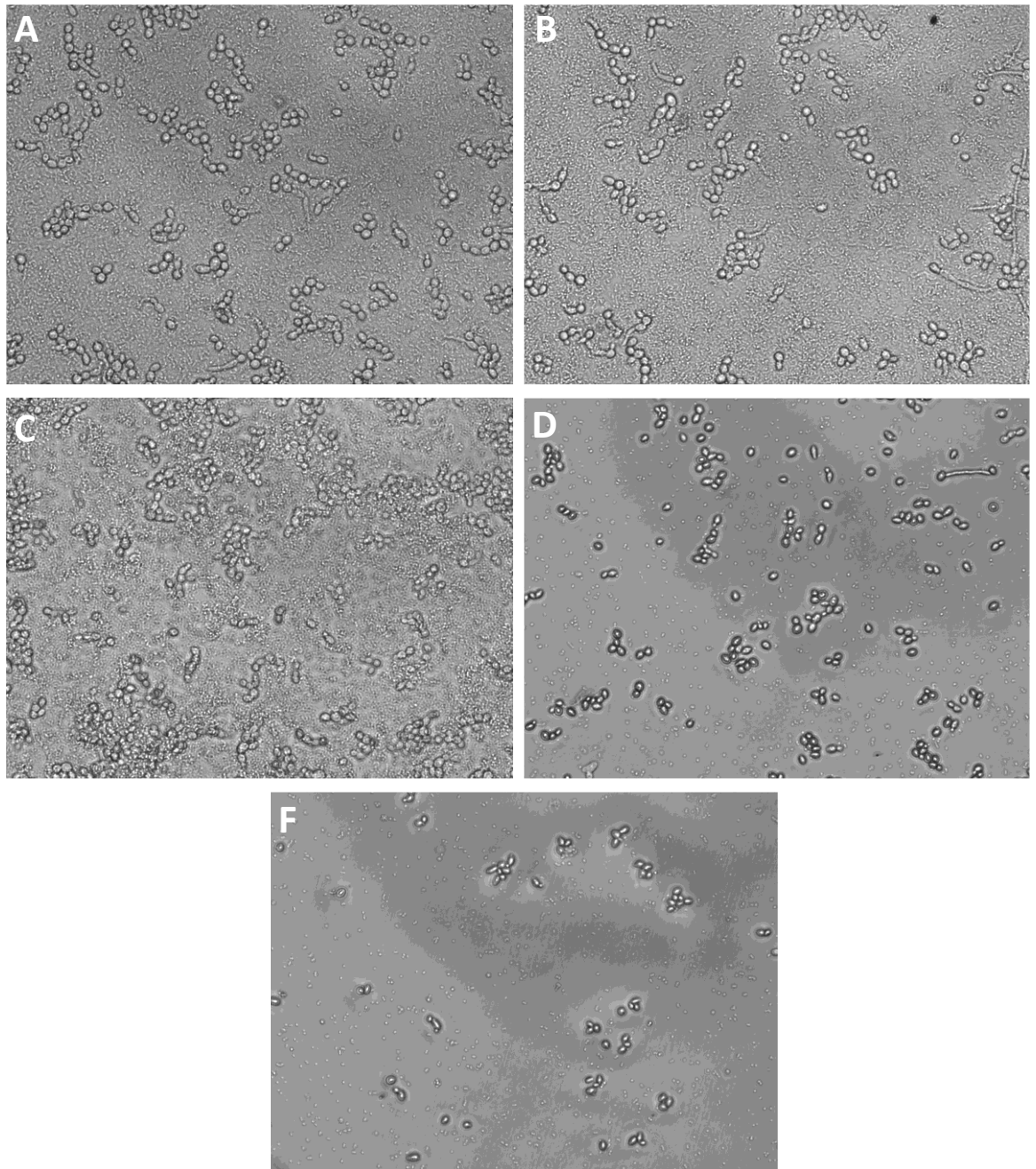


Figure 4.33: Light microscope images of *C. albicans* and *E. faecalis* ER5/1 dual-species biofilm inhibition with and without treatment with darapladib. *E. faecalis* clinical strain ER5/1 single-species biofilm and *C. albicans* laboratory strain SC5314 (A-E) was grown in THB:RPMI media for 24 hours with darapladib at 4 µg/mL (B) and 8 µg/mL (C) and 16 µg/mL (D) and 32 µg/mL (E) and without treatment as PCs (A). Images are representatives of three replicates. Biofilms were examined using EVOS cell imaging system at 400X magnification.

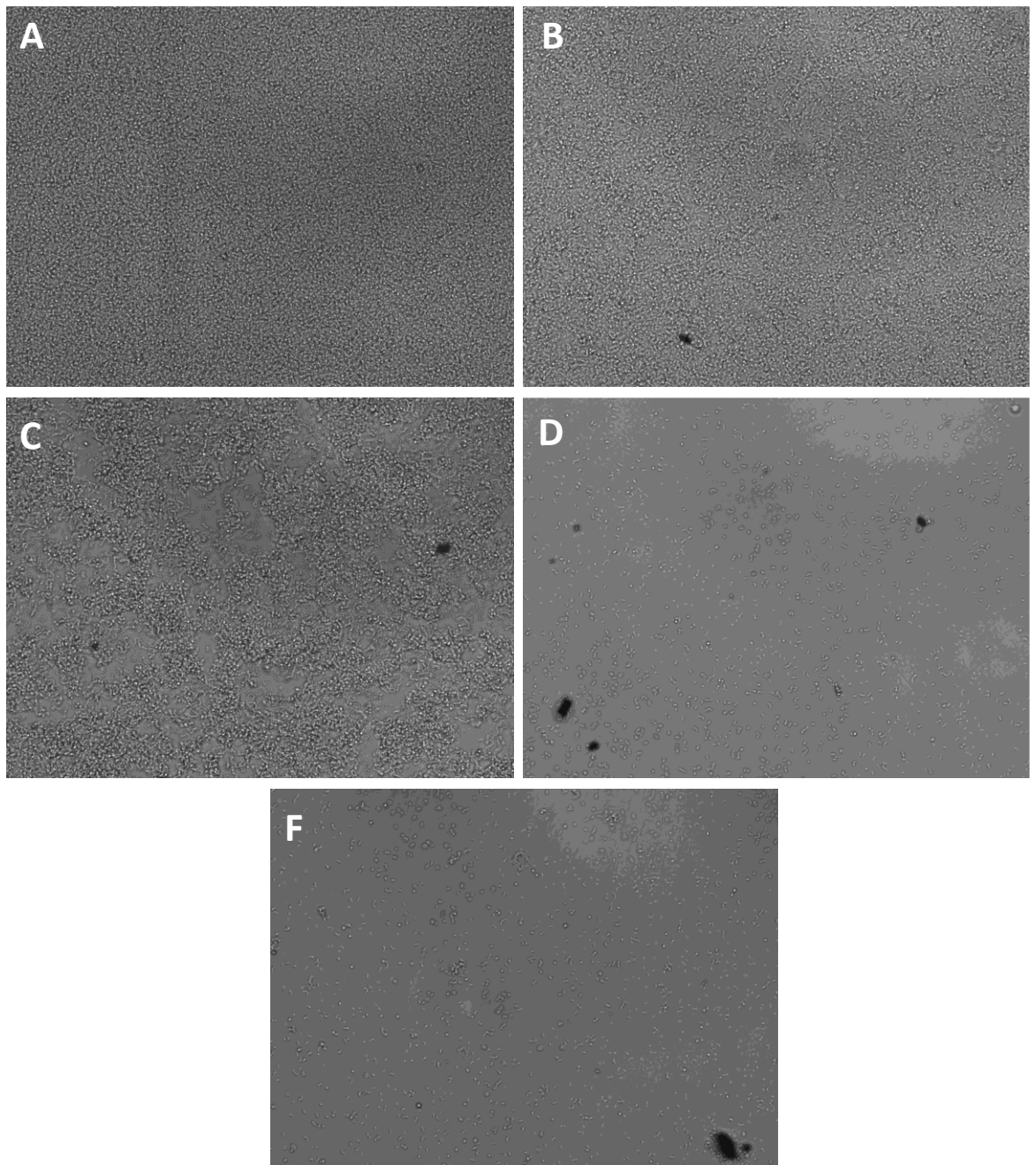


Figure 4.34: Light microscope images of *E. faecalis* E2 single-species biofilm inhibition with and without treatment with darapladib. *E. faecalis* clinical strain E2 single-species biofilm (A-E) was grown in THB:RPMI media for 24 hours with darapladib at 4 µg/mL (B) and 8 µg/mL (C) and 16 µg/mL (D) and 32 µg/mL (E) and without treatment as PCs (A). Biofilms were examined using EVOS cell imaging system at 400X magnification.

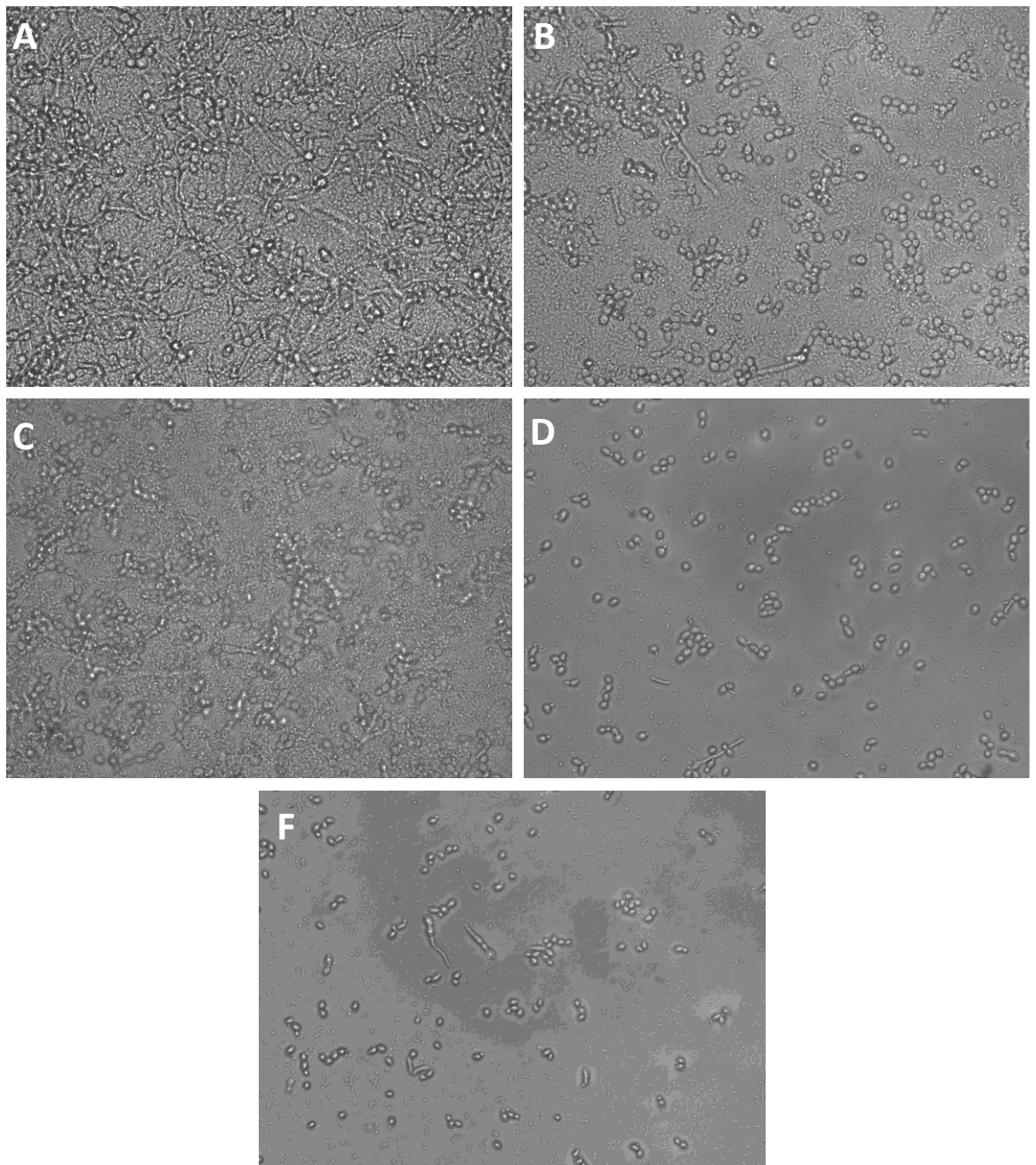


Figure 4.35: Light microscope images of *C. albicans* and *E. faecalis* E2 dual-species biofilm inhibition with and without treatment with darapladib. *E. faecalis* clinical strain E2 single-species biofilm and *C. albicans* laboratory strain SC5314 (A-E) was grown in THB:RPMI media for 24 hours with darapladib at 4 $\mu\text{g}/\text{mL}$ (B) and 8 $\mu\text{g}/\text{mL}$ (C) and 16 $\mu\text{g}/\text{mL}$ (D) and 32 $\mu\text{g}/\text{mL}$ (E) and without treatment as PCs (A). Images are representatives of three replicates. Biofilms were examined using EVOS cell imaging system at 400X magnification.

4.4.12 Biofilm disruption activity of KHS101 and darapladib against single and dual-species biofilm combined with NDs

After biofilm inhibition activity, the biofilm disruption capability of these compounds was assessed. In addition, NDs were combined with the drugs to explore the combined antimicrobial effect they would exert on *C. albicans* and *E. faecalis* in single and dual-species biofilms. Biofilms are intrinsically resistant to antimicrobial agents, and so a higher concentration of drugs are required to disrupt biofilm and kill microbes compared to their planktonic counterparts. Thus, for the following experiments the highest concentrations of the most effective compounds KHS101 hydrochloride, darapladib and NDs were selected for further investigation.

The metabolic activity and the biomass of biofilms were assessed after 24 hours of treatment. In *C. albicans* single-species biofilm, NDs alone reduced biofilm viability by 66%. KHS101 alone or in combination with NDs completely reduced metabolic activity of biofilm ($p < 0.01$). Darapladib reduced the metabolic activity of *C. albicans* single-species biofilm by 82% and the viability was further reduced when combined with NDs for up to 90% ($p < 0.05$) (Figure 4.36: A). Biofilm biomass of *C. albicans* single-species biofilm was not significantly reduced amongst treatment conditions in comparison to PC. The highest reduction was seen in darapladib treatment whether alone or combined with NDs. (Figure 4.37:A).

In *E. faecalis* single-species biofilm, NDs did not reduce the viability of biofilm. In ER5/1 HVS single-species biofilm, KHS101 reduced biofilm viability by 99% and darapladib completely reduced biofilm viability by 100% ($p < 0.0001$). However, when KHS101 hydrochloride and darapladib were combined with NDs, the viability of biofilms was reduced by 61% and 73% ($p < 0.001$) respectively (Figure 4.36:: B). The biofilm biomass was significantly reduced in KHS101 hydrochloride treatment by 33% ($p < 0.05$) and darapladib treatment by 51% ($p < 0.001$) (Figure 4.37: B). For *E. faecalis* E2 LVS single-species biofilm, KHS 101 hydrochloride reduced biofilm viability by 99% as in HVS *E. faecalis* ER5/1 ($p < 0.05$). When it was combined with NDs, it reduced the efficacy of KHS101 hydrochloride and the viability was only reduced by 59%. Darapladib reduced biofilm viability by 77% ($p < 0.05$). When combined with NDs, it slightly reduced darapladib efficacy and biofilm viability

was reduced by 64% (Figure 4.36: D). The biofilm biomass was significantly reduced by 50% upon darapladib treatment only ($p<0.05$) (Figure 4.37: D).

In dual-species biofilm, NDs alone did not reduce viability of dual-species biofilm. When *C. albicans* SC5314 was cocultured with ER5/1 HVS, KHS101 and darapladib reduced biofilm viability by 83% and 96% respectively ($p<0.0001$). However, the combinations NDs-KHS101 hydrochloride and NDs-darapladib reduced further the biofilm viability to 52% and 63% respectively ($p<0.001$) (Figure 1.36: C). When *C. albicans* SC5314 was cocultured with E2 LVS, KHS101 hydrochloride reduced biofilm viability by 99%, ($p<0.01$), but darapladib was less effective than ER5/1 dual-species biofilm and showed reduction in viability by 69%. Combining NDs with KHS101 hydrochloride reduced biofilm viability to 54%. However, the efficacy of darapladib remained unchanged after combining NDs to darapladib (Figure 4.36: E). Biofilm biomass of dual-species biofilms were only significantly reduced when biofilms were treated with KHS101 hydrochloride and darapladib. In ER5/1 HVS dual-species biofilm, biofilm biomass was reduced by 30% ($p<0.05$) and darapladib reduced biofilm biomass by 34% ($p<0.01$) (Figure 4.37: C). In *E. faecalis* E2 dual-species biofilm, a significant 37% reduction in biofilm biomass was observed in KHS101 hydrochloride treatment ($p<0.05$); and a significant 41% reduction in biofilm biomass was revealed for darapladib ($p<0.05$) (Figure 4.37: E).

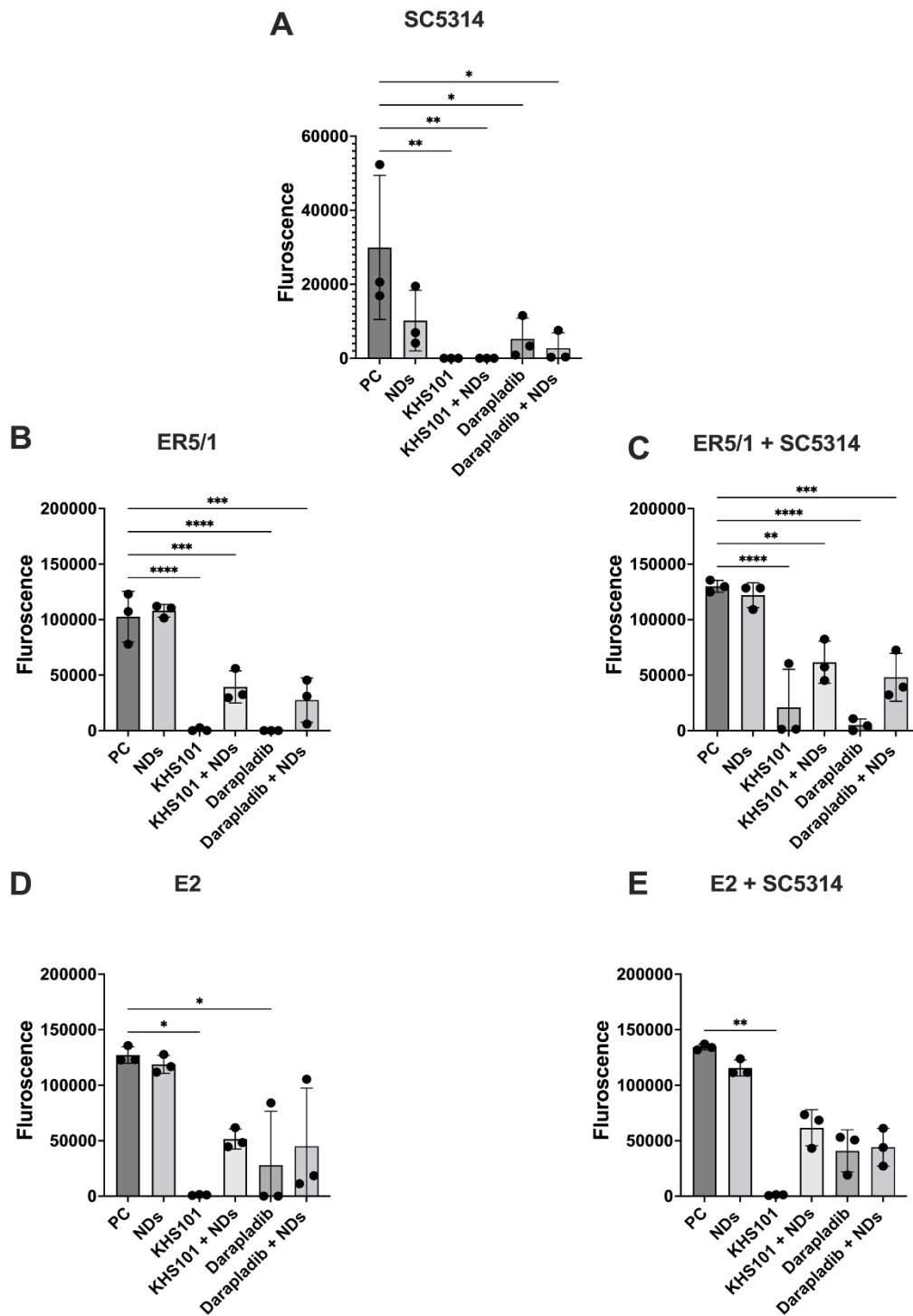


Figure 4.36: Metabolic activity of *C. albicans* and two *E. faecalis* strains single and dual-species after biofilm disruption treatment by KHS101 hydrochloride, Darapadib, NDs and combinational treatment. Single and dual-species biofilms were grown as the following A: *C. albicans* SC5314 single-species, B: *E. faecalis* ER5/1 single-species, C: *C. albicans* SC5314 + *E. faecalis* ER5/1 dual-species, D: *E. faecalis* E2 single-species, E: *C. albicans* SC5314 + *E. faecalis* E2 dual-species for 24 hours and biofilms were then treated with NDs alone at 5000 mg/L concentration, KHS101 hydrochloride 64 µg/mL, KHS101 hydrochloride 64 µg/mL and NDs 5000 mg/L, darapladib 32 µg/mL, darapladib 32 µg/mL and NDs 5000 mg/L. After 24 hours, biofilms metabolic activity (A-E) was determined using AlamarBlue™. Data represented as mean ± SD in triplicate on three separate occasions. An Analysis of Variance (ANOVA) statistical test and Dunnett's post-test was used to assess significance between treated samples and PCs when data were normally distributed and A Kruskal-Wallis statistical test with Dunn's post-test was used to assess significance between treated samples and PCs (* $p < 0.05$, ** $p < 0.01$, *** $p < 0.001$, **** $p < 0.0001$).

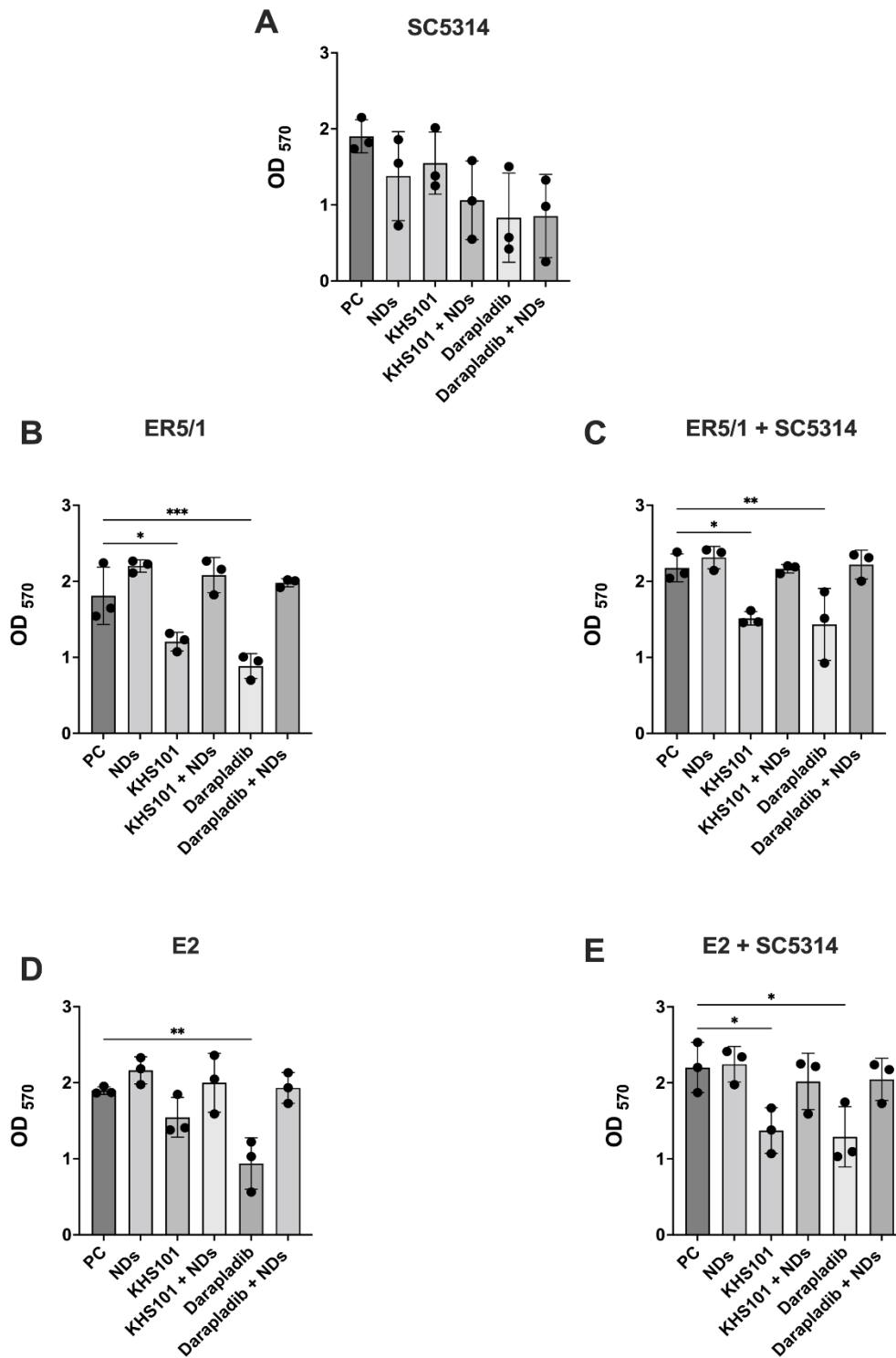


Figure 4.37: Biofilm biomass of *C. albicans* and two *E. faecalis* strains single and dual-species after biofilm disruption treatment by KHS101 hydrochloride, Darapadib, NDs and combinational treatment. Single and dual-species biofilms were grown as the following A: *C. albicans* SC5314 single-species, B: *E. faecalis* ER5/1 single-species, C: *C. albicans* SC5314 + *E. faecalis* ER5/1 dual-species, D: *E. faecalis* E2 single-species, E: *C. albicans* SC5314 + *E. faecalis* E2 dual-species for 24 hours and biofilms were then treated with NDs alone at 5000 mg/L concentration, KHS101 hydrochloride 64 µg/mL, KHS101 hydrochloride 64 µg/mL and NDs 5000 mg/L, darapladib 32 µg/mL, darapladib 32 µg/mL and NDs 5000 mg/L. After 24 hours, biofilms metabolic activity (A-E) was determined using CV. Data represented as mean ± SD in triplicate on three separate occasions. An Analysis of Variance (ANOVA) statistical test and Dunnett's post-test was used to assess significance between treated samples and PCs when data were normally distributed and A Kruskal-Wallis statistical test with Dunn's post-test was used to assess significance between treated samples and PCs (* $p < 0.05$, ** $p < 0.01$, *** $p < 0.001$).

Biofilm analysis revealed that *C. albicans* CFUs were reduced by 0.7 logs when treated with NDs. KHS101 hydrochloride reduced CFUs by two logs ($p<0.001$) but when combined with NDs the reduction was decreased to 1.4 logs ($p<0.05$). Darapladib reduced CFUs by 1.5 logs ($p<0.01$) and the combination with NDs reduced CFUs by 1.4 log reduction ($p<0.05$) (Figure 4.38: A).

In dual-species biofilm with *E. faecalis* ER5/1, generally, less reduction was seen in all treatment conditions except for NDs that were ineffective in reducing *C. albicans* CFUs in dual-species biofilm. KHS101 hydrochloride reduced CFUs by 1.16 ($p<0.05$). When NDs were combined, 0.8-fold reduction was observed. Darapladib also reduced CFUs of *C. albicans* by 1 log, however, when combined with NDs it reduced CFUs by 0.3 only (Figure 4.38: B).

When *C. albicans* was cocultured with *E. faecalis* E2 LVS, KHS101 significantly reduced *C. albicans* CFUs by 1.9 ($p<0.5$). However, when combined with NDs this efficacy was reduced and 0.7 log reduction was noticed. Interestingly, darapladib was the least efficient and only reduced CFUs by 0.3 log and this effect was completely abolished when darapladib was combined with NDS (Figure 4.38: C). NDs treatment alone was also ineffective in reducing *C. albicans* CFUs.

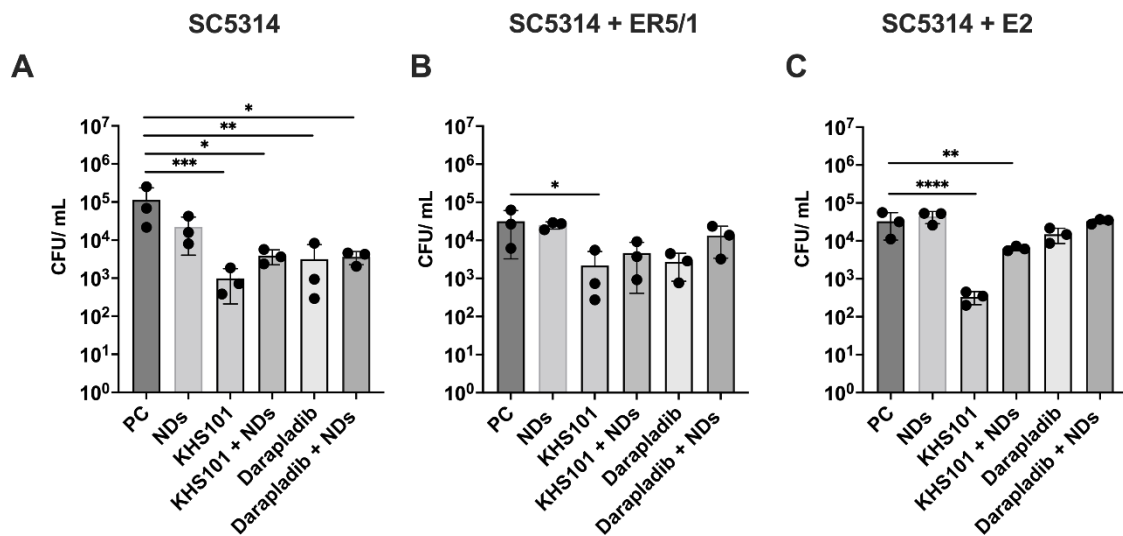


Figure 4.38: *C. albicans* colony forming units after biofilm disruption treatment by KHS101 hydrochloride, darapadib, NDs and combinational treatment. Biofilms were grown in (THB: RPMI) media on 24 well plate in single and dual-species biofilm states with different treatment conditions (NDs alone at 5000 mg/L concentration, KHS101 hydrochloride 64 $\mu\text{g}/\text{mL}$, KHS101 hydrochloride 64 $\mu\text{g}/\text{mL}$ and NDs 5000 mg/L, darapladib 32 $\mu\text{g}/\text{mL}$, darapladib 32 $\mu\text{g}/\text{mL}$ and NDs 5000 mg/L). After 24 hours, Mean colony forming units of *C. albicans* were determined in SC5314 single-species biofilm (A), dual-species when cocultured with HVS ER5/1 (B), dual-species when cocultured with HVS ER5/1 (C), untreated biofilms were determined as PCs. Data represented as mean \pm SD in triplicate on three separate occasions. An Analysis of Variance (ANOVA) statistical test and Dunnett's post-test was used to assess significance between treated samples and PCs when data were normally distributed and A Kruskal-Wallis statistical test with Dunn's post-test was used to assess significance between treated samples and PCs (* $p < 0.05$, ** $p < 0.01$, *** $p < 0.001$, **** $p < 0.0001$).

In single-species biofilm of *E. faecalis* ER5/1 HVS, NDs reduced CFUs of ER5/1 by 0.6 log reduction only. KHS101 hydrochloride reduced ER5/1 CFUs by 1.9 logs ($p < 0.05$). When combined with NDs, the efficacy of KHS101 was reduced to only one log. In darapladib treatment, ER5/1 CFUs were reduced by 1.8 log reductions ($p < 0.01$). When combined with NDs, darapladib reduced CFUs by 1.4 log ($p < 0.05$) (Figure 4.39: A). In ER5/1 dual-species biofilm, NDs reduced CFUs by 0.7 log reduction ($p < 0.05$) and KHS101 hydrochloride reduced ER5/1 CFUs by 2.1 log reduction ($p < 0.0001$). When NDs were added to KHS101 hydrochloride, its efficiency was reduced to 0.9 log reduction ($p < 0.01$). darapladib treatment reduced ER5/1 CFUs by 1.4 log reduction ($p < 0.0001$) and when treatment was combined with NDs log reductions were reduced to 0.96 ($p < 0.01$) (Figure 4.39: B).

In *E. faecalis* E2 single-species biofilm, NDs reduced CFUs by 0.6 log reduction. KHS101 hydrochloride treatment reduced E2 CFUs by 1.5 logs ($p<0.05$). When treatment was combined with NDs, log reductions were only 1. Darapladib reduced E2 CFUs by 3 log reductions ($p<0.01$) and when NDs were combined to darapladib the log reduction was lowered to 1.4 (Figure 4.39: C). In E2 dual-species biofilm, NDs produced significant reductions to E2 CFUs by 0.9 log ($p<0.05$). KHS101 hydrochloride was the most potent in reducing E2 CFUs by 2.8 logs ($p<0.0001$). However, when NDs were added, the reduction was lowered to 1 only ($p<0.05$). In darapladib treatment, E2 CFUs were reduced by 1.3 only ($p<0.01$) compared to single-species biofilm. Combining NDs to darapladib did not affect its efficiency and CFUs were reduced by 1.6 ($p<0.01$) (Figure 4.39: D).

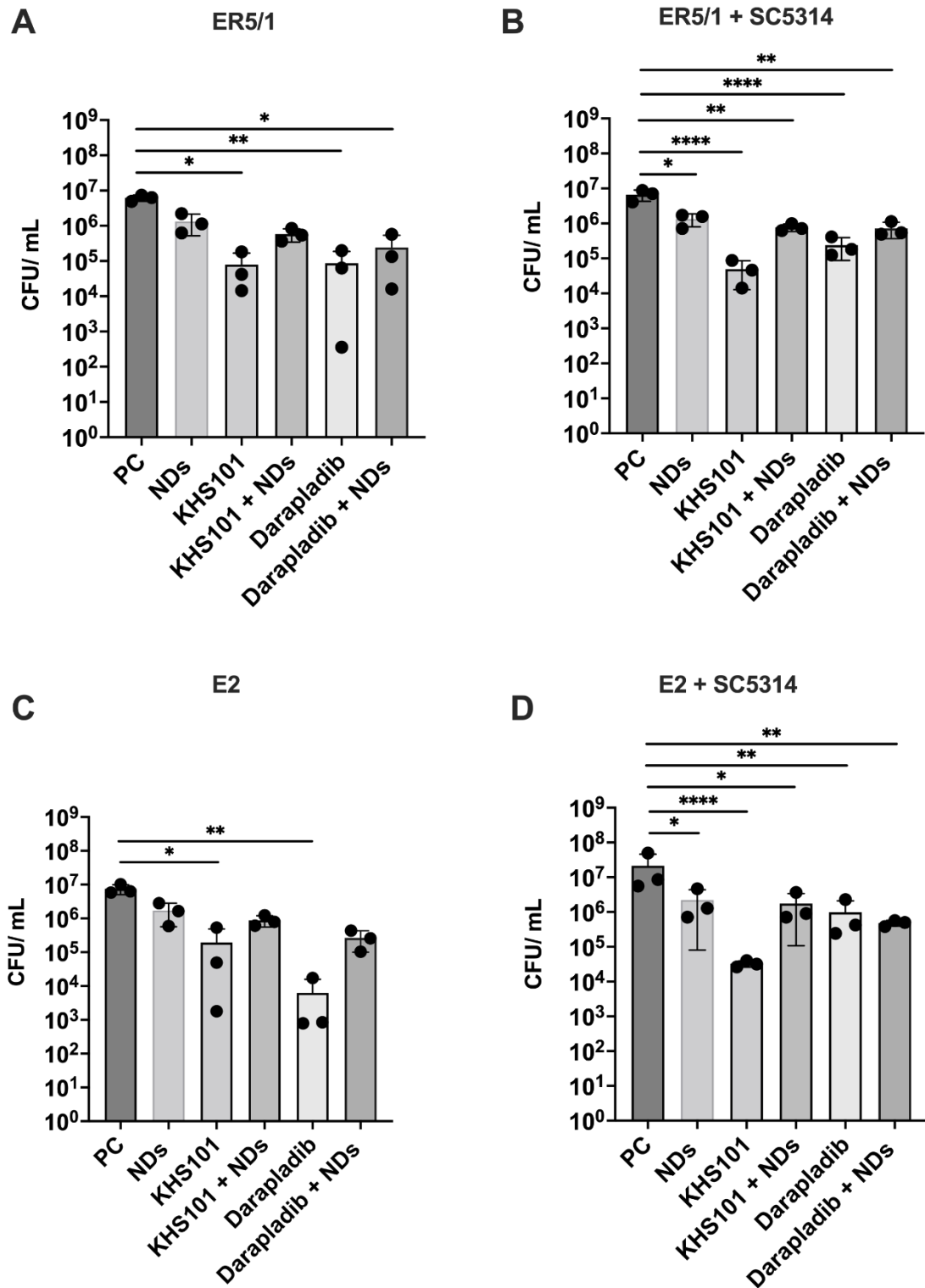


Figure 4.39: *E. faecalis* colony forming units after biofilm disruption treatment by KHS101 hydrochloride, darapadib, NDs and combinational treatment. Biofilms were grown in (THB:RPMI) media on 24 well plate in single and dual-species biofilm states with different treatment conditions (NDs alone at 5000 mg/L concentration, KHS101 hydrochloride 64 μ g/mL, KHS101 hydrochloride 64 μ g/mL and NDs 5000 mg/L, darapladib 32 μ g/mL, darapladib 32 μ g/mL and NDs 5000 mg/L). After 24 hours, mean colony forming units of *E. faecalis* were determined in ER5/1 single-species biofilm (A), ER5/1 dual-species when cocultured with SC5314 (B), E2 single-species biofilm (C), E2 dual-species biofilm when cocultured with SC5314. Untreated biofilms were determined as PCs. Data represented as mean \pm SD in triplicate on three separate occasions. An Analysis of Variance (ANOVA) statistical test and Dunnett's post-test was used to assess significance between treated samples and PCs when data were normally distributed and A Kruskal-Wallis statistical test with Dunn's post-test was used to assess significance between treated samples and PCs (* p <0.05, ** p <0.01, *** p <0.001, **** p <0.0001).

Lastly, darapladib anti-biofilm efficacy was examined by microscopy. NDs slightly disrupted *C. albicans* biofilm compared to untreated controls (Figure 4.40: A, B). There was a reduction in *C. albicans* biofilm when treated with KHS101 64 µg/mL compared to PC. However, some *C. albicans* cells remained attached to the bottom of the well. These cells looked phenotypically different from their untreated counterparts (Figure 4.36: C). Combining NDs with KHS101 hydrochloride reduced biofilm, and it was shown that *C. albicans* cells and their hyphae were coated with NDs (Figure 4.36: D). Darapladib had the same effect as KHS101, where a reduction in biofilm was noted after treatment. Cells were shrunken and phenotypically different compared to the PC (Figure 4.36: E). Combination treatment composed of darapladib and NDs exerted the same effect as KHS101 hydrochloride, where biofilm was reduced upon treatment and *C. albicans* cells, and their hyphae were coated with NDs (Figure 4.36: F).

In ER5/1 single-species biofilm, no significant difference was observed under the microscope for all treatment conditions compared to PC biofilm (Figure 4.43: A-F). Treatment of dual-species biofilm composed of *C. albicans* and *E. faecalis* HVS ER5/1 with NDs did not seem to have any effect on biofilm reduction and some of *C. albicans* cells were coated with NDs and some other cells were not (Figure 4.42: B). Upon treatment with KHS101, *C. albicans* cells were shrunken compared to their untreated counterparts in PC biofilm. In addition, slight disruption amongst *E. faecalis* colonies was seen (Figure 4.42: A,C). The effect of KHS101 remained the same when combined with NDs and did not prevent the change in *C. albicans* cells phenotype compared to KHS101 treatment only (Figure 4.42: D). Darapladib had the same effect on dual-species biofilm as in KHS101 and when combined with NDs biofilm disruption was evident (Figure 4.42: E, F).

As with *E. faecalis* ER5/1, no significant difference was seen with E2 *E. faecalis* single-species biofilm disruption compared to untreated controls (Figure 4.43: A-F). In dual-species biofilm of SC5314 and E2 LVS treatment with NDs, slight disruption was observed and NDs were coating *C. albicans* cells and their hyphae (Figure 4.44: B). Upon treatment with KHS101 *C. albicans* cells were shrunk and biofilm disruption was evident (Figure 4.44: C). When combining NDs, enhanced disruption was seen and NDs were coating *C. albicans* cells (Figure 4.44: D). Darapladib was also effective in disrupting dual-species biofilm and *C. albicans* cells phenotype looked shrunk compared to untreated biofilm (Figure 4.44: E).

When combining NDs with darapladib, disruption was still evident and NDs were coating *C. albicans* cells and their hyphae (Figure 4.44: F).

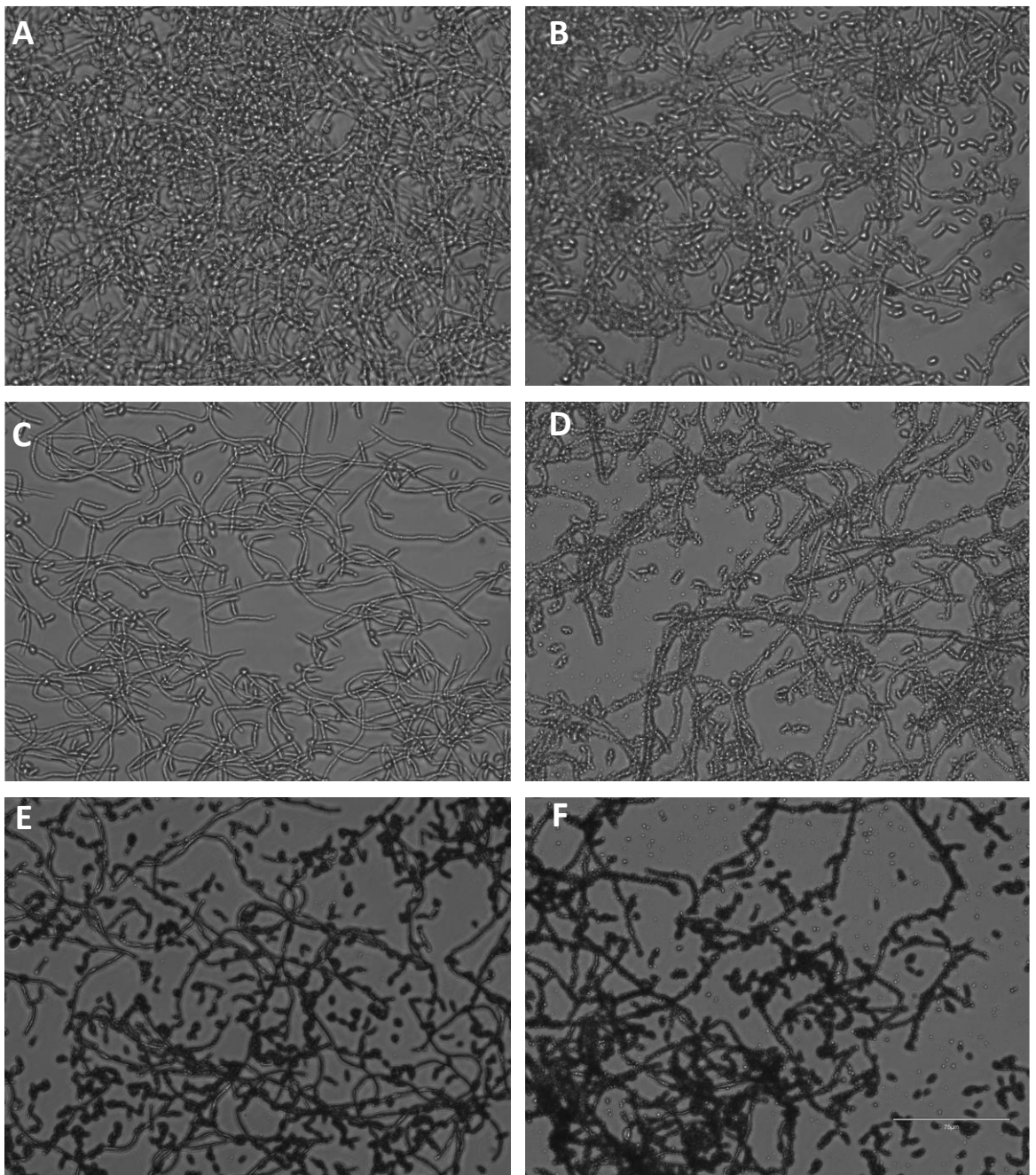


Figure 4.40: Light microscope images of single-species biofilm disruption of *C. albicans* with and without different treatment conditions. *C. albicans* laboratory strain SC5314 single-species biofilm (A-F) was grown for 24 hours in THB: RPMI media. . Untreated biofilm was used as a PC (A) Biofilms were treated with 5000 mg/L NDs (B), KHS101 64 µg/mL (C), KHS101 hydrochloride 64 µg/mL and NDs 5000 mg/L (D), darapladib 32 µg/mL (E) and darapladib 32 µg/mL and NDs 5000 mg/L (F) for 24 hours. Images are representatives of three replicates. Biofilms were examined using EVOS cell imaging system at 400X magnification.

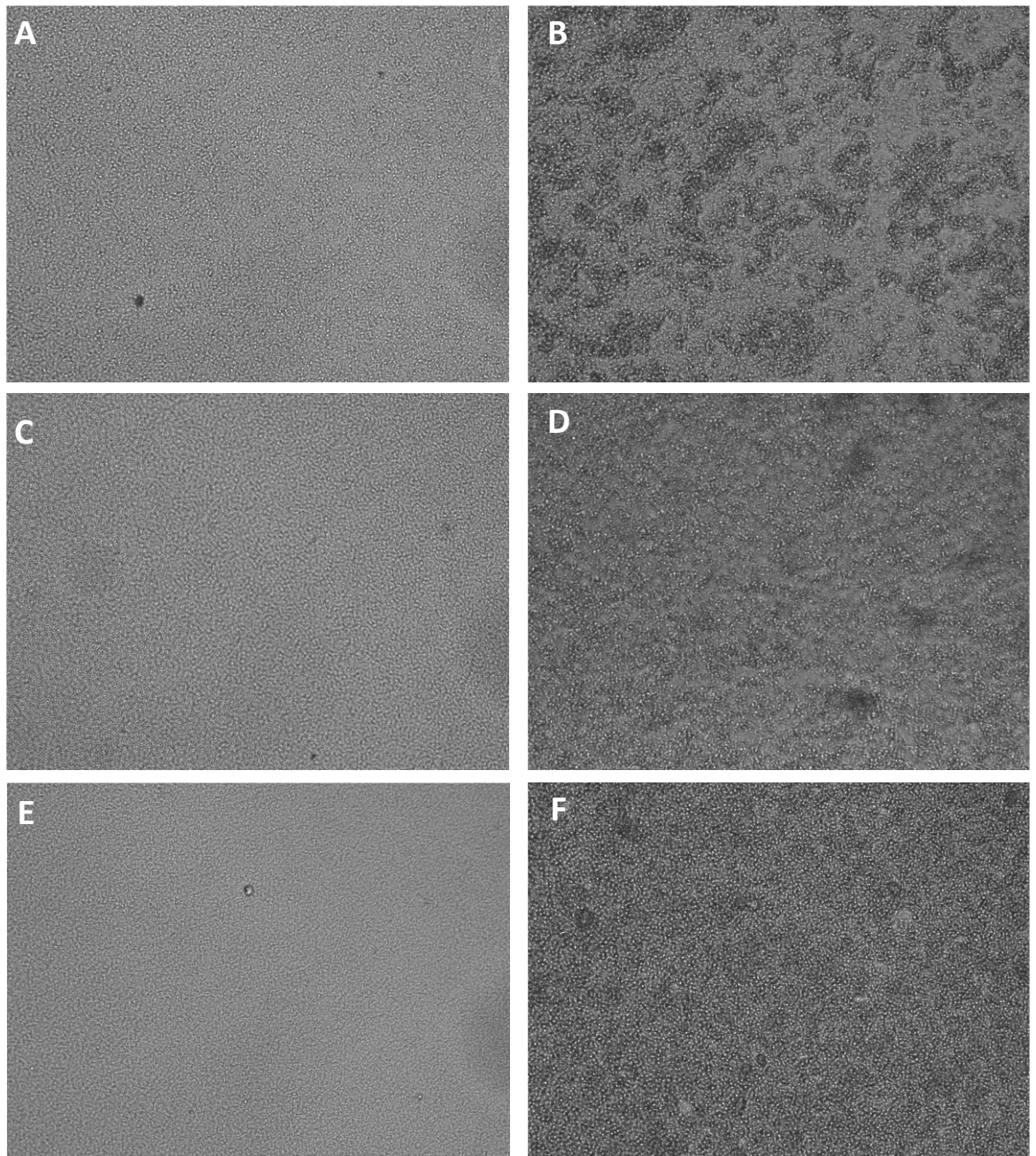


Figure 4.41: Light microscope images of single-species biofilm disruption of *E. faecalis* ER5/1 with and without different treatment conditions. *E. faecalis* clinical strain ER5/1 single-species biofilm (A-F) was grown for 24 hours in THB: RPMI media. Untreated biofilm was used as a PC (A) Biofilms were treated with 5000 mg/L NDs (B), KHS101 64 µg/mL (C), KHS101 hydrochloride 64 µg/mL and NDs 5000 mg/L (D), darapladib 32 µg/mL (E) and darapladib 32 µg/mL and NDs 5000 mg/L (F) for 24 hours. Images are representatives of three replicates. Biofilms were examined using EVOS cell imaging system at 400X magnification.

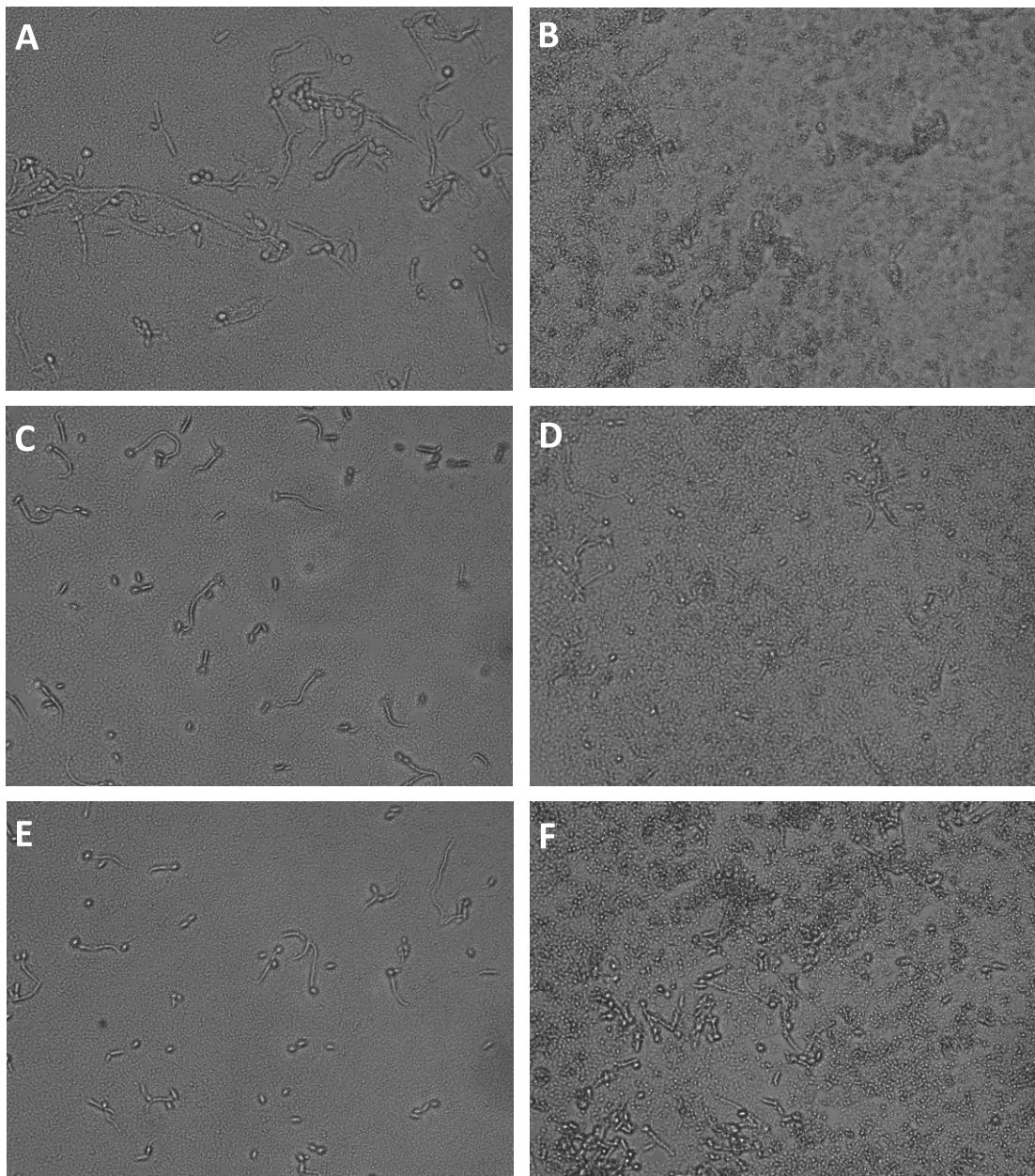


Figure 4.42: Light microscope images of *C. albicans* and *E. faecalis* ER5/1 dual-species biofilm disruption with and without different treatment conditions. *C. albicans* laboratory strain SC5314 and *E. faecalis* clinical strain ER5/1 dual-species biofilm (A-F) was grown for 24 hours in THB : RPMI media. . Untreated biofilm was used as a PC (A) Biofilms were treated with 5000 mg/L NDs (B), KHS101 64 $\mu\text{g}/\text{mL}$ (C), KHS101 hydrochloride 64 $\mu\text{g}/\text{mL}$ and NDs 5000 mg/L (D), darapladib 32 $\mu\text{g}/\text{mL}$ (E) and darapladib 32 $\mu\text{g}/\text{mL}$ and NDs 5000 mg/L (F) for 24 hours. Images are representatives of three replicates. Biofilms were examined using EVOS cell imaging system at 400X magnification.

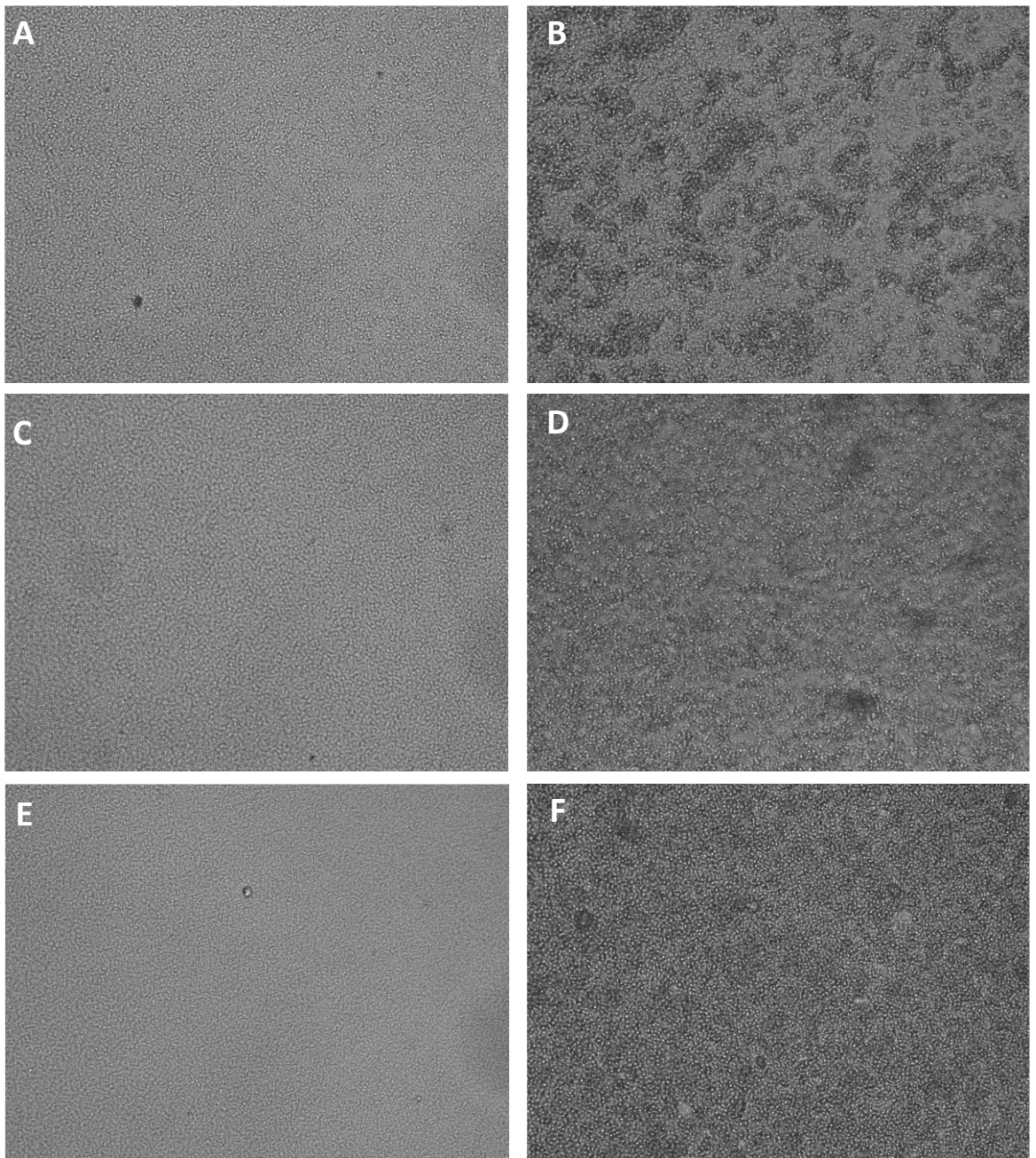


Figure 4.43: Light microscope images of single-species biofilm disruption of *E. faecalis* E2 with and without different treatment conditions. *E. faecalis* clinical strain E2 single-species biofilm (A-F) was grown for 24 hours in THB : RPMI media. . Untreated biofilm was used as a PC (A) Biofilms were treated with 5000 mg/L NDs (B), KHS101 64 $\mu\text{g}/\text{mL}$ (C), KHS101 hydrochloride 64 $\mu\text{g}/\text{mL}$ and NDs 5000 mg/L (D), darapladib 32 $\mu\text{g}/\text{mL}$ (E) and darapladib 32 $\mu\text{g}/\text{mL}$ and NDs 5000 mg/L (F) for 24 hours. Images are representatives of three replicates. Biofilms were examined using EVOS cell imaging system at 400X magnification.

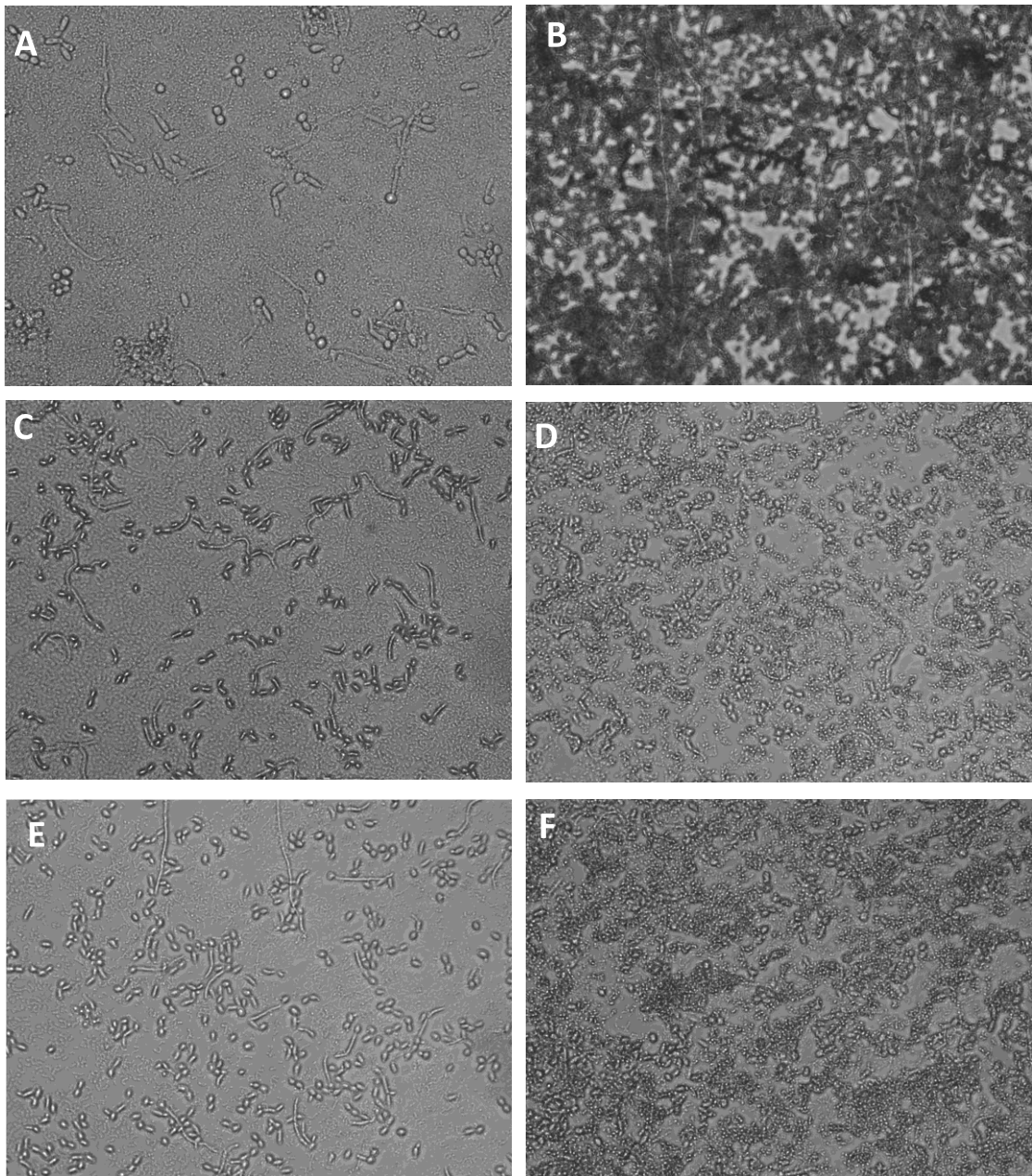


Figure 4.44: Light microscope images of *C. albicans* and *E. faecalis* E2 dual-species biofilm disruption with and without treatment conditions. *C. albicans* laboratory strain SC5314 and *E. faecalis* clinical strain E2 dual-species biofilm (A-F) was grown for 24 hours in THB : RPMI media. . Untreated biofilm was used as a PC (A) Biofilms were treated with 5000 mg/L NDs (B), KHS101 64 µg/mL (C), KHS101 hydrochloride 64 µg/mL and NDs 5000 mg/L (D), darapladib 32 µg/mL (E) and darapladib 32 µg/mL and NDs 5000 mg/L (F) for 24 hours. Images are representatives of three replicates. Biofilms were examined using EVOS cell imaging system at 400X magnification.

4.5 Discussion

Previous literature shows varying antimicrobial responses to NDs, which has been attributed to many factors, such as the types of NDs and their surface modifications and species being investigated. (Szunerits *et al.*, 2016, Fouda *et al.*, 2019, Iyer *et al.*, 2018, Norouzi *et al.*, 2020, Wehling *et al.*, 2014, Zhang *et al.*, 2021a). The current results show that NDs had no killing effect against *C. albicans* or *E. faecalis* isolates as demonstrated by the metabolic activity test and disk diffusion assay. Results were in line with a previous study that showed NDs antibacterial activity was due to particle aggregation behaviour and bacterial clumping which led to a bacteriostatic effect of NDs attachment which played a significant role in the reduction of colony forming units reported (Norouzi *et al.*, 2020).

Results have confirmed the anti-adhesion effect and the resultant biofilm inhibition by NDs on *C. albicans* and *E. faecalis* for both clinical and laboratory isolates as demonstrated by light microscopy and viable plate counts. Microscopy showed NDs coating *C. albicans* cells and their hyphae and aggregating with *E. faecalis* cells. In addition, significantly fewer cells attached to the bottom of the plate compared to untreated controls. This led to the speculation that NDs exhibited an anti-adhesion effect against *C. albicans* and *E. faecalis* and thus the biofilm inhibition was seen under the microscope. It was then decided to count the mean colony forming units of planktonic and attached cells when incubated with NDs. The CFU data shows an increase in planktonic cell number in the case of *C. albicans* cells compared to controls. In addition, attached cell counts were significantly reduced by more than 70% which confirms the anti-adhesion effect seen on *C. albicans*. The antibiofilm effect of NDs was also confirmed in previous studies. One study coated chamber slides with NDs and showed its antibiofilm effect on bacterial and fungal pathogens. Results showed that NDs inhibited the formation of the biofilm by *C. albicans*, *C. glabrata*, *S. mutans* and *P. gingivalis* biofilms (Zhang *et al.*, 2021a). Another study evaluated the effect of different concentrations of NDs added to PMMA denture base material on *C. albicans* adhesion. These studies showed that the addition of NDs decreased *C. albicans* counts (Fouda *et al.*, 2019).

Studies on the antimicrobial effect of NDs on dual or multispecies biofilms are limited. Since infections are rarely found single-species, it is important to explore the response of multispecies biofilms to NDs. Therefore, assessment of the antibiofilm potential of NDs against dual-species biofilm was carried out. Assessing the response of *C. albicans* and *E. faecalis* in dual-species biofilm to NDs will help unravel certain aspects in their interkingdom interaction. The present results showed that NDs inhibited dual-species cell attachment as seen in single-species biofilm. The effect was seen across all dual-species biofilms tested with high and low biofilm formers cocultured with either high or low virulent strains of *E. faecalis*. NDs coated *C. albicans* cells and hyphae and aggregated to *E. faecalis* cells in the same manner seen in single-species biofilm. Moreover, mean CFUs of planktonic *C. albicans* cells was higher when biofilms were incubated with NDs, and less attached cells were seen. However, due to the antagonistic effect of *E. faecalis* on *C. albicans* as well as the anti-adhesion effect of NDs on *C. albicans*, it was expected that NDs will have an additional effect in reducing *C. albicans* cell attachment. This was not evident as results showed higher and more significant reduction when *C. albicans* was in single-species biofilm. Furthermore, microscopic images revealed that *C. albicans* hyphae was relatively longer in dual-species biofilms incubated with NDs compared to untreated controls. This was confirmed later in gene expression analysis.

The potential mechanism by which NDs inhibited biofilm adhesion can be explored via gene expression analysis. It has been reported that NDs play specific roles in modulating *C. albicans* virulence through modulation of adhesion and biofilm formation pathways (Fouda *et al.*, 2019, Zhang *et al.*, 2021a). Here, key virulence genes involved in modulating virulence of *C. albicans* were chosen as in the previous chapters. Results in this chapter revealed that NDs modulated virulence behaviour of *C. albicans*. It was clear that NDs treatment led to downregulation of genes involved in adhesion and biofilm formation. These genes were further explored when *C. albicans* was subject to NDs treatment in dual-species biofilm. In previous chapters, it was demonstrated that *E. faecalis* downregulated key virulence genes in *C. albicans*. Given the downregulation of virulence genes seen by NDs, it was expected that NDs would lead to enhanced downregulation in virulence genes expression. However, this was not evident as minimum downregulation occurred. In fact, one gene, SAP5 was upregulated when *C.*

albicans was in dual-species biofilm of both strains of *E. faecalis*. SAP5 is a hyphae specific protease whose expression is induced upon hyphal formation *in vitro* and during experimental infection *in vivo* (Hube *et al.*, 1994, Staib *et al.*, 2000). This suggests that the effect of NDs on *C. albicans* virulence is modulated by the presence of *E. faecalis*. Gene expression analysis goes in line with what was seen phenotypically.

To explore further the applicability of NDs in endodontics, NDs were incorporated to Biodentine™. It has long been known that Biodentine™ exhibits antimicrobial activity due to high alkalinity resulting from the release of calcium hydroxide ions (Esteki *et al.*, 2021, Deveci *et al.*, 2019, Bhavana *et al.*, 2015). However, several studies have reported that Biodentine™ was unable to show any antimicrobial activity. Therefore, suggestions were proposed to enhance Biodentine™ with different types of materials such as nanoparticles to improve its antimicrobial effect (Elsaka *et al.*, 2019, Jardine *et al.*, 2019, Abusrewil *et al.*, 2021). Here, NDs were incorporated with Biodentine™ and regrowth of single and dual-species biofilm on their surfaces was assessed. The current results showed that *C. albicans* colonised Biodentine™ more than dentine which was consistent with what was shown in previous studies (Abusrewil *et al.*, 2021). NDs were able to reduce *C. albicans* colonisation when in single-species biofilm only. However, comparable level of colonisation was seen between dentine, Biodentine™ and Biodentine™ incorporated with NDs when *C. albicans* was cocultured with *E. faecalis*. In *E. faecalis*, the incorporation of NDs to dentine did not show any reduction in its colonisation whether in single or dual-species biofilm. In fact, ER5/1 HVS strain of *E. faecalis* colonisation was enhanced when cocultured with *C. albicans* but not with E2 LVS. This shows synergy between *C. albicans* and *E. faecalis* by increasing the later colonisation which was in line with a previous study and this was strain dependent (Du *et al.*, 2021).

Another novel antimicrobial approach to overcome drug resistance is drug repurposing. Drug repurposing has emerged as an alternative to traditional drug discovery processes involving *de novo* synthesis. It involves screening drugs that are currently approved or under development for the intention of non-antibiotic use that may possess some antimicrobial properties. These drugs may have repurposing potential by themselves or in combination with other antimicrobials.

During initial screening, compounds were identified as hits when they inhibited more than 99% of *C. albicans* SC5314 biofilm formation at concentration of 0.1mM. The starting concentration was 1:100 dilution of the stock concentration. The reason behind this is that screening at low to medium concentrations normally identifies compounds that provide more relevant biological starting point as with levels of starting concentrations of antimicrobials. Screening at higher concentrations might lead to the identification of more positive signals which might lead to false positive results. Amongst the 1280 compounds screened 85 initial hits were identified from Tocriscreen™ 2.0 library.

Amongst the 11 compounds confirmed, some compounds did not show the antifungal effect as was observed during library screening. This can be due to the false positive rates referred to compound impurities (Goodnow, 2001). Which is the rate that screening samples appear active during screening but later they prove inactive in follow-up assays. Although the purchased compounds purity level was claimed to be high (>99%), many organizations do not specify explicitly the manner in which purity is defined (Goodnow, 2001).

The results showed that Polygodial and Toyocamycin exhibited antifungal effect which is in accordance with previous studies that reported antifungal effect of Polygodial against *C. albicans* and other several fungal pathogens (Lee *et al.*, 1999, Kipanga *et al.*, 2021, Kubo *et al.*, 2001). One single study showed the antifungal effect of Toyocamycin (Nishimura *et al.*, 1956). The rest of the confirmed drugs showed dual-species antimicrobial efficacy; M62812 is a TLR4 signal transduction inhibitor of which TLR4 signal transduction has been recognised as a key pathway for LPS induced activation of various immune cells and coagulation cascades. As suggested by the results, M62812 had an antifungal and an antibacterial effect against *E. faecalis*. This achieved dual effect might be helpful in reducing inflammation and producing simultaneous fungicidal and bactericidal effects (Nakamura *et al.*, 2007).

In addition, retinoic acid compounds (CD437, LE135, CH55) exhibited more potency towards Gram positive bacteria *E. faecalis* than *C. albicans*. CD437, a synthetic retinoid, that has been reported to be used as a potential antibiotic. Kim *et al.*, (2018) performed a high throughput screen of compound library of about 82,000 synthetic molecules using a *Caenorhabditis elegans* methicillin-

resistant *Staphylococcus aureus* (MRSA) infection model. These studies selected synthetic retinoids CD437 and CD1530 and explored their activity against Gram-positive and Gram-negative bacteria and revealed that they can effectively kill growing and persistent methicillin-resistant *S. aureus* cells by disrupting the lipid bilayer, were potent killers at MIC $1\mu\text{g}/\text{ml}^{-1}$ and antimicrobial against Gram-positive but not against major Gram-negative pathogens (Fauvart et al., 2018, Kim et al., 2018). Another study investigated bactericidal and antibiofilm activity of CD437 against *E. faecalis* (Tan et al., 2019). They reported that the synthetic retinoid compound CD437 had potent bactericidal effect against *E. faecalis*. It also inhibited biofilm formation by *E. faecalis* and exerted bactericidal effect on mature biofilm. While no bactericidal action of CD437 was observed against gram negative bacteria. The results revealed that CD437 was also potent against *E. faecalis* strains at $1\mu\text{g}/\text{mL}$ however against *C. albicans*, higher concentrations were needed to exhibit its antifungal effect. Results showed that CD437 exhibited a paradoxical effect, where it was potent at lower concentrations and this effect was reversed when concentrations were increased (Smith et al., 2012b). The paradoxical effect shown along with the fact that it is a highly toxic compound were strong reasons for this drug to be excluded from subsequent experiments.

Darapladib is a lipoprotein associated phospholipase A2 inhibitor that was developed as a treatment for atherosclerosis. Phospholipase is one of the key hydrolytic enzymes used by *C. albicans* during infection of mammalian host. It plays an important role in nutrient acquisition and tissue invasion as well as host immune response modulation (Ghannoum, 2000). Targeting this enzyme in *C. albicans* might reduce its virulence. Furthermore, phase III study with darapladib has failed because it did not achieve the primary endpoint of a reduction of major coronary events versus placebo (O'Donoghue et al., 2014, Investigators et al., 2014, White et al., 2010). The overall safety profile for darapladib showed no major safety concerns as was reported in a previous study (Mohler et al., 2008). Therefore, it is now approved to be used globally. This approval is another valid reason to consider repurposing darapladib for another potential use. KHS101 hydrochloride induces neuronal differentiation in cultured hippocampal neural progenitor cells by interacting with TACC3 which is a known regulator for cell division. It is a potential drug to be used to reduce tumour cells growth by disrupting energy metabolism in mitochondria of human glioblastoma cancer cells

(Wurdak *et al.*, 2010). Moreover, KHS101 hydrochloride exerted no cytotoxic effect against non-cancerous cell lines (Polson *et al.*, 2018).

Darapladib and KHS101 hydrochloride were chosen to investigate further their potency in dual-species biofilm given their activity against *E. faecalis* and *C. albicans*. These experiments are the first *in vitro* assays to be carried out to assess potential antimicrobial activity of KHS101 hydrochloride against planktonic, biofilm formation and biofilm disruption of *C. albicans* and *E. faecalis* species. Thus far, no studies have been carried out to assess the antimicrobial activity of KHS101 and darapladib against any microbes. The present results show that they exhibit MIC values against planktonic cells at 32 - 64 µg/mL for KHS101 and at 4-16 µg/mL for darapladib. These doses were also effective for biofilm disruption in single and dual-species biofilms.

The current results have also revealed that darapladib and KHS101 hydrochloride exerted a dose-dependent inhibitory effect on *C. albicans* single-species biofilm. In this regard, at lower doses they did not completely inhibit biofilm formation however, they reduced yeast to hyphae transition and thus reduced the virulence. This may serve as a potential drug to be used at lower doses in combination with other antifungals therapeutics. Within a dual-species biofilm, *C. albicans* displayed, a dose-dependent response. However, the number of cells recovered when cocultured with HVS ER5/1 was higher than LVS E2 and single-species alone when biofilms were treated with both drugs. Given the antagonistic effect which *E. faecalis* had on *C. albicans*, it would be expected to be more susceptible to drug treatment, however, this was not the case. In fact, the response of *C. albicans* differed when in dual-species biofilm that was more resistant to both drugs. Its response also differed according to *E. faecalis* strain and treatment type, being more susceptible when cocultured with LVS type of *E. faecalis*. This also suggests that *C. albicans* had a synergistic effect with *E. faecalis* by being more tolerant to these drugs.

E. faecalis single-species were resistant to lower doses of both darapladib and KHS101 drugs. Higher doses were more effective in inhibiting their biofilm formation. Strain type played a role in *E. faecalis* susceptibility. HVS ER5/1 was generally more resistant to KHS101 and darapladib than LVS E2. When treating dual-species biofilm with KHS101, ER5/1 responded in the same manner whether

in single or dual-species biofilm. However, in darapladib treatment, ER5/1 HVS was more susceptible while in dual-species than when in single-species biofilm. This suggests that ER5/1 interaction with *C. albicans* rendered it more susceptible to drug. For E2 LVS, it was more resistant when in dual-species biofilm compared to being in single-species biofilm when exposed to KHS101 hydrochloride as well as darapladib treatments. This suggests that *C. albicans* might have played a role in E2 resistance development when this biofilm was subject to treatment.

After testing biofilm inhibition, the drug's efficacy was assessed against biofilm disruption of single and dual-species biofilms. NDs were used in combination with drugs to explore their mutual effect on each other and on microorganisms. Owing to their size, NDs are very well-known drug carriers and able to penetrate tissue models and ECM (Yu *et al.*, 2019b, Su *et al.*, 2019, Perevedentseva *et al.*, 2019, Tchoryk *et al.*, 2019, Chauhan *et al.*, 2020). These reasons make NDs as an attractive candidates to be used in combination with small molecule drugs to facilitate drug proximity to microbial cells.

As seen in biofilm inhibition, results of biofilm disruption analysis under different treatment conditions showed that *C. albicans* was more resistant when coexisting with *E. faecalis* and a higher resistance was shown when cocultured with the HVS ER5/1. However, *E. faecalis* was rendered more susceptible when in dual-species biofilm than in single-species biofilm. This is further evidence that species interaction plays a significant role in biofilm virulence and response to different treatments. It should be noted that the combination of NDs has reduced the drug efficacy in exerting their effect on microbial cells. A finding that should be taken into consideration before utilising NDs as drug carriers or potential combinations for antimicrobial therapy.

One concern regarding these drugs is the heterogeneity observed in response to their treatment. This response is species and strain dependent. It has been shown in literature that gut microbiota can metabolise non antimicrobial drugs that are administered orally (Weersma *et al.*, 2020) and thus alter their efficacy. *E. faecalis* is a common resident in the gut and might inherently be able to metabolise drugs as well (Maini Rekdal *et al.*, 2019). One study assessed the metabolism of darapladib by human gut microbiota (Dave *et al.*, 2014). They observed the effects of incubating 5 μM of darapladib with *E. faecalis* under

anaerobic conditions and reported negligible metabolism by *E. faecalis* and other bacterial species. However, their dose was equal to 3.3 ug/ml a concentration that is lower than the effective dose that was used in the experiments described in this chapter (Dave *et al.*, 2014). To date, no studies have shown drug metabolism by *C. albicans*. The fact that certain doses showed various responses can also be explained by the effective dosages needed to activate such metabolic response.

In addition, results showed that interspecies interaction affected each species tolerance to the drug. One explanation might be that inter-species interactions involve many alterations in each microorganism's metabolic behaviour; these alterations may play a significant role in microbial response to drugs (Bottery *et al.*, 2022, Aranda-Diaz *et al.*, 2020, Zimmermann *et al.*, 2021). Consequently, microorganisms become able to metabolise certain groups in the drug structure and renders the drug ineffective (Hitchings and Kelly, 2019, Maini Rekdal *et al.*, 2019, Wallace *et al.*, 2010, Zimmermann *et al.*, 2019).

Lastly, further analysis should be done to assess KHS101 hydrochloride and darapladib broad-spectrum activity against different fungal pathogens, Gram negative bacterial species and other gram-positive bacterial species. Further tests should be carried out to assess cytotoxic effect of these drugs against human cell lines. Moreover, to determine their mechanism of action, gene expression analysis should be done to explore possible virulence mechanisms that may be targeted by these drugs. Transcriptomic analysis can also be done to identify genes involved in certain metabolic pathways, that are majorly differentially expressed, and help understand each species response and targeted therapy. Moreover, the transcriptomic analyses performed in the previous chapter analysing interkingdom interaction at the transcriptomic level might provide an insight on differentially expressed genes that might have an impact on drug metabolism. This may provide an explanation to response differences seen in single and dual-species biofilms and reveal mechanisms of interkingdom interaction between *C. albicans* and *E. faecalis*.

4.6 Conclusion

In this chapter, an antibiofilm activity of NDs against *C. albicans* and *E. faecalis* single and dual-species biofilm was reported. In addition, a new bioactive activity for KHS101 hydrochloride and darapladib as antimicrobials against *E. faecalis* and *C. albicans* species was reported.

- NDs produced an anti-adhesion effect on *C. albicans* and a bacteriostatic effect on *E. faecalis*.
- NDs downregulated key genes involved in virulence of *C. albicans*. However, this alteration was not observed when *E. faecalis* was cocultured with *C. albicans*.
- The antimicrobial activity of KHS101 hydrochloride and darapladib was effective against clinical isolates and strains of both species forming high and low biofilms of *C. albicans* and high and low virulent strains of *E. faecalis*.
- KHS101 hydrochloride and darapladib were antimicrobial against monoculture and polymicrobial coculture.
- KHS101 hydrochloride and darapladib had antimicrobial activity against *C. albicans*, and *E. faecalis*. Therefore, they are promising antimicrobial agents that may be repurposed against diverse microbial species.
- NDs and small molecule compounds helped in understanding cross-kingdom interaction and in revealing synergistic tolerance to different types of treatment. However, this was dose and agent dependent.
- The virulence of *E. faecalis* strain played a role in the response to treatment.
- The results reported in this chapter echo the complexity of interkingdom interaction of *C. albicans* and *E. faecalis*.

Chapter 5: General Discussion

5.1 Introduction

The complex microbial communities that exist in any given host has increased the urge to understand interactions across species boundaries. Whether antagonistic or synergistic, these interactions influence the microbiogeography of species within microbial communities (Stacy *et al.*, 2016). Spatial patterning of microorganisms can draw the shape of the disease by either progressive and enhanced tolerance to treatment or dampening its virulence and increasing susceptibility to treatment (Figure 5.1). The underlying mechanisms behind these interactions are now further explored due to the enhanced resolution in imaging techniques and higher throughput of available techniques (Earle *et al.*, 2015, Stahl *et al.*, 2016). Comparisons of transcriptome outcomes from mono-species and multispecies biofilms have allowed identification of genes and proteins of which expression is affected by the presence of other strains (He *et al.*, 2017, Wolf *et al.*, 2018). Therefore, the underlying mechanisms and consequences of interspecies interaction could be revealed.

Fungal and bacterial kingdoms are engaged in complex interactions that lead to microbial critical behavioural shifts ranging from mutualism to antagonism (Peters *et al.*, 2012, Hogan and Kolter, 2002). The interaction between *C. albicans* and *E. faecalis* is an example of a complex interkingdom relationship. These microorganisms share key similarities like being opportunistic pathogens after their long commensal existence in host microbiome niches. (ZERVOS *et al.*, 1987, Quindos, 2014). Infections that arise from these organisms are often linked to ecological disruptions resulting from a change in microenvironment or exposure to antibiotics or chemotherapeutic agents.

Comprehensive RNA-sequencing technologies have contributed to understanding the communications within microbial communities during health and disease (Duran-Pinedo *et al.*, 2014). Omics approaches have helped reveal important information on microbial response with their interacting partner (Shokeen *et al.*, 2021).

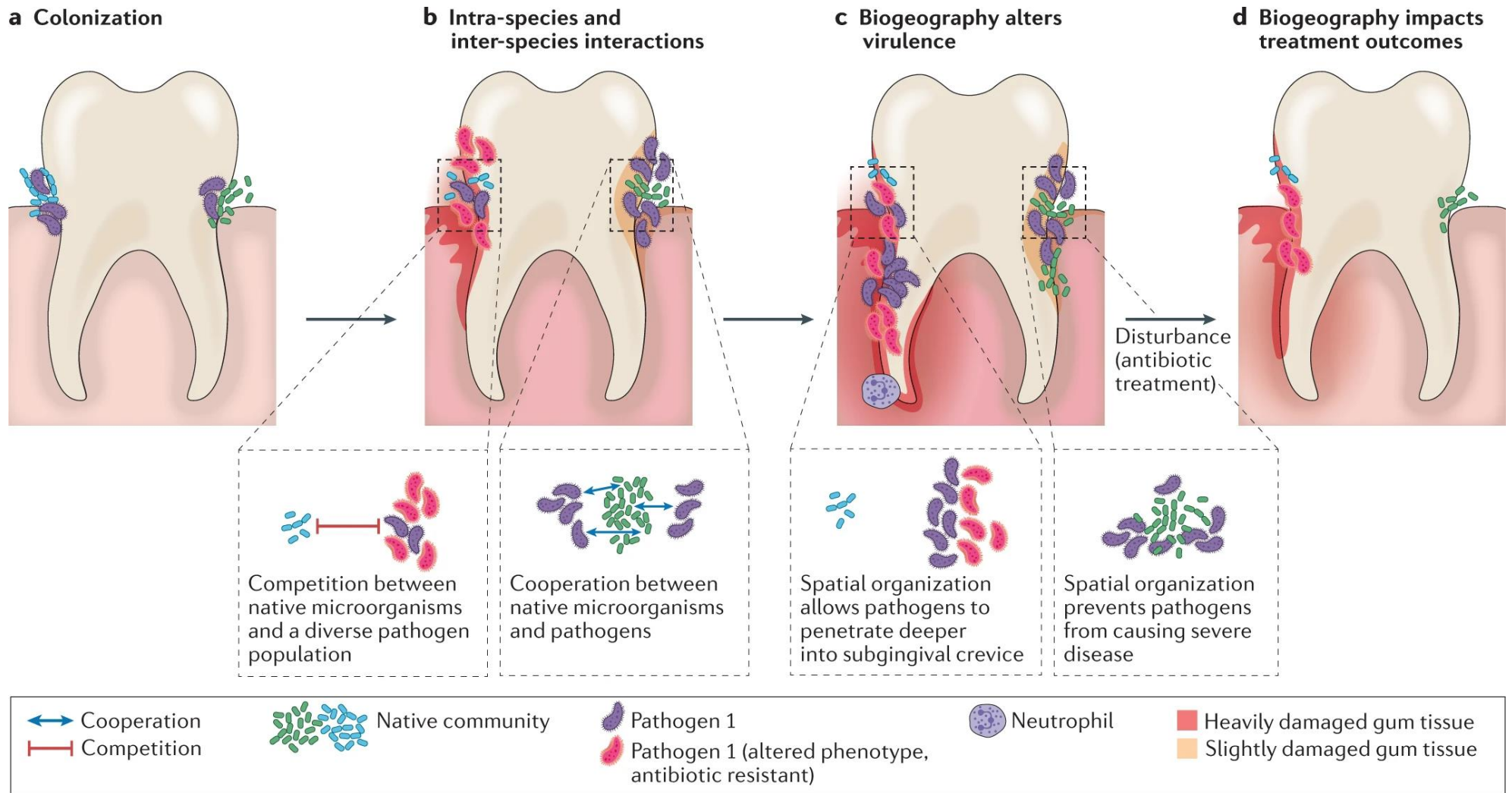


Figure 5.1: Spatial patterning of microorganisms (microbiogeography) determines the fate of infection. A schematic diagram showing the importance of interspecies communication in driving disease pathogenicity and the response to antimicrobial treatment (Azimi *et al.*, 2022)

5.2 Building dual-species biofilm model

To mimic the clinical scenario, the selected strains had been isolated from clinical infections. The *E. faecalis* ER5/1 was characterised as a HVS and had been clinically isolated from recurrent root canal infections. *Candida albicans* SC5314 is isolated from a urinary tract infection and was a HBF. Thus, the strains involved in this study have already been isolated from an active disease that do not harbour commensals, which serves to aid understanding dual-species behaviour within the pathogenicity of endodontic infections.

To mimic the root canal environment, *E. faecalis* was assessed under different oxygen tension conditions and its virulence characterised accordingly. Moreover, this was essential to have further insight on any possible alteration in virulence behaviour specially when *E. faecalis* candidate strains are cocultured with *C. albicans* since biofilms of the latter provide a hypoxic environment (Fox *et al.*, 2014).

5.3 Antagonism in health, but synergy in disease

Several models have been used to study *C. albicans* and *E. faecalis* interkingdom interaction. These have ranged from *in vitro* studies involving different colonisation substrates like dentine (Du *et al.*, 2021) and mucosal surfaces (Krishnamoorthy *et al.*, 2020) to *in vivo* studies that used *C. elegans* (Cruz *et al.*, 2013, Graham *et al.*, 2017a) and murine models (Mason *et al.*, 2012a, Mason *et al.*, 2012b). These models studied the commensal as well as pathogenic behaviours.

The reported synergism between both species have been reported by several authors (Mason *et al.*, 2012a, Mason *et al.*, 2012b). They studied the effect of the bacterial microbiome on the colonisation of *C. albicans* in stomach and used an *in vivo* murine model to colonise *C. albicans* in germ free mice and mice with disturbed microbiome post antibiotic treatment. The results showed that gastritis induced by *C. albicans* was much worse in germ free mice compared to gastritis in antibiotic-treated normal mice. The results indicate that even an impaired bacterial microbiota can suppress *C. albicans*-associated pathology.

To study the effect of *C. albicans* on bacterial microbiota, the microbiome has been disturbed by exposing mice to the antibiotic cefoperazone for 7 days. Then, the recolonisation of bacteria with and without the presence of *C. albicans* have been assessed. In untreated mice, Lactobacilli were the dominant lactic acid producing bacteria. However, upon antibiotic treatment, Enterococci were dominant at day 7 but was dominated by Lactobacilli when recovered at day 21. Recolonisation differed significantly post treatment when *C. albicans* was introduced; Enterococci were the dominant species at day 7 and day 21 (Mason *et al.*, 2012a). This finding was confirmed in a caecum murine model in which the ability of *C. albicans* to alter the bacterial microbiota during nonpathogenic colonization was proven (Mason *et al.*, 2012b). These results can be interpreted by either of the two possibilities: *C. albicans* was antagonised with the growth of *Lactobacilli* or they had a synergistic effect favouring the colonisation and growth of *E. faecalis*. This finding reflects that any change in microenvironment can disrupt normal microbiome and species interactions.

Cruz *et al.* (2013) studied interspecies interaction *in vitro* and *in vivo* using a *C. elegans* model (Cruz *et al.*, 2013). They discovered that *E. faecalis* and *C. albicans* displayed a negative impact on each other's virulence. The negative impact was manifested mainly in *C. albicans*, in the form of inhibition of hyphal morphogenesis and biofilm formation. This inhibition was partially dependent on the Fsr quorum-sensing system, a major virulence regulator in *E. faecalis*, and the two proteases regulated by this sensing system namely GelE, SerE. Later, the bacteriocin EntV was identified to be responsible for the inhibition hyphal morphogenesis (Graham *et al.*, 2017a). In this study, they exposed the gut of *C. elegans* and colonised it with both species. The results showed a commensal relationship may have existed whereby coinfection inhibits *C. albicans* filamentation and killing of the worm. The authors developed a synthetic version of EntV (sEntV) and assessed its efficacy in biofilm inhibition and in protection of *C. elegans* against *candida* infections (Graham *et al.*, 2017a). In the same study, they further studied this relationship in the context of murine pathogenic model. They observed that sEntV reduced epithelial invasion the resulting tissue inflammation and fungal burden in murine model of oropharyngeal candidiasis. Also, the bacteriocin reduced the depth and biomass of mature biofilms without killing or inhibiting *C. albicans* growth. In addition, it inhibited *C. albicans* hyphal

morphogenesis and biofilm formation at sub-nanomolar concentrations. They claimed that sEntV was 3,000-fold more effective at inhibiting biofilm formation than the unprocessed peptide. This pathogenic inhibition was also found in a study that used heat killed *E. faecalis* to treat patients with oral candidiasis. Subjects took a powder containing heat-killed *E. faecalis* once a day before bedtime for seven consecutive days. A 55% decrease of *C. albicans* load was noticed (Graham et al., 2017a).

Synergism in virulence was investigated in other infection models. Carlson et. al in (1983), studied the role of *C. albicans* in the stimulation of infection by *S. aureus* and *E. faecalis* in mice with intraperitoneal inoculation of bacterial species along with non-lethal doses of *C. albicans*. *S. aureus* alone did not establish infection; however, infection was induced in mice when they were injected with *C. albicans* and *S. aureus*. Furthermore, *E. faecalis* was recovered from blood and tissues of animals that were dually injected with *C. albicans*. However no *E. faecalis* was recovered from mice that were injected with *E. faecalis* alone (Carlson, 1983).

Krishmnoorthy et al. (2020) studied this interaction on biotic surfaces using a human oral mucosal model (Krishnamoorthy et al., 2020). Colonisation on oral epithelium revealed profound surface erosion by dual-species biofilm which was similar to that induced by *C. albicans* SC5314 but greater than what was induced by *E. faecalis*. In contrast, using a clinical isolate enhanced invasion of tissues compared to that to that of *C. albicans* alone since the clinical isolate formed neither dense biofilms nor hyphae in mono-species biofilm. The invasion of both species together was deeper into mucosal compartments than that of either species alone. It was noted that the majority of *E. faecalis* cells appeared to be located extracellularly within the disrupted epithelial tissues which was later confirmed by gene expression analysis whereby downregulation of key genes involved in biofilm formation and adhesion was noted. This mutualistic interactions between both microorganisms in pathogenesis was also demonstrated by a recent study. Du et al., (2021) in *in vitro* and *in vivo* biofilm models of post-treatment endodontic disease (PTED) to explore if dual-species model exacerbates periapical lesions (Du et al., 2021). SEM images showed enhanced biofilm formation on dentine substrates compared to either species alone. In contrast to

the results of (Krishnamoorthy *et al.*, 2020). *C. albicans* enhanced the adherence of *E. faecalis* to dentine, which was confirmed by enhanced expression of adhesion related genes of *E. faecalis*. *In vivo* results showed that co-inoculation of *E. faecalis* and *C. albicans* increased the extent of periapical lesions compared to either species infection alone. This was attributed to increased periapical bone resorption and suppressed bone formation as well as upregulation of inflammatory cytokines. The data demonstrated a synergistic effect between *C. albicans* and *E. faecalis* to form endodontic biofilm of high virulence which may increase periapical lesion formation.

Although dual-species biofilm increased tissue invasion, inflammation, and destruction, the predominance of *C. albicans* yeast has been confirmed in dual-species models in several studies (Krishnamoorthy *et al.*, 2020, Du *et al.*, 2021).

These contradictory findings may indicate a complex interkingdom relationship which may be attributed to many influential factors like substrate type, microbial strain, colonisation surface and clinical picture. The interkingdom relationship may be further complicated when *E. faecalis* and *C. albicans* are part of polymicrobial infection. One study showed that *C. albicans* was synergistic with *S. sanguinis*, *S. gordonii*, *Actinomyces odontolyticus* and *Actinomyces viscosus*, however, its virulence was dramatically reduced once *P. gingivalis* was introduced (Morse *et al.*, 2019).

Where does this thesis' results stand in the context of previous literature?

This thesis work confirmed antagonism between *C. albicans* and *E. faecalis* in an *in vitro* model. Phenotypically, hyphal morphogenesis and biofilm formation was inhibited compared to *C. albicans* single species biofilm. *E. faecalis* growth and biofilm was not affected by *C. albicans* presence. Gene expression analysis revealed antagonism at later time points and synergism at earlier time points in key genes involved in *C. albicans* virulence. Upregulation in *E. faecalis* genes was observed. A literature review revealed that no previous studies have utilised RNA-Seq technology to investigate the cross-kingdom relationship in question. RNA-Seq revealed significant alteration in the transcriptome of *C. albicans*. *E. faecalis* altered carbon and nitrogen assimilation in *C. albicans*. The alteration was evident by downregulation of glycolytic genes and upregulation of genes involved in carbon

assimilation from alternative carbon sources. Moreover, *C. albicans* had nitrogen starvation via upregulation of amino acid biosynthesis pathway. In addition, key transcription factors genes were upregulated; GCN4 and ACE2 are two transcription factors involved in *C. albicans* adhesion and biofilm formation (Nadeem *et al.*, 2013, Holland *et al.*, 2014, Finkel *et al.*, 2012). Metabolic adaptation is one of the key virulence factors in *C. albicans* (Brown *et al.*, 2014). Metabolic adaptation can rely on different carbon and nitrogen sources and alter biofilm formation and affect cell wall biogenesis (Lok *et al.*, 2021, Silao and Ljungdahl, 2021). This has been seen in transcriptomics results by the downregulation of genes involved in mannosylation of cell wall mannoproteins.

Carbon adaptation can modulate stress resistance by enhancing stress adaptation indirectly (Lok *et al.*, 2021). This increases the survival of fungal cells by reducing their vulnerability to environmental stresses. Moreover, metabolism contributes to stress adaptation by generating molecules such as osmolyte glycerol, antioxidants like glutathione (González-Párraga *et al.*, 2003) which was evident in this thesis transcriptomics data. Furthermore, HSPs were released as stress response adaptation. HSP70 and HSP90 were upregulated in transcriptomics data, and they have major roles in biofilm formation. Alcohol dehydrogenases that act negatively on biofilm matrix were down regulated (*ifd6*, *csh1*). This has led to the speculation that *C. albicans* may enhance the stress response of dual-species biofilm. In addition, metabolic adaptability yielded an alteration of certain genes involved in biofilm formation and biofilm matrix.

Lastly, results from transcriptomics data have confirmed the fact that changes in microenvironment in which both species reside in either of commensalism or antagonism statuses can alter their overall behaviour. The Arginine biosynthetic pathway was upregulated, and Arginine catabolic pathway was downregulated. This results in generation of less ammonia which alkalise surrounding media that eventually triggers hyphal switch in *C. albicans* (Vylkova and Lorenz, 2014). This finding was supported by the strong upregulation of the ammonium transporter MEP2 that has led to the speculation that the cytosolic pH of *C. albicans* is acidic (Biswas and Morschhauser, 2005).

It has been established that low pH favours yeast growth form in *C. albicans* (Buffo *et al.*, 1984, Nadeem *et al.*, 2013). Thus, it was hypothesized that adjusting the pH of dual-species biofilm media to alkaline state will induce hyphal morphogenesis. This hypothesis was proved by the work of our group (Alshanta *et al.*, 2022). The pH media of dual-species biofilm was (5) and upon alkalisating the media to pH (6 or 7), *C. albicans* was able to induce hyphae again. This also confirms that the hyphal inhibition seen is not solely based on a bacteriocin generated by *E. faecalis*. These findings should be reflected on clinical scenarios whereby microenvironment within host varies and any changes in its elements can cause alterations in *C. albicans* behaviour.

5.4 Does antagonism increase sensitivity of microbial cells towards treatment?

Antagonism between species increased susceptibility of microbial cells to environmental stresses and antimicrobial drugs. Transcriptomic results revealed enhanced stress response by upregulation of genes involved in HSPs, antioxidants and fungal biofilm matrix. To assess the efficiency of this stress response, novel therapeutics were employed to exert stress on dual-species biofilm. These therapeutics can target virulence behaviour in *C. albicans*.

The resistance of dual-species biofilm has been reported previously in literature. A recent study demonstrated in that coculturing both species yielded a biofilm that is more tolerant to several stresses such as a starvation alkalinity environment, mechanical shear force and bactericidal chemicals (Du *et al.*, 2021). Furthermore, a dual-species biofilm model was established and allowed to grow in PBS for the starvation assay in order to mimic the starvation environment in root filled canal. *E. faecalis* showed more resistance to starvation in the presence of *C. albicans* than when present alone (Gao *et al.*, 2016). In addition, common endodontic treatment modalities along with antifungals and antibiotics responded differently to dual-species compared to single species biofilms (Zancan *et al.*, 2019). Therefore, the need for novel antimicrobial treatments is urgent and essential to tackle certain behaviour of microorganisms and avoid drug tolerance. The aim is to utilise novel therapies like NDs and small molecule from HTS of FDA approved drug library to further understand cross-kingdom interaction and search for the possible targeting of virulence mechanisms in both species. This aim was

fulfilled. Antagonism did not render either species more susceptible than each species alone and treatment modalities were effective against single and dual-species biofilm inhibition and disruption. Even low doses helped in inhibiting virulence of both species. These novel therapies can be incorporated in endodontic clinical practice by many means. NDs as antimicrobial particles should be assessed carefully even for non-antimicrobial use if implemented in clinical practice as it has displayed antagonistic effect with drugs and decreased efficiency. However, they still can be utilised in coating surfaces like gutta percha or fiberposts to prevent recolonisation of biofilms after root canal treatment. Small molecules were efficient and deemed to be safe for clinical use. Therefore, they can be used as intracanal medicaments given that they produced an effect in 24-hour biofilm and was efficient in reducing virulence of microbes in planktonic form just before establishing a biofilm. Thus, their use would be complementary to cleaning and shaping stage when established biofilms are mechanically disrupted.

5.5 Concluding remarks and future work

The high mortality rate owing to *C. albicans* and *E. faecalis* biofilm associated infections is a big challenge in the medical field. The work embodied in this thesis highlighted the importance of studying *C. albicans* and *E. faecalis* interkingdom interaction. In addition, it shed light on the complexity of this relationship by explaining some significant changes in *C. albicans* transcriptome induced by its interacting partner *E. faecalis*. It is accepted that interkingdom interaction seen *in vitro* might be a simplistic overview of this relationship which may be even more complicated in *in vivo* models as both species may alter colonisation ability of each other leading to promotion or inhibition of disease.

Cross-kingdom interaction is an understudied issue. The few previous studies have established an essential foundation in investigating *C. albicans* and *E. faecalis* cross-kingdom interaction and the work of this project is a small but significant part in the foundation. Advancements in omics approaches should facilitate further and accelerate research on the composition of the oral polymicrobial biofilm community. Transcriptomics and proteomics approaches have already started to provide insight on the complexities of vast inter-species interactions.

Utilising these approaches on *C. albicans* and *E. faecalis* dual-species models on different colonisation surfaces that better simulate root canal environment can serve as a starting point.

The improvement of new biomaterials with anti-adhesive properties, high throughput phenotypic screening of small-molecule inhibitors and the discovery and repurposing of FDA-approved drugs are targets of active research. Therefore, polymicrobial biofilms should be extensively studied with a focus on the interaction of microbial biofilm residents to target different phenotypic character change that play a major role in biofilm formation. It is assumed that the work and results presented in this thesis can serve a baseline for further research that employ different novel therapies against *C. albicans*, *E. faecalis* and other dual-species biofilm and establish a potent treatment regime against polymicrobial infections.

Potential antimicrobial drugs investigated in this work namely KHS101 hydrochloride and darapladib, must undergo further assessments in terms of efficiency as antimicrobial agents against species associated with endodontic infections other than *C. albicans* and *E. faecalis*. In addition, their effect on human cell lines requires evaluation. Despite being proved safe for human use, cell culture work can discover potential side effects at certain doses and time points. Finally, studying microbial transcriptome alteration in response to these drugs can assist in resolving their mechanism of action and in target-based therapy.

List of References

- ABBASZADEGAN, A., NABAVIZADEH, M., GHOLAMI, A., ALEYASIN, Z. S., DOROSTKAR, S., SALIMINASAB, M., GHASEMI, Y., HEMMATEENEJAD, B. & SHARGHI, H. 2015. Positively charged imidazolium-based ionic liquid-protected silver nanoparticles: a promising disinfectant in root canal treatment. *Int Endod J*, 48, 790-800.
- ABIODUN-SOLANKE, I., AJAYI, D. & ARIGBEDE, A. 2014. Nanotechnology and its application in dentistry. *Annals of medical and health sciences research*, 4, 171-177.
- ABUSREWIL, S., BROWN, J. L., DELANEY, C., BUTCHER, M. C., TIBA, M., SCOTT, J. A., RAMAGE, G. & MCLEAN, W. 2021. Chitosan Enhances the Anti-Biofilm Activity of Biodentine against an Interkingdom Biofilm Model. *Antibiotics*, 10, 1317.
- ABUSREWIL, S., BROWN, J. L., DELANEY, C. D., BUTCHER, M. C., KEAN, R., GAMAL, D., SCOTT, J. A., MCLEAN, W. & RAMAGE, G. 2020. Filling the Void: An Optimized Polymicrobial Interkingdom Biofilm Model for Assessing Novel Antimicrobial Agents in Endodontic Infection. *Microorganisms*, 8.
- AEBI, M. 2013. N-linked protein glycosylation in the ER. *Biochim Biophys Acta*, 1833, 2430-7.
- AHAMED, M., KARNS, M., GOODSON, M., ROWE, J., HUSSAIN, S. M., SCHLAGER, J. J. & HONG, Y. 2008. DNA damage response to different surface chemistry of silver nanoparticles in mammalian cells. *Toxicol Appl Pharmacol*, 233, 404-10.
- AHIMOU, F., SEMMENS, M. J., HAUGSTAD, G. & NOVAK, P. J. 2007. Effect of protein, polysaccharide, and oxygen concentration profiles on biofilm cohesiveness. *Applied and environmental microbiology*, 73, 2905-2910.
- AKPATA, E. S. & BLECHMAN, H. 1982. Bacterial invasion of pulpal dentin wall in vitro. *J Dent Res*, 61, 435-8.
- AKTENER, B. O. & BILKAY, U. 1993. Smear layer removal with different concentrations of EDTA-ethylenediamine mixtures. *J Endod*, 19, 228-31.
- AKYILDIZ, I., TAKE, G., UYGUR, K., KIZIL, Y. & AYDIL, U. 2013. Bacterial biofilm formation in the middle-ear mucosa of chronic otitis media patients. *Indian J Otolaryngol Head Neck Surg*, 65, 557-61.
- ALAOHALI, A., SALZLECHNER, C., ZAUGG, L. K., SUZANO, F., MARTINEZ, A., GENTLEMAN, E. & SHARPE, P. T. 2022. GSK3 Inhibitor-Induced Dentinogenesis Using a Hydrogel. *J Dent Res*, 101, 46-53.
- ALBERTI, A., CORBELLA, S., TASCHIERI, S., FRANCETTI, L., FAKHRUDDIN, K. S. & SAMARANAYAKE, L. P. 2021. Fungal species in endodontic infections: A systematic review and meta-analysis. *PLoS One*, 16, e0255003.
- ALBUQUERQUE, P. & CASADEVALL, A. 2012. Quorum sensing in fungi--a review. *Med Mycol*, 50, 337-45.
- ALLONSIUS, C. N., VAN DEN BROEK, M. F., DE BOECK, I., KIEKENS, S., OERLEMANS, E. F., KIEKENS, F., FOUBERT, K., VANDENHEUVEL, D., COS, P. & DELPUTTE, P. 2017. Interplay between *Lactobacillus rhamnosus* GG and *Candida* and the involvement of exopolysaccharides. *Microbial biotechnology*, 10, 1753-1763.
- ALSHANTA, O. A., ALBASHAIREH, K., MCKLOUD, E., DELANEY, C., KEAN, R., MCLEAN, W. & RAMAGE, G. 2022. *Candida albicans* and *Enterococcus*

- faecalis biofilm frenemies: When the relationship sours. *Biofilm*, 4, 100072.
- AMBARDAR, S., GUPTA, R., TRAKROO, D., LAL, R. & VAKHLU, J. 2016. High Throughput Sequencing: An Overview of Sequencing Chemistry. *Indian J Microbiol*, 56, 394-404.
- ANDERS, S., PYL, P. T. & HUBER, W. 2015. HTSeq—a Python framework to work with high-throughput sequencing data. *bioinformatics*, 31, 166-169.
- ANDERSON, A. C., HELLWIG, E., VESPERMANN, R., WITTMER, A., SCHMID, M., KARYGIANNI, L. & AL-AHMAD, A. 2012. Comprehensive analysis of secondary dental root canal infections: a combination of culture and culture-independent approaches reveals new insights. *PLoS One*, 7, e49576.
- ANDERSON, A. C., JONAS, D., HUBER, I., KARYGIANNI, L., WOLBER, J., HELLWIG, E., ARWEILER, N., VACH, K., WITTMER, A. & AL-AHMAD, A. 2015. Enterococcus faecalis from Food, Clinical Specimens, and Oral Sites: Prevalence of Virulence Factors in Association with Biofilm Formation. *Front Microbiol*, 6, 1534.
- ANTIMICROBIAL RESISTANCE, C. 2022. Global burden of bacterial antimicrobial resistance in 2019: a systematic analysis. *Lancet*.
- ANTUNES, L. C. M., FERREIRA, R. B. R., BUCKNER, M. M. C. & FINLAY, B. B. 2010. Quorum sensing in bacterial virulence. *Microbiology (Reading)*, 156, 2271-2282.
- APPLEGATE, D. H. & BRYERS, J. D. 1991. Effects of carbon and oxygen limitations and calcium concentrations on biofilm removal processes. *Biotechnol Bioeng*, 37, 17-25.
- ARANDA-DIAZ, A., OBADIA, B., DODGE, R., THOMSEN, T., HALLBERG, Z. F., GUVENER, Z. T., LUDINGTON, W. B. & HUANG, K. C. 2020. Bacterial interspecies interactions modulate pH-mediated antibiotic tolerance. *Elife*, 9.
- ARBELOA, A., SEGAL, H., HUGONNET, J. E., JOSSEAUME, N., DUBOST, L., BROUARD, J. P., GUTMANN, L., MENGIN-LECREULX, D. & ARTHUR, M. 2004. Role of class A penicillin-binding proteins in PBP5-mediated beta-lactam resistance in Enterococcus faecalis. *J Bacteriol*, 186, 1221-8.
- ARIAS, C. A., PANESSO, D., MCGRATH, D. M., QIN, X., MOJICA, M. F., MILLER, C., DIAZ, L., TRAN, T. T., RINCON, S., BARBU, E. M., REYES, J., ROH, J. H., LOBOS, E., SODERGREN, E., PASQUALINI, R., ARAP, W., QUINN, J. P., SHAMOO, Y., MURRAY, B. E. & WEINSTOCK, G. M. 2011. Genetic basis for in vivo daptomycin resistance in enterococci. *N Engl J Med*, 365, 892-900.
- ASHBURN, T. T. & THOR, K. B. 2004. Drug repositioning: identifying and developing new uses for existing drugs. *Nat Rev Drug Discov*, 3, 673-83.
- AYON, N. J. & GUTHEIL, W. G. 2019. Dimensionally Enhanced Antibacterial Library Screening. *ACS Chem Biol*, 14, 2887-2894.
- AZIMI, S., LEWIN, G. R. & WHITELEY, M. 2022. The biogeography of infection revisited. *Nature Reviews Microbiology*, 1-14.
- BABIOR, B. M., KIPNES, R. S. & CURNUTTE, J. T. 1973. Biological defense mechanisms. The production by leukocytes of superoxide, a potential bactericidal agent. *The Journal of clinical investigation*, 52, 741-744.
- BACHTIAR, E. W., DEWIYANI, S., SURONO AKBAR, S. M. & BACHTIAR, B. M. 2016. Inhibition of Candida albicans biofilm development by unencapsulated Enterococcus faecalis cps2. *J Dent Sci*, 11, 323-330.

- BAISHYA, J., BISHT, K., RIMBEY, J. N., YIHUNIE, K. D., ISLAM, S., AL MAHMUD, H., WALLER, J. E. & WAKEMAN, C. A. 2021. The Impact of Intraspecies and Interspecies Bacterial Interactions on Disease Outcome. *Pathogens*, 10.
- BAMFORD, C. V., D'MELLO, A., NOBBS, A. H., DUTTON, L. C., VICKERMAN, M. M. & JENKINSON, H. F. 2009. *Streptococcus gordonii* Modulates *Candida albicans* Biofilm Formation through Intergeneric Communication. *Infection and Immunity*, 77, 3696-3704.
- BANERJEE, D., SHIVAPRIYA, P., GAUTAM, P. K., MISRA, K., SAHOO, A. K. & SAMANTA, S. K. 2020. A review on basic biology of bacterial biofilm infections and their treatments by nanotechnology-based approaches. *Proceedings of the National Academy of Sciences, India Section B: Biological Sciences*, 90, 243-259.
- BANERJEE, M., THOMPSON, D. S., LAZZELL, A., CARLISLE, P. L., PIERCE, C., MONTEAGUDO, C., LOPEZ-RIBOT, J. L. & KADOSH, D. 2008. UME6, a novel filament-specific regulator of *Candida albicans* hyphal extension and virulence. *Mol Biol Cell*, 19, 1354-65.
- BAPAT, R. A., CHAUBAL, T. V., JOSHI, C. P., BAPAT, P. R., CHOUDHURY, H., PANDEY, M., GORAIN, B. & KESHARWANI, P. 2018. An overview of application of silver nanoparticles for biomaterials in dentistry. *Mater Sci Eng C Mater Biol Appl*, 91, 881-898.
- BARBOSA-RIBEIRO, M., DE-JESUS-SOARES, A., ZAIA, A. A., FERRAZ, C. C., ALMEIDA, J. F. & GOMES, B. P. 2016. Antimicrobial Susceptibility and Characterization of Virulence Genes of *Enterococcus faecalis* Isolates from Teeth with Failure of the Endodontic Treatment. *J Endod*, 42, 1022-8.
- BARNARD, A. S., RUSSO, S. & SNOOK, I. 2003. Structural relaxation and relative stability of nanodiamond morphologies. *Diamond and related materials*, 12, 1867-1872.
- BARRAS, A., MARTIN, F. A., BANDE, O., BAUMANN, J. S., GHIGO, J. M., BOUKHERROUB, R., BELOIN, C., SIRIWARDENA, A. & SZUNERITS, S. 2013. Glycan-functionalized diamond nanoparticles as potent *E. coli* anti-adhesives. *Nanoscale*, 5, 2307-16.
- BAUMGARTNER, J. C., WATTS, C. M. & XIA, T. 2000. Occurrence of *Candida albicans* in infections of endodontic origin. *J Endod*, 26, 695-8.
- BECHERELLI, M., TAO, J. & RYDER, N. S. 2013a. Involvement of heat shock proteins in *Candida albicans* biofilm formation. *J Mol Microbiol Biotechnol*, 23, 396-400.
- BECHERELLI, M., TAO, J. & RYDER, N. S. 2013b. Involvement of heat shock proteins in *Candida albicans* biofilm formation. *Microbial Physiology*, 23, 396-400.
- BELDA-FERRE, P., ALCARAZ, L. D., CABRERA-RUBIO, R., ROMERO, H., SIMON-SORO, A., PIGNATELLI, M. & MIRA, A. 2012. The oral metagenome in health and disease. *ISME J*, 6, 46-56.
- BELDA-FERRE, P., WILLIAMSON, J., SIMÓN-SORO, Á., ARTACHO, A., JENSEN, O. N. & MIRA, A. 2015. The human oral metaproteome reveals potential biomarkers for caries disease. *Proteomics*, 15, 3497-3507.
- BELSTRØM, D., JERSIE-CHRISTENSEN, R. R., LYON, D., DAMGAARD, C., JENSEN, L. J., HOLMSTRUP, P. & OLSEN, J. V. 2016. Metaproteomics of saliva identifies human protein markers specific for individuals with periodontitis and dental caries compared to orally healthy controls. *PeerJ*, 4, e2433.

- BENNETT, R. J. & JOHNSON, A. D. 2003. Completion of a parasexual cycle in *Candida albicans* by induced chromosome loss in tetraploid strains. *EMBO J*, 22, 2505-15.
- BENNETT, R. J. & JOHNSON, A. D. 2005. Mating in *Candida albicans* and the search for a sexual cycle. *Annu Rev Microbiol*, 59, 233-55.
- BENSEN, E. S., CLEMENTE-BLANCO, A., FINLEY, K. R., CORREA-BORDES, J. & BERMAN, J. 2005. The mitotic cyclins Clb2p and Clb4p affect morphogenesis in *Candida albicans*. *Mol Biol Cell*, 16, 3387-400.
- BERGENHOLTZ, G. D., G. 2004. Advances in the study of endodontic infections: Introduction. *Endod. Top*, 9, 1-4.
- BERMAN, J. & SUDBERY, P. E. 2002. *Candida Albicans*: a molecular revolution built on lessons from budding yeast. *Nat Rev Genet*, 3, 918-30.
- BEYTH, N., HOURI-HADDAD, Y., DOMB, A., KHAN, W. & HAZAN, R. 2015. Alternative antimicrobial approach: nano-antimicrobial materials. *Evid Based Complement Alternat Med*, 2015, 246012.
- BHATTY, M., CRUZ, M. R., FRANK, K. L., GOMEZ, J. A., ANDRADE, F., GARSIN, D. A., DUNNY, G. M., KAPLAN, H. B. & CHRISTIE, P. J. 2015. Enterococcus faecalis pCF10-encoded surface proteins PrgA, PrgB (aggregation substance) and PrgC contribute to plasmid transfer, biofilm formation and virulence. *Mol Microbiol*, 95, 660-77.
- BHAVANA, V., CHAITANYA, K. P., GANDI, P., PATIL, J., DOLA, B. & REDDY, R. B. 2015. Evaluation of antibacterial and antifungal activity of new calcium-based cement (Biodentine) compared to MTA and glass ionomer cement. *J Conserv Dent*, 18, 44-6.
- BINDEA, G., MLECNIK, B., HACKL, H., CHAROENTONG, P., TOSOLINI, M., KIRILOVSKY, A., FRIDMAN, W. H., PAGES, F., TRAJANOSKI, Z. & GALON, J. 2009. ClueGO: a Cytoscape plug-in to decipher functionally grouped gene ontology and pathway annotation networks. *Bioinformatics*, 25, 1091-3.
- BIRJANDI, A. A., SUZANO, F. R. & SHARPE, P. T. 2020. Drug Repurposing in Dentistry; towards Application of Small Molecules in Dentin Repair. *Int J Mol Sci*, 21.
- BISWAS, K. & MORSCHHAUSER, J. 2005. The Mep2p ammonium permease controls nitrogen starvation-induced filamentous growth in *Candida albicans*. *Mol Microbiol*, 56, 649-69.
- BOLES, B. R. & HORSWILL, A. R. 2011. Staphylococcal biofilm disassembly. *Trends Microbiol*, 19, 449-55.
- BOLGER, A. M., LOHSE, M. & USADEL, B. 2014. Trimmomatic: a flexible trimmer for Illumina sequence data. *Bioinformatics*, 30, 2114-20.
- BONHOMME, J., CHAUVEL, M., GOYARD, S., ROUX, P., ROSSIGNOL, T. & D'ENFERT, C. 2011. Contribution of the glycolytic flux and hypoxia adaptation to efficient biofilm formation by *Candida albicans*. *Molecular microbiology*, 80, 995-1013.
- BONNET, M., LAGIER, J. C., RAOULT, D. & KHELAIFIA, S. 2020. Bacterial culture through selective and non-selective conditions: the evolution of culture media in clinical microbiology. *New microbes and new infections*, 34, 100622.
- BOR, B., CEN, L., AGNELLO, M., SHI, W. & HE, X. 2016. Morphological and physiological changes induced by contact-dependent interaction between *Candida albicans* and *Fusobacterium nucleatum*. *Scientific Reports*, 6, 27956.

- BOTTERY, M. J., MATTHEWS, J. L., WOOD, A. J., JOHANSEN, H. K., PITCHFORD, J. W. & FRIMAN, V. P. 2022. Inter-species interactions alter antibiotic efficacy in bacterial communities. *ISME J*, 16, 812-821.
- BOUILLAGUET, S., MANOIL, D., GIRARD, M., LOUIS, J., GAIA, N., LEO, S., SCHRENZEL, J. & LAZAREVIC, V. 2018. Root Microbiota in Primary and Secondary Apical Periodontitis. *Front Microbiol*, 9, 2374.
- BOWEN, W. H., BURNE, R. A., WU, H. & KOO, H. 2018. Oral Biofilms: Pathogens, Matrix, and Polymicrobial Interactions in Microenvironments. *Trends Microbiol*, 26, 229-242.
- BRAND, A., SHANKS, S., DUNCAN, V. M., YANG, M., MACKENZIE, K. & GOW, N. A. 2007. Hyphal orientation of *Candida albicans* is regulated by a calcium-dependent mechanism. *Curr Biol*, 17, 347-52.
- BRAUER, M. J., HUTTENHOWER, C., AIROLDI, E. M., ROSENSTEIN, R., MATESE, J. C., GRESHAM, D., BOER, V. M., TROYANSKAYA, O. G. & BOTSTEIN, D. 2008. Coordination of growth rate, cell cycle, stress response, and metabolic activity in yeast. *Molecular biology of the cell*, 19, 352-367.
- BRECKENRIDGE, A. & JACOB, R. 2019. Overcoming the legal and regulatory barriers to drug repurposing. *Nat Rev Drug Discov*, 18, 1-2.
- BREHMER, D., GREFF, Z., GODL, K., BLENCHE, S., KURTENBACH, A., WEBER, M., MULLER, S., KLEBL, B., COTTEN, M., KERI, G., WISSING, J. & DAUB, H. 2005. Cellular targets of gefitinib. *Cancer Res*, 65, 379-82.
- BROWN, A. J., BROWN, G. D., NETEA, M. G. & GOW, N. A. 2014. Metabolism impacts upon *Candida* immunogenicity and pathogenicity at multiple levels. *Trends in microbiology*, 22, 614-622.
- BROWN, G. D., DENNING, D. W., GOW, N. A., LEVITZ, S. M., NETEA, M. G. & WHITE, T. C. 2012. Hidden killers: human fungal infections. *Sci Transl Med*, 4, 165rv13.
- BROWN, J. L., YATES, E. A., BIELECKI, M., OLCZAK, T. & SMALLEY, J. W. 2018. Potential role for *Streptococcus gordonii*-derived hydrogen peroxide in heme acquisition by *Porphyromonas gingivalis*. *Molecular Oral Microbiology*, 33, 322-335.
- BROWN, V., SEXTON, J. A. & JOHNSTON, M. 2006. A glucose sensor in *Candida albicans*. *Eukaryot Cell*, 5, 1726-37.
- BROXTON, C. N. & CULOTTA, V. C. 2016. An Adaptation to Low Copper in *Candida albicans* Involving SOD Enzymes and the Alternative Oxidase. *PLoS One*, 11, e0168400.
- BUFFO, J., HERMAN, M. A. & SOLL, D. R. 1984. A characterization of pH-regulated dimorphism in *Candida albicans*. *Mycopathologia*, 85, 21-30.
- BUKHARI, S., KIM, D., LIU, Y., KARABUCAK, B. & KOO, H. 2018. Novel endodontic disinfection approach using catalytic nanoparticles. *Journal of endodontics*, 44, 806-812.
- BURMEISTER, A. & GRUNBERGER, A. 2020. Microfluidic cultivation and analysis tools for interaction studies of microbial co-cultures. *Curr Opin Biotechnol*, 62, 106-115.
- BURMOLLE, M., REN, D., BJARNSHOLT, T. & SORENSEN, S. J. 2014. Interactions in multispecies biofilms: do they actually matter? *Trends Microbiol*, 22, 84-91.
- BURNIE, J. P., CARTER, T. L., HODGETTS, S. J. & MATTHEWS, R. C. 2006. Fungal heat-shock proteins in human disease. *FEMS microbiology reviews*, 30, 53-88.

- CAMPILLOS, M., KUHN, M., GAVIN, A.-C., JENSEN, L. J. & BORK, P. 2008. Drug target identification using side-effect similarity. *Science*, 321, 263-266.
- CARLSON, E. 1983. Enhancement by *Candida albicans* of *Staphylococcus aureus*, *Serratia marcescens*, and *Streptococcus faecalis* in the establishment of infection in mice. *Infect Immun*, 39, 193-7.
- CAVALLA, D. & SINGAL, C. 2012. Retrospective clinical analysis for drug rescue: for new indications or stratified patient groups. *Drug Discov Today*, 17, 104-9.
- CHATTERJEE, A., PEREVEDENTSEVA, E., JANI, M., CHENG, C. Y., YE, Y. S., CHUNG, P. H. & CHENG, C. L. 2015. Antibacterial effect of ultrafine nanodiamond against gram-negative bacteria *Escherichia coli*. *J Biomed Opt*, 20, 051014.
- CHATTERJEE, K., SARKAR, S., JAGAJJANANI RAO, K. & PARIA, S. 2014. Core/shell nanoparticles in biomedical applications. *Adv Colloid Interface Sci*, 209, 8-39.
- CHAUDHARY, A., WELCH, J. O. & JACKMAN, R. B. 2010. Electrical properties of monodispersed detonation nanodiamonds. *Applied Physics Letters*, 96, 242903.
- CHAUHAN, S., JAIN, N. & NAGAICH, U. 2019. Nanodiamonds with powerful ability for drug delivery and biomedical applications: Recent updates on in vivo study and patents. *Journal of Pharmaceutical Analysis*, Volume 10, 1-12.
- CHAUHAN, S., JAIN, N. & NAGAICH, U. 2020. Nanodiamonds with powerful ability for drug delivery and biomedical applications: Recent updates on in vivo study and patents. *J Pharm Anal*, 10, 1-12.
- CHAVEZ DE PAZ, L. E. 2007. Redefining the persistent infection in root canals: possible role of biofilm communities. *J Endod*, 33, 652-62.
- CHAVEZ DE PAZ, L. E., DAHLEN, G., MOLANDER, A., MOLLER, A. & BERGENHOLTZ, G. 2003. Bacteria recovered from teeth with apical periodontitis after antimicrobial endodontic treatment. *Int Endod J*, 36, 500-8.
- CHEN, L. & WEN, Y. M. 2011. The role of bacterial biofilm in persistent infections and control strategies. *Int J Oral Sci*, 3, 66-73.
- CHEUNG, G. S. & HO, M. W. 2001. Microbial flora of root canal-treated teeth associated with asymptomatic periapical radiolucent lesions. *Oral Microbiol Immunol*, 16, 332-7.
- CHIANG, A. P. & BUTTE, A. J. 2009. Systematic evaluation of drug-disease relationships to identify leads for novel drug uses. *Clin Pharmacol Ther*, 86, 507-10.
- CHONG, P. P., CHIN, V. K., WONG, W. F., MADHAVAN, P., YONG, V. C. & LOOI, C. Y. 2018. Transcriptomic and Genomic Approaches for Unravelling *Candida albicans* Biofilm Formation and Drug Resistance-An Update. *Genes (Basel)*, 9.
- CHU, Z., ZHANG, S., ZHANG, B., ZHANG, C., FANG, C. Y., REHOR, I., CIGLER, P., CHANG, H. C., LIN, G., LIU, R. & LI, Q. 2014. Unambiguous observation of shape effects on cellular fate of nanoparticles. *Sci Rep*, 4, 4495.
- CHWALIBOG, A., SAWOSZ, E., HOTOWY, A., SZELIGA, J., MITURA, S., MITURA, K., GRODZIK, M., ORLOWSKI, P. & SOKOLOWSKA, A. 2010. Visualization of interaction between inorganic nanoparticles and bacteria or fungi. *International Journal of Nanomedicine*, 5, 1085.
- CLSI 2022. Performance Standards for Antimicrobial Susceptibility Testing, 32nd Edition. *Clinical and Laboratory Institute*, 362.

- COCO, B., BAGG, J., CROSS, L., JOSE, A., CROSS, J. & RAMAGE, G. 2008a. Mixed *Candida albicans* and *Candida glabrata* populations associated with the pathogenesis of denture stomatitis. *Oral microbiology and immunology*, 23, 377-383.
- COCO, B. J., BAGG, J., CROSS, L. J., JOSE, A., CROSS, J. & RAMAGE, G. 2008b. Mixed *Candida albicans* and *Candida glabrata* populations associated with the pathogenesis of denture stomatitis. *Oral Microbiol Immunol*, 23, 377-83.
- CONCEIÇÃO, K., DE ANDRADE, V. M., TRAVA-AIROLDI, V. & CAPOTE, G. 2019. High antibacterial properties of DLC film doped with nanodiamond. *Surface and Coatings Technology*, 375, 395-401.
- CONCEICAO, N., DA SILVA, L. E., DARINI, A. L., PITONDO-SILVA, A. & DE OLIVEIRA, A. G. 2014. Penicillin-resistant, ampicillin-susceptible *Enterococcus faecalis* of hospital origin: pbp4 gene polymorphism and genetic diversity. *Infect Genet Evol*, 28, 289-95.
- CONSORTIUM, G. T. 2015. Human genomics. The Genotype-Tissue Expression (GTEx) pilot analysis: multitissue gene regulation in humans. *Science (New York, N.Y.)*, 348, 648-660.
- COTE, P., HOGUES, H. & WHITEWAY, M. 2009. Transcriptional analysis of the *Candida albicans* cell cycle. *Mol Biol Cell*, 20, 3363-73.
- COUSIN, M. A., EBBERT, J. O., WIINAMAKI, A. R., URBAN, M. D., ARGUE, D. P., EKKER, S. C. & KLEE, E. W. 2014. Larval zebrafish model for FDA-approved drug repositioning for tobacco dependence treatment. *PLoS One*, 9, e90467.
- COX, G. & WRIGHT, G. D. 2013. Intrinsic antibiotic resistance: mechanisms, origins, challenges and solutions. *Int J Med Microbiol*, 303, 287-92.
- CRUZ, M. R., GRAHAM, C. E., GAGLIANO, B. C., LORENZ, M. C. & GARSIN, D. A. 2013. *Enterococcus faecalis* inhibits hyphal morphogenesis and virulence of *Candida albicans*. *Infect Immun*, 81, 189-200.
- CUÉLLAR-CRUZ, M., LÓPEZ-ROMERO, E., RUIZ-BACA, E. & ZAZUETA-SANDOVAL, R. 2014. Differential response of *Candida albicans* and *Candida glabrata* to oxidative and nitrosative stresses. *Current microbiology*, 69, 733-739.
- CUGINI, C., SHANMUGAM, M., LANDGE, N. & RAMASUBBU, N. 2019. The Role of Exopolysaccharides in Oral Biofilms. *J Dent Res*, 98, 739-745.
- DAGISTAN, S., AKTAS, A. E., CAGLAYAN, F., AYYILDIZ, A. & BILGE, M. 2009. Differential diagnosis of denture-induced stomatitis, *Candida*, and their variations in patients using complete denture: a clinical and mycological study. *Mycoses*, 52, 266-71.
- DAKSHANAMURTHY, S., ISSA, N. T., ASSEFNIA, S., SESHASAYEE, A., PETERS, O. J., MADHAVAN, S., UREN, A., BROWN, M. L. & BYERS, S. W. 2012. Predicting new indications for approved drugs using a proteochemometric method. *J Med Chem*, 55, 6832-48.
- DANILENKO, V. V. 2004. On the History of the Discovery of Nanodiamond Synthesis. *Physics of the Solid State*, Vol. 46, pp. 595-599.
- DAVE, M., NASH, M., YOUNG, G. C., ELLENS, H., MAGEE, M. H., ROBERTS, A. D., TAYLOR, M. A., GREENHILL, R. W. & BOYLE, G. W. 2014. Disposition and metabolism of darapladib, a lipoprotein-associated phospholipase A2 inhibitor, in humans. *Drug Metab Dispos*, 42, 415-30.
- DAVIES, D. 2003. Understanding biofilm resistance to antibacterial agents. *Nat Rev Drug Discov*, 2, 114-22.

- DAVIS, D. A. 2009. How human pathogenic fungi sense and adapt to pH: the link to virulence. *Curr Opin Microbiol*, 12, 365-70.
- DAY, A. M., COVE, J. H. & PHILLIPS-JONES, M. 2003. Cytolysin gene expression in *Enterococcus faecalis* is regulated in response to aerobiosis conditions. *Molecular Genetics and Genomics*, 269, 31-39.
- DE CARVALHO, F. G., SILVA, D. S., HEBLING, J., SPOLIDORIO, L. C. & SPOLIDORIO, D. M. 2006. Presence of mutans streptococci and *Candida* spp. in dental plaque/dentine of carious teeth and early childhood caries. *Arch Oral Biol*, 51, 1024-8.
- DEFRANCESCO, A. S., MASLOBOEVA, N., SYED, A. K., DELOUGHERY, A., BRADSHAW, N., LI, G.-W., GILMORE, M. S., WALKER, S. & LOSICK, R. 2017. Genome-wide screen for genes involved in eDNA release during biofilm formation by *Staphylococcus aureus*. *Proceedings of the National Academy of Sciences*, 114, E5969-E5978.
- DELANEY, C., KEAN, R., SHORT, B., TUMELTY, M., MCLEAN, W., NILE, C. J. & RAMAGE, G. 2018. Fungi at the scene of the crime: innocent bystanders or accomplices in oral infections? *Current Clinical Microbiology Reports*, 5, 190-200.
- DESAI, J. V., BRUNO, V. M., GANGULY, S., STAMPER, R. J., MITCHELL, K. F., SOLIS, N., HILL, E. M., XU, W., FILLER, S. G., ANDES, D. R., FANNING, S., LANNI, F. & MITCHELL, A. P. 2013. Regulatory role of glycerol in *Candida albicans* biofilm formation. *mBio*, 4, e00637-12.
- DEVECI, C., TUZUNER, T., CINAR, C., ODABAS, M. & BURUK, C. 2019. Short-term antibacterial activity and compressive strength of biodentine containing chlorhexidine/cetirizide mixtures. *Nigerian Journal of Clinical Practice*, 22, 227-227.
- DI BELLA, J. M., BAO, Y., GLOOR, G. B., BURTON, J. P. & REID, G. 2013. High throughput sequencing methods and analysis for microbiome research. *J Microbiol Methods*, 95, 401-14.
- DI RESTA, C., GALBIATI, S., CARRERA, P. & FERRARI, M. 2018. Next-generation sequencing approach for the diagnosis of human diseases: open challenges and new opportunities. *EJIFCC*, 29, 4-14.
- DIDEM, K., ÇİFTÇİ, S. Y. & NEMUTLU, E. 2021. Metabolomics-driven approaches on interactions between *Enterococcus faecalis* and *Candida albicans* biofilms. *Turkish Journal of Pharmaceutical Sciences*, 18, 557.
- DIEKEMA, D. J., HSUEH, P. R., MENDES, R. E., PFALLER, M. A., ROLSTON, K. V., SADER, H. S. & JONES, R. N. 2019. The Microbiology of Bloodstream Infection: 20-Year Trends from the SENTRY Antimicrobial Surveillance Program. *Antimicrob Agents Chemother*, 63.
- DONLAN, R. M. 2000. Role of biofilms in antimicrobial resistance. *ASAIO J*, 46, S47-52.
- DONLAN, R. M. 2002. Biofilms: microbial life on surfaces. *Emerg Infect Dis*, 8, 881-90.
- DOUGLAS, L. J. 2003. *Candida* biofilms and their role in infection. *Trends in microbiology*, 11, 30-36.
- DRAGOS, A. & KOVACS, A. T. 2017. The Peculiar Functions of the Bacterial Extracellular Matrix. *Trends Microbiol*, 25, 257-266.
- DU, Q., YUAN, S., ZHAO, S., FU, D., CHEN, Y., ZHOU, Y., CAO, Y., GAO, Y., XU, X., ZHOU, X. & HE, J. 2021. Coexistence of *Candida albicans* and *Enterococcus faecalis* increases biofilm virulence and periapical lesions in rats. *Biofouling*, 37, 964-974.

- DUDLEY, J. T., DESHPANDE, T. & BUTTE, A. J. 2011. Exploiting drug-disease relationships for computational drug repositioning. *Brief Bioinform*, 12, 303-11.
- DUMANI, A., YOLDAS, O., YILMAZ, S., KOKSAL, F., KAYAR, B., AKCIMEN, B. & SEYDAOGLU, G. 2012. Polymerase chain reaction of enterococcus faecalis and candida albicans in apical periodontitis from Turkish patients. *J Clin Exp Dent*, 4, e34-9.
- DUNSEATH, O., SMITH, E. J. W., AL-JEDA, T., SMITH, J. A., KING, S., MAY, P. W., NOBBS, A. H., HAZELL, G., WELCH, C. C. & SU, B. 2019. Studies of Black Diamond as an antibacterial surface for Gram Negative bacteria: the interplay between chemical and mechanical bactericidal activity. *Sci Rep*, 9, 8815.
- DURAN-PINEDO, A. E., CHEN, T., TELES, R., STARR, J. R., WANG, X., KRISHNAN, K. & FRIAS-LOPEZ, J. 2014. Community-wide transcriptome of the oral microbiome in subjects with and without periodontitis. *The ISME journal*, 8, 1659-1672.
- DUSCHINSKY, R., PLEVEN, E. & HEIDELBERGER, C. 1957. The synthesis of 5-fluoropyrimidines. *Journal of the American Chemical Society*, 79, 4559-4560.
- DUTTA, P. K., DUTTA, J. & TRIPATHI, V. 2004. Chitin and chitosan: Chemistry, properties and applications.
- DUTTON, L. C., PASZKIEWICZ, K. H., SILVERMAN, R. J., SPLATT, P. R., SHAW, S., NOBBS, A. H., LAMONT, R. J., JENKINSON, H. F. & RAMSDALE, M. 2016. Transcriptional landscape of trans-kingdom communication between *Candida albicans* and *Streptococcus gordonii*. *Molecular oral microbiology*, 31, 136-161.
- EARLE, K. A., BILLINGS, G., SIGAL, M., LICHTMAN, J. S., HANSSON, G. C., ELIAS, J. E., AMIEVA, M. R., HUANG, K. C. & SONNENBURG, J. L. 2015. Quantitative Imaging of Gut Microbiota Spatial Organization. *Cell Host Microbe*, 18, 478-88.
- EGAN, M. W., SPRATT, D. A., NG, Y. L., LAM, J. M., MOLES, D. R. & GULABIVALA, K. 2002. Prevalence of yeasts in saliva and root canals of teeth associated with apical periodontitis. *Int Endod J*, 35, 321-9.
- ELIOPOULOS, G. M. 1993. Aminoglycoside resistant enterococcal endocarditis. *Infect Dis Clin North Am*, 7, 117-33.
- ELLEPOLA, K., LIU, Y., CAO, T., KOO, H. & SENEVIRATNE, C. 2017. Bacterial GtfB augments *Candida albicans* accumulation in cross-kingdom biofilms. *Journal of dental research*, 96, 1129-1135.
- ELLEPOLA, K., TRUONG, T., LIU, Y., LIN, Q., LIM, T., LEE, Y., CAO, T., KOO, H. & SENEVIRATNE, C. 2019a. Multi-omics analyses reveal synergistic carbohydrate metabolism in *Streptococcus mutans*-*Candida albicans* mixed-species biofilms. *Infection and immunity*, 87, e00339-19.
- ELLEPOLA, K., TRUONG, T., LIU, Y., LIN, Q., LIM, T. K., LEE, Y. M., CAO, T., KOO, H. & SENEVIRATNE, C. J. 2019b. Multi-omics Analyses Reveal Synergistic Carbohydrate Metabolism in *Streptococcus mutans*-*Candida albicans* Mixed-Species Biofilms. *Infect Immun*, 87.
- ELSAKA, S. E., ELNAGHY, A. M., MANDORAH, A. & ELSHAZLI, A. H. 2019. Effect of titanium tetrafluoride addition on the physicochemical and antibacterial properties of Biodentine as intraorifice barrier. *Dental Materials*, 35, 185-193.

- ENE, I. V., HEILMANN, C. J., SORGO, A. G., WALKER, L. A., DE KOSTER, C. G., MUNRO, C. A., KLIS, F. M. & BROWN, A. J. 2012. Carbon source-induced reprogramming of the cell wall proteome and secretome modulates the adherence and drug resistance of the fungal pathogen *Candida albicans*. *Proteomics*, 12, 3164-3179.
- ENJALBERT, B., NANTEL, A. & WHITEWAY, M. 2003. Stress-induced gene expression in *Candida albicans*: absence of a general stress response. *Mol Biol Cell*, 14, 1460-7.
- ENJALBERT, B., SMITH, D. A., CORNELL, M. J., ALAM, I., NICHOLLS, S., BROWN, A. J. & QUINN, J. 2006. Role of the Hog1 stress-activated protein kinase in the global transcriptional response to stress in the fungal pathogen *Candida albicans*. *Mol Biol Cell*, 17, 1018-32.
- ERTEM, E., GUTT, B., ZUBER, F., ALLEGRI, S., LE OUAY, B., MEFTI, S., FORMENTIN, K., STELLACCI, F. & REN, Q. 2017. Core-Shell Silver Nanoparticles in Endodontic Disinfection Solutions Enable Long-Term Antimicrobial Effect on Oral Biofilms. *ACS Appl Mater Interfaces*, 9, 34762-34772.
- ESCOBAR, I. E., POSSAMAI ROSSATTO, F. C., KIM, S. M., KANG, M. H., KIM, W. & MYLONAKIS, E. 2021. Repurposing Kinase Inhibitor Bay 11-7085 to Combat *Staphylococcus aureus* and *Candida albicans* Biofilms. *Front Pharmacol*, 12, 675300.
- ESTEKI, P., JAHROMI, M. Z. & TAHMOURESPOUR, A. 2021. In vitro antimicrobial activity of mineral trioxide aggregate, Biodentine, and calcium-enriched mixture cement against *Enterococcus faecalis*, *Streptococcus mutans*, and *Candida albicans* using the agar diffusion technique. *Dental Research Journal*, 18.
- EUROPEAN-COMMISSION. 2011. *Commission recommendation of 18 October 2011 on the definition of nanomaterial* [Online]. Available: <http://data.europa.eu/eli/reco/2011/696/oj>. [Accessed 24th of March 2022].
- EVANS, L. V. 2000. *Biofilms: recent advances in their study and control*, CRC press.
- FABRICIUS, L., DAHLEN, G., HOLM, S. E. & MOLLER, A. J. 1982a. Influence of combinations of oral bacteria on periapical tissues of monkeys. *Scand J Dent Res*, 90, 200-6.
- FABRICIUS, L., DAHLEN, G., OHMAN, A. E. & MOLLER, A. J. 1982b. Predominant indigenous oral bacteria isolated from infected root canals after varied times of closure. *Scand J Dent Res*, 90, 134-44.
- FAKRUDDIN, M., CHOWDHURY, A., HOSSAIN, M. N., MANNAN, K. & MAZUMDA, R. 2012. Pyrosequencing-principles and applications. *Int J Life Sci Pharma Res*, 2, L-65-L-76.
- FAN, Y., HE, H., DONG, Y. & PAN, H. 2013. Hyphae-specific genes HGC1, ALS3, HWP1, and ECE1 and relevant signaling pathways in *Candida albicans*. *Mycopathologia*, 176, 329-335.
- FANNING, S., XU, W., SOLIS, N., WOOLFORD, C. A., FILLER, S. G. & MITCHELL, A. P. 2012. Divergent targets of *Candida albicans* biofilm regulator Bcr1 in vitro and in vivo. *Eukaryotic cell*, 11, 896-904.
- FARSHAD, M., ABBASZADEGAN, A., GHAHRAMANI, Y. & JAMSHIDZADEH, A. 2017. Effect of Imidazolium-Based Silver Nanoparticles on Root Dentin Roughness in Comparison with Three Common Root Canal Irrigants. *Iran Endod J*, 12, 83-86.

- FAUVART, M., VAN DEN BERGH, B. & MICHIELS, J. 2018. Stabbed while Sleeping: Synthetic Retinoid Antibiotics Kill Bacterial Persister Cells. *Mol Cell*, 70, 763-764.
- FELK, A., KRETSCHMAR, M., ALBRECHT, A., SCHALLER, M., BEINHAEUER, S., NICHTERLEIN, T., SANGLARD, D., KORTING, H. C., SCHAFER, W. & HUBE, B. 2002. *Candida albicans* hyphal formation and the expression of the Efg1-regulated proteinases Sap4 to Sap6 are required for the invasion of parenchymal organs. *Infection and immunity*, 70, 3689-3700.
- FERNANDES CDO, C., RECHENBERG, D. K., ZEHNDER, M. & BELIBASAKIS, G. N. 2014. Identification of Synergistetes in endodontic infections. *Microb Pathog*, 73, 1-6.
- FERNANDES, T. R., SEGORBE, D., PRUSKY, D. & DI PIETRO, A. 2017. How alkalinization drives fungal pathogenicity. *PLoS pathogens*, 13, e1006621.
- FIEHN, O. 2002. Metabolomics--the link between genotypes and phenotypes. *Plant Mol Biol*, 48, 155-71.
- FINKEL, J. S. & MITCHELL, A. P. 2011. Genetic control of *Candida albicans* biofilm development. *Nature Reviews Microbiology*, 9, 109-118.
- FINKEL, J. S., XU, W., HUANG, D., HILL, E. M., DESAI, J. V., WOOLFORD, C. A., NETT, J. E., TAFF, H., NORICE, C. T. & ANDES, D. R. 2012. Portrait of *Candida albicans* adherence regulators. *PLoS pathogens*, 8, e1002525.
- FIORI, A., KUCHARÍKOVÁ, S., GOVAERT, G., CAMMUE, B. P., THEVISSSEN, K. & VAN DIJCK, P. 2012. The heat-induced molecular disaggregase Hsp104 of *Candida albicans* plays a role in biofilm formation and pathogenicity in a worm infection model. *Eukaryotic cell*, 11, 1012-1020.
- FISHER, K. & PHILLIPS, C. 2009. The ecology, epidemiology and virulence of *Enterococcus*. *Microbiology (Reading)*, 155, 1749-1757.
- FLAHAUT, S., FRERE, J., BOUTIBONNES, P. & AUFRAY, Y. 1996. Comparison of the bile salts and sodium dodecyl sulfate stress responses in *Enterococcus faecalis*. *Appl Environ Microbiol*, 62, 2416-20.
- FLAHAUT, S., HARTKE, A., GIARD, J. C. & AUFRAY, Y. 1997. Alkaline stress response in *Enterococcus faecalis*: adaptation, cross-protection, and changes in protein synthesis. *Appl Environ Microbiol*, 63, 812-4.
- FLEMMING, H.-C., WINGENDER, J., SZEWZYK, U., STEINBERG, P., RICE, S. A. & KJELLEBERG, S. 2016. Biofilms: an emergent form of bacterial life. *Nature Reviews Microbiology*, 14, 563-575.
- FLEMMING, H. C. & WINGENDER, J. 2010. The biofilm matrix. *Nat Rev Microbiol*, 8, 623-33.
- FONZI, W. A. & IRWIN, M. 1993. Isogenic strain construction and gene mapping in *Candida albicans*. *Genetics*, 134, 717-728.
- FOUDA, S. M., GAD, M. M., ELLAKANY, P., AL-THOBITY, A. M., AL-HARBI, F. A., VIRTANEN, J. I. & RAUSTIA, A. 2019. The effect of nanodiamonds on *Candida albicans* adhesion and surface characteristics of PMMA denture base material - an in vitro study. *J Appl Oral Sci*, 27, e20180779.
- FOURIE, R., CASON, E. D., ALBERTYN, J. & POHL, C. H. 2021. Transcriptional response of *Candida albicans* to *Pseudomonas aeruginosa* in a polymicrobial biofilm. *G3 (Bethesda)*, 11.
- FOURIE, R., ELLS, R., SWART, C. W., SEBOLAI, O. M., ALBERTYN, J. & POHL, C. H. 2016. *Candida albicans* and *Pseudomonas aeruginosa* Interaction, with Focus on the Role of Eicosanoids. *Front Physiol*, 7, 64.
- FOURIE, R. & POHL, C. H. 2019. Beyond Antagonism: The Interaction Between *Candida* Species and *Pseudomonas aeruginosa*. *J Fungi (Basel)*, 5.

- FOX, E., COWLEY, E., NOBILE, C., HARTOONI, N., NEWMAN, D. & JOHNSON, A. 2014. Anaerobic bacteria grow within *Candida albicans* biofilms and induce biofilm formation in suspension cultures. *Current biology*, 24, 2411-2416.
- FREITAS, R. A., JR. 2000. Nanodentistry. *J Am Dent Assoc*, 131, 1559-65.
- FRIEDEN, T. R., MUNSIFF, S. S., WILLIAMS, G., FAUR, Y., KREISWIRTH, B., LOW, D., WILLEY, B., WARREN, S. & EISNER, W. 1993. Emergence of vancomycin-resistant enterococci in New York City. *The Lancet*, 342, 76-79.
- FUX, C. A., COSTERTON, J. W., STEWART, P. S. & STOODLEY, P. 2005. Survival strategies of infectious biofilms. *Trends Microbiol*, 13, 34-40.
- GALE, C. A., LEONARD, M. D., FINLEY, K. R., CHRISTENSEN, L., MCCLELLAN, M., ABBEY, D., KURISCHKO, C., BENSON, E., TZAFRIR, I., KAUFFMAN, S., BECKER, J. & BERMAN, J. 2009. SLA2 mutations cause SWE1-mediated cell cycle phenotypes in *Candida albicans* and *Saccharomyces cerevisiae*. *Microbiology (Reading)*, 155, 3847-3859.
- GAO, Y., JIANG, X., LIN, D., CHEN, Y. & TONG, Z. 2016. The Starvation Resistance and Biofilm Formation of *Enterococcus faecalis* in Coexistence with *Candida albicans*, *Streptococcus gordonii*, *Actinomyces viscosus*, or *Lactobacillus acidophilus*. *J Endod*, 42, 1233-8.
- GARBE, E. & VYLKOVA, S. 2019. Role of amino acid metabolism in the virulence of human pathogenic fungi. *Current Clinical Microbiology Reports*, 6, 108-119.
- GARBEROGLIO, R. & BECCE, C. 1994. Smear layer removal by root canal irrigants. A comparative scanning electron microscopic study. *Oral Surg Oral Med Oral Pathol*, 78, 359-67.
- GARBEROGLIO, R. & BRANNSTROM, M. 1976. Scanning electron microscopic investigation of human dentinal tubules. *Arch Oral Biol*, 21, 355-62.
- GARSIN, D. A. & LORENZ, M. C. 2013. *Candida albicans* and *Enterococcus faecalis* in the gut: synergy in commensalism? *Gut Microbes*, 4, 409-15.
- GATTI, J. J., DOBECK, J. M., SMITH, C., WHITE, R. R., SOCRANSKY, S. S. & SKOBE, Z. 2000. Bacteria of asymptomatic periradicular endodontic lesions identified by DNA-DNA hybridization. *Endod Dent Traumatol*, 16, 197-204.
- GAWRON, K., WOJTOWICZ, W., LAZARZ-BARTYZEL, K., LAMASZ, A., QASEM, B., MYDEL, P., CHOMYSZYN-GAJEWSKA, M., POTEMPA, J. & MLYNARZ, P. 2019. Metabolomic Status of The Oral Cavity in Chronic Periodontitis. *In Vivo*, 33, 1165-1174.
- GHANNOUM, M. A. 2000. Potential role of phospholipases in virulence and fungal pathogenesis. *Clin Microbiol Rev*, 13, 122-43, table of contents.
- GHANNOUM, M. A., JUREVIC, R. J., MUKHERJEE, P. K., CUI, F., SIKAROODI, M., NAQVI, A. & GILLEVET, P. M. 2010. Characterization of the oral fungal microbiome (mycobiome) in healthy individuals. *PLoS Pathog*, 6, e1000713.
- GIAOURIS, E., HEIR, E., DESVAUX, M., HEBRAUD, M., MORETRO, T., LANGSRUD, S., DOULGERAKI, A., NYCHAS, G. J., KACANIOVA, M., CZACZYK, K., OLMEZ, H. & SIMOES, M. 2015. Intra- and inter-species interactions within biofilms of important foodborne bacterial pathogens. *Front Microbiol*, 6, 841.

- GIARD, J. C., HARTKE, A., FLAHAUT, S., BENACHOUR, A., BOUTIBONNES, P. & AUFRAY, Y. 1996. Starvation-induced multiresistance in *Enterococcus faecalis* JH2-2. *Curr Microbiol*, 32, 264-71.
- GOLDBERG, M., KULKARNI, A. B., YOUNG, M. & BOSKEY, A. 2011. Dentin: structure, composition and mineralization. *Front Biosci (Elite Ed)*, 3, 711-35.
- GOMES, C. C., GUIMARAES, L. S., PINTO, L. C. C., CAMARGO, G., VALENTE, M. I. B. & SARQUIS, M. I. M. 2017. Investigations of the prevalence and virulence of *Candida albicans* in periodontal and endodontic lesions in diabetic and normoglycemic patients. *J Appl Oral Sci*, 25, 274-281.
- GONZÁLEZ-PÁRRAGA, P., HERNÁNDEZ, J. A. & ARGÜELLES, J. C. 2003. Role of antioxidant enzymatic defences against oxidative stress (H₂O₂) and the acquisition of oxidative tolerance in *Candida albicans*. *Yeast*, 20, 1161-1169.
- GOODNOW, R. A., JR. 2001. Current practices in generation of small molecule new leads. *J Cell Biochem Suppl*, Suppl 37, 13-21.
- GÖRAN SUNDQVIST & FIGDOR, D. 2003. *Life as an endodontic pathogen: Ecological differences between the untreated and root-filled root canals.*
- GRAHAM, C. E., CRUZ, M. R., GARSIN, D. A. & LORENZ, M. C. 2017a. *Enterococcus faecalis* bacteriocin EntV inhibits hyphal morphogenesis, biofilm formation, and virulence of *Candida albicans*. *Proceedings of the National Academy of Sciences*, 114, 4507-4512.
- GRAHAM, C. E., CRUZ, M. R., GARSIN, D. A. & LORENZ, M. C. 2017b. *Enterococcus faecalis* bacteriocin EntV inhibits hyphal morphogenesis, biofilm formation, and virulence of *Candida albicans*. *Proc Natl Acad Sci U S A*, 114, 4507-4512.
- GRASSL, N., KULAK, N. A., PICHLER, G., GEYER, P. E., JUNG, J., SCHUBERT, S., SINITCYN, P., COX, J. & MANN, M. 2016. Ultra-deep and quantitative saliva proteome reveals dynamics of the oral microbiome. *Genome medicine*, 8, 1-13.
- GREEN, C. B., ZHAO, X., YEATER, K. M. & HOYER, L. L. 2005. Construction and real-time RT-PCR validation of *Candida albicans* PALS-GFP reporter strains and their use in flow cytometry analysis of ALS gene expression in budding and filamenting cells. *Microbiology*, 151, 1051-1060.
- GREENE, C. S. & VOIGHT, B. F. 2016a. Pathway and network-based strategies to translate genetic discoveries into effective therapies. *Human molecular genetics*, 25, R94-R98.
- GREENE, C. S. & VOIGHT, B. F. 2016b. Pathway and network-based strategies to translate genetic discoveries into effective therapies. *Hum Mol Genet*, 25, R94-R98.
- GRIFFEN, A. L., BEALL, C. J., CAMPBELL, J. H., FIRESTONE, N. D., KUMAR, P. S., YANG, Z. K., PODAR, M. & LEYS, E. J. 2012. Distinct and complex bacterial profiles in human periodontitis and health revealed by 16S pyrosequencing. *ISME J*, 6, 1176-85.
- GULHAN, T., BOYNUKARA, B., CIFTCI, A., SOGUT, M. & FINDIK, A. 2015. Characterization of *Enterococcus faecalis* isolates originating from different sources for their virulence factors and genes, antibiotic resistance patterns, genotypes and biofilm production. *Iranian Journal of Veterinary Research*, 16, 261.

- GUTMANN, J. L. & MANJARRES, V. 2018. Historical and Contemporary Perspectives on the Microbiological Aspects of Endodontics. *Dent J (Basel)*, 6.
- HAAPASALO, M., SHEN, Y. & RICUCCI, D. 2008. Reasons for persistent and emerging post-treatment endodontic disease. *Endodontic Topics*, 18, 31-50.
- HALL, C. W. & MAH, T. F. 2017. Molecular mechanisms of biofilm-based antibiotic resistance and tolerance in pathogenic bacteria. *FEMS Microbiol Rev*, 41, 276-301.
- HALL, R. A., TURNER, K. J., CHALOUPKA, J., COTTIER, F., DE SORDI, L., SANGLARD, D., LEVIN, L. R., BUCK, J. & MUHLSCHLEGEL, F. A. 2011. The quorum-sensing molecules farnesol/homoserine lactone and dodecanol operate via distinct modes of action in *Candida albicans*. *Eukaryot Cell*, 10, 1034-42.
- HALL-STOODLEY, L., COSTERTON, J. W. & STOODLEY, P. 2004. Bacterial biofilms: from the natural environment to infectious diseases. *Nat Rev Microbiol*, 2, 95-108.
- HAN, T.-L., CANNON, R. D., GALLO, S. M. & VILLAS-BÔAS, S. G. 2019. A metabolomic study of the effect of *Candida albicans* glutamate dehydrogenase deletion on growth and morphogenesis. *NPJ biofilms and microbiomes*, 5, 1-14.
- HARPF, V., RAMBACH, G., WURZNER, R., LASS-FLORL, C. & SPETH, C. 2020. *Candida* and Complement: New Aspects in an Old Battle. *Front Immunol*, 11, 1471.
- HARTMANN, M., BETZ, P., SUN, Y., GORB, S. N., LINDHORST, T. K. & KRUEGER, A. 2012. Saccharide-modified nanodiamond conjugates for the efficient detection and removal of pathogenic bacteria. *Chemistry*, 18, 6485-92.
- HE, J., KIM, D., ZHOU, X., AHN, S.-J., BURNE, R. A., RICHARDS, V. P. & KOO, H. 2017. RNA-seq reveals enhanced sugar metabolism in *Streptococcus mutans* co-cultured with *Candida albicans* within mixed-species biofilms. *Frontiers in microbiology*, 8, 1036.
- HERMANN, C., HERMANN, J., MUNZEL, U. & RUCHEL, R. 1999. Bacterial flora accompanying *Candida* yeasts in clinical specimens. *Mycoses*, 42, 619-27.
- HEYERAAS, K. J. 1989. Pulpal hemodynamics and interstitial fluid pressure: balance of transmicrovascular fluid transport. *J Endod*, 15, 468-72.
- HIRANO, H. & TAKEMOTO, K. 2019. Difficulty in inferring microbial community structure based on co-occurrence network approaches. *BMC Bioinformatics*, 20, 329.
- HITCHINGS, R. & KELLY, L. 2019. Drug metabolism as a community effort. *Cell metabolism*, 30, 235-237.
- HOGAN, D. A. & KOLTER, R. 2002. *Pseudomonas-Candida* interactions: an ecological role for virulence factors. *Science*, 296, 2229-32.
- HOLLAND, L. M., SCHRÖDER, M. S., TURNER, S. A., TAFF, H., ANDES, D., GRÓZER, Z., GÁCSEK, A., AMES, L., HAYNES, K. & HIGGINS, D. G. 2014. Comparative phenotypic analysis of the major fungal pathogens *Candida parapsilosis* and *Candida albicans*. *PLoS pathogens*, 10, e1004365.
- HOLLENBECK, B. L. & RICE, L. B. 2012. Intrinsic and acquired resistance mechanisms in enterococcus. *Virulence*, 3, 421-33.
- HONG, B. Y., LEE, T. K., LIM, S. M., CHANG, S. W., PARK, J., HAN, S. H., ZHU, Q., SAFAVI, K. E., FOUAD, A. F. & KUM, K. Y. 2013. Microbial analysis in

- primary and persistent endodontic infections by using pyrosequencing. *J Endod*, 39, 1136-40.
- HOOD, M. I. & SKAAR, E. P. 2012. Nutritional immunity: transition metals at the pathogen-host interface. *Nat Rev Microbiol*, 10, 525-37.
- HORNER, C., MUSHTAQ, S., ALLEN, M., HOPE, R., GERVER, S., LONGSHAW, C., REYNOLDS, R., WOODFORD, N. & LIVERMORE, D. M. 2021. Replacement of *Enterococcus faecalis* by *Enterococcus faecium* as the predominant enterococcus in UK bacteraemias. *JAC-Antimicrobial Resistance*, 3, dlab185.
- HOYER, L. L. 2001. The ALS gene family of *Candida albicans*. *Trends Microbiol*, 9, 176-80.
- HOYER, L. L., OH, S.-H., JONES, R. & COTA, E. 2014. A proposed mechanism for the interaction between the *Candida albicans* Als3 adhesin and streptococcal cell wall proteins. *Frontiers in microbiology*, 5, 564.
- HUANG, H., PIERSTORFF, E., OSAWA, E. & HO, D. 2008. Protein-mediated assembly of nanodiamond hydrogels into a biocompatible and biofunctional multilayer nanofilm. *ACS nano*, 2, 203-212.
- HUANG, Y., FUJII, K., CHEN, X., IWATANI, S., CHIBANA, H., KOJIMA, S. & KAJIWARA, S. 2020. Fungal NOX is an essential factor for induction of TG2 in human hepatocytes. *Med Mycol*, 58, 679-689.
- HUANG, Y. H. & VAKOC, C. R. 2016. A Biomarker Harvest from One Thousand Cancer Cell Lines. *Cell*, 166, 536-537.
- HUBE, B., MONOD, M., SCHOFIELD, D. A., BROWN, A. J. & GOW, N. A. 1994. Expression of seven members of the gene family encoding secretory aspartyl proteinases in *Candida albicans*. *Mol Microbiol*, 14, 87-99.
- HUBE, B., STEHR, F., BOSSENZ, M., MAZUR, A., KRETSCHMAR, M. & SCHAFFER, W. 2000. Secreted lipases of *Candida albicans*: cloning, characterisation and expression analysis of a new gene family with at least ten members. *Arch Microbiol*, 174, 362-74.
- HUNT, C. P. 1998. The emergence of enterococci as a cause of nosocomial infection. *British Journal of Biomedical Science*, 55, 149-156.
- HURLE, M. R., YANG, L., XIE, Q., RAJPAL, D. K., SANSEAU, P. & AGARWAL, P. 2013. Computational drug repositioning: from data to therapeutics. *Clin Pharmacol Ther*, 93, 335-41.
- HUYCKE, M. M., ABRAMS, V. & MOORE, D. R. 2002. *Enterococcus faecalis* produces extracellular superoxide and hydrogen peroxide that damages colonic epithelial cell DNA. *Carcinogenesis*, 23, 529-536.
- HWANG, G., MARSH, G., GAO, L., WAUGH, R. & KOO, H. 2015. Binding force dynamics of *Streptococcus mutans*-glucosyltransferase B to *Candida albicans*. *Journal of dental research*, 94, 1310-1317.
- ILJIN, K., KETOLA, K., VAINIO, P., HALONEN, P., KOHONEN, P., FEY, V., GRAFSTROM, R. C., PERALA, M. & KALLIONIEMI, O. 2009. High-throughput cell-based screening of 4910 known drugs and drug-like small molecules identifies disulfiram as an inhibitor of prostate cancer cell growth. *Clin Cancer Res*, 15, 6070-8.
- INVESTIGATORS, S., WHITE, H. D., HELD, C., STEWART, R., TARKA, E., BROWN, R., DAVIES, R. Y., BUDAJ, A., HARRINGTON, R. A., STEG, P. G., ARDISSINO, D., ARMSTRONG, P. W., AVEZUM, A., AYLWARD, P. E., BRYCE, A., CHEN, H., CHEN, M. F., CORBALAN, R., DALBY, A. J., DANCHIN, N., DE WINTER, R. J., DENCHEV, S., DIAZ, R., ELISAF, M., FLATHER, M. D., GOUDEV, A. R., GRANGER, C. B., GRINFELD, L., HOCHMAN, J. S., HUSTED,

- S., KIM, H. S., KOENIG, W., LINHART, A., LONN, E., LOPEZ-SENDON, J., MANOLIS, A. J., MOHLER, E. R., 3RD, NICOLAU, J. C., PAIS, P., PARKHOMENKO, A., PEDERSEN, T. R., PELLA, D., RAMOS-CORRALES, M. A., RUDA, M., SEREG, M., SIDDIQUE, S., SINNAEVE, P., SMITH, P., SRITARA, P., SWART, H. P., SY, R. G., TERAMOTO, T., TSE, H. F., WATSON, D., WEAVER, W. D., WEISS, R., VIIGIMAA, M., VINEREANU, D., ZHU, J., CANNON, C. P. & WALLENTIN, L. 2014. Darapladib for preventing ischemic events in stable coronary heart disease. *N Engl J Med*, 370, 1702-11.
- IOANNIDIS, K., NIAZI, S., MYLONAS, P., MANNOCCI, F. & DEB, S. 2019. The synthesis of nano silver-graphene oxide system and its efficacy against endodontic biofilms using a novel tooth model. *Dent Mater*, 35, 1614-1629.
- IORIO, F., ISACCHI, A., DI BERNARDO, D. & BRUNETTI-PIERRI, N. 2010. Identification of small molecules enhancing autophagic function from drug network analysis. *Autophagy*, 6, 1204-5.
- IORIO, F., RITTMAN, T., GE, H., MENDEN, M. & SAEZ-RODRIGUEZ, J. 2013. Transcriptional data: a new gateway to drug repositioning? *Drug Discov Today*, 18, 350-7.
- IYER, J. K., DICKEY, A., ROUHANI, P., KAUL, A., GOVINDARAJU, N., SINGH, R. N. & KAUL, R. 2018. Nanodiamonds facilitate killing of intracellular uropathogenic E. coli in an in vitro model of urinary tract infection pathogenesis. *PLoS One*, 13, e0191020.
- IZADI, Z., DERA KHSHANKHAH, H., ALAEI, L., KARKAZIS, E., JAFARI, S. & TAYEBI, L. 2020. Recent Advances in Nanodentistry. *Applications of Biomedical Engineering in Dentistry*. Springer.
- JACOBSEN, I. D., WILSON, D., WACHTLER, B., BRUNKE, S., NAGLIK, J. R. & HUBE, B. 2012. Candida albicans dimorphism as a therapeutic target. *Expert Rev Anti Infect Ther*, 10, 85-93.
- JAIN, C., PASTOR, K., GONZALEZ, A. Y., LORENZ, M. C. & RAO, R. P. 2013. The role of Candida albicans AP-1 protein against host derived ROS in in vivo models of infection. *Virulence*, 4, 67-76.
- JAKUBOVICS, N. S. 2015. Intermicrobial Interactions as a Driver for Community Composition and Stratification of Oral Biofilms. *J Mol Biol*, 427, 3662-75.
- JANDA, J. M., ATANG-NOMO, S., BOTTONI, E. J. & DESMOND, E. P. 1980. Correlation of proteolytic activity of Pseudomonas aeruginosa with site of isolation. *J Clin Microbiol*, 12, 626-8.
- JARDINE, A. P., MONTAGNER, F., QUINTANA, R. M., ZACCARA, I. M. & KOPPER, P. M. P. 2019. Antimicrobial effect of bioceramic cements on multispecies microcosm biofilm: a confocal laser microscopy study. *Clin Oral Investig*, 23, 1367-1372.
- JAVORKA, P., RAXWAL, V. K., NAJVAREK, J. & RIHA, K. 2019. art MAP: A user-friendly tool for mapping ethyl methanesulfonate-induced mutations in Arabidopsis. *Plant Direct*, 3, e00146.
- JEEVANANDAM, J., BARHOUM, A., CHAN, Y. S., DUFRESNE, A. & DANQUAH, M. K. 2018. Review on nanoparticles and nanostructured materials: history, sources, toxicity and regulations. *Beilstein J Nanotechnol*, 9, 1050-1074.
- JENSEN, P. B., JENSEN, L. J. & BRUNAK, S. 2012. Mining electronic health records: towards better research applications and clinical care. *Nat Rev Genet*, 13, 395-405.
- JIMÉNEZ-LÓPEZ, C., COLLETTE, J. R., BROTHERS, K. M., SHEPARDSON, K. M., CRAMER, R. A., WHEELER, R. T. & LORENZ, M. C. 2013. Candida albicans

- induces arginine biosynthetic genes in response to host-derived reactive oxygen species. *Eukaryotic Cell*, 12, 91-100.
- JIN, Y., SAMARANAYAKE, L. P., SAMARANAYAKE, Y. & YIP, H. K. 2004. Biofilm formation of *Candida albicans* is variably affected by saliva and dietary sugars. *Archives of Oral Biology*, 49, 789-798.
- JOHNSON, E. M., FLANNAGAN, S. E. & SEDGLEY, C. M. 2006. Coaggregation interactions between oral and endodontic *Enterococcus faecalis* and bacterial species isolated from persistent apical periodontitis. *Journal of Endodontics*, 32, 946-950.
- JORTH, P., TURNER, K. H., GUMUS, P., NIZAM, N., BUDUNELI, N. & WHITELEY, M. 2014. Metatranscriptomics of the human oral microbiome during health and disease. *mBio*, 5, e01012-14.
- JOSE, A., COCO, B. J., MILLIGAN, S., YOUNG, B., LAPPIN, D. F., BAGG, J., MURRAY, C. & RAMAGE, G. 2010. Reducing the incidence of denture stomatitis: are denture cleansers sufficient? *J Prosthodont*, 19, 252-7.
- JOWKAR, Z., HAMIDI, S. A., SHAFIEI, F. & GHAHRAMANI, Y. 2020. The effect of silver, zinc oxide, and titanium dioxide nanoparticles used as final irrigation solutions on the fracture resistance of root-filled teeth. *Clinical, cosmetic and investigational dentistry*, 12, 141.
- KAKEHASHI, S., STANLEY, H. R. & FITZGERALD, R. J. 1965. The Effects of Surgical Exposures of Dental Pulps in Germ-Free and Conventional Laboratory Rats. *Oral Surg Oral Med Oral Pathol*, 20, 340-9.
- KANDASWAMY, D. & VENKATESHBABU, N. 2010. Root canal irrigants. *J Conserv Dent*, 13, 256-64.
- KARYGIANNI, L., REN, Z., KOO, H. & THURNHEER, T. 2020. Biofilm Matrixome: Extracellular Components in Structured Microbial Communities. *Trends Microbiol*, 28, 668-681.
- KARYGIANNI, L., RUF, S., FOLLO, M., HELLWIG, E., BUCHER, M., ANDERSON, A. C., VACH, K. & AL-AHMAD, A. 2014. Novel Broad-Spectrum Antimicrobial Photoinactivation of In Situ Oral Biofilms by Visible Light plus Water-Filtered Infrared A. *Appl Environ Microbiol*, 80, 7324-36.
- KAYAOGU, G. & ORSTAVIK, D. 2004. Virulence factors of *Enterococcus faecalis*: relationship to endodontic disease. *Crit Rev Oral Biol Med*, 15, 308-20.
- KEIJSER, B. J., ZAURA, E., HUSE, S. M., VAN DER VOSSEN, J. M., SCHUREN, F. H., MONTIJN, R. C., TEN CATE, J. M. & CRIELAARD, W. 2008. Pyrosequencing analysis of the oral microflora of healthy adults. *J Dent Res*, 87, 1016-20.
- KEISER, M. J., SETOLA, V., IRWIN, J. J., LAGGNER, C., ABBAS, A. I., HUFSEIN, S. J., JENSEN, N. H., KUIJER, M. B., MATOS, R. C., TRAN, T. B., WHALEY, R., GLENNON, R. A., HERT, J., THOMAS, K. L., EDWARDS, D. D., SHOICHET, B. K. & ROTH, B. L. 2009. Predicting new molecular targets for known drugs. *Nature*, 462, 175-81.
- KELLY, M. T., MACCALLUM, D. M., CLANCY, S. D., ODDS, F. C., BROWN, A. J. & BUTLER, G. 2004. The *Candida albicans* CaACE2 gene affects morphogenesis, adherence and virulence. *Mol Microbiol*, 53, 969-83.
- KEREN, I., KALDALU, N., SPOERING, A., WANG, Y. & LEWIS, K. 2004. Persister cells and tolerance to antimicrobials. *FEMS Microbiol Lett*, 230, 13-8.
- KESKIN, C., DEMIRYUREK, E. O. & ONUK, E. E. 2017. Pyrosequencing Analysis of Cryogenically Ground Samples from Primary and Secondary/Persistent Endodontic Infections. *J Endod*, 43, 1309-1316.
- KHAN, I., SAEED, K. & KHAN, I. 2019. Nanoparticles: Properties, applications and toxicities. *Arabian journal of chemistry*, 12, 908-931.

- KHARISOV, B. I., KHARISSOVA, O. V. & CHÁVEZ-GUERRERO, L. 2010. Synthesis techniques, properties, and applications of nanodiamonds. *Synthesis and Reactivity in Inorganic, Metal-Organic, and Nano-Metal Chemistry*, 40, 84-101.
- KIM, E. B., KOPIT, L. M., HARRIS, L. J. & MARCO, M. L. 2012. Draft genome sequence of the quality control strain *Enterococcus faecalis* ATCC 29212. *J Bacteriol*, 194, 6006-7.
- KIM, J. H., CHENG, L. W., CHAN, K. L., TAM, C. C., MAHONEY, N., FRIEDMAN, M., SHILMAN, M. M. & LAND, K. M. 2020a. Antifungal Drug Repurposing. *Antibiotics (Basel)*, 9.
- KIM, M.-A., ROSA, V. & MIN, K.-S. 2020b. Characterization of *Enterococcus faecalis* in different culture conditions. *Scientific Reports*, 10, 21867.
- KIM, W., ZHU, W., HENDRICKS, G. L., VAN TYNE, D., STEELE, A. D., KEOHANE, C. E., FRICKE, N., CONERY, A. L., SHEN, S., PAN, W., LEE, K., RAJAMUTHIAH, R., FUCHS, B. B., VLAHOVSKA, P. M., WUEST, W. M., GILMORE, M. S., GAO, H., AUSUBEL, F. M. & MYLONAKIS, E. 2018. A new class of synthetic retinoid antibiotics effective against bacterial persisters. *Nature*, 556, 103-107.
- KIPANGA, P. N., DEMUYSER, L., VRIJDAG, J., ESKES, E., D'HOOGHE, P., MATASYOH, J., CALLEWAERT, G., WINDERICKX, J., VAN DIJCK, P. & LUYTEN, W. 2021. Investigating the Antifungal Mechanism of Action of Polygodial by Phenotypic Screening in *Saccharomyces cerevisiae*. *Int J Mol Sci*, 22.
- KISHEN, A., SHRESTHA, S., SHRESTHA, A., CHENG, C. & GOH, C. 2016. Characterizing the collagen stabilizing effect of crosslinked chitosan nanoparticles against collagenase degradation. *Dent Mater*, 32, 968-77.
- KITCHEN, D. B., DECORNEZ, H., FURR, J. R. & BAJORATH, J. 2004. Docking and scoring in virtual screening for drug discovery: methods and applications. *Nat Rev Drug Discov*, 3, 935-49.
- KLIPPEL, N., CUI, S., GROEBE, L. & BILITEWSKI, U. 2010. Deletion of the *Candida albicans* histidine kinase gene *CHK1* improves recognition by phagocytes through an increased exposure of cell wall beta-1,3-glucans. *Microbiology (Reading)*, 156, 3432-3444.
- KLOSINSKA, M. M., CRUTCHFIELD, C. A., BRADLEY, P. H., RABINOWITZ, J. D. & BROACH, J. R. 2011. Yeast cells can access distinct quiescent states. *Genes & development*, 25, 336-349.
- KLOTZ, S. A., GAUR, N. K., DE ARMOND, R., SHEPPARD, D., KHARDORI, N., EDWARDS JR, J. E., LIPKE, P. N. & EL-AZIZI, M. 2007. *Candida albicans* Als proteins mediate aggregation with bacteria and yeasts. *Medical Mycology*, 45, 363-370.
- KOHLER, J. R., ACOSTA-ZALDIVAR, M. & QJ, W. 2020. Phosphate in Virulence of *Candida albicans* and *Candida glabrata*. *J Fungi (Basel)*, 6.
- KOMOROWSKI, R., GRAD, H., WU, X. Y. & FRIEDMAN, S. 2000. Antimicrobial substantivity of chlorhexidine-treated bovine root dentin. *J Endod*, 26, 315-7.
- KONG, E. F., TSUI, C., KUCHARIKOVA, S., VAN DIJCK, P. & JABRA-RIZK, M. A. 2017. Modulation of *Staphylococcus aureus* Response to Antimicrobials by the *Candida albicans* Quorum Sensing Molecule Farnesol. *Antimicrob Agents Chemother*, 61.

- KONG, M., CHEN, X. G., XING, K. & PARK, H. J. 2010. Antimicrobial properties of chitosan and mode of action: a state of the art review. *Int J Food Microbiol*, 144, 51-63.
- KONG, X. L., HUANG, L. C., HSU, C. M., CHEN, W. H., HAN, C. C. & CHANG, H. C. 2005. High-affinity capture of proteins by diamond nanoparticles for mass spectrometric analysis. *Anal Chem*, 77, 259-65.
- KOO, H., FALSETTA, M. L. & KLEIN, M. I. 2013. The exopolysaccharide matrix: a virulence determinant of cariogenic biofilm. *J Dent Res*, 92, 1065-73.
- KOO, H. & YAMADA, K. M. 2016. Dynamic cell-matrix interactions modulate microbial biofilm and tissue 3D microenvironments. *Curr Opin Cell Biol*, 42, 102-112.
- KRISHNAMOORTHY, A. L., LEMUS, A. A., SOLOMON, A. P., VALM, A. M. & NEELAKANTAN, P. 2020. Interactions between *Candida albicans* and *Enterococcus faecalis* in an organotypic oral epithelial model. *Microorganisms*, 8, 1771.
- KRUPPA, M., GOINS, T., CUTLER, J. E., LOWMAN, D., WILLIAMS, D., CHAUHAN, N., MENON, V., SINGH, P., LI, D. & CALDERONE, R. 2003. The role of the *Candida albicans* histidine kinase [CHK1] gene in the regulation of cell wall mannan and glucan biosynthesis. *FEMS Yeast Res*, 3, 289-99.
- KUBO, I., FUJITA, K. & LEE, S. H. 2001. Antifungal mechanism of polygodial. *J Agric Food Chem*, 49, 1607-11.
- KUMAMOTO, C. A. 2008. Molecular mechanisms of mechanosensing and their roles in fungal contact sensing. *Nat Rev Microbiol*, 6, 667-73.
- KURAMITSU, H. K., HE, X., LUX, R., ANDERSON, M. H. & SHI, W. 2007. Interspecies interactions within oral microbial communities. *Microbiology and molecular biology reviews : MMBR*, 71, 653-670.
- LAI, L. & BARNARD, A. S. 2011. Modeling the thermostability of surface functionalisation by oxygen, hydroxyl, and water on nanodiamonds. *Nanoscale*, 3, 2566-75.
- LAMB, J., CRAWFORD, E. D., PECK, D., MODELL, J. W., BLAT, I. C., WROBEL, M. J., LERNER, J., BRUNET, J.-P., SUBRAMANIAN, A. & ROSS, K. N. 2006. The Connectivity Map: using gene-expression signatures to connect small molecules, genes, and disease. *science*, 313, 1929-1935.
- LECLERC, R. 1990. [Sodium hypochlorite in endodontics]. *J Dent Que*, 27, 13-6.
- LECLERCQ, R. 1997. Enterococci acquire new kinds of resistance. *Clinical Infectious Diseases*, 24, S80-S84.
- LEE, D. K., KEE, T., LIANG, Z., HSIU, D., MIYA, D., WU, B., OSAWA, E., CHOW, E. K., SUNG, E. C., KANG, M. K. & HO, D. 2017. Clinical validation of a nanodiamond-embedded thermoplastic biomaterial. *Proc Natl Acad Sci U S A*, 114, E9445-E9454.
- LEE, D. K., KIM, S. V., LIMANSUBROTO, A. N., YEN, A., SOUNDIA, A., WANG, C. Y., SHI, W., HONG, C., TETRADIS, S., KIM, Y., PARK, N. H., KANG, M. K. & HO, D. 2015. Nanodiamond-Gutta Percha Composite Biomaterials for Root Canal Therapy. *ACS Nano*, 9, 11490-501.
- LEE, K., SILVA, E. A. & MOONEY, D. J. 2011. Growth factor delivery-based tissue engineering: general approaches and a review of recent developments. *J R Soc Interface*, 8, 153-70.
- LEE, S. H., LEE, J. R., LUNDE, C. S. & KUBO, I. 1999. In vitro antifungal susceptibilities of *Candida albicans* and other fungal pathogens to polygodial, a sesquiterpene dialdehyde. *Planta Med*, 65, 204-8.

- LEFTEROVA, M. I., SUAREZ, C. J., BANAEI, N. & PINSKY, B. A. 2015. Next-Generation Sequencing for Infectious Disease Diagnosis and Management: A Report of the Association for Molecular Pathology. *J Mol Diagn*, 17, 623-34.
- LI, F., SVAROVSKY, M. J., KARLSSON, A. J., WAGNER, J. P., MARCHILLO, K., OSHEL, P., ANDES, D. & PALECEK, S. P. 2007. Eap1p, an adhesin that mediates *Candida albicans* biofilm formation in vitro and in vivo. *Eukaryotic cell*, 6, 931-939.
- LI, H., HANDSAKER, B., WYSOKER, A., FENNEL, T., RUAN, J., HOMER, N., MARTH, G., ABECASIS, G., DURBIN, R. & GENOME PROJECT DATA PROCESSING, S. 2009. The Sequence Alignment/Map format and SAMtools. *Bioinformatics*, 25, 2078-9.
- LI, L., HSIAO, W. W., NANDAKUMAR, R., BARBUTO, S. M., MONGODIN, E. F., PASTER, B. J., FRASER-LIGGETT, C. M. & FOUAD, A. F. 2010. Analyzing endodontic infections by deep coverage pyrosequencing. *J Dent Res*, 89, 980-4.
- LI, L., MENDIS, N., TRIGUI, H., OLIVER, J. D. & FAUCHER, S. P. 2014. The importance of the viable but non-culturable state in human bacterial pathogens. *Front Microbiol*, 5, 258.
- LI, X. & SUN, S. 2016. Targeting the fungal calcium-calcineurin signaling network in overcoming drug resistance. *Future Science*.
- LI, X., YEH, Y. C., GIRI, K., MOUT, R., LANDIS, R. F., PRAKASH, Y. S. & ROTELLO, V. M. 2015. Control of nanoparticle penetration into biofilms through surface design. *Chem Commun (Camb)*, 51, 282-5.
- LIEBSCH, C., PITCHIKA, V., PINK, C., SAMIETZ, S., KASTENMÜLLER, G., ARTATI, A., SUHRE, K., ADAMSKI, J., NAUCK, M. & VÖLZKE, H. 2019. The saliva metabolome in association to oral health status. *Journal of dental research*, 98, 642-651.
- LINDBERG, E., HAMMARSTROM, H., ATAOLLAHY, N. & KONDORI, N. 2019. Species distribution and antifungal drug susceptibilities of yeasts isolated from the blood samples of patients with candidemia. *Sci Rep*, 9, 3838.
- LINDER, M. C. & HAZEGH-AZAM, M. 1996. Copper biochemistry and molecular biology. *Am J Clin Nutr*, 63, 797S-811S.
- LINDQUIST, S. 1992. Heat-shock proteins and stress tolerance in microorganisms. *Curr Opin Genet Dev*, 2, 748-55.
- LIU, W., RODER, H. L., MADSEN, J. S., BJARNSHOLT, T., SORENSEN, S. J. & BURMOLLE, M. 2016. Interspecific Bacterial Interactions are Reflected in Multispecies Biofilm Spatial Organization. *Front Microbiol*, 7, 1366.
- LIU, Y. & FILLER, S. G. 2011. *Candida albicans* Als3, a multifunctional adhesin and invasin. *Eukaryot Cell*, 10, 168-73.
- LLEO, M. M., BONATO, B., TAFI, M. C., SIGNORETTO, C., BOARETTI, M. & CANEPARI, P. 2001. Resuscitation rate in different enterococcal species in the viable but non-culturable state. *J Appl Microbiol*, 91, 1095-102.
- LOK, B., ADAM, M. A. A., KAMAL, L. Z. M., CHUKWUDI, N. A., SANDAI, R. & SANDAI, D. 2021. The assimilation of different carbon sources in *Candida albicans*: Fitness and pathogenicity. *Med Mycol*, 59, 115-125.
- LOVE, M. I., HUBER, W. & ANDERS, S. 2014. Moderated estimation of fold change and dispersion for RNA-seq data with DESeq2. *Genome Biol*, 15, 550.
- LOVE, R. M., MCMILLAN, M. D. & JENKINSON, H. F. 1997. Invasion of dentinal tubules by oral streptococci is associated with collagen recognition

- mediated by the antigen I/II family of polypeptides. *Infect Immun*, 65, 5157-64.
- LU, J.-J., CHANG, T.-Y., PERNG, C.-L. & LEE, S.-Y. 2005. The vanB2 gene cluster of the majority of vancomycin-resistant *Enterococcus faecium* isolates from Taiwan is associated with the pbp5 gene and is carried by Tn 5382 containing a novel insertion sequence. *Antimicrobial agents and chemotherapy*, 49, 3937-3939.
- MACHADO DE OLIVEIRA, J. C., SIQUEIRA, J. F., JR., ROCAS, I. N., BAUMGARTNER, J. C., XIA, T., PEIXOTO, R. S. & ROSADO, A. S. 2007. Bacterial community profiles of endodontic abscesses from Brazilian and USA subjects as compared by denaturing gradient gel electrophoresis analysis. *Oral Microbiol Immunol*, 22, 14-8.
- MACIEL, E. I., VALLE AREVALO, A., ZIMAN, B., NOBILE, C. J. & OVIEDO, N. J. 2020. Epithelial Infection With *Candida albicans* Elicits a Multi-System Response in Planarians. *Front Microbiol*, 11, 629526.
- MAINI REKDAL, V., BESS, E. N., BISANZ, J. E., TURNBAUGH, P. J. & BALSUS, E. P. 2019. Discovery and inhibition of an interspecies gut bacterial pathway for Levodopa metabolism. *Science*, 364, eaau6323.
- MANOIL, D., AL-MANEI, K. & BELIBASAKIS, G. N. 2020. A Systematic Review of the Root Canal Microbiota Associated with Apical Periodontitis: Lessons from Next-Generation Sequencing. *Proteomics Clin Appl*, 14, e1900060.
- MARSH, P. D. 2005. Dental plaque: biological significance of a biofilm and community life-style. *J Clin Periodontol*, 32 Suppl 6, 7-15.
- MARSH, P. D., DO, T., BEIGHTON, D. & DEVINE, D. A. 2016. Influence of saliva on the oral microbiota. *Periodontol 2000*, 70, 80-92.
- MARTIN, R., ALBRECHT-ECKARDT, D., BRUNKE, S., HUBE, B., HÜNNIGER, K. & KURZAI, O. 2013. A core filamentation response network in *Candida albicans* is restricted to eight genes. *PLoS one*, 8, e58613.
- MARTÍNEZ-MARTÍNEZ, L., PASCUAL, A. & JACOBY, G. A. 1998. Quinolone resistance from a transferable plasmid. *The Lancet*, 351, 797-799.
- MASON, K. L., DOWNWARD, J. R. E., FALKOWSKI, N. R., YOUNG, V. B., KAO, J. Y., HUFFNAGLE, G. B. & DEEPE, G. S. 2012a. Interplay between the Gastric Bacterial Microbiota and *Candida albicans* during Postantibiotic Recolonization and Gastritis. *Infection and Immunity*, 80, 150-158.
- MASON, K. L., ERB DOWNWARD, J. R., MASON, K. D., FALKOWSKI, N. R., EATON, K. A., KAO, J. Y., YOUNG, V. B. & HUFFNAGLE, G. B. 2012b. *Candida albicans* and bacterial microbiota interactions in the cecum during recolonization following broad-spectrum antibiotic therapy. *Infect Immun*, 80, 3371-80.
- MAYER, F. L., WILSON, D. & HUBE, B. 2013. *Candida albicans* pathogenicity mechanisms. *Virulence*, 4, 119-28.
- MAYER, F. L., WILSON, D., JACOBSEN, I. D., MIRAMON, P., GROSSE, K. & HUBE, B. 2012. The novel *Candida albicans* transporter Dur31 is a multi-stage pathogenicity factor. *PLoS Pathog*, 8, e1002592.
- MCCALL, A. D., PATHIRANA, R. U., PRABHAKAR, A., CULLEN, P. J. & EDGERTON, M. 2019. *Candida albicans* biofilm development is governed by cooperative attachment and adhesion maintenance proteins. *NPJ Biofilms Microbiomes*, 5, 21.
- MCCLURE, R. S. 2019. Toward a better understanding of species interactions through network biology. *Msystems*, 4, e00114-19.

- MCCLURE, R. S., OVERALL, C. C., HILL, E. A., SONG, H. S., CHARANIA, M., BERNSTEIN, H. C., MCDERMOTT, J. E. & BELIAEV, A. S. 2018. Species-specific transcriptomic network inference of interspecies interactions. *ISME J*, 12, 2011-2023.
- MCKLOUD, E., DELANEY, C., SHERRY, L., KEAN, R., WILLIAMS, S., METCALFE, R., THOMAS, R., RICHARDSON, R., GERASIMIDIS, K., NILE, C. J., WILLIAMS, C. & RAMAGE, G. 2021. Recurrent Vulvovaginal Candidiasis: a Dynamic Interkingdom Biofilm Disease of *Candida* and *Lactobacillus*. *mSystems*, 6, e0062221.
- MEDERSKI-SAMORAJ, B. D. & MURRAY, B. E. 1983. High-level resistance to gentamicin in clinical isolates of enterococci. *Journal of Infectious Diseases*, 147, 751-757.
- MERGONI, G., PERCUDANI, D., LODI, G., BERTANI, P. & MANFREDI, M. 2018. Prevalence of *Candida* Species in Endodontic Infections: Systematic Review and Meta-analysis. *J Endod*, 44, 1616-1625 e9.
- MERRILL, A. T. & CLARK, W. M. 1928. Some conditions affecting the production of gelatinase by *Proteus* bacteria. *Journal of bacteriology*, 15, 267-296.
- METZGER, Z., SOLOMONOV, M. & KFIR, A. 2013. The role of mechanical instrumentation in the cleaning of root canals. *Endodontic Topics*, 29, 87-109.
- MICHELICH, V., PASHLEY, D. H. & WHITFORD, G. M. 1978. Dentin permeability: a comparison of functional versus anatomical tubular radii. *J Dent Res*, 57, 1019-24.
- MILES, A. A., MISRA, S. S. & IRWIN, J. O. 1938. The estimation of the bactericidal power of the blood. *The Journal of Hygiene*, 38, 732-749.
- MOCHALIN, V. N., SHENDEROVA, O., HO, D. & GOGOTSI, Y. 2012. The properties and applications of nanodiamonds. *Nature nanotechnology*, 7, 11-23.
- MOFFAT, J. G., VINCENT, F., LEE, J. A., EDER, J. & PRUNOTTO, M. 2017. Opportunities and challenges in phenotypic drug discovery: an industry perspective. *Nat Rev Drug Discov*, 16, 531-543.
- MOHAMMADI, Z. & ABBOTT, P. V. 2009. The properties and applications of chlorhexidine in endodontics. *Int Endod J*, 42, 288-302.
- MOHAMMADI, Z. & SHALAVI, S. 2013. Antimicrobial activity of sodium hypochlorite in endodontics. *J Mass Dent Soc*, 62, 28-31.
- MOHAMMADI, Z., SHALAVI, S., MOEINTAGHAVI, A. & JAFARZADEH, H. 2017. A Review Over Benefits and Drawbacks of Combining Sodium Hypochlorite with Other Endodontic Materials. *Open Dent J*, 11, 661-669.
- MOHLER, E. R., 3RD, BALLANTYNE, C. M., DAVIDSON, M. H., HANEFELD, M., RUILOPE, L. M., JOHNSON, J. L., ZALEWSKI, A. & DARAPLADIB, I. 2008. The effect of darapladib on plasma lipoprotein-associated phospholipase A2 activity and cardiovascular biomarkers in patients with stable coronary heart disease or coronary heart disease risk equivalent: the results of a multicenter, randomized, double-blind, placebo-controlled study. *J Am Coll Cardiol*, 51, 1632-41.
- MOLINA, D. M., JAFARI, R., IGNATUSHCHENKO, M., SEKI, T., LARSSON, E. A., DAN, C., SREEKUMAR, L., CAO, Y. & NORDLUND, P. 2013. Monitoring drug target engagement in cells and tissues using the cellular thermal shift assay. *Science*, 341, 84-87.
- MOLLER, A. J. 1966. Microbiological examination of root canals and periapical tissues of human teeth. Methodological studies. *Odontol Tidskr*, 74, Suppl:1-380.

- MOLLER, A. J., FABRICIUS, L., DAHLEN, G., SUNDQVIST, G. & HAPPONEN, R. P. 2004. Apical periodontitis development and bacterial response to endodontic treatment. Experimental root canal infections in monkeys with selected bacterial strains. *Eur J Oral Sci*, 112, 207-15.
- MOLOBELA, I. P. & ILUNGA, F. M. 2012. Impact of bacterial biofilms: the importance of quantitative biofilm studies. *Annals of Microbiology*, 62, 461-467.
- MOLVEN, O., OLSEN, I. & KEREKES, K. 1991. Scanning electron microscopy of bacteria in the apical part of root canals in permanent teeth with periapical lesions. *Endod Dent Traumatol*, 7, 226-9.
- MONTELONGO-JAUREGUI, D., SRINIVASAN, A., RAMASUBRAMANIAN, A. K. & LOPEZ-RIBOT, J. L. 2016. An in vitro model for oral mixed biofilms of *Candida albicans* and *Streptococcus gordonii* in synthetic saliva. *Frontiers in microbiology*, 7, 686.
- MONZAVI, A., ESHRAGHI, S., HASHEMIAN, R. & MOMEN-HERAVI, F. 2015. In vitro and ex vivo antimicrobial efficacy of nano-MgO in the elimination of endodontic pathogens. *Clin Oral Investig*, 19, 349-56.
- MOREILLON, P. & QUE, Y. A. 2004. Infective endocarditis. *Lancet*, 363, 139-49.
- MORSE, D. J., WILSON, M. J., WEI, X., BRADSHAW, D. J., LEWIS, M. A. O. & WILLIAMS, D. W. 2019. Modulation of *Candida albicans* virulence in in vitro biofilms by oral bacteria. *Lett Appl Microbiol*, 68, 337-343.
- MORSE, D. R. 1970. The endodontic culture technique: a critical evaluation. *Oral Surg Oral Med Oral Pathol*, 30, 540-4.
- MOYES, D. L., WILSON, D., RICHARDSON, J. P., MOGAVERO, S., TANG, S. X., WERNECKE, J., HOF, S., GRATACAP, R. L., ROBBINS, J., RUNGLALL, M., MURCIANO, C., BLAGOJEVIC, M., THAVARAJ, S., FORSTER, T. M., HEBECKER, B., KASPER, L., VIZCAY, G., IANCU, S. I., KICHIK, N., HADER, A., KURZAI, O., LUO, T., KRUGER, T., KNIEMEYER, O., COTA, E., BADER, O., WHEELER, R. T., GUTSMANN, T., HUBE, B. & NAGLIK, J. R. 2016. Candidalysin is a fungal peptide toxin critical for mucosal infection. *Nature*, 532, 64-8.
- MUKHERJEE, P. K., MOHAMED, S., CHANDRA, J., KUHN, D., LIU, S., ANTAR, O. S., MUNYON, R., MITCHELL, A. P., ANDES, D., CHANCE, M. R., ROUABHIA, M. & GHANNOUM, M. A. 2006. Alcohol dehydrogenase restricts the ability of the pathogen *Candida albicans* to form a biofilm on catheter surfaces through an ethanol-based mechanism. *Infect Immun*, 74, 3804-16.
- MULLER, E. E., GLAAB, E., MAY, P., VLASSIS, N. & WILMES, P. 2013. Condensing the omics fog of microbial communities. *Trends Microbiol*, 21, 325-33.
- MUNRO, C. A., WHITTON, R. K., HUGHES, H. B., RELLA, M., SELVAGGINI, S. & GOW, N. A. 2003. CHS8-a fourth chitin synthase gene of *Candida albicans* contributes to in vitro chitin synthase activity, but is dispensable for growth. *Fungal Genet Biol*, 40, 146-58.
- MUNSON, M. A., PITT-FORD, T., CHONG, B., WEIGHTMAN, A. & WADE, W. G. 2002. Molecular and cultural analysis of the microflora associated with endodontic infections. *J Dent Res*, 81, 761-6.
- MURAD, A. M., LENG, P., STRAFFON, M., WISHART, J., MACASKILL, S., MACCALLUM, D., SCHNELL, N., TALIBI, D., MARECHAL, D., TEKAIA, F., D'ENFERT, C., GAILLARDIN, C., ODDS, F. C. & BROWN, A. J. 2001. NRG1 represses yeast-hypha morphogenesis and hypha-specific gene expression in *Candida albicans*. *EMBO J*, 20, 4742-52.

- MURAKAMI, S., MEALEY, B. L., MARIOTTI, A. & CHAPPLE, I. L. C. 2018. Dental plaque-induced gingival conditions. *J Clin Periodontol*, 45 Suppl 20, S17-S27.
- MURPHY, M. P. 2009. How mitochondria produce reactive oxygen species. *Biochemical journal*, 417, 1-13.
- MURRAY, B. E. 1990. The life and times of the Enterococcus. *Clinical microbiology reviews*, 3, 46-65.
- MURRAY, C. J., IKUTA, K. S., SHARARA, F., SWETSCHINSKI, L., AGUILAR, G. R., GRAY, A., HAN, C., BISIGNANO, C., RAO, P. & WOOL, E. 2022. Global burden of bacterial antimicrobial resistance in 2019: a systematic analysis. *The Lancet*.
- NADEEM, S. G., SHAFIQ, A., HAKIM, S. T., ANJUM, Y. & KAZM, S. U. 2013. Effect of growth media, pH and temperature on yeast to hyphal transition in *Candida albicans*. *Open Journal of Medical Microbiology*, 3.
- NAENNI, N., THOMA, K. & ZEHNDER, M. 2004. Soft tissue dissolution capacity of currently used and potential endodontic irrigants. *Journal of endodontics*, 30, 785-787.
- NAGAOKA, S., MIYAZAKI, Y., LIU, H. J., IWAMOTO, Y., KITANO, M. & KAWAGOE, M. 1995. Bacterial invasion into dentinal tubules of human vital and nonvital teeth. *J Endod*, 21, 70-3.
- NAGLIK, J. R., CHALLACOMBE, S. J. & HUBE, B. 2003. *Candida albicans* secreted aspartyl proteinases in virulence and pathogenesis. *Microbiol Mol Biol Rev*, 67, 400-28, table of contents.
- NAGLIK, J. R., GAFFEN, S. L. & HUBE, B. 2019. Candidalysin: discovery and function in *Candida albicans* infections. *Curr Opin Microbiol*, 52, 100-109.
- NAIR, P. N. 2004. Pathogenesis of apical periodontitis and the causes of endodontic failures. *Crit Rev Oral Biol Med*, 15, 348-81.
- NAIR, P. N. 2006. On the causes of persistent apical periodontitis: a review. *Int Endod J*, 39, 249-81.
- NAIR, P. R. 1987. Light and electron microscopic studies of root canal flora and periapical lesions. *Journal of endodontics*, 13, 29-39.
- NAJEEB, S., KHURSHID, Z., AGWAN, A. S., ZAFAR, M. S., ALRAHABI, M., QASIM, S. B. & SEFAT, F. 2016. Dental applications of nanodiamonds. *Science of Advanced Materials*, 8, 2064-2070.
- NAKAMURA, M., SHIMIZU, Y., SATO, Y., MIYAZAKI, Y., SATOH, T., MIZUNO, M., KATO, Y., HOSAKA, Y. & FURUSAKO, S. 2007. Toll-like receptor 4 signal transduction inhibitor, M62812, suppresses endothelial cell and leukocyte activation and prevents lethal septic shock in mice. *Eur J Pharmacol*, 569, 237-43.
- NALLAPAREDDY, S. R., QIN, X., WEINSTOCK, G. M., HOOK, M. & MURRAY, B. E. 2000. Enterococcus faecalis adhesin, ace, mediates attachment to extracellular matrix proteins collagen type IV and laminin as well as collagen type I. *Infect Immun*, 68, 5218-24.
- NARAYANAN, L. L. & VAISHNAVI, C. 2010. Endodontic microbiology. *J Conserv Dent*, 13, 233-9.
- NETT, J. E., LEPAK, A. J., MARCHILLO, K. & ANDES, D. R. 2009. Time course global gene expression analysis of an in vivo *Candida* biofilm. *J Infect Dis*, 200, 307-13.
- NETT, J. E., SANCHEZ, H., CAIN, M. T. & ANDES, D. R. 2010. Genetic basis of *Candida* biofilm resistance due to drug-sequestering matrix glucan. *The Journal of infectious diseases*, 202, 171-175.

- NGUYEN, N. T., GRELLING, N., WETTELAND, C. L., ROSARIO, R. & LIU, H. 2018. Antimicrobial Activities and Mechanisms of Magnesium Oxide Nanoparticles (nMgO) against Pathogenic Bacteria, Yeasts, and Biofilms. *Sci Rep*, 8, 16260.
- NICHOLLS, S., MACCALLUM, D. M., KAFFARNIK, F. A., SELWAY, L., PECK, S. C. & BROWN, A. J. 2011. Activation of the heat shock transcription factor Hsf1 is essential for the full virulence of the fungal pathogen *Candida albicans*. *Fungal Genet Biol*, 48, 297-305.
- NISHIMURA, H., KATAGIRI, K., SATO, K., MAYAMA, M. & SHIMAOKA, N. 1956. Toyocamycin, a new anti-candida antibiotics. *J Antibiot (Tokyo)*, 9, 60-2.
- NOBILE, C. J., FOX, E. P., NETT, J. E., SORRELLS, T. R., MITROVICH, Q. M., HERNDAY, A. D., TUCH, B. B., ANDES, D. R. & JOHNSON, A. D. 2012. A recently evolved transcriptional network controls biofilm development in *Candida albicans*. *Cell*, 148, 126-38.
- NOBILE, C. J. & MITCHELL, A. P. 2006. Genetics and genomics of *Candida albicans* biofilm formation. *Cellular microbiology*, 8, 1382-1391.
- NOBILE, C. J., NETT, J. E., HERNDAY, A. D., HOMANN, O. R., DENEALD, J. S., NANTEL, A., ANDES, D. R., JOHNSON, A. D. & MITCHELL, A. P. 2009. Biofilm matrix regulation by *Candida albicans* Zap1. *PLoS Biol*, 7, e1000133.
- NOBILE, C. J., SCHNEIDER, H. A., NETT, J. E., SHEPPARD, D. C., FILLER, S. G., ANDES, D. R. & MITCHELL, A. P. 2008. Complementary adhesin function in *C. albicans* biofilm formation. *Curr Biol*, 18, 1017-24.
- NOOR, E., CHERKAOUI, S. & SAUER, U. 2019. Biological insights through omics data integration. *Current Opinion in Systems Biology*, 15, 39-47.
- NORONHA, V. T., PAULA, A. J., DURAN, G., GALEMBECK, A., COGO-MULLER, K., FRANZ-MONTAN, M. & DURAN, N. 2017. Silver nanoparticles in dentistry. *Dent Mater*, 33, 1110-1126.
- NOROUZI, N., ONG, Y., DAMLE, V. G., HABIBI NAJAFI, M. B. & SCHIRHAGL, R. 2020. Effect of medium and aggregation on antibacterial activity of nanodiamonds. *Mater Sci Eng C Mater Biol Appl*, 112, 110930.
- NOVERR, M. C. & HUFFNAGLE, G. B. 2004. Regulation of *Candida albicans* morphogenesis by fatty acid metabolites. *Infect Immun*, 72, 6206-10.
- O'DONNELL, L. E., SMITH, K., WILLIAMS, C., NILE, C. J., LAPPIN, D. F., BRADSHAW, D., LAMBERT, M., ROBERTSON, D. P., BAGG, J. & HANNAH, V. 2016. Dentures are a reservoir for respiratory pathogens. *Journal of Prosthodontics*, 25, 99-104.
- O'DONOGHUE, M. L., BRAUNWALD, E., WHITE, H. D., LUKAS, M. A., TARKA, E., STEG, P. G., HOCHMAN, J. S., BODE, C., MAGGIONI, A. P., IM, K., SHANNON, J. B., DAVIES, R. Y., MURPHY, S. A., CRUGNALE, S. E., WIVIOTT, S. D., BONACA, M. P., WATSON, D. F., WEAVER, W. D., SERRUYS, P. W., CANNON, C. P., INVESTIGATORS, S.-T. & STEEN, D. L. 2014. Effect of darapladib on major coronary events after an acute coronary syndrome: the SOLID-TIMI 52 randomized clinical trial. *JAMA*, 312, 1006-15.
- O'MEARA, T. R. & COWEN, L. E. 2014. Hsp90-dependent regulatory circuitry controlling temperature-dependent fungal development and virulence. *Cellular microbiology*, 16, 473-481.
- O'MEARA, T. R., ROBBINS, N. & COWEN, L. E. 2017. The Hsp90 Chaperone Network Modulates *Candida* Virulence Traits. *Trends in microbiology*, 25, 809-819.

- OKONECHNIKOV, K., CONESA, A. & GARCÍA-ALCALDE, F. 2016. Qualimap 2: advanced multi-sample quality control for high-throughput sequencing data. *Bioinformatics*, 32, 292-294.
- OKSHEVSKY, M. & MEYER, R. L. 2015. The role of extracellular DNA in the establishment, maintenance and perpetuation of bacterial biofilms. *Critical reviews in microbiology*, 41, 341-352.
- ONG, S. Y., CHIPAUX, M., NAGL, A. & SCHIRHAGL, R. 2017. Shape and crystallographic orientation of nanodiamonds for quantum sensing. *Phys Chem Chem Phys*, 19, 10748-10752.
- ONG, S. Y., VAN HARMELEN, R. J. J., NOROUZI, N., OFFENS, F., VENEMA, I. M., HABIBI NAJAFI, M. B. & SCHIRHAGL, R. 2018. Interaction of nanodiamonds with bacteria. *Nanoscale*, 10, 17117-17124.
- ONO, S., MURATANI, T. & MATSUMOTO, T. 2005. Mechanisms of resistance to imipenem and ampicillin in *Enterococcus faecalis*. *Antimicrob Agents Chemother*, 49, 2954-8.
- OPPENHEIMER-SHAANAN, Y., SIBONY-NEVO, O., BLOOM-ACKERMANN, Z., SUISSA, R., STEINBERG, N., KARTVELISHVILI, E., BRUMFELD, V. & KOLODKIN-GAL, I. 2016. Spatio-temporal assembly of functional mineral scaffolds within microbial biofilms. *NPJ biofilms and microbiomes*, 2, 1-10.
- OPREA, T. I., TROPSHA, A., FAULON, J. L. & RINTOUL, M. D. 2007. Systems chemical biology. *Nat Chem Biol*, 3, 447-50.
- ORSTAVIK, D. & HAAPASALO, M. 1990. Disinfection by endodontic irrigants and dressings of experimentally infected dentinal tubules. *Endod Dent Traumatol*, 6, 142-9.
- PAIK, H., CHUNG, A. Y., PARK, H. C., PARK, R. W., SUK, K., KIM, J., KIM, H., LEE, K. & BUTTE, A. J. 2015. Repurpose terbutaline sulfate for amyotrophic lateral sclerosis using electronic medical records. *Sci Rep*, 5, 8580.
- PALMER, K. L., KOS, V. N. & GILMORE, M. S. 2010. Horizontal gene transfer and the genomics of enterococcal antibiotic resistance. *Curr Opin Microbiol*, 13, 632-9.
- PALMITER, R. D. 1998. The elusive function of metallothioneins. *Proc Natl Acad Sci U S A*, 95, 8428-30.
- PANÁČEK, A., KVÍTEK, L., SMÉKALOVÁ, M., VEČEŘOVÁ, R., KOLÁŘ, M., RÖDEROVÁ, M., DYČKA, F., ŠEBELA, M., PRUCEK, R. & TOMANEC, O. 2018. Bacterial resistance to silver nanoparticles and how to overcome it. *Nature Nanotechnology*, 13, 65-71.
- PARK, O. J., YI, H., JEON, J. H., KANG, S. S., KOO, K. T., KUM, K. Y., CHUN, J., YUN, C. H. & HAN, S. H. 2015. Pyrosequencing Analysis of Subgingival Microbiota in Distinct Periodontal Conditions. *J Dent Res*, 94, 921-7.
- PARK, S. Y., KIM, K. M., LEE, J. H., SEO, S. J. & LEE, I. H. 2007. Extracellular gelatinase of *Enterococcus faecalis* destroys a defense system in insect hemolymph and human serum. *Infect Immun*, 75, 1861-9.
- PASSERI, D., RINALDI, F., INGALLINA, C., CARAFA, M., ROSSI, M., TERRANOVA, M. L. & MARIANECCI, C. 2015. Biomedical Applications of Nanodiamonds: An Overview. *J Nanosci Nanotechnol*, 15, 972-88.
- PASTER, B. J., OLSEN, I., AAS, J. A. & DEWHIRST, F. E. 2006. The breadth of bacterial diversity in the human periodontal pocket and other oral sites. *Periodontol 2000*, 42, 80-7.
- PATEL, B., COCKERILL, F., BRADFORD, P., ELIOPOULOS, G., HINDLER, J. & JENKINS, S. 2015. M07-A10 Methods for Dilution Antimicrobial

- Susceptibility Tests for Bacteria That Grow Aerobically; Approved Standard—. Clinical and Laboratory Standards Institute.
- PATIDAR, R. K., GUPTA, M. K. & SINGH, V. 2013. Phenotypic detection of virulence traits and antibiotic susceptibility of endodontic *Enterococcus faecalis* isolates. *American Journal of Microbiological Research*, 1, 4-9.
- PATRA, J. K. & BAEK, K. H. 2017. Antibacterial Activity and Synergistic Antibacterial Potential of Biosynthesized Silver Nanoparticles against Foodborne Pathogenic Bacteria along with its Anticandidal and Antioxidant Effects. *Front Microbiol*, 8, 167.
- PATTERSON, M. J., MCKENZIE, C. G., SMITH, D. A., DA SILVA DANTAS, A., SHERSTON, S., VEAL, E. A., MORGAN, B. A., MACCALLUM, D. M., ERWIG, L.-P. & QUINN, J. 2013. Ybp1 and Gpx3 signaling in *Candida albicans* govern hydrogen peroxide-induced oxidation of the Cap1 transcription factor and macrophage escape. *Antioxidants & redox signaling*, 19, 2244-2260.
- PAYNE, D. J., GWYNN, M. N., HOLMES, D. J. & POMPLIANO, D. L. 2007. Drugs for bad bugs: confronting the challenges of antibacterial discovery. *Nat Rev Drug Discov*, 6, 29-40.
- PECIULIENE, V., REYNAUD, A. H., BALCIUNIENE, I. & HAAPASALO, M. 2001. Isolation of yeasts and enteric bacteria in root-filled teeth with chronic apical periodontitis. *Int Endod J*, 34, 429-34.
- PEREVEDENTSEVA, E., ALI, N., KARMENYAN, A., SKOVORODKIN, I., PRUNSKAITE-HYYRYLAINEN, R., VAINIO, S., CHENG, C. L. & KINNUNEN, M. 2019. Optical Studies of Nanodiamond-Tissue Interaction: Skin Penetration and Localization. *Materials (Basel)*, 12.
- PERLMUTTER, J. I., FORBES, L. T., KRYSAN, D. J., EBSWORTH-MOJICA, K., COLQUHOUN, J. M., WANG, J. L., DUNMAN, P. M. & FLAHERTY, D. P. 2014. Repurposing the antihistamine terfenadine for antimicrobial activity against *Staphylococcus aureus*. *J Med Chem*, 57, 8540-62.
- PERSOON, I. F., BUIJS, M. J., OZOK, A. R., CRIELAARD, W., KROM, B. P., ZAURA, E. & BRANDT, B. W. 2017a. The mycobiome of root canal infections is correlated to the bacteriome. *Clin Oral Investig*, 21, 1871-1881.
- PERSOON, I. F., CRIELAARD, W. & OZOK, A. R. 2017b. Prevalence and nature of fungi in root canal infections: a systematic review and meta-analysis. *Int Endod J*, 50, 1055-1066.
- PERSOON, I. F. & OZOK, A. R. 2017. Definitions and Epidemiology of Endodontic Infections. *Curr Oral Health Rep*, 4, 278-285.
- PETERS, B. M., OVCHINNIKOVA, E. S., KROM, B. P., SCHLECHT, L. M., ZHOU, H., HOYER, L. L., BUSSCHER, H. J., VAN DER MEI, H. C., JABRA-RIZK, M. A. & SHIRTLIFF, M. E. 2012. *Staphylococcus aureus* adherence to *Candida albicans* hyphae is mediated by the hyphal adhesin Als3p. *Microbiology*, 158, 2975.
- PETERSON, B. W., HE, Y., REN, Y., ZERDOUM, A., LIBERA, M. R., SHARMA, P. K., VAN WINKELHOFF, A.-J., NEUT, D., STOODLEY, P. & VAN DER MEI, H. C. 2015. Viscoelasticity of biofilms and their recalcitrance to mechanical and chemical challenges. *FEMS microbiology reviews*, 39, 234-245.
- PETERSON, E. & KAUR, P. 2018. Antibiotic Resistance Mechanisms in Bacteria: Relationships Between Resistance Determinants of Antibiotic Producers, Environmental Bacteria, and Clinical Pathogens. *Front Microbiol*, 9, 2928.

- PETROSINO, J. F., HIGHLANDER, S., LUNA, R. A., GIBBS, R. A. & VERSALOVIC, J. 2009. Metagenomic pyrosequencing and microbial identification. *Clin Chem*, 55, 856-66.
- PIERCE, C. G., UPPULURI, P., TRISTAN, A. R., WORMLEY, F. L., JR., MOWAT, E., RAMAGE, G. & LOPEZ-RIBOT, J. L. 2008. A simple and reproducible 96-well plate-based method for the formation of fungal biofilms and its application to antifungal susceptibility testing. *Nat Protoc*, 3, 1494-500.
- PINU, F. R., BEALE, D. J., PATEN, A. M., KOUREMENOS, K., SWARUP, S., SCHIRRA, H. J. & WISHART, D. 2019a. Systems Biology and Multi-Omics Integration: Viewpoints from the Metabolomics Research Community. *Metabolites*, 9.
- PINU, F. R., GOLDANSAZ, S. A. & JAINE, J. 2019b. Translational Metabolomics: Current Challenges and Future Opportunities. *Metabolites*, 9.
- PIRES-BOUCAS, P. D., IZUMI, E., FURLANETO-MAIA, L., STURION, L. & SUZART, S. 2010. Effects of environmental and nutritional factors on gelatinolytic activity by *Enterococcus faecalis* strains isolated from clinical sources. *African Journal of Microbiology Research*, 4, 969-976.
- POLSON, E. S., KUCHLER, V. B., ABBOSH, C., ROSS, E. M., MATHEW, R. K., BEARD, H. A., DA SILVA, B., HOLDING, A. N., BALLEREAU, S., CHUNTHARPURSAT-BON, E., WILLIAMS, J., GRIFFITHS, H. B. S., SHAO, H., PATEL, A., DAVIES, A. J., DROOP, A., CHUMAS, P., SHORT, S. C., LORGER, M., GESTWICKI, J. E., ROBERTS, L. D., BON, R. S., ALLISON, S. J., ZHU, S., MARKOWETZ, F. & WURDAK, H. 2018. KHS101 disrupts energy metabolism in human glioblastoma cells and reduces tumor growth in mice. *Sci Transl Med*, 10.
- PONDE, N. O., LORTAL, L., RAMAGE, G., NAGLIK, J. R. & RICHARDSON, J. P. 2021. *Candida albicans* biofilms and polymicrobial interactions. *Crit Rev Microbiol*, 47, 91-111.
- PORTELA, C. A., SMART, K. F., TUMANOV, S., COOK, G. M. & VILLAS-BOAS, S. G. 2014. Global metabolic response of *Enterococcus faecalis* to oxygen. *J Bacteriol*, 196, 2012-22.
- PRADA, I., MICO-MUNOZ, P., GINER-LLUESMA, T., MICO-MARTINEZ, P., COLLADO-CASTELLANO, N. & MANZANO-SAIZ, A. 2019. Influence of microbiology on endodontic failure. Literature review. *Med Oral Patol Oral Cir Bucal*, 24, e364-e372.
- PREDA, V. G. & SĂNDULESCU, O. 2019. Communication is the key: biofilms, quorum sensing, formation and prevention. *Discoveries*, 7.
- PRILL, S. K., KLINKERT, B., TIMPEL, C., GALE, C. A., SCHROPPEL, K. & ERNST, J. F. 2005. PMT family of *Candida albicans*: five protein mannosyltransferase isoforms affect growth, morphogenesis and antifungal resistance. *Mol Microbiol*, 55, 546-60.
- PRISTOV, K. E. & GHANNOUM, M. A. 2019. Resistance of *Candida* to azoles and echinocandins worldwide. *Clin Microbiol Infect*, 25, 792-798.
- PROCTOR, R. A., VON EIFF, C., KAHL, B. C., BECKER, K., MCNAMARA, P., HERRMANN, M. & PETERS, G. 2006. Small colony variants: a pathogenic form of bacteria that facilitates persistent and recurrent infections. *Nat Rev Microbiol*, 4, 295-305.
- PUSHPAKOM, S., IORIO, F., EYERS, P. A., ESCOTT, K. J., HOPPER, S., WELLS, A., DOIG, A., GUILLIAMS, T., LATIMER, J., MCNAMEE, C., NORRIS, A., SANSEAU, P., CAVALLA, D. & PIRMOHAMED, M. 2019. Drug repurposing:

- progress, challenges and recommendations. *Nat Rev Drug Discov*, 18, 41-58.
- QUINDOS, G. 2014. Epidemiology of candidaemia and invasive candidiasis. A changing face. *Rev Iberoam Micol*, 31, 42-8.
- RABE, A., GESELL SALAZAR, M., MICHALIK, S., FUCHS, S., WELK, A., KOCHER, T. & VÖLKER, U. 2019. Metaproteomics analysis of microbial diversity of human saliva and tongue dorsum in young healthy individuals. *Journal of oral microbiology*, 11, 1654786.
- RAMACHANDRAN NAIR, P. N. 1987. Light and electron microscopic studies of root canal flora and periapical lesions. *J Endod*, 13, 29-39.
- RAMAGE, G., SAVILLE, S. P., WICKES, B. L. & LÓPEZ-RIBOT, J. L. 2002. Inhibition of *Candida albicans* biofilm formation by farnesol, a quorum-sensing molecule. *Applied and environmental microbiology*, 68, 5459-5463.
- REUTER, J. A., SPACEK, D. V. & SNYDER, M. P. 2015. High-throughput sequencing technologies. *Mol Cell*, 58, 586-97.
- REYNAUD AF GEIJERSSTAM, A., CULAK, R., MOLENAAR, L., CHATTAWAY, M., ROSLIE, E., PECIULIENE, V., HAAPASALO, M. & SHAH, H. N. 2007. Comparative analysis of virulence determinants and mass spectral profiles of Finnish and Lithuanian endodontic *Enterococcus faecalis* isolates. *Oral Microbiol Immunol*, 22, 87-94.
- RHOADS, A. & AU, K. F. 2015. PacBio Sequencing and Its Applications. *Genomics Proteomics Bioinformatics*, 13, 278-89.
- RICHARDS, D., DAVIES, J. K. & FIGDOR, D. 2010. Starvation survival and recovery in serum of *Candida albicans* compared with *Enterococcus faecalis*. *Oral Surg Oral Med Oral Pathol Oral Radiol Endod*, 110, 125-30.
- RICHTER, K., HASLBECK, M. & BUCHNER, J. 2010. The heat shock response: life on the verge of death. *Mol Cell*, 40, 253-66.
- RICKARD, A. H., GILBERT, P., HIGH, N. J., KOLENBRANDER, P. E. & HANDLEY, P. S. 2003. Bacterial coaggregation: an integral process in the development of multi-species biofilms. *Trends Microbiol*, 11, 94-100.
- RICUCCI, D. & SIQUEIRA, J. F., JR. 2010. Biofilms and apical periodontitis: study of prevalence and association with clinical and histopathologic findings. *J Endod*, 36, 1277-88.
- RICUCCI, D., SIQUEIRA, J. F., JR., BATE, A. L. & PITT FORD, T. R. 2009. Histologic investigation of root canal-treated teeth with apical periodontitis: a retrospective study from twenty-four patients. *J Endod*, 35, 493-502.
- RIGGLE, P. J. & KUMAMOTO, C. A. 2000. Role of a *Candida albicans* P1-type ATPase in resistance to copper and silver ion toxicity. *J Bacteriol*, 182, 4899-905.
- RINDUM, J. L., STENDERUP, A. & HOLMSTRUP, P. 1994. Identification of *Candida albicans* types related to healthy and pathological oral mucosa. *J Oral Pathol Med*, 23, 406-12.
- ROBERTSON, S. N., GIBSON, D., MACKAY, W. G., REID, S., WILLIAMS, C. & BIRNEY, R. 2017. Investigation of the antimicrobial properties of modified multilayer diamond-like carbon coatings on 316 stainless steel. *Surface and Coatings Technology*, 314, 72-78.
- RODRIGUES, C. T., DE ANDRADE, F., DE VASCONCELOS, L., MIDENA, R., PEREIRA, T., KUGA, M., DUARTE, M. & BERNARDINELLI, N. 2018. Antibacterial properties of silver nanoparticles as a root canal irrigant against

- Enterococcus faecalis biofilm and infected dentinal tubules. *International Endodontic Journal*, 51, 901-911.
- ROLPH, H. J., LENNON, A., RIGGIO, M. P., SAUNDERS, W. P., MACKENZIE, D., COLDERO, L. & BAGG, J. 2001. Molecular identification of microorganisms from endodontic infections. *J Clin Microbiol*, 39, 3282-9.
- ROMAN, E., CORREIA, I., SALAZIN, A., FRADIN, C., JOUAULT, T., POULAIN, D., LIU, F. T. & PLA, J. 2016. The Cek1 mediated MAP kinase pathway regulates exposure of alpha1,2 and beta1,2mannosides in the cell wall of *Candida albicans* modulating immune recognition. *Virulence*, 7, 558-77.
- RONAGHI, M., UHLEN, M. & NYREN, P. 1998. A sequencing method based on real-time pyrophosphate. *Science*, 281, 363, 365.
- ROSHDY, N. N., KATAIA, E. M. & HELMY, N. A. 2019. Assessment of antibacterial activity of 2.5% NaOCl, chitosan nano-particles against *Enterococcus faecalis* contaminating root canals with and without diode laser irradiation: an in vitro study. *Acta Odontologica Scandinavica*, 77, 39-43.
- RUTHERFORD, S. T. & BASSLER, B. L. 2012. Bacterial quorum sensing: its role in virulence and possibilities for its control. *Cold Spring Harb Perspect Med*, 2.
- SAGATOVA, A. A., KENIYA, M. V., WILSON, R. K., SABHERWAL, M., TYNDALL, J. D. & MONK, B. C. 2016. Triazole resistance mediated by mutations of a conserved active site tyrosine in fungal lanosterol 14alpha-demethylase. *Sci Rep*, 6, 26213.
- SAHM, D. F., KISSINGER, J., GILMORE, M. S., MURRAY, P. R., MULDER, R., SOLLIDAY, J. & CLARKE, B. 1989. In vitro susceptibility studies of vancomycin-resistant *Enterococcus faecalis*. *Antimicrob Agents Chemother*, 33, 1588-91.
- SAKAMOTO, M., ROCAS, I. N., SIQUEIRA, J. F., JR. & BENNO, Y. 2006. Molecular analysis of bacteria in asymptomatic and symptomatic endodontic infections. *Oral Microbiol Immunol*, 21, 112-22.
- SAMIEI, M., GHASEMI, N., DIVBAND, B., BALAEI, E., HOSIEN SOROUSH BARHAGHI, M. & DIVBAND, A. 2015. Antibacterial efficacy of polymer containing nanoparticles in comparison with sodium hypochlorite in infected root canals. *Minerva Stomatol*, 64, 275-81.
- SANDAI, D., TABANA, Y. & SANDAI, R. 2018. Carbon sources attribute to pathogenicity in *Candida albicans*. *Candida albicans*.
- SANGER, F., NICKLEN, S. & COULSON, A. R. 1977. DNA sequencing with chain-terminating inhibitors. *Proc Natl Acad Sci U S A*, 74, 5463-7.
- SANSEAU, P., AGARWAL, P., BARNES, M. R., PASTINEN, T., RICHARDS, J. B., CARDON, L. R. & MOOSER, V. 2012. Use of genome-wide association studies for drug repositioning. *Nature biotechnology*, 30, 317-320.
- SASSONE, L. M., FIDEL, R. A., FIDEL, S. R., DIAS, M. & HIRATA, R. J. 2003. Antimicrobial activity of different concentrations of NaOCl and chlorhexidine using a contact test. *Braz Dent J*, 14, 99-102.
- SAVILLE, S. P., LAZZELL, A. L., MONTEAGUDO, C. & LOPEZ-RIBOT, J. L. 2003. Engineered control of cell morphology in vivo reveals distinct roles for yeast and filamentous forms of *Candida albicans* during infection. *Eukaryot Cell*, 2, 1053-60.
- SCHAUDINN, C., CARR, G., GORUR, A., JARAMILLO, D., COSTERTON, J. W. & WEBSTER, P. 2009. Imaging of endodontic biofilms by combined microscopy (FISH/cLSM - SEM). *J Microsc*, 235, 124-7.

- SCHLEIFER, K. H. & KILPPERBALZ, R. 1984. Transfer of *Streptococcus-Faecalis* and *Streptococcus-Faecium* to the Genus *Enterococcus* Nom Rev as *Enterococcus-Faecalis* Comb-Nov and *Enterococcus-Faecium* Comb-Nov. *International Journal of Systematic Bacteriology*, 34, 31-34.
- SCHRAND, A. M., HUANG, H., CARLSON, C., SCHLAGER, J. J., OMACR SAWA, E., HUSSAIN, S. M. & DAI, L. 2007. Are diamond nanoparticles cytotoxic? *J Phys Chem B*, 111, 2-7.
- SEASHORE-LUDLOW, B., REES, M. G., CHEAH, J. H., COKOL, M., PRICE, E. V., COLETTI, M. E., JONES, V., BODYCOMBE, N. E., SOULE, C. K., GOULD, J., ALEXANDER, B., LI, A., MONTGOMERY, P., WAWER, M. J., KURU, N., KOTZ, J. D., HON, C. S., MUNOZ, B., LIEFELD, T., DANCİK, V., BITTKER, J. A., PALMER, M., BRADNER, J. E., SHAMJI, A. F., CLEMONS, P. A. & SCHREIBER, S. L. 2015. Harnessing Connectivity in a Large-Scale Small-Molecule Sensitivity Dataset. *Cancer Discov*, 5, 1210-23.
- SEDGLEY, C., BUCK, G. & APPELBE, O. 2006. Prevalence of *Enterococcus faecalis* at Multiple Oral Sites in Endodontic Patients Using Culture and PCR. *Journal of Endodontics*, 32, 104-109.
- SEDGLEY, C. M., LENNAN, S. L. & CLEWELL, D. B. 2004. Prevalence, phenotype and genotype of oral enterococci. *Oral Microbiol Immunol*, 19, 95-101.
- SEDGLEY, C. M., MOLANDER, A., FLANNAGAN, S. E., NAGEL, A. C., APPELBE, O. K., CLEWELL, D. B. & DAHLEN, G. 2005a. Virulence, phenotype and genotype characteristics of endodontic *Enterococcus* spp. *Oral Microbiol Immunol*, 20, 10-9.
- SEDGLEY, C. M., NAGEL, A. C., SHELBURNE, C. E., CLEWELL, D. B., APPELBE, O. & MOLANDER, A. 2005b. Quantitative real-time PCR detection of oral *Enterococcus faecalis* in humans. *Arch Oral Biol*, 50, 575-83.
- SERRA-CARDONA, A., PETREZSELYOVA, S., CANADELL, D., RAMOS, J. & ARINO, J. 2014. Coregulated expression of the Na⁺/phosphate Pho89 transporter and Ena1 Na⁺-ATPase allows their functional coupling under high-pH stress. *Mol Cell Biol*, 34, 4420-35.
- SERRAGE, H. J., JEPSON, M. A., ROSTAMI, N., JAKUBOVICS, N. S. & NOBBS, A. H. 2021. Understanding the Matrix: The Role of Extracellular DNA in Oral Biofilms. *Front Oral Health*, 2, 640129.
- SERRANO, R., RUIZ, A., BERNAL, D., CHAMBERS, J. R. & ARIÑO, J. 2002. The transcriptional response to alkaline pH in *Saccharomyces cerevisiae*: evidence for calcium-mediated signalling. *Molecular microbiology*, 46, 1319-1333.
- SHANNON, P., MARKIEL, A., OZIER, O., BALIGA, N. S., WANG, J. T., RAMAGE, D., AMIN, N., SCHWIKOWSKI, B. & IDEKER, T. 2003. Cytoscape: a software environment for integrated models of biomolecular interaction networks. *Genome Res*, 13, 2498-504.
- SHE, P., WANG, Y., LI, Y., ZHOU, L., LI, S., ZENG, X., LIU, Y., XU, L. & WU, Y. 2021. Drug Repurposing: In vitro and in vivo Antimicrobial and Antibiofilm Effects of Bithionol Against *Enterococcus faecalis* and *Enterococcus faecium*. *Front Microbiol*, 12, 579806.
- SHEKH, R. M. & ROY, U. 2012. Biochemical characterization of an anti-*Candida* factor produced by *Enterococcus faecalis*. *BMC Microbiol*, 12, 132.
- SHEMER, R., MEIMOUN, A., HOLTZMAN, T. & KORNITZER, D. 2002. Regulation of the transcription factor Gcn4 by Pho85 cyclin PCL5. *Mol Cell Biol*, 22, 5395-404.

- SHEPARD, B. D. & GILMORE, M. S. 1999. Identification of aerobically and anaerobically induced genes in *Enterococcus faecalis* by random arbitrarily primed PCR. *Appl Environ Microbiol*, 65, 1470-6.
- SHIN, J., LEE, S., GO, M.-J., LEE, S. Y., KIM, S. C., LEE, C.-H. & CHO, B.-K. 2016. Analysis of the mouse gut microbiome using full-length 16S rRNA amplicon sequencing. *Scientific reports*, 6, 1-10.
- SHIN, J. M., LUO, T., LEE, K. H., GUERREIRO, D., BOTERO, T. M., MCDONALD, N. J. & RICKARD, A. H. 2018. Deciphering Endodontic Microbial Communities by Next-generation Sequencing. *J Endod*, 44, 1080-1087.
- SHOKEEN, B., DINIS, M. D. B., HAGHIGHI, F., TRAN, N. C. & LUX, R. 2021. Omics and interspecies interaction. *Periodontol 2000*, 85, 101-111.
- SHORT, B., DELANEY, C., MCKLOUD, E., BROWN, J. L., KEAN, R., LITHERLAND, G. J., WILLIAMS, C., MARTIN, S. L., MACKAY, W. G. & RAMAGE, G. 2021. Investigating the Transcriptome of *Candida albicans* in a Dual-Species *Staphylococcus aureus* Biofilm Model. *Front Cell Infect Microbiol*, 11, 791523.
- SHRESTHA, A., SHI, Z., NEOH, K. G. & KISHEN, A. 2010. Nanoparticulates for antibiofilm treatment and effect of aging on its antibacterial activity. *J Endod*, 36, 1030-5.
- SHRESTHA, S. & KISHEN, A. 2017. Bioactive Molecule Delivery Systems for Dentin-pulp Tissue Engineering. *J Endod*, 43, 733-744.
- SILAO, F. G. S. & LJUNGDAHL, P. O. 2021. Amino Acid Sensing and Assimilation by the Fungal Pathogen *Candida albicans* in the Human Host. *Pathogens*, 11.
- SILAO, F. G. S., RYMAN, K., JIANG, T., WARD, M., HANSMANN, N., MOLENAAR, C., LIU, N.-N., CHEN, C. & LJUNGDAHL, P. O. 2021. Correction: Glutamate dehydrogenase (Gdh2)-dependent alkalization is dispensable for escape from macrophages and virulence of *Candida albicans*. *PLoS pathogens*, 17, e1009877.
- SILVA, P. V., GUEDES, D. F., NAKADI, F. V., PECORA, J. D. & CRUZ-FILHO, A. M. 2013. Chitosan: a new solution for removal of smear layer after root canal instrumentation. *Int Endod J*, 46, 332-8.
- SILVA, S., RODRIGUES, C. F., ARAUJO, D., RODRIGUES, M. E. & HENRIQUES, M. 2017. *Candida* Species Biofilms' Antifungal Resistance. *J Fungi (Basel)*, 3.
- SINGH, K. V. & MURRAY, B. E. 2005. Differences in the *Enterococcus faecalis* *lsa* locus that influence susceptibility to quinupristin-dalfopristin and clindamycin. *Antimicrobial agents and chemotherapy*, 49, 32-39.
- SIQUEIRA, J. F., JR. 2002. Endodontic infections: concepts, paradigms, and perspectives. *Oral Surg Oral Med Oral Pathol Oral Radiol Endod*, 94, 281-93.
- SIQUEIRA, J. F., JR., ANTUNES, H. S., ROCAS, I. N., RACHID, C. T. & ALVES, F. R. 2016. Microbiome in the Apical Root Canal System of Teeth with Post-Treatment Apical Periodontitis. *PLoS One*, 11, e0162887.
- SIQUEIRA, J. F., JR. & ROCAS, I. N. 2004. Polymerase chain reaction-based analysis of microorganisms associated with failed endodontic treatment. *Oral Surg Oral Med Oral Pathol Oral Radiol Endod*, 97, 85-94.
- SIQUEIRA, J. F., JR. & ROCAS, I. N. 2007. Bacterial pathogenesis and mediators in apical periodontitis. *Braz Dent J*, 18, 267-80.
- SIQUEIRA, J. F., JR. & ROCAS, I. N. 2008. Clinical implications and microbiology of bacterial persistence after treatment procedures. *J Endod*, 34, 1291-1301 e3.

- SIQUEIRA, J. F., JR. & ROCAS, I. N. 2009a. Community as the unit of pathogenicity: an emerging concept as to the microbial pathogenesis of apical periodontitis. *Oral Surgery, Oral Medicine, Oral Pathology, Oral Radiology, and Endodontology*, 107, 870-878.
- SIQUEIRA, J. F., JR. & ROCAS, I. N. 2009b. Distinctive features of the microbiota associated with different forms of apical periodontitis. *J Oral Microbiol*, 1.
- SIQUEIRA, J. F., JR. & ROCAS, I. N. 2009c. Diversity of endodontic microbiota revisited. *J Dent Res*, 88, 969-81.
- SIQUEIRA, J. F., JR. & ROCAS, I. N. 2013a. As-yet-uncultivated oral bacteria: breadth and association with oral and extra-oral diseases. *J Oral Microbiol*, 5.
- SIQUEIRA, J. F., JR. & ROCAS, I. N. 2013b. Microbiology and treatment of acute apical abscesses. *Clin Microbiol Rev*, 26, 255-73.
- SIQUEIRA, J. F., JR. & ROCAS, I. N. 2017. The Oral Microbiota in Health and Disease: An Overview of Molecular Findings. *Methods Mol Biol*, 1537, 127-138.
- SIQUEIRA, J. F., JR. & ROCAS, I. N. 2021. Present status and future directions: Microbiology of endodontic infections. *Int Endod J*.
- SIQUEIRA, J. F., JR., ROCAS, I. N., RICUCCI, D. & HULSMANN, M. 2014. Causes and management of post-treatment apical periodontitis. *Br Dent J*, 216, 305-12.
- SIQUEIRA, J. F., JR., ROCAS, I. N. & ROSADO, A. S. 2004. Investigation of bacterial communities associated with asymptomatic and symptomatic endodontic infections by denaturing gradient gel electrophoresis fingerprinting approach. *Oral Microbiol Immunol*, 19, 363-70.
- SIQUEIRA, J. F., JR. & SEN, B. H. 2004. Fungi in endodontic infections. *Oral Surg Oral Med Oral Pathol Oral Radiol Endod*, 97, 632-41.
- SIQUEIRA, J. J. & FOUAD, A. F. 2014. Endodontic microbiology. *Endodontics - E-Book: Principles and Practice*. St. Louis, Missouri: Saunders.
- SIROTA, M., DUDLEY, J. T., KIM, J., CHIANG, A. P., MORGAN, A. A., SWEET-CORDERO, A., SAGE, J. & BUTTE, A. J. 2011. Discovery and preclinical validation of drug indications using compendia of public gene expression data. *Sci Transl Med*, 3, 96ra77.
- SMITH, S. B., DAMPIER, W., TOZEREN, A., BROWN, J. R. & MAGID-SLAV, M. 2012a. Identification of common biological pathways and drug targets across multiple respiratory viruses based on human host gene expression analysis. *PLoS One*, 7, e33174.
- SMITH, S. W., HAUBEN, M. & ARONSON, J. K. 2012b. Paradoxical and bidirectional drug effects. *Drug Saf*, 35, 173-89.
- SPARLING, P. F. 1983. Bacterial virulence and pathogenesis: an overview. *Rev Infect Dis*, 5 Suppl 4, S637-46.
- SPENCER, H. R., IKE, V. & BRENNAN, P. A. 2007. Review: the use of sodium hypochlorite in endodontics--potential complications and their management. *Br Dent J*, 202, 555-9.
- STACY, A., MCNALLY, L., DARCH, S. E., BROWN, S. P. & WHITELEY, M. 2016. The biogeography of polymicrobial infection. *Nat Rev Microbiol*, 14, 93-105.
- STAHL, P. L., SALMEN, F., VICKOVIC, S., LUNDMARK, A., NAVARRO, J. F., MAGNUSSON, J., GIACOMELLO, S., ASP, M., WESTHOLM, J. O., HUSS, M., MOLLBRINK, A., LINNARSSON, S., CODELUPPI, S., BORG, A., PONTEN, F., COSTEA, P. I., SAHLEN, P., MULDER, J., BERGMANN, O., LUNDEBERG, J. &

- FRISEN, J. 2016. Visualization and analysis of gene expression in tissue sections by spatial transcriptomics. *Science*, 353, 78-82.
- STAIB, P., KRETSCHMAR, M., NICHTERLEIN, T., HOF, H. & MORSCHHAUSER, J. 2000. Differential activation of a *Candida albicans* virulence gene family during infection. *Proc Natl Acad Sci U S A*, 97, 6102-7.
- STAIB, P. & MORSCHHAUSER, J. 2007. Chlamydospore formation in *Candida albicans* and *Candida dubliniensis*--an enigmatic developmental programme. *Mycoses*, 50, 1-12.
- STEHR, F., FELK, A., GACSER, A., KRETSCHMAR, M., MAHNSS, B., NEUBER, K., HUBE, B. & SCHAFFER, W. 2004. Expression analysis of the *Candida albicans* lipase gene family during experimental infections and in patient samples. *FEMS Yeast Res*, 4, 401-8.
- STURTEVANT, J., DIXON, F., WADSWORTH, E., LATGE, J.-P., ZHAO, X.-J. & CALDERONE, R. 1999. Identification and cloning of GCA1, a gene that encodes a cell surface glucoamylase from *Candida albicans*. *Medical mycology*, 37, 357-366.
- SU, L.-J., LIN, H.-H., WU, M.-S., PAN, L., YADAV, K., HSU, H.-H., LING, T.-Y., CHEN, Y.-T. & CHANG, H.-C. 2019. Intracellular delivery of luciferase with fluorescent nanodiamonds for dual-modality imaging of human stem cells. *Bioconjugate Chemistry*, 30, 2228-2237.
- SUDBERY, P. E. 2011. Growth of *Candida albicans* hyphae. *Nat Rev Microbiol*, 9, 737-48.
- SUN, J. N., SOLIS, N. V., PHAN, Q. T., BAJWA, J. S., KASHLEVA, H., THOMPSON, A., LIU, Y., DONGARI-BAGTZOGLU, A., EDGERTON, M. & FILLER, S. G. 2010. Host cell invasion and virulence mediated by *Candida albicans* Ssa1. *PLoS pathogens*, 6, e1001181.
- SUNDQVIST, G. 1976. *Bacteriological Studies of Necrotic Dental Pulps*. Ph.D, University of Umea, Sweden. .
- SUNDQVIST, G. 1994. Taxonomy, ecology, and pathogenicity of the root canal flora. *Oral Surg Oral Med Oral Pathol*, 78, 522-30.
- SUZUKI, T. Y. U., GALLEGO, J., ASSUNCAO, W. G., BRISO, A. L. F. & DOS SANTOS, P. H. 2019. Influence of silver nanoparticle solution on the mechanical properties of resin cements and intraradicular dentin. *PLoS One*, 14, e0217750.
- SWIMBERGHE, R. C. D., COENYE, T., DE MOOR, R. J. G. & MEIRE, M. A. 2019. Biofilm model systems for root canal disinfection: a literature review. *Int Endod J*, 52, 604-628.
- SZTUKOWSKA, M. N., DUTTON, L. C., DELANEY, C., RAMSDALE, M., RAMAGE, G., JENKINSON, H. F., NOBBS, A. H. & LAMONT, R. J. 2018. Community development between *Porphyromonas gingivalis* and *Candida albicans* mediated by InlJ and Als3. *MBio*, 9, e00202-18.
- SZUNERITS, S., BARRAS, A. & BOUKHERROUB, R. 2016. Antibacterial Applications of Nanodiamonds. *Int J Environ Res Public Health*, 13, 413.
- TAGLIALEGNA, A., NAVARRO, S., VENTURA, S., GARNETT, J. A., MATTHEWS, S., PENADES, J. R., LASA, I. & VALLE, J. 2016. Staphylococcal Bap Proteins Build Amyloid Scaffold Biofilm Matrices in Response to Environmental Signals. *PLoS Pathog*, 12, e1005711.
- TAN, F., SHE, P., ZHOU, L., LIU, Y., CHEN, L., LUO, Z. & WU, Y. 2019. Bactericidal and Anti-biofilm Activity of the Retinoid Compound CD437 Against *Enterococcus faecalis*. *Front Microbiol*, 10, 2301.

- TANNER, A. C., KRESSIRER, C., FALLER, L., LAKE, K., DEWHIRST, F., KOKARASB, A., PASTER, B. & FRIAS-LOPEZ, J. 2017. Bacterial metatranscriptome of dentin caries. *Journal of Oral Microbiology*, 9, 1325194.
- TASSEL, D. & MADOFF, M. A. 1968. Treatment of Candida sepsis and Cryptococcus meningitis with 5-fluorocytosine: a new antifungal agent. *Jama*, 206, 830-832.
- TCHORYK, A., TARESCO, V., ARGENT, R. H., ASHFORD, M., GELLERT, P. R., STOLNIK, S., GRABOWSKA, A. & GARNETT, M. C. 2019. Penetration and Uptake of Nanoparticles in 3D Tumor Spheroids. *Bioconjug Chem*, 30, 1371-1384.
- TESCHLER, J. K., ZAMORANO-SANCHEZ, D., UTADA, A. S., WARNER, C. J., WONG, G. C., LININGTON, R. G. & YILDIZ, F. H. 2015. Living in the matrix: assembly and control of Vibrio cholerae biofilms. *Nat Rev Microbiol*, 13, 255-68.
- TINWALA, H. & WAIRKAR, S. 2019. Production, surface modification and biomedical applications of nanodiamonds: A sparkling tool for theranostics. *Mater Sci Eng C Mater Biol Appl*, 97, 913-931.
- TOLEDO-ARANA, A., VALLE, J., SOLANO, C., ARRIZUBIETA, M. A. J., CUCARELLA, C., LAMATA, M., AMORENA, B., LEIVA, J., PENADÉS, J. R. & LASA, I. 2001. The enterococcal surface protein, Esp, is involved in Enterococcus faecalis biofilm formation. *Applied and environmental microbiology*, 67, 4538-4545.
- TORRES SANGIAO, E., HOLBAN, A. M. & GESTAL, M. C. 2019. Applications of Nanodiamonds in the Detection and Therapy of Infectious Diseases. *Materials (Basel)*, 12.
- TRIPATHI, G., WILTSHIRE, C., MACASKILL, S., TOURNU, H., BUDGE, S. & BROWN, A. J. 2002. Gcn4 co-ordinates morphogenetic and metabolic responses to amino acid starvation in Candida albicans. *EMBO J*, 21, 5448-56.
- TURCHENIUK, V., RAKS, V., ISSA, R., COOPER, I. R., CRAGG, P. J., JIJIE, R., DUMITRASCU, N., MIKHALOVSKA, L. I., BARRAS, A. & ZAITSEV, V. 2015. Antimicrobial activity of menthol modified nanodiamond particles. *Diamond and Related Materials*, 57, 2-8.
- TURNBULL, L., TOYOFUKU, M., HYNEN, A. L., KUROSAWA, M., PESSI, G., PETTY, N. K., OSVATH, S. R., CARCAMO-OYARCE, G., GLOAG, E. S., SHIMONI, R., OMASITS, U., ITO, S., YAP, X., MONAHAN, L. G., CAVALIERE, R., AHRENS, C. H., CHARLES, I. G., NOMURA, N., EBERL, L. & WHITCHURCH, C. B. 2016. Explosive cell lysis as a mechanism for the biogenesis of bacterial membrane vesicles and biofilms. *Nat Commun*, 7, 11220.
- TZANETAKIS, G. N., AZCARATE-PERIL, M. A., ZACHAKI, S., PANOPOULOS, P., KONTAKIOTIS, E. G., MADIANOS, P. N. & DIVARIS, K. 2015. Comparison of Bacterial Community Composition of Primary and Persistent Endodontic Infections Using Pyrosequencing. *J Endod*, 41, 1226-33.
- TZUNG, K. W., WILLIAMS, R. M., SCHERER, S., FEDERSPIEL, N., JONES, T., HANSEN, N., BIVOLAREVIC, V., HUIZAR, L., KOMP, C., SURZYCKI, R., TAMSE, R., DAVIS, R. W. & AGABIAN, N. 2001. Genomic evidence for a complete sexual cycle in Candida albicans. *Proc Natl Acad Sci U S A*, 98, 3249-53.
- UPPULURI, P., CHATURVEDI, A. K., SRINIVASAN, A., BANERJEE, M., RAMASUBRAMANIAM, A. K., KÖHLER, J. R., KADOSH, D. & LOPEZ-RIBOT, J. L. 2010a. Dispersion as an important step in the Candida albicans biofilm developmental cycle. *PLoS pathogens*, 6, e1000828.

- UPPULURI, P., PIERCE, C. G., THOMAS, D. P., BUBECK, S. S., SAVILLE, S. P. & LOPEZ-RIBOT, J. L. 2010b. The transcriptional regulator Nrg1p controls *Candida albicans* biofilm formation and dispersion. *Eukaryot Cell*, 9, 1531-7.
- VAN HOEK, A. H., MEVIUS, D., GUERRA, B., MULLANY, P., ROBERTS, A. P. & AARTS, H. J. 2011. Acquired antibiotic resistance genes: an overview. *Front Microbiol*, 2, 203.
- VAN TYNE, D., MARTIN, M. J. & GILMORE, M. S. 2013. Structure, function, and biology of the *Enterococcus faecalis* cytolysin. *Toxins*, 5, 895-911.
- VANDERMEULEN, M. D. & CULLEN, P. J. 2022. Gene by Environment Interactions reveal new regulatory aspects of signaling network plasticity. *PLoS Genet*, 18, e1009988.
- VASUDEVAN, R. 2014. Biofilms: microbial cities of scientific significance. *J Microbiol Exp*, 1, 00014.
- VENGERFELDT, V., SPILKA, K., SAAG, M., PREEM, J. K., OOPKAUP, K., TRUU, J. & MANDAR, R. 2014. Highly diverse microbiota in dental root canals in cases of apical periodontitis (data of illumina sequencing). *J Endod*, 40, 1778-83.
- VERSTREPEN, K. J. & KLIS, F. M. 2006. Flocculation, adhesion and biofilm formation in yeasts. *Mol Microbiol*, 60, 5-15.
- VESIĆ, D. & KRISTICH, C. J. 2012. MurAA is required for intrinsic cephalosporin resistance of *Enterococcus faecalis*. *Antimicrobial agents and chemotherapy*, 56, 2443-2451.
- VIANNA, M. E., GOMES, B. P., BERBER, V. B., ZAIA, A. A., FERRAZ, C. C. & DE SOUZA-FILHO, F. J. 2004. In vitro evaluation of the antimicrobial activity of chlorhexidine and sodium hypochlorite. *Oral Surg Oral Med Oral Pathol Oral Radiol Endod*, 97, 79-84.
- VIEIRA, A. P. M., ARIAS, L. S., DE SOUZA NETO, F. N., KUBO, A. M., LIMA, B. H. R., DE CAMARGO, E. R., PESSAN, J. P., DELBEM, A. C. B. & MONTEIRO, D. R. 2019. Antibiofilm effect of chlorhexidine-carrier nanosystem based on iron oxide magnetic nanoparticles and chitosan. *Colloids and Surfaces B: Biointerfaces*, 174, 224-231.
- VINOGRADOV, A., WINSTON, M., RUPP, C. J. & STOODLEY, P. 2004. Rheology of biofilms formed from the dental plaque pathogen *Streptococcus mutans*. *Biofilms*, 1, 49-56.
- VLAMAKIS, H., CHAI, Y., BEAUREGARD, P., LOSICK, R. & KOLTER, R. 2013. Sticking together: building a biofilm the *Bacillus subtilis* way. *Nat Rev Microbiol*, 11, 157-68.
- VYLKOVA, S. & LORENZ, M. C. 2014. Modulation of phagosomal pH by *Candida albicans* promotes hyphal morphogenesis and requires Stp2p, a regulator of amino acid transport. *PLoS pathogens*, 10, e1003995.
- WAAR, K., VAN DER MEI, H. C., HARMSSEN, H. J. M., DEGENER, J. E. & BUSSCHER, H. J. 2002. *Enterococcus faecalis* surface proteins determine its adhesion mechanism to bile drain materials. *Microbiology (Reading)*, 148, 1863-1870.
- WALLACE, B. D., WANG, H., LANE, K. T., SCOTT, J. E., ORANS, J., KOO, J. S., VENKATESH, M., JOBIN, C., YEY, L. A., MANI, S. & REDINBO, M. R. 2010. Alleviating cancer drug toxicity by inhibiting a bacterial enzyme. *Science*, 330, 831-5.
- WALTON, R. E. & TORABINEJAD, M. 2015. *Endodontics : principles and practice*.

- WANG, C., HOU, J., VAN DER MEI, H. C., BUSSCHER, H. J. & REN, Y. 2019. Emergent properties in *Streptococcus mutans* biofilms are controlled through adhesion force sensing by initial colonizers. *MBio*, 10, e01908-19.
- WANG, J., QI, J., ZHAO, H., HE, S., ZHANG, Y., WEI, S. & ZHAO, F. 2013. Metagenomic sequencing reveals microbiota and its functional potential associated with periodontal disease. *Sci Rep*, 3, 1843.
- WANG, L., DONG, M., ZHENG, J., SONG, Q., YIN, W., LI, J. & NIU, W. 2011. Relationship of biofilm formation and *gelE* gene expression in *Enterococcus faecalis* recovered from root canals in patients requiring endodontic retreatment. *J Endod*, 37, 631-6.
- WANG, Z., GERSTEIN, M. & SNYDER, M. 2009. RNA-Seq: a revolutionary tool for transcriptomics. *Nat Rev Genet*, 10, 57-63.
- WANG, Z., MONTEIRO, C. D., JAGODNIK, K. M., FERNANDEZ, N. F., GUNDERSEN, G. W., ROUILLARD, A. D., JENKINS, S. L., FELDMANN, A. S., HU, K. S., MCDERMOTT, M. G., DUAN, Q., CLARK, N. R., JONES, M. R., KOU, Y., GOFF, T., WOODLAND, H., AMARAL, F. M. R., SZETO, G. L., FUCHS, O., SCHUSSLER-FIORENZA ROSE, S. M., SHARMA, S., SCHWARTZ, U., BAUSELA, X. B., SZYMKIEWICZ, M., MAROULIS, V., SALYKIN, A., BARRA, C. M., KRUTH, C. D., BONGIO, N. J., MATHUR, V., TODORIC, R. D., RUBIN, U. E., MALATRAS, A., FULP, C. T., GALINDO, J. A., MOTIEJUNAITE, R., JUSCHKE, C., DISHUCK, P. C., LAHL, K., JAFARI, M., AIBAR, S., ZARAVINOS, A., STEENHUIZEN, L. H., ALLISON, L. R., GAMALLO, P., DE ANDRES SEGURA, F., DAE DEVLIN, T., PEREZ-GARCIA, V. & MA'AYAN, A. 2016. Extraction and analysis of signatures from the Gene Expression Omnibus by the crowd. *Nat Commun*, 7, 12846.
- WARENDA, A. J. & KONOPKA, J. B. 2002. Septin function in *Candida albicans* morphogenesis. *Mol Biol Cell*, 13, 2732-46.
- WATAMOTO, T., EGUSA, H., SAWASE, T. & YATANI, H. 2015. Screening of Pharmacologically Active Small Molecule Compounds Identifies Antifungal Agents Against *Candida* Biofilms. *Front Microbiol*, 6, 1453.
- WAYNE, P. 2002. Reference method for broth dilution antifungal susceptibility testing of yeasts, approved standard. *CLSI document M27-A2*.
- WEERSMA, R. K., ZHERNAKOVA, A. & FU, J. 2020. Interaction between drugs and the gut microbiome. *Gut*, 69, 1510-1519.
- WEHLING, J., DRINGEN, R., ZARE, R. N., MAAS, M. & REZWAN, K. 2014. Bactericidal activity of partially oxidized nanodiamonds. *ACS nano*, 8, 6475-6483.
- WEINER-LASTINGER, L. M., ABNER, S., EDWARDS, J. R., KALLEN, A. J., KARLSSON, M., MAGILL, S. S., POLLOCK, D., SEE, I., SOE, M. M., WALTERS, M. S. & DUDECK, M. A. 2020. Antimicrobial-resistant pathogens associated with adult healthcare-associated infections: Summary of data reported to the National Healthcare Safety Network, 2015-2017. *Infect Control Hosp Epidemiol*, 41, 1-18.
- WEINSTEIN, J. N. 2012. Drug discovery: Cell lines battle cancer. *Nature*, 483, 544-5.
- WEISBURG, W. G., BARNS, S. M., PELLETIER, D. A. & LANE, D. J. 1991. 16S ribosomal DNA amplification for phylogenetic study. *J Bacteriol*, 173, 697-703.
- WEISS, E. L., KURISCHKO, C., ZHANG, C., SHOKAT, K., DRUBIN, D. G. & LUCA, F. C. 2002. The *Saccharomyces cerevisiae* Mob2p-Cbk1p kinase complex promotes polarized growth and acts with the mitotic exit network to

- facilitate daughter cell-specific localization of Ace2p transcription factor. *The Journal of cell biology*, 158, 885-900.
- WEISSMAN, Z. & KORNITZER, D. 2004. A family of Candida cell surface haem-binding proteins involved in haemin and haemoglobin-iron utilization. *Mol Microbiol*, 53, 1209-20.
- WHALEY, S. G., BERKOW, E. L., RYBAK, J. M., NISHIMOTO, A. T., BARKER, K. S. & ROGERS, P. D. 2016. Azole Antifungal Resistance in Candida albicans and Emerging Non-albicans Candida Species. *Front Microbiol*, 7, 2173.
- WHITE, H., HELD, C., STEWART, R., WATSON, D., HARRINGTON, R., BUDAJ, A., STEG, P. G., CANNON, C. P., KRUG-GOURLEY, S., WITTES, J., TRIVEDI, T., TARKA, E. & WALLENTIN, L. 2010. Study design and rationale for the clinical outcomes of the STABILITY Trial (STabilization of Atherosclerotic plaque By Initiation of darapLadlb TherapY) comparing darapladib versus placebo in patients with coronary heart disease. *Am Heart J*, 160, 655-61.
- WIGHTMAN, R., BATES, S., AMORNRATTANAPAN, P. & SUDBERY, P. 2004. In Candida albicans, the Nim1 kinases Gin4 and Hsl1 negatively regulate pseudohypha formation and Gin4 also controls septin organization. *J Cell Biol*, 164, 581-91.
- WILKINS, M. R., SANCHEZ, J. C., GOOLEY, A. A., APPEL, R. D., HUMPHERY-SMITH, I., HOCHSTRASSER, D. F. & WILLIAMS, K. L. 1996. Progress with proteome projects: why all proteins expressed by a genome should be identified and how to do it. *Biotechnol Genet Eng Rev*, 13, 19-50.
- WILSON, J. W., SCHURR, M. J., LEBLANC, C. L., RAMAMURTHY, R., BUCHANAN, K. L. & NICKERSON, C. A. 2002. Mechanisms of bacterial pathogenicity. *Postgrad Med J*, 78, 216-24.
- WINAND, R., BOGAERTS, B., HOFFMAN, S., LEFEVRE, L., DELVOYE, M., BRAEKEL, J. V., FU, Q., ROOSENS, N. H., KEERSMAECKER, S. C. & VANNESTE, K. 2019. Targeting the 16s Rna Gene for Bacterial Identification in Complex Mixed Samples: Comparative Evaluation of Second (Illumina) and Third (Oxford Nanopore Technologies) Generation Sequencing Technologies. *Int J Mol Sci*, 21.
- WINGETT, S. W. & ANDREWS, S. 2018. FastQ Screen: A tool for multi-genome mapping and quality control. *F1000Res*, 7, 1338.
- WINTER, M. B., SALCEDO, E. C., LOHSE, M. B., HARTOONI, N., GULATI, M., SANCHEZ, H., TAKAGI, J., HUBE, B., ANDES, D. R., JOHNSON, A. D., CRAIK, C. S. & NOBILE, C. J. 2016. Global Identification of Biofilm-Specific Proteolysis in Candida albicans. *mBio*, 7.
- WISPLINGHOFF, H., BISCHOFF, T., TALLENT, S. M., SEIFERT, H., WENZEL, R. P. & EDMOND, M. B. 2004. Nosocomial bloodstream infections in US hospitals: analysis of 24,179 cases from a prospective nationwide surveillance study. *Clin Infect Dis*, 39, 309-17.
- WOLF, T., KAMMER, P., BRUNKE, S. & LINDE, J. 2018. Two's company: studying interspecies relationships with dual RNA-seq. *Curr Opin Microbiol*, 42, 7-12.
- WONG, J., MANOIL, D., NASMAN, P., BELIBASAKIS, G. N. & NEELAKANTAN, P. 2021a. Microbiological Aspects of Root Canal Infections and Disinfection Strategies: An Update Review on the Current Knowledge and Challenges. *Front Oral Health*, 2, 672887.
- WONG, J., ZOU, T., LEE, A. H. C. & ZHANG, C. 2021b. The Potential Translational Applications of Nanoparticles in Endodontics. *Int J Nanomedicine*, 16, 2087-2106.

- WONG, K. H., HYNES, M. J. & DAVIS, M. A. 2008. Recent advances in nitrogen regulation: a comparison between *Saccharomyces cerevisiae* and filamentous fungi. *Eukaryot Cell*, 7, 917-25.
- WU, D., FAN, W., KISHEN, A., GUTMANN, J. L. & FAN, B. 2014. Evaluation of the antibacterial efficacy of silver nanoparticles against *Enterococcus faecalis* biofilm. *J Endod*, 40, 285-90.
- WURDAK, H., ZHU, S., MIN, K. H., AIMONE, L., LAIRSON, L. L., WATSON, J., CHOPIUK, G., DEMAS, J., CHARETTE, B., HALDER, R., WEERAPANA, E., CRAVATT, B. F., CLINE, H. T., PETERS, E. C., ZHANG, J., WALKER, J. R., WU, C., CHANG, J., TUNTLAND, T., CHO, C. Y. & SCHULTZ, P. G. 2010. A small molecule accelerates neuronal differentiation in the adult rat. *Proc Natl Acad Sci U S A*, 107, 16542-7.
- XIAO, J., HOOK, M., WEINSTOCK, G. M. & MURRAY, B. E. 1998. Conditional adherence of *Enterococcus faecalis* to extracellular matrix proteins. *FEMS Immunol Med Microbiol*, 21, 287-95.
- YAJKO, D. M., MADEJ, J. J., LANCASTER, M. V., SANDERS, C. A., CAWTHON, V. L., GEE, B., BABST, A. & HADLEY, W. K. 1995. Colorimetric method for determining MICs of antimicrobial agents for *Mycobacterium tuberculosis*. *Journal of clinical microbiology*, 33, 2324-2327.
- YAMAZAKI, T., USHIKOSHI-NAKAYAMA, R., SHIRONE, K., SUZUKI, M., ABE, S., MATSUMOTO, N., INOUE, H. & SAITO, I. 2019. Evaluation of the effect of a heat-killed lactic acid bacterium, *Enterococcus faecalis* 2001, on oral candidiasis. *Beneficial Microbes*, 10, 661-669.
- YIN, I. X., ZHANG, J., ZHAO, I. S., MEI, M. L., LI, Q. & CHU, C. H. 2020. The Antibacterial Mechanism of Silver Nanoparticles and Its Application in Dentistry. *Int J Nanomedicine*, 15, 2555-2562.
- YOO, Y. J., KIM, A. R., PERINPANAYAGAM, H., HAN, S. H. & KUM, K. Y. 2020. *Candida albicans* Virulence Factors and Pathogenicity for Endodontic Infections. *Microorganisms*, 8.
- YU, M. K., KIM, M. A., ROSA, V., HWANG, Y. C., DEL FABBRO, M., SOHN, W. J. & MIN, K. S. 2019a. Role of extracellular DNA in *Enterococcus faecalis* biofilm formation and its susceptibility to sodium hypochlorite. *J Appl Oral Sci*, 27, e20180699.
- YU, Y., YANG, X., LIU, M., NISHIKAWA, M., TEI, T. & MIYAKO, E. 2019b. Amphipathic Nanodiamond Supraparticles for Anticancer Drug Loading and Delivery. *ACS Appl Mater Interfaces*, 11, 18978-18987.
- ZANCAN, R. F., CALEFI, P. H. S., BORGES, M. M. B., LOPES, M. R. M., DE ANDRADE, F. B., VIVAN, R. R. & DUARTE, M. A. H. 2019. Antimicrobial activity of intracanal medications against both *Enterococcus faecalis* and *Candida albicans* biofilm. *Microsc Res Tech*, 82, 494-500.
- ZENG, X., SHE, P., ZHOU, L., LI, S., HUSSAIN, Z., CHEN, L. & WU, Y. 2021. Drug repurposing: Antimicrobial and antibiofilm effects of penfluridol against *Enterococcus faecalis*. *Microbiologyopen*, 10, e1148.
- ZERVOS, M. J., KAUFFMAN, C. A., THERASSE, P. M., BERGMAN, A. G., MIKESSELL, T. S. & SCHABERG, D. R. 1987. Nosocomial infection by gentamicin-resistant *Streptococcus faecalis*: an epidemiologic study. *Annals of Internal Medicine*, 106, 687-691.
- ZHANG, T., KALIMUTHU, S., RAJASEKAR, V., XU, F., YIU, Y. C., HUI, T. K., NEELAKANTAN, P. & CHU, Z. 2021a. Biofilm inhibition in oral pathogens by nanodiamonds. *Biomaterials Science*.

- ZHANG, T., KALIMUTHU, S., RAJASEKAR, V., XU, F., YIU, Y. C., HUI, T. K. C., NEELAKANTAN, P. & CHU, Z. 2021b. Biofilm inhibition in oral pathogens by nanodiamonds. *Biomater Sci*, 9, 5127-5135.
- ZHANG, Y., SHI, W., SONG, Y. & WANG, J. 2019. Metatranscriptomic analysis of an in vitro biofilm model reveals strain-specific interactions among multiple bacterial species. *J Oral Microbiol*, 11, 1599670.
- ZHENG, J. X., WU, Y., LIN, Z. W., PU, Z. Y., YAO, W. M., CHEN, Z., LI, D. Y., DENG, Q. W., QU, D. & YU, Z. J. 2017. Characteristics of and Virulence Factors Associated with Biofilm Formation in Clinical *Enterococcus faecalis* Isolates in China. *Front Microbiol*, 8, 2338.
- ZHENG, X., WANG, Y. & WANG, Y. 2004. Hgc1, a novel hypha-specific G1 cyclin-related protein regulates *Candida albicans* hyphal morphogenesis. *EMBO J*, 23, 1845-56.
- ZHU, X., WANG, Q., ZHANG, C., CHEUNG, G. S. & SHEN, Y. 2010. Prevalence, phenotype, and genotype of *Enterococcus faecalis* isolated from saliva and root canals in patients with persistent apical periodontitis. *Journal of endodontics*, 36, 1950-1955.
- ZHU, Y., LI, J., LI, W., ZHANG, Y., YANG, X., CHEN, N., SUN, Y., ZHAO, Y., FAN, C. & HUANG, Q. 2012. The biocompatibility of nanodiamonds and their application in drug delivery systems. *Theranostics*, 2, 302.
- ZIMMERMANN, M., PATIL, K. R., TYPAS, A. & MAIER, L. 2021. Towards a mechanistic understanding of reciprocal drug-microbiome interactions. *Mol Syst Biol*, 17, e10116.
- ZIMMERMANN, M., ZIMMERMANN-KOGADEEVA, M., WEGMANN, R. & GOODMAN, A. L. 2019. Mapping human microbiome drug metabolism by gut bacteria and their genes. *Nature*, 570, 462-467.
- ZOLETTI, G. O., PEREIRA, E. M., SCHUENCK, R. P., TEIXEIRA, L. M., SIQUEIRA, J. F. & DOS SANTOS, K. R. N. 2011. Characterization of virulence factors and clonal diversity of *Enterococcus faecalis* isolates from treated dental root canals. *Research in Microbiology*, 162, 151-158.